7th edition

of the international scientific conference

ForestSAT 2016

15th to 18th

of November 2016

Santiago, Chile

OTERRA

Centro de Estudios de Recursos Naturales

Universidad Mayor

Universidad Mayor

para espíritus emprendedores

Facultad de Ciencias

Escuela de Ingeniería Forestal

Título: Proceedings Book 7th edition of the International Scientific Conference ForestSAT 2016

Editores: Claudio Muñoz Riveros,
Paulina Javiera Vidal Páez,
Waldo Antonio Pérez Martínez,
Pablo Christian Cruz Johnson,
Markus Frederick Keusch,
Jesús Torralba Pérez.

ISBN: 978-956-7459-49-0

Edita: Universidad Mayor

Printed in Chile
Imprime: CUPOLICAN Servicios Gráficos - Fono 226716467
Dieciocho Nº 786, Santiago, Chile
ventas@caupolican.cl

Hosts

Sponsors

Organizing Committee

Claudio Muñoz
OTERRA, Universidad Mayor, Chile.

Pablo Cruz
OTERRA, Universidad Mayor, Chile.

Waldo Perez
OTERRA, Universidad Mayor, Chile.

Paulina Vidal
OTERRA, Universidad Mayor, Chile.

Jesús Torralba
OTERRA, Universidad Mayor, Chile.

Markus Frederick Keusch
OTERRA, Universidad Mayor, Chile.

Steering Committee

David Miranda,
Universidad Santiago Compostela, Spain.

Gherardo Chirici,
Universidad de Firenze, Italy.

Hakan Olsson,
Swedish University of Agricultural Sciences, Sweden.

Javier Cano,
Corporación Nacional Forestal, Chile.

Juan Suarez,
Forest Research, UK.

Maureen Duane,
Oregon State, USA.

Pablo Cruz,
OTERRA, Universidad Mayor, Chile.

Ronald McRobert,
USDA Forest Service, USA.

Ross Hill,
Bournemouth University, UK.

Tatjana Koukal,
BOKU, Austria.

Warren Cohen,
USDA Forest Service, USA.

Scientific Committee

Alfonso Condal,
Laval University, Québec, Canada.

Alvaro Gutiérrez,
Universidad de Chile, Chile.

Angela de Santis,
Centro Científico Regional Fundación CEQUA, Chile.

Annemarie Bastrup-Birk,
European Environmental Agency, Denmark.

Carlos Cárdenas,
Universidad de Magallanes, Chile.

Cristian Mattar,
Universidad de Chile, Chile.

Damiano Gianelle,
Fondazione Edmund Mach, Italy.

Daniel McInerney,
Coillte Teoranta (State Forest Board), Ireland.

Esteban Vojkovic,
CIREN, Chile.

Hubert Hasenauer,
BOKU, Austria.

Hugo Rivera,
Corporación Nacional Forestal, Chile.

Jaime Hernandez,
Universidad de Chile, Chile.

Joao Roberto dos Santos,
INPE, Brazil.

Juan Carlos Jiménez-Muñoz,
UVEG, Spain.

Juan de la Riva,
Universidad de Zaragoza, Spain.

Juan Pablo Flores,
CIREN, Chile.

Juan Suarez,
Forest Research, UK.

Lars T. Waser,
Swiss Federal Research Institute WSL, Switzerland.

Laszlo Pancel,
GIZ, Germany.

Lin Cao,
Nanjing Forestry University, China.

Lori D. Daniels,
Forestry UBC, Canada.

Lucio Castro,
Embrapa, Brazil.

Luis Morales,
Universidad de Chile, Chile.

Marcelo Miranda,
Universidad Católica, Chile.

Marcelo Scavuzzo,
Comisión Nacional de Actividades Espaciales CONAE, Argentina.

Maria Augusta Doetzer,
Embrapa, Brazil.

Maria Pilar Martin,
CSIC, Spain.

Michael Koehl,
World Forest Institute, Germany.

Nicholas C. Coops,
Forestry UBC, Canada.

Patricio Acevedo,
Universidad de la Frontera, Chile.

Richard Fournier,
Université de Sherbrooke, Canada.

Ross Hill,
Bournemouth University, UK.

Ruben Valbuena,
University of Eastern Finland, Finland.

Tatjana Koukal,
BOKU, Austria.

Victor Sandoval,
Universidad Austral, Chile.

Warren Cohen,
USDA Forest Service, USA.

Yony Ormazábal,
Universidad de Talca, Chile.

Presentation

Dear all,
We are pleased to introduce you the scientific programme of the 7th edition of ForestSAT. The international conference of Spatial Application Tools in Forestry is the continuation of an idea that started in back in 2002. An idea that has been growing progressively into an international movement of foresters, scientists and developers around the use of Earth Observation in forestry. This year, the organisation of this conference is happening outside the traditional venues in Europe or North America. Chile, one of the countries with important forest resources, some of them unique and well protected in a long list of National Parks and Reserves of the Biosphere, is our impressive venue this year. With just 18 million population, the 796,000 km2 has 23% forested, where 19% are native forests supporting high endemism of flora and fauna. This conference also happens at the time the Chilean parliament approved their National Strategy for Climate Change and Vegetation Resources for 2017-2025. This is an important step forward in the rationalization and protection of the unique and sensitive environmental resources of this country. The strategy, coordinated by the Chilean Forest Service, CONAF, contemplates the use of Earth Observation and others sources of spatial information as fundamental tools for the implementation and management of policies.

As always, the scientific team has made a selection of topics based on the global interest of our community that focused on Forest Monitoring, REDD+ and FLEGT, the usual Forest Inventory and Mapping, Forest Management and Development Methods. This year, the organisation wanted to introduce specific subjects of interest for the Latin American community with some of the presentations in Spanish to allow other scientists to break language barriers and contribute with their unique experiences.

Three keynote speakers where selected because of the relevance of their work for the international community.

Dr Warren Cohen, from the US Forest Service based in Oregon, is a well know scientist that has been working for many years in the development of tools to monitor the trajectories of change in the forest. His work has created important applications for the US Forest Service to map changes, the impact of disturbances and the recovery of the vegetation. In a time where the EU has launched the new Sentinel-2 sensors that join the Landsat series of satellites, his tools are one of the most important for a continuous and complete monitoring of the forested parts of this planet.

Professor Pang Yong, from the Chinese Academy of Forestry, is presenting all the interesting work that they have been developing over many years in partnership with the Chinese Academy of Sciences and their own Space programme. He will be talking about the, mostly unknown outside China, Gaofen sensor and the way is being used by the forest service to monitor their constantly expanding forest resources. Also, he will be talking about the integration of LiDAR, Hyperspectral and video sensors under the LiCHy programme. This is a highly portable group of sensors that aims

to explore the strengths of each one for a comprehensive monitoring of the forest resources from an airborne platform.

Dr. María Pilar Martin, Spanish National Research Council, will be talking about her experience in the monitoring of grasslands and forest fires in the Mediterranean using spectro-radiometric sensors. She has an extensive career as a researcher that has participated in many national and international projects with a long list of peer-reviewed papers. She will be talking about the techniques she has been pioneering over these years and provide an overview of what is going to be the future in the use of spectral analysis.

Finally, the organisation of the conference will like to pay tribute to Dr. Thomas Hilker, sadly missed a few months before. At the age of just 40 years old, Thomas has left us full of sorrow but with an important legacy of scientific work in his prolific career that covered almost every technique from LiDAR to Satellite imagery, hyperspectral analysis, modelling, data mining, multi-angle analysis, data fusion and even as an editor of Remote Sensing of the Environment. He was a brilliant scientist and our friend. Professor Nicholas Coops will present a summary of his valuable contribution to our science in a special session.

We all hope that the list of oral presentations, posters and training courses become an enjoyable experience for you.

Best wishes,

Juan Suárez and Claudio Muñoz, conference conveners.

Index

■ EXPOSITOR ■ POSTER

ForestSAT 2016

Development of Methods

OTERRA
CENTRO DE ESTUDIOS DE RECURSOS NATURALES
UNIVERSIDAD MAYOR

UNIVERSIDAD MAYOR
para espíritus emprendedores

Facultad de Ciencias
ESCUELA DE INGENIERÍA FORESTAL

A novel sampling strategy for applying ALS-based plot imputation to Australian native eucalypt forests

Gavin Melville[1], Christine Stone[2] and Mike Sutton[3]

[1]Trangie Agricultural Research Centre, Mitchell Hwy, Trangie 2823, Australia.
Email: gavin.melville@dpi.nsw.gov.au
[2]NSW Department of Industry - Lands, Forest Research, Level 12, 10 Valentine Ave., Parramatta 2124, Australia.
Email: christine.stone@industry.nsw.gov.au
[3]Forestry Corporation of NSW, PO Box 100, Beecroft NSW 2119, Australia

Keywords: LiDAR; plot sampling design; nearest centroid; imputation; native eucalypt forests; inventory; New South Wales.

Abstract

A new sampling design method, termed 'Nearest Centroid' (NC), based on k-means clustering, is applied to ALS data captured over a native eucalypt forest on the south coast of New South Wales, Australia. The NC method has been specifically designed for imputation and optimizes the survey design by using the distance properties of the sample in the space defined by the auxiliary variables. A total of 338 ground plots, 6 inventory variables and 44 ALS predictor variables were used in the study. Reference plots were chosen from candidate plots according to the sampling strategies: simple random; locally balanced and NC. Specifications in the imputation prediction process were also varied and compared. In all cases, NC sampling was more efficient.

Introduction

Significant progress has been made in the utilisation of airborne laser scanning (ALS) data (also referred to as LiDAR data) to predict forest inventory variables across a range of conditions. It is now well established that the use of imputation in Australian softwood plantations provides better precision than traditional inventory methods [Melville et al., 2015; Rombouts et al. 2015, Melville and Stone, 2016]. However, when ALS data are used on naturally generated forests, such as native eucalypt forests, the correlation between the LiDAR metrics and the key forest attributes is not as pronounced as it is with softwood plantations. There are several reasons for this, including the diversity of species, combined with different canopy heights, ages and stem characteristics, all of which lead to a complex three-dimensional structure which is encapsulated in the LiDAR information.

Imputation is commonly used in conjunction with LiDAR-based forest inventory and assessment [McRoberts et al., 2015]. In the context of ALS-enhanced forest inventory, usually the target observations are comprised of pixel-level ALS metrics from a LiDAR acquisition campaign. Specific information relating to key attributes, such as timber volume, is assigned to non-measured plots from the most closely related measured plots as defined by the similarity structure. In order to be effective, ground reference plots selected for the LiDAR imputation process must cover the full range of variability in the targeted attributes.

There are several sampling methods which are suited to a modelling approach including the widely used grid-based sampling approach and/or strategies which employ stratification, including stratification based on LiDAR variables [e.g. Hawbaker et al., 2009]. In addition to these conventional approaches,

there are methods based on spatial segregation such as the generalized random tessellation stratified sampling (GRTS) method [Stevens and Olsen, 2004] and methods based on multiple associated variables. For example, the sensor-directed response surface (SDRS) approach [Lesch, 2005], constructs a sample using a principal components analysis of variables correlated with the variable of interest, whereas the locally balanced sampling method [Grafström et al., 2014] selects a subset of plots which are simultaneously balanced over multiple auxiliary variables. The new sampling method examined in this paper relies on a cluster analysis which is carried out in the multi-dimensional space defined by the auxiliary variables, and is termed the nearest centroid (NC) approach [Melville and Stone, 2016].

Methodology

Study area: The study area of 120,000 ha comprises several State Forests close to the coastal town of Eden on the south coast of New South Wales (Latitude ranging from -36°20′ to -37°30′ and Longitude ranging from 149°13′ and 150°00′). The forests are dominated by a suite of native eucalypt species that include *Eucalyptus sieberi*, *E. muellerana*, *E. agglomerata* and *E. fastigata* and managed by the Forestry Corporation of New South Wales (FCNSW) for the sustainable extraction of sawlogs and pulpwood. The silvicultural practices in this region include a combination of thinning and alternate compartment harvesting which results in a mosaic of multiple aged stands across the landscape.

Plot inventory and ALS data: Inventory data obtained from 338 ha plots were collected during June to September 2014 by Forest Data PL according to FCNSW's standard inventory specifications. Each plot was 0.1 ha in size and established on a systematic grid with random start at an approximate density of 1 plot per 250 ha. Six response variables derived from the inventory plot data were used in this study, specifically: merchantable volume (m^3) (MVol); merchantable volume for trees over 60cm (m^3) (MVol60), basal area (m^2ha^{-1}) (BA) , stems ha^{-1} (SPH), stems ha^{-1} for trees over 60cm (SPH60) and quadratic mean of mean dominant height for trees over 60cm (m) (QMMDH60).

Discrete return ALS data were acquired over the Eden forests in July 2013 by RPS Australia East PL using a Harrier 68i LiDAR mapping system. The 44 potential predictor variables in the ALS data were reduced to around 8 by selecting variables which minimised the mean squared prediction error.

Nearest Centroid sampling method: The Nearest Centroid (NC) sampling method was developed specifically with imputation in mind. It is assumed that a reference plot well suited to imputation would ideally have many nearest neighbours among the target plots, that is, it is 'well connected' in the covariate space [Melville and Stone, 2016; Melville et al. 2016]. The NC method is based on the arrangement of the virtual plots in the multi-dimensional space defined by the standardized auxiliary variables (i.e. the LiDAR variables which are selected for imputation). A suitable clustering algorithm is employed, such as k-means clustering [Hartigan & Wong, 1979] to segregate the virtual plots into n clusters, where n is the sample size. Within each cluster, the virtual plot closest to the cluster centroid is chosen as the reference plot. When the reference plots are sufficiently close to the cluster centroids, these plots also become the nearest neighbour plots within their respective clusters during imputation. The method is illustrated in Figure 1 which displays a series of target plots arranged into eight clusters, based on the auxiliary variables p1m (proportion of heights greater than 1 m) and mqh (mean quadratic height). The centroid of each cluster is displayed as an asterisk. In each cluster the reference plot closest (in the auxiliary space) to the centroid is selected as the reference plot.

Simulation approach: The simulations were performed by separating the available plots at random into a candidate set (N_C=138 plots) and a target set (N=200 plots), a process which was repeated for each realization. A sample of reference plots (n=25) was chosen from the candidate set according to one of three sampling strategies; simple random sampling, locally balanced sampling [Grafström et al., 2014] and NC sampling. Irrespective of the sampling method chosen, both the candidate plots and the target plots are part of an overall grid sample, as described above, which was used as the original inventory. The reference plots were used to predict the response variables in the target set and the predicted values of the response variables were compared to their actual values in order to evaluate the sampling strategies in terms of relative root mean square error (RRMSE), relative bias (RB) and mean absolute deviation (MAD). The sample size

was then varied from *n*=10 to *n*=75 so as to observe the relationship between precision and the number of reference plots.

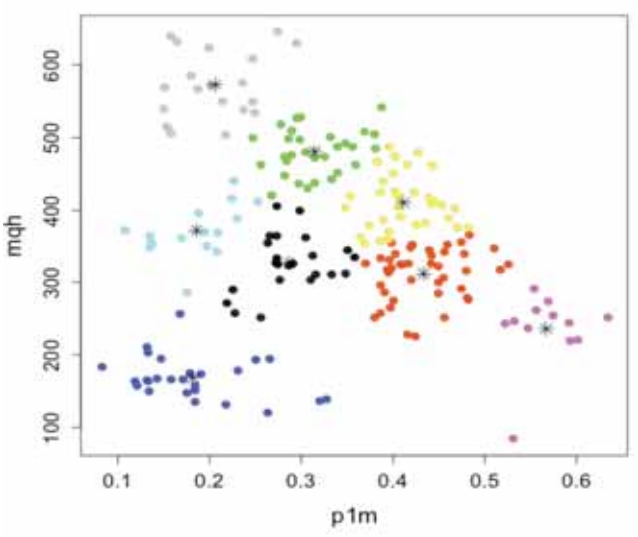

Fig 1. Illustration of nearest centroid (NC) sampling method

Results

NC sampling was the most efficient strategy for all the response variables (Table 1). For example the best precision for MVol occurs with NC sampling which is 1.36 times more efficient than random sampling (12.0% vs 14.0% RRMSE). Relative efficiencies across all variables range from 1.52 (SPH) to 1.20 (QMDBH60). The effect of sample size on the prediction of MVol is shown in Figure 2, where once again the NC sampling method gave the best precision.

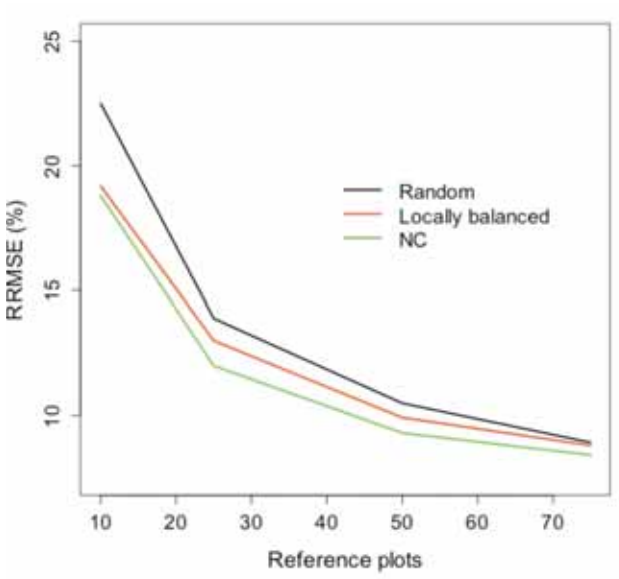

Figure 2. Relative RMSE (%) of MVol vs sample size for three sampling strategies

Table 1. Precision and bias of three sampling strategies using six response variables (n=25, k=1)

Variable	Sample method	RRMSE (%)	RBias (%)	RMAD (%)
MVol	random	14.0	-0.4	11.1
	balanced	13.0	-0.1	10.4
	NC	12.0	-0.9	9.5
MVol60	random	16.7	1.4	13.3
	balanced	15.0	1.2	11.9
	NC	13.9	-3.9	11.3
SPH	random	12.1	3.2	9.6
	balanced	11.3	3.8	9.1
	NC	9.8	1.4	7.8
BA	random	7.2	0.9	5.7
	balanced	6.7	1.2	5.3
	NC	6.2	1.2	5.0
SPH60	random	22.2	-1.7	17.9
	balanced	20.1	-1.1	16.1
	NC	19.1	3.3	15.1
QMDBH60	random	4.6	-0.2	3.9
	balanced	4.6	-0.3	3.7
	NC	4.2	-0.5	3.3

Conclusions

Both NC and balanced sampling were more efficient than random sampling when they were used with imputation in the Eden native eucalypt forest, with NC sampling the most efficient. Efficiency gains of up to 1.5 or more were achieved, depending on the response variable and sample size. This would allow the sample size to be reduced by 33% without any adverse effect on the prediction errors.

References

Grafström, A., Saarela, S., Ene, L.T. (2014) - *Efficient sampling strategies for forest inventories by spreading the sample in auxiliary space.* Canadian Journal of Forest Research, 44: 1156-1164. http://dx.doi.org/10.1139/cjfr-2014-0202.

Hartigan, J.A., Wong, M.A. (1979) - *A k-means clustering algorithm.* Applied Statistics, 28: 104-108.

Hawbaker, T.J., Keuler, N.S., Lesak, A.A., Gobakken, T., Contrucci, K., Radeloff, V.C. (2009) - *Improved estimates of forest vegetation structure and biomass with a LiDAR-optimized sampling design.* Journal of Geophysical Research,114**:** GE00E04. http://dx.doi.org/10.1029/2008JG000870.

Lesch, S.M. (2005) - *Sensor-directed response surface sampling designs for characterizing spatial variation in soil properties.* Computers and Electronics in Agriculture, 46**:** 153-179. http://dx.doi.org/10.1016/j.compag.2004.11.004.

McRoberts, R.E., Næsset, E., Gobakken T. (2015) - *Optimizing the k-Nearest Neighbors technique for estimating forest aboveground biomass using airborne laser scanning data.* Remote Sensing of Environment, 163: 13-22. http://dx.doi.org/10.1016/j.rse.2015.02.026.

Melville, G.J., Stone, C., Turner, R. (2015) - *Application of LiDAR data to maximise the efficiency of inventory plots in softwood plantations.* New Zealand Journal of Forestry Science, 45. doi: 10.1186/s40490-015-0038-7.

Melville, G., Stone, C. (2016) - *Optimizing nearest neighbour information – a simple, efficient sampling strategy for forestry plot imputation using remotely sensed data*. Australian Forestry, 79:3, 217-228. http://dx.doi.org/10.1080/00049158.2016.1218265.

Melville, G, Stone, C., Rombouts, J. (2016) - *Survey designs which maximize efficiency gains in ALS-based forestry plot imputation.* Proceedings of Spatial Accuracy, July 5-8, 2016, Montpellier, France, pp. 52-59.

Rombouts, J., Melville, G., Kathuria, A., Rawley, B., Stone, C. (2015) – *Operational deployment of LiDAR derived information into softwood resource systems.* Forest and Wood Products Australia Ltd.

Stevens, D.L. Jr., Olsen, A.R. (2004) - *Spatially balanced sampling of natural resources.* Journal of the American Statistical Association, 99**:** 262-278. http://dx.doi.org/10.1198/016214504000000250.

POSTER

Airborne Dual Band Radar for Rural Cadastre

Dieter Lübeck[1], Rafael A. S. Rosa[1], Christian Wimmer[1], Karlus A. C. Macedo[1], Juliano Lázaro[1]

[1]Bradar Indústria S.A.

Keywords: rural cadastre, synthetic aperture radar, SAR, X-band, P-band.

The land ownership and land use rights are high on the global agenda. 50% of the sustainable development goals for 2030 are land related. A very rough estimation for reaching these goals with traditional approaches in cadastral data acquisition ends up in over 500 years of cadastral survey work. This estimation makes clear that breakthrough techniques will be necessary to overcome this demand.

A well-known approach for surveying big areas in a short time is airborne or space borne remote sensing. In Fit-For-Purpose approaches for land administration printed imagery is used in the field for boundary identification in a participatory way. The question is, if radar image data can support the mapping of cadastral boundaries in an efficient way. A promising new approach in this area is using airborne dual band InSAR (X- and P-Band). Due to the known advantages, like cloud penetration, sun light independency and foliage penetration, radar imagery is increasingly being used for large scale mapping and monitoring over the last decade.

Bradar´s airborne dual band Radar uses X- and P-band because they have the most complementary mapping characteristics. While X-band, with 3 cm wavelength, maps exclusively the surface, P-band, with 70 cm wavelength, penetrates the foliage and allows mapping the topography below vegetation. In the former days, the main application of this technology was the interferometric phase processing for the topographic mapping. Nowadays the high quality images from the amplitudes are opening new horizons for planimetric feature extraction in scales up to 1:5.000 with the big advantage of cloud penetration and a wide mapping swath. The mentioned airborne radar systems combines all these characteristics and could already map an area of about 2.3 million km² in Central and South America and Europe.

Detect fences

New studies, realized by Bradar in Brazil, are showing that P-Band is not only capable to detect boundaries demarked by roads, river or vegetation, but also very small wire fences, which are commonly used for example in South America for demarking land (Figure 1). Applying this technology to supporting land registration and cadastral survey could be the solution for speeding up registration processes. This brings help to the local people in protecting them from land grabbing.

Figure 1: Wire fence constructions are very often cadastral boundaries. Those fences can be easily detected with radar.

Surprising results

Tests showed that the feature extraction of these fences can be realized with a high planimetric accuracy of up to 20 cm in the P-Band imagery (Figure 2), which meets the requirements for support in land administration in many developing countries. This surprisingly result can be achieved because the horizontal wires of the wire fences act like small antennas for the horizontal polarized P-Band radiation. With the presence of the ground we have the effect of the so called double-bounce of the wave back to the radar. Due to this effect the signal of all horizontal wires of the fence sum up and the fence appears in the image as one line only with its origin at the vertical projection of the fence on the ground. Figure 3 shows an example of a P-Band image with a fence network in a deforested area. Beside the fences, other important features can be extracted, like forest, road, construction, single trees and animals.

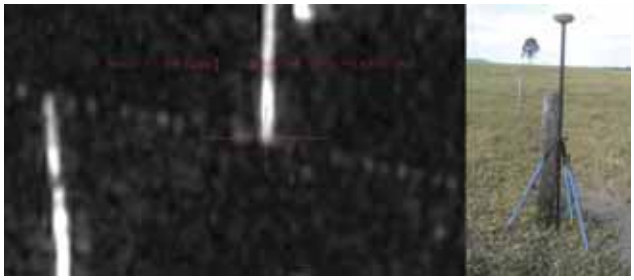

Figure 2: Planimetric accuracy for fence detection in P band imagery – the fence can be projected to the surface of the earth.

Application

The radar imagery can be applied for integral cadastral boundary detection. Mostly those boundaries are visible features - defined by roads, vegetation, rivers, fences and constructions in a very efficient way. Even rivers covered by vegetation can be extracted. Figure 4 shows an example of an area in Brazil, including orthoimages X, P, X/P colour, and extracted boundaries overlaid to P-band image (from left to right). Additionally, digital terrain and/or surface models can be provided by applying interferometric flights to obtain altimetric information for contour lines generation and drainage networks, including 3D simulations. This information is not only useful for supporting the land administration but also the rural development, infrastructure projects, forest certification and rural environmental cadastre, risk mapping, area preservation, land us mapping, and topographic mapping, among many other applications.

Change detection

For change detection the radar imagery has another big advantage, which is the constant illumination between different flights. This allows, on the contrary to optical imagery, systematic comparisons of the images supported by image processing software. Changes in the land use can be detected automatically, as well as in any type of construction. This provides the option to reconstruct "replaced" cadastral boundaries.

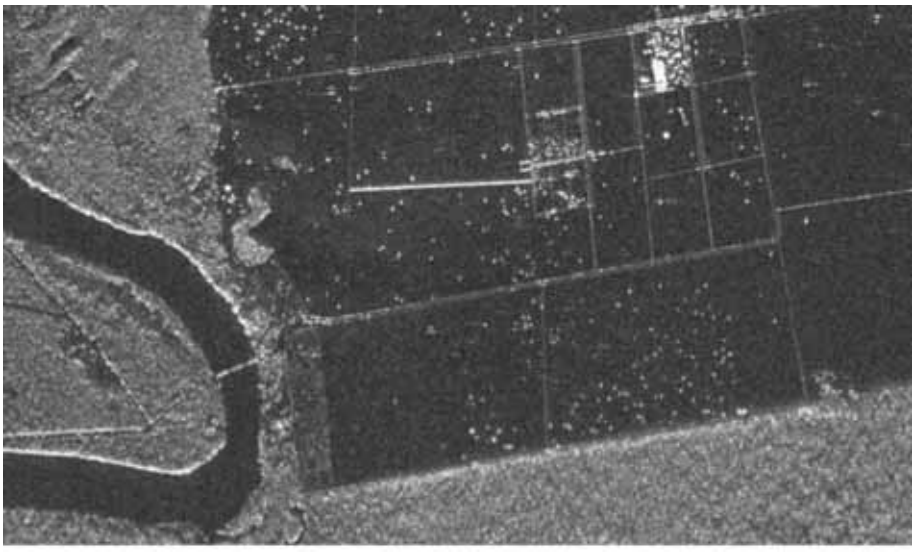

Figure 3: P-Band Image of rural area. Many of the line shaped features are cadastral boundaries.

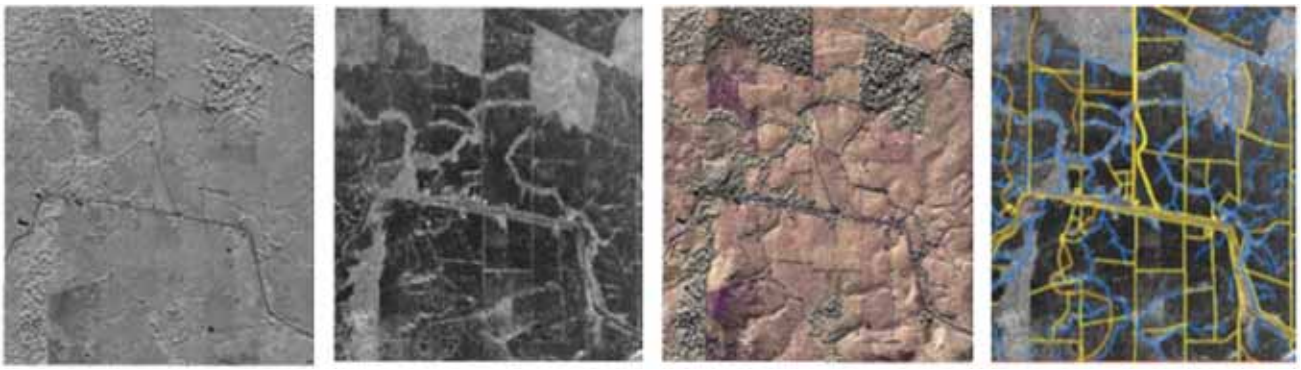

Figure 4: Example of boundary extracting from radar imagery.

Experience in Brazil

Two technological viability projects, one close to the hydropower station of Belo Monte and one in the district of São José dos Campos already demonstrated the applicability of this approach.

The planimetric accuracy was measured with differential GPS at both sites. Wire fences presented an RMSE error of around 20 cm and water boundaries of around 1 m. The radar survey will not completely substitute the ground survey, but it allows the general definition of the ground boundaries and their vectorization before going to the field.

In Brazil, for example, the interview with the ground owner, the review of the ground boundaries and the demarking must be carried out by the ground survey. The radar could reduce from 3 to 5 times the effort and execution time of the conventional field work.

Fit-For-Purpose

Agencies in Brazil and Latin America never considered remote sensing for the development of land administration. Actual governmental regulations do even not allow it without performing a complete ground survey. Radar survey accelerates such ground survey and serves as a control method. In Fit-For-Purpose approaches the Radar imagery is considered to be as sufficient in order to collect cadastral boundary data fast, quick and cheap. It means that the printed imagery can be taken to the field to compare the automatically extracted features with the real cadastral boundaries. Those boundaries can be marked with pen on top of the image. Back in office the polygons for spatial units (parcels) can be easily identified and included with expected accuracy.

An approximation for non-parametric bootstrapping to assess uncertainties in imputation mapping of forest vegetation

David M. Bell, USDA Forest Service, Pacific Northwest Research Station
Matthew Gregory, Oregon State University, College of Forestry

Keywords: bootstrapping; *k*-nearest neighbor imputation; Landsat; precision; uncertainty

Abstract

Satellite-based vegetation maps are an increasingly common source of information for natural resource planning, but the utility of these products is unclear without an understanding of their limitations. Nearest neighbor imputation methods for mapping forest attributes across broad geographic areas have been employed extensively, motivating research into uncertainties associated with imputed maps. While uncertainties can be quantified in a variety of ways, non-parametric bootstrapping has emerged as a potential alternative to parametric methodologies, especially when plots are directly imputed to pixels (i.e., *k*-nearest neighbor with $k = 1$). However, bootstrapping methods for examining uncertainties in imputations for large regions requires substantial computational power and data storage, limiting the usefulness of bootstrapping for assessing uncertainties over the large areas required for regional planning and monitoring activities. In this research, we describe a new approximation for a non-parametric bootstrapping approach for *k*NN with $k = 1$ methods (hereafter, bootstrap approximation). Our objectives were to (1) assess the capacity of the bootstrap approximation method to reproduce results based on non-parametric bootstrapping and (2) examine regional variation in imputation uncertainties in forest attributes in landscapes of California, Oregon, and Washington, USA. We performed *k*-NN with $k = 1$ imputation mapping with 4000 bootstrap samples of field plot data and generated several metrics of prediction uncertainty and central tendency. In contrast, our bootstrap approximation was based on a weighted sample of the seven nearest neighbors in environmental and Landsat spectral space. Our results indicate that the bootstrap approximation are essentially equivalent with results produced by non-parametric bootstrapping for measures of central tendency (means and medians), presence of structural elements (e.g., attribute greater than zero), and measures of precision (width of confidence intervals), with coefficients of determination (r^2) ranging from 0.996 to 1.000. Using our bootstrap approximation, we found that spatial variation in climate, ownership, and disturbance history explained geospatial patterns in predicted forest attributes as well as the variability in the imputation process. The bootstrap approximation presented in this research provides a useful new tool for examining the limitations of *k*NN with $k = 1$ imputation, informing both scientists and managers of the limitations of consequent vegetation mapping products.

POSTER

Analysis of land cover classes separability using optical and SAR data in areas of high cloud content in northern South America

Sebastián Palomino-Ángel
Catedrático, Facultad de Ingeniería, Universidad de Medellín, Cra 87 Nº 30 – 65, Medellín, Colombia, spalomino@udem.edu.co
Jesús A. Anaya-Acevedo
Profesor Titular, Facultad de Ingeniería, Universidad de Medellín, Cra 87 Nº 30 – 65, Medellín, Colombia, janaya@udem.edu.co

Keywords: Land cover, high cloud content, optical data, radar data, Jeffries-Matusita

Abstract

Land cover classification in tropical regions is challenging because of the dynamics of land cover change, persistent cloud cover, and presence of small patches. Due to its location and topography, Colombia has different physical conditions which favors the formation of cloud cover almost over the full extent of the country. This complexity is more pronounced to the west because of the interaction of the humid currents of the Pacific Ocean and the Andes mountains. Northwest Colombia, is an interesting region due to its forest and biodiversity, but those natural resources have been affected by drivers of forest loss, mainly cattle grazing and agricultural activities. It is estimated that 70% of native forest has been subject to land cover change in the last 40 years.

The main objective of this work was to assess the ability of radar data in separating land cover classes, and the potential of optical and radar combination for improving classification accuracy in a region of high cloud content in northwest Colombia. Landsat 5 and Phase Array L-Band SAR (PALSAR) were used as input data. Jeffries-Matusita (JM) distance was used as a separability measure for the analysis. In order to perform the classification of satellite images, we used maximum likelihood classification algorithm for optical data and Wishart Supervised Classification for radar data. High resolution images, aerial photographs and field information were used as reference data for training and validation.

A total of 22 classes were evaluated using JM analysis: 3 crops classes, 15 vegetation cover classes (including different forests types and typical wetland vegetation), 3 pastures classes and 1 urban class. The JM distance ranges from 0 to 2, being 0 the value for low separable classes and 2 the value for high separable classes. It was found that higher JM values were obtained for optical and radar combination, with a mean value of 1.94 JM distance for all classes. Optical data presented a mean value of 1.90 JM distance and radar data presented a mean value of 1.16. Additionally, accuracy assessment was performed using error matrix method. Optical, radar, and the combination of optical and radar resulted in different overall accuracies: 75%, 50% and 76% respectively. The combination of optical and radar not only has the best accuracy, it also reduces optical invalid data due to cloud content. The classification problems were evaluated, focused on determining the causes of error, and identifying techniques to improve results in areas of high cloud content.

Analyzing some factors affecting the extraction of full-waveform LiDAR metrics and their effect in forest structure variable estimates

Ruiz, Luis A.[1], Crespo-Peremarch, Pablo [1], Estornell, Javier [1], Balaguer-Beser, Angel [1]

[1] Geo-Environmental Cartography and Remote Sensing Group, Universitat Politècnica de València, Camino de Vera, s/n, 46022 Valencia, Spain.
email: laruiz@cgf.upv.es

Keywords: full-waveform; forest structure; fuel parameters; LiDAR metrics.

Abstract

Introduction

Full-waveform LiDAR is a promising technique to analyze vertical structure of forest stands., and derived metrics provide better forest structure and fuel variables estimates than using discrete LiDAR (Hermosilla et al., 2014; Cao et al., 2014). However, full-waveform derived metrics are more sensitive to side-lap effects during data acquisition than discrete LiDAR and data are usually subject to voxelization processes in which some methodological parameters, such as voxel size and voxel value assigning criteria, affect the final forest structure models (Crespo-Peremarch et al., 2016).

The objectives of this work are: (i) to assess the effect of two full-waveform parameters, voxel size and voxel value assigning method, on the estimation of forest structure and fuel variables; (ii) to compare these methodological parameters in two different types of forest areas, Mediterranean and temperate US Pacific Northwest; and (iii) to explore the full-waveform LiDAR data side-lap effect on the derived metrics.

Data and methods

Full-waveform LiDAR data were acquired in a temperate US Pacific Northwest forest in Panther Creek, Oregon, and in a Mediterranean forest located in Sierra de Espadán (Spain), using a Leica ALS60 and a LiteMapper 6800, resulting in pulse densities of >8m^{-2} and >11m^{-2}, respectively. Inventory field measurements were collected in 84 circular plots (16m radius) in Panther Creek, and in 55 circular plots (15m radius) in Espadán. In the first area, the dominant species is Douglas-fir (*Pseudotsuga menziesii*), occasionally mixed with other conifers, such as western hemlock (*Tsuga heterophylla*), western red cedar (*Thuja plicata*) and grand fir (*Abies grandis*), or deciduous species such as red alder (*Alnus rubra*) and bigleaf maple (*Acer macrophyllum*). In the second area, the dominant forest species is *Pinus halepensis*, occasionally mixed with *Quercus suber*, with the common presence of understory shrub vegetation. LiDAR metrics were extracted as described by Duong (2010) and Cao et al. (2014) after a voxelization process (Hermosilla et al., 2014). They were used to create regression models for six forest structure and fuel variables in both areas (aboveground biomass, basal area, quadratic mean diameter, canopy height, canopy base height and canopy fuel load). Four voxel sizes (0.25m, 0.5m, 1m and 2m), and six different types of voxel assigning methods (maximum, mean, median,

mode, percentiles 90 and 95) were tested, computing the adjusted coefficient of determination R2 and root-mean-square error (RMSE) and using leave-one-out cross-validation for evaluation. The effect of LiDAR density variations within and around side-lap areas was also analyzed using pairwise samples in the Panther Creek study site.

Results

When small voxel sizes are used (0.25m and even 0.5m), there are very few waves contained in each individual voxel, and the different voxel assignation methods yield very similar R^2 results. Voxel sizes near 0.5 m are, in general, the most efficient in generating accurate models. Using voxels sizes over 1m increases the influence of the voxel value assigning method. Maximum and high percentiles (95%) are usually the most efficient assigning criteria. Table 1 shows, as an example, the R^2 values of the aboveground biomass when these methodological parameters are varied.

The R^2 of forest structure variables related to height, such as canopy height and canopy base height, are not significantly affected by the voxel size and voxel value assigning criteria tested. In these cases, the influence of the values of internal voxels is negligible. This suggests that the use of full-waveform LiDAR does not increase the accuracy of these height variables models in comparison to the use of discrete LiDAR. Results obtained in both areas are consistent, some differences are found probably due to the presence of different species and canopy types.

Regarding the side-lap effect, metrics such as number of peaks of the wave (NP), roughness of outermost canopy (ROUGH) and front slope angle (FS) are the most affected by density differences. Using the mean value as voxel assigning method reduces this effect. Metrics height of median energy (HOME), height to median ratio (HTMR) and waveform distance (WD) are the most efficient and robust in modeling forest structure attributes.

Main conclusions

When using full-waveform LiDAR data for modeling forest structure variables following a voxelization process, voxel size should be chosen based on the density of LiDAR data by ensuring the presence of waves within the voxels but avoiding an overload of values. For medium pulse densities (8-12 m^{-2}), voxel sizes around 0.5 m are recommended. Assigning the maximum wave value to each voxel, the negative effect of increasing the pixel size is reduced. Some full-waveform derived metrics are more efficient and less affected by density differences than others, especially when side-lap effect exists. This fact should be considered when creating the models, by employing those metrics less affected. Voxel value assigning criteria should be selected attending to the voxel size and the heterogeneity of the LiDAR point density in the study area. Further work will be focused in density homogeneization techniques to avoid side-lap effect.

Table 1. R^2 values of the forest stand variable *Aboveground biomass* when modifying the full-waveform methodological parameters voxel size (0.25, 0.5, 1 and 2m) and voxel assigning methods (maximum, mean, median, mode, p90 and p95) in the two study areas.

	Aboveground biomass							
	Panther Creek				Espadan			
	0.25m	0.5m	1m	2m	0.25m	0.5m	1m	2m
Maximum	0,84	0,85	0,85	0,84	0,79	0,79	0,79	0,80
Mean	0,84	0,84	0,84	0,83	0,79	0,79	0,78	0,76
Median	0,84	0,84	0,83	0,82	0.78	0,79	0,77	0,72
Mode	0,84	0,82	0,82	0,82	0,79	0,79	0,75	0,69
p90	0,84	0,85	0,84	0,84	0,79	0,79	0,78	0,78
p95	0,84	0,85	0,85	0,84	0,78	0,79	0,79	0,78

References

Cao, L., Coops, N.C., Hermosilla, T., Innes, J., Dai, J., She, G., 2014. Using small-footprint discrete and full-waveform airborne LiDAR metrics to estimate total biomass and biomass components in subtropical forests. *Remote Sensing*, 6, 7110-7135.

Crespo-Peremarch, P., Ruiz, L.A., Balaguer-Beser, A., Estornell, J., 2016. Analysis of the side-lap effect on full-waveform LiDAR data acquisition for the estimation of forest structure variables. Int. Arch. Photogramm. Remote Sens. Spatial Inf. Sci., 12-19 July, Prague, XLI-B8, pp. 603-610.

Duong, H.V., 2010. Processing and application of ICESat large footprint full waveform laser range data. Ph.D. Thesis, Delft University of Technology, Netherlands.

Hermosilla, T., Ruiz, L.A., Kazakova, A.N., Coops, N.C, Moskal, L.M., 2014. Estimation of forest structure and canopy fuel parameters from small-footprint full-waveform LiDAR data. *International Journal of Wildland Fire,* 23(2), 224-233.

Analyzing the Lorenz Curve of Tree Growth Dominance with Multi-temporal Airborne Lidar in Wytham Forest (UK)

Rubén Valbuena[1, 2], Matti Maltamo[1], Lauri Mehtätalo[1], David Coomes[2]

[1] University of Eastern Finland. Faculty of Forest Sciences. Yliopistokatu 7. 80100 Joensuu, Finland
[2] University of Cambridge. Department of Plant Sciences. Downing St. CB2 3EA Cambridge, UK.

Keywords: Airborne laser scanning; Tree competition; Metabolic scaling theory

Abstract

Growth dominance curves are employed to study the relative shares of the total growth accounted for each tree in the forest community (Binkley, 2004). These relations can be used to define patterns of tree competition: symmetric or asymmetric (Pretzsch & Biber, 2010). Growth dominance curves are one specific type of Lorenz curve, and therefore their associated growth dominance coefficient is also a particular type of Gini coefficient (GC). Relations of tree size inequality are determined by these patterns of competition, and hence the GC can be valuable to study asymmetric competition (Cordonnier & Kunstler, 2015). After a concentrating our research on static studies applying the Lorenz curve and derived indicators and determining the means for predicting them with airborne Lidar (Valbuena et al., 2013), our research objectives are now on the study of growth dominance using multi-temporal datasets. We studied the growth dominance curves that should correspond to predictions by the metabolic scaling theory (MST) of tree growth (Enquist et al. 1999), which provides grounds for predicting structure and dynamics of an average idealized natural forest. Empirical divergences from MST predictions have been, however, considered to be caused by forest disturbance, asymmetric competition among trees in the forest community, and the allocation of different types of resources (Coomes, 2012). Lidar is a valuable tool in order to investigate the relations of competitive dominance among trees in the forest community, since it allows to model the light environment, and investigate forest structure and disturbance.

Our research was structured in two phases. The first phase consisted in a deductive approach to determine mathematically the growth dominance curve that corresponds to MST predictions, and therefore determine a scenario of pure symmetric competition. Empirical divergences from that ideal situation were analysed in a second inductive phase, which consisted in quantifying these divergences and predicting them using standard area-based Lidar approaches. This second phase was carried out at the Wytham Woods, Oxfordshire (UK), a woodland comprised mainly of ash, oak and sycamore trees, for which were obtained detailed data measured in 2008 and 2010. We calculated wall-to-wall growth dominance coefficients over an 18-hectare plot, and estimated them using airborne Lidar. The underlying envisaged goal is to enable the use of Lidar for determining whether symmetric or asymmetric competition processes apply to a given area of forest.

References

Binkley, D. (2004) A hypothesis about the interaction of tree dominance and stand production through stand development. *Forest Ecology and Management* 190(2):265–271

Cordonnier, T., & Kunstler, G. (2015). The Gini index brings asymmetric competition to light. *Perspectives in Plant Ecology, Evolution and Systematics*, 17 (2), 107-115.

Coomes, D. A., Holdaway, R. J., Kobe, R. K., Lines, E. R. and Allen, R. B. (2012), A general integrative framework for modelling woody biomass production and carbon sequestration rates in forests. *Journal of Ecology*, 100: 42–64.

Enquist, B., West, G., Charnov, E. & Brown, J. (1999) Allometric scaling of production and life-history variation in vascular plants. *Nature*, 401, 907–911.

Pretzsch, H., Biber, P. (2010) Size-symmetric versus size-asymmetric competition and growth partitioning among trees in forest stands along an ecological gradient in central Europe. *Canadian Journal of Forest Research* 40:370–384

Valbuena, R., Packalen, P., Mehtätalo, L., García-Abril, A., Maltamo, M., 2013a. Characterizing forest structural types and shelterwood dynamics from Lorenz-based indicators predicted by airborne laser scanning. *Canadian Journal of Forest Research* 43, 1063–1074.

Change detection techniques for development of compatible height growth and site index models using repeated Airborne Laser Scanning Data

Jarosław Socha[*1], Marcin Pierzchalski [1], Radomir Bałazy[2], Mariusz Ciesielski[2]*
[1] University of Agriculture in Krakow, Faculty of Forestry, Al. 29 Listopada, Krakow, 32-425 Poland
[2] Forest Research Institute, Braci Leśnej 3, Sękocin Stary, 05 – 090 Poland
[*]Speaker, e-mail: rlsocha@cyf-kr.edu.pl

Keywords: Change detection, height growth, Norway spruce, LiDAR, dynamic site index model, site productivity

Abstract

Forest site productivity, which is a quantitative estimate of the potential of a site to produce plant biomass remains a fundamental variable in forestry (Bontemps and Bouriaud, 2013; Skovsgaard and Vanclay, 2008). The most commonly used and widely accepted method of evaluating site productivity is site index (Bontemps and Bouriaud, 2013; Coops et al., 2011; Hägglund and Lundmark, 1977; Sharma et al., 2012; Skovsgaard and Vanclay, 2008). Therefore the construction of site index models remains a fundamental task for site productivity differentiation (Cieszewski and Strub, 2007; Mathiasen et al., 2006; Sharma et al., 2011).

To date three main data sources were used for site index model development: 1) PSP - repeated measurements on permanent sample plots (PSP); 2) Temporary Sample Plots data (TSP) from periodic inventories that usually cover most of the forested areas of a given territory (Raulier et al., 2003); 3) Stem analysis (SA) data. SA deduces past height growth from growth ring observations made on dissected sample trees.

Recently, a number of remote sensing technologies have emerged that offer alternative approaches for forest inventories, with potential of improving the accuracy and precision of stand-based measurements while reducing data acquisition cost (Hilker et al., 2008). Laser scanning of forest stands provides the mean canopy height of dominant and codominant trees. Hyyppä *et al.* (2003) demonstrated that multi-temporal ALS data could be used to measure forest growth and the standard error when estimating height growth at stand level was less than 5 cm. St-Onge and Vepakomma (2004) used ALS with the density data acquired in 1998 and 2003 to detect tree growth within a 6.8 ha study site in Québec, Canada. Hopkinson *et al.* (2008) evaluated the estimation of plot level mean tree height growth using four ALS acquisitions of a pine plantation in Toronto and found that the 100th height percentile provided the most robust overall direct estimate of field measured forest growth, and demonstrated that there was no statistically significant difference between all plot-level field and Lmax ALS mean growth rate estimates. Yu et al. (2004) provided an assessment of Norway spruce (Picea abies (L.) Karst.) and Scots pine (Pinus sylvestris L.) canopy growth from two lidar acquisitions 21 months apart. Precision of plot-level growth estimated by differences in raster canopy height models (CHMs) was of 10 to 15 cm. Repeated LiDAR observations enable measurement of tree and stand height growth over time ((Hopkinson et al., 2008; Yu et al., 2006)Yu et al. 2006, 2008; Næsset and Nelson 2007). However, to date,

repeated LIDAR height measurements data have not been used in modelling height growth and site index models development, and as it was stated by Coops in recent review concerning Characterizing of Forest Growth and Productivity using Remotely Sensed Data (Coops, 2015) considerable research is required to determine the appropriate design of repeat LIDAR surveys for measurement of tree height growth. In his detailed review Coops (Coops, 2015) indicated also need to better understand the amount of time needed for sufficient growth to excess noise and other uncertainties within LIDAR systems. Presented research is the example of successful attempt of answer for both above mentioned questions.

The objective of this research is to describe the new application for change detection using airborne laser scanners and present the procedure for the development of compatible height growth - site index models using repeated ALS data. We showed how wall-to-wall light detection and ranging (LiDAR) data obtained for large forest area exceeding 70 thousand ha could be used in development site index model, which appropriately reflects unique region and site-specific growth trajectories. LIDAR measurements may be biased as a result of several factors, including instrument specifications, flying height, species architecture, and the measurement method used (Wulder et al., 2008. We hypothesized that in spite of possible errors observed in case of single area units (raster plots), that can range from a few centimetres up to a few meters (e.g., Aldred and Bonnor 1985, Chen and Ni 1993, Ritchie 1995, Latypov 2002, (Yu et al., 2006)) repeated complete LIDAR coverage on large areas should give unbiased mean height growth trend and increment estimates and therefore may be recognised as new fully valuable data source for stand height development modelling. Developed using repeated ALS data compatible height growth and site index models were validated using independent data sets consisting 156 height growth trajectories obtained by stem analysis of dominant trees collected on the research area.

To the best of our knowledge, out study constitutes the first practical application of change detection by airborne laser scanners for the development of compatible height growth - site index models using repeated ALS data.

Combining remote sensing and dendrochronology to assess the effect of groundwater extraction on Prosopis tamarugo: from tree to aquifer level

Mathieu Decuyper[1,2], Roberto O. Chávez[3], Jan Clevers[1], Martin Herold[1]*

[1] Laboratory of Geo-Information Science and Remote Sensing, Wageningen University, Droevendaalsesteeg 3, 6708 PB Wageningen, The Netherlands
[2] Forest Ecology and Forest Management Group, Wageningen University, Droevendaalsesteeg 3, 6708 PB Wageningen, The Netherlands
[3] Institute of Geography, Pontificia Universidad Catolica de Valparaíso, Valparaiso, Chile

Abstract

Groundwater dependent ecosystems are sensitive to changes in groundwater availability, and therefore, threatened by desertification as a consequence of global warming. In this study, we combined remote sensing and dendrochronology to assess drought stress on *Prosopis tamarugo* Phil, endemic to the Atacama Desert in Northern Chile. This unique ecosystem is threatened by groundwater (GW) overexploitation due to mining and urban consumption. We first performed a spatio-temporal assessment of Tamarugos' water condition for the whole Pampa del Tamarugal aquifer (comprising the Tamarugo ecosystem) using two NDVI (Normalized Difference Vegetation Index) -derived parameters: NDVI in winter (NDVIw) and the difference between NDVI in summer and winter (NDVIws). These were calculated using Landsat satellite imagery. Based on this aquifer level assessment, we selected two representative sites (control versus high-depletion site) to perform more detailed remote sensing based estimations of canopy growth and water condition at the stand level, and tree-ring based analysis of stem growth on both the stand and tree level. Also at the tree level the Green Canopy Fraction (GCF), obtained from a Worldview2 image was used as an indicator of the canopy greenness.

Radial stem growth was determined for the same period after cross-correlating the tree rings per site. Time-series analysis was done over a period of 26 years and both NDVI-derived parameters showed significant negative trends in the high-depletion site, indicating drought stress. Radial stem growth of viable *P. tamarugo* trees was 48% lower in the high-depletion site. At the tree level, the GCF also indicated drought stress since a larger percentage of trees fell within lower GCF classes.

On the aquifer level, NDVIw and NDVIws of the *P. tamarugo* forest declined on average 19% and 51%, respectively, while GW depleted on average 3 m over the period 1988-2013. About 730,000 trees were identified in the study area, from which 5.2% showed a GCF < 0.25 associated with severe drought stress. A GW level > 12 m increasingly limited the paraheliotropic leaf movement, leading to dehydration and foliage loss. This is in line with the indications at plot level for both remote sensing as well as radial stem growth. Overall we can conclude that *P. tamarugo* trees at 12-16 m GW level suffered moderate drought stress while a GW level of 16-20 m implied severe drought stress. Combining dendrochronology and remote sensing allows us to understand the effects of drought stress on two different carbon pools (crown and stem, respectively), providing more insights on the physiological response of the species to drought and on potential management actions to minimize the impacts of water extraction.

Comparison of forest canopy point-measurement methods from above and below

Jaan Liira, Marta Mõistus, Kertu Lõhmus

In remote-sensing, mayor effort has been paid to the estimation of LAI and canopy height of the stand overstory to quantify the timber volume and carbon storage. Many forest ecosystems in the World, however, consist of multiple layers in understory, which play as important or even more important role in provision of ecosystem services and human welfare than just the first layer of trees. Understory is widely ignored in remote sensing because of various reasons, but in conditions of increasing quantity of remote sensing sources and methods, the methodological differences should be estimated. We compared different areal LiDAR and ground-based methods to evaluate the estimation bias of canopy density between them. We capitalized on understory management gradient from mature forest to old parks, that to avoid stand growth related side effects. We observed that all methods suffer from the hiding effect of distant layers in multi-layered stands. Therefore, more elaborated or complex measured should be implemented to reduce the stand characterization bias, including overall carbon storage or biodiversity.

Generation of a Landsat image mosaic over the Amazon rainforest

Jasper Van doninck, Hanna Tuomisto
Amazon Research Team, Department of Biology, University of Turku, Finland

Keywords: Amazonia, ETM+, TM, preprocessing, BRDF, per-pixel compositing

Although Amazonian forests may at first sight seem one homogenous mass, field surveys have revealed high floristic heterogeneity, even over short distances. The combination of this high local-scale variability with the enormous extent of the Amazon forest makes satellite remote sensing an indispensable tool in Amazonian biodiversity monitoring. Landsat imagery offers the desired combination between high spatial resolution and basin-wide coverage, but the use of this dataset over Amazonian forests is hampered by some practical issues. A first obvious problem is the persistent cloud cover over tropical forests. Consequently, only an extremely small fraction of the available Landsat images over Amazonian forests are entirely cloud-free, and per-pixel multi-temporal image compositing is a necessity in order to obtain a basin-wide mosaic. In case multiple cloud-free observations are available for a pixel, the choice of the compositing may influence the radiometric consistency of the final mosaic. A second issue is the large spectral similarity between floristically distinct forest types. Because of this, even small radiometric artefacts can impede image interpretation or classification. One of these artefacts is an across-track reflectance gradient, caused by the bidirectional reflectance distribution function (BRDF). Failure to remove directional effects will result in clearly discernible edges between adjacent Landsat scenes in a larger mosaic.

We here present a preprocessing chain for generating a radiometrically consistent Landsat TM/ETM+ image mosaic. First, atmospherically corrected surface reflectance products are corrected for directional effects using the Ross-Li BRDF model calibrated with multi-angular Landsat observations. The directional normalization is validated using the overlap area of Landsat images in adjacent paths. The validation shows that directional effects over Amazonian forest can cause surface reflectance differences up to 4% in the near-infrared band over the Landsat swath, but that these are eliminated after normalization. In a second step, multi-temporal Landsat images are combined in a per-pixel image compositing. It is shown that, depending on the used compositing method, radiometric consistency of the composite image may improve drastically with an increasing availability of clear observations. The resulting image mosaic reveals clear floristic and geological patterns within Amazonia at both the local and the basin-wide scale.

Detection of Dead Standing Eucalyptus for managing biodiversity using full-waveform LiDAR data

Milto Miltiadou[1,2,3], Neill D.F. Campbell[1], Matthew Brown[1], Susana Gonzalez Aracil[3], Tony Brown[4], Darren Cosker[1] and Michael Grant[2]
[1]The Centre for Digital Entertainment, University of Bath, Bath, UK
[2]Remote Sensing Group, Plymouth Marine Laboratory, Plymouth, UK
[3]Interpine Group Ltd, Rotorua, NZ
[4]Forestry Corporation of NSW, Wauchope, Australia

Keywords: full-waveform LiDAR data, voxelisation, biodiversity, dead trees

The value of dead standing Eucalyptus Camaldulensis (Red Gum) from a biodiversity management perspective is large. In Australia, many arboreal mammals and birds, of which some of them are close to extinct, inhabit hollow trees (Lindenmayer, 2002). Studies have shown in some forests there is likely to be a shortage of hollows available for colonisation. (Goldingay, 2009) (Gibbons and Lindenmayer, 2010). Dead standing Eucalyptuses are more likely to be aged and have hollows, therefore automated detection of them plays a significant role in protecting those animals.

The full-waveform (FW) LiDAR data used for this project are supplied by RPS Australia East Pty Ltd and they were collected in March 2015 using the Trimble AX60 Airborne LiDAR sensor. In addition, the field plots used for the classifications are provided by Forestry Corporation of NSW and contain around 1000 Eucalyptuses of which 10% are dead.

The standard method of using the higher resolution of full-waveform LIDAR would be to generate and extract a denser point cloud (Neuenschwander, 2009) (Reitberger, 2006). While this identifies significant features as points, the full waveform data also contains information in single shots that may be below the significance threshold. These data can be accumulated from multiple shots into a voxelised volume, e.g. Persson et al, 2005, who used voxelisation to visualise the waveforms. We have implemented and improved on the voxelisation approach in DASOS, an open source software for managing FW LiDAR data (Miltiadou et al, 2015). DASOS further normalises the intensities so that equal pulse length exists inside each voxel, making intensities more meaningful and it exports forestry metrics (i.e. intensity distribution and height differences within a radius relevant to canopy heights) into a single vector for fast interpretation in advanced statistical tools like R and Matlab.

Addressing the dead Eucalyptus case, we have generated 3D priors characterizing dead standing Eucalyptuses. These 3D dead standing tree priors are run over the voxelised FW LiDAR data using the Random Forest and the Nearest Neighbour algorithms in order to detect the locations of candidate trees. A comparison between the LiDAR point cloud and the voxelised FW LiDAR data is further performed to demonstrate the increased survey accuracy obtained with the voxelisation.

References:

Gibbons, P. & Lindenmayer, D. (2002), Tree Hollows and Wildlife Conservation in Australia, CSIRO Publishing.

Goldingay, R. L. (2009), 'Characteristics of tree hollows used by australian birds and bats', Wildlife Research 36(5), 394–409.

Lindenmayer, D. B. & Wood, J. T. (2010), 'Long-term patterns in the decay, collapse, and abundance of trees with hollows in the mountain ash (eucalyptus regnans) forests of victoria, southeastern australia', Canadian Journal of Forest Research 40(1), 48–54.

Miltiadou, M., Warren, M. A., Grant, M. & Brown, M. (2015), 'Alignment of hyperspectral imagery and full-waveform lidar data for visualisation and classification purposes', The International Archives of Photogrammetry, Remote Sensing and Spatial Information Sciences 40(7), 1257.

Neuenschwander, A., Magruder, L. & Tyler, M. (n.d.), 'Landcover classification of small-footprint full-waveform lidar data', Jounal of Applied Remote Sensing 3(1), 033544–033544.

Persson, A., Soderman, U., Topel, J. & Ahlberg, S. (2005), Visualisation and Analysis of full-waveform airborne laser scanner data, V/3 Workshop, Laser scanning 2005.

Reitberger, J., Krzystek, P. & Stilla, U. (2008), 'Analysis of full waveform LiDAR data for tree species classification', International Journal of Remote Sensing 29(5), 1407–1431.

Detection of dead trees by machine learning techniques in temperate forests of the Bavarian Forest National Park

Peter Krzystek, Przemyslaw Polewski

Dept. Of Geoinformatics, Munich University of Applied Sciences, 80333 Munich, Germany Keywords: Dead tree, machine lerrning, segmentation, classification The study highlights experiments conducted in the Bavarian Forest National Park for the areawide extraction of standing and fallen trees from ALS LiDAR data and aerial imagery. Full waveform LiDAR data were captured in leaf-on situation with the Riegl LMS Q-860i scanner at a point density of 30 points/m^2. Multispectral airborne data were acquired with the DMC camera at a GSD of 20 cm. ALS 3D points clouds were obtained by a waveform decomposition using a sum of Gaussian functions. Clusters for single standing trees are found by a wall-towall technique for single 3D segmentation in advance. Single dead tree trunks without a crown known as snags are captured just using the segmented tree point cloud. A MSAC-based line fitting preselects the best samples which are subsequently classified by kernelized logistic regression using free shape contexts (FSC) as features. FSCs are 3D shape descriptors which quantify the distribution of points around the principal axis. Standing dead trees with existing crowns are identified from images with green, blue and infrared channels as spectral bands. The 3D clusters from the tree segmentation are used at object level to find the corresponding enclosing polygon in the image. The means of the 3 channels and 6 independent elements of the 3x3 channel covariance matrix are used in the kernelized logistic regression to classify the dead trees. For both types of dead trees a training set of 100 samples is selected. The two methods are combined with a novel active and supervised learning technique to achieve best classification results at a minimum of training costs. The active learning using a Renyi entropy regularized expected error reduction (EER) achieves 90 % of the final classification performance using around 60 % of the number of queries required by standard EER. If the full training set is used the overall accuracy of the dead tree detection is 87 % and 88 %, resp. Finally, a new approach for fallen dead trees detection is based on the idea to first segment the fallen stems in parts and to subsequently combine them into the entire stems. First, potential stem points are identified using point descriptors known from computer vision and a logistic regression. Then, features are calculated from the stem points by shape descriptors and are utilized in a logistic regression to estimate potential stem segments. To this end, the segments are merged to entire stems by a normalized cut segmentation whose control parameters and classifier-based stopping criterion are learned from a simulated virtual fallen tree scenario. In case of beeches, the correctness and completeness of the method amounts at average to 85 % and 79 %, resp. For spruces we end up at 86 % and 57 %.

The paper demonstrates that techniques from machine learning and computer vision are the key to an object-based segmentation and classification of forest parameters. The presented methods have been successfully applied to map dead trees on a large scale forest area (ca. 300 km^2).

Development of an energy balance model for estimating canopy stomatal conductance from airborne thermal data

Juan Suárez, Georgios Xenakis and Roberto Antolín.
Centre for Sustainable Forestry and Climate Change, Forest Research, Northern Research Station, Roslin, Midlothian EH25 9SY, UK.

Keywords: Thermal, LiDAR, Tree physiology, Windflow modelling, Thermolidar, QGIS

Declining tree health is a concern due to the impact of climate change and tree diseases that have profound impacts on commercial activities and the ecological quality of the ecosystems. In this context, the early detection of signs of physiological stress in trees becomes increasingly important in order to plan management interventions. Forest monitoring over large areas is labour intensive in the field and earth observation is frequently restricted to the detection of late-stage visible symptoms. However, sensors have the potential to early detect some subtle changes in leaf biochemistry and the other processes linked to the physiological activity of the foliage. One of those processes is the alterations in stomata activity.

For many years, scores of researchers have used thermal sensors to measure temperature differences used as a proxy of constrained stomatal conductance. Stomatal closure is influenced by the water condition of the plant, modifying energy dissipation as heat. Therefore, a reduce rate of gas exchange of the foliage can be detected as increasing canopy temperatures. Nevertheless, this methodology is constrained by to the lack of sensors at higher spatial resolutions (<1-2 m), the aggregation of combined thermal responses (shadows, ground features and other plant constituent elements) and the air boundary layer above the foliage. All these elements combined increase the noise to signal ratio for an effective detection of thermal differences that can be associated to stomata activity.

This work has reformulated the energy balance model primarily suggested by Blonquist et al (2009) that now estimates canopy stomatal conductance by using a series of standard meteorological and airborne thermal data. The model calculates canopy stomatal conductance (gC , mol m−2 ground area s−1) from canopy temperature, air temperature, barometric pressure, relative humidity, net radiation, wind speed and plant canopy height. Canopy temperature has been measured using a thermal sensor on a plane platform in a study area in the Trossachs and Ben Lomond National Park of Scotland. Measurements took place at the time of maximum stomata activity at 10 a.m. in May, July and September and calibrated with field data. Wind speed has been calculated using reference anemometers and the airflow model WAsP. The meteorological variables (air temperature, barometric pressure and relative humidity) have been measured in two stations in the field closed to the monitoring plots used as validation. Vegetation height was extracted from airborne LiDAR. Incoming shortwave radiation at the top of the canopy has been calculated as a function of latitude, elevation, slope and aspect, monthly air temperature, relative humidity and total precipitation to calculate the solar radiation first at the top of the atmosphere, then corrected it for atmospheric conditions and finally corrected it for topographic exposure and inclination. Net assimilation has been estimated from incoming solar radiation and a constant value obtained from the literature.

The model has been implemented in QGIS using a combination of C++ and Phython. This development has been part of the EU-funded project Thermolidar.

The outputs of the model were validated against field measurements by measuring stomatal conductance on a number of trees at the time of thermal data collection. The canopy of each sample tree was divided in several layers (approximately three levels) and at least four samples (two sunlit and two shaded

branches). In each, leaf stomatal conductance was measured using an infrared gas analyser (IRGA, LiCOR 6400). The results showed the potential of this methodology for creating thematic cartography showing the distribution of stomatal conductance across a forested area. More work is being underway at the time of the submission of this abstract that will be presented during the conference.

Development of precision forestry applications for New Zealand plantations using remotely sensed datasets

Michael S Watt[1], Jonathan P Dash[2], Grant Pearse[2], David Pont[2], Heidi Dungey[2], Mark Kimberley[2], Marie Heaphy[2]*

[1]Scion, PO Box 29237, Fendalton, Christchurch, New Zealand
[2]Scion, PO Box 3020, Rotorua, New Zealand

Keywords: ALS; light detection and ranging; *Pinus radiata*; radiata pine; stocking

Precision forestry is the deployment of high resolution remotely sensed data to support decision making. Remotely sensed information is now at a cost and availability that allows precision forestry to become a reality within New Zealand plantations. Implementation of precision forestry will provide the necessary information for managers to make decisions that optimise plantation growth and value at a fine (sub-stand to stand) scale across broad spatial extent. The objective of this research is to describe current and potential precision forestry applications within New Zealand plantations.

Using LiDAR and satellite imagery as input data the following precision forestry applications are likely to be implemented within New Zealand plantation forestry operations over the next decade:

- Spatial optimisation of final crop stand density using a model based on the productivity indices Site Index and 300 Index, which in turn are derived from remotely sensed information (GIS layers, satellite imagery; LiDAR)
- Characterisation of weed competition in young plantation stands, using multispectral data (acquired from satellite imagery or UAV's) to guide decision making around weed control using aerially applied herbicides
- Regional monitoring of key needle cast diseases at a fine scale using satellite imagery allowing targeted disease control measures
- Area based phenotyping where LiDAR data can be used spatially quantify genetic gain. This information can be used to precisely identity the optimal location of individual genotypes throughout a forestry estate to optimise growth, disease resistance and wood quality
- Determination of plantation areas where fertiliser application is likely to result in the highest growth gains, based on estimates of predicted leaf area index derived from LiDAR

At the time of writing a model describing spatial optimisation of final crop density has been developed and is currently being operationalised using remotely sensed data as input. Remotely sensed multispectral imagery has been successfully used to characterise weed competition and the disease red needle cast (second and third listed applications). Research assessing the utility of area based phenotyping across a major plantation estate is currently underway and expected to be completed within a year. LiDAR data has been successfully used to describe leaf area index and the utility of this layer for predicting areas where fertilisation will be most effective is currently being assessed across a major plantation estate. This research will be completed within a year.

Datasets that support precision forestry are becoming increasingly affordable within New Zealand. Free regional LiDAR datasets are available within New Zealand and the cost of airborne LiDAR has over recent years declined to a level that makes acquisition cost effective for most major plantation growers. Recent satellite launches (e.g. Sentinel 2) that provide freely available imagery on a regular basis are also providing a useful source of information for precision forestry applications.

Estimating the regional resource supply of forests in south-west Germany for a future lignocellulose-based bioeconomy using airborne LiDAR, Landsat 7 and National Forest Inventory data

Joachim Maack[1], Marcus Lingenfelder[2], Thomas Smaltschinski[2], Dirk Jaeger[2], Barbara Koch[1]

[1]University of Freiburg, Chair of Remote Sensing and Landscape Information Systems (FeLis), Germany
[2]University of Freiburg, Chair of Forest Operations, Germany

Keywords: LiDAR, Landsat 7, National Forest Inventory, Timber Volume Modelling, Bioeconomy

Abstract

In the endeavour to move towards sustainable development, one essential goal is to replace fossil-fuel-based materials with bio-based products derived from algae, crops and wood. There is a strong interest in estimating biomass or timber volume because to assess the prospects of a future bioeconomy it is important to calculate the potential supply of resources. Remote sensing-based timber volume estimation is essential to modelling the regional potential, accessibility and price of lignocellulosic raw material for an emerging bioeconomy. We used a unique wall-to-wall airborne LiDAR dataset and Landsat 7 satellite images in combination with terrestrial inventory data derived from the German National Forest Inventory (NFI), and applied generalized additive models (GAM) to estimate spatially explicit timber distribution and volume in the federal state of Baden-Württemberg (~35000 km^2). The NFI data showed an underlying structure regarding size and ownership of the different wooded areas that reflect various management impacts in terms of cultivation, timber stocks and logging. We further correlated the estimated timber volume with the annual regional timber harvest for different forest sizes and ownership classes to analyze the regional economic potential. In the final step we will propose optimized locations for possible biomass conversion plants with varying catchment areas using routing-enabled infrastructure data. As it is still largely unknown which size, throughput and resource demand a conversion-plant will feature, we developed an adaptive workflow that allows for future adjustments of the approach. The results demonstrate the usefulness of remote sensing techniques for mapping timber volume towards a future lignocellulose-based bioeconomy.

Estimation of canopy cover in hemi-boreal broad-leaved forests in Estonia using hemispherical photography and lidar data

Tauri Arumäe [1,2], Mait Lang [1,3], Ave Kodar [3]*

*[1]Institute of Forestry and Rural Engineering, Estonian University of Life Sciences, Kreutzwaldi 5, 51014, Tartu, Estonia; *e-mail: tauri.arumae@rmk.ee;*
[2]State Forest Management Centre, 10149, Tallinn, Estonia;
[3]Tartu Observatory, 61602, Tõravere, Tartumaa, Estonia;

Keywords: airborne laser data, canopy cover, living crown-base height, leaf-on and leaf-off canopy cover

Introduction & aim

Estonia has a country-wide regular airborne laser scanning cycle and with two years the whole country is covered with lidar data. By the end of 2015 the whole country had a repetitive layer of airborne lidar coverage. As approximately 50% of land in Estonia is covered with forests, then the understanding and application of lidar data in practical forest management is essential.

The aim of the study was to estimate canopy cover (CC) in dense broadleaved hemi-boreal forests in Estonia using airborne lidar data. The estimates were validated by using hemispherical photos for validation data. CC is a key parameter for estimating standing volume, biomass and leaf area index. We tested different height breaks up to living crown base height and first or all reflections for calculating CC using ALS.

Materials and methods

The test site is located in south-eastern part of Estonia, near Laeva (Figure 1). The test site was 15x15 km and mostly covered (>50%) with broad-leaved forests (Appendix 1), mainly dominated by Silver birch (Betula pendula Roth), Norway spruce (Picea Abies L.), Trembling aspen (Populus tremula L.) and Black Alder (Alnus Glutinosa L.). The forests are mostly multi-layered with Norway spruce in the second layer.

Figure 1. Test site location.

Forest-Observation-System.net – towards global reference database for forest biomass

Dmitry Schepaschenko (IIASA, Laxenburg, Austria), Jerome Chave (CNRS, Toulouse, France), Oliver L. Phillips (University of Leeds, UK), Stuart J. Davies (STRI, Washington, USA), Steffen Fritz (IIASA, Laxenburg, Austria), Christoph Perger (IIASA, Laxenburg, Austria), Christopher Dresel (IIASA, Laxenburg, Austria), Simon Lewis (University of Leeds, UK), Klaus Scipal (ESA, Netherlands)

Keywords: Forest biomass, remote sensing, permanent plots, calibration and validation, BIOMASS mission

The Forest Observation System (FOS) is an international cooperation implemented at the initiative of the ESA BIOMASS mission, to establish and maintain a global in-situ forest biomass database to support earth observation and to encourage investment in relevant field-based science. It is designed to be able eventually fulfil the ground data requirements for algorithm training and validation of spaceborne forest related missions, i.e. ESA Sentinel-1, BIOMASS and SAOCOM-CS; NASA GEDI and NISAR; JAXA PALSAR, etc.

The FOS serves as an interface between the remote sensing and ecological communities. Data sharing nowadays is one of the biggest problem despite of the fact that everyone can benefit. Ecologists sometimes do not realize how important their data are for calibration/validation of remote sensing products. Remote sensing community can provide additional rationality and arguments for investments in measurements on sample plots.

The implementation of the FOS is guided by four principles. First, the ground data should be of high quality and collected on permanent plots from 0.25 ha upwards by size. Second, the selection of the sites should be realistic, i.e. proposed at sites where previous expertise and capacity have been built. Third, sites should cover a broad range of geographical and environmental conditions, so as to maximize the robustness of models. Fourth, the procedures for ground data acquisition and database compilation should be transparent and proofed extensively.

Project web portal (http://forest-observation-system.net/) presents besides several base maps, two types of data: (1) metadata: where and what were measured on permanent sample plots; (2) sample plot data for subset of plots where authors agreed to share the data: aggregated to 50x50 m live biomass, tree height, wood density and tree composition. In the proof-of-concept phrase, FOS includes the Center for Tropical Forest Science (CTFS-ForestGEO), RAINFOR, AfriTRON and IIASA networks. FOS is an open initiative and we expect more networks to join for common benefits, incl. joint publications and application for funding of fieldwork.

POSTER

Fractal Volumetric Bouligand-Minkowski Classification of Forest Trees

João Paulo Herrera - EMBRAPA Instrumentação
João do Espírito Santo Batista Neto – Universidade de São Paulo
Lúcio André de Castro Jorge – EMBRAPA Instrumentação

Keywords: Texture, descriptor, fractal, Bolingand-Minkowski, tropical, forests, fourier, classification

Abstract:

The fractal theory is a well-known technique for representing complex structures of nature. In this work, a recent fractal texture descriptor is evaluated in aerial images of tropical forests obtained by an unmanned aerial vehicle. The first results show that the method is able to efficiently characterize some areas. However, additional studies are needed to enhance its performance.

Introduction

Texture is an important physical and visual attribute and is intrinsically involved with properties that define a surface [1]. In Computer Vision, this attribute is defined by the distribution of image reflectance indices and is widely used to characterize a particular region of interest.

There are several models of texture extraction. Recently, researchers of University of São Paulo developed a new texture descriptor based on the Fractal model [2] which is widely known by its good representation of high complex structures and is generally associated with objects of nature. In this context, others authors [3, 4] investigated the performance of this method in different vegetation databases. However, these studies focus only on the analysis of the micro texture on the leaf surface of the plants. In addition, the authors used a very high statistical accuracy for the selection of the samples. In this work, the investigation is based on the analysis of the performance of volumetric Bouligand-Minkowski in aerial images of Brazilian tropical forests. The automatic recognition will enable the mapping of preservation zones and provide new tools for monitoring practices.

Volumetric Bouligand-Minkowski

Theoretically, a fractal is made by infinite self-similar fragments and its characterization is given by fractal dimension measure [5]. In practice, the physical limits of the fractal objects make difficult to compute its exact value of fractal dimension, so it must be estimated.

The volumetric Bouligand-Minkowski method is an estimator of the fractal dimension of textures. Basically, a grey level image is transformed into a three dimensional surface so that the coordinates and are preserved and refers to the grey intensities values. Then each voxel of the surface is successively dilated by a sphere until its radius size reaches a pre-determined value, as shown in Figure 1. At each step the total volume of the surface is computed. The fractal dimension value is given by:

$$Df = 3 - \lim_{r \to 0} \frac{\log\big(V(S,r)\big)}{\log\,(r)},$$

such that:

$$\in S: \sqrt{(v'_x - \ v_x)^2 + \left(v'_y - \ v_y\right)^2 + (v'_z - \ v_z)^2} \ \leq r\},$$

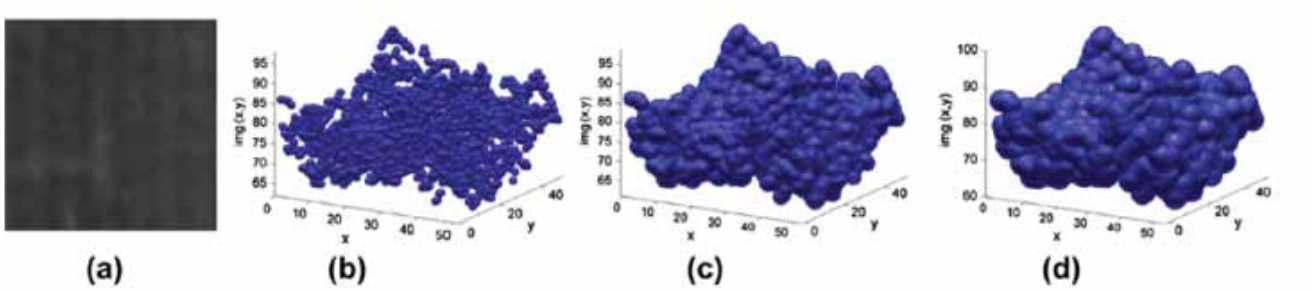

Figure 1 – Dilatation process of the Volumetric Bouligand-Minkowski method. (a) Refers to a grey-level image.(b) Dilatation of with . (c) Dilatation of with. (d) Dilatation of with. Source: Florindo *et al*. (2014)

where $(v_x, v_y, v_z) \in S$ a point of interest on the surface and the limit is the angular coefficient of the line fitted to the log-log curve.

Methodology

The experiment consisted in take aerial images of tropical forests located in São Carlos city, Brazil. The images were captured by a SONY ILCE-5100 camera docked on a fixed wing UAV model ECHAR 20B, which was managed to work at approximately 300 meters in height. The characteristics extraction was performed locally once the image has different textured regions. Thus, each side of the image was divided into 32 equal parts, resulting in a grid of 1024 textured regions.

The volumetric Bouligand-Minkowski extraction was based on the methodology suggested by [2]. They propose to create a three-dimensional Euclidean distance map of the surface in order to facilitate the dilation process of the spheres. Thus, it is not necessary to centralize them in each voxel of, only to count the number of values smaller or equal to its radius. In addition, [3] showed that only the value of the fractal dimension is not enough to describe a texture. This is because different textures can have the same fractal dimension [6]. Therefore, a vector of characteristics was used as a texture signature. This vector is composed by the values of for each increment of the distance value to the limit which in this case was defined as 30:

$$\psi(r_{max}) = \left[\log V(S,1), \log V(S,\sqrt{2}), \log V\left(S,\sqrt{3}\right), \ldots, \log V(S,r_{max})\right]$$

In addition to the proposed approach, four other methods were used: Grey-Level Co-occurrence Matrices (GLCM), Local Binary Patterns (LBP), Local Binary Patterns Rotation Invariation Uniform () and Fourier Descriptors.

At the training stage, 510 tree samples and 490 samples from other areas, such as grass, road, soil and rocks were selected and their textures were extracted by the five descriptors.

In the classification stage, 4 images with 1024 textured regions were classified using the Linear Discriminant Analysis (LDA) classifier.

Preliminary Results

The first results obtained from the 4 images are presented in Table 1. The best performance was the Fourier Descriptors, with global accuracy of 95.7% and kappa = 0.94 and the worst was the Bouligand-Minkowski volumetric, with overall accuracy of 87.1 % and kappa = 0.84. The LDA and SVM classifiers were used to calculate the kappa coefficient.

The preliminary results of the volumetric Bouligand-Minkowski technique suggest further studies to leverage its discriminative power in textures of tropical forests distributed over aerial images. Finding the optimal value of is a fundamental key to a better performance. Furthermore, the time and computational resources consumed were high. Figures 2 and 3 illustrate some regions classified by the method.

Table 1 – Classification accuracies

Descriptor	Overall Accuracy	Kappa
Bouligand-Minkowski	87,1%	0.84
GLCM	94,7%	0.93
LBP	93,1%	0.85
LBP^{riu2}	89,0%	0.93
Fourier	95,7%	0.94

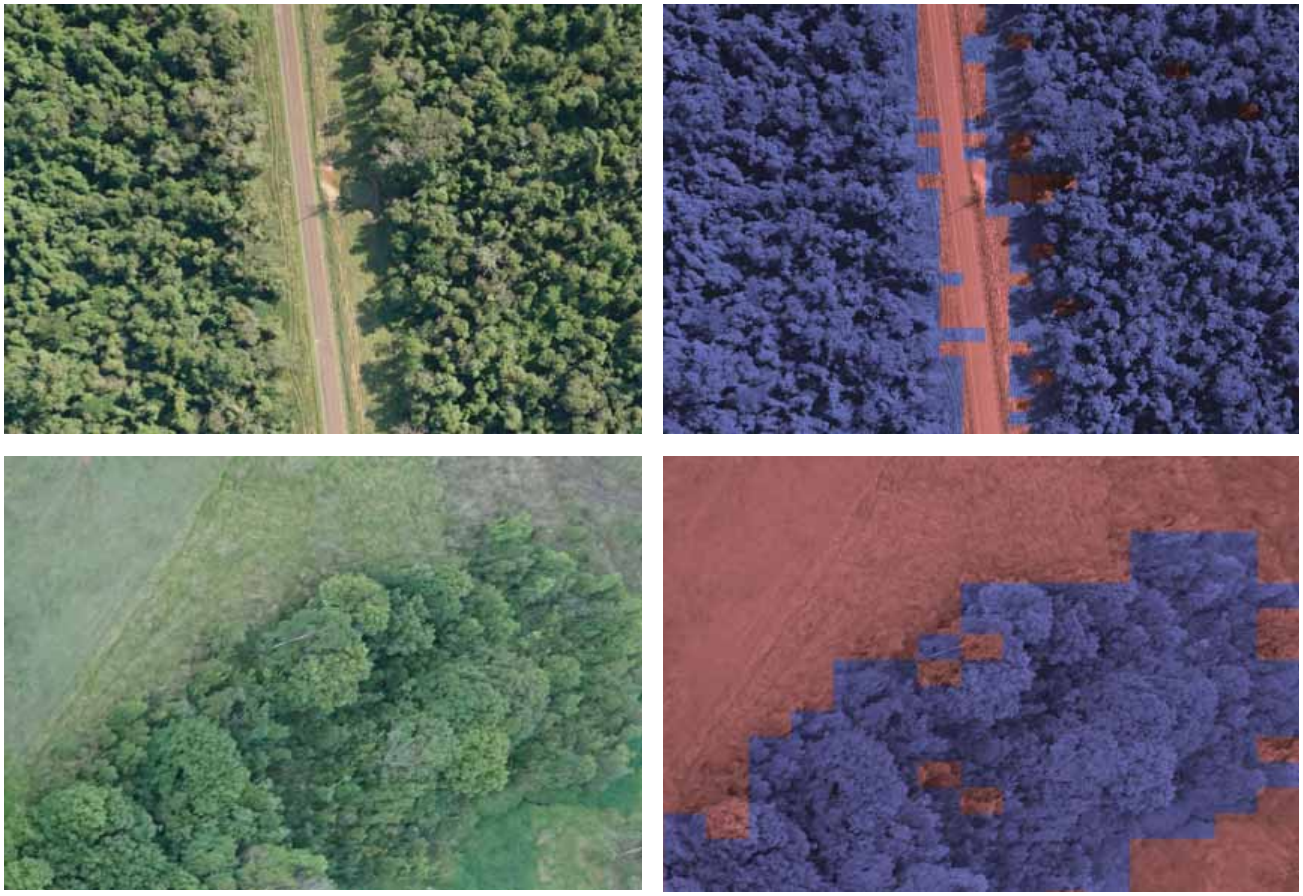

Figure 2 – Examples of good segmentation using the proposed method

Conclusões

In this work, the texture of tropical forests in aerial images was extracted through the recent volumetric Bouligand-Minkowski fractal descriptor. Despite the good representation that a fractal has on structures of nature, the preliminary results did not show good performance against the other texture descriptors already diffused in the literature. Further studies are needed in order to find the maximum radius of the structuring element ideal for this type of texture.

Figure 3 – Examples of poor segmentation using the proposed method

References:

1. Petrou, M; Sevilla, P.G - "Image Processing, dealing with texture", John Wiley and Sons, 2006.
2. Backes, A. R; Casanova, D; Bruno, O. M - "Plant leaf identification based on volumetric fractal dimension", 2009.
3. Florindo, J. B; Da Silva, N. R; Romualdo, L. M; Da Silva, F. F; Luz, P. H. de C; Herling, V. R; Bruno, O. M – "Brachiaria species identification using imaging techniques based on fractal descriptors", Computers and Electronics in Agriculture, 2014.
4. Florindo, J. B; De Castro, M; Bruno, O. M - "Enhancing Volumetric Bouligand-Minkowski Fractal Descriptors by using Functional Data Analysis", International Journal of Modern Physics C, 22:9, 2012.
5. Mandelbrot, B. - "How long is the coast of Britain? Statistical self-similarity and fractional dimension", Science, New series, vol. 156, No 3775, 1967, pp. 636-638.
6. Florindo, J. B; Bruno, O. M – "Descritores fractais aplicados à análise de texturas", Universidade de São Paulo, 2013

Full waveform LiDAR and the new PulseWaves format

Abstract:

The earliest airborne Light Detection And Ranging (LiDAR) scanners delivered just a single elevation return per laser shot. Later systems produced a return for the first and the last interaction between the laser and the landscape below. Today, discrete return LiDAR commonly produces up to 4 or more returns. This allows picking up hits of electricity or telephone wires and captures more information about the vegetation structure.

Recently, waveform digitizers have become popular that capture the reflection of the emitted laser pulse with much more detail: The waveform returning to the plane is digitized up to one billion times per second so that the intensity of the laser pulse's reflection is recorded every nanosecond giving a vertical resolution of one sample of digitized amplitude each 15 centimeters for the returning waveform.

Since 2012 rapidlasso GmbH has been working with the LiDAR community and hardware vendors to create and support the PulseWaves format - a new data exchange format that is similar to the popular LAS format but aimed at storing the entire digitized waveform instead of discrete LiDAR returns in a fully georeferenced manner. In particular it allows storing the outgoing waveform that was "shot" at the aircraft in addition to one or multiple samplings of the returning waveform.

In this talk we will provide a quick intuitive look at how full waveform LiDAR is different from discrete LiDAR, introduce the key features of the PulseWaves format, how to obtain data in this format, and how to use the existing API to read and process it. We look at the current set of PulseTools that are already available for processing full waveform data in PulseWaves (and other full waveform formats), summarize scenarios where operating directly on the full waveform already lead to superior results, and conclude with an outlook on what other full wabeform exploits may lie ahead.

Isolation of obscured forest tree stems using TLS data

Johannes Heinzel

Swiss Federal Institute for Forest, Snow and Landscape Research WSL, Zürcherstraße 111, 8903 Birmensdorf, Switzerland

Keywords: Tree stems, Obstruction, Terrestrial laser scanning, 3D images, 3D mathematical morphology

Abstract

The presented study aims at the detection of obscured tree stems, which often appear hidden by leaves and branches of the regeneration layer. We make use of the high information density in the lower forest layers achieved by terrestrial laser scanning (TLS). The method builds on 3D volumetric images and requires the original point vector data to be transferred into a regular volumetric grid. The actual object detection workflow consists of two major steps. The first one applies a generalized three-dimensional template of a tree stem to probe the complete dataset for vertically elongated structures. The second step comprises a logical processing chain, which combines split stem segments and closes gaps between segments belonging to the same tree stem.

Introduction

The extraction of forest tree stems from laser scanning data provides an important basis for deriving forest stand characteristics. Most existing approaches are limited to the extraction of distinct stems from mature trees, which are not obscured by other vegetation [Eysn et al., 2013; Lovell et al., 2011; Reitberger et al., 2007]. Others reconstruct stems from completely isolated trees, which are separated from any forest environment [Hosoi et al., 2013; Raumonen et al., 2013]. The latter studies concentrate on stem details and less on the detection of stems by number and location within a forest environment. Contrary to those approaches, in many naturally regenerated forests the understory forms a dense and unordered structure. It is characterized by leaves and branches obscuring the tree stems of both mature trees and those of the regeneration layer. Only few studies attend to these difficulties, but still show unfavourable restrictions [Brolly et al., 2013; Xia et al., 2015]. From the perspectives of the scanner positions, stems are often not visible in their total extend and only parts or small fragments can be captured. The challenge is to separate those fragments from the surrounding objects and to combine all segments belonging to the same tree stem.

Methodology

Detecting the tree stems in dense and obscured forest environments is subject to the present method. A special characteristic of the presented method is that it aims at the stem extraction from both mature and regeneration trees within a single dataset. While with airborne laser scanning (ALS) data it is difficult to obtain enough reflections from the lower forest layers, terrestrial laser scanners (TLS) produce a much higher information density due to the different perspective. This results in a better data coverage of the tree stems. However, TLS data is not suitable for capturing continuous wide area information as ALS does. Instead, TLS is often used on a sample plot basis for forestry applications and possibly can be combined with area wide data.
Making use of the perspective advantages of TLS, data has been captured on nine spatially independent plots, located in the canton of Grisons, Switzerland. The plots resemble diverse and often dense forest

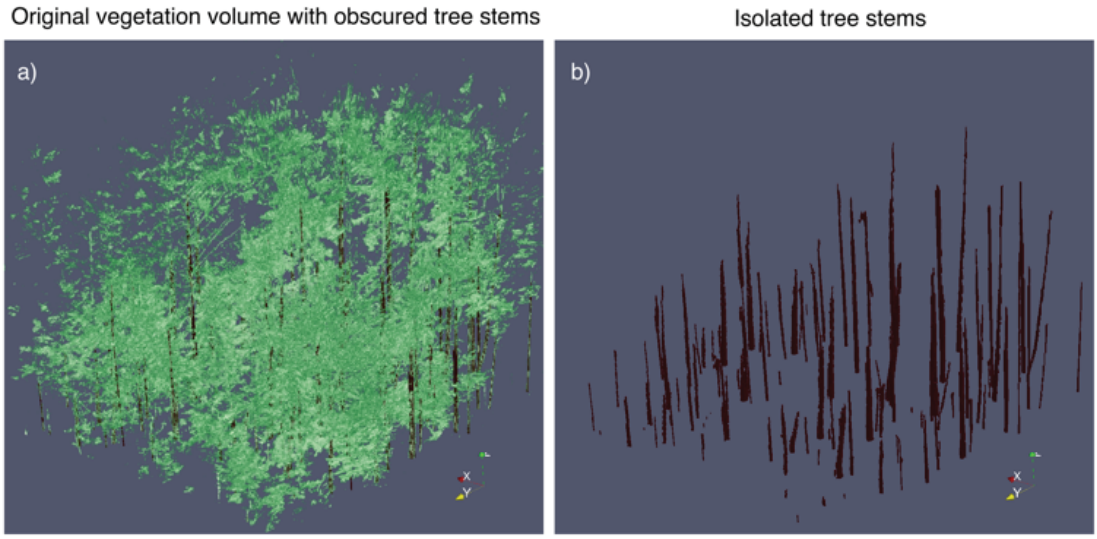

Figure 1. The illustration shows the original vegetation volume and the extracted tree stems. Part a) depicts the partly transparent volume grid of the complete vegetation dataset with obscured stems in the background. In b) green vegetation and branches are removed and only isolated stems remain.

conditions, including different numbers of structural layers. The quadratic plots are centred on grid nodes used by the forest inventory and have a dimension of 25 m edge length. On each plot five scans from different positions have been captured.

Processing of the data covers pre-processing and subsequently two major steps of image analysis. The pre-processing includes the registration of the single scans, the three-dimensional (3D) thinning of the point cloud and the normalization by terrain elevation. The most important part of the pre-processing is the transfer of the point cloud data into a volume grid. All further processing builds on the advantages of the ordered structure of 3D grids. The first major step for stem detection uses techniques from mathematical morphology to separate non-stem vegetation parts from tree stem objects. We apply a series of structuring elements for spatially variant and directional openings of the original volume data. The results are combined into a binary volume, including only stem candidate segments. The second step combines labelling techniques with a logical processing chain in order to aggregate all segments, which belong to a single stem. Finally we receive multiple 3D connected components for all tree stems within a plot. Figure 1 shows the original vegetation data in comparison to the isolated tree stems.

Results

Automatically derived tree stem objects are verified for all nine plots by comparing the number and position of the stems against the reference. For mature trees we verified all stems as measured by the forest inventory, while for regeneration trees only randomly selected individuals were available. Mature trees with a diameter at breast height (DBH) of more than 12 cm show an almost complete detection rate of 97.4 %. Stems from regeneration trees with a minimum crown top height of more than 130 cm and a DBH of less than 12 cm show an overall accuracy of 84.6 %.

Conclusions

In conclusion, the presented method allows practical and reliable extraction of tree stems from mixed mature and regeneration trees. The method is transferable to diverse and dense forest structures and could support applications, such like the management of protective forest against natural hazards, forest inventory or regeneration mapping.

Acknowledgments: This study was conducted within the framework of the Swiss National Forest Inventory. The author would like to thank Markus Huber for project management, Natalia Rehush and Björn Dreier for support during fieldwork, Christian Ginzler for expertise in GNSS technology and Susette Haegi for scan registration. The forest administration of the canton Grisons, Switzerland, gave important assistance to this project.

References

Brolly Gá., Király Gé., Czimber K. (2013) - Mapping Forest Regeneration from Terrestrial Laser Scans. Acta Silv. Lign. Hung., 9: 135-146. DOI: 10.2478/aslh-2013-0011.

Eysn L., Pfeifer N., Ressl C., Hollaus M., Grafl A., Morsdorf F. (2013) - A Practical Approach for Extracting Tree Models in Forest Environments Based on Equirectangular Projections of Terrestrial Laser Scans. Remote Sens., 5: 5424-5448. DOI: 10.3390/rs5115424.

Hosoi F., Nakai Y., Omasa K. (2013) - 3-D voxel-based solid modeling of a broad-leaved tree for accurate volume estimation using portable scanning lidar. ISPRS J. Photogramm. Remote Sens., 82: 41-48. DOI: 10.1016/j.isprsjprs.2013.04.011.

Lovell J., Jupp D., Newnham G., Culvenor D. (2011) - Measuring tree stem diameters using intensity profiles from ground-based scanning lidar from a fixed viewpoint. ISPRS J. Photogramm. Remote Sens., 66: 46-55. DOI: 10.1016/j.isprsjprs.2010.08.006.

Raumonen P., Kaasalainen M., Åkerblom M., Kaasalainen S., Kaartinen H., Vastaranta M., Holopainen M., Disney M., Lewis P. (2013) - Fast Automatic Precision Tree Models from Terrestrial Laser Scanner Data. Remote Sens., 5: 491-520. DOI: 10.3390/rs5020491.

Reitberger J., Krzystek P., Stilla U. (2007) - Combined tree segmentation and stem detection using full waveform lidar data. ISPRS Workshop on Laser Scanning 2007 and SilviLaser 2007, XXXVI-3/W52. Espoo, Finland. pp. 332-337.

Xia S., Wang C., Pan F., Xi X., Zeng H., Liu H. (2015) - Detecting stems in dense and homogeneous forest using single-scan TLS. Forests, 6: 3923-3945. DOI: 10.3390/f6103923.

LiDAR- and SAR-based mapping of structural attributes of deciduous savannahs and woodlands in the southern African region

Renaud Mathieu[1,2], Russell Main[1,2], Laven Naidoo[1,2], Konrad Wessels[3,2], Greg Asner[4]

[1]Ecosystem Earth Observation, Natural Resources and the Environment, CSIR, Pretoria, South Africa
[2]Department of Geography, Geoinformatics, and Meteorology, University of Pretoria, Pretoria, South Africa
[3]Remote Sensing Research Unit, Meraka Institute, CSIR, Pretoria, South Africa
[4]Department of Global Ecology, Stanford University, Stanford, CA, USA
Corresponding author contact details: RMathieu@csir.co.za; (+27)12 841 4089

Keyword: multi-frequency SAR, optical, woody cover, above ground biomass

Abstract

Savannahs and woodlands are the largest forested biome in southern Africa, accounting for 35-45% of the land. These are open forests, with a continuous grass layer and a discontinuous low biomass woody layer (< 60T/ha). Excessive harvesting of woody plants and land use changes can threaten the sustainability of the provision of grass, timber, fuelwood, edible fruits and roots to poorest rural communities. On the other hand, bush encroachment (or thickening) is increasingly seen as a major regional threat for food security via a reduction of grassland for meat production. In South Africa tree cover in savannahs is believed to have increased at a rate of 5-6% per decade and to encroach in grasslands; bush encroachment affects 10-20 million ha. Despite these drastic changes and the legal requirement to report on the forest status every three years at national scale (Forest Act 1998, SA), there is yet limited information on spatial patterns of woody vegetation. We assessed the use of multi-frequency Synthetic Aperture Radar (SAR) and optical datasets acquired at various seasons to map structural attributes (woody cover, above ground biomass) in southern African deciduous woodlands and savannahs. Imagery included X-band TerraSAR, C-band RADARSAT-2 and ENVISAT ASAR, L-band ALOS PALSAR, and Landsat. Methods were based on the integration of field data, airborne LiDAR, and satellite imagery. Field plots were used to calibrate and validate extensive LiDAR-based maps of structural metrics, which were then used to upscale the metrics at satellite level using random forest. Results demonstrated that L-band data acquired in winter performs much better than any other SAR frequency or Landsat optical data, acquired at any seasons. Structural metric retrievals can be can improved by ca. 10% using the combination of L-band with C-band or Landsat reflectance, but L-band remains the most important datasets to monitor woody resource in the region, including for woody cover. Dense time series of winter C-band imagery were shown to be a suitable substitute when L-band data are not available. In addition, the research led to the development of a LiDAR/SAR processing platform, and the production of unique 1-ha maps of woody cover for the entire land mass of South Africa and Namibia, totalling 2 million km2. The maps were produced using extensive regional LiDAR datasets for local calibration/validation and the JAXA ALOS PALSAR mosaic. They are a significant improvement on the global products which were until recently the only available datasets in the region.

Linking remotely sensed functional diversity with phylogenetic structure of a temperate forest

Carla Guillén Escribà[1], Fabian D. Schneider[1], Felix Morsdorf[1], Andy Tedder[2], Eri Yamasaki[2], Kentaro K. Shimizu[2], Bernhard Schmid[2], Michael E. Schaepman[1]

[1.] Department of Geography, Remote Sensing Laboratories, University of Zurich, Zurich, Switzerland.
[2.] Institute of Evolutionary Biology and Environmental Studies, Evolutionary and Ecological Genomics, University of Zurich, Zurich, Switzerland.

Keywords: functional diversity, genetic diversity, imaging spectroscopy, laser scanning, intraspecific variation.

Understanding the forces driving forest biodiversity under global environmental change conditions is an important goal for plant ecologists (Pereira et al. 2012). One of the metrics that is commonly used for the assessment of forest diversity is functional diversity (FD), that is the diversity of functional traits in a given community (Díaz and Cabido 2001; Cadotte et al. 2011, Cardinale et al. 2012). Some studies have found evidence of the strong link between the FD and the phylogenetic composition (PD) of a community (Petchey and Gaston, 2002a; Cadotte et al. 2009). Other studies such as Flynn et al. (2011) and Wang et al. (2015) have delved into the understanding of the mechanistic link between diversity, community functioning and provision of services, and the mechanisms explaining patterns of local FD and PD. To understand these interactions detailed observations are needed. Traditional in-situ approaches have provided very useful data, but are usually spatially constrained (Duro et al. 2007), hence exhibit limited possibilities to be extrapolated to larger scales (Pereira et al. 2013). With the advent of emerging remote sensing methods for functional traits mapping at regional to global scales, the gap of missing trait distribution at larger scales is to be filled (Jetz et al., 2016). We propose to contribute to filling this gap at regional scale by using remote sensing data in combination with in-situ sampling at different spatial and temporal scales.

Here, we investigate the relevance of remotely sensed local interspecific functional variation of a temperate forest (9-hectare plot located on the south-facing slope of the Lägern mountain, Switzerland) to differentiate vegetation types and species at distant and close phylogenetic distances. Phylogeny of the species was constructed using DNA barcode data. Biochemical and architectural plant traits were retrieved by using canopy spectra and point clouds from airborne imaging spectroscopy and laser scanning data respectively. Additionally, trait responses along environmental gradients were detected at intraspecific level to attribute sources of functional diversity within species.

Preliminary results focus on the retrieval of different functional traits. Figure 1 shows the potential of trait clustering for vegetation types classification. Three different biochemical plant traits have been used for this: Chlorophyll, Carotenoid and Leaf water relative abundance. Conifers such as Abies alba present higher leaf water content values while deciduous trees have higher pigment content. Figure 2 shows inter- and intraspecific variation of 3 different architectural traits. Preliminary results seem to indicate that*fraction of single echoes* could be one of the architectural traits performing better vegetation type classification and *maximum height* could be a good predictor for species.

References

Cadotte, M. W., Carscadden, K. & Mirotchnick, N. (2011). Beyond species: Functional diversity and the maintenance of ecological processes and services. J.Appl.Ecol., 48, 1079-1087.

Cadotte, M.W., Cavender-Bares, J., Tilman, D. & Oakley, T.H. (2009). Using phylogenetic,

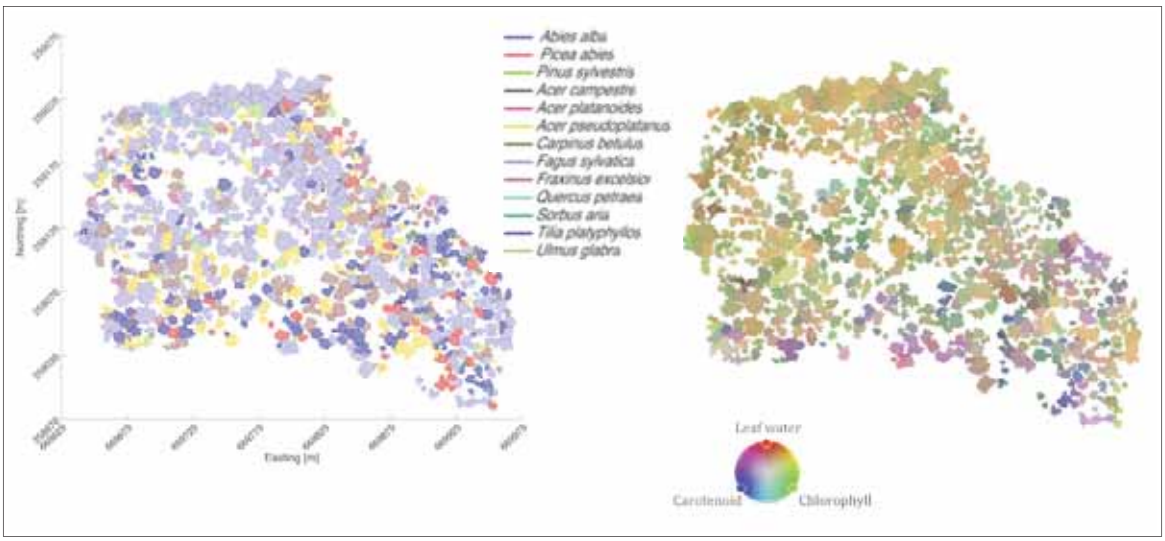

Figure 1. (a) Individual tree crowns at the test site coloured by species and (b) by abundance in relative units [0-1%] of three biochemical functional traits (red=carotenoid, green= chlorophyll and blue= leaf water).

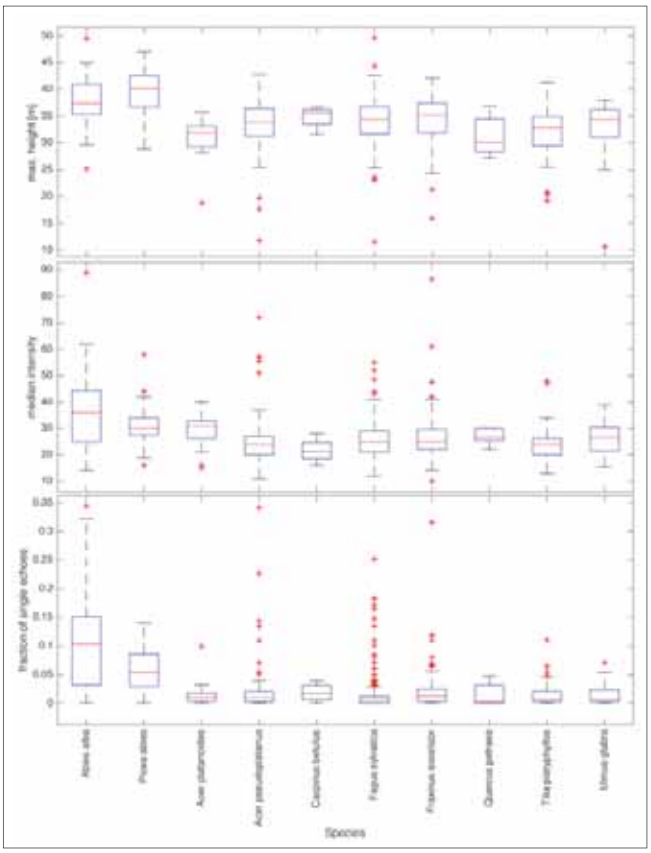

Figure 2. Boxplots of intra- and interspecific architectural trait variation for each of the species at the test site. Traits are: maximum height, median intensity and fraction of single echoes.

functional and trait diversity to understand patterns of plant community productivity. PLoS ONE, 4, e5695

Cardinale BJ., Duffy JE., Gonzalez A., Hooper DU., Perrings C., Venail P., Narwani A., Mace GM., Tilman D., Wardle DA. & Kinzig AP. (2012). Biodiversity loss and its impact on humanity. Nature. Jun 7, 486, no. 7401: 59-67.

Diaz, S. and Cabido, M. (2001). Vive la difference: plant functional diversity matters to ecosystem processes. Trends Ecol. Evol. 18: 646- 655

Duro, D., Coops, N., Wulder, M., and Han, Tian., (2007). Development of a large area biodiversity monitoring system driven by remote sensing. Progress in Physical Geography, 31: 2

Flynn, D.F.B., Mirotchnick, N., Jain, M., Palmer, M.I. & Naeem, S. (2011). Functional and phylogenetic diversity as predictors of biodiversity-ecosystem-function relationships. Ecology 92, 1573 – 1581.

Jetz, W., Cavender-Bares, J., Schimel, D., Pavlik, R., Davis, F., Asner, G.P., Guralnick, R., Kattge, J., Latimer, A.M., Moorcroft, P., Schaepman, M.E., Schildhauer, M.P., Schneider, F.D., Schrodt, F., Ustin S.L., & Turner W. (2016). A global remote sensing mission to detect and predict plant functional biodiversity change. Nature Plants

Pereira, H.M., Ferrier, S., Walters, M., Geller, G.N., Jongman, R.H.G., Scholes, R.J., Bruford, M.W., Brummitt, N., Butchart, S.H.M., Cardoso, A.C., Coops, N.C., Dulloo, E., Faith, D.P., Freyhof, J., Gregory, R.D., Heip, C., Höft, R., Hurtt, G.,

Jetz, W., Karp, D., McGeoch, M.A., Obura, D., Onoda, Y., Pettorelli, N., Reyers, B., Sayre, R., Scharlemann, J.P.W., Stuart, S.N., Turak, E., Walpole, M. and Wegmann, M. (2013). Essential Biodiversity Variables. Science, 339:277-278

Pereira, H.M., Navarro, L.M., Martins, I.S. (2012). Global biodiversity change: the bad, the good, and the unknown. Annu. Rev. Environ. Resour. 37, 25–50

Petchey, O. L. and Gaston, K. J. (2002). Functional diversity (FD), species richness and community composition. Ecology Letters, 5: 402–411.

Wang X., Wiegand T., Swenson N. G., Wolf A. T., Howe R. W., Hao Z., et al. (2015). Mechanisms underlying local functional and phylogenetic beta diversity in two temperate forests. Ecology96:1062–1073.

POSTER

Local pivotal method sampling design combined with micro stands utilizing airborne laser scanning data in a long term forest management planning setting

Rami Saad, Jörgen Wallerman, Johan Holmgren and Tomas Lämås

Keywords: local pivotal method (LPM); segmentation; most similar neighbor (MSN) imputation; forest management planning; suboptimal loss; Lidar; Heureka; decision support system

Abstract

A new sampling design, the local pivotal method (LPM), was combined with the micro stand approach and compared with the traditional systematic sampling design for estimation of forest stand variables. The LPM uses the distance between units in an auxiliary space – in this case airborne laser scanning (ALS) data – to obtain a well-spread sample. Two sets of reference plots were acquired by the two sampling designs and used for imputing data to evaluation plots. The first set of reference plots, acquired by LPM, made up four imputation alternatives (varying number of reference plots) and the second set of reference plots, acquired by systematic sampling design, made up two alternatives (varying plot radius). The forest variables in these alternatives were estimated using the nonparametric method of most similar neighbor imputation, with the ALS data used as auxiliary data. The relative root mean square error (RelRMSE), stem diameter distribution error index and suboptimal loss were calculated for each alternative, but the results showed that neither sampling design, i.e. LPM vs. systematic, offered clear advantages over the other. It is likely that the obtained results were a consequence of the small evaluation dataset used in the study (n = 30). Nevertheless, the LPM sampling design combined with the micro stand approach showed potential for improvement and might be a competitive method when considering the cost efficiency.

Machine learning regression algorithms for biophysical parameter retrieval from spectral properties to detect different levels of ash vitality in Central Europe

Michael Foerster[1], Nele Steinmetz[1], Stephan Pflugmacher[3], Kyle Pipkins[1] and Anne Clasen[1, 2]

[1]Geoinformation in Environmental Planning Lab, Technische Universität Berlin, Straße des 17. Juni 145, D-10623 Berlin, Germany
[2]Helmholz Centre Potsdam-GFZ German Research Centre for Geosciences, Telegrafenberg, 14473 Potsdam, Germany
[3]Department of Ecological Impact Research and Ecotoxicology, Technische Universität Berlin, Ernst-Reuter-Platz 1, D-10587 Berlin, Germany

Keywords: Support Vector Regression, Gaussian Process Regression, Ash dieback, tree mortality

Abstract

The north-East of Europe is affected by the ash (Fraxinus excelsior) dieback caused by the fungal pathogen *Hymenoscyphus pseudoalbidus.* The presented study will show the relation between the biophysical parameters of different levels of ash mortality and their spectral properties, taken from ASD spectral measurements and a CIR aerial image. Just in this way, the biophysical relation of this disease can be related to remote sensing properties.

The study was performed for three ash damage levels, evaluated by forest experts of the federal forestry institution. For each of the three damage levels 40 samples were taken. Close range spectral measurements of the canopy and single leaves were taken at the at the 17th and 18th of July 2014 with an ASD FieldSpec instrument mounted to a crane measurement platform situated in a temperate deciduous forest in North-East Germany. Simultaneously, in the 2014 field campaign, data was collected by CIR airborne campaign. As biophysical variables for the three mortality levels, measurements of Chlorophyll a/b, leaf water content, carotenoids were taken as well as SPAD values. Machine learning regression algorithms (MLRA) have been introduced recently for biophysical parameter retrieval with remote sensing. This study will utilize the Support Vector Regression (SVR) and Gaussian Process Regression (GPR) to predict the biophysical parameters and relate the outcome to the different mortality rates.

Both machine learning algorithms show clear relations to the spectral measurements as well as to the CIR aerial imagery. For both tests of the data-sets, the r^2 of all parameters varies between 0.34 and 0.48 with the exception of leaf water contents, which provides limited predictive power. The relative RMSE is especially low for Carotenoid (4.6 %) as well as the SPAD measurements (4.7 %).

A clear distribution of the different levels of damage can be seen in the scatterplots (see Fig. 1) and can be transferred to map the biophysical parameters to larger areas. The MLRA algorithms were applied to simulated EnMap and Sentinel-2 spectral values, derived by the ASD measurements. The transfer functions could be used to show the level of damage applied on a real Sentinel-2 scene of the summer 2016.

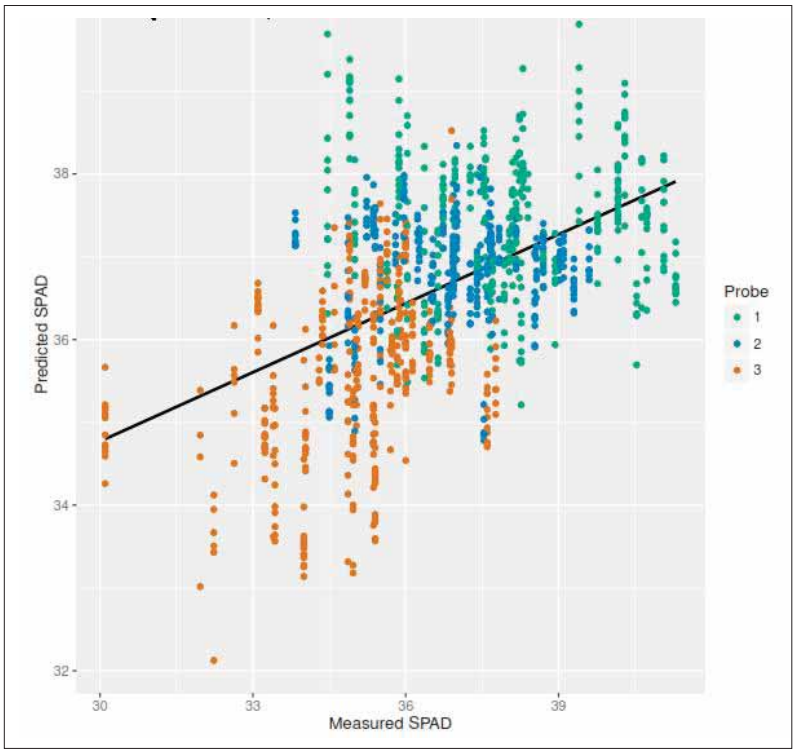

Fig. 1: Scatterplot of predicted versus measured SPAD values for CIR data yielded by SVR (1 = good status of ash health; 2 = medium; 3 = bad)

POSTER

Mapping the 3D structure of a tropical rainforest using terrestrial laser scanning – a quality assessment

Fabian D. Schneider, Daniel Kükenbrink, Michael E. Schaepman and Felix Morsdorf
Remote Sensing Laboratories, University of Zurich, Winterthurerstrasse 190, CH-8057, Zurich, Switzerland

Keywords: terrestrial laser scanning, lidar, forest structure, occlusion mapping, ray tracing

Terrestrial laser scanning (TLS) has emerged as a state-of-the-art measurement technology of forest canopy structure and the three-dimensional (3D) distribution of plant material. The detailed and accurate measurements of scatterer location and abundance have been used for forest reconstruction, forest monitoring, and modeling of radiative transfer or biomass (e.g., Calders et al., 2015; Newnham et al., 2015)we develop an approach to estimate AGB from TLS data, which does not need any prior information about allometry. We compare these estimates against destructively harvested AGB estimates and AGB derived from allometric equations. We also evaluate tree parameters, diameter at breast height (DBH. When measuring a forest plot with TLS, the quality and completeness of the data is mainly determined by the applied measurement setup. The goal of reducing occlusion and reaching a complete coverage among all vertical layers of the canopy has to be traded against number of scan locations and hence costly operation time. Occlusion has been identified as a major source of uncertainty in forest reconstruction (Béland, Baldocchi, Widlowski, Fournier, & Verstraete, 2014)we investigate the optimal voxel dimensions for estimating the spatial distribution of within crown leaf area density. We analyzed LiDAR measurements from two field sites, located in Mali and in California, with trees having different leaf sizes during periods with and without leaves.We found that there is a range of voxel sizes, which satisfy three important conditions. The first condition is related to clumping and requires voxels small enough to exclude large gaps between crowns and branches. The second condition requires a voxel size large enough for the conditions postulated by the Poisson law to be valid, i.e., a turbid medium with randomly positioned leaves. And, the third condition relates to the appropriate voxel size to pinpoint the location of those volumes within the canopy which were insufficiently sampled by the LiDAR instrument to derive reliable statistics (occlusion effects, but very few studies have specifically investigated the effects of occlusion on TLS data quality.

In this study, we applied a ray tracing based method developed by Kükenbrink, Leiterer, Schneider, Schaepman, & Morsdorf (under review) to map occlusion in a 1 ha forest plot. The method uses a voxel-traversal algorithm and traces each laser pulse to determine sampled and occluded, empty or filled voxels. We scanned 1 ha of tropical rainforest in the Lambir Hills National Park (Sarawak, Malaysia) from 93 positions on the ground, with an average horizontal spacing of 10 m. Additionally, we performed 32 TLS scans from four platforms of a canopy crane at 24, 39, 59 and 76 m above ground. Our main research questions are: (1) How is occlusion distributed in the vertical canopy layers in (a) scans from the ground and (b) scans from the canopy crane? (2) What is the benefit of combining ground based and above-ground TLS measurements for forest reconstruction? (3) How is occlusion influenced by the number of scan positions?

Preliminary results are presented in Figure 1. The voxel grid shows parts of the canopy crane on the left and a 1 m deep transect through the surrounding trees. It shows that most of the vegetated voxels have only been covered by one or two scans. Therefore, it is crucial to have many different scan positions to cover trees in a tropical forest with their full extent. Furthermore, it shows that parts of the upper canopy are occluded in more than four out of seven scans. This suggests that the scans from the canopy crane are the main contribution to the coverage and quality of the data in the uppermost canopy layers. By extending the analysis to the whole forest plot, we want to assess the quality of

ground and above-ground TLS measurements in a tropical rainforest and provide some guidelines to establish a best performing measurement setup.

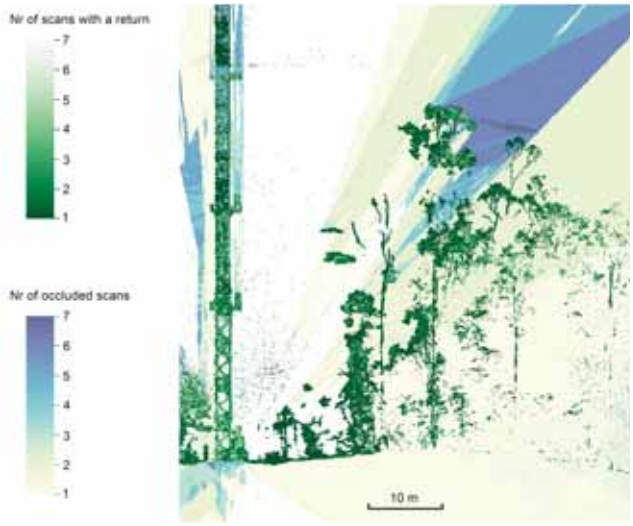

Figure 1. Vertical profile of a 10 cm voxel grid showing voxels with laser returns and occluded voxels. The color scale indicates the number of different scans producing a laser return or occlusion. For this example, seven scans have been co-registered, three of them are located on the lower three crane platforms.

References

Béland, M., Baldocchi, D. D., Widlowski, J. L., Fournier, R. a., & Verstraete, M. M. (2014). On seeing the wood from the leaves and the role of voxel size in determining leaf area distribution of forests with terrestrial LiDAR. *Agricultural and Forest Meteorology*, *184*, 82–97. http://doi.org/10.1016/j.agrformet.2013.09.005

Calders, K., Newnham, G., Burt, A., Murphy, S., Raumonen, P., Herold, M., … Kaasalainen, M. (2015). Nondestructive estimates of above-ground biomass using terrestrial laser scanning. *Methods in Ecology and Evolution*, *6*(2), 198–208. http://doi.org/10.1111/2041-210X.12301

Kükenbrink, D., Leiterer, R., Schneider, F. D., Schaepman, M. E., & Morsdorf, F. (under review). Quantification of hidden canopy volume of airborne laser scanning data using a voxel traversal algorithm. *Remote Sensing of Environment*, (Special Issue of the SilviLaser 2015 Conference).

Newnham, G. J., Armston, J. D., Calders, K., Disney, M. I., Lovell, J. L., Schaaf, C. B., … Danson, F. M. (2015). Terrestrial Laser Scanning for Plot-Scale Forest Measurement. *Current Forestry Reports*, 239–251. http://doi.org/10.1007/s40725-015-0025-5

POSTER

Measuring stem diameters - a comparison of three methods

Susann Klatt, Thünen Institute of Forest Ecosystems
Johannes Breidenbach, Norwegian Institute of Bioeconomy Research
Rasmus Astrup, Norwegian Institute of Bioeconomy Research

Keywords: Close-range photogrammetry, Criterion, Gator Eyes

Abstract

As descriptors of stem taper and allometry, breast height and upper diameters (dbh, du) are input parameters to estimte tree volume and biomass. Therefore, the measurement of diameters is essential in forest inventories. Here, we compared three devices to measure dbh and an upper diameter in approx. 30% of tree height for 50 trees in south eastern Norway. The devices were: (1) images taken with two reflex cameras mounted on a stereo rig (RCS), (2) a Criterion dendrometer (CRD) mounted on a tripod and a handheld Gator Eye caliper (GEC). RCS images were taken simultaneously from seven positions on a hemisphere with five meters distance to the tree.

Close-range photogrammetry data were processed using Python scripting for wokflow automation. The dbh and du were measured in 3D dense point clouds using open source software. For dbh, the devices were compared to reference measurements with a caliper.

Preliminary analysis for dbh resulted in root mean squared deviances (RMSDs) of 9.8 mm and 8.2 mm for CRD and GEC, respectively. Systematic deviances were less than 2 mm for both methods. First analysis of the close-range photogrammetry data were promising, as the image-matching point cloud resembles data generated by terrestrial laser scanners. The photogrammetric method allows for the documentation of the trees' status and future re-processing with more advanced methods. However, the number of pictures taken would need to be reduced to save time and storage capacity in most forest inventory settings. Random and systematic deviances of the measurements based on the three methods will be compared and discussed.

Multi-Year Comparison of Tree Species Discrimination from Formosat-2 Satellite Image Time Series

M. Fauvel[1], D. Sheeren[1,], J.-F. Dejoux[2], J. Willm[1]*

[1]DYNAFOR Lab., INP Toulouse/INRA, University of Toulouse, France
[2]CESBIO Lab., CNES/UPS/IRD/CNRS, University of Toulouse, France

Keywords: Tree species, forest, time series, classication, uncertainty.

Abstract

Mapping forest composition is essential for forest management, biodiversity conservation and predicting potential shifts of tree species under the context of climate change. However, operational production of accurate species maps is still challenging in remote sensing. In this study, the ability of dense high spatial resolution multispectral Formosat-2 satellite image time-series (SITS) to discriminate tree species in temperate forests is investigated. Using height years of satellite data, we compared the performance of single-year classications to map thirteen dominant tree species in a study area of southwest France. Formosat time-series were composed of eleven to fourty-three dates acquired across one year from 2006 to 2014. Canopy species were identied using parametric (GMM) and nonparametric (k-NN, RF, SVM) machine learning algorithms at three class hierarchy levels, after ltering noisy pixels using B-Splines. The classiers were trained and cross-validated from 1235 eld-collected plots by applying a random data-splitting procedure repreated 25 times. The results showed a very high suitability of the SITS to identify the forest tree species based on phenological dierences. Accuracy of single-year classications varied from 0.85 (k_{mean} in 2008 for GMM) to 0.95 (k_{mean} in 2014 for SVM) with a decrease in performance as the classication became more specic from level 1 to level 3. SVM outperformed systematically the other classiers with a higher stability in accuracy between the years. However, a spatial analysis of the interannual variability revealed disagreements between the single-year classications in complex mixed forests, suggesting a higher uncertainty in these areas. By contrast, a good stability was observed within monospecic plantations (e.g. for aspen or eucalyptus). Our ndings suggest that time-series data is a promising approach for mapping forest types. It also demonstrates the potential contribution of the Sentinel-2 satellites for large scale forest monitoring.

Corresponding author
Email address: david.sheeren@ensat.fr (D. Sheeren)
Preprint submitted to ForestSAT'2016 May 9, 2016

POSTER

Multiscale forest health mapping: the potential of air- and space-borne sensors

Iurii Shendryk[1,], Mark Broich[1], Mirela G. Tulbure[1], Andrew McGrath[2], David Keith[3], Sergey V. Alexandrov[4]*

[1]School of Biological, Earth and Environmental Sciences, University of New South Wales, Kensington NSW 2052, Australia.
[2]Airborne Research Australia, Flinders University, Salisbury South, 5106, Australia.
[3]Centre for Ecosystem Science, School of Biological, Earth and Environmental Sciences, University of New South Wales, Kensington NSW 2052, Australia and New South Wales Office of Environment and Heritage, Hurstville NSW 2220, Australia.
[4]Automation and Control Institute, Vienna University of Technology, Vienna, Austria
** Corresponding author: iurii.shendryk@unsw.edu.au*

Keywords: tree health, LiDAR, imaging spectroscopy, random forest, object-oriented classification, Australia, flooding frequency, dieback, eucalypt, individual trees, WorldView-2, SAR

Abstract

Full-waveform airborne LiDAR scanning and imaging spectroscopy data were collected in May-June 2014 to cover 100 sq. km of the largest eucalypt, river red gum forest in the world, located in the south-east of Australia. The objective was to delineate individual trees, characterize their health using airborne remotes sensing data, and investigate spatial relation of forest health to flooding frequency. In addition we tested the ability of optical and SAR satellite imagery as well as low density discrete-return airborne LiDAR scans in upscaling forest health metrics in terms of basal area. Here we present the processing methodology and results of our analysis with the main focus on upscaling forest health metrics.

Introduction

During the past 60 years sizeable areas of forest in Australia have experienced dieback, mostly caused by drought and high temperatures. In order to restore the extent and distribution of healthy forest there is a need in developing a high-tech accounting system of trees. In this respect airborne LiDAR and imaging spectroscopy are two potentially complementary remote sensing technologies that provide comprehensive structural and spectral characteristics of forests over large areas. Focusing on the largest eucalypt, river red gum (RRG) forest in the world (Barmah-Millewa forest) in this study we aimed to (1) develop algorithms for individual tree delineation using full-waveform LiDAR scans and (2) characterize health of delineated trees utilizing LiDAR scans and imaging spectroscopy in a structurally complex floodplain eucalypt forest, (3) characterize the relationship between tree health and flooding frequency derived from Landsat time-series, and (4) extrapolate spatially non-contiguous tree health map derived from LiDAR and imaging spectroscopy datasets (covering ~14% of the study area) to cover the whole extent of this forest using optical and SAR imagery as well as low density discrete-return airborne LiDAR scans. Once developed, this methodology can be a starting point in the development of a nationwide forest health monitoring framework in Australia and applied to other forests worldwide.

Methodology

We conducted experiments in the largest (737 sq. km) eucalypt, river red gum forest in the world, located in the south-east of Australia that experienced severe dieback over the past six decades. For detection of individual trees from full-waveform LiDAR scans we developed a novel bottom-up approach based on Euclidean distance clustering to detect

tree trunks and random walks segmentation to further delineate tree crowns. The proposed algorithm presents a stepwise procedure, where firstly tree trunks are identified based on the spatial arrangement of points in the lowest part of the LiDAR point cloud. Secondly, the points representing identified tree trunks are labelled within the point cloud. Thirdly, a 3D graph is built by connecting all points within a certain radius. Finally based on the spatial connectivity of points to the labelled ones, using so-called random walks algorithm, the point cloud is segmented into individual trees (Fig. 1). The detailed description of the individual delineation algorithm can be found in Shendryk, Broich et al. (2016).

The accurate delineation of trees allowed us to classify the health of this forest using machine learning and field-measured tree crown dieback ratios, which was a good predictor of tree health and crown density, respectively, in this forest. Although tree health is a subjective term, in Barmah-Millewa it is best approximated by dieback levels (i.e. the proportion of dead branches to the total number of branches), which were visually assessed in the field and grouped into three classes. The LiDAR indices were calculated for segmented tree crowns exploiting the full range of full-waveform LiDAR attributes and tree geometry, and used as predictor variables in object-oriented random forest classification. Random forest is a supervised non-parametric machine learning technique, and was particularly suitable for this study as it is able to achieve superior classification performance as compared to other ensemble learning algorithms with small training samples. The detailed description of the individual tree health classification can be found in Shendryk, Broich et al. (2016)"B.

The decrease in flooding has been frequently identified as the main cause of tree health decline in Australia's floodplains. In order to tease out the causes of unhealthy forest we overlaid the flooding frequency map derived from time series of Landsat imagery (1986-2011) (Tulbure, Broich et al. 2016) with our individual tree health maps.

Finally, we utilized very high resolution satellite imagery (i.e. WorldView-2) in combination with SAR imagery (i.e. Sentinel-1 and ALOS-2/PALSAR-2 imagery) and low density discrete-return airborne LiDAR scans as a substrate for extrapolating LiDAR and imaging spectroscopy derived individual tree health. Similarly to individual tree health classification, we developed object-oriented random forest regressions to quantify live and dead basal area (BA) in 60m cells using zonal statistics as predictor variables.

Results

Overall, our individual tree delineation algorithm was able to detect 67% of tree trunks with diameter larger than 13 cm. We assessed the accuracy of tree delineations in terms of crown height and width, with correct delineation of 68% of tree crowns. The increase in LiDAR point density from ~12 to ~24 points/sq. m. resulted in tree trunk detection and crown delineation increase of 11% and 13%, respectively (Shendryk, Broich et al. 2016). Trees with incorrectly delineated crowns were generally attributed to areas with high tree density.

Returned pulse width, intensity and density related LiDAR indices were the most important predictors in the individual tree health classifications. At the forest level in terms of tree crown dieback, 77% of trees were classified as healthy, 14% as declining and 9% as dying or dead with 81% mapping accuracy. Landsat derived flooding frequency map for over 26 years showed that trees in areas that were flooded less than 5% of the time a pixel was observed

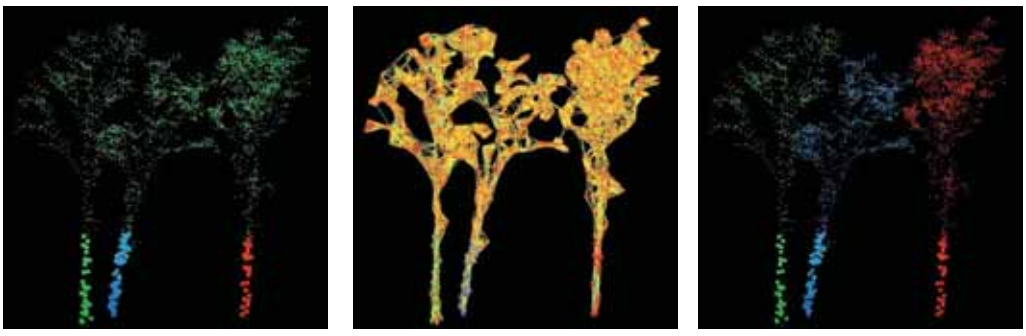

Fig 1: Individual tree segmentation procedure

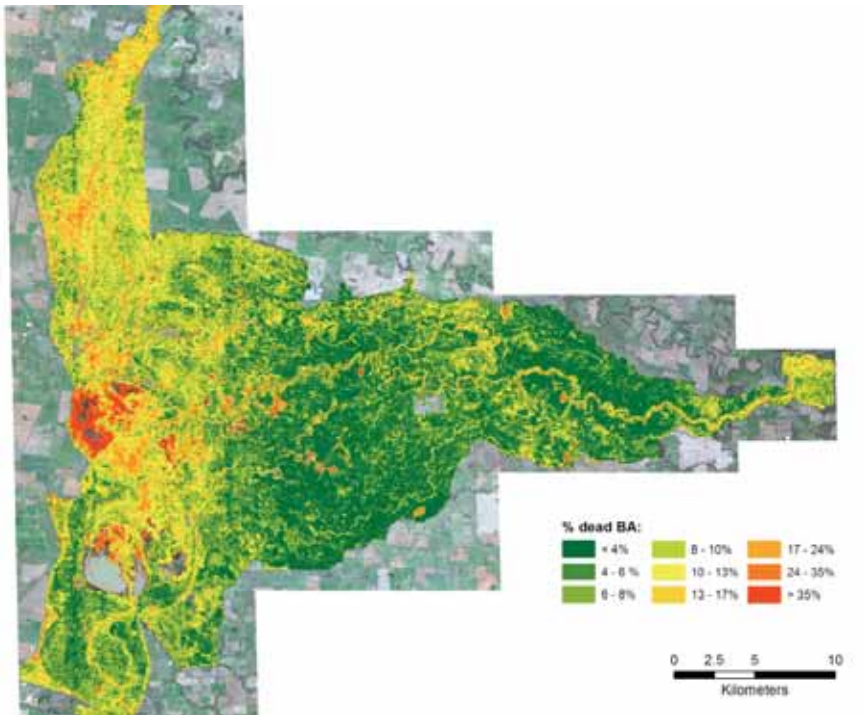

Fig. 1: Preliminary LiDAR, SAR- and WorldView2-derived tree mortality map of the Barmah-Millewa forest, Australia. Areas with canopy cover <10% are masked out. Map pixels are aggregated to 60m spatial resolution and WorldView-2 imagery is shown as a background.

were most susceptible to dieback (Shendryk, Broich et al. 2016).

Our preliminary results also suggest that very high resolution optical and SAR satellite imagery in combination with low density discrete-return LiDAR scans are effective in upscaling individual tree health of this mono-specific forest to a stand level (i.e. 60m resolution). The object-oriented random forest regressions allowed us to quantify total, live, dead and %dead basal area (BA) with R^2 of 0.74, 0.73, 0.41 and 0.46, respectively. The most important variables in predicting total and live BA were zonal statistics extracted from LiDAR derived canopy height model (CHM) and canopy cover (CC) rasters as well as ALOS-2/PALSAR-2 HV- and HH- polarized imagery, and WorldView-2 derived near-infrared (NIR2) to red edge (RE) derived NDVI. While the most important variables in predicting dead and %dead BA were zonal statistics extracted from LiDAR derived CHM and CC as well as Sentinel-1 VH-polarized imagery and WorldView-2 derived NIR2/RE NDVI. Fig. 1 shows the preliminary LiDAR-, SAR- and WorldView2-derived tree mortality map of the Barmah-Millewa forest in terms of %dead BA.

Conclusions

Our results provide algorithms that accurately delineate and classify the health of trees in a structurally complex forest, enabling us to prioritize areas for forest health promotion and biodiversity conservation. We suggest using optical and SAR satellite imagery as well as low-density discrete LiDAR as a possible substrate for extrapolating full-waveform LiDAR and imaging spectroscopy derived individual tree health in order to reduce the cost of larger scale studies.

References

Shendryk, I., M. Broich, M. G. Tulbure and S. V. Alexandrov (2016). "Bottom-up delineation of individual trees from full-waveform airborne laser scans in a structurally complex eucalypt forest." Remote Sensing of Environment **173**: 69-83.

Shendryk, I., M. Broich, M. G. Tulbure, A. McGrath, D. Keith and S. V. Alexandrov (2016). "Mapping individual tree health using full-waveform airborne laser scans and imaging spectroscopy: A case study for a floodplain eucalypt forest." Remote Sensing of Environment **187**: 202-217.

Tulbure, M. G., M. Broich, S. V. Stehman and A. Kommareddy (2016). "Surface water extent dynamics from three decades of seasonally continuous Landsat time series at subcontinental scale in a semi-arid region." Remote Sensing of Environment **178**: 142-157.

Near Real-Time Detection of Forest Changes using Google Earth Engine® and Sentinel-2 Imagery: A Case Study in Curacutin region, Chile

Nils Nölke[1], Hans Fuchs[1] , Victor Sandoval[2], Patricio Acevedo[3], Guillermo Trincado[2], Manuel Castro[3], Nolwenn Boucher[2], Hugo Zerda[4], Christoph Kleinn[1]

[1]Chair of Forest Inventory and Remote Sensing, Georg-August-Universität Göttingen, Germany
[2]Instituto de Bosques y Sociedad, Universidad Austral de Chile, Valdivia, Chile
[3]Departamento de Ciencias Físicas, Universidad de la Frontera, Temuco, Chile 4Facultad de Ciencias Forestales, Universidad Nacional de Santiago del Estero, Argentina

Keywords: forest change, Google Earth Engine, Sentinel-2

Human induced changes in forest area (deforestation, reforestation) and forest condition (forest degradation) are of great significance in national and international policy processes - both in the context of regularly planned forest management and illegal or accidental interventions.

The magnitude and spatial distribution of these activities vary within a country and are difficult to monitor in particular for larger areas. Remote sensing is the only source of information that can be used to identify these activities in larger areas and shorter time intervals. The use of high-resolution imagery acquired on airborne or UAV platforms is time-consuming when it comes to processing, and requires very high-performance computers. Similarly, the processing of satellite imagery acquired at short time intervals on national and subnational scale is very resource-intensive. Nevertheless, the latter may be the only practical approach if one seeks to identify forest changes in the context if implementing efficient "early warning systems".

The Google Earth Engine® provides a powerful means for identifying changes in forests by combining high-performance cloud computing with the automated retrieval of satellite imagery from a vast depository of images.

Our case study is conducted in Curacautín, Chile, and this presentation aims to present results from the initial phase of the study and to evaluate the use of the Google Earth Engine® for identifying areas of forest change at an early point in time. We distinghuish between forest conversion (deforestation) and changes in forest conditions (forest degradation), and match and compare the changes with the corresponding forest management plans in order to provide a reliable interpretation. An Earth Engine® JavaScript was written to access the Sentinel-2 imagery archive of the Engine and serves to detect changes within two consecutive months with a minimum mapping unit of 0.1 ha. The Sentinel-2 satellite imagery was then analyzed using the built-in image processing functions; threshold criteria were identified and used to reliably indicate the occurrence of forest changes.

To illustrate the findings of our study, the presentation compares the results of our automated approach (with the Google Earth Engine® cloud processing) to the results of independent analyses of aerial photographs and satellite imagery. Finally, the potential of high temporal revisits of the only recently available Sentinel-2 imagery for the detection of human induced changes in forests is explored.

POSTER

Optimization of dynamic a global vegetation model at a land cover remote sensing data for better representation of Russian forests

Sergey Venevsky Tsinghua University, Beijing, China
Sergey Khvostikov, Space Research Institute, Moscow, Russia
Sergey Bartalev, Space Research Institute, Moscow, Russia

Dynamic global vegetation model SEVER has been regionally adapted using a remote sensing data derived land cover map in order to improve reconstruction conformity of vegetation functional types distribution over Russia, particularly forests. The SEVER model was modified to address noticeable divergences between modelling results and the land cover map. The model modification included a light competition method elaboration and introduction into the model a tundra class. The rigorous optimisation of key model parameters was done using two-steps procedure. First approximate global optimum was found with Efficient Global Optimisation algorithm, afterwards local search in vicinity of approximate optimum was done with quasi-Newton algorithm BFGS. The regionally adapted model shows significant improvement of the vegetation distribution reconstruction over Russia with better matching with the satellite derived TerraNorte land cover map, which was confirmed by both a visual comparison and a formal conformity criterion.

The closest fit of the model to the remote sensing data derived plant functional types distribution is seen in the Asian part of Russia, which got human activities mainly in the most southern part near the border. Especially important is geographically correct representation of areas for boreal needle-leaved deciduous forests (*Larix* forests) and tundra in the Asian part of Russia. This confirms that *Larix* forests and tundra are determined mainly by climatic variables. Differences in vegetation distribution between optimised version of SEVER DGVM and the TerraNorte land cover map seen in the European part of Russia also provide us with important insight. We conclude that areas, climatically suitable for boreal and temperate broad-leaved forests, are converted to agricultural lands (described as grassland PFTs in SEVER DGVM) by human activities.

Predicting Single Tree Species Diameter Distribution by Airborne Laser Scanning Using Different Modeling Alternatives

Maltamo, M.[1], Mehtätalo, L.[2], Valbuena, R.[1], Vauhkonen, J.[1] and Packalen, P.[1]*

[1] University of Eastern Finland, Faculty of Science and Forestry, School of Forest Sciences, P.O. BOX 111, FI-80101 Joensuu, Finland.
[2] University of Eastern Finland, Faculty of Science and Forestry, School of Computing, P.O. BOX 111, FI-80101 Joensuu, Finland.
** Corresponding author. E-mail address: matti.maltamo@uef.fi*

Keywords: LiDAR, tree size distribution, Weibull, *k-nn*, plantation, parameter prediction, parameter recovery

Abstract

Diameter distribution is a stand-level indicator of the structure of the tree stock and, in forest inventory applications, the information on diameter distribution allows the calculation of timber assortments. However, diameter distribution is usually not included in the field measurements of stand-level management inventory systems. In such cases, the diameter distribution can be predicted using field assessed stand attributes as predictors in theoretical distribution functions, such as Weibull (e.g. Bailey and Dell 1973), or k-nearest neighbor (*k-nn*) imputation (e.g. Maltamo and Kangas 1998).

The emergence of airborne laser scanning (ALS) techniques has had major impact on stand level management inventories (e.g. White et al. 2013). However, there are still primary information needs concerning diameter distribution but it cannot be directly produced by the inventory, and thus, it must be predicted (Maltamo and Gobakken 2014). So far, ALS data have been utilized to predict aggregated stand-level diameter distribution applying Weibull distribution and *k-nn* imputation in some earlier works (Gobakken and Næsset 2004, Maltamo et al. 2009) but the existence of several tree species and irregular distribution shapes usually hampers the prediction (Packalen and Maltamo 2008).

This study aims to examine the ability of metrics of area based approach of ALS to estimate single tree species diameter distribution in an even-aged monoculture plantation, which provides disturbance free conditions to analyze the relationship between ALS and diameter distribution due to the missing minor tree species or undergrowth. The test area is located in Bahia, Brazil and the considered tree species is *Eucalyptus urograndis*. We compare different methods to predict diameter distribution, namely parameter prediction, parameter recovery and distribution matching based on the Weibull function form, in addition to a non-parametric *k-nn* imputation. We also include such a parameter prediction alternative, where Weibull distribution is predicted using field attributes which are typically available in plantations' stand register data. The criteria of the goodness-of-fit are based on the shape of the distribution, i.e. error indices of diameter classes and third powers of diameters of proportional frequencies between 0 and 1.

In general, the results showed that ALS information can predict diameter distribution with an error of slightly more than 10% of relative root mean square error of third power of diameter class frequencies and error index values between 50-60%. The reliability figures of the most accurate ALS based alternatives are also close to the field information based estimates. The results showed strong relationship between ALS information and diameter distribution but the results concerning the comparison between different prediction methods varied regarding the reliability criteria used.

References

Bailey, R.L. and Dell, T.R. 1973. Quantifying diameter distributions with the Weibull function. For. Sci. 19: 97–104.

Gobakken, T. and Næsset, E. 2004. Estimation of diameter and basal area distributions in coniferous forest by means of airborne laser scanner data. Scand. J. For. Res. 19: 529–542.

Maltamo, M. and Gobakken, T. 2014. Predicting tree diameter distributions. In Forestry Applications of Airborne Laser Scanning –concepts and case studies by Maltamo, M., Næsset, E. and Vauhkonen, J. Managing Forest Ecosystems vol 27. Springer, pp.177-191

Maltamo, M. and Kangas, A. 1998. Methods based on k-nearest neighbor regression in the estimation of basal area diameter distribution. Can. J. For. Res. 28: 1107-1115.

Maltamo, M., Næsset, E., Bollandsås, O.-M., Gobakken, T. and Packalén, P. 2009. Non-parametric estimation of diameter distributions by using ALS data. Scand. J. For. Res. 24: 541-553.

Packalén, P. and Maltamo, M. 2008. The estimation of species-specific diameter distributions using airborne laser scanning and aerial photographs. Can. J. For. Res. 38: 1750-1760.

White, J.C., Wulder, M.A., Varhola, A., Vastaranta, M., Coops, N.C., Cook, B.D., Pitt, D., and Woods, M. 2013. A best practices guide for generating forest inventory attributes from airborne laser scanning data using an area-based approach. Forest Chron. 89(6): 722-723.

POSTER

Quality control and quality assessment of LiDAR data

Assis, M.[1]; Cantinho, R. Z.[1]; Oliveira, P. V. C.[1]; dos-Santos, M. N.[2]; Gorgens, E. B.[3]; Ometto, J. P.[1]

[1] Earth System Science Center, National Institute for Space Research. Av. dos Astronautas, 1758, Jardim da Granja, 3º andar. São José dos Campos, São Paulo, CEP 12227-010, Brazil.
[2] Empresa Brasileira de Pesquisa Agropecuária (EMBRAPA-CNPTIA) Av. Dr. André Tosello, 209 - Cidade Universitária, Campinas - SP, Brazil.
[3] Universidade Federal dos Vales do Jequitinhonha e Mucuri. Rodovia MGT 367 - Km 583, nº 5000, Alto da Jacuba CEP 39100-000, Brazil.

Keywords: ALS, LiDAR, data validation, MDT, point cloud, QAQC

A consistent and reliable biomass map for the whole Brazilian Amazon forest is one of the primary objectives of the research project Estimation of Biomass in the Amazon (EBA). A total of 625 randomly distributed lidar flight transects covering an area of 300mx12500m each is being collected since 2016 February. To establish a systematic and consistent data collection methodology, the vendor was required to meet a strict pre-defined set of requirements and specifications. Although primary quality assessment and quality control of the data are typically a responsibility of the vendor, confirming the integrality of the data received became necessary. We developed a protocol to assess return density, return homogeneity, footprint, completeness of the data, the range of values, spatial coverage, scan angle, datum (vertical and horizontal), projection, linear unit and overall adherence to accuracy requirements.

It is indispensable to predetermine which products are considered deliverables: point cloud and its file format (usually .las or a compacted version, laz); digital models (commonly terrain and surface) and file format (generally .asc). For algorithms, it is important to define which ones will be used for the deliverables production and the processing degree (data interference) performed by the contractor (i.e. outliers removal, ground filtering and digital terrain modeling). Furthermore, it is important to define how to proceed in case an unexpected event occurs, especially for large campaigns as ours. Our study presents Python scripts for data validation to be applied by those who are contracting ALS data. Phyton is a free software development platform, and its use is increasing fast in Data Science processing. It also includes laspy, a library that enables lidar data direct accessing and processing. Finally, aiming at raising awareness of the lidar data users community, we present the problems commonly found during the validation process.

Shadow compensation for imaging spectroscopy data using a radiative transfer approach

Daniel Kükenbrink, Fabian D. Schneider, Andreas Hueni, Felix Morsdorf, Michael E. Schaepman
Remote Sensing Laboratories, University of Zurich, Winterthurerstrasse 190, CH-8057, Zurich, Switzerland

Keywords: imaging spectroscopy, airborne laser scanning, radiative transfer, shadow compensation, target reflectance, forestry, raytracing

The retrieval of accurate target reflectance values from imaging spectroscopy data in forest ecosystems is a challenging task due to their structural complexity, largely influencing the measured radiance at sensor level. Topographic and tree crown shadowing effects highly limit accurate biophysical and biochemical parameter retrievals from imaging spectroscopy data. Current approaches trying to overcome these limitations often exclude shadowed areas, significantly reducing the study area, or rely on simple, but often inaccurate shadow compensation approaches based on histogram thresholding, band ratios or matched filters.

In this contribution, we introduce a novel approach to compensate shadowed areas in imaging spectroscopy reflectance data using a radiative transfer approach based on the radiative transfer model DART (Gastellu-Etchegorry et al., 2015). DART is able to estimate the three-dimensional radiative budget, from which we can extract the surface irradiance per image pixel. We parameterised the DART model using airborne laser scanning and in-situ data for a Swiss temperate forest following the approach proposed by Schneider et al. (2014). A shadow compensation factor was retrieved per spectral band and pixel based on the surface and the top of scene irradiance unaffected by shadowing effects, both extracted from the three-dimensional radiative budget output of DART.

The proposed shadow compensation approach was tested on simulated (using DART) and real imaging spectroscopy data derived from the Airborne Prism Experiment (APEX) sensor (Schaepman et al., 2015)its calibration and subsequent radiometric measurements as well as Earth science applications derived from this data. APEX is a dispersive pushbroom imaging spectrometer covering the solar reflected wavelength range between 372 and 2540nm with nominal 312 (max. 532. The approach showed promising results in successfully compensating the reflectance values of ground pixels affected by shadows, which were cast by trees. Figure 1 shows the preliminary results derived from a DART simulation of a simple scene composed by a single tree located in the middle of a meadow with a homogenous known reflectance of 20% in the simulated band (560±1 nm). These preliminary results show that the proposed compensation approach is able to successfully extract target reflectance inside the core shadow. However, the complex light scattering mechanisms inside the forest canopy remain difficult to model, rendering successful target reflectance retrieval as well as its validation challenging. Nevertheless, we argue that the proposed shadow compensation approach significantly improves target reflectance estimation, as well as the retrieval of biochemical and biophysical parameters from high resolution imaging spectroscopy data.

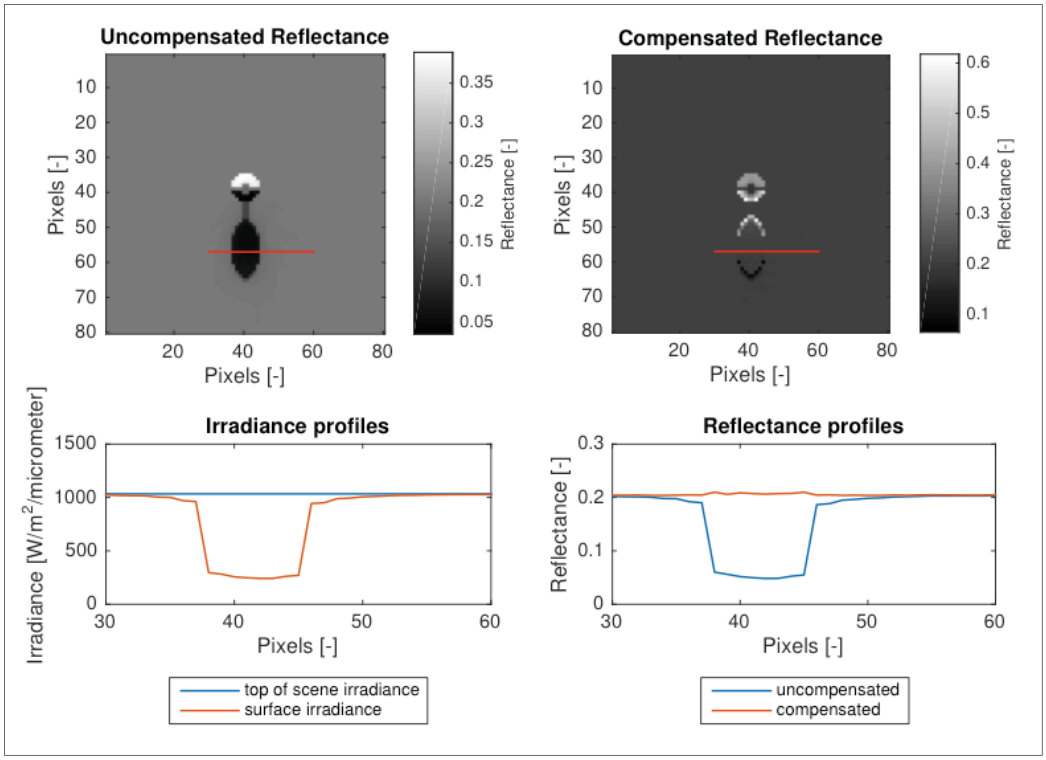

Figure **1**: Preliminary results of the shadow compensation approach applied to a synthetic scene composed by a single tree located in the middle of a meadow with known homogenous reflectance of 20% in the simulated band. The scene was parameterised and the image was simulated using DART at a single spectral band in the green spectrum (560±1 nm). The sun azimuth and zenith angles were defined as 180º and 48º respectively. Top left shows the uncompensated original reflectance image at the given band. The bottom left shows the top of scene irradiance and the surface irradiance for the profile denoted by the red line. Top right shows the compensated image and the bottom right the reflectance profile along the red line for the uncompensated and compensated image.

References:

Gastellu-Etchegorry, J.-P., Yin, T., Lauret, N., Cajgfinger, T., Gregoire, T., Grau, E., … Ristorcelli, T. (2015). Discrete Anisotropic Radiative Transfer (DART 5) for Modeling Airborne and Satellite Spectroradiometer and LIDAR Acquisitions of Natural and Urban Landscapes. *Remote Sensing*, *7*(2), 1667–1701. doi:10.3390/rs70201667

Schaepman, M. E., Jehle, M., Hueni, A., D'Odorico, P., Damm, A., Weyermann, J., … Itten, K. I. (2015). Advanced radiometry measurements and Earth science applications with the Airborne Prism Experiment (APEX). *Remote Sensing of Environment*, *158*, 207–219. doi:10.1016/j.rse.2014.11.014

Schneider, F. D., Leiterer, R., Morsdorf, F., Gastellu-Etchegorry, J.-P., Lauret, N., Pfeifer, N., & Schaepman, M. E. (2014). Simulating imaging spectrometer data: 3D forest modeling based on LiDAR and in situ data. *Remote Sensing of Environment*, *152*, 235–250. doi:10.1016/j.rse.2014.06.015

Simulating the spectral response of tropical tree species with 3-D radiative transfer modeling

Matheus Pinheiro Ferreira[1], Jean-Baptiste Féret[2], Eloi Grau[2], Yosio Edemir Shimabukuro[1], Carlos Roberto de Souza Filho[3]

[1] National Institute for Space Research (INPE), São José dos Campos, Brazil - (mpf; yosio)@dsr.inpe.br
[2] Irstea, Land, environment, remote sensing and spatial information (TETIS), Montpellier, France, - (jean-baptiste.feret; eloi.grau)@teledetection.fr
[3] Institute of Geosciences, University of Campinas, Campinas, Brazil - beto@ige.unicamp.br

Abstract

Spatial and temporal information on biochemical and biophysical attributes of forest areas are key for global and regional studies of ecosystem processes. In this purpose, hyperspectral remote sensing combined with physically-based radiative transfer models (RTMs) has been widely used. However, such approach requires an accurate simulation of the remote sensing signal, which is challenging due to the complex structure and spectral diversity of forest canopies, particularly in tropical environments. This issue can be addressed using three-dimensional (3D) RTMs such as the Discrete Anisotropic Radiative Transfer (DART) model. In this study, the DART model was used to simulate the spectral response of tropical tree species at the canopy level. We tested the influence of a simplified crown structure and optical properties leading to realistic simulations. A look-up table of individual tree crown (ITC) reflectance was built using combinations of DART parameters derived from *in situ* measurements. Then, measured spectral characteristics of individual trees were compared to their simulated counterparts in terms of Root Mean Square Deviation (RMSD). Finally, a sensitivity analysis was performed to understand how the DART parameters affect the simulated canopy reflectance. Differences between experimental and simulated data reached RMSD values from 0.2 to 0.9% in the visible (VIS, 450-650 nm), 0.4 to 1.2% in the red edge (RE, 700-750 nm) and 0.2 to 1.8% in the near-infrared (NIR, 750-920 nm). The sensitivity analysis showed that structural parameters are dominantly responsible for the variation observed in the NIR range, where the highest disagreements between simulated and experimental data were observed. Our study shows that the simulation of the spectral response of tropical tree species is feasible with 3D RTMs, which is the first step to inversely retrieve biophysical and biochemical attributes of tropical forest canopies using physically-based methods.

1. Introduction

Retrieval of biophysical and biochemical vegetation properties using remotely sensed data has long been performed with empirical models. These models relate a measure of reflectance or a vegetation index (VI) to the variable of interest measured in the field. Although these methods are simple and fast, they have some unresolved drawbacks such as: (i) the validity of the model is limited to the environmental conditions where it has been developed, (ii) variables influencing the radiation regime such as the canopy structure are neglected and (iii) the relationship between VIs and the variable of interest is established using costly fieldwork data. 3D Radiative Transfer Models (RTMs) offer the possibility to encompass these limitations by integrating the canopy architecture and simulating remote sensing data in a variety of acquisition and environmental conditions. The retrieval of canopy variables from measured signals is performed by inversion of the model. The inversion basically consists of finding the best set of model parameters that generate the most similar spectrum to a given experimental spectrum (e.g. the spectral response of a pixel). This procedure mainly depends on a good agreement between simulated and measured data. However, little is known about the accuracy of simulations of hyperspectral images as acquired over tropical forests.

In this study we designed a methodology aiming at comparing experimental imaging spectroscopy acquired over a complex tropical forest with DART simulations obtained after application of a certain number of simplifying hypotheses. This methodology is based on the generation of a look-up table (LUT) of individual tree crown (ITC) reflectance using DART simulations obtained by realistic combinations of biophysical and chemical vegetation properties derived from field observations, and a simplified geometric architecture of the trees. We then compared simulations with experimental data in terms of spectral similarity. Finally, a sensitivity analysis was performed to understand how each DART parameter affects the simulated canopy spectral response.

2. Material and Methods

2.1 Study area

The study area is a well-preserved tropical seasonal semi-deciduous forest located in the municipality of Campinas, São Paulo State, southeastern Brazil (22°49'13.4"S 47°06'43.6"W). It is an old-growth forest area, about 630 m a.s.l, subjected to a 5-month dry season (May to September) and characterized by deciduous and evergreen tree species.

2.2 Hyperspectral data

Hyperspectral data was acquired under clear sky conditions on June 7, 2010, using the AisaEAGLE (Spectral Imaging, Inc., Oulu, Finland) sensor that covers the visible/near-infrared (VNIR, 400-970 nm) wavelength range. 122 VNIR spectral bands spaced by 5 nm were acquired with a radiometric resolution of 12 bits. Ten flight-lines in the North-South direction were necessary to cover the whole study area (251.8 ha). The data collected were atmospherically and geometrically corrected according to the procedures described in Ferreira et al. (2016). The spectral bands located below 450 and above 920 nm were discarded due to their low signal-to-noise ratio (SNR). Then, 99 bands covering the 450-920 nm spectral range were retained for further use.

2.3 Field data

2.3.1 Individual tree crown and leaf optical properties data

In this work, we used the ITC dataset of Ferreira et al. (2016), which was produced by visual interpretation of the hyperspectral data and field work. A total of 234 ITCs were identified, corresponding to seven tree species. Additionally, leaves of these species were collected at the beginning of the dry season (end May 2015) for reflectance measurements. The spectroradiometer ASD/FieldSpec®4 (Analytical Spectral Devices (ASD), Inc., Boulder, Colorado) with the Plant Probe accessory, combined with the Leaf Clip assembly, was used to measure leaf reflectance in the 350 to 250 nm range.

3. Methods

3.1 DART radiative transfer

DART is a 3D radiative transfer model that simulates radiation propagation in urban and natural landscapes (Gastellu-Etchegorry et al., 2015). In this work, to simulate the spectral response of tropical tree species at the ITC level, a single tree located at the center of a 10x10 m scene was used. The crown was of round shape with a diameter of 10 m, centered at 20 m height. The canopy was represented by 0.5 m^3 cells filled with foliage and woody branches modeled with two separated turbid media, defined by two densities, spectra and proportion of full cells. Branch reflectance spectra were set to a measured bark spectra. The forest understory was represented by a turbid plot of 2.5 m height (±0.5 m) covering a flat ground. Standard spectra from the DART database were used to characterize optical properties of the understory vegetation, braches and litter. Leaf optical properties were simulated with the PROSPECT-5 model (Féret et al., 2008).

3.2 LUT generation

We generated a LUT by varying 11 DART parameters (Table 2), which can be divided into three main categories: canopy structural properties, leaf biophysical properties (corresponding to the input parameters of PROSPECT-5) and scene optical properties.

3.3 Sensitivity analysis

We are interested to identify the most influential DART parameters and quantify how much they contribute to the variability in the simulated canopy reflectance. To do this, we performed a one at a time sensitivity analysis (OAT-SA) and computed a set of sensitivity indices. The OAT-SA aimed to understand how the DART parameters individually affect the spectral response of the simulated tree. Thus, we varied the DART parameters one at a time

Table 2 DART + PROSPECT parameters, their ranges, and increments and nature used to build the LUT

Canopy structural parameters	Unit/Type	Min	Max	Increment	Increment OAT-SA[a]	Base-case	Nature
Leaf Angle Distribution (LAD)	*planophile*	-	-	-	-	*planophile*	Categorical
	erectophile	-	-	-	-		
	plagiophile	-	-	-	-		
	extremophile	-	-	-	-		
	spherical	-	-	-	-		
	uniform	-	-	-	-		
Density of branches per voxel (DBF)	volume %	0	0.75	0.25	0.25	10	Categorical
Density of leaves per voxel (DLF)	m^2/m^3	0.5	3	0.5	0.5	1	Continuous
Proportion of full cells within the tree crown (pCells)	%	40	100	20	20	70	Categorical
Scene optical parameters							
Optical reflectance factor of branches (OBF)	-	0	1	0.5	0.5	1	Categorical
Optical reflectance factor of the ground (OGF)	-	0	1.5	0.5	0.5	1	Categorical
PROSPECT-5 parameters							
Chlorophyll *a+b* (C_{ab})	µg/cm²	10	100	-	20	40	Continuous
Carotenoids (C_{xc})	µg/cm²	5	25	-	5	10	Continuous
Equivalent Water Thickness (C_w)	g/cm²	0.002	0.042	-	0.01	0.012	Continuous
Dry Matter Content (C_m)	g/cm²	0.003	0.033	-	0.005	0.009	Continuous
Leaf Structure (N)	-	1.4	3.4	-	0.5	1.8	Continuous

[a] Increment used for the one at a time sensitivity analysis (OAT-SA)

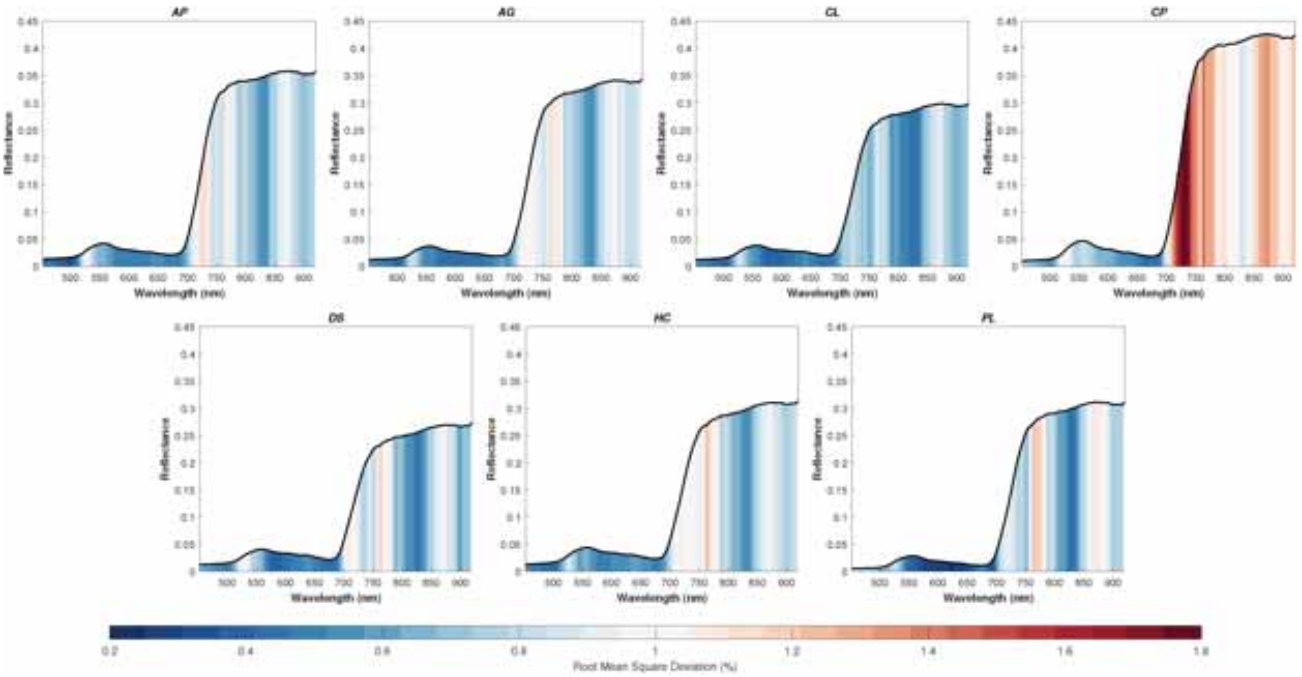

Fig. 1 Root Mean Square Deviation (%) between the simulated and the measured spectral response of seven tree species from a tropical seasonal semi-deciduous forest formation. The mean spectral response of the species are plotted for clarity. AP=*Aspidosperma polyneuron;* AG=*Astronium graveolens;* CL=*Cariniana legalis*; CP=*Croton piptocalyx;* DS= *Diatenopteryx sorbifolia;* HC=*Hymenaea courbaril;* PL= *Pachystroma longifolium.*

by specific increments, keeping all other parameters at their base-case values, which yielded a factorial design of size 56 (Table 2).

3.4 Comparison between experimental and simulated data

Pixels from the manually delineated ITCs were extracted from the hyperspectral image and averaged to compose an experimental dataset of 234 spectra. We selected only sunlit crown pixels within each ITC to compute its mean spectral response. Sunlit pixels were defined as those presenting high NIR reflectance (>0.2). This choice was motivated by the fact that sunlit pixels are less influenced by shadows and thus present high signal-to-noise ratios. We averaged the reflectance corresponding to sunlit pixels for each ITC and obtained an experimental dataset of 234 spectra. Similarly, the mean spectral response of each simulated tree was computed, resulting in a simulated dataset of 3518 spectra. We then compared simulated with measured spectra, using the Root Mean Square Deviation (RMSD) as a criterion for spectral similarity.

4. Results

4.1 Spectral similarity

Spectral differences between experimental spectra and their simulated counterpart (based on minimized RMSD criterion) and averaged per species varied from 0.2 to 1.8% over the VNIR domain. More specifically, RMSD reached values from 0.2 to 1% in the visible (VIS, 450-700 nm), 0.5 to 1.8% in the red-edge (RE, 700-750 nm) and 0.4 to 1.4% in the near-infrared (NIR, 750-920 nm) (Fig.1). Regardless of the species, there was an increasing trend in RMSD from VIS to NIR, which can be noted starting at 750 nm, and due to the lower overall values of reflectance in the VIS domain due to saturating absorption from photosynthetic pigments. Overall, simulated and experimental spectra showed a better agreement in the VIS than in the NIR.

4.2 Sensitivity analysis

The sensitivity analysis provided the opportunity to better understand how each DART parameter affected the crown spectral response (Fig. 2). The VIS range is more influenced by the leaf optical properties than by the canopy structural parameters. Most notably, C_{ab} variations changed the spectra from 500 to 750 nm, impacting more severely the green peak and the red-edge (Fig. 2).

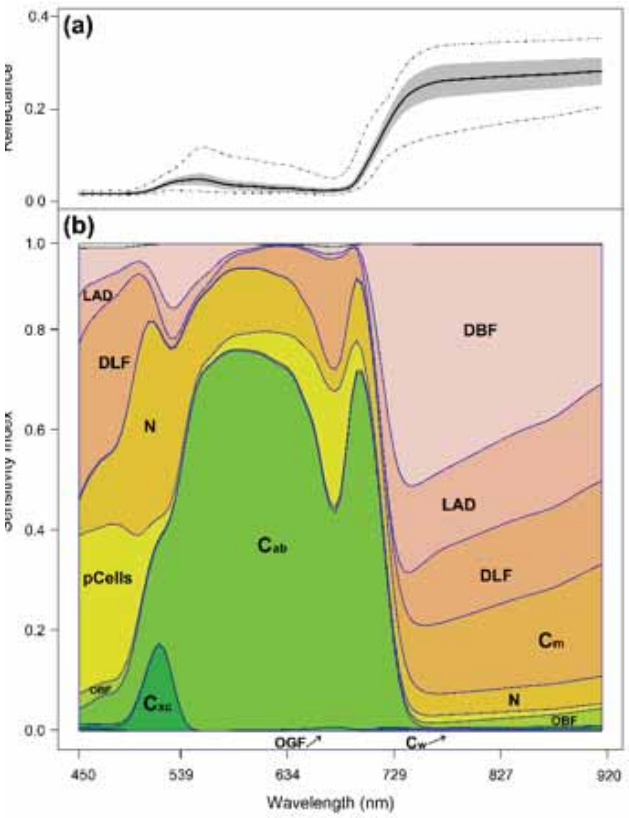

Fig. 3 (a) Extreme (dotdashed lines), inter-quartile (grey) and median (bold line) of DART simulated reflectance values, obtained after varying each parameter in turn keeping all other parameters fixed at their reference values (one at a time sensitivity analysis (OAT-SA)) (see Table 2). (b) Dynamics of the sensitivity indices computed for the OAT-SA over the 450-920 nm wavelength range.

More subtly, C_{xc} and N also affected the VIS, while N impact the entire region by increasing the amplitude of the spectra, C_{xc} produced variations only in the vicinity of 525 nm. C_m and C_w made a negligible contribution to variations in the visible, with the former affecting intensely the NIR and the latter producing no variations at all.

5. Conclusions

Our study demonstrates the feasibility of using 3D radiative transfer modeling to simulate airborne hyperspectral data acquired over high diversity tropical forest areas. We performed simulations of the spectral response of tree species with small

RMSD (≤ 1.8%), using a simplified geometrical crown filled with turbid media characterized by leaves and branches optical properties. The highest disagreements between experimental and simulated data were found at the NIR, which was influenced mainly by canopy structural DART parameters.

Acknowledgements

This work was supported by the São Paulo Research Foundation (FAPESP) grant no. 2013/11.589-5.

References

Féret, J.B., François, C., Asner, G. P., Gitelson, A. A., Martin, R. E., Bidel, L. P., Ustin, S.L., Marie, G., & Jacquemoud, S. (2008). PROSPECT-4 and 5: Advances in the leaf optical properties model separating photosynthetic pigments. Remote Sensing of Environment, 112, 3030-3043.

Ferreira, M. P., Zortea, M., Zanotta, D. C., Shimabukuro, Y. E., & de Souza Filho, C. R. (2016). Mapping tree species in tropical seasonal semi-deciduous forests with hyperspectral and multispectral data. Remote Sensing of Environment, 179, 66-78.

Gastellu-Etchegorry, J-P, et al., (2015). Discrete Anisotropic Radiative Transfer (DART 5) for modeling airborne and satellite spectroradiometer and LIDAR acquisitions of natural and urban landscapes. Remote Sensing, 7, 1667-1701.

Single tree detection with weak canopy shape constraints

Ruedi Boesch, Mauro Marty
Swiss Federal Institute for Forest, Snow and Landscape Research WSL, Birmensdorf, Switzerland-
(ruedi.boesch, mauro.marty)@wsl.ch

Keywords: tree, detection, shape, gradient

Abstract:

Deriving object features like single trees from point cloud data is crucial to understand the structure and function of forest ecosystems. The recognition process of single trees is still a challenge due to different forest types, varying acquisition conditions and often difficult terrain conditions.

Nowadays acquisition campaigns using airborne laser scanning or aerial images allow to derive georeferenced point clouds with high spatial resolution and nearly uniform point density, even over large areas.

Due to established uniform point density we propose a raster-based method to derive single trees from point cloud data with minimized spatial constraints for tree crowns.

Initially a candidate of a single tree crown is found at a local height maximum. Starting from this candidate location, 8 compass directions (separated by 45 degrees) are investigated, if the height gradient values conform to a tree crown shape.

The vast number of tree species at different growing seasons requires to be very restrictive concerning shape assumptions in point cloud data. Therefore the single gradient values can be varying, either convex or concave, but must be positive. Gradients are positive if the height is constantly decreasing in one of the 8 compass directions starting from the center location.

Due to filtering or matching errors during point cloud generation and varying acquisition problems, digital surface models of point clouds are not as smooth as expected or simply contain data generation errors. Therefore the strict gradient criteria for the 8 directions must be relaxed. Following one of the 8 compass directions, the gradient must be positive, but can be interrupted by small local maxima. Small local maxima are represented by a short sequence of negative gradients. Search directions with positive gradients can therefore be interrupted by negative gradients and still be classified as valid tree crown direction. This relaxed shape constraint in one dimension must be fulfilled by all search directions.

The proposed method will be evaluated with the available data from the NEWFOR-benchmark, published by Eysn, Hollaus et al.,Forests 2015, 6, 1721-1747; doi:10.3390/f6051721.

Study on Removal of Atmospheric Effect on Normalized Difference Vegetation Index

Authors: Haitao Lv[1], and Yong Wang[1,2,3]*

[1]School of Resources and Environment, University of Electronic and Science Technology of China (UESTC)
2006 Xiyuan Avenue, West Hi-tech Zone, Chengdu, Sichuan 611731, China
[2]Department of Geography, Planning, and Environment, East Carolina University
Greenville, NC 27858, USA
[3]Institute of Remote Sensing Big Data, Big Data Research Center of UESTC
2006 Xiyuan Avenue, West Hi-tech Zone, Chengdu, Sichuan 611731, China
[*]Corresponding author, wangy@ecu.edu

Keywords: Empirical analysis; Radiative transfer model; atmosphere effect removal.

Abstract:

The normalized difference vegetation index (NDVI) is a popular and widely-used indicator in the land application using visible and NIR data. Unfortunately, the presence of atmosphere (especially clouds) affects red and NIR reflectance. With the increasing of atmospheric optical thickness, NDVI values are obtained in lower panels. An empirical and radiative transfer algorithm is developed to remove atmosphere effect on NDVI. We first assume that under the atmosphere-free condition, the top-of-atmosphere reflectance values from ground targets between any two visible bands have a linear relationship. The relationship is independent from different terrain types. We then assume that the influences on any two visible bands caused by the atmosphere are linearly related. Finally, under the cloud-cover water pixels, the reflectance values of a visible band caused by atmosphere are linear related to the reflectance values of a near infrared band (NIR). After validating the assumptions and solving six unknown parameters, the NDVI values after removal of atmospheric effect are obtained. The effectiveness of the algorithm has been evaluated in forest areas using the Landsat 8 data. In comparison with the data before and after the algorithm, the effect of atmosphere on NDVI disappears visually. The values of mean increases. The increase of the mean values is further supported by the rightward shift of the histogram curve for NDVI. Overall, the removal of atmosphere effect on NDVI was quantitatively and quantitatively satisfactory.

Synergism of SAR and optical data for land use mapping in the Amazonia transition landscape

João Arthur Pompeu Pavanelli[1], João Roberto dos Santos[1], Lênio Soares Galvão[1], Maristela Ramalho Xaud[2], Haron Abrahim Magalhães Xaud[2]*

[1]National Institute for Space Research - INPE, Astronautas Av., 1758, São José dos Campos, São Paulo, Brazil
[2]Brazilian Agricultural Research Corporation - EMBRAPA, BR-174, Boa Vista, Roraima, Brazil
**Corresponding author: joao.pompeu@inpe.br*

Keywords: Random Forest, Land use, SAR data, Savannah, Tropical forest

Abstract

The aim of this study was to analyse the integration of OLI/Landsat-8 optical and PALSAR/ALOS-2 images to characterize the landscape of ecological tension between forest and savannah in northern Brazilian Amazonia using the Random Forest classifier. Landsat-8/OLI surface reflectance and ALOS-2/PALSAR-2 HH and HV amplitude were tested for classification purposes. In addition, NDVI and EVI were calculated from OLI data, and GLCM metrics were determined from PALSAR-2 images for both HH and HV polarizations. Five polarization PALSAR-2 indices were also extracted. Random Forest was calibrated for optimal "ntree" and "mtry" parameters. Results showed an overall classification accuracy of 82.41% and a Kappa of 0.8. The synergistic use of OLI and PALSAR-2 data improved the classification of a great number of classes (17) in the study area.

Introduction

Land use and land cover mapping in tropical landscapes are key components for management, conservation and better understanding on the anthropogenic impacts over natural ecosystems. However, the complexity of these fragmented landscapes due to the transition between vegetation physiognomies (savannahs and forests), forming a mosaic of land use for agriculture and/or pasture often, affects their characterization using optical remote sensing data (LU *et al.*, 2007). In addition, persistent cloud cover creates difficulties for obtaining cloud-free optical data over the region.

In this sense, the synergistic use of optical and SAR satellite data is relevant because it generally improves the quality of land use/land cover maps (LAURIN *et al.*, 2013). The objective of this study was to analyse the integration of Operational Land Imager (OLI)/Landsat-8 and Phased Array type L-band Synthetic Aperture Radar (PALSAR)/ALOS-2 images to map landscapes of ecological tension between forests and savannah in northern Amazonia, in Brazil, using the Random Forest (RF) classifier.

Methodology

The study area is located in the Roraima state, in northern Brazilian Amazon (Figure 1). The region is characterized by the contact of tropical forests and savannah physiognomies, including also classes of anthropogenic land uses such as smallholder's activities and large-scale commodity-driven agriculture. These classes form a complex landscape from a remote sensing perspective. The forest and savannah domains are separated by the Mucajaí River, composing an ecological tension zone.

Seventeen classes were defined during fieldwork and tested for RF classification: (1) agriculture; (2) waterbodies; (3) *campinarana*; (4) wooded savannah; (5) savannah grassland; (6) shrub savannah; (7) initial secondary succession (SS1); (8) intermediate

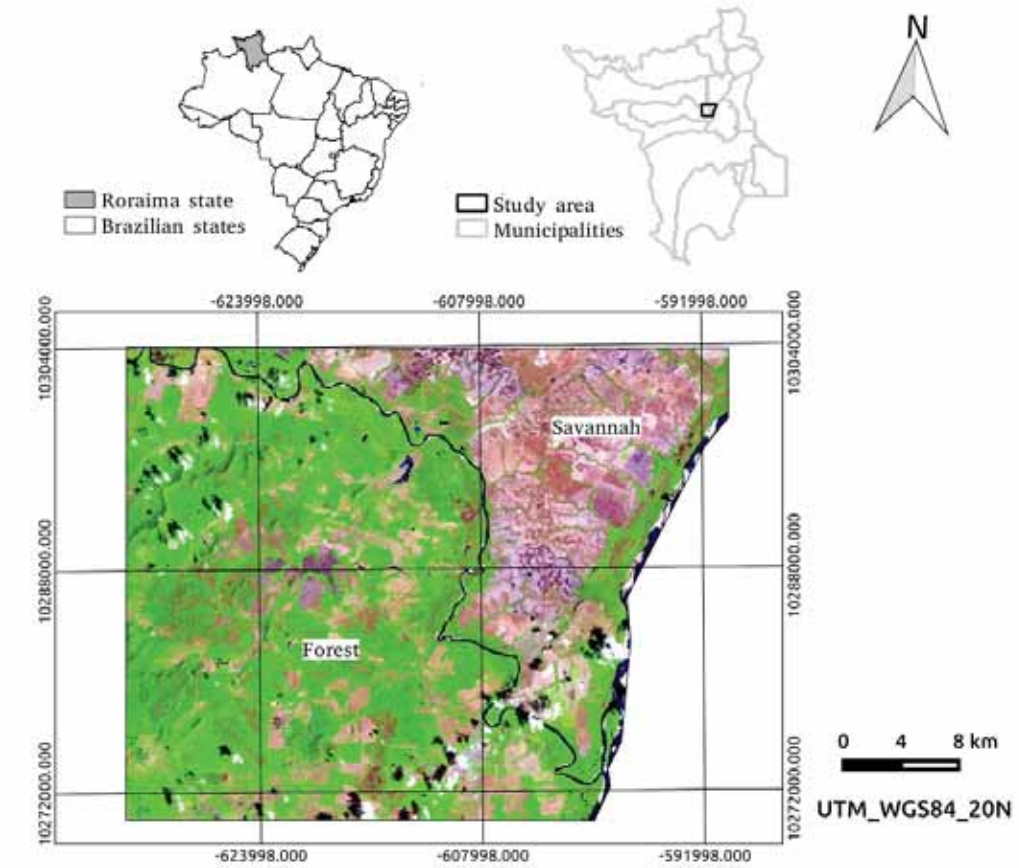

Figure 1. Location of study area highlighting the transition between tropical forests and savannah physiognomies, separated by the Mucajaí River.

secondary succession (SS2); (9) burned savannah; (10) woodland savannah; (11) mature forest; (12) clean pasture; (13) overgrown (dirty) pasture; (14) silviculture; (15) clear-cut silviculture; (16) bare soil; and (17) palm swamps.

Landsat-8/OLI CDR surface reflectance data (30 metres of spatial resolution) and PALSAR-2/ALOS dual (HH+HV), level 1.5, CEOS format (10 metres of spatial resolution) were used for classification. From the OLI dataset, the Normalized Difference Vegetation Index (NDVI) and the Enhanced Vegetation Index (EVI) were generated. The PALSAR-2 image was filtered for speckle using a 3 x 3 Lee filter. After that, Grey Level Co-occurrence Matrix (GLCM) textures metrics were extracted from each HH and HV polarization image. We also calculated five polarizations indices: HH+HV, HH-HV, HH/HV, HV/HH and a SAR Index = (HH*HV)/(HH+HV) (Lu et al., 2013). In total, we tested 35 attributes for RF classification: 8 optical reflectance-derived attributes and 27 SAR amplitude-derived metrics. All the images were co-registered using an ortho-rectified OLI image subsequently resampled to 10 meters.

The thematic classification was performed using the data mining RF algorithm. In order to improve classification accuracy, a previous calibration step was required to define the parameters "ntree" (number of trees in the forest) and "mtry" (number of variables at each split node) (MILLARD and RICHARDSON 2015). By default, the "ntree" parameter is 500 trees and "mtry" is the square root of the number of input variables, in this case 6.

RF was processed by combining the "ntree" and "mtry" in order to obtain the lowest classification error, starting with "ntree" = 100 and "mtry" =1, and changing "ntree" from 100, 200, 300... 1000 and mtry from 1 to 35. The set of combined attributes with the minimum error was used for land use mapping.

Validation of the classification results was assessed using a separate set of samples supported by ground-truth information.

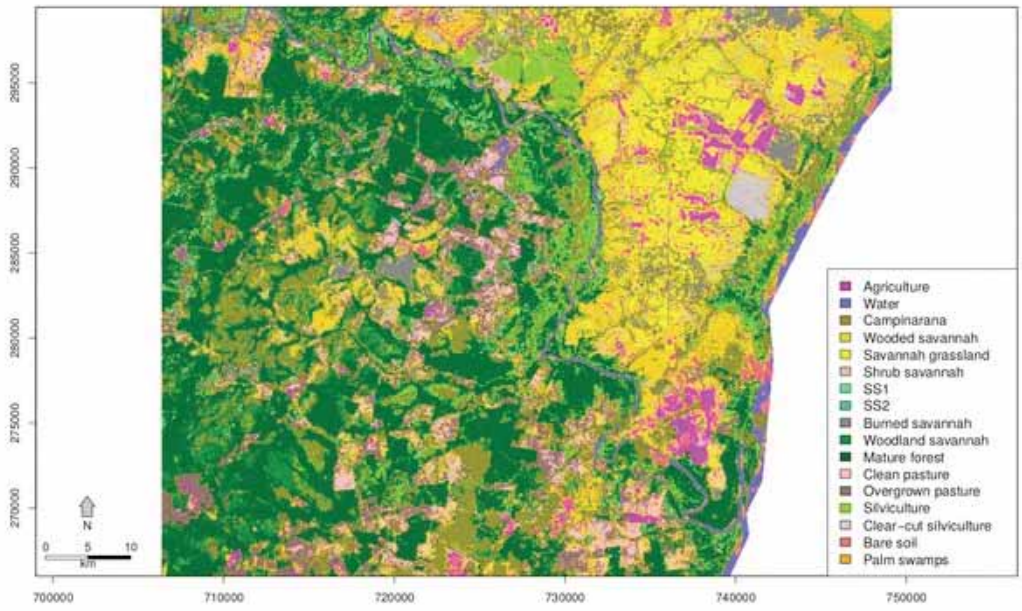

Figure 2. Land use/land cover map derived from the Random Forest classification using the hybrid set of PALSAR-2 and OLI attributes.

Results

The hybrid PALSAR-2 and OLI classification (Figure 2) produced an overall accuracy of 82.41% and a Kappa of 0.8, which is a good result due to the large number and complexity of the classes.

The parameters "ntree" and "mtry" that produced the lowest error in the RF calibration were 900 trees and 11 variables at each split node, respectively. This result highlights the importance of the previous step of RF calibration to find the optimal parameters for land use classification. The most important RF variables, according to the mean decrease in accuracy of the variables, were the reflectance of band 5, followed by the EVI. For PALSAR-2, the most important attributes were the GLCM metrics of contrast for the HV and HH polarizations, respectively.

Conclusions

The synergistic use of OLI and PALSAR-2 attributes improved the classification of a complex transition landscape, formed by a large number of classes (17). The most important optical attributes for RF classification were the reflectance of band 5 and the EVI, whereas the most important SAR metric was the GLCM contrast for the HV and HH polarizations.

References

LAURIN, G. V.; LIESENBERG, V.; CHEN, Q.; GUERRIERO, L.; FRATE, F. D.; BARTOLINI, A.; COOMES, D.; WILEBORE, B.; LINDSELL, J.; VALENTINI, R. Optical and sar sensor synergies for forest and land cover mapping in a tropicals ite in west africa. **International Journal of Applied Earth Observation and Geoinformation,** v. 21, p. 7–16, 2013.

LU, D.; BATISTELLA, M.; MORAN, E. Land-cover classification in the Brazilian Amazon with the integration of Landsat ETM+ and RADARSAT data. **International Journal of Remote Sensing,** v. 28, p. 5447–5459, 2007.

LU, D.; LI, G.; MORAN, E.; DUTRA, L.; BATISTELLA, M. A comparison of multisensor integration methods for land cover classification in the Brazilian Amazon. **GIScience & Remote Sensing,** Taylor & Francis, v. 48, n. 3, p. 345–370, 2013.

MILLARD, K.; RICHARDSON, M. On the importance of training data sample selection in random forest image classification: A case study in peatland ecosystem mapping. **Remote Sensing,** v. 7, n. 7, p. 8489–8515, 2015.

Tandem-L Global Observation of forests with Two L-Band SAR Satellites - Tandem-L

Andreas Huth[1], Rico Fischer[1], Friedrich Bohn[1], Nikolai Knapp[1], Sebastian Lehmann[1], Sebastian Paulick[1], Edna Roedig[1], Peter Biber[2], Kostas Papathanassiou[3]

[1] Helmholtz Centre of Environmental Research – UFZ, Leipzig, Germany
[2] Technical University of Munich, Chair of Forest Growth and Yield Science, Germany
[3] German Aerosopace Center (DLR), Microwaves and Radar Institute, Germany

Tandem-L is a proposal for a highly innovative L-band SAR satellite mission for the global observation of dynamic processes on the Earth's surface with hitherto unparalleled quality and resolution (10 m). Main mission goals are the global measurement of 3-D forest structure and biomass for a better understanding of ecosystem dynamics and the carbon cycle, and high-resolution measurement of variations in soil moisture close to the surface. In addition the satellite mission can be used for systematic recording of deformations of the Earth's surface for earthquake research (with millimeter accuracy) and quantification of glacier movements and melting processes. For this mission different bio/geo-physical information products have been developed and evaluated based on a larger number of field campaigns in the HGF Alliance "Remote Sensing and Earth System Dynamics" (EDA) .

The presentation will give an overview on the Tandem-L project and main results of the field campaigns concerning forest structure and biomass. Based on the German forest inventory (including 9000 forest plots, 4 km grid) and remote sensing data (L-Band Radar, Lidar) we calculated two indices describing the vertical and horizontal structure of forests (16 classes). Forests in Germany feature a low heterogeneity in vertical structure and a high diversity concerning horizontal structures. Classification by remote sensing can be compared to ground-based classifications. For 89 % (57 %) of the forest plots the correct vertical (horizontal) structure type could be predicted by remote sensing. In addition, we show that height-biomass relationships for forests can be improved by including forest structure indices.

Temporal Albedo Dynamics in Boreal Forest Fire Scars Using Higher Resolution Albedo Products from Landsat and Sentinel 2A

Angela M. Erb [1], Zhan Li[1], Yan Liu[1], Yanmin Shuai[1], Qingsong Sun[1], Crystal B. Schaaf [1], Zhuosen Wang [2], Ian Paynter[1]

[1] School for the Environment, University of Massachusetts Boston, Boston, MA, USA
[2] NASA Postdoctoral Program Fellow, Goddard Space Flight Center, Greenbelt, MD, USA

Keywords: Albedo, Landsat, Sentinel-2, Boreal

The Landsat Albedo Product provides higher resolution albedo values by coupling 30m Landsat surface reflectances with concurrent 500m Bidirectional Reflectance Distribution Functions (BRDF) Products from the Moderate Resolution Imaging Spectroradiometer (MODIS) (Shuai et al., 2011, 2014, Wang et al 2015). This approach has been extended to generate a 20-m resolution albedo product from Sentinel-2A MultiSpectral Instrument (MSI) reflectance bands with configurations similar to Landsat sensors. In addition, the 12-bit radiometric fidelity of both the Sentinel-2A and Landsat-8 satellites allows for the inclusion of high-quality, unsaturated surface reflectance and albedo calculations over snow covered surfaces. The validation of these products over spatially representative tower sites has shown the albedo values from both Landsat-8 OLI and Sentinel-2A MSI agree well with the ground measurements, with snow and snow-free RMSEs for OLI of 0.0426 (n=28) and 0.0191 (n=89) respectively (Wang et al., 2015) and a snow-free RMSE of 0.004 (n=4) for MSI (Schaaf et al., 2016). MSI snow albedo is under assessment and will be presented at ForestSAT 2016. The increased temporal resolution provided by multiple instruments allows a better understanding of albedo dynamics in historically difficult imaging locations.

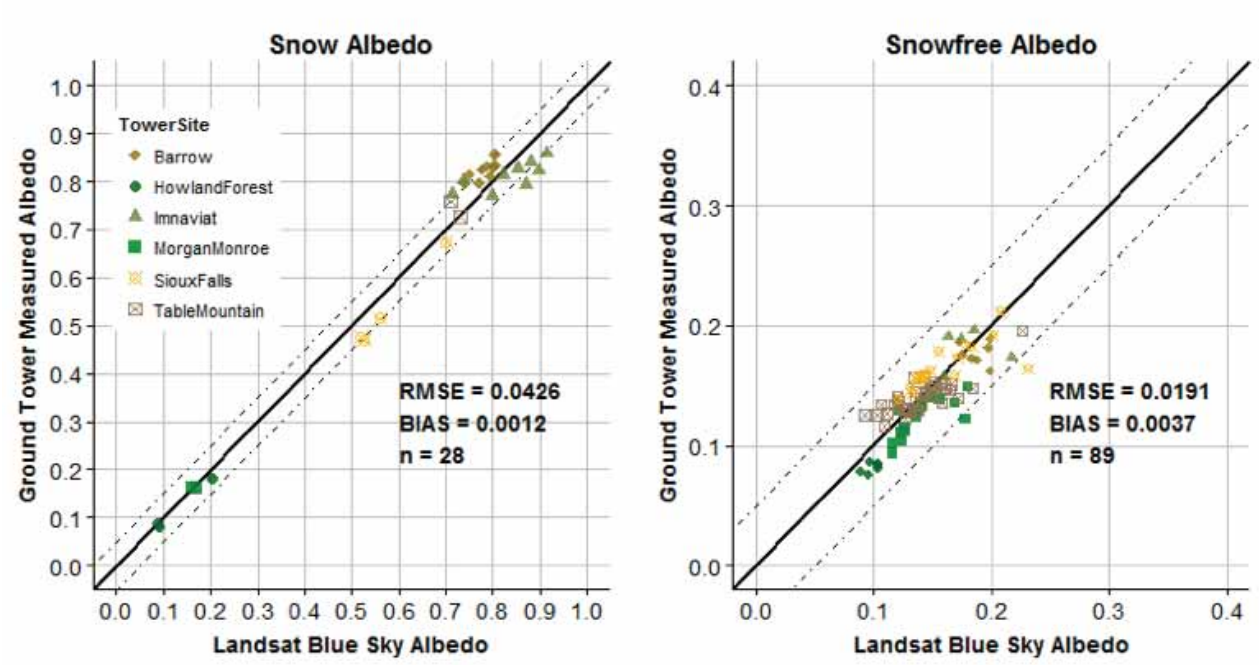

Figure 1: Validation of the Landsat-8 Blue Sky Albedo Product at six tower sites in North America. The overall RMSE for the combined product is 0.0267

North American boreal forest fires have increased in both frequency and severity over the past four decades. This trend is expected to continue as surface temperatures continue to rise and fire season lengthens. As such, understanding both the immediate and long term effects of these fires on radiative forcing and the carbon budget will become increasingly more important. We focus this investigation on the seasonal variation within several recent boreal forest fires scars in Alaska and central Canada. We examine the impact of landscape heterogeneity and fire severity on the albedo in the growing and dormant seasons and quantify the effects of over story canopy loss and changes in snow exposure on radiative forcing. Recent work on early spring albedo of fire scars has illustrated that both burn severity and early spring albedo show significant post-fire spatial heterogeneity at the landscape scale and highlights the need for a continued high temporal and spatial resolution data record. This synergistic approach, combining multiple data sources to create a more comprehensive data record of land surface albedo, will enhance our understanding and projection of the carbon cycling and radiative forcing of these spatially heterogeneous and temporally dynamic ecosystems under a changing climate.

References

Schaaf, C.B., Li, Z., Liu, Y., Wang, Z., Erb, A.M., Sun, Q., Shuai, Y., Paynter, I.L. (2016). The Use of Higher Resolution Albedo Product from Landsat and Sentinel 2A to assess Landscape Heterogeneity and Temporal Albedo Dynamics. International Living Planet Symposium.

Shuai, Y., Masek, J. G., Gao, F., & Schaaf, C. B. (2011). An algorithm for the retrieval of 30-m snow-free albedo from Landsat surface reflectance and MODIS BRDF. *Remote Sensing of Environment*, *115*(9), 2204–2216. http://doi.org/10.1016/j.rse.2011.04.019

Shuai, Y., Masek, J. G., Gao, F., Schaaf, C. B., & He, T. (2014). An approach for the long-term 30-m land surface snow-free albedo retrieval from historic Landsat surface reflectance and MODIS-based a priori anisotropy knowledge. *Remote Sensing of Environment*, *152*, 467–479. http://doi.org/10.1016/j.rse.2014.07.009

Román, M. O., Schaaf, C. B., Lewis, P., Gao, F., Anderson, G. P., Privette, J. L., ... Barnsley, M. (2010). Assessing the coupling between surface albedo derived from MODIS and the fraction of diffuse skylight over spatially-characterized landscapes. *Remote Sensing of Environment*, *114*(4), 738–760.

Wang, Z., Erb, A.M., Schaaf C.B., Sun, Q., Liu, Y., Yang, Y., Roman, M.O., Shuai, Y., Casey

K. (2015). Early spring post-fire snow albedo dynamics in high latitude boreal forests using Landsat-8 OLI data. *Remote Sensing on Environment.* In press.

Terrestrial LiDAR and 3D Reconstruction Models for Estimation of Large Individual Tree Biomass in Tropics

Alvaro Lau Sarmiento[1,3], Jose Gonzalez de Tanago[1,3], Harm Bartholomeus[1], Martin Herold[1], Pasi Raumonen[2], Valerio Avitabile[1], Christopher Martius[3], Rosa Goodman[4] and Solichin Manuri[5]*

[1]Laboratory of Geo-Information Science and Remote Sensing, Wageningen University, Wageningen, the Netherlands
[2]Tampere University of Technology, Tampere, Finland
[3]Center for International Forestry Research – CIFOR, Bogor, Indonesia
[4]Yale School of Forestry and Environment Studies, New Haven, United States of America
[5]Fenner School of Environment and Society, The Australian National University, Canberra, Australia
[*]Email correspondent author: alvaro.lausarmiento@wur.nl

Key words: terrestrial laser scanning, 3D Reconstruction Models, quantitative structure models, aboveground biomass, large trees, tropical forest

Abstract:

Tropical forest biomass is a crucial component on the estimation of carbon emissions in context of REDD+. However, calibration and validation of such estimates requires accurate and effective methods for in-situ estimation of above ground biomass – AGB. The most common method uses allometric equation to indirectly estimate AGB from tree parameters as diameter, species and height. This approach has been reported as major source of uncertainty in tropical large trees. On the other hand, terrestrial LiDAR (Light Detection and Ranging) has demonstrated to be more accurate to infer forest AGB in a non-destructive and more direct approach. This method has been applied and validated in an open Eucalyptus in Australia. Nevertheless, application on tropical forest trees still has its challenges, mostly due to occlusion, tree structural complexity and large scale application. We propose a method to estimate AGB from individual tropical trees by estimating tree volume from terrestrial LiDAR point clouds.

Nine plots of 30 x 40 m were scanned with a Riegl VZ-400 terrestrial laser scanner – TLS following a spatial grid covering three study sites (Peru, Indonesia and Guyana). We identified the largest tree per plot, extracted its point cloud and calculated tree wood volume by modelling 3D tree architecture using quantitative structure models (TLS-QSM method). To validate our method, we harvested the scanned trees, took detailed measurements of stems and all branches up to 10cm and reconstructed tree volume as well. Then, tree wood volume was converted to AGB using species-specific wood density values. To compare TLS estimates with present methods, we estimated AGB using

The Global Ecosystems Dynamics Investigation: Current Status

Spaceborne lidar has been identified as a key technology by the international ecosystem science community because it enables accurate estimates of canopy structure and biomass and forms the basis for fusion approaches with existing and planned missions, such as the NASA's ICESat2, ECOSTRESS and OCO_3 missions, and extends the capabilities of radar missions such as the NASA-ISRO SAR, Tandem-X and the ESA BIOMASS missions. The Global Ecosystems Dynamics Investigation (GEDI) is a space-based lidar instrument scheduled for launch in late 2018. From its vantage point on the International Space Station, GEDI will provide high-resolution observations of forest vertical. These data will be used to address three core science questions: What is the aboveground carbon balance of the land surface? What role will the land surface play in mitigating atmospheric CO_2 in the coming decades? How does ecosystem structure affect habitat quality and biodiversity? GEDI informs these science questions by making billions of lidar waveform observations per year. These canopy measurements are then used to estimate biomass and in fusion with radar and other remote sensing data to quantify changes in biomass resulting from disturbance and recovery. GEDI further marries ecosystem structure from lidar with ecosystem and habitat modeling to evaluate the impact of changes in land use and climate on carbon sequestration and biodiversity. In this talk we present an overview of the GEDI mission and its current implementation status. We first review its major science objectives and planned data sets. We then summarize GEDI algorithms and our approach to calibration and validation. Lastly, we provide the status of the instrument hardware build, as well as expected technical performance details.

The Potential of Multitemporal and Polarimetric Features Derived From Sentinel-1 Data for Forest Parameters Retrieval

Ziolkowski Dariusz[1], Hoscilo Agata[1], Lewandowska Aneta[1], Sterenczak Krzysztof[2]

[1]Institute of Geodesy and Cartography, [2]Forest Research Institute

Keywords: Sentinel-1, Above_ground biomass, multitemporal analysis, polarimetry

The aim of the study is to show potential of multitemporal and polarimetric analysis of Sentinel-1 data for forest parameters retrieval within various forests of temperate zone. The C-band SAR data are not commonly used for forest parameters retrieval, especially for biomass studies, due to the saturation effect of backscattering coefficient even for low biomass values. The launch of Sentinel-1 data with 12-day's temporal resolution gives the possibility for new methodological approaches to overcome this problem, especially using multitemporal analysis of the data.

The research was carried out on two study areas in Poland: Supraśl and Pieńsk. There are various types of forests on both test sites: deciduous, mixed and coniferous, each of them located on fresh and wet habitats. Two sets of ground truth data were used: data from Forest Digital Maps which offers many forest parameters determined for forest plots and field measurements for 500 sample plots of 25m radius for each study area. For each of them many various forest parameters were available i.e. tree height, DBH (diameter at breast height), stock volume, AGB (Above-ground biomass), density and species. Meteorological data were also collected for the whole period.

The set of 30 dual-polarization (VV and VH) successive Sentinel-1 images acquired in 2015 were used. The data were co-registered, calibrated and then divided into two sets of images (trees with leaves and without leaves). Then each of sets of images was filtered separately using multitemporal filters. Then various temporal statistics were generated for both sets of the data. Independently polarimetric processing of the data was also performed.

The change of backscattering coefficient during the whole season and its correlation with forest parameters (AGB, tree height and DBH) were analyzed for the all sample plots together and also separately for the particular forest types. The analysis was performed in conjunction with the variability of meteorological conditions. Next spatial variability of temporal statistics for individual pixels and its relation with forest parameters were studied. The results of temporal analysis were compared with spatial and temporal behavior of polarimetric signatures.

First results show that the correlation of backscattering coefficient with forest parameters is changing a lot during the year. They are in accordance with variation of hydrothermal index. The best correlation of VH polarization with stem volume was observed at the beginning of October 2015 during the very dry conditions. The character and strength of the correlation is different for particular forest types, what can be seen in the best way in the case of coniferous forests located on fresh and wet habitats. Both of them are characterized by the strongest correlations with backscattering coefficient but the second one is negative. Great spatial variation of multi-temporal features even within the same forest types suggests big heterogeneity of forests which is confirmed by spatial and temporal variability of scattering mechanisms derived from H/A/Alpha decomposition. Both methods have great potential for improvements of the results.

Towards an "all-in-one sensor" for forestry applications – estimating forest density, species composition and biomass from stereo WorldView-2 data

Fabian Ewald Fassnacht[1], Daniel Mangold[1], Jannika Schäfer[1], Hooman Latifi[2]

[1] Institute of Geography and Geoecology, Karlsruhe Institute of Technology (KIT), Kaiserstraße 12, 76131 Karlsruhe, Germany
[2] University of Wuerzburg, Department of Remote Sensing in Cooperation with German Aerospace Center, Oswald-Kuelpe-Weg 86, 97074 Wuerzburg, Germany.

Keywords: WorldView-2, photogrammetric height information, very high resolution data, biomass, forest density, tree species.

Over the last years, efforts were made to estimate forest inventory attributes from airborne LiDAR, multispectral and hyperspectral data. Although, airborne data were found to be suitable for many applications they are still commonly regarded as being expensive compared to the cost of satellite products. Since recently, the application of stereo pairs of very high-resolution multispectral sensors (VHRMS) such as WorldView-2 has been discussed as an alternative to spatially estimate forest inventory parameters. The VHRMS enable the simultaneous collection of spectral and structural information via stereo photogrammetric approaches.

In this study, we used VHRMS data to spatially estimate forest biomass with an approach that imitates the field measured biomass estimations. In a first step, the three key-parameters of forest type (tree species), forest density (stem count per ha) and height (as a proxy for DBH) were estimated from a pair of WorldView-2 images acquired in 2013 over a temperate central European forest in Germany. In the second step, the obtained parameters served as an input to a regression model of aboveground forest biomass. Corresponding field data were collected in three surveys during the period between 2013 and 2015.

Preliminary results of Random Forest models and few predictor variables representing spectral, textural and structural information resulted in moderate to good estimates of forest density (r^2 = 0.68) . Classification of forest types using Support Vector Machines led to high accuracies, including kappa > 0.95 when considering only four classes (broadleaved, coniferous, shadow and soil) and kappa = 0.77 when considering 7 tree species. The subsequent estimation of aboveground forest biomass using forest type, density and additional height information derived from a photogrammetric point cloud returned reasonable results (r^2 = 0.58 obtained with Random Forest). The wall-to-wall predictions (Figs. 1 + 2) agreed well with the expected

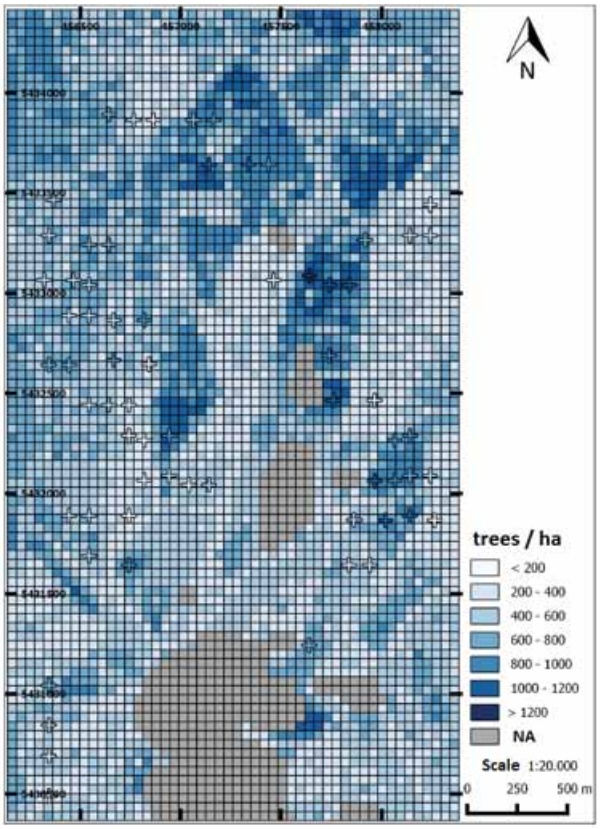

Fig 1: Forest density map.

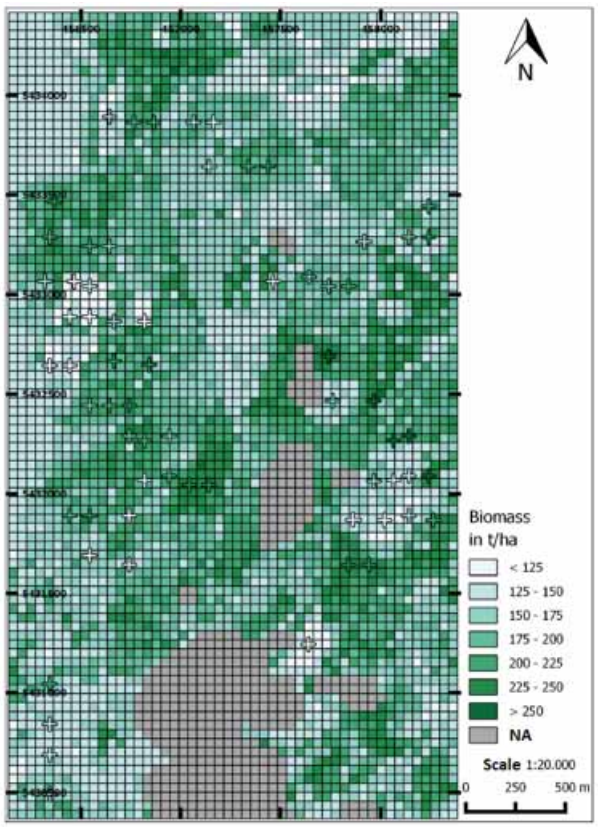

Fig 2: Biomass estimated for the study area.

spatial distributions of stand densities and biomass within the study area.

Further refinements of the described methodology by integrating pre-knowledge on the relationships amongst forest density, forest type and height in the biomass models are foreseen. In addition, variables describing the average crown diameters of the reference areas will be integrated to further improve the biomass models.

Our preliminary results suggest VHRMS data as viable alternatives to airborne data to obtain useful estimations of forest inventory parameters. Further investigations, including more diverse forest scenarios and varying sensor settings are required to draw more consistent conclusions on the suitability of the presented approach.

Tropical forest degradation monitoring: Radiometric issues of using both Landsat 8 and Sentinel 2 in one time series

Manuela Hirschmugl, Mathias Schardt, Roland Perko
Joanneum Research Forschungsgesellschaft mbH
8010 Graz, Austria
manuela.hirschmugl@joanneum.at

Viktoria Schell, Carina Sobe
Graz University of Technology
Graz, Austria

Keywords: forest monitoring, remote sensing, geometric and radiometric adjustment

Abstract

For continuous monitoring of forest disturbance and re-growth dynamics with high temporal and spatial resolution, a dense time series of data is needed. Sentinel-2 and Landsat8 are the sensors, which are currently delivering optical data globally and free of charge. This study investigates, how data from both sensors can be integrated in a time series analysis for forest degradation monitoring in tropical areas in Malawi and Peru. Geometric inconsistencies exist and need to be eliminated before considering a time series classification approach. The differences could be removed by an automated image matching procedure. Radiometric differences in the raw data are reduced by using surface reflectance products (Landsat8) and Sen2Cor results (for Sentinel-2). The still remaining differences, mainly in the NIR and SWIR band, could be corrected by relative radiometric adjustment. First analysis of time series data show, that the magnitude of these remaining differences is much smaller than the magnitude of forest changes. Therefore, data from both sensors can be jointly used in a time series classification.

Introduction

The aim of the EOMonDis project is to develop a system which allows spatial-explicit, wall-to-wall, continuous monitoring of forest disturbance and re-growth dynamics with high temporal and spatial resolution. In order to do so, a dense time series is needed, which can only be achieved by employing multiple sensors in tropical conditions with frequent cloud cover. Although Sentinel 2 will – once the 2B satellite is in orbit too – deliver images every 5 days, there are still some limitations. First, in order to monitor changes, the natural variations need to be understood and these variations can only be observed in the past, where Sentinel data had not yet been available. Further, even with a high revisit rate such as the one from Sentinel 2, there is still the matter of cloud cover, which may be reduced by more frequent images taken from different sensors. Therefore, the objective of this study is to integrate Landsat 8 and Sentinel 2 data in one time series data stack for follow-up joint processing. The issues are investigated in two testsites: Malawi and Peru.

Methods

Geometric adjustment

While in some areas and test sites, the geometric accuracy between Landsat 8 and Sentinel 2 orthorectified images is already sufficiently high, others still show significant geometric shifts, which have to be corrected before moving on to investigating radiometric issues. In order to correct geometric differences, a multi-modal matching technique was used. The developed fully automatic image matching procedure [1] using the mutual information method (based on [2]) leads to

improved geometric congruence between the two data sets. The specific matching strategy proposed for this project starts with a pre-processing step that upscales the Landsat data to the reference Sentinel – 2 data. Next, the histograms of the filtered images are compressed using a quantile processing. A lower and upper threshold representing a given quantile of the data distribution (e.g. 1% and 99%) are calculated and used to compress the histogram to a given number of values. This technique helps the following up matching procedure as the joint histograms are then better populated and thus a larger number of correct matches are found. A compression to 64 bins yields best results. The areal matching paradigm is based on mutual-information maximization. The main idea is that the joint entropy of two image patches is minimized, when the patches are correctly aligned. Therefore, a maximization of the MI measure corresponds to a maximization of clusters in the joint entropy and to a minimization of the joint entropy's dispersion. To get normalized similarity measurements the entropy correlation coefficient is used, which maps the normalized mutual-information to the domain [0,1],

$$ECC(X,Y) = 2 - \frac{2H(X,Y)}{H(X) + H(Y)} \quad (1)$$

with H(X) and H(Y) being the individual entropies and H(X,Y) the joint entropy of image patches X and Y (cf. [2]). In contradiction to e.g. the normalized cross-correlation (NCC) method, which is just invariant to linear mappings between the values of the images to be matched, the MI method can also handle non-linear dependencies. In our tests best results are achieved with 151x151 pixel windows for MI calculation. A sub-pixel measurement is achieved by fitting a polynomial using the 3x3 neighborhood of the entropy's correlation peak and analytical calculation of its maxima. Since, a rigid transformation between the two datasets is assumed, it is sufficient to match points on a regular grid (dense image matching would be an overkill for this application). Using these vectors, a rigid transformation is estimated by solving an over- determined equation system in the least-squares sense. The parameters of the estimated transformation are then used to register the Landsat data to the reference Sentinel - 2 data. In the last step of the adjustment, a resampling from 30 to 10m resolution is performed.

Radiometric evaluation

Radiometric differences need to be investigated, as the gray level differences between intact and degraded forests can be very small. For Landsat 8, the surface reflectance product [3] has been used, processed before July, 1st, 2016, i.e. there are still some artifacts in the resulting images, which are mainly problematic in the blue band, which has not been used in the current analysis. For Sentinel 2, both the raw data as well as the result of the Sen2Cor atmospheric correction [4] are analyzed. For the radiometric analysis, reference areas, which have not been visibly changed between the image acquisition dates, were selected from VHR data and Landsat / Sentinel images for both test sites. For the three classes: water, bare soil and pine plantations (Malawi) and natural forest (Peru), areas were selected and mean values obtained from two Sentinel images and one Landsat image. Different statistical values were calculates such as: Coefficient of correlation, mean absolute difference and difference in percent of the variation of each land cover class. These values were calculated both for the comparison between the two Sentinel images as well as between Sentinel and Landsat. Relative radiometric adjustment was applied in order to see, if the remaining differences can be reduced. The regression coefficients for the relative radiometric adjustment are calculated within areas which define so-called pseudo-invariant features (PIFs). The program uses an automated process where PIFs are derived by utilizing a correlation coefficient within a certain window size. This allows to use images with remaining cloud areas without an effect on the radiometric adjustment.

Finally, for the Peru test site, a time series involving both Sentinel and Landsat images was build. Several intact forest areas are compared to degradation areas during the same time period in order to analyze the magnitude of difference between the sensors in comparison to the magnitude of the change to be detected.

Results

Geometric adjustment results

The automatic geometric adjustment worked very well in both test sites. Fig. 1 shows the Sentinal-2 image on the left and the Landsat image on the right side for the Peru test site. In the top comparison, a clear north-south shift is visible, which could successfully be corrected by our automatic adjustment procedure (bottom).

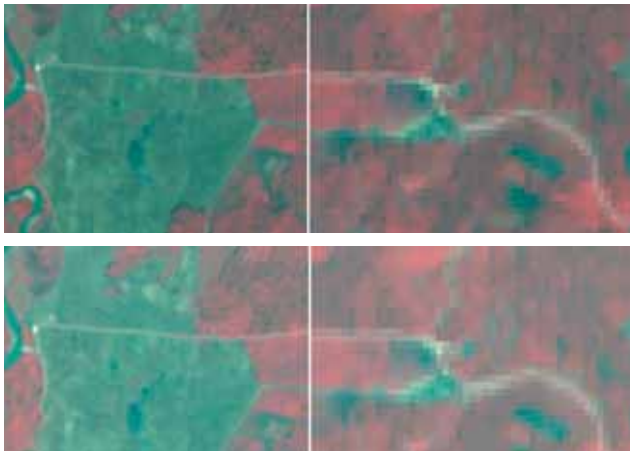

Fig. 1. top: Geometric shift between Sentinel (left) and Landsat 8, bottom: Landsat image adjusted to Sentinel 2 geometry

Radiometric evaluation results - Malawi

For the three classes: water, bare soil and pine plantations, areas were selected and mean values obtained from two Sentinel images (26.12.2015 and 05.01.2016) and one Landsat 8 image (12.11.2015). The results show that the raw Sentinel 2 data sets are already radiometrically stable. For the shorter wavelengths, the difference is higher due to atmospheric influences than for the longer wavelengths (R^2 = 0.83 in blue band vs. 0.93 in the NIR band). After atmospheric correction with Sen2Cor, the R^2 value changed only marginally. Comparing the two Sentinel images, the mean of absolute differences for all selected areas is higher in the raw data (blue band: 1152; NIR band: 1871) compared to the Sen2Cor result (blue band: 477; NIR band: 285). Despite the differences in band width, the compliance between Sentinel 2 Sen2Cor result of 2015 to the Landsat8 data showed an R^2 of 0.97 for the NIR band and 0.73 for the blue band. The mean of absolute difference for all selected areas is 344 (blue) and 423 (NIR).

In order to get a better evaluation of the magnitude of these values, we calculated the variance for each class (water, bare soil and pine plantations) solely in the Sentinel reference scene from 05.01.2016 (Table I – second column). This variance is defined as the difference between the maximum and the minimum mean value per polygon for each land cover class in the reference data set. It shows that bare soil has the highest variance in all bands, followed by water areas and pine plantation. This is logical, as plantations tend to be very homogeneous. In the next step, the difference values per polygon between the Sentinel (Ref) and the Landsat8 respectively Sentinel (In) were calculated. Next, each of these difference values is expressed in percent of its land cover's variance. Some polygons show a high difference, some a low one. This led to the values shown in Table I - columns three and four. The table reads: the difference between the same water areas in Landsat8 image and Sentinel reference image in the red band shows between 5 and 88% of the difference within all water areas in the Sentinel reference scene alone. As long as the values are below 100% it means that involving an additional image would not add to the variance of the land cover class. Considering this, it can be seen that for the two Sentinel images, the values remain below 100, while for Landsat, the differences are higher. In case of the pine plantations, the differences are about 20 % higher, for bare soil, it is similar in red and SWIR, but higher in the NIR band. The difference in water areas in the NIR and SWIR bands are extremely high. One reason for these larger differences may be found in the different time of data acquisition, as the Landsat image and the Sentinel reference image are almost two months apart.

TABLE I. DIFFERENCES PER LAND COVER BETWEEN SENTINEL & SENTINEL AS WELL AS LANDSAT & SENTINEL FOR MALAWI

Band	Variance per LC (Sentinel reference image only)	Difference as % of Variance	
		Sentinel (In) (26.12.2015)– **Sentinel** (Ref) (05.01.2016)	**Landsat** (12.11.2015) – **Sentinel** (Ref) (05.01.2016)
RED	Water: 877	2 – 64 %	5 – 88 %
	Bare soil: 1929	2 – 62 %	10 – 51 %
	Pines: 179	29 – 87 %	19 – 113 %
NIR	Water: 225	5 - 80 %	246 – 390 %
	Bare soil: 1621	10 – 63 %	16 - 116 %
	Pines: 2105	1 – 84 %	2 – 102 %
SWIR	Water: 260	6 – 33 %	188 – 282 %
	Bare soil: 3399	15 – 39 %	9 - 44 %
	Pines: 774	13 – 80 %	31 – 107 %

Radiometric evaluation results - Peru

In the Peru testsite, also two Sentinel 2 scenes and one Landsat 8 scene were used for the radiometric comparison. Sentinel data were acquired on 11.12.2015 and on 10.01.2016. The Landsat 8 scene was acquired on 06.12.2015. Thus the time difference between Landsat and Sentinel is only six days. The differences in percentage of the variance per land cover are shown in Table II (same calculation method as for Table I). The values indicate that the time difference between the image acquisitions is as

important as the sensor. Also there is a difference in the different bands: while the red band of Landsat and Sentinel corresponds very well, the NIR band is worse. The SWIR bands show similar difference values for Landsat-Sentinel as for Sentinel-Sentinel. After application of relative radiometric calibration, the values change in different band differently. While the red band becomes worse, especially in forest areas, the NIR values are improved. Based on this statistics, no definite recommendation on the improvement by relative radiometric adjustment can be given.

TABLE II. DIFFERENCES PER LAND COVER BETWEEN SENTINEL & SENTINEL; LANDSAT & SENTINEL AND LANDSAT CALIBRATED & SENTINEL FOR PERU

Band	Variance per LC (Sentinel reference image only)	Difference as % of Variance		
		Sentinel (In) (10.01.2016)– **Sentinel** (Ref) (11.12.2015)	**Landsat** (06.12.2015) – **Sentinel** (Ref) (11.12.2015)	**Landsat calib** (06.12.2015) – **Sentinel** (Ref) (11.12.2015)
RED	Water: 86	184– 265%	9 – 120 %	9 – 117 %
	Bare soil: 735	15 – 82 %	5 – 58 %	93 – 147 %
	Forest: 21	31 – 197 %	5 – 57 %	303 – 363 %
NIR	Water: 39	382 - 489 %	370 – 581 %	431 – 730 %
	Bare soil: 1060	36 – 90 %	68 - 121 %	42 - 93 %
	Forest: 544	3 – 34 %	29 – 115 %	3 – 56 %
SWIR	Water: 159	73 – 145 %	19 – 140 %	7 – 44 %
	Bare soil: 1329	46 – 96 %	35 - 92 %	52 -115 %
	Forest: 222	5 – 37 %	5 – 66 %	2 – 46 %

Time series results

In order to apply the values in a time series, a first attempt was performed in the Peru test site for intact forests and changed areas. Normalized difference infrared index 7 (NDII7) was calculated for all images and printed in a timeline. The time series consists of five Sentinel 2 images (22.10.2015, 11.12.2015; 10.01.2016; 10.03.2016; 18.06.2016) and three Landsat scenes (06.12.2015; 15.06.2016; 01.07.2016). The timeline without additional relative radiometric adjustment for the Landsat scenes is plotted in Fig.2. It can be seen, that the values of the Landsat image show clear differences from the Sentinel time series, but the magnitude of the difference is smaller than the magnitude of the change. Fig. 3 shows the same timeline with the calibrated Landsat images. The timeline is much smother, the sharp turns mostly gone or at least smaller in magnitude. From this first analysis it appears that classification from a combined time series is possible to detect degradation features in forest areas, because the spectral difference in a change area is of a much larger magnitude than the difference by the sensors. It also shows that relative radiometric adjustment improves the continuity of the data in the time series. This will be even more important, if the degradation features are not as clear as in Peru, where degradation is basically small patches of deforestation (smaller than the minimum mapping unit for deforestation and therefore considered as degradation). In other tropical areas, other degradation patterns such as selective logging occur. They are more difficult to detect. In such cases, a consistent time series is a prerequisite. In general, integration of more scenes and testing in other areas has yet to be applied to draw a final conclusion.

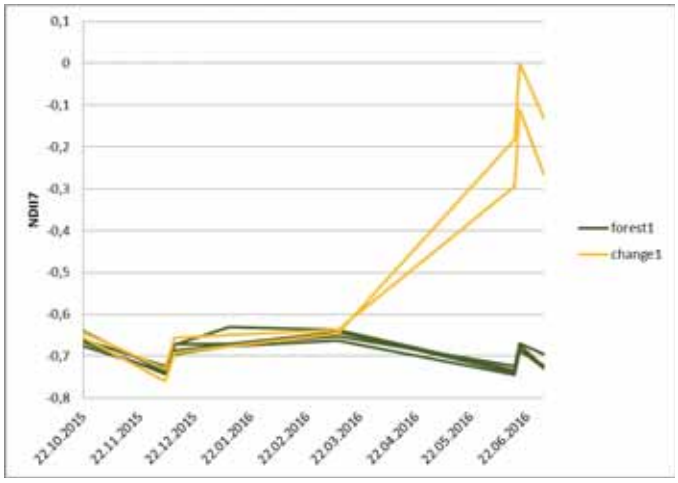

Fig. 2. Forest and changed areas in a combined Landsat – Sentinel timeseries

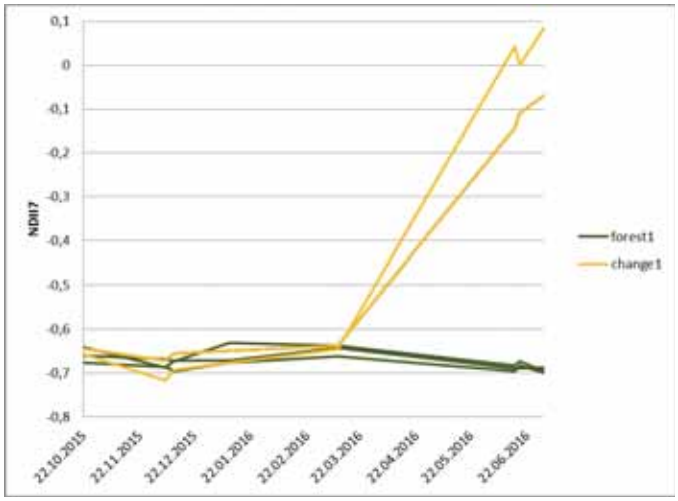

Fig. 3. Forest and changed areas in a combined Landsat – Sentinel timeseries with additional radiometric calibration of Landsat images

Conclusion and Outlook

In a preliminary conclusion, the combination of Landsat8 surface reflectance product and the Sentinel-2 Sen2Cor result in one time series is possible. Remaining differences can be reduced by application of relative radiometric adjustment. Further work to be done consists of improved cloud elimination, as the existing cloud masks from Sentinel-2 and also Landsat 8 still do not cover all cloud areas. These remaining cloud areas need to be classified through the time series classification, as manual delineation is too tedious and too expensive for the large amounts of images to be processed. Further, a temporal filtering approach to fill the cloud gaps is already available and needs to be applied before finally moving on to classification of the change areas. This classification will be done in a trajectory fitting approach [5].

Acknowledgment

This project has received funding from the European Union's Horizon 2020 research and innovation programme under grant agreement No 685761 (Project EOMonDis).

References

[1] R. Perko, H. Raggam, K. Gutjahr, and M. Schardt. Using worldwide available TerraSAR-X data to calibrate the geo-location accuracy of optical sensors. In *IEEE International Geoscience and Remote Sensing Symposium Proceedings*, pages 2551–2554, Vancouver, Canada, 2011.

[2] J.P.W. Pluim, J.B.A. Maintz, and M.A. Viergever. Mutual information based registration of medical images: A survey. *IEEE Transactions on Medical Imaging*, pages 986–1004, 2003.

[3] Department of the Interior U.S. Geological Survey. *PRODUCT GUIDE: PROVISIONAL LANDSAT 8 SURFACE REFLECTANCE CODE (LASRC) PRODUCT*, version 3.2 edition, 2016.

[4] Uwe Mueller-Wilm. *Sentinel-2 MSI - Level-2A Prototype Processor Installation and User Manual*, 2016.

[5] Manuela Hirschmugl, Martin Steinegger, Heinz Gallaun, and Mathias Schardt. Mapping Forest Degradation due to Selective Logging by Means of Time Series Analysis: Case Studies in Central Africa. *Remote*, 6 (1)(ISSN 2072-4292):756–775, 2014.

POSTER

Tropical forest height and structure estimation from AfriSAR campaign PolInSAR data in Gabon

Marco Lavalle[1], Ralph Dubayah[2] and Lola Fatoymbo[3]

[1] Jet Propulsion Laboratory, California Institute of Technology
[2] University of Maryland
[3] Goddard Space Flight Center

Keywords: Tropical forests, vertical structure, PolInSAR algorithms, radar tomography

Aim

The goal of this contribution is to present our first results of canopy height and vertical structure estimation from polarimetric-interferometric radar (PolInSAR) data collected in Gabon during the February 2016 AfriSAR campaign. The AfriSAR campaign was a joint effort between NASA and the European Space Agency (ESA) to acquire airborne and field data over African tropical forests in support to forthcoming spaceborne missions, including NISAR, GEDI and BIOMASS. NASA acquired 39.6 flight hours of data with the JPL's L-band UAVSAR radar instrument and 32.4 flight hours of data with the LVIS lidar instrument over 5 different sites in Gabon for calibration, validation, and new algorithm demonstration of various ecosystem science products.

Materials

Here we focus on the UAVSAR dataset of 9 PolInSAR images (~20 km x 40 km, 0.6m x 1.8 m level-1 resolution) acquired over the northern part of the Lope National Park in Central Gabon to demonstrate extraction of canopy height and vertical structure. The gradient of forest biomass from the forest-savanna boundary (< 100 Mg/ha) to dense undisturbed humid tropical forests (> 400 Mg/ha) makes Lope an ideal site for PolInSAR algorithm assessment. The UAVSAR dataset is fully polarimetric and has been acquired by incrementing the aircraft altitude by 20 m at each flight track in order to acquire data from different look angles and resolve vertical structure. Several LVIS lidar flights have been also conducted contemporary to UAVSAR to retrieve canopy height and structure. Field data are available from previous field campaigns as well as from the current the 2016 campaign.

Methods

We apply model-based PolInSAR technique (Cloude and Papathanassiou, 1998) and polarization coherence tomography (PCT) technique (Cloude, 2006) to extract canopy and vertical structure of tropical forests from UAVSAR data. In PolInSAR, wave polarization (e.g, HH, HV, VV or arbitrary combinations of these channels) is used to identify distinct structural components of the forest (understory, stem, foliage, etc.) and interferometry is used to locate the vegetation component along the vertical direction – thus providing a measurement of 3D vegetation structure. PolInSAR models such as the RVoG or RMoG models (Lavalle and Khun, 2014; Lavalle and Hensley, 2015) allow for direct estimation of canopy height. PCT technique, instead, assumes arbitrary vertical structure with enhanced flexibility in parameter retrieval at the expenses of data processing.

Results

We will show maps of canopy height and vertical structure estimated via PolInSAR and PCT techniques from multi-baseline UAVSAR data. Error on the radar-derived canopy height is expected to be ~15-25% and will be accurately assessed against LVIS lidar-derived canopy height. Radar-derived vertical structure and lidar-derived vertical structure will be compared to assess the relative differences as well as explore complementarity that may lead to new radar-lidar fusion algorithms. Field data will be also considered for assessing the quality of the

radar-derived structural parameters, as well as to convert maps of radar-derived structural parameters to above-ground biomass.

Cloude, S.R., "Polarization Coherence Tomography" (2006), *Radio Science*, 41, RS4017.

Cloude, S. R., and Papathanassiou, K. P. (1998). "Polarimetric SAR Interferometry". *Geoscience and Remote Sensing, IEEE Transactions on*, 36(5), 1551-1565.

Lavalle, M., and Hensley, S. (2015), "Extraction of structural and dynamic properties of forests from polarimetric-interferometric SAR data affected by temporal decorrelation," *IEEE Transactions on Geoscience and Remote Sensing*, vol.53, no.9, pp.4752-4767.

Lavalle, M., and Khun, K. (2014), "Three-baseline InSAR Estimation of Forest Height," *Geoscience and Remote Sensing Letters, IEEE*, vol. 11, no. 10, pp. 1737–1741.

Two Phase Assessment System for the Effective Monitoring of Tropical Forests

Mathias Schardt, Forschungsgesellschaft Joanneum Research, Austria

Based on increasing demands for information on forests new methods for effective forest inventories in tropical countries are to be developed in order to save costs and / or to increase accuracies. Research in this field has been very dynamic in recent years producing a wealth of new ideas and approaches including state-of-the-art technologies such as remote sensing, mapping as well as inventory designs. The challenge, particularly in the context of tropical and sub-tropical countries is how to make such comprehensive assessments most cost-effective while achieving desired international standards.

Behind this background a pilot project was initiated by the Austrian Natural Resources Management and International Cooperation Agency (ANRICA) and the Surinamese Foundation for Forest Management and Production Control (SBB) aiming at the development of an effective forest inventory system. The proposed approach is based on two main concepts: a) comprehensive statistical sampling methodologies (to dramatically reduce costs by meeting high international accuracy standards at the same time) and a two phase approach by combining aerial and terrestrial data. The cost reduction is achieved by substantially reducing field work due to a reduced number of field plots to be measured.

The remote sensing phase was composed by CIR aerial photos and 3D canopy models derived from photogrammetry. Additionally a LiDAR campaign will be carried out in autumn this year in order to derive tree heights and digital terrain models. Aerial based acquisition of remote sensing data in countries without any local facilities for data acquisition is very cost intensive since a special airplane needs to be transferred to the country which causes high additional costs. To overcome this problem Joanneum Research has developed the mapping system ADAM-C (airborne data acquisition and mapping for Cessna) that can be mounted on the wing strut of any Cessna 182 and 206 and, therefore can be operated worldwide. The system consists of a Phase One Camera (80MP), Riegl Laserscanner 580, IMU (inertial measuring unit) and a GPS system receiver. The terrestrial phase of the inventory system comprises of terrestrial sampling, whereas the sampling intensity was set up based upon the national accuracy requirements for the data collected on timber stocks and Above Ground Biomass (generally set at no less than 5% accuracy). That's why for the pilot project, primarily data on these two parameters was collected. The terrestrial phase was carried out by measuring field plots according to good forest inventory standards for terrestrial field inventory defined by the FAO.

The proposed two phase sampling approach uses parameters extracted from photogrammetric models to be correlated to with AGB and timber volume, thus helping to reduce the number of plots which need to be measured in the field.The key challenge for this investigation was to find the most suitable parameters that can be extracted from the aerial imagery. As a source for this investigation the following basic data sets were used:

- CIR ortho image mosaic (20 cm resolution)
- DSM from multiple stereo images (20 cm resolution)
- SRTM terrain estimation
- In future also LiDAR data

Overall the tested parameters can be grouped in the following way:

- Vegetation indices, Texture parameters, Forest canopy density, Volume of DSM – DTM difference, Number of trees, Size of the crowns by segmentation, Statistical features based on nDSM

Mathematical models combining airborne and field data on above ground biomass were established and statistical data analysis has shown that the number of highly expensive ground plots can be substantially reduced and, thus, costs of forest inventories decreased.

The presentation will concentrate on the methods for the remote sensing based assessment of the forest parameters described above, the correlation of these parameters with terrestrial AGB assessments (from terrestrial plot sampling) and on the selection of the best performing parameters.

UAV-Borne and Airborne Remote Sensing for Tree Disease Symptom Detection

Magdalena Smigaj[1], Rachel Gaulton[1], Stuart L. Barr[1], Juan C. Suarez[2]

[1] School of Civil Engineering and Geosciences, Newcastle University, Newcastle upon Tyne, NE1 7RU, UK
Contact: m.smigaj@ncl.ac.uk
[2] Forest Research, Northern Research Station, Roslin, Midlothian, EH25 9SY, UK

Keywords: stress detection, unmanned aerial vehicle, UAV, thermal, hyperspectral

Abstract

Climate change has a major influence on forest health by indirectly affecting the distribution and abundance of pathogens, as well as the severity of tree diseases. Changing weather conditions may also result in the introduction of non-native invasive pest species. The detection and robust monitoring of affected forest stands is therefore crucial for allowing management interventions to reduce the spread of infections.

Stress induced by an invasion of insects or onset of disease manifests itself in tree foliage, and may result in a variety of changes to plant's physiological processes. When a plant is under stress, stomatal closure occurs to help reduce water losses and prevent the entry of microbes and host tissue colonisation. This mechanism can cause an increase in leaf and canopy temperature.

Nevertheless, there has been limited research into the use of thermal remote sensing for tree health monitoring as required high spatial resolution data is usually obtained with low temporal frequency. Newly emerging technologies, such as unmanned aerial vehicles (UAVs), could supplement aerial data acquisition, but sensor development is still in the early stages. This project investigates the use of airborne and UAV-borne sensors for detection of disease symptoms, in particular low-cost UAV-borne microbolometer thermal system for monitoring disease-induced canopy temperature rise.

The research is based in Queen Elizabeth Forest Park, Scotland, where research plots were established in pine stands, exhibiting various stages of stress. Extensive structural measurements of sample trees were collected, including visual estimation of red band needle blight infection level. Infection level was expressed as percentage of total unsuppressed crown volume in 10% steps, where a score of 20 indicates that 20% of crown was diseased. To compliment this, a number of needle samples were collected for leaf spectral reflectance measurements. These measurements accompany airborne hyperspectral, thermal and LiDAR data, as well as a thermal UAV-borne imagery collected in 2014.

Initially, calibration of the microbolometer camera was performed in laboratory, revealing non-uniformity across the imagery, which was minimised using a two-point calibration technique. Further laboratory trials involved altering the camera's temperature throughout imaging. These indicated that the imager maintains stable radiometric calibration across different temperatures, unless exposed to very rapid changes (> 0.2 K/min).

The derived calibration parameters were applied to test datasets of UAV-borne imagery. These were georeferenced by registration to a LiDAR-derived canopy height model. At canopy level, the comparison of tree crown temperature recorded by the thermal camera suggests a small temperature increase related to disease progression; indicating that UAV-borne cameras might be able to detect sub-degree temperature differences induced by disease onset. The influence of acquisition timing on the signal was tested with repeated flights over the survey plot during summer 2015 at different times of the day.

This paper will present results of UAV-borne thermal imaging for detection of disease-induced canopy temperature increase, as well as preliminary analysis of the acquired airborne data.

Updating of lidar based forest attribute maps using digital photogrammetry combined with the lidar data

H. Olsson[1], N. Lindgren[1], J. Bohlin[1], J. Jonzen[1], I. Bohlin[1], E., Willén[2], M. Nilsson[1]

[1]Department of Forest Resource Management, Swedish University of Agricultural Sciences, Umeå, Sweden, firstname.lastname@slu.se
[2]Skogforsk, Uppsala, Sweden, firstname.lastname@skogforsk.se

Keywords: lidar, laser scanning, digital photogrammetry, forest attribute maps, updating

Abstract

The Swedish national land survey (Lantmäteriet) has scanned all of Sweden with airborne lidar. Based on these data, the Swedish University of Agricultural Sciences (SLU) and the Swedish Forest Agency, has made nationwide forest attribute maps, which are freely available over internet. These prediction maps were made using the area based method and regression functions with national forest inventory plot data as response variables (Nilsson *et al.*, 2016). In addition, most large forest companies in Sweden have made similar lidar based prediction maps from the same national lidar data, but using their own reference plots and ancillary information from their existing forest maps. The existence of the national lidar data has changed the practice in the forest sector, since essential variables such as stem volume, basal area, mean stem diameter and Lorey's mean height, can be automatically predicted with at least as good accuracy as traditional methods based on field work and air photo interpretation. The national lidar scanning did however start year 2009 and most forest areas were scanned during the years 2010 – 2012. There is no decision yet to repeat the national lidar scanning, but Lantmäteriet has an ambitious air photo program. Point clouds from digital photogrammetry provides good height estimates, but compared to lidar, less good estimates of the canopy density (Bohlin *et al.* 2016). Hence, for example volume and basal area are estimated less accurately.

In this presentation, we will therefore present the results from a study were lidar data from 2010 and 2011 is combined with point clouds from digital air photos acquired year 2015. Among the evaluated methods are the use the old lidar metrics in combination with the height difference obtained when new photogrammetry data is added. The test area is 1 million ha area 100 km north Stockholm. The estimations will be trained with national forest inventory plot data from 2015 and the validation will be done for 100 stands which are field surveyed with 8 – 10 plots per stand. The products will be produced in two versions: using only commonly available data which corresponds to a possible future nationwide product; and using also company specific information, which corresponds to possible future products to be used internally in the forest companies.

References

Bohling, J., Bohlin, I., Jonzén, J., Nilsson, M. 2016. National forest attribute map using stereophotogrammetry of aerial images, the national terrain model and data from the national forest inventory. Submitted.

Nilsson, M., Nordkvist, K., Jonzen, J., Lindgren, N., Axensten, P., Wallerman, J., Egberth, M., Larsson, S., Nilsson, L., Eriksson, J., Olsson, H. 2016. A nationwide forest attribute map of Sweden using airborne laser scanning data and field data from the national forest inventory. Submitted.

Use of Hybrid Model-Based Inference with a Sample of Lidar Measurements to Produce Gridded Biomass Estimates

Paul L. Patterson, Sean P. Healey, Göran Ståhl, Sören Holm, Steen Magnussen, Ralph O. Dubayah, Steven Hancock, Hans-Erik Andersen*

**Speaker: United States Forest Service, Statistician*

Keywords: Space-based Lidar, Hybrid, Model-based Inference, Biomass

The forthcoming NASA GEDI (Global Ecosystem Dynamics Investigation) mission will install a full-waveform lidar instrument on the International Space Station for the purpose of measuring global forest structure. The resulting waveform data is expected to be strongly correlated with aboveground forest biomass, and one of the mission's primary science products will be a 1-km gridded biomass product. Grid cell-level estimates must be accompanied by formally estimated precision. Waveforms will be collected in spatially discontinuous "footprints" that will sample, instead of census, each 1-km cell. Biomass will be modeled at each footprint using relationships derived from sets of co-located field and lidar measurements. GEDI's spatially discontinuous measurements, combined with the fact that biomass will be modeled instead of measured at each footprint, argues for methods based upon a hybrid of design- and model-based inference.

Hybrid estimators (*sensu* Ståhl *et al.*, 2016) have been employed in large-area estimation problems, but their performance at the scale of 1-km grid cells has not been thoroughly demonstrated. Two activities are under way to assess such estimators for use with GEDI waveforms. First, a simulation-based study is investigating the general relationship between estimator performance and variables such as the size of an estimation unit and spatial autocorrelation of model residual error. Second, an empirical study is assessing proposed estimators using GEDI waveforms simulated from small-footprint airborne lidar data collected in six diverse sites in the United States. This latter study addresses GEDI-specific concerns such as density of instrument overpasses and strength of the footprint-level biomass relationship. Relevance of these studies extends to estimation of biomass across irregularly shaped areas (e.g. watersheds or countries), as well as to other sensors that collect high-quality but spatially discontinuous forest structure information.

Use of partial-coverage UAV data as a sampling tool for large scale forest inventories

Stefano Puliti, Terje Gobakken, Liviu Theodor Ene, and Erik Næsset*
Department of Ecology and Natural Resource Management, Norwegian University of Life Sciences, P. O. Box 5003, NO-1432 Ås, Norway,
Stefano.puliti@nmbu.no, terje.gobakken@nmbu.no, liviu.ene@nmbu.no, erik.naesset@nmbu.no.

Keywords: Unmanned aerial vehicle; Structure-from-Motion; partial-coverage; hybrid; large-scale forest inventory.

Abstract

Use of image based three dimensional data from unmanned aerial vehicles (UAV) has proven effective for forest inventories; however limitations in the range of operations of UAV hinder their use in large scale applications. Use of partial-coverage UAV data may increase precision of purely field based estimates of forest resource parameters and offer a cost-effective alternative to wall-to-wall acquisition. In this study, data from UAV collected in systematically distributed blocks and combined with ground observations in a two-phase design with hybrid inference (UAV_{HYB}) were used to estimate mean volume and its standard error (precision) for a 7330 ha forest area of interest (AOI). Hybrid inference (HYB) rests on probabilistic sampling of auxiliary data (the UAV data) and a prediction model calibrated with field data that predicts volume across the areas covered with auxiliary data. In the uncertainty analysis, the sampling variability of the UAV data collection is added to the uncertainty induced by the prediction model. Because the field data need not come from a probability sample, the method offers great flexibility in field data collection while it can benefit from the great value of strongly correlated remotely sensed data to improve precision of estimates. The estimate of precision of UAV_{HYB} was compared with precision of estimates with from alternative inventory, in terms of design (one-phase) and estimators (design-based and model-based). Relative efficiency (RE), calculated as the ratio between the estimated variances of two alternative methods, was used as measure for improvement in precision between two alternative methods. Additionally the study addressed the flexibility of HYB inference by including external ground reference observations. The comparison against a method where a one-phase, design-based estimate based purely on field data revealed that the use of UAV increased the precision of the estimates (RE = 1.2). The alternative sampling design was one-phase sampling and the alternative estimators were design-based (DB) and model-based (MB), respectively. For DB only field-data ($FIELD_{DB}$) was available while for MB also wall-to-wall airborne laser scanning (ALS) data (ALS_{MB}) were acquired. Relative efficiency (RE), calculated as the ratio between the estimated variances of two different methods, was used as measure for improvement in efficiency for one method over the other. Comparison of UAV_{HYB} against $FIELD_{DB}$ revealed that the use of the former four times more efficient than the latter (RE=4.4) when external observations were used. This translates to a need for 4.4 times as many field plots under simple random sampling for a $FIELD_{DB}$ estimate to be equally precise as the UAV_{HYB} estimate. However, when including only observations from the AOI the RE decreased to 1.2, indicating only a slight increase in precision. Also, the comparison against the ALS_{MB} revealed that for the latter the increase in efficiency compared to UAV_{HYB} was limited (RE = 1.6). The study also demonstrated that the precision under UAV_{HYB} can be improved when including additional field data from other inventories, highlighting the flexibility of HYB. Cost estimates for each inventory approach were also compared and discussed, revealing that UAV may be a cost-effective tool for landscape level forest resource assessment.

Using LiDAR remote sensing for identifying suitable habitat. Case: Darwin´s Fox

G. Carrasco[1], R. Briones[2]*

[1]Landscape ecology program, Ecosystemic management division, Bioforest S.A.
[2]Fauna conservation program, Ecosystemic management division, Bioforest S.A.

Keywords: LIDAR, Camera-trap, Lycalopex fulvipes, Caramavida.

Abstract

The range of Nahuelbuta has an outstanding biogeographic importance and high endemism of flora and fauna. In this range, the Valdivian temperate forest extends north along the maritime watershed, while the sclerophyllous forest extends south along the continental slope and northern coastal plain. The L. fulvipes that inhabits this habitat is considered at high extinction risk due to both demographic and ecological factors, such as disease, predation by cougars or other fox species. Our study was conducted in Caramávida using camera traps (N = 84) during October 2011-March 2012 to observe L. fulvipes, this information was correlated with LIDAR data to generate: elevation model, forest height; and the raw data were used to estimate the vertical vegetation coverage for seven different layers of height, cover, leaf area index and vertical complexity index. Our results indicate the presence of 17 positive results with L. fulvipes watch. The presence data and vegetation analyzes indicate correlations with tree cover larger than 20 meters high and with a high diversity of vegetation in the vertical profile , which may propose the presence of sites with potential presence and corridors for this species. We conclude that this methodology can generate highly accurate and relevant vegetation variables that may provide some guidance regarding which are the areas where a species is potentially distributed and the design of corridors that may enrich their habitat.

Introduction

The biogeographic situation of Nahuelbuta Range and its geomorphological and climatic characteristics have given rise to environmental heterogeneity establishing a wide variety of habitats (Mardones 2005, Luebert & Pliscoff 2005). Its peaks higher than 1,200 masl are covered by Araucaria araucana and Nothofagus pumilio forests, as well as wetlands. Both of the areas protected by the State in Nahuelbuta Range, the Nahuelbuta National Park (PNN) and the Contulmo Natural Monument (MNC), besides the protected area Piedra del Águila, are clearly insufficient to preserve this biodiversity, due to their small surface and location in high regions, above 600 masl (Contulmo with 82 ha) and above 1,000 masl (Nahuelbuta with 6,800 ha) (Ibarra-Vidal et al. 2005, Ortiz & Ibarra-Vidal 2005).

Lycalopex fulvipes (Martin, 1837) is an endemic canid of Chile at high extinction risk (Macdonald et al. 2004, Cofré & Marquet 1998). This species was originally considered Vulnerable (Glade 1993) and then as Endangered (MINSEGPRES 2007) and Critically Endangered at global level by UICN (Jiménez et al. 2008). It is included in Appendix II of CITES, being considered as one of the canids with most serious conservation problems (Macdonald & Sillero-Zubiri 2004).

It was considered that its distribution was restricted to the west part of the Great Island of Chiloé and Nahuelbuta National Park located at approximately 600 km from Chiloé Island. This disjoint pattern is now being questioned because of the recent finding of individuals using camera traps in the Alerce Costero National Park, Valdivian Coastal Reserve,

Oncol Park and Chanchan near Valdivia, as well as the presence of a dead specimen in Lastarria, near Gorbea (Farias et al. 2014, D´elía et al. 2013, Vilà et al. 2004, Medel et al. 1990, Jaksic et al. 1990, Jiménez et al. 1990). This evidence leads to the hypothesis that the Darwin fox distribution may be more continuous, associated with the remaining coastal forests.

The biological information about this species is scarce, it is found mainly in studies conducted in Chiloé Island (Jiménez et al. 2008, Jiménez 2007, Jiménez & McMahon 2004, McMahon 2002). On this regard, Yahnke et al. (1996) describe home ranges and they inform a population of 500 individuals for Chiloé (Yahnke et al. 1996). Jiménez & McMahon (2004), based on intensive capture inside the Nahualbuta National Park (PNN), made a population estimate of 78 individuals by extrapolating from a density of 1.14 ind/km2. This estimate is based on captures in the southeast section of the PNN (sectors: Pehuenco, Piedra del Águila and Coimallín). This scenario has become more complex because in general the areas adjacent to the PNN have high degradation and human impact levels (Armesto et al. 2010) turning them unsuitable for the L. fulvipes to have a viable population (Mella 1994, Shaffer 1981).

The species distribution is mathematically or statistically associated with different independent variables that describe the environmental conditions. If it is so, this relationship is extrapolated to the rest of the study area and then a value is derived for each place which is usually construed as the presence probability of the species in that spot. The "presence probability" is, therefore, an abusive interpretation of the environmental similarity measure which should be construed, at the most, as a suitability value for the species to develop. These models use variables and among them the forest variables are widely used; however, they are often estimated categorically.

Using the LIDAR technology (Light Detection and Ranging) and some process algorithms vegetation variables can be generated (e.g. coverage, leaf area index, vertical profile and height) with high precision. Aerial LIDAR is a sensor installed in an airplane that emits pulses while flying and these pulses hit an object (e.g. bare ground, building, stone, vegetation, water). Part of this energy is reflected by the ground or the objects on the surface and this energy is detected by the sensor.

The sensor calculates the distance to the ground or object; and each one of these pulses is stored together with coordinates by means of the differential GPS system and the inertial navigation system installed in the airplane, so that the position of a spot can be determined in three dimensions with high precision (Dubayah & Drake 2000). When these points hit the vegetation, they can be intercepted at different heights and if the pulse density is high (around 4 pulse/m2) the vertical structure of vegetation can be determined very precisely by means of a set of algorithms (Ko 2012, McGaughey 2007, McGaughey 2003).

The purpose of this study is to use a methodology associated with the LIDAR technology in order to generate variables intended to be used in the biodiversity area and applied to endangered species such as L. fulvipes.

Methodology

Study area and data

The study area is located in the Nahuelbuta Range in the central zone of Chile, in the sector called Caramavida, characterized by temperate forest vegetation and the presence of a wide animal diversity. The area is topographically steep and scarped with 900 m mean height above sea level, and the range going from 500 to 1200 m.

In 2010, flights were performed over the area among the activities of a cartographic improvement project of Forestal Arauco and the study area surface is 500 km2. The data were collected using the LIDAR Optech sensor, the scanning angle was ± 15º and the footprint was around 0.5 m. The final pulse density was 3.5 pls/m2. The data were processed by the owner company of the flight producing a high-resolution digital elevation model (1x1m resolution), surface model and orthorectified images (0.5x0.5 m resolution). The raw data were gathered in LAS format including X, Y, Z coordinates and intensity.

Determination of distribution range

To estimate the quantity of stations, the monitoring information of Quebrada Caramávida performed by Forestal Arauco was used (Briones et al. 2011) (Zuñiga 2012), based on which a minimum number

of spots was determined in order to have significant estimates of the parameters being studied (standard error lower than 0.04; see Mackenzie et al. 2005), using the native forest registry (CONAF-CONAMA-BIRF, 1999). Within each coverage, the stations will be randomly distributed at a distance of ≥ 0.3 kilometres to promote spatial independence (based on the home range radius by Jiménez 2007). The proportion of sampling units in each coverage was related with the size of each coverage, and the design was balanced in order to minimize variance in the results, which might occur in a coverage with small surface.

A total of 84 sampling stations were installed being made up by a camera trap. They were deployed in micro-habitat conditions suitable for L. fulvipes, as close as possible to the selected spot, but considering the following restrictions: ≥ 300m from houses, and ≥ 50m from trails and roads. The cameras were installed at 0.5 m high and they remained active during 15 consecutive days in each station. Considering that detection rates could be low for this species, baits will be used to attract them (synthetic urine and jack mackerel). The camera trap study was carried out in spring and summer (from October 2011 to March 2012). Both seasons are critical periods after winter for recovering the energetic demands and reproduction, increasing the carnivore activity (Muñoz-Pedreros et al. 1995, Jaksic et al. 1990, Jiménez et al. 1990). On the other hand, the previous study with cameras conducted between 2009 and 2011 in the study area confirms a higher activity of L. fulvipes in spring-summer, compared to autumn-winter (Zuñiga 2012)(Fig. 1b).

Determination of core patches

With the elevation model (bare land) and the surface model, the crown height model was calculated using the difference between both surfaces (Fisk et al. 2009). After that, the surface with a vegetation height above 4 m was identified, in order to get the core patches in the area; subsequently, the patches with a surface larger than 100 ha. were isolated since these are the areas that may potentially support a sustainable habitat (Santos & Tellería 1998).

Additionally, a model of morphology patterns (Vogt et al. 2007) was used to classify the patches in 7 shape classes in order to determine which patches are actual patches or which participate in other connectivity functions.

Processing raw LIDAR data

The data were processes with the software program FUSION (McGaughey 2007) and the Gridmetrics algorithm. The resolution or cell size for calculation was 20x20 m (container) since at lower resolution the process tends to identify trees and generate gaps in the vegetation coverage and therefore the coverage estimate of the area cannot be determined. The points intercepted at seven height ranges were obtained (0 – 2, 2 – 4, 4 – 8, 8 – 12, 12 – 20, 20 – 32 and >32 m.), which are those used by the national registry of native forest (CONAF-CONAMA-BIRF 1999).

The coverage (Cob) was estimated for each height range as follows:

$$\mathbf{Cob} = \frac{\sum \mathbf{x_{int\ veget}}}{\sum \mathbf{x_{totales}}}$$

$\sum x_{\text{int veget}}$ stands for the pulses intercepted by vegetation and $\sum x_{\text{totales}}$ is the total pulses intercepted in that height range. Based on this, the vegetation coverage for each layer could be estimated. Besides, the total coverage for the entire vertical profile was estimated.

The effective leaf area index (IAF) is calculated with the Beer law equation:

$$\mathbf{IAF} = -\mathbf{ln\ x}\ (\mathbf{1} - \mathbf{Cob})$$

The LIDAR system is classified as an active remote sensing system, that is, it emits its own light source. This characteristic means that vegetation can be illuminated by means of pulses or infrared light beams and comparing the light that is intercepted with the light that reaches the forest ground it is possible to apply the Beer law in order to estimate the area where light was intercepted; and that area is then the effective leaf area.

The vertical complexity index (ICV) is based on diversity measurement indexes that measure the heterogeneity within a specific system (Van Ewijk et al. 2011) in this case, the vertical structure of vegetation.

$$\mathbf{ICV} = (-\sum_{\mathbf{i=1}}^{\mathbf{HB}}[(\mathbf{p_i} * \mathbf{ln}(\mathbf{p_i}))])/\mathbf{ln}\ (\mathbf{HB})$$

Where HB is the total number of pulses in the container and is the pulse ratio in the container at height i.

Statistical analysis

There is a variety of models in order to predict the potential habitat of species; however, a logistic regression model was selected due to the nature of the dependent variable and also because these models can provide a probabilistic prediction of L. fulvipes presence and in this way our analysis with LIDAR can be prioritized. Additionally, unlike most of the multivariate procedures, it does not require variables to be normally distributed. The logistic function is expressed as:

$$\mathbf{P} = \mathbf{e^u}/(\mathbf{1} + \mathbf{e^u})$$

Where P is the estimated probability of occurrence of an event, e is the inverse of the natural logarithm and u is the linear model:

$$\mathbf{u} = \mathbf{b_0} + \mathbf{b_1X_1} + \mathbf{b_2X_2} + \cdots + \mathbf{b_nX_n}$$

Where is the regression coefficients and is the independent variables.

Nine variables based on surfaces were used: understory vegetation coverage, mean, maximum and modal height of vegetation, total coverage, leaf area index, elevation and vertical complexity index. Since there are different scales in the variables, some of them were converted in order to generate a better adjustment ($elev_t$ =elev/1000). A stepwise process was performed to select the variables that generate the best estimate of the L. fulvipes distribution. The statistics used for the selection was the Chi-square test and the correct percentage of model classification.

Results

From the 84 sampling stations consisting of camera traps, 17 had positive results for the L. fulvipes presence (Fig. 1b). A total of seven carnivore species were found during the sampling period: L. fulvipes, Lycalopex culpeus (Molina, 1782), Lycalopex griseus (Gray, 1837), Puma concolor (Linnaeus, 1771), Conepatus chinga (Molina, 1782), Galictis cuja (Molina, 1782). The occupancy values, occupancy corrected for detectability and detectability of L. fulvipes show that the proportion of stations where the species was detected was 11%, but the actual proportion would reach 14% after correcting for detectability.

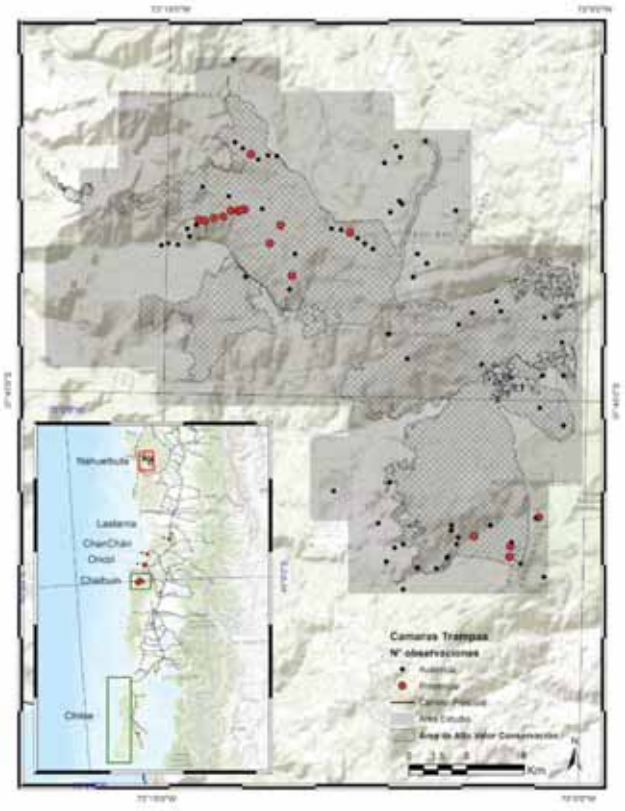

Figure 1: Study area in Caramávida zone located at 30 km from Cañete. The grey zone is the area that has raw LIDAR data and the hatched zone is Caramávida, the area with high conservation value belonging to Forestal Arauco. The points indicate the 84 cameras installed in the study area and those in red are the ones that detected the presence of L. fulvipes.

The stepwise process carried out by means of forward selection, backward elimination and subset selection, gave as a result that the best prediction model includes the following as main variables: modal height, vertical complexity index and elevation (Fig. 2). The chi-square value for the model is 49.60 (Table 2).

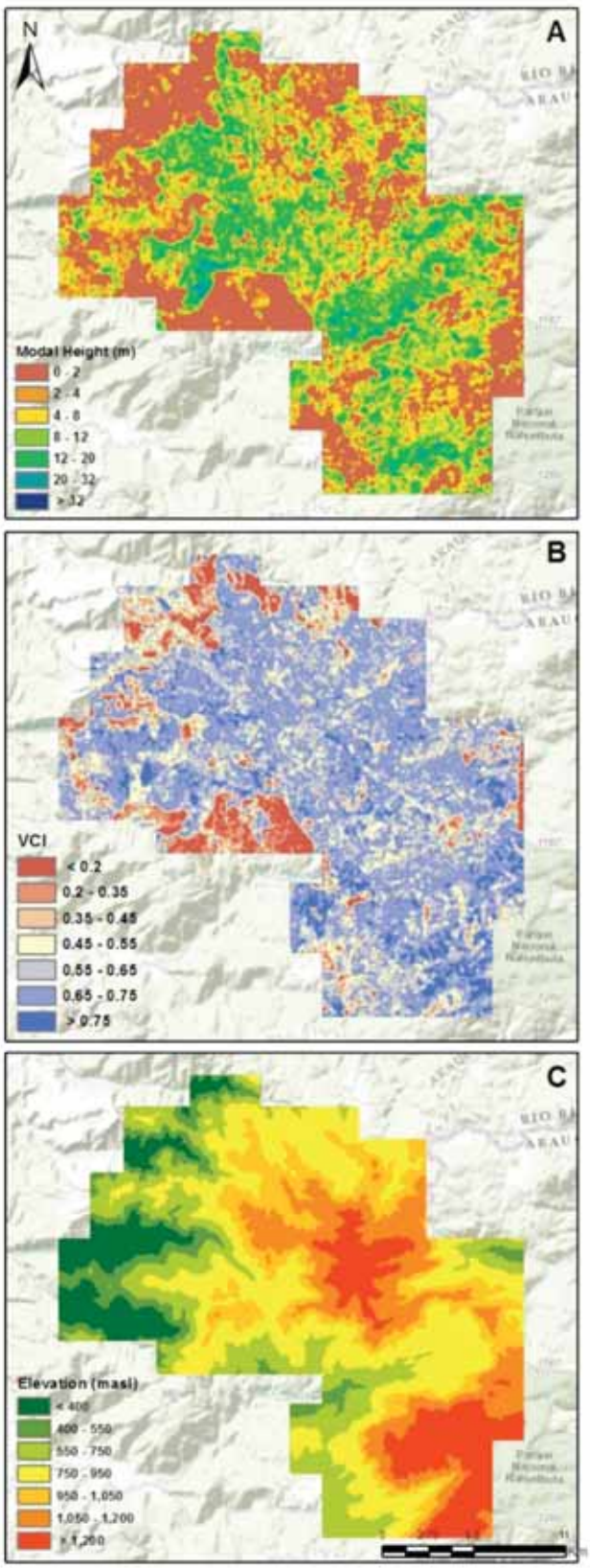

Figure 2: a) Modal height (m) which characterizes the most frequent height, indicating the homogeneous forest height. b) Vertical complexity index, derived from diversity indexes that allow characterizing the vertical structure of the forest. Closer to zero means that only a few height layers have vegetation and closer to 1 means that all the height layers have the same quantity of vegetation or coverage, showing that there is a high diversity in the vertical profile of vegetation. c) Elevation above sea level.

These three variables were selected as the best indicators or independent variables explaining the presence of L. fulvipes.

The probability of occurrence increases as long as there are core patches present and the most important predictor variables are the modal height, representing the most frequent height, that is the most homogeneous height of the core patch, and then the ICV variable that reflects the distribution of vegetation at different heights; closer to zero indicates areas where vegetation is concentrated at certain heights, such as the case of forest plantation, but when the value is near 1, vegetation is distributed homogeneously in the entire vertical profile, indicating the presence of forests with different composition or age, which show a high diversity in the zone. Subsequently, elevation indicates an altitudinal gradient for the presence of L. fulvipes.

Variable	Parameter	Chi-Square	Value - p
Constant	8.875		0.0000437
Modal Height	-0.194	29.75	0.0000004
ICV	-7.634	13.17	0.0140017
Elevation	-1.959	6.67	0.0154766

Table 2: Parameters derived from the best predictor variables of the regression model.

The classification matrix showed that the model has a high prediction rate (79.07%), which means that from every 5 observation 4 are virtually successful, also, the odds ratio was 16, indicating that there is a high probability of occurrence or presence (16:1) of L. fulvipes in the zones shown by the model (Fig. 3).

Conclusions

The Caramávida cleft, Trongol and their surroundings are the most relevant areas in Nahuelbuta, since they still have primary and secondary forest fractions. These native forests, preserved in different degrees, constitute the laurifolia ecosystem in the Nahuelbuta Range (Pauchard 2011). In its low areas Gomortega keule (Molina, 1782) Baill., 1869 and Berberidopsis corallina Hook, 1862, can be found, and in its high areas Araucaria araucana (Molina) K. Koch dominating the landscape. The Caramávida ecosystems are considered as priority sites for regional preservation by the Chilean governmental bodies.

Generating reliable information about the geographic distribution of species is one of the main requirements to establish effective preservation policies. However, after decades of taxonomic and faunistic work, we only have approximate data about the total of species that inhabit Chilean lands and we do not have convincing information that enables us to know the current distribution of most species (Briones et al. 2012). These insufficiencies become evident when we include vegetable coverage in our study. For our study area we have generated information layers regarding the understory vegetation coverage, mean, maximum and modal height of vegetation, total coverage, leaf area index, elevation and vertical complexity index. This information gives us more variables making our analysis statistically more robust.

The species distribution models are in full development and expansion with new methods and strategies for their treatment and interpretation. Consequently, there is a large number of articles building up with significant methodological and theoretic contributions for the modelling of species distribution (see Mateo et al. 2011). There are several information restrictions for these models, such as the lack of presence/absence data, cartography, environmental variables. With this the predicting capacity of the models is affected.

Acknowledgements
The authors thank Forestal Arauco centre zone for their funding and support in the field. The authors are also grateful to the researchers Patricio Viluñir, Rodolfo Figueroa, Felipe Hernandez, Alfonso Jara, Alfredo Zuñiga, Dario Moreira and Javier Cabello for their support in the field and methodological inputs.

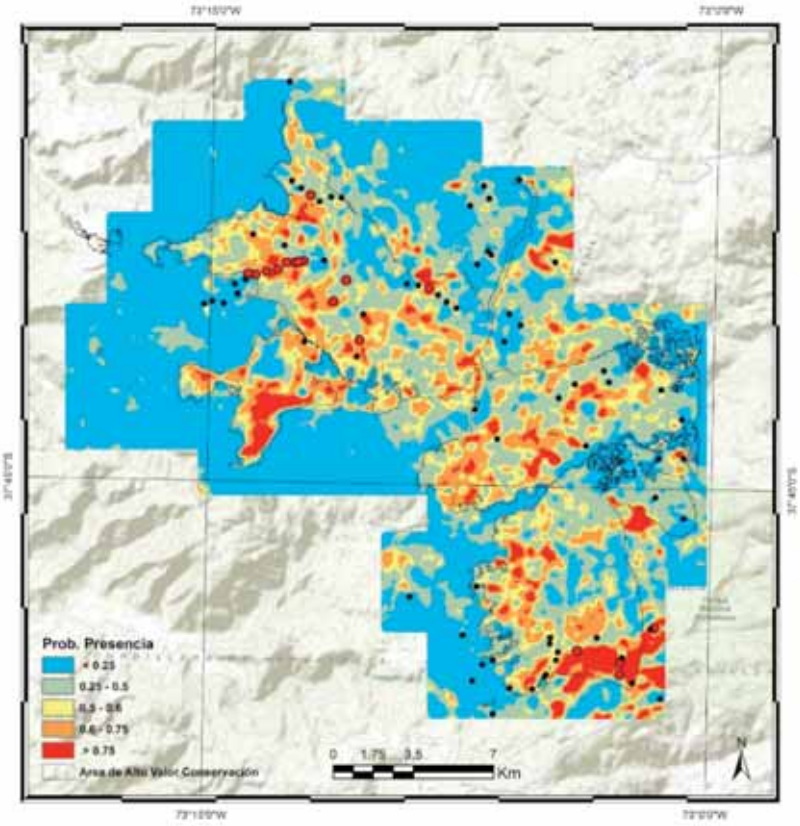

Figure 3: Map showing the probability of L. fulvipes presence, derived from the output of the logistic model. The variables used in the model were modal height, ICV and elevation; the correct classification percentage was 79.07%.

Bibliography

ARMESTO, J.J., D. MANUSCHEVICHA, A. MORA, C. SMITH-RAMIREZ, R. ROZZI, A.M. ABARZÚA & MARQUET, P.A. 2010. From the Holocene to the Anthropocene: A historical framework for land cover change in southwestern South America in the past 15,000 years. Land Use Policy 27 148–160.

BRIONES, R., F. GARATE-FLORES & JEREZ, V. 2012. Insectos de Chile nativos, introducidos y con problemas de conservación. Guía de Campo. Ed. Corporación Chilena de la Madera, Concepción, Chile. 256 pp.

BRIONES, R. 2011. Diversidad de Carnívoros de transectos con trampas cámaras en AAVC Caramavida. Documento interno Forestal Arauco. 30 pp.

IUCN 2012. IUCN red list categories and criteria, version 3.1, 2nd edn. IUCN, Gland.

COFRÉ, H. & MARQUET, P.A. 1999. Conservation status, rarity, and geographic priorities for conservation of Chilean mammals: an assessment. Biological Conservation 88: 53-68.

CONAF-CONAMA. 1999. Catastro y Evaluación de Recursos Vegetacionales Nativos de Chile. Informe Regional Décima Región. Proyecto CONAF-CONAMA-BIRF. Santiago. Chile.

D'ELÍA, G., A. ORTLOFF, P. SÁNCHEZ, B. GUIÑEZ & VARAS, V. 2013. A new geographic record of the endangered Darwin's fox Lycalopex fulvipes (Carnivora: Canidae): filling the distributional gap. Revista Chilena de Historia Natural 86:485–488.

FARIAS, A.A., M.A. SEPÚLVEDA, E.A. SILVA-RODRÍGUEZ, A. EGUREN, D. GONZÁLEZ, N.I. JORDÁN, E. OVANDO, P. STOWHAS & SVENSSON, G.L. 2014. A new population of Darwin's fox (Lycalopex fulvipes) in the Valdivian Coastal Range. Revista Chilena de Historia Natural 87: 1:3.

FISK, H., P. MAUS & DALE, S. 2009. Derived Lidar products and forestry applications: Crawford study area—White Mountain National Forest. RSAC-0999-BRIEF3. Salt Lake City, UT: U.S. Department of Agriculture Forest Service, Remote Sensing Applications Center. 6 p.

GLADE, A. 1993. Libro rojo de los vertebrados terrestres de Chile. Corporación Nacional Forestal, Santiago, Chile. 68 pp.

IBARRA-VIDAL, H., C. SEPÚLVEDA, D. SAAVEDRA & MALDONADO, E. 2005. Propuestas de conservación de los bosques nativos en la cordillera del Maule y Biobío (VII y VIII Regiones). In Smith-Ramírez C., J. Armesto & Valdovinos, C. eds. Historia, biodiversidad y ecología de los bosques costeros de Chile. Santiago, Chile. Editorial Universitaria. p. 617-631.

JAKSIĆ, F.M., J.E. JIMÉNEZ, R.G. MEDEL & MARQUET, P. A. 1990. Habitat and diet of Darwin´s fox (Pseudalopexfulvipes) on the Chilean mainland. Journal of Mammalogy, 71(2), 246–248.

JIMÉNEZ, J.E. 2000. Viability of the endangered Darwin´s fox (Pseudalopex fulvipes): assessing ecological factors in the last mainland population. Progress report for the Lincoln Park Zoo Neotropic Fundation. Chicago, Illinois, USA. 68 pp.

JIMÉNEZ, J. E. & MCMAHON, E. 2004. Pseudalopex fulvipes. In: Sillero-Zubiri, C., Hoffmann. M., & Macdonald, D.W. (eds.). Canids: Foxes, wolves, jackals and dogs. Status survey and conservation action plan. IUCN/SSC Canid Specialist Group. Gland, Switzerland and Cambridge, UK. Pg. 50-55.

JIMÉNEZ, J. E. 2007. Ecology of a coastal population of the critically endangered Darwin´s fox (Pseudalopex fulvipes) on Chiloe Island, southern Chile. Journal of Zoology, 271(1), 63-77.

JIMENEZ, J. E., YÁÑEZ, J.L., TABILO, E. & JAKSIC, F. M. 1996. Niche-complementarity of South American foxes: reanalysis and test of a hypothesis. Revista Chilena de Historia Natural, 69: 113–123.

JIMÉNEZ, J.E. 1993. Comparative ecology of Dusicyon foxes at the Chinchilla National Reserve in northcentral Chile. Master of Science thesis. University of Florida, Gainesville, FL.

JIMÉNEZ, J.E., LUCHERINI, M., & NOVARO, A.J. 2008. Pseudalopex fulvipes. IUCN Red List of Threatened Species.Version 2010.4.<www.iucnredlist.org>. Downloaded on 09 May 2011.

JIMÉNEZ, J.E., MARQUET, P.A., MEDEL, R.G., & JAKSIC, F.M. 1990.Comparative ecology of Darwin's fox (Pseudalopex fulvipes) in mainland and island settings of southern Chile. Revista Chilena de Historia Natural, 63, 177-186.

JIMENEZ J.E., C. BRICEÑO, H. ALCAÍNO, P. VÁSQUEZ, S. FUNK & GONZÁLEZ-ACUÑA D. 2012. Coprologic survey of endoparasites from Darwin's fox (Pseudalopex fulvipes) in Chiloé, Chile. Archivos de Medicina Veterinaria 44: 93-97

KO, C., T.K. REMMEL, & SOHN, G. 2012. Mapping tree genera using discrete LiDAR and geometric tree metrics. BOSQUE 33(3):313-319.

LUEBERT, F. & PLISCOFF, P. 2005. Bioclimas de la Cordillera de la Costa del centro-sur de Chile. In: Historia, biodiversidad y ecología de los bosques costeros de Chile (Smith, C., Armesto, J. y Valdovinos, C. eds.), pp. 60-73. Editorial Universitaria, Santiago.

SILLERO-ZUBIRI, C., M. HOFFMANN & MACDONALD, D.W. (eds). 2004. Canids: Foxes, Wolves, Jackals and Dogs. Status Survey and Conservation Action Plan. IUCN/SSC Canid Specialist Group. Gland, Switzerland and Cambridge, UK

MCMAHON, E. 2002. Status and conservation of the zorro chilote on mainland Chile. Progress report for SAG and CONAF, Temuco, Chile.

MACKENZIE, D. I., & ROYLE, J. A. 2005. Designing occupancy studies: general advice and allocating survey effort. Journal of Applied Ecology, 42 (6), 1105-1114.

MARDONES, M. 2005. La Cordillera de la Costa: caracterización físico-ambiental y regiones morfoestructurales. En: Historia, biodiversidad y ecología de los bosques costeros de Chile (Eds. C. Smith-Ramírez, J.J. Armesto& C. Valdovinos), pp. 39-59. Editorial Universitaria, Santiago de Chile.

MCGAUGHEY, R. J. & CARSON, W.W. 2003. Fusing LIDAR data, photographs, and other data using 2D and 3D visualization techniques, In: Proceedings of Terrain Data: Applications and Visualization – Making the Connection, October 28-30, 2003; Charleston, South Carolina: Bethesda, MD: American Society for Photogrammetry and Remote Sensing. pp. 16-24.

MCGAUGHEY, R.J. 2007. USDA Forest Service, FUSION manual, version 2.60.

MEDEL, R.G., J.E. JIMÉNEZ & JAKSIC, F. 1990. Discovery of a continental population of the rare Darwin´s fox, Dusicyonfulvipes (Martin, 1837) in Chile. Biological Conservation, 51(1), 71–77.

MINSEGPRES (Ministerio Secretaría General de la Presidencia). 2007. Decreto supremo 151/2007. Oficializa primera clasificación de especies silvestres según estado de conservación.

MUÑOZ-PEDREROS, A., J. RAU, M. VALDEBENITO, V. QUINTANA & MARTINEZ, D. 1995. Densidad relativa de pumas (Felis concolor) en un ecosistema forestal del sur de Chile. Revista Chilena de Historia Natural, 68: 501–507.

ORTIZ JC & IBARRA-VIDAL H. 2005. Anfibios y reptiles de la cordillera de Nahuelbuta. En: Smith-Ramirez C, JJ Armesto, C Valdovinos (eds.). Historia, Biodiversidad y Ecología de los Bosques Costeros de Chile. Editorial Universitaria, Santiago, Chile. Pp 427-440.

SANTOS, T. & TELLERÍA, J.L. 1998. Efectos de la fragmentación de los bosques sobre los vertebrados de las mesetas ibéricas. MIMA, Madrid.

SHAFFER, M.L. 1981. "Minimum population sizes for species conservation". BioScience (American Institute of Biological Sciences) 31 (2): 131–134.

STOWHAS, P. 2012. Conflicto Entre Carnívoros Silvestres y Campesinos en el sur de Chile, DVM thesis. Universidad Mayor, Santiago, Chile.

MELLA, J. 1994. Conservación de mamíferos en las áreas silvestres protegidas de Chile: Representación y poblaciones viables. Ambiente y Desarrollo, Vol X (3): 72-78.

VAN EWIJK, K. Y., P. M. TREITZ & SCOTT, N.A. 2011. Characterizing Forest Succession in Central Ontario using Lidar-derived Indices. Photogrammetric Engineering and Remote Sensing 77:261-269.

VILÀ, C., J.A. LEONARD, A. IRIARTE, S.J. O´BRIEN, W.E. JOHNSON & WAYNE, R. K. 2004. Detecting the vanishing populations of the highly endangered Darwin´s fox, Pseudalopex fulvipes. Animal Conservation, 7(2), 147-153.

VOGT, P., RIITTERS, K., IWANOWSKI, M., ESTREGUIL, C., KOZAK, J. & SOILLE, P. 2007. Mapping Landscape Corridors Ecological Indicators 7, issue 2, pp. 481-488.

YAHNKE, C. J., W.E. JOHNSON, E. GEFFEN, D. SMITH, F. HERTEL, M.S. ROY, C.F. BONACIC, T.K. FULLER, B. VAN VALKENBURGH & WAYNE RK. 1996. Darwin´s Fox: A Distinct Endangered Species in a Vanishing Habitat. Conservation Biology, 10(2), 366-375.

ZUÑIGA, A. 2012. Ensamble de carnívoros de la Cordillera de Nahuelbuta: ¿Condicionado por el tipo de hábitat o las relaciones interespecificas?. Tesis para optar al grado de Magíster en Ciencias, mención Manejo, Producción y Conservación de Recursos Naturales. Universidad de Los Lagos, Chile. pp 106.

Why Your Next Mapping Project Will Probably Use Stacking

Sean P. Healey[1], Warren B. Cohen[1], Zhiqiang Yang[2], Todd Schroeder[1], Noel Gorelick[3], Gretchen Moisen[1]*

**Speaker*
Affiliations: [1-] United States Forest Service [2-] Oregon State University [3-] Google, Inc.

Ensemble prediction methods have become popular for many classification tasks, including those related to remote sensing of forest resources. Foremost among these methods is a "bagging" technique called Random Forests, which trains an ensemble of decision trees with random subsets of the training data, and uses a voting procedure to integrate across output classifications. This approach is thought to improve classification accuracy through reduction of overfitting. An alternative approach called "stacking" (or "stacked generalization,") starts with an ensemble of classifiers that use completely independent methods instead of replicating the same model with random subsets of training data. Stacking is accomplished by comparing alternative classification results with the training data to explicitly weight ensemble members in producing a meta-classification. Typically, parametric methods such as logistic regression are used to identify the classifier biases used in this process.

We suggest that alternative forest maps can be effectively integrated by a stacking process governed by a non-parametric model such as Random Forests instead of a parametric approach. A Random Forests integration rule eliminates the variable-selection processes required with parametric approaches, and theoretically would also improve performance and robustness by reducing overfitting of ensemble member weights. This approach was recently tested with several leading forest change detection algorithms and a broad reference dataset that included even very subtle and/or slow changes. Judged against this definition of disturbance, which is admittedly broader than the definition built into some of the original classifiers, ensemble integration with a Random Forests stacking rule outperformed both the original maps and stacking with logistic regression. Performance (rates of disturbance omission and commission) also improved when unrelated spatial products were added to the ensemble, including: forest cover classifications, topography, and pre- and post-disturbance Landsat reflectance values.

Stacking provides a means to integrate the signal carried by alternative maps in addressing complex classification tasks, but as implemented here, it also requires tremendous computing capacity and the ability to make maps using several different classification approaches. Increasingly popular cloud-based remote sensing platforms are at once 1) improving our ability to share mapping algorithms, and 2) raising our capacity to run several mapping processes in parallel. When implemented with a Random Forests integration rule on a cloud-based system, stacking can offer significant performance gains in a variety of mapping tasks.

POSTER

3-D Model of a Mediterranean Tree-Grass Ecosystem for Remote Sensing Applications

Pacheco-Labrador, Javier[1], Gajardo, John[2], Riaño, David1[1,3], Martín, M. Pilar[1]

[1] Environmental Remote Sensing and Spectroscopy Laboratory (SpecLab), Institute of Economic, Geography and Demography (IEGD-CCHS), Spanish National Research Council (CSIC), C/Albasanz 26-28, 28037 Madrid, Spain.
[2] Facultad de Ciencias Forestales Universidad de Talca, Avenida Lircay S/N Talca, Chile.
[3] Center for Spatial Technologies and Remote Sensing (CSTARS), University of California, Davis, One Shields Avenue, 139 Veihmeyer Hall, Davis, CA 95616, USA.

Keywords: Tree-grass, savanna, LiDAR, Remote sensing, BRDF, shadow

Abstract

Tree-grass ecosystems are mixed woody-herbaceous systems characterized by a low density and disperse distribution of woody vegetation. Such heterogeneity in physiology, phenology and structure represent a challenge for modelers of different communities. Remote sensing applications usually need to determine the fraction of trees and grass canopies observed; whereas Proximal Sensing systems have the challenge of measure separately woody and grass elements. This becomes more difficult in the case of multi-angular hyperspectral systems dedicated to the retrieval of BRDF, since usual kernel-based functions are no longer valid.

In this work we present a geometrical 3-D model of a Tree-grass ecosystem located in Majadas del Tiétar, Spain. The site is subject of research from remote sensors, Eddy Covariance systems and features multi-angular hyperspectral systems (AMSPEC-MED). The model is developed to contribute to the abovementioned applications. The 3-D model was built from Airborne laser scanning (ALS) data, provided by Spanish Program of Aerial Orthophotography (PNOA). TerraScan (Terrasolid Ltd., Finland) classified ground and tree canopy points to obtain a 0.5 m Digital Ground (DGM) and a Surface (DSM) Model. Circular Hough transform-based algorithm identified single crowns in the DSM; then an ellipsoid was fit to ALS returns identified in each crown. Additionally, terrestrial laser scanning (TLS) data of some crowns and a voxel model were used to predict crown transmittance at different illumination angles.

The model covered an area of 2,328 Km^2, where tree density was ~ 21.6 trees\ha. It provides detailed structure of tree crowns and grass surface, and an additional probability of transmission as a function of observation/zenith angle. Current applications are the unmix of trees and grass BRDF from the AMSPEC-MED system, estimation of the tree/grass/shadow fractions as observed from mid and coarse resolution remote sensors and ecosystem shadow fraction estimation for biogeochemical modeling and energy balances.

3D measurement of tree health using multispectral intensity data from terrestrial laser scanners

Samuli Junttila[1,2], Mikko Vastaranta[1,2], Riikka Linnakoski[1], Junko Sugano[3], Harri Kaartinen[2,4], Antero Kukko[2,4], Markus Holopainen[1,2], Hannu Hyyppä[2,5], and Juha Hyyppäb,[4]

[1] Department of Forest Sciences, University of Helsinki, 00014 Helsinki, Finland.
[2] Centre of Excellence in Laser Scanning Research, Finnish Geospatial Research Institute FGI, 02431 Masala, Finland.
[3] Department of Biology, University of Turku, 20014 Turku, Finland.
[4] Department of Remote Sensing and Photogrammetry, Finnish Geospatial Research Institute FGI, 02431 Masala, Finland.
[5] Department of Built Environment, Aalto University, P.O.Box 15800, 00076 Aalto, Finland.

Keywords: Forest health, terrestrial laser scanning, LiDAR, multispectral laser scanning, leaf water content, monitoring.

Abstract

Equivalent water thickness (EWT), a measure of leaf water content, and leaf chlorophyll content (Cab) are important early indicators of tree stress caused by a variety of factors including pest insects, pathogens and drought. Early detection of pest insects and pathogens is vital in reducing the damages and costs of decreased tree growth and tree mortality. Recent investigations have explored the use of backscatter intensity information from terrestrial laser scanners (TLSs) in order to obtain EWT and Cab, but few studies have investigated the use of multiple wavelengths or TLSs.

Here we tested the ability of three-wavelength terrestrial laser scanning in detecting leaf water content from Norway spruce seedlings (n = 90). To simulate a drought event, the seedlings were subjected to different levels of watering during 8 weeks resulting in variation in tree health. During this period a sub-sample of seedlings were randomly selected for laser scanning and destructive measurements of EWT at 10 time intervals. The relationship between the measured EWT from needle samples and laser intensity features, using 690 nm, 905 nm and 1550 nm wavelengths, were determined. The results showed a relationship of R2 = 0.72 (RMSE = 0.006 g/cm2) between the measured EWT and the ratio of mean backscattered laser intensity from 905 nm and 1550 nm wavelengths. In addition to EWT measurements, needle samples from 30 seedlings were collected for analysis of chlorophyll a and b content. These analyzes are under process and the results will be presented in ForestSAT 2016.

3D modeling of below-canopy global irradiance using terrestrial LiDAR data and ray tracing

Renato Cifuentes La Mura[1, 3], Dimitry Van der Zande[2], Christian Salas[3], Laurent Tits[1, 4], Jamshid Farifteh[1], Pol Coppin[1]

[1] KU Leuven, Department of Biosystems, Division of Crop Biotechnics, Willem de Croylaan 34, BE-3001 Leuven, Belgium
[2] Directorate Natural Environment, Royal Belgian Institute of Natural Sciences, Gulledelle 100, BE-1200 Brussels, Belgium
[3] Laboratorio de Biometría, Departamento de Ciencias Forestales, Universidad de La Frontera, PO Box 54-D, Temuco, Chile
[4] Flemish Institute for Technological Research (VITO), Remote Sensing Unit, Boeretang 200, BE-2400 Mol, Belgium

Keywords: canopy structure, 3D modeling, terrestrial LiDAR, ray tracing

Phase-based terrestrial LiDAR (PTL) measurements were collected on two broadleaved forest to i) generate the 3D models of their canopies and estimate leaf area index (LAI), clumping index (CI) and canopy openness (CO), and to ii) feed a ray-tracing system to analyze distribution of global irradiance, specifically photosynthetically active radiation (PAR), below the canopy. Data were collected on a pure beech (*Fagus sylvatica* L.) and on a mixed (beech, oak (*Quercus robur* L.) and birch (*Betula pendula* Roth)) forest. A total of nine scans were taken per forest on a 400 m^2 area using a FARO® LS880 PTL scanner (λ=785 nm, maximum range=76 m). Digital hemispherical photographs were collected as reference data. Leaves and trunks spectra were also recorded on a FieldSpec® 3 spectroradiometer. Similarly, global irradiance was measured in the field using a remote cosine-corrected receptor. This light measurements were taken on every cross point of a 1m grid within the 400 m^2 area. For three-dimensional (3D) canopy modeling, the PTL data was filtered (i.e., noise correction), classified in green and non-green elements, and voxelized using four different voxel side lengths (VS) i.e., 10 mm, 20 mm, 26 mm and 30 mm. A series of forest scenes, emulating hemispherical images, were then built using the open source Persistence of Vision Raytracer (POV-Ray) for LAI, CI and CO calculation. These estimates were later compared with the reference data. Likewise, the Physically-Based Ray Tracer (PBRT) was used for light distribution simulations and PAR analysis. Results after simple linear regression modeling (α=0.01) indicate that predicted values of canopy structural variables are consistent with the observed ones at particular zenith angle ranges (ZAR) and parametrization for 3D modeling. In the mixed forest, LAI was better predicted using VS 10 mm at 30°-60° ZAR, CI was not significantly influenced by VS but showed differences in slope and intercept at different ZAR, and CO was accordingly predicted using VS 10 mm at all ZARs. In the beech forest, LAI predictions were consistent at 20°-60° ZAR using VS 20 mm, CI presented similar trends as in the mixed forest but VS had an impact at narrower ZAR (e.g., VS 20 mm at 40°-60°), while CO was better predicted with several VS (e.g., 20 mm, 26 mm, and 30 mm) at both 5°-25° and 5°-30° ZAR. Consequently, the parameters required for the suitable specification of the 3D model for light simulation and analysis of PAR in PBRT were adopted after this structural analysis. PAR results from both mixed and beech forest reflected that predictions were biased in relation to observed values. In the mixed forest, predictions underestimated PAR up to a certain level, where the trend was then shifted to overestimation (*RMSD* = 0,23). On the other hand, predicted values on the beech forest, systematically underestimated PAR (*RMSD* = 0,19).

ForestSAT 2016

Forest Mapping & Inventory

OTERRA
CENTRO DE ESTUDIOS DE RECURSOS NATURALES
UNIVERSIDAD MAYOR

UNIVERSIDAD MAYOR
para espíritus emprendedores

Facultad de Ciencias
ESCUELA DE INGENIERÍA FORESTAL

POSTER

A web service proposal for forest inventory of fast-growing species in areas with small-size property using free software: GRASS GIS,WPS and LiDAR

Miguel Cordero , Eduardo Corbelle David Miranda

Land Laboratory – Department of Agroforestry Engineering, University of Santiago de Compostela, Escuela Politécnica Superior, R/Benigno Ledo, Campus Universitario, 27002 Lugo, Spain
Miguel Cordero (miguel.cordero@usc.es)

Keywords (5-8), forest inventory, small property, lidar, WPS, free software

Abstract,

Estimating timber volume of very small stands (e.g. less than 2000 m2) of fast-growing species by means of automated inventory techniques can be really challenging. Lack of adequate means to easily estimate volume in those circunstances result in less transparent timber markets and generally hampers planning and sustainable forest management. This is tipically the case of areas in Northwestern Spain, where most property lots are usually very small. While methods for LiDAR-based volume estimation in this geographic area have already been published (mainly for Pinus radiata D. Don, and Eucaliptus globlulus Labill stands), their use has been largely restricted to research purposes and they have only been used operationally in forest stands of medium to large area. In this work, we outline the characteristics of a public web service based on free software that builds on existing methods and publicly available LiDAR data to automate estimation of timber volume in small plots of fast-growing species. The service would be implemented in GRASS GIS, use WPS protocol, and build on public low-density LiDAR data, available filtering algorithms, and already published volume-assessment equations for P. radiata and E. globulus. We tested the system with real data from small woodlots harvested in the same year of LiDAR data acquisition. A basic description of the proposed design is presented, along with an assessment of the achieved degree of functionality, main obstacles found, and an assessment of final error in volume estimation.

Introduction

Estimating timber volume of very small stands (e.g. less than 2000 m2) of fast-growing species by means of automated inventory techniques can be really challenging. Lack of adequate means to easily estimate volume in those circunstances result in less transparent timber markets and generally hampers planning and sustainable forest management. This is tipically the case of areas in Northwestern Spain, where most property lots are usually very small. While methods for LiDAR-based volume estimation in this geographic area have already been published (mainly for Pinus radiata D. Don, and Eucaliptus globlulus Labill stands), their use has been largely restricted to research purposes and they have only been used operationally in forest stands of medium to large area. In this work, we outline the characteristics of a public web service based on free software that builds on existing methods and publicly available LiDAR data to automate estimation of timber volume in small plots of fast-growing species. The service would be implemented in GRASS GIS, use WPS protocol, and build on public low-density LiDAR data, available filtering algorithms, and already published volume-assessment equations for

P. radiata and E. globulus. We tested the system with real data from small woodlots harvested in the same year of LiDAR data acquisition. A basic description of the proposed design is presented, along with an assessment of the achieved degree of functionality, main obstacles found, and an assessment of final error in volume estimation.

Methodology, The service would be implemented in GRASS GIS, use WPS protocol, and build on public low-density LiDAR data, available filtering algorithms, and already published volume-assessment equations for P. radiata and E. globulus. We used data from two public sources; cadastral plot and details of the lidar from PNOA (a natioanl program of remote data acquisition). Both data sets are freely downloadable and vector data supplied high quality in terms of spatial accuracy. In the case of lidar with low density points (0.5 points / m2).

As the tools we chose to use software for easy access to internal documents and the gratuitous licensing to implement the service; OpenLayers v3.0 as map viewer, PyWPS v5.0 as implementation of the protocol and Web Processing Service and GRASS GIS v7.0 as computing GIS platform.

For the validation of the system results were compared with values of timber companies that buy wood in the area conducting field inventory plots.

In order to maximize the transparency of the process, the system is based on data and public access software and hardware.

For the estimation of timber in each plot, a GIS system was prepared that from the polygon of land cut the plot data, filter the corresponding points to the terrain, and apply the existing volume estimation equations to lidar data. This process was automated from scripts in the GIS.

Through PyWPS was connected to the web server so that the previous GIS script became available as a web service hosted on a public server.

Through Open Layers an interface is provided to the user to select the parcel of interest and to be able to request its timber estimation. This interface transmits to PyWPS the parameters that the service needs (limit of the plot or zone to be measured).

Results, We tested the system with real data from small woodlots harvested in the same year of lidar data acquisition. In plots with raw data (without information of age, forestry, etc.) the system can estimate between 40-60 percent of the total value. Taking into account that they are raw data can be an important margin of improvement without deteriorate user experience.

We also tested the system with real users, owners of small plots, detecting that there may be a problem, not of handling the tool but of continuity or familiarity of use, since the measurements are sporadic uses, with years without intermediate use. Therefore, it may be necessary to take actions towards their generalization in the sector.

References.

[1] E. Gonz´alez-Ferreiro, U. Dí eguez-Aranda, and D. Miranda.
Estimation of stand variables in pinus radiata d. don plantations using different lidar pulse densities.
Forestry, 85(2):281–292, 2012.

[2] L. Gon¸calves-Seco, E. Gonz´alez-Ferreiro, U. Di´eguez-Aranda, B. Fraga-Bugallo, R. Crecente, and D. Miranda.
Assessing the attributes of high-density eucalyptus globulus stands using airborne laser scanner data.
International Journal of Remote Sensing, 32(24):9821–9841, 2011.

Above ground biomass related to field measurement errors

Trucíos C., R.[1] ; Paudel, P.[2], Kleinn, C.[3]

[1] PhD student Faculty of Forest Sciences and Forest Ecology, Georg-August-Universität, Göttingen.
[2] M. Sc. formed in Tropical and International Forestry, Faculty of Forest Sciences and Forest Ecology, Georg-August-Universität, Göttingen.
[3] Prof. Dr. and Head of Chair of Forest Inventory and Remote Sensing, Faculty of Forest Sciences and Forest Ecology, Georg-August-Universität, Göttingen.

Key words: measurement error, discrepancy, training, biomass

Measurement errors are generally not reported in the dasometric data, in this case specifically measurements in national forest inventories. Measuring the field variables and know the measurement error makes known the accuracy of the measured variable and those estimates derived variables expressing forest productivity as basal area, volume, forest biomass, stored carbon, among others. This document presents a case study in a forests owned by the federal state of Lower Saxony, north of Göttingen, Germany. In this study, we compared the accuracy of above ground biomass estimates developing skills through training teams in field measurement variables (DBH, total height, azimuth and horizontal distance). Similarly, the accuracy between measurements of two instruments for diameter and height variables used in the estimation models of forest biomass was compared. To analyze the random measurement errors, clear protocols for the use of devices were established, in addition to calibrated instruments used to avoid deviations due to bias measurements. Part of the analysis was to compare field measurements of the two work teams: experienced and no experience in dasometric measurement variables. After a training period, the teams re-measured the plots and the effects of training were analyzed on the accuracy of the measurements. Measurements of the two teams were made with the same instruments and compared to a control data consisting of the average of 5 mensurations (using the same instrument). The second part of the analysis corresponds to the re-measurement of trees (Control two) with different precision equipment and its comparison with Control data. After second training, mean of the difference in DBH measurement decreased for both groups, -0.08 cm to 0.0002 cm for inexperienced and -0.107 cm to 0.02 cm for experienced in first and second measurements, respectively. However, mean of difference in height measurement for experienced observers was very low compared to inexperienced observers in both measurements. Large errors (outliers) in measurement of DBH in both measurements were randomly distributed regardless of tree size. A higher deviation was noticed in measurement of height for taller and bigger trees measured by inexperienced observer in both measurement, however such deviation only found in first measurement in case of experienced observer. One of the parameters used to compare control data was the relative standard deviation of the analyzed variables which was less than 6%, indicating acceptable accuracy measurements. Using the law of error propagation will be estimated uncertainty of the measured variables and their impact on the estimation of above ground biomass through allometric models used in this study.

Above-ground biomass estimation using calibrated multispectral aerial images in grasslands. Do calibration targets matter?

*Miguel Marabel, Flor Alvarez-Taboada**

**corresponding author. flor.alvarez@unileon.es*

Affiliation of all the authors: GEOINCA research group. Department of Mining Technology, Topography and Structures, University of León, Ponferrada Campus, Avenida de Astorga s/n, 24400, Ponferrada, León, Spain.

Key words: grasslands; vicarious calibration; spectro-radiometer; Partial least squares regression; Ultracam XP/WA

Abstract

The main objectives of this research work were: (i) to establish a procedure for the radiometric calibration of images from the airborne photogrammetric camera UltraCam-Xp WA and (ii) to estimate the above-ground biomass (dry weight of the green fraction) in grasslands using those calibrated images. The empirical line calibration and three multispectral images (A, B, C) were used. Three different types of calibration targets were used: (i) 1 m x 1 m portable rigid targets (gray scale), (ii) 2 m x 2 m non rigid targets made of fabric (gray scale and colour) and (iii) target areas (not portable). 27 different combinations of these targets were tested to calibrate the images. The most suitable calibrations were used to obtain the at-surface reflectance images (Ar, Br, Cr), which were used to estimate the biomass. The calibration targets consisting of portable rigid panels provided the most accurate radiometric calibration (R^2=0.99; RMSE≤0.014 %; RMSE (%)=3.64). The most accurate estimation of above-ground biomass was obtained by using Partial Least Squares Regression (PLSR) and at-surface reflectance of the Cr image (R^2=0.90; RMSE=4.096 g/m^2; RMSE (%)=12.92), although the differences between images were not significantly different. Using the vegetation indices NDVI (R^2=0.80; RMSE=5.593 g/m^2; RMSE (%)=18.81), SR (R^2= 0.78; RMSE=5.864g/m^2; RMSE (%)=18.49), NLI (R^2=0.88; RMSE=4,267g/m^2; RMSE (%)=13.46) or SAVI (R^2=0.85; RMSE=4.867 g/m^2; RMSE (%)=15.35) the estimates were less accurate.

When PLRS was used for the biomass estimation, the differences between using different calibration sets ranged from 0.1% to 2.5% for the RMSE (%). However, when vegetation indices were used (NDVI, SR, NLI, SAVI), the differences derived from using different calibration sets ranged from 1.6% to 19.2% for the RMSE. NDVI and SAVI were the least sensitive to the changes in the calibration (<5% difference), while SR was the most affected (10%-19% difference). These results were obtained in the tree images.

The calibration equations adjusted for image A and for image C were applied to image B, and the differences in the biomass estimation after using those calibrations or the calibration obtained specifically for B were smaller than 1% (RMSE%). Thus, the calibration of one image can be successfully used for adjacent images.

The images of the UltraCam-Xp WA are therefore suitable for estimating the above-ground biomass once they have been calibrated to at-surface reflectance, using PLSR and the spectral information of the 4 bands of the image.

Introduction

Above-ground biomass refers to the part of vegetation which grows above the ground, and some of it corresponds to grasslands. The importance of grasslands is remarkable, since they cover 37% of the terrain and they are able to capture CO_2 and transform it into biomass through photosynthetic processes. It is also noticeable the role of grassland biomass in silvopastoralism, as well as its energetic value, since they are biofuels. Moreover, these areas are crucial to protect soils from erosion. On the other hand, digital aerial cameras are suitable to record multispectral images, with high radiometric and geometric accuracy, which need however to be calibrated to extract qualitative and quantitative thematic information (Honkavaara et al., 2004). Along those lines, the estimation of biophysical variables like biomass requires an absolute radiometric calibration of those images, so that at-surface reflectance values are obtained (Jensen, 2005) and they can be used an input data in the estimation models.

Therefore, the main objectives of this research work were: (i) to establish a procedure for the radiometric calibration of images from the airborne photogrammetric camera UltraCam-Xp WA and (ii) to estimate the above-ground biomass (dry weight of the green fraction) in grasslands using those calibrated images.

Methodology

The general workflow is showed in Figure 1. It starts with the radiometric calibration of the multispectral images using an empirical line calibration and its validation, and it is followed by the biomass estimation using the calibrated image and field measurements, by means of reflectance values or vegetation indices.

Radiometric calibration

The empirical line calibration and three multispectral images (A, B, C) were used. The images were gathered with the metric aerial camera UltraCam-Xp WA, with a spectral resolution covering the Red (R), Green (G), Blue (B) and Near Infrared (NIR) regions of the electromagnetic spectrum, a GSD of 18 cm, and a radiometric resolution of 16 bits. The flight was carried out in 23/07/2012, and the three adjacent photograms were taken following a N-S flight-line.

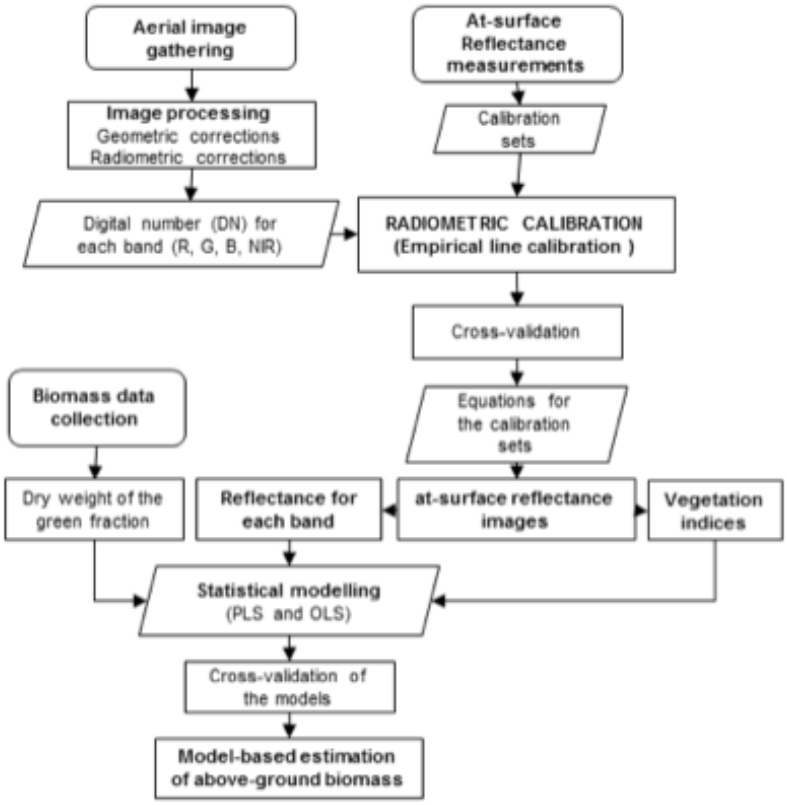

Figure 1. General workflow.

To avoid possible bilinear reflectance effects, the geometric center of the images was close to the calibration targets. The images were processed from level 1 to level 2 and orthorectified using ground control points measured with a GNSS receiver.

Three different types of calibration targets were used: (i) 1 m x 1 m portable rigid targets (gray scale), (ii) 2 m x 2 m non rigid targets made of fabric (gray scale and colour) and (iii) target areas (not portable). 27 different combinations of these targets were tested to calibrate the images (Table 1). Each target was radiometrically characterized by 30 measurements done by using the ASD Fieldspec3 spectro-radiometer. The same procedure was followed to characterize thirty 1 m x 1 m plots, which consisted mainly of *Lolium perenne, Poa pratensis* and *Trifolium repens*. The aboveground biomass (defined as the dry weight of the green fraction in $g/m^{2)}$ was obtained as described in Marabel & Álvarez-Taboada (2013, 2014). The biomass average value was 31.71 g/m^2 ±12.63.

The digital numbers obtained for each target in the multispectral image were compared with the at-surface reflectance values gathered with the spectro-radiometer. The difference in spectral resolution of the data (4 wide multispectral bands for the la UltraCam-Xp WA versus 1nm spectral bands for the radiometer) was taken into account by calculating the weighed reflectance corresponding to 20 nm simulated bands for the UltraCam-Xp WA, considering the sensibility curve for each multispectral band. Therefore the weighed reflectance for the R-G-B-NIR bands was obtained for each target.

A linear regression was carried out between the at-surface reflectance values (dependent variable) and the digital numbers (independent variable) for each target and for each multispectral band, as showed in Del Pozo et al. (2014). A full cross-validation was carried out (Geladi & Kowalski, 1986). The criteria to choose the most suitable calibration set were to minimize the RMSE and to maximize the R^2 in the validation.

Biomass estimation using radiometrically corrected images

The most suitable calibrations were used to obtain the at-surface reflectance images (Ar, Br, Cr), which were used to estimate the biomass. Two approaches were followed, (i) using the reflectances for bands R, G, B, NIR or (ii) using vegetation indices as independent variables. The vegetation indices considered in this study were: NDVI (Rouse et al., 1974), Simple Ratio (Birth & McVey, 1968), Soil Adjusted Vegetation Index (Huete, 1988), and Non-Lineal Vegetation Index (Goel & Qin, 1994). The prediction models based on reflectance bands were adjusted by using Partial Least Squares Regression (PLSR) (Geladi & Kowalski, 1986), due to its suitability for collinear data (Marabel & Álvarez-Taboada, 2013). Later on a Leave-One-Out Cross validation was carried out. The criteria to choose the most suitable model were: minimize the number of factors, maximize R^2, minimize RMSE and %RMSE of the validation. The biomass estimation using vegetation indices was done by using Ordinary Least Squares Regression (OLSR), using as criteria to maximize R^2, and minimize RMSE and %RMSE of the validation. All statistical analyses were performed by Unscrambler® X10.2 (CAMO Software Inc., Woodbridge).

Results

Radiometric calibration

The calibration targets consisting of portable rigid panels provided the most accurate radiometric calibration for the three images (R^2=0.99; RMSE≤0.014 %; %RMSE (%)<3,80%), therefore that set can be used for calibration (Table 1). This set consists of portable rigid targets with 0%, 25%, 50%, 75%, 100% nominal reflectance. These results are similar to the ones obtained by Álvarez *et al*. (2010) and Honkavaara & Markelin, (2007) for the ADS40, DMC, UltraCamD and DSS multispectral sensors.

Tabla 1. Empirical line calibration accuracy for each band for the suggested set. RMSE values in % (reflectance)

BAND	IMAGE A			IMAGE B			IMAGE C		
	R^2	RMSE	%RMSE	R^2	RMSE	%RMSE	R^2	RMSE	%RMSE
B	0.996	0.0178	5.31	0.996	0.0169	5.03	0.996	0.0169	5.03
G	0.999	0.0092	2.69	0.999	0.0086	2.52	0.999	0.0084	2.48
R	0.997	0.0146	4.33	0.995	0.0174	5.13	0.996	0.0150	4.42
NIR	0.998	0.0107	2.34	0.998	0.0108	2.36	0.997	0.0121	2.64
AVERAGE	0.997	0.0131	3.67	0.997	0.0134	3.76	0.997	0.0131	3.64

Table 2. Results for the cross-validation of the models for biomass estimation in the three images, using reflectances, vegetation indices and the recommended calibration set. P=Image; F: latent factors; E=RMSE: g/m²; %E=%RMSE: %.

	R, G, NIR				NDVI			SR			NLI			SAVI		
P	R^2	E	F	%E	R^2	E	%E	R^2	E	%E	R^2	E	%E	R^2	E	%E
Ar	0,873	4,5741	2	14,42	0,793	5,6500	17,82	0,725	6,5181	20,56	0,851	4,7869	15,10	0,843	4,9163	15,50
Br	0,878	4,4842	2	14,14	0,767	5,9964	18,91	0,710	6,6939	21,11	0,830	5,1158	16,13	0,830	5,1163	16,13
Cr	0,898	4,0958	2	12,92	0,797	5,9635	18,81	0,701	6,7929	21,42	0,839	4,9887	15,73	0,841	4,9541	15,62

Tabla 3. Validation of the biomass estimation models obtained when the radiometric calibration equations adjusted for image B were applied to image A and C, using reflectances, vegetation indices and the recommended calibration set. P=Image; F: latent factors; E=RMSE: g/m²; %E=%RMSE: %.

	R. G. NIR				NDVI			SR			NLI			SAVI		
P	R^2	E	F	%E	R^2	E	%E	R^2	E	%E	R^2	E	%E	R^2	E	%E
B_B	0.878	4.4842	2	14.14	0.767	5.9964	18.91	0.710	6.6939	21.11	0.830	5.1158	16.13	0.830	5.1163	16.13
A_B	0.884	4.4938	2	14.17	0.775	5.8883	18.47	0.729	6.4613	20.38	0.841	4.9582	15.64	0.835	5.0497	15.92
C_B	0.884	4.4938	2	14.17	0.778	5.8575	18.47	0.747	6.2529	19.72	0.844	4.9044	15.47	0.835	5.0441	15.91

Biomass estimation

The most accurate estimation of above-ground biomass was obtained by using PLSR and at-surface reflectance of the Cr image (R^2=0.90; RMSE=4.096 g/m²; %RMSE (%)=12.92), although the differences between images were not significantly different. Using the vegetation indices the estimates were less accurate (Table 2).

These results were obtained in the tree images (Ar, Br, Cr). However the vegetation indices NLI or SAVI can be used if a simplified prediction model is aimed, since the similar accuracy in the results, with differences in %RMSE smaller than 1.6% (regardless the considered image) showed the suitability of the calibration method and the model to estimate biomass. When PLRS was used for the biomass estimation, the differences between using different calibration sets ranged from 0.1% to 2.5% for the RMSE (%) (results not showed). However, when vegetation indices were used (NDVI, SR, NLI, SAVI), the differences derived from using different calibration sets ranged from 1.6% to 19.2% for the RMSE. NDVI and SAVI were the least sensitive to the changes in the calibration (<5% difference), while SR was the most affected (10%-19% difference). These results were obtained in the tree images.

The calibration equations adjusted for image B were applied to image A and C, and the differences in the biomass estimation after using those calibrations or the calibration obtained specifically for B were smaller than 1% (RMSE%) (Table 3).

Conclusions

The images of the UltraCam-Xp WA are therefore suitable for estimating the above-ground biomass once they have been calibrated to at-surface reflectance, using PLSR and the spectral information of the four bands of the image. Moreover, the calibration of one image can be successfully used for adjacent images.

References

Álvarez, F., Catanzarite, T., Rodríguez-Pérez, J.R., Nafría, D., 2010a. Radiometric Calibration and Evaluation of the Ultracam Xp using Portable Reflectance Targets and Spectroradiometer Data. Application: to Extract Thematic Data from the Imagery Gathered by the National Plan of Arial Orthophotography (PNOA). En: Colomina, I.

Birth, G.S., and McVey, C. 1968. Measuring the color of growing turf with a reflectance spectroradiometer, Agronomy Journal, 60: 640-643.

CAMO, Technologies Inc., 2013. The Unscrambler appendices: method references. PDFdocument. Available at: http://www.camo.com/ (09/11/2016).

Del Pozo, S., Rodríguez-Gonzálvez, P., Hernández-López, D., Felipe-García, B. 2014. Vicarious Radiometric Calibration of a Multispectral Camera on Board an Unmanned Aerial System. Remote Sensing, 6: 1918-1937.

Geladi, P., Kowalski, B.R. 1986. Partial leastsquares regression: a tutorial. Analytica Chimica Acta, 185: 1-17.

Goel, N.S., Qi, W., 1994. Influences of canopy architecture on relation- ships between various vegetation indices and LAI and FPAR: A computer simulation. Remote Sens. Rev., 10: 309-347.

Honkavaara, J., Siitari, H., Viitala, J. 2004. Fruit color preferences of redwings (Turdus iliacus): experiments with hang-raised juveniles and wild-caught adults. Ethology, 110: 445-457.

Honkavaara, E., Markelin, L., 2007. Radiometric Performance of Digital Image Data Collection. A Comparison of ADS40/DMC/UltraCam and EmergeDSS, Photogrammetric Week. (Fritsch, D., Ed.), Wichmann Verlag, Heidelberg, Germany, pp. 117-129.

Huete, A.R., Jackson, R. D., Post, D.F., 1988. Spectral response of a plant canopy with different soil backgrounds. Remote Sensing of Environment, 17: 37-53.

Jensen, J. R., 2005. Introductory to Digital Image Processing: A remote sensing perspective (3rd ed.). Upper Saddle River, NJ, USA, Prentice Hall, 526 p. ISBN: 0-13-145361-0.

Marabel, M. y Álvarez-Taboada F. 2013. Spectroscopic Determination of Aboveground Biomass in Grasslands Using Spectral Transformations, Support Vector Machine and Partial Least Squares Regression. Sensors, 13: 10027-10051.

Marabel-García, M. y Álvarez-Taboada F. 2014. Estimación de biomasa en herbáceas a partir de datos hiperespectrales, regresión PLS y la transformación continuum removal. Revista de la Asociación Española de Teledeteción (AET) 42:49-60.

Rouse, J.W., Haas, R.H., Schell, J.A., y Deering, D.W. 1974. Monitoring vegetation systems in the Great Plains with ERTS, In: S.C. Freden, E.P. Mercanti, and M. Becker (eds) Third Earth Resources Technology Satellite–1 Syposium. Technical Presentations, NASA SP-351, NASA, Washington, D.C., 1: 309-317.

ALS-based forest inventory data and stem data from harvester to predict timber quality of Norway spruce structural timber

Carolin Fischer[1], Marius Hauglin[1], Terje Gobakken[1], Olav Høibø[1], Geir I. Vestøl[1]

[1] Norwegian University of Life Sciences, Department of Ecology and Natural Resource Management, P.O. Box 5003, NO-1432 As, Norway.

Keywords: Strength grading, timber properties, forest inventory

The properties of structural timber vary significantly at different levels, making strength grading of each single board crucial. Norway spruce (Picea abies) is the main species for the production of structural timber in Norway, and most of the strength grading machines used account for only parts of the great variation. In order to meet the requirements of timber properties from all subsamples, the grading has to be conservative, resulting in a poor utilization of the properties of the timber resource. The yield of higher strength classes can potentially be improved by combining machine strength grading with knowledge about the timber resource, and thereby improve the competitiveness for timber as a structural material. Different methods to predict timber properties prior to sawing have been investigated, and one possibility is to use more information about the origin of the timber. The aim of the current study is to predict the distribution of timber properties at the sawmill based on ALS data, forest inventory data and stem data from the harvester.

We collected timber from four sites in southeastern Norway. On each site, 20 trees were selected and the timber was graded in a local sawmill. We developed single-tree models predicting timber strength using variables derived from ALS and harvester data. These models provide valuable insight in the potential of forest inventory and remote sensingdata to predict important timber properties to improve strength grading.

Characterization of forest structures through the synergetic fusion of airborne LiDAR and multispectral sensor-derived difference vegetation index.

Manzanera, JA., García-Abril, A., Pascual, C, Tejera, R, Martín-Fernández S, Martínez-Falero E, Valbuena, R[2].

Affiliation(s) & Corresponding Author(s):
Research Group for Sustainable Management SILVANET FoReStLab, College of Forestry and Natural Environment, Technical University of Madrid, Ciudad Universitaria, 28040 Madrid, Spain.
[2] University of Eastern Finland. Faculty of Forest Sciences. Yliopistokatu 7. 80100 Joensuu, Finland; and: University of Cambridge. Department of Plant Sciences. Downing St. CB2 3EA Cambridge, UK.
Corresponding author: J.A. Manzanera (joseantonio.manzanera@upm.es).

Keywords (5-8) Airborne laser scanning; Data fusion; Difference Vegetation Index; Forest Structural Types; multispectral imagery; Stand structure.

Abstract

The aim of this contribution is the incorporation of complementary multispectral information from optical sensors to Light Detection and Ranging (LiDAR), particularly through the incorporation of complementary multispectral information from optical sensors by back-projecting the LIDAR points onto the multispectral image. Canonical Correlation Analysis (CCA) was performed to relate multivariate data sets of both LIDAR and multispectral metrics with structural variables measured in a Scots pine stand. The correlation coefficient between pairs of canonical variables ranged from 0.997 to 0.949 for the four significant pairs. The amount of explained variance in the response component ranged from 99.39% to 90.1%, and an 86.2% accumulated variance was explained. We related indicators of stand development, i.e. height and volume, with LIDAR elevation metrics, tree size and stand density, representing maturity of the stand, and LIDAR elevation metrics and three red edge index-based multispectral metrics with Lorenz curve-derived attributes, which represent size heterogeneity within the stand, in the first three pairs of canonical variables. The third pair of canonical variables was interpreted as an indicator of size variability, discriminating even-sized from uneven-sized stands, which also benefited from the multispectral information. In the fourth pair of canonical variables, four red edge index metrics significantly explained the heterogeneity of the stand. We may conclude that metrics from the optical sensor complemented information of the LIDAR sensor.

Introduction

Initial studies of forest structure inferred from LIDAR advanced incorporating predictors derived from satellite multispectral datasets (Pascual et al., 2010). Data fusion of both LIDAR and optical passive sensors, such as multispectral photography, have synergic capabilities for providing reliable inventories for operational forestry (Packalén et al., 2009; Valbuena et al., 2013). Estimation of forest parameters from ALS can also be assisted by image analysis, increasing the potential of multispectral imagery for thematic classification and index calculation (St-Onge and Achaichia, 2001).

Appropriate automated geometric correspondence of simultaneously acquired LIDAR and aerial multispectral imagery, plus the positioning of LIDAR points on the conical projection of uncorrected aerial pictures is a method known as back-projecting, which successfully permitted allocating the original radiometric information in the LIDAR point cloud (Valbuena et al 2011, 2013).

Therefore, our purpose is to analyze the canonical relationship between two coincident multivariate datasets, one containing both LIDAR and passive optical sensor measurements, and the other containing field measurements of forest stands.

Materials and Methodology

The study area is the Valsaín forest (Spain; latitude: 40°53′ – 41°15′ N; longitude: 3°59′ – 4°18′ W; altitude 1300 – 1500 m above sea level), which is attached to the Sierra de Guadarrama National Park, with Scots pine (*Pinus sylvestris* L.) as the main species. Field survey consisted of 37 circular plots of 20 m-radius sampled in a cluster design, where the standard dasometric variables were inventoried.

Remote sensing data was simultaneously acquired with a discrete-pulse multi-return airborne laser scanner ALS50-II (Leica Geosystems, Switzerland), and a digital mapping camera DMC (Zeiss-Intergraph, Germany) system consisting of four charge-coupled device (CCD) frame array sensors. With Red and NIR data we generated the Red edge (*redge*) index (Gautam et al., 2010):

$$redge = NIR - Red \quad (1)$$

Canonical Correlation Analysis (CCA) was performed to assess the interrelationships between two data sets of variables: LIDAR and multispectral metrics, on one side (the predictor dataset), and forest structure indicators, on the other.

Results

A multivariate data set of both LiDAR and multispectral metrics could be related with a multivariate data set of stand structural variables measured in a Scots pine forest through Canonical Correlation Analysis. Four statistically significant pairs of canonical variables were found, which explained 84.2% accumulated variance. The first pair of canonical variables related indicators of stand development, i.e. height and volume, with LiDAR height metrics. The second pair related stand density to LiDAR variables determining canopy coverage. The third and fourth pairs of canonical variables pertained to Lorenz curve-derived attributes, which are measures of within-stand tree size variability and heterogeneity, able to discriminate even-sized from uneven-sized stands. The most relevant result was to find that metrics derived from the multispectral sensor showed significant explanatory potential for the prediction of these structural attributes.

Conclusions

In light of the obtained results, we concluded that metrics derived from the optical sensor have potential for complementing the information from the LiDAR sensor in describing structural properties of forest stands. We therefore recommend the use of back-projecting for jointly exploiting the synergies of both sensors using similar types of metrics as they are customary in forestry applications of LiDAR.

References

Gautam B.R., Tokola T., Hamalainen J., Gunia M., Peuhkurinen J., Parviainen H. (2010) - Integration of airborne LiDAR, satellite imagery, and field measurements using a two-phase sampling method for forest biomass estimation in tropical forests. In: International Symposium on "Benefiting from Earth Observation". Kathmandu, Nepal.

Packalén P, Suvanto A, Maltamo M (2009) A two stage method to estimate species-specific growing stock. Photogramm Eng Remote Sens 75:1451–1460

Pascual C., A. Garcıa-Abril, L.G. Garcıa-Montero, S. Martın-Fernandez, W.B. Cohen. Object-based semi-automatic approach for forest structure characterization using lidar data in heterogeneous Pinus sylvestris stands. Forest Ecology and Management 255 (2008) 3677–3685.

St-Onge, A., and Achaichia, N. (2001). - Measuring forest canopy height using a combination of LIDAR and aerial photography data. International Archives of Photogrammetry and Remote Sensing, 343 W4, pp.131-137

Valbuena R., Mauro F., Arjonilla F. and Manzanera J. A., Comparing Airborne Laser Scanning-Imagery Fusion Methods Based on Geometric Accuracy in Forested Areas. Remote Sensing of Environment. 115 (2011) 1942–1954.

Valbuena, R., De Blas, A., Martín Fernández, S., Maltamo, M., Nabuurs, G.J., & Manzanera, J.A. (2013) Within-species benefits of back-projecting laser scanner and multispectral sensors in monospecific Pinus sylvestris forests. European Journal of Remote Sensing 46: 491 – 509.

POSTER

Characterization of forest structures through the synergic fusion of airborne LiDAR and multispectral sensor-derived difference vegetation index

Manzanera, JA., García-Abril, A., Pascual, C, Tejera, R, Martín-Fernández S, Martínez-Falero E, Valbuena, R.

Affiliation:
Research Group for Sustainable Management SILVANET FoReStLab, College of Forestry and Natural Environment, Technical University of Madrid, Ciudad Universitaria, 28040 Madrid, Spain.

Key words Airborne laser scanning; Data fusion; Difference Vegetation Index; Forest Structural Types; multispectral imagery; Stand structure.

Abstract

The aim of this contribution is the incorporation of complementary multispectral information from optical sensors to Light Detection and Ranging (LiDAR), particularly through data fusion by back-projecting the LiDAR points onto the multispectral image.
Materials and methods used:
A multivariate data set of both LiDAR and multispectral metrics was related with a multivariate data set of stand structural variables measured in a Scots pine forest through Canonical Correlation Analysis.

Main Results:
Four statistically significant pairs of canonical variables were found, which explained 84.2% accumulated variance. The first pair of canonical variables related indicators of stand development, i.e. height and volume, with LiDAR height metrics. The second pair related stand density to LiDAR variables determining canopy coverage. The third and fourth pairs of canonical variables pertained to Lorenz curve-derived attributes, which are measures of within-stand tree size variability and heterogeneity, able to discriminate even-sized from uneven-sized stands. The most relevant result was to find that metrics derived from the multispectral sensor showed significant explanatory potential for the prediction of these structural attributes. Therefore, we concluded that metrics derived from the optical sensor have potential for complementing the information from the LiDAR sensor in describing structural properties of forest stands. We therefore recommend the use of back-projecting for jointly exploiting the synergies of both sensors using similar types of metrics as they are customary in forestry applications of LiDAR.

Effect of flying altitude, scanning angle and scanning mode on the accuracy of ALS based forest inventory

Juha Keränen[1], Matti Maltamo[1], Petteri Packalen[1]

Affiliation and address (including e-mail address) for each author
[1]Faculty of Science and Forestry, School of Forest Sciences. University of Eastern Finland, P.O. Box 111, FI-80101 Joensuu, Finland. FAX: +358 29 4457 316.
Email: juha.keranen@uef.fi; matti.maltamo@uef.fi; petteri.packalen@uef.fi

Keywords: ALS, flying altitude, scanning angle, scanning mode, bootstrap approach, forest inventory

Abstract

Many countries are nowadays collecting airborne laser scanning (ALS) data nation-wide to produce high quality elevation data. While ALS data is used in the forest inventory, the ALS data acquisition costs form a remarkable proportion of the total inventory costs. Also the accuracy of the ALS based forest inventory is closely dependent on ALS data. That is the reason why ALS data collection parameters must be carefully defined. These extrinsic parameters have been assessed in numerous studies about a decade ago, but since then ALS devices have developed and it is possible that previous findings do not hold true with newer technology.

In this study the effect of flying altitudes (2000, 2500 or 3000 m), scanning angles (±15° and ±20° off nadir) and scanning modes (single- and multiple pulses in air) with the area-based approach using a Leica ALS70HA-laser scanner was studied. The study was conducted in a managed pine-dominated forest area in Finland, where eight separate discrete-return ALS data were acquired with the same aerial coverage. With these ALS data sets and field data comprising 47 field sample plots the estimates for plot-level volume and mean height were calculated. The comparison of results of the different data sets was based on the bootstrap approach with 5-fold cross validation.

Results indicated that the narrower scanning angle (±15° i.e. 30°) led to slightly more accurate estimates of plot volume (RMSE%: 21-24 vs. 22.5-25) and mean height (RMSE%: 8.5-11 vs. 9-12). In addition, the results indicated that a moderate increase in flying altitude does not directly decrease the accuracy of the prediction. This is the situation not only with the narrower scanning angle but also with the wider scanning angle. This can be considered as a positive finding because it means that (almost) the same RMSE% can be obtained at a lower cost. Our analysis also indicated that contemporary ALS technology enables the use of multiple pulses in air mode.

Forest aboveground biomass mapping in Mexico using SAR, optical and airborne LiDAR data

Mikhail Urbazaev[1], Christiane Schmullius[1], Christian Thiel[1], Bruce Cook[2], Ralph Dubayah[3], Mirco Migliavacca[4], Markus Reichstein[4]

[1]Friedrich-Schiller-University, Jena, Germany
[2] NASA Goddard Space Flight Center, Greenbelt, MD, USA
[3] University of Maryland, College Park, MD, USA
[4]Max-Planck-Institute for Biogeochemistry, Jena, Germany

Keywords: aboveground biomass, Mexico, remote sensing, ALOS PALSAR, Landsat, airborne LiDAR

Abstract

Information on the spatial distribution of aboveground biomass (AGB) over large areas is needed for understanding and managing the processes involved in the carbon cycle, and supporting international policies for climate change mitigation and adaption. Furthermore, these products provide local stakeholders with important baseline data for the development of sustainable management strategies. Using remote sensing techniques it is possible to provide spatially explicit information of AGB from local to global scales. In this work we present a twostage upscaling approach to estimate forest aboveground biomass in Mexico at national scale based on multi-sensor remote sensing data. For this, we estimate firstly AGB along the airborne LiDAR transects using Mexican National Forest Inventory data collected by CONAFOR and very high resolution NASA G-LiHT LiDAR data. We calculated from discrete-return LiDAR data more than 80 LiDAR metrics that are then related to field-estimated AGB. In the next step, we calibrate active (ALOS PALSAR) and passive satellite imagery (Landsat) with LiDAR-based AGB estimates in a non-parametric Random Forest model to create a national wall-to-wall AGB map. Finally, the generated AGB product is validated using independent Mexican National Forest Inventory data that were not used for model training. Furthermore, we modeled AGB at national scale using satellite imagery and National Forest Inventory data only and compared to the results from the two-stage up-scaling approach in order to show a benefit of using airborne LiDAR data for large-area mapping. With airborne LiDAR data we increase a number of calibration data, which leads to a robust estimation of AGB. Moreover, since field measurements are limited to point measurements, they cannot adequately describe patterns at different spatial scales. In contrast, airborne LiDAR data captures spatial variability of forest structure and improves estimation of AGB.

GEDI Biomass Model Development in Tropical Forests

Laura Duncanson[1], Jim Kellner[2], Steve Hancock[3], John Armston[3], Hao Tang[3], Suzanne Marselis[3], Ralph Dubayah[3]

[1]Biospheric Sciences Laboratory, Goddard Space Flight Center (GSFC), NASA
[2]Institute at Brown for Environment and Society, Brown University
[3]Department of Geographical Sciences, University of Maryland, College Park

Key Words: GEDI, waveform LiDAR, biomass, tropics

The Global Ecosystem Dynamics Investigation (GEDI) is a NASA funded, University of Maryland (UMD) led mission to measure forest structure from the International Space Station. GEDI will be launched in early 2019 and provide waveform LiDAR measurements of Earth's forests between ~51 degrees North and South. One of the mission's primary goals is to produce an empirically derived map of aboveground biomass (AGB). To estimate biomass from GEDI data, models are being developed from existing spatially and temporally coincident airborne LiDAR and field measurements. Airborne LiDAR are processed to simulate GEDI waveforms, from which waveform metrics are extracted. These metrics, (e.g. height percentiles), are empirically related to field estimates of AGB. Here, we present first results from tropical forests in Africa, Central and South America. This presentation includes results from Tanzania, Gabon, the Democratic Republic of Congo, Costa Rica, Panama, Borneo, Brazil, French Guyana, and Columbia. We develop models both at the footprint (25 m diameter circle) and multi-footprint level to assess the sensitivity of modeling results to spatial scale. We test cross-validated model accuracy using different regression modeling frameworks including multiple linear, stepwise linear, hierarchical Bayesian, and random forests. Accuracies are assessed as a function of topography, height, canopy cover, biomass, and eco-region. Preliminary results show that modeling accuracy decreases with increasing biomass, and increases with increasing plot size.

Improved forest cover mapping based on MODIS time series and landscape stratification

Jean-Philippe Denux[1], Véronique Chéret[1], Emmanuelle Cano[1], Mar Bisquert[2] and Laurence Hubert-Moy[3]*

[1] Dynafor, Université de Toulouse, INRA, INPT, INP-EI Purpan, Toulouse, France
[2] Universidad de Castilla-la-Mancha, Ciudad Real, Spain
[3] Laboratoire LETG COSTEL, Université de Rennes 2, Rennes, France
[*]Corresponding author, e-mail address: veronique.cheret@purpan.fr

Keywords: classification; stratification; MODIS; time series; object based image analysis; forest cover mapping

Introduction

In Europe most of the forest inventories focus on forest only without giving detailed information other natural vegetation. Forest maps use mainly a vector-based approach where polygons consider forest stands as homogeneous. They updated approximatively every 10 years. Nomenclatures and classes definition change over different countries, even over different provinces. We aim to use remote sensing image as complementary source of information to take into account more types of forests and natural vegetation, to consider mixed forest stands and gradients, to propose updates regularly, and to homogenize nomenclatures. But detailed forest cover mapping at a regional scale by supervised classification is technically limited by various factors. In a heterogeneous mountain area, this study presents three points: the ability of an OBIA landscape stratification method to improve classification accuracy, the impact of time compositing and finally the interest of studying temporal consistency for accuracy assessment.

Materials

The study area is the Pyrenees mountain range located at the border of France, Spain and Andorra, covering a 75000 km² area. The elevation rises from sea level to over 3000 m, with climatic influences from Atlantic Ocean and Mediterranean Sea. We processed MOD13Q1 products of Terra-MODIS, using both NDVI (Rouse et al. 1973) and EVI (Huete et al. 2002) in 16-day composite images, at 250 m spatial resolution. The time series spans from 2000 to 2014, with 23 synthesis per year. We used as a reference a synthesis of existing forest inventories, namely the "Inventaire Forestier National" (IFN, http://inventaire-forestier.ign.fr/spip/) for France, the "Mapa Forestal de España" (MFE, www.magrama.gob.es/es/biodiversidad/servicios/banco-datos-naturaleza/informacion-disponible/mfe50.aspx) for Spain and the "Mapa Forestal del Principat d'Andorra" (MFPA, http://www.iea.ad/mapa-forestal-del-principat-dandorra) for Andorra. An harmonized forest type nomenclature was created from this database, composed of 22 forest and natural vegetation classes.

Methodology

Stratification

The supervised classification was based on Maximum Likelihood algorithm (ML). ML is parametric approach, based on the hypothesis that the values of each class are normally distributed in a multidimensional features space (Richards 2013). This may be a limitation to classify heterogeneous natural vegetation over wide areas. To deal with this problem an approach using spatial strafication to divide each class into more homogeneous sub-classes is frequently used (Richards and Kingsbury 2014). The first step of the stratification was to delineate radiometrically homogeneous regions considered as landscape units using the object segmentation method developed by (Bisquert et al. 2015). Principal component analysis was apply to monthly synthesis of EVI to select the 3 most representative dates. Haralick textural indices (homogeneity, contrast, dissimilarity, entropy and second moment) were

Table 1: Combination of variety and frequency

			Variety	
			1	2 to maximum
			Stable	Unstable
Frequency	Maximum (every year)	Always classified as the reference	*Stable and classified as the reference*	-
	Intermediate values		-	*Errors and change*
	0	Never classified as the reference	*Stable affected to a class different from the reference*	*Errors and change*

processed on a 5x5 pixels window. Then, the best combination of EVI and textural index and optimal scale parameters for segmentation, were chosen with unsupervised evaluation methods (Johnson and Xie 2011; Zhang et al. 2012). The second step was to simplify the 56 homogeneous landscape units created. Non-forested units were eliminated. Each units with too small an area was merged with the most similar nearby unit. Finally 25 homogeneous landscape units were kept as strata. Classification accuracies with and without stratification were compared globally and per strata. Indices describing the topographical and landscape of the strata were used to identify characteristics related with improvement of classification's quality (Cano et al. 2017).

Input data and time compositing

Previously to the stratification, we analyzed the effect of the organization of input data on the quality of the classification, we compared:

- NDVI and EVI
- Annual temporal compositing: 3 dates, all the dates, all dates except winter
- Inter-annual compositing: all the images for 1, 2 or 3 years, and calculating average images for each date over 2 or 3 years.

Classifications with different combinations were compared.

Temporal consistency

Kappa, producer's and user's accuracy and reject fraction were used to assess the classification quality (Congalton 1991). These indicators were calculated using the synthesis of forest inventories as a reference, selecting the pixels fully included in forest polygons. Particular emphasis was made on the temporal consistency of the results (Darren et al. 2012). Frequency, variety and their combination were caculated as indicator of temporal consistency using all the classifications processed from 2000 to 2014. Frequency indicates the number of years a pixel is classified as the reference. Variety shows the number of different classes are assigned to a pixel. Their combination allows to identify 3 categories of results:

- Stable and classified as the reference
- Stable assigned to a class different from the reference
- All others cases considered as error or change

Results

Input data and time compositing

Kappa values presented (figure 1) show clearly the interest of using all the available dates, aside from winter, for 3 years. Kappa value rises from 0.35 to more than 0.50 between a data set composed of 3 dates of NDVI for 1 year and the one composed of all available dates, aside from winter, for 3 years. Furthermore classifications based on NDVI systematically show better results than the one based on EVI.

Stratification

We compare classification for 2007-2009 and 2009-2011 three years period, for NDVI. Kappa index values increased similarly for both periods, respectively, from 0.53 to 0.65 and from 0.52 to 0.64. Meanwhile, reject fraction (RF) value increased from 6 to 13%. Results per strata (figure 2) show that higher Kappa are usually accompanied by high reject fraction.

Most of the topographical and landscape indices have no particular influence on the classifications quality (table 2). The area and the forest cover rate for each stratum are the only indices correlated with the

Figure 1: Effect of time compositing on Kappa

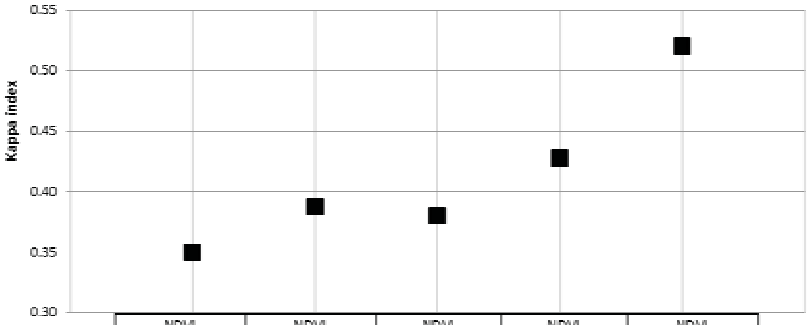

NDVI	NDVI	NDVI	NDVI	NDVI
3 dates	no winter (9 months)	complete year	Complete year, no winter	Complete year, no winter
1 year	1 year	1 year	3 years averaged	3 years
3 images	17 images	23 images	17 images	51 images

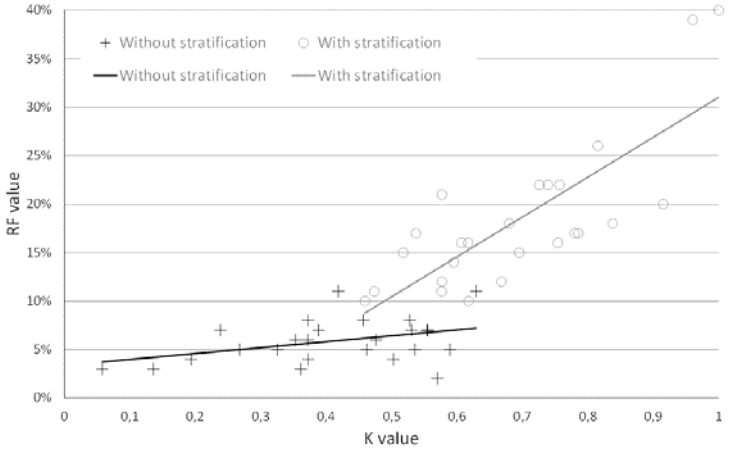

Figure 2: Effect of stratification on Kappa and reject fraction per strata

Index	K difference	RF difference
Topographical indices		
Stratum area (ha)	**(-) 0.32**	**(-) 0.35**
Elevation (standard deviation) (m)	**(-) 0.38**	**(-) 0.31**
Slope (mean) (°)	**(-) 0.28**	(-) 0.18
Area-derived landscape indices		
Total forest cover rate	(-) 0.09	(-) 0.11
Patch area (average) (ha)	(+) 0.07	(+) 0.003
Patch area (standard deviation) (ha)	**(+) 0.64**	**(+) 0.59**
Composition landscape indices		
Number of classes	**(-) 0.34**	**(-) 0.42**
Diversity Shannon index	(-) 0.10	(-) 0.15

Table 2: Coefficient of determination (R^2) between the stratum indicators and the perstratum K and RF differences for the 2007-2009 period (bold: significant for α=0.01; (+): positive correlation; (-): negative correlation).

increase in classification quality. The interpretation of these indices allows to identify thresholds which leads to differentiate 3 groups:

- Strata with area >450 000 ha and forest area >120 000 ha: with no effect on classification quality
- Strata with area <100 000 ha and forest area <5 000 ha: very high reject fraction
- Intermediate strata presents an enhancement of the classification quality.

Temporal consistency

Mapping the results of the combination of frequency and variety displays a spatial organization of these indicators (figure 3). Groups of pixels identified as stable and misclassified seems to indicate errors in the reference map based on the forest inventories. Unstable pixels are often localized on the border between polygons of two different classes. Our hypothesis is that we may have some noisy data with misregistration or acquisition angle problems. On wider area these unstable pixels may indicate a gradient and mixed pixels where the forest inventories drew a linear limit.

Conclusion

Time series composing shows clearly the advantage of using a three year series as input data for the classification.

The object based stratification is easy to process and useful to improve Maximum Likelihood results. The landscape analysis stratification approach has

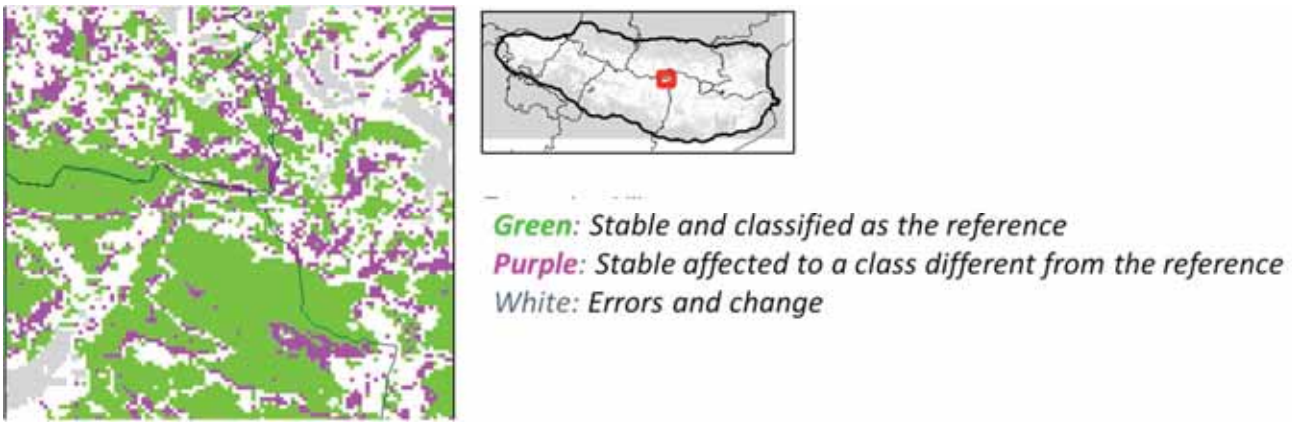

Figure 3: Extract of the map showing the combination of frequency and variety

the same efficiency level as the usual approaches encountered in literature. Only easily accessible remote sensing data have been used and this method does not have to rely on existent thematic map or on expert knowledge. The analysis of the strata landscape characteristics leads to strata definition operational items that could be used to adjust the parameters while creating HLU and defining the strata. Strata area and the forest cover rate are determining attributes to strata delineation. Segmentation parameters can be adjusted to produce an optimized stratification.

Accuracy assessment indicators processed from confusion matrix are limited to the available references. Reject fraction can be used for algorithm quality assessment, furthermore it could be useful for training evaluation and update. Temporal consistency is an original point developed here. It is complementary to existing accuracy assessment. Variability can always be calculated. Frequency is limited to reference availability but allows to benefit from imperfect reference data. Thematic interpretation of their combination needs to be developed to distinguish errors from change.

References

Bisquert, M., Bégué, A., & Deshayes, M. (2015). Object-based delineation of homogeneous landscape units at regional scale based on MODIS time series. *International Journal of Applied Earth Observation and Geoinformation,* 37, 72-82

Cano, E., Denux, J.-P., Bisquert, M., Hubert-Moy, L., & Chéret, V. (2017). Improved forest cover mapping based on MODIS time series and landscape stratification. *International Journal of Remote Sensing, accepted* Congalton, R.G. (1991). A review of assessing the accuracy of classifications of remotely sensed data. Remote *Sensing of Environment,* 37, 35-46

Darren, P., Rasim, L., Ian, O., & Robert, F. (2012). Supervised Classification Approaches for the Development of Land-Cover Time Series. *Remote Sensing of Land Use and Land Cover* (pp. 177-190): CRC Press

Huete, A., Didan, K., Miura, T., Rodriguez, E.P., Gao, X., & Ferreira, L.G. (2002). Overview of the radiometric and biophysical performance of the MODIS vegetation indices. *Remote Sensing of Environment, 83,* 195-213 Johnson, B., & Xie, Z. (2011). Unsupervised image segmentation evaluation and refinement using a multi-scale approach. ISPRS *Journal of Photogrammetry and Remote Sensing, 66,* 473-483

Richards, J.A. (2013). Supervised Classification Techniques. R*emote Sensing Digital Image Analysis* (pp. 247- 318): Springer Berlin Heidelberg

Richards, J.A., & Kingsbury, N.G. (2014). Is There a Preferred Classifier for Operational Thematic Mapping? Ieee Transactions on Geoscience and Remote Sensing, 52, 2715-2725 Rouse, J.W., Haas, R.H., Schell, J.A., & Deering, D.W. (1973). Monitoring Vegetation Systems in the Great

Plains with ERTS. In NASA (Ed.), *Third ERTS Symposium.* Washington, DC, USA

Zhang, X., Xiao, P., & Feng, X. (2012). An Unsupervised Evaluation Method for Remotely Sensed Imagery Segmentation. *Geoscience and Remote Sensing Letters, IEEE,* 9, 156-160

Improving assessment of fire risk in Yunnan Province, China using remote sensing

Jacqueline Rosette[1], Iain Bye[1], Bowei Chen[2], Yongjie Xia[2], Juan Suárez[4], Shengxi Liao[3], Huaiqing Zhang[2], Yong Pang[2], Peter North[1]

[1]Swansea University, Singleton Park, Swansea SA2 8PP, UK
[2]Chinese Academy of Forestry, Institute for Forest Resources and Information Techniques (IFRIT), Beijing, China.
[3]Chinese Academy of Forestry, Resource Institute for Resources and Insects (RIRI), Kunming, China.
[4]Forest Research, Northern Research Station, Roslin EH25 9SY, UK

Key words: fuel model, fire risk, lidar, forest structure, fuelbed characterisation

The Newton Fund aims to strengthen research and innovation partnerships between the UK and emerging knowledge economies, and forms part of the UK's Official Development Assistance (ODA) commitment. A research partnership was developed between collaborators from Swansea University and Forest Research in the UK, and the Chinese Academy of Forestry (IFRIT and RIRI), and funded through a Newton Agritech Project and the Royal Society University Research Fellowship.

Lidar remote sensing was used to produce forest structure, density and canopy profile-based inputs for a fuel model. These enabled potential fuels to be better-characterised using spatial variability of vegetation and canopy structure, reducing assumptions from field data sampling, and improving the resolution of fire risk information.

The project included an intensive, collaborative month-long field campaign in Yunnan Province, China. Remote sensing analysis was used to segment and stratify the landscape using representative land cover classes and age distribution, enabling the impartial selection of field plot locations. The four vegetation classes comprised broadleaf forest, conifer forest, bamboo stands, and economic shrubs (tea and coffee). Broadleaves and conifers were further subcategorised into young, pole and mature classes.

The project adapts and applies the US Forest Service Fuel Characteristic Classification System (FCCS) to the Chinese context. Lidar permitted direct observations and estimates of the spatial variability of canopy structure, fractional cover, and dynamic vegetation parameters which are key to the successful estimation of fire risk. Understorey shrubs, ladder fuels, herb layer and litter were less easily estimated using remote sensing and were therefore characterised using mean static values from field investigation for each vegetation class. SMAP data were additionally incorporated in order to assess seasonal variability of susceptibility of a fuelbed to surface and crown fires, and to consume fuels.

The methodology reduces the assumptions based purely on vegetation type that would otherwise be typically formed from a coarse, ground-based sampling scheme and conventional field procedures. The results can inform management decisions regarding risk potential and containment, allowing specific at-risk stands to be managed or monitored accordingly e.g. using fire breaks or managing undergrowth. The proximity of shrub and forest agriculture to rural dwellings, and the spatial assessment of fire susceptibility and behaviour potential, can have societal implications, both for economic security (i.e. loss of potential revenue) and for population safety.

Industrial forest mapping: a Landsat Spatial and Temporal Approach

Luigi Boschetti, Lian-Zhi Huo*, Nuria Sanchez Lopez*, Andrew Hudak**, Alistair Smith*, Robert Keefe**

** College of Natural Resources, University of Idaho, Moscow, ID 83844, USA*
*** Rocky Mountain Research Station, US Forest Service, Moscow, ID 83844, USA*

Keywords: Forest Mapping and Inventory, Landsat, Automatic processing, Object Oriented, Deforestation, Industrial Forestry

Abstract

Remote sensing has been widely used for mapping and characterizing changes in forest cover, but the available remote sensing forest change products are not discriminating between deforestation (permanent transition from forest to non-forest), industrial forest management (logging followed by regrowth, with no land use change) and natural disturbances such as insect damage and fires (forest cover loss followed by regrowth, also with no land use change) (Hansen et al, 2010). Current estimates of carbon-equivalent emissions report the contribution of deforestation as 12% of total anthropogenic carbon emissions (van der Werf et al., 2009), but accurate monitoring of forest carbon balance should discriminate between land use change related to forest natural disturbances, and forest management. The total change in forest cover (Gross Forest Cover Loss, GFLC) needs to be characterized based on the cause (natural/human) and on the outcome of the change (regeneration to forest/transition to non/forest)(Kurtz et al, 2010). Industrial forestry is nowadays highly optimized: economic profitability forces the adoption of standard practices resulting in very clear spatial patterns evident to human interpreter, but hardly detectable with traditional satellite mapping approaches. To overcome these challenges, we propose a methodology for post-processing forest cover change maps (Hansen et al., 2013) by classifying each forest cover loss detection as either (a) deforestation, (b) fire and insect disturbances or (c) forest management practices. The classification methodology combines the use of multitemporal Landsat data time series, and object-oriented analysis of shapes, textures, and spatial relationships of the areas of forest cover loss. The methods are demonstrated by wall-to-wall classification of the forest cover loss in the conterminous United States for the 2002-2011 period.

References

Hansen, M.C., Stehman, S.V., & Potapov, P.V. (2010). Reply to Wernick et al.: Global scale quantification of forest change. Proceedings of the National Academy of Sciences, 107, E148-E148

Hansen, M. C., Potapov, P. V., Moore, R., Hancher, M., Turubanova, S. A., Tyukavina, A., ... & Kommareddy, A. (2013). High-resolution global maps of 21st-century forest cover change. science, 342(6160), 850-853.

Kurz, W.A. (2010). An ecosystem context for global gross forest cover loss estimates. Proceedings of the National Academy of Sciences, 107, 9025-9026

van der Werf, G.R., Morton, D.C., DeFries, R.S., Olivier, J.G., Kasibhatla, P.S., Jackson, R.B., Collatz, G.J., & Randerson, J. (2009). CO_2 emissions from forest loss. Nature Geoscience, 2, 737-738

POSTER

Improving merchantable timber volume accuracy for balsam fir plots by analyzing the spatial distribution of airborne LiDAR returns

Sarah Yoga B., Jean Bégin, Benoît St-Onge, Martin Riopel

Sarah Yoga B. (sarah.yoga-bengbate.1@ulaval.ca), Department of Wood and Forest Sciences, Laval University, Quebec City, QC, Canada.
Jean Bégin (jean.begin@sbf.ulaval.ca), Department of Wood and Forest Sciences, Laval University, Quebec City, QC, Canada.
Benoît St-Onge (st-onge.benoit@uqam.ca), Department of Geography, Université du Québec à Montréal, QC, Canada.
Martin Riopel (martin.riopel.1@ulaval.ca), Department of Wood and Forest Sciences, Laval University, Quebec City, QC, Canada.

Keywords: Lidar, merchantable volume, balsam fir, spatial distribution, density, residual variance.

Abstract

Airborne Laser Scanning data (ALS) are now regularly used to characterize forest structure. In this study, we determined the effects of the scanning angle settings of an ALS system and those of the point spacing on the accuracy of merchantable timber volume estimates of balsam fir plots in eastern Canada. We used the ALS point cloud to compute predictor variables of the merchantable volume in a nonlinear model. Our best model included ALS mean height, the proportion of first returns below 2 m and the rumple index. Our analysis showed a high correlation (pseudo-R^2 = 0.91, RSE = 27.5 $m^3.ha^{-1}$) between ALS and field data of 119 plots. A more accurate merchantable volume estimate was obtained from ALS data by focusing in the explanation of the residual variance of a standard prediction model. We reduced the RSE (residual standard error) from 27.5 $m^3.ha^{-1}$ to 13.5 $m^3.ha^{-1}$ by including a variable accounting for the spatial distribution of the ALS returns in our model. There was, however, no effect of the ALS returns density on the merchantable volume models (p=0.74). This suggests that the spatial distribution of ALS returns rather than the point density should be considered when deriving merchantable volume estimates from ALS data.

Industrial forest mapping: a Landsat Spatial and Temporal Approach

Luigi Boschetti[1], Lian-Zhi Huo[1], Nuria Sanchez Lopez[1], Andrew Hudak[2], Alistair Smith[1], Robert Keefe[1]

[1] College of Natural Resources, University of Idaho, Moscow, ID 83844, USA
[2] Rocky Mountain Research Station, US Forest Service, Moscow, ID 83844, USA

Keywords Forest Mapping and Inventory, Landsat, Automatic processing, Object Oriented, Deforestation, Industrial Forestry

Abstract

Remote sensing has been widely used for mapping and characterizing changes in forest cover, but the available remote sensing forest change products are not discriminating between deforestation (permanent transition from forest to non-forest), industrial forest management (logging followed by regrowth, with no land use change) and natural disturbances such as insect damage and fires (forest cover loss followed by regrowth, also with no land use change) (Hansen et al, 2010). Current estimates of carbon-equivalent emissions report the contribution of deforestation as 12% of total anthropogenic carbon emissions (van der Werf et al., 2009), but accurate monitoring of forest carbon balance should discriminate between land use change related to forest natural disturbances, and forest management. The total change in forest cover (Gross Forest Cover Loss, GFLC) needs to be characterized based on the cause (natural/human) and on the outcome of the change (regeneration to forest/transition to non/forest)(Kurtz et al, 2010). Industrial forestry is nowadays highly optimized: economic profitability forces the adoption of standard practices resulting in very clear spatial patterns evident to human interpreter, but hardly detectable with traditional satellite mapping approaches. To overcome these challenges, we propose a methodology for post-processing forest cover change maps (Hansen et al., 2013) by classifying each forest cover loss detection as either (a) deforestation, (b) fire and insect disturbances or (c) forest management practices. The classification methodology combines the use of multitemporal Landsat data time series, and object-oriented analysis of shapes, textures, and spatial relationships of the areas of forest cover loss. The methods are demonstrated by wall-to-wall classification of the forest cover loss in the conterminous United States for the 2002-2011 period.

References

Hansen, M.C., Stehman, S.V., & Potapov, P.V. (2010). Reply to Wernick et al.: Global scale quantification of forest change. Proceedings of the National Academy of Sciences, 107, E148-E148

Hansen, M. C., Potapov, P. V., Moore, R., Hancher, M., Turubanova, S. A., Tyukavina, A., ... & Kommareddy, A. (2013). High-resolution global maps of 21st-century forest cover change. science, 342(6160), 850-853.

Kurz, W.A. (2010). An ecosystem context for global gross forest cover loss estimates. Proceedings of the National Academy of Sciences, 107, 9025-9026

van der Werf, G.R., Morton, D.C., DeFries, R.S., Olivier, J.G., Kasibhatla, P.S., Jackson, R.B., Collatz, G.J., & Randerson, J. (2009). CO2 emissions from forest loss. Nature Geoscience, 2, 737-738

Inventory of Small Forest Areas Using an Unmanned Aerial System

Stefano Puliti, Hans Ole Ørka, Terje Gobakken, and Erik Næsset

Department of Ecology and Natural Resource Management, Norwegian University of Life Sciences, PO Box 5003, NO-1432 Ås, Norway

Keywords: UAS; forest inventory; area-based approach; structure from motion; photogrammetry

Abstract

Acquiring high spatial and temporal resolution imagery from small unmanned aerial systems (sUAS) provides new opportunities for inventorying forests at small scales. Only a few studies have investigated the use of UASs in forest inventories, and the results are inconsistent and incomplete. The present study used three-dimensional (3D) variables derived from UAS imagery in combination with ground reference data to fit linear models for Lorey's mean height (h_L), dominant height (h_{dom}), stem number (N), basal area (G), and stem volume (V). Plot-level cross validation revealed adjusted R2 values of 0.71, 0.97, 0.60, 0.60, and 0.85 for h_L, h_{dom}, N, G, and V, respectively, with corresponding RMSE values of 1.4 m, 0.7 m, 538.2 ha^{-1}, 4.5 $m^2 \cdot ha^{-1}$, and 38.3 $m^3 \cdot ha^{-1}$. The respective relative RMSE values were 13.3%, 3.5%, 39.2%, 15.4%, and 14.5% of the mean ground reference values. The mean predicted values did not differ significantly from the reference values. The results revealed that the use of UAS imagery can provide relatively accurate and timely forest inventory information at a local scale. In addition, the present study highlights the practical advantages of UAS-assisted forest inventories, including adaptive planning, high project customization, and rapid implementation, even under challenging weather conditions.

Large scale timber volume prediction with digital aerial photogrammetry and national forest inventory data

Johannes Rahlf[1], Johannes Breidenbach[1], Svein Solberg[1], Erik Næsset[2], Rasmus Astrup[1]

[1] National Forest Inventory, Norwegian Institute of Bioeconomy Research, Postboks 115, NO-1431 Ås, Norway
[2] Norwegian University of Life Sciences, Postboks 5003, NO-1432 Ås, Norway

Digital aerial photogrammetry (DAP) is a relatively new source of high resolution 3D information for remote sensing assisted forest inventories. Forest parameters have been predicted with similar accuracy as with airborne laser scanning (ALS) on small study areas with homogeneous conditions. Accuracies for large scale applications, however, have not yet been reported. In our study we used DAP and national forest inventory (NFI) data to fit a timber volume prediction model on a large area with varying terrain and forest vegetation. Based on this model, we tested the influence of various factors on the accuracy.

Aerial images were acquired in 2010 and 2013 over two adjacent areas in central Norway. The total area was 24 473 km2. The two image blocks were processed separately to point clouds using different matching strategies. A digital terrain model based on ALS data was used to extract vegetation heights. Timber volume measurements of 513 National Forest inventory plots which had been collected during a period of five years were used as reference data. We calculated numerical metrics describing the height distribution of the DAP data at the sample plots. A linear model was fitted to the timber volume measurements using DAP height metrics as explanatory variables. Cross validation was used to calculate R^2 and RMSE (root mean squared error) of the model. Additionally, we calculated a range of variables describing the time difference between inventory and image acquisition, the color of the point cloud, and terrain and light conditions. The effect of these additional variables on the model accuracy was used to investigate the influence of the heterogeneous conditions caused by large area coverage.

The model based on the DAP height metrics had a R^2 of 0.83 and a RMSE of 38 m3 ha-1, which corresponded to 49% of the mean observed timber volume. Including relative sun inclination during the image acquisition at the inventory plot, as well as the time difference between the inventory and the aerial image acquisition showed the largest influence on the model accuracy. The R^2 increased to 0.85 and the RMSE was reduced to 35 m3 ha-1 (45%). The time difference of the two image acquisitions in combination with different matching strategies had only a marginal influence on the accuracy.

Large-Scale Prediction of Aboveground Biomass in Mountain Forests Utilizing Airborne Laser Scanning

Maltamo, M.[1], Bollandsås, O.M.[2], Gobakken, T.[2] and Næsset E.[2]

[1] University of Eastern Finland, Finland. P.O.Box 111, 80101 Joensuu, Finland.
[2] Norwegian University of Life Sciences, Department of Ecology and Natural Resource Management, Norway. P.O.Box 5003, N-1432 Ås, Norway.

Keywords: LiDAR, forest biomass, montane forests, allometry, climatic variation, elevation

Abstract

For most forest attributes (timber volume, biomass, mean height etc.) airborne laser scanning (ALS) has been shown to be the remotely sensed source of auxiliary information that provides the most accurate estimates (e.g. Zolkos et al. 2013). In the case of aboveground biomass (AGB), variation in crown allometry is largely accounted for by the ALS data since the echo distribution resulting from the collection of ALS data is directly dependent on the three-dimensional biomass distribution of the different crown components (e.g., Magnussen & Boudewyn 1998). ALS based forest biomass studies has reported considerably larger errors for the biomass estimates than those found in studies conducted in productive low-land forests (e.g. Montagnoli et al. 2015). The reason may be that montane forests, on small spatial scales, are more heterogeneous with respect to growing conditions and terrain. On a larger scale, climate will also affect growing conditions and allometry.

This study consider ALS based AGB prediction in mountain forests. The objectives of this study were 1) to test the accuracy of ALS-based AGB models calibrated on data comprising high levels of small-scale variation in tree allometry as well as large-scale variation in the underlying growing conditions, 2) to test the additional effect of proxies for growing conditions in models for AGB based on ALS variables, and 3) to test the additional effect of species information in models for AGB based on ALS variables and proxies for growing conditions.

The study area consisted of a long transect from southern Norway to northern parts of the country with wide ranges of elevation and latitude. The transect was covered by ALS data and field data from 238 plots. AGB was modeled using different types of predictor variables, namely ALS metrics, variables related to growing conditions and tree species information. To represent growing conditions, we used climatic metrics, elevation and latitude as predictor variables. We applied both linear regression modeling and *k* nearest neighbor (*k*-nn) imputation. The *k*-nn approach was applied to examine the predicting power of different types of variables, whereas linear regression analysis was performed to construct general and dominant species level ALS-based biomass prediction models.

Modelling of AGB in the long transect covering diverse mountainous forest conditions was challenging, the RMSE values being rather large (37-70%). The effect of growing conditions was minor in predictions. Furthermore, we did not find good proxy variables for different tree forms and climatic conditions that potentially could have provided additional information beyond the tree allometry-related information reflected by the ALS metrics. However, species information was essential to improve accuracy. The analysis revealed that when doing inventories of spruce dominated areas, all plots should be pooled together when the models are developed, whereas if pines or deciduous dominate the area in question, separate dominant species-wise models should be constructed.

References

Magnussen, S., and Boudewyn, P. 1998. Derivations of stand heights from airborne laser scanner data with canopy-based quantile estimators. Can. J. For. Res. 28: 1016-1031.

Montagnoli, A., Fusco, S. Terzaghi, M., Kirsrchbaum, A., Pflugmacher, D, Cohen, W.B., Scippa, G.S., and Chiatanrte, D., 2015. Estimating forest aboveground biomass by low density lidar data in mixed broad-leaved forests in Italian Pre-Alps. Forest Ecosystems 2. doi:10.1186/s40663-015-0035-6.

Zolkos, S.G., Goetz, S.J., and Dubayah, R. 2013. A meta-analysis of terrestrial aboveground biomass estimation using lidar remote sensing. Remote Sens. Environ. 128: 289–298.

Mapping Amazonian biodiversity and geology using basin-wide fern species inventories and Landsat imagery

Jasper Van doninck, Gabriela Zuquim, Hanna Tuomisto
Amazon Research Team, Department of Biology, University of Turku, Finland

Keywords: Amazonia, Landsat TM/ETM+, species composition, soil, classification

Fern species composition has been found to be a predictor of species composition of other plant groups, as well as soil properties. The University of Turku Amazon Research Team and the Brazilian Program for Biodiversity Research have developed rapid fern species inventories methods based on long plots. Collecting 1000 plots over the past 30 years, we have accumulated an exceptionally large and internally consistent data set of fern species composition and soil properties. These field inventories have allowed us to document high local-scale plant heterogeneity, and to identify the interface of geological formations. Evidently, these field inventories are labour intensive and can only cover certain selected regions of the Amazon basin. Satellite remote sensing is an indispensable tool in order to achieve a comprehensive mapping of Amazonian forest biodiversity and geology. Due to the high heterogeneity at the local scale, such mapping requires high resolution images like those acquired by the Landsat satellites. Previous research has shown that spectral patterns in individual Landsat images reflect patterns in fern species composition and geology, but radiometric artefacts in Landsat imagery –caused by, e.g., atmospheric contamination or the bidirectional reflectance distribution function– have for a long time hampered the use of Landsat over larger areas. Recent advances in image preprocessing (atmospheric correction, directional normalization and image compositing) and processing capabilities have now allowed us to generate a radiometrically consistent, cloud-free Landsat TM/ETM+ image composite covering the entire Amazon basin. We here combine this Landsat mosaic with our entire dataset of fern species inventories to obtain a wall-to-wall mapping of plant biodiversity and the underlying soil properties at an unprecedented spatial resolution.

Mapping certified forests for sustainable management - a tool for information improvement through citizen science

Florian Kraxner (International Institute for Applied Systems Analysis - IIASA, Laxenburg, Austria), Dmitry Schepaschenko[*] (IIASA, Laxenburg, Austria), Sabine Fuss (Mercator Research Institute on Global Commons and Climate Change, Berlin, Germany), Anders Lunnan (Norwegian University of Life Sciences, Aas, Norway), Georg Kindermann (Austrian Research and Training Centre for Forests, Natural Hazards and Landscape, Vienna, Austria), Kentaro Aoki (Shinshu University, Nagano, Japan), Martina Dürauer (IIASA, Laxenburg, Austria), Anatoly Shvidenko (IIASA, Laxenburg, Austria), Linda See (IIASA, Laxenburg, Austria)

[*] *Presenting author*

Keywords: forest certification mapping, FSC, PEFC, citizen science, Geo-Wiki

About 10% of forest area has been certified globally, however, the speed of certification has slowed down and the vast majority of certified forests are located in the northern hemisphere. There are currently no spatially explicit, openly accessible data available on forest certification below national level so understanding the drivers of these developments, examining the scope for further certification and using this information for development of future sustainable forest management strategies are challenging. We present a methodology for the development of a spatially explicit global map of certified forest areas as well as an online tool (http://forest.geo-wiki.org) for visualization and interactive improvement of the map, which is aimed at a range of stakeholders including certification bodies, third-party certifiers, green NGOs, forestry organizations, decision-makers, scientists and local experts. A new methodology for downscaling national forest certification statistics has resulted in the first spatially explicit global forest certification map at a 1km resolution. Regional validation (Russia) suggests an overall accuracy of 89%. By building such a community-based online tool, more accurate information on forest certification will become available, promoting the sharing of data and encouraging more transparent and sustainable forest management. Such an approach is intended to encourage transparency in the forest certification arena but will also provide benefits to multiple users, e.g. in monitoring, marketing and in the development of targeted policy strategies.

POSTER

Mapping forest degradation caused by fires in 2010 in Mato Grosso State, Brazilian Amazon using Landsat TM fraction images

Yosio E. Shimabukuro[1,], Egidio Arai[1], Liana O. Anderson[2], Luiz Eduardo Aragão[1], Valdete Duarte[1]*

[1] Instituto Nacional de Pesquisas Espaciais – INPE
Caixa Postal 515 - 12245-970 - São José dos Campos - SP, Brasil
[2] Centro Nacional de Monitoramento de Desastres Naturais – CEMADEN
Parque Tecnológico de São José dos Campos, Estrada Doutor Altino Bondensan, 500,
São José dos Campos - São Paulo, 12247-016
[*] Corresponding author – yosio@dsr.inpe.br

Keywords: Remote Sensing, Image Processing, Forest Degradation, Burned Areas, Forest Fires, Fraction Images.

Abstract

The objective of this work is to assess the extent of forest degraded areas due to fires in 2010 in Mato Grosso State, southern Amazonia. Mato Grosso State has experienced high deforestation rates and therefore forest degradation activities due to fires do occur. For this work, we selected 42 Landsat TM images acquired during the dry season of year 2010**.** The proposed method is based on (i) linear spectral mixing model applied to TM images to derive soil, vegetation and shade fraction images and (ii) image segmentation and classification applied to the shade fraction images. In a first step, a map of forest/non forest areas are derived from Hansen et al. (2013) dataset. Then burned areas are identified and mapped from the shade fraction images. These mapped areas are then distributed in the three land cover types, i.e., forest, non forest (cerrado and old deforestation), and deforested areas from 2001 to 2010. Our results showed that 32% of forests in Mato Grosso were burned during year 2010 (22,633 km^2) likely degrading the forest ecosystem. In addition, 5,175 km^2 (7%) of burning occurred in the areas deforested from 2001 to 2010 and 42,510 km^2 (61%) occurred in the Cerrado and old deforestation areas. The proposed method is efficient for mapping degraded forest areas due to fires. The information is important for the carbon emission estimation.

Introduction

A large part of the gross carbon emissions into the atmosphere due to land cover changes is attributable to deforestation in the tropics (Achard *et al*., 2014). Forest degradation, defined as long-term disturbance in forested areas, is considered to represent up to 40% of the gross emissions from deforestation in the Brazilian Amazon (Aragão *et al*., 2014). In this region deforestation is defined as forest clear cut with conversion to other land uses (INPE, 2008), while forest degradation is related to a combination of selective logging and forest fires (Asner *et al*., 2009, Berenguer *et al*., 2014).

Hansen *et al.* (2013) mapped global tree cover extent, loss, and gain for the period from 2000 to 2012 at a spatial resolution of 30 m, with loss allocated annually. Then from this dataset, the forest/non forest map can be extracted for the year 2000 to 2012 by selecting some tree cover threshold value.

Fraction images derived from different remote sensing sensors have been used for many tropical forest applications, especially in the Brazilian Amazon. Specifically the ones derived from the Landsat Thematic Mapper were tested for this region for mapping areas of degraded forests due to the following characteristics: a) vegetation fraction images highlight the forest cover conditions and allow

differentiating between forest and non-forest areas similarly to vegetation indices such as the Normalized Difference Vegetation Index (NDVI) and the Enhanced Vegetation Index (EVI); b) shade fraction images highlight areas with low reflectance values such as water, shadow and burned areas; and c) soil fraction images highlight areas with high reflectance values such as bare soil and clear-cuts (Shimabukuro *et al.*, 2014). In this context the main purpose of this study is to present an estimate of the extent of degraded forest due to fires in Mato Grosso State, Brazilian Amazon, using a semi-automated procedure based on fraction images derived from TM sensor.

Methodology

The study area corresponds to Mato Grosso State located in the Brazilian Amazon region. Due to variable climate, terrain relief, precipitation patterns, and length of the dry season, the State of Mato Grosso comprises parts of three Brazilian biomes, the Amazon, the Cerrado, and a portion of the Pantanal, and has a naturally very high biodiversity with vegetation types ranging from dense evergreen forest to deciduous open forest, savannas, natural grasslands and seasonal wetlands. This region has taken place a high rate on conversion of vegetation cover not only due to the recent use of mechanized agriculture but also due to deforestation processes, selective logging and burning (INPE, 2005, 2008).

For this work, we selected 42 Landsat TM images at 30 m spatial resolution acquired during the dry season of year 2010 to adapt a methodology developed by Shimabukuro *et al*. (2009) for burned area estimation.

The proposed method for mapping the forest degradation by fire consists in four steps. The first step (i) of our approach is to obtain a forest mask. In this case, we used the Hansen *et al*. (2013) dataset. The second step (ii) consisted in the generation of fraction images (Shimabukuro and Smith, 1991) for the 42 Landsat TM images selected during the dry season of year 2010. The burned areas are assessed from the shade fraction images considering that the shade fraction images highlight areas with low reflectance corresponding to burned areas.

The third step (iii) of our approach was divided in two parts. First, a shade fraction image was segmented and then an unsupervised classification algorithm was applied in order to derive individual and explicit objects (polygons). Secondly, the resulting clusters of objects were assigned as unburned or burned areas from their spectral and textural properties derived from shade fraction images.

The fourth step consists in producing the forest degradation areas due to forest fires (burned forest), by combining the resulting maps of forest/non-forest areas (first step) with the burned area maps (from the third step), i.e. the forested areas that were burned without clear cut during the year 2010.

Results

The forest/non forest map derived from Hansen et al. (2013) shows that forest cover (>50% of tree cover) is 458,677 km^2 and 74,129 km^2 of forest loss from 2000 to 2010 (5,403 km^2 from 2010). Our results (Figure 1) showed that 70,317 km^2 was burned in the State of Mato Grosso during the year 2010. From this amount 5,175 km^2 was deforested and burned and 22,633 km^2 was forest burned, i.e. forest degraded by fire. The most burned areas (42,510 km2) occurred in the non-forest areas (Cerrado and old deforested areas).

The depicted burned areas in Amazonia are related to management activities using fire, to deforestation process, or to a degradation process: in the case of deforestation the forest cover is first clear cut and then the remaining vegetation is burned to allow using the land for agriculture (cropland or grassland). In the case of forest degradation, the forest cover is burned through an uncontrolled fire without removal of wood nor conversion to another land use. This makes the use of a forest/non-forest map essential for differentiating between deforestation and forest degradation processes. Deforested areas will appear as non-forest areas (cropland or grassland) in the successive months or years after the initial deforestation event while burned forests (degraded forest) will recover as forest regrowth (Shimabukuro *et al.*, 2014).

Conclusions

The proposed method is efficient for mapping burned forest areas (degraded forest areas due to fires). An initial forest/non forest map is essential for developing a procedure for mapping degradation areas due to forest fires.

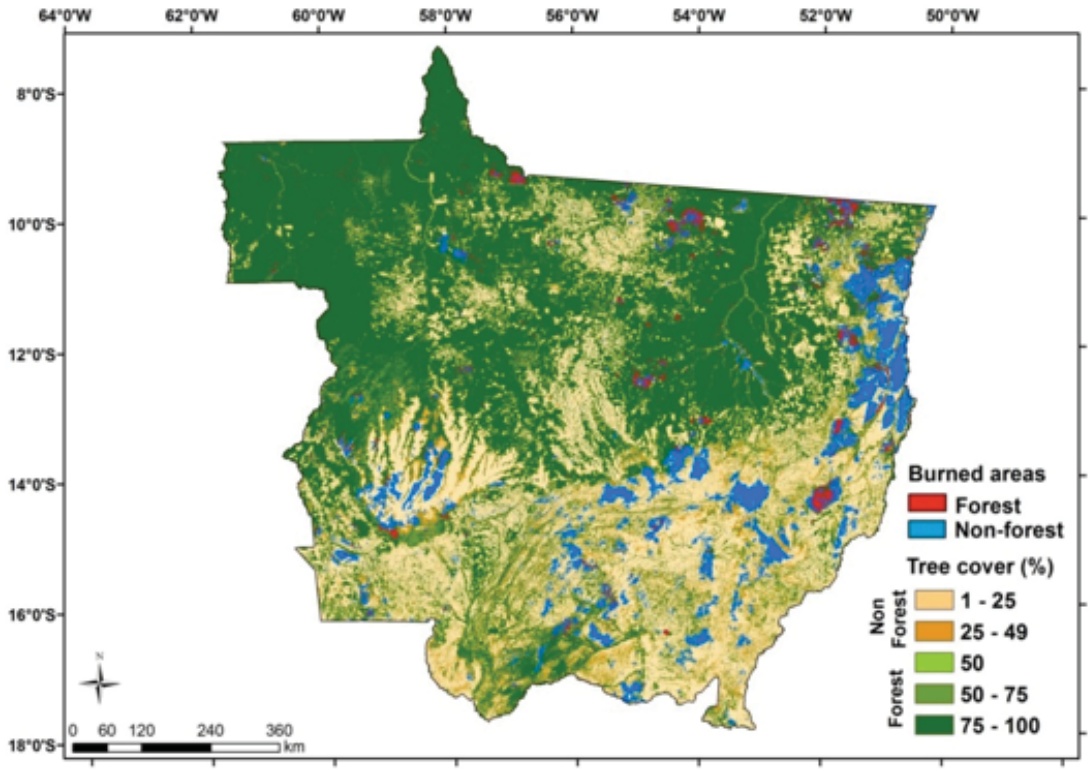

Fig.1 - Burned areas depicted by our method: in red over the forest areas and in blue over the non-forest areas.

The shade fraction image generated from the application of spectral linear mixing model on Landsat TM images allowed to identify and to map burned areas semi automatically. Then combining the burned areas result with the forest/non forest map derived from Hansen *et al.* (2013) dataset allowed to estimate the degradation forest areas due to forest fire. These information are very important for the carbon emission estimation.

References

Achard, F., Beuchle, R., Mayaux, P., Stibig, H.-J., Bodart, C., Brink, A., Carboni, S., Desclée, B., Donnay, F., Eva, H. D., Lupi, A., Raši, R., Seliger, R., Simonetti, D. Determination of Tropical Deforestation Rates and Related Carbon Losses from 1990 to 2010." **Global Change Biology** 20: 2540–2554, 2014. doi:10.1111/gcb.12605.

Aragão, L. E. O. C., Poulter, B., Barlow, J. B., Anderson, L. O., Malhi, Y., Saatchi, S., Phillips, O. L., Gloor, E. Environmental change and the carbon balance of Amazonian forests. **Biological Reviews** (2014).

Asner, G. P., Knapp, D. E., Balaji, A., Páez-Acosta, G. Automated mapping of tropical deforestation and forest degradation: CLASlite. **Journal of Applied Remote Sensing**, 3, 033543, 2009.

Berenguer, E., Ferreira, J., Gardner, T. A., Aragão, L. E. O. C., Camargo, P. B., Cerri, C. E., Durigan, M., Oliveira, R. C., Vieira, I. C. G., Barlow, J. A large-scale field assessment of carbon stocks in human-modified tropical forests. **Global Change Biology**, doi: 10.1111/gcb.12627, 2014.

Hansen, M., Potapov, P. V., Moore ,R., Hancher, M., Turubanova, S. A., Tyukavina, A., Thau, D., Stehman, S. V., Goetz, S. J., Loveland, T. R., Kommareddy, A., Egorov, A., Chini, L., Justice, C. O., Townshend, J. R. G. High-Resolution Global Maps of 21st-Century Forest Cover Change. **Science**, 342, 850-853, 2013.

INPE (Instituto Nacional de Pesquisas Espaciais). **Monitoramento da floresta Amazônica brasileira por satellite. Seminário de avaliação.** Disponivel on-line: <http://www.obt.inpe.br/prodes/seminario2005/>(Acessado em 12 de Agosto de 2005), 2005.

INPE(Instituto Nacional de Pesquisas Espaciais). **Monitoramento da cobertura florestal da amazônia por satélites: sistemas PRODES,**

DETER, DEGRAD E QUEIMADAS 2007-2008. INPE, São José dos Campos. 47p., 2008.

Shimabukuro, Y. E., Smith, J. A. The least squares mixing models to generate fraction images derived from remote sensing multispectral data. **IEEE Transactions on Geoscience and Remote Sensing**, 29, 16-20, 1991.

Shimabukuro, Y. E., Duarte, V., Arai, E., Freitas, R. M., Lima, A., Valeriano, D. M., Brown, I. F., Maldonado, M. L. R. Fraction images derived from Terra MODIS data for mapping burnt areas in Brazilian Amazonia. **International Journal of Remote Sensing**, 30, 1537-1546, 2009.

Shimabukuro, Y.E., Beuchle, R., Grecchi, R., Achard, F. Assessment of forest degradation in Brazilian Amazon due to selective logging and fires using time series of fraction images derived from Landsat ETM+ images. **Remote Sensing Letters**, Vol. 5, No. 9, 773–782, http://dx.doi.org/10.1080/2150704X.2014.967880, 2014.

Mapping forest height and biomass of the Chocó region, Colombia, combining stratified random sampling of Lidar data and spaceborne remote sensing data

Victoria Meyer[1,2], Sassan, Saatchi[1], Antonio Ferraz[1], Alan Xu[3], Alvaro Duque[4], Mailyn Gonzalez[5], Jérôme Chave[2]

[1] Jet Propulsion Laboratory, California Institute of Technology, Pasadena, CA. USA
[2] Laboratoire Evolution et Diversité Biologique UMR 5174, CNRS Université Paul Sabatier, Toulouse, France
[3] Institute of the Environment and Sustainability, University of California, Los Angeles, CA 90095-1496
[4] Departamento de Ciencias Forestales, Universidad Nacional de Colombia, Calle 59A No. 63-20, Medellín, Colombia
[5] Instituto de Investigación de Recursos Biológicos, Alexander von Humboldt, Bogotá, D.C., Colombia

Keywords: Lidar, Biomass, Forest Height, Tropical Forest, Remote Sensing, Random Forest

Abstract

Mapping aboveground biomass using remote sensing has been proven to be accurate at local scales, especially when relying on small footprint lidar data and their derived height metrics. Extending these biomass estimations to larger areas that are not covered by lidar is a challenge that has yet to be resolved. In this study, we show that developing a forest height map based on multiple remote sensing sources can be the first step to producing a biomass map at a regional scale. Focusing on mapping forest height prior to estimate biomass circumvents the issues of having errors related to local forest structure and differences in allometry.

We are testing a random forest algorithm based on spaceborne remote sensing layers over the Chocó region, located along the Pacific coast of Colombia, combining information on topography (SRTM), forest structure (ALOS) and spectral signature (Landsat). Forty-seven small footprint lidar scenes of 20km^2 each, based on stratified random sampling over the whole Chocó region as part of a BioREDD project, are used as the training data. The result is a forest height map covering the Chocó region, for which the uncertainties are reported at the pixel level. The effect of spatial resolution is also being analyzed. The last step of the analysis consists in determining allometric equations based on available ground data in the region and local parameters such as wood density. We test the hypothesis that biomass can be estimated at a regional scale if based on an accurate forest height map and wood density information.

Mapping of forest attributes across Canada using Landsat pixel composites and LiDAR plots

*Giona Matasci[1], Michael A. Wulder[2], Joanne C. White[2], Geordie W. Hobart[2], Harold S. J. Zald[3], Txomin Hermosilla[1], Nicholas C. Coops**

[1] Integrated Remote Sensing Studio, Department of Forest Resources Management, University of British Columbia, Vancouver, British Columbia V6T 1Z4, Canada
[2] Pacific Forestry Centre, Canadian Forest Service, Natural Resources Canada, Victoria, British Columbia V8Z 1M5, Canada
[3] Department of Forest Engineering Resources and Management, College of Forestry, Oregon State University, Corvallis OR 97331, USA

Keywords: LiDAR, Landsat, forest mapping, large-scale, random forest, monitoring

Large-area mapping of forest structural attributes is a critical information need for national forest reporting. Landsat time series data provide key long-term information on land cover and land cover change, including forest cover and disturbance characteristics. Passive optical data alone however are limited in their capacity to estimate forest structural attributes such as height and biomass.

In this contribution, we present a large-scale mapping approach to estimate key forest structural variables across the forested area of Canada by leveraging the Landsat archive (TM/ETM+ sensors) and LiDAR plots (airborne laser-based observations of the forest structure). A cross-country LiDAR transect acquired in 2010 provided the response variables describing the vertical structure of the forest. Spatially comprehensive pixel-based image composites (cloud-free, radiometrically and phenologically consistent surface reflectance composites), derived vegetation indices and forest disturbance history combined with topographic variables provided the predictors. The random forest framework, a widely accepted, robust and accurate approach was used to impute stand height over the entire forested area. Such a statistical model was developed and validated on a set of more than 80,000 LiDAR plots.

With the full availability of the Landsat archive, these wall-to-wall predictions can inform models of stand development over time, and provide critical information to national monitoring programs and forest management policies.

Mapping the efficacy of fuel reduction burns using image-based point clouds

Luke Wallace[1,2], Karin Reinke[1,2], Christine Spits[1], Bryan Hally[1,2] and Simon Jones[1,2]

[1.] School of Sciences, Mathematical and Geospatial Sciences, RMIT University, Melbourne, Australia, Luke.Wallace2@rmit.edu.au
[2.] Bushfire and Natural Hazards Cooperative Research Centre, Melbourne, Australia

Keywords: Fuel reduction burns, Image-based point clouds, Terrestrial Laser Scanners, multi-temporal monitoring

Fuel reduction burns are commonly used in fire-prone forests to reduce the risk of wildfire, or to maintain ecosystem condition and diversity. As such, producing quantified assessments of fire-induced change is important to understanding the outcomes of the intervention. This study aims to quantify the changes in fuel structure generated by a fuel reduction burn using image-based point clouds. Colocated image sets are collected pre and post burn within a dry sclerophyll forest in South East Australia. These image sets are used to produce point clouds, from which metrics representing fuel volume, horizontal connectivity, and vertical stratification are derived. Fire-induced change in these metrics is assessed and the efficacy of the burn in relation to fuel hazard is described. The method is assessed against two sets of data, (1) the results of visual fuel hazard and fire severity assessments following standard guidelines used by Australian land managers, and (2) the point clouds generated using Terrestrial Laser Scanning (TLS) data collected from a similar fire-altered forest plot. It is shown that a similar correlation between fuel load and image-based point cloud estimated volume (r2 = 0.70 to 0.87) and TLS estimated volume (r2 = 0.69 to 0.81) exists. Furthermore, similarities between the image-based and TLS point clouds in mapping fuel depths (root mean square deviation (rmsd) less than 0.03 m) and horizontal coverage (rmsd less than 5%) indicate that the fire-induced change can be mapped using image-based point clouds with similar detail and accuracy to that achieved with TLS. The method utilises a low-cost consumer grade camera and has similar in field requirements to the visual assessments. As such the method presented can be easily adapted for use by land managers to provide routine and quantified assessments of fuel hazard and fire severity.

Prediction of height, basal-area and stem volume in boreal forest using Pléiades or WorldView-2 acquisitions

Henrik J. Persson[1], Håkan Olsson[1], Johan E.S. Fransson[1]*

[1]Department of Forest Resource Management, Swedish University of Agricultural Sciences, Umeå, Sweden
**Corresponding author: henrik.persson@slu.se*

Keywords: stereo, satellite, forest, WorldView, Pléiades

Abstract

This paper evaluates predictions of Lorey's mean height (H_L), basal-area (BA) and stem volume (VOL) of boreal forest at two Swedish test sites, Krycklan and Remningstorp. Forest heights derived from very high resolution stereo matched satellite data from the Pléiades sensor or the WorldView-2 sensor were trained with 10 m field plots and then predictions and evaluations were performed on independently inventoried 40 m field plots. The best prediction results were found in Krycklan with WorldView-2 data, with H_L = 3.4% RMSE, VOL = 9.8% RMSE and BA with 9.7% RMSE. In conclusion, both sensors delivered robust and accurate imagery for both the evaluated test sites. Moreover, the presented approach appears suitable for operational forestry planning, especially at remote locations with limited or no other remote sensing data.

Introduction

There is a steady need of establishing and updating information about the forest. Airborne laser scanning (ALS) has for more than one decade been considered the most accurate remote sensing technique that in combination with field samples can be used to create wall-to-wall estimations of typical forest variables, like Lorey's mean height (HL), stem volume (VOL) or basal-area (BA). Many countries, including Sweden, can now offer complete national terrain models based on ALS, which has enabled also other techniques for estimations of this type of variables. One such technique uses images acquired from at least two directions which enables stereogrammetric image matching to derive heights. For this purpose, aerial images or very high resolution (VHR) satellite images are suitable, as they often possess resolutions below one meter. The image matched result is a digital surface model (DSM) from which the terrain model can be subtracted to obtain the forest canopy height, which can be correlated with different forest variables. One main advantage of using stereo matched VHR images over ALS data, is the significant lower price (\$40/km^2 compared to >\$200/km^2), and the high repetition frequency of the satellites passing the region of interest (often within days or a few weeks). The VHR imagery have hence appeared as an attractive option to the more expensive ALS data. The stereo matched heights have been investigated in a number of papers, but very few have compared the sensors Pléiades and WorldView-2, both with image ground sampling distances of about 0.5 m, in boreal forest (Persson & Perko 2016; Persson 2016; Immitzer et al. 2016; Yu et al. 2015; Shamsoddini et al. 2013).

This work evaluates and compares the estimation of the forest variables Lorey's mean height, stem volume and basal-area, using stereogrammetrically matched VHR imagery from the Pléiades or WorldView-2 sensors.

Methods

VHR imagery have been stereogrammetrically matched, using the software Remote Sensing Package Graz, which utilizes the semi-global matching algorithm, to derive height rasters. The processing is further described in (Persson & Perko 2016; Persson 2016). The terrain height (obtained from a national laser scanning for the duration of

2009 to 2016) was subtracted to obtain canopy heights. From the derived height rasters, different metrics, e.g., mean height, standard deviation, and numerous height percentiles, were extracted for field plots located on the two test sites. These metrics were furthermore used as explanatory variables in multiple linear regression models, where the models were trained on plots with 10 m radius, and hereafter the models were evaluated on independently inventoried 40 m plots.

The performance of respective VHR sensor was evaluated and compared at two Swedish test sites illustrated in Figure 1 (Krycklan, Lat. 64°16′N, Long. 19°46′E, and Remningstorp, Lat. 58°30′N, Long. 13°40′E). Systematic 10 m field plots were distributed at the respective test sites, from which the field variables in question have been computed, using established allometric equations. The estimated variables were HL, BA and VOL. In Krycklan, the five hundred 10 m plots were inventoried during the fall 2015, while the thirty-two 40 m plots were inventoried primarily before the 2016 vegetation season. In Remningstorp, both the two hundred sixty 10 m plots and the forty 40 m plots were inventoried during the fall 2014. At all inventoried plots, only trees with diameter breast height ≥0.04 m were calipered. Both the Pléiades and WV2 data were acquired during 2015.

Results

From inspection of the model coefficients and extracted heights, it appears that most WV2 height percentiles are similar to each other, located close to the top height, while the Pleiades height percentiles differ more. That is, the Pléiades sensor appears to catch a larger dynamic range compared to the WV2 sensor. Moreover, the detected top height appears generally higher for the WV2 sensor compared to the Pleiades. However, this might be due to possible differences on how the acquired bands are used in the matching. The WV2 images used in this study were acquired as panchromatic images at 450-800 nm, while the Pléiades images were acquired in four spectral bands, blue, green, red, and near-infrared, with the possible (but not used) panchromatic range of 480-830 nm, and possibly only a single band was used in the image matching, which might cause the larger height differences. This is to be clarified.

Estimation results from both sensors at the two test sites indicate robust and similar results at both test sites, despite the differences in the forests. The heights were estimated with an RMSE below one meter in Krycklan, corresponding to 3% to 6% RMSE, while the accuracy was almost identical in Remningstorp, with 5% RMSE (Table 1). As height was the only variable directly derived from the VHR

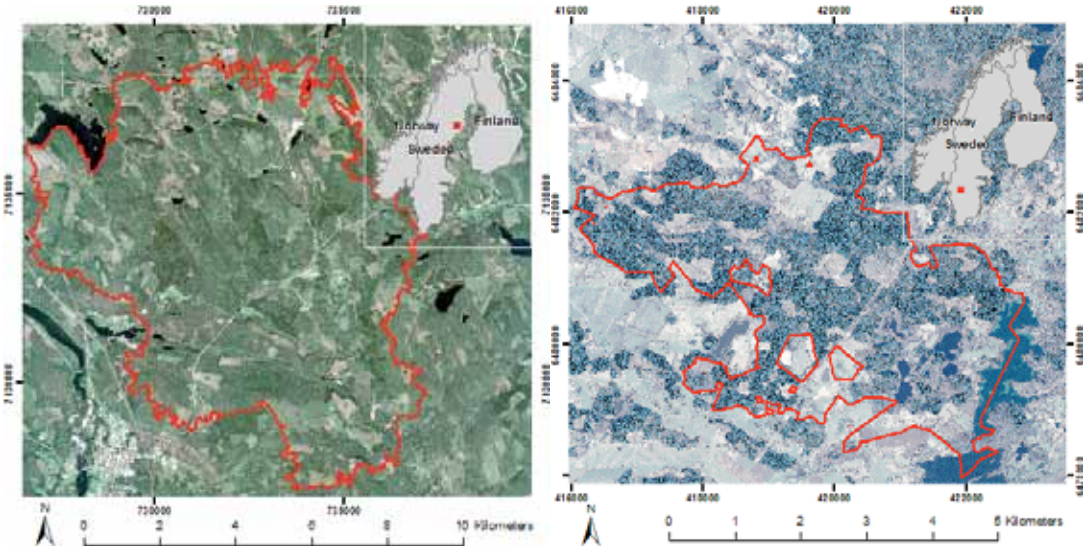

(a) **(b)**

Figure 1. Ortho-rectified Pléiades images of the two test sites superimposed in red. Krycklan (a) and Remningstorp (b), located in northern (64°N) and southern (58°N) Sweden, respectively, projected in the UTM 33N coordinate system on the WGS84 reference ellipsoid. ©CNES_2015, distribution Astrium Services / Spot Image S.A, France, all rights reserved

imagery, the same source of explanatory variables (sometimes in transformed forms) were used to predict H_L, VOL and BA. Therefore, the similarity in the height results is reflected also for the variables VOL and BA, with almost identical results for respective sensor, at the respective test site. However, the across test site values differ slightly, which might be due to several reasons, including sampling errors, differences in time for the image acquisitions and the field samples, and moreover due to the differences of the forest types. One observation was that the estimation accuracy of basal-area and stem volume was highly correlated, despite that stem volume is considered a threedimensional unity (including both height and density of the forest) while basal-area often functions as one measure of forest density.

The scatter plots were similar between the variables and sensors, and hence an example on scatter plots of the H_L, VOL and BA estimated from Pléiades are illustrated in Figure 2 a,c,d and in addition, the height estimation from WV2 data is also included (Figure 2 b) for comparison.

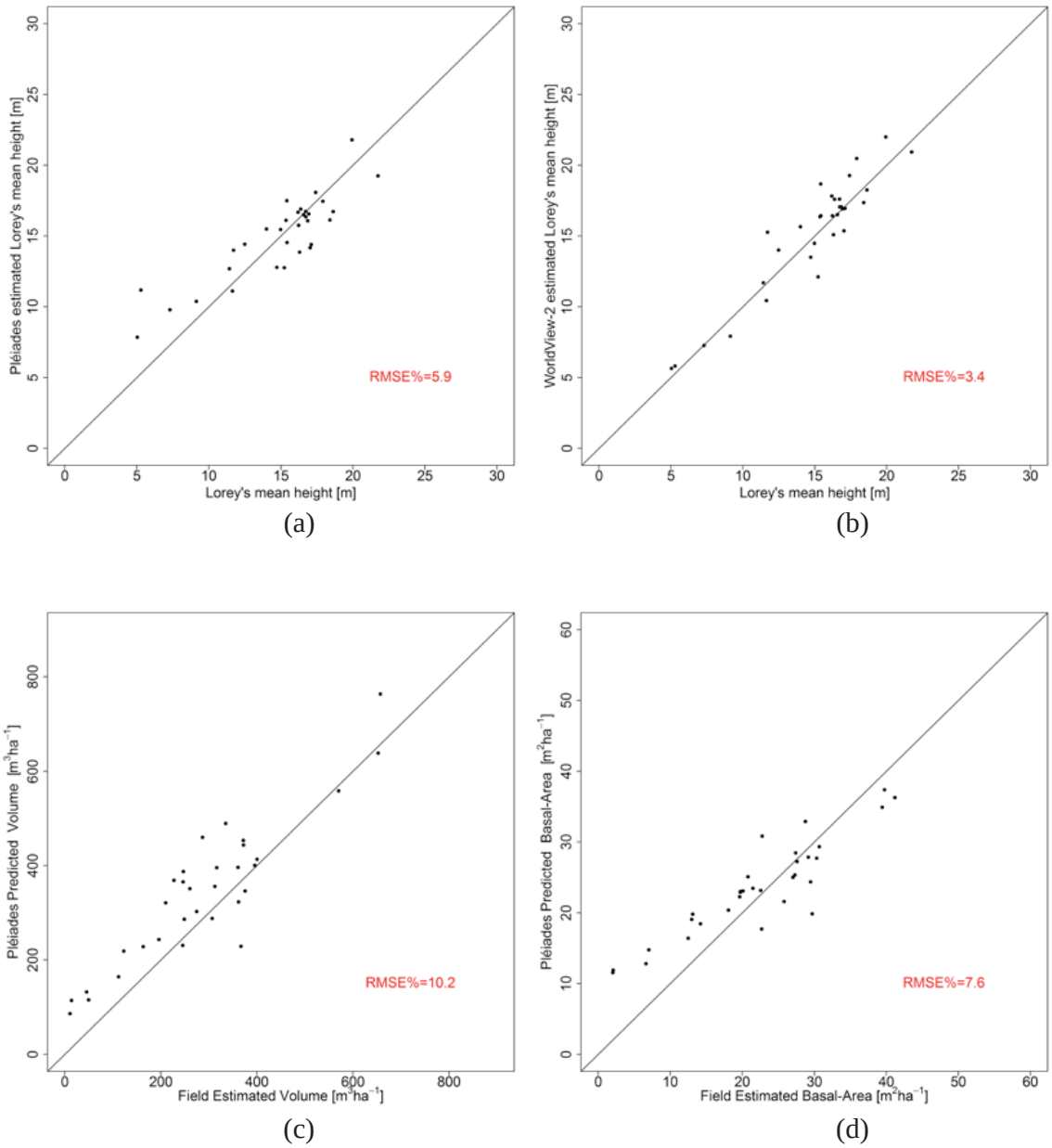

Figure 2. Scatter plots of the evaluated predictions from the Krycklan test site. a,c,d are estimations with the Pléiades sensor and b from the WV2 sensor. a) HL, b) HL, c) VOL, d) BA

Table 1 –Results from evaluation of the independently inventoried plots with 40 m radius.

Test site	Sensor	Variable	Unit	RMSE	RMSE%
Krycklan	Pléiades	H_L	m	0.876	5.88
Krycklan	Pléiades	VOL	m^3/ha	29.1	10.2
Krycklan	Pléiades	BA	m^2/m^2	1.69	7.61
Krycklan	WorldView-2	H_L	m	0.502	3.38
Krycklan	WorldView-2	VOL	m^3/ha	27.9	9.80
Krycklan	WorldView-2	BA	m^2/m^2	1.51	9.67
Remningstorp	Pléiades	H_L	m	1.09	4.84
Remningstorp	Pléiades	VOL	m^3/ha	36.1	10.9
Remningstorp	Pléiades	BA	m^2/m^2	3.06	10.1
Remningstorp	WorldView-2	H_L	m	1.10	4.88
Remningstorp	WorldView-2	VOL	m^3/ha	38.4	11.6
Remningstorp	WorldView-2	BA	m^2/m^2	3.41	11.2

Conclusions

The conclusion is that stereo matching of VHR satellite images is a promising method for estimating forest variables, when a high-resolution terrain model is available. The results from this study, indicated that the dynamic range of Pléiades heights is larger than the heights obtained fromWV2 data. The BA and the VOL were highly correlated, considering prediction accuracy, and both sensors are giving robust and accurate acquisitions at both the evaluated test sites.

Acknowledgments
The authors would like to thank the AdvancedSAR FP 7 project under Grant 606971 for financial support and to enable access to WorldView-2 imagery. The Swedish National Space Board is acknowledged for providing the Pléiades images. This work has also received funding from the Hildur and Sven Wingquist foundation.

References

Immitzer, M. et al., 2016. Forest Ecology and Management Use of WorldView-2 stereo imagery and National Forest Inventory data for wall-to-wall mapping of growing stock. Forest Ecology and Management, 359, pp.232–246. Available at: http://dx.doi.org/10.1016/j.foreco.2015.10.018.

Persson, H., 2016. Estimation of Boreal Forest Attributes from Very High Resolution Pléiades Data. Remote Sensing, 8(9), p.736. Available at: http://www.mdpi.com/2072-4292/8/9/736/ [Accessed September 6, 2016].

Persson, H.J. & Perko, R., 2016. Assessment of boreal forest height from WorldView-2 satellite stereo images. Remote Sensing Letters, 7(12), pp.1150–1159. Available at: https://www.tandfonline.com/doi/full/10.1080/2150704X.2016.1219424.

Shamsoddini, A., Trinder, J.C. & Turner, R., 2013. Pine plantation structure mapping using WorldView-2 multispectral image. International Journal of Remote Sensing, 34(11), pp.3986–4007. Available at: <Go to ISI>://WOS:000315384500016.

Yu, X. et al., 2015. Comparison of laser and stereo optical, SAR and InSAR point clouds from air- and space-borne sources in the retrieval of forest inventory attributes. Remote Sensing, 7(12), pp.15933–15954.

POSTER

Regional predictive mapping of paludification black spruce forests in the north eastern Canada using remote sensing and statistical modeling

Osvaldo Valeria[1], Nicolas Mansuy[1], Ahmed Laamrani[2], Nicole Fenton[1] and Yves Bergeron[1]*

[1]Forest research institute, Université du Québec en Abitibi Témiscamingue, Québec, Canada.
[2] Agriculture and Agri-Food Canada: Guelph Research and Development Centre, Ontario, Canada.
Osvaldo.valeria@uqat.ca

Abstract

The black spruce forests in north eastern Canada are considered as a potential source of wood fibre. However, a considerable volume of timber in this region is located in areas that are prone to gradual accumulation of surface organic matter deposits over time (paludification). Paludification is a natural process where organic material accumulates on the ground surface over time, resulting in higher soil moisture levels and elevated water tables (Crawford et al., 2003; Vygodskaya et al., 2007). These conditions alter dynamic succession and favour the invasion of Sphagnum moss species (Fenton et al., 2005), which can lead to the development of forested peatlands and substantial decreases in forest productivity (Simard et al., 2007). Many parts of the world, including interior Alaska, the western Siberian plain, and the Hudson Bay-James Bay Lowlands of Canada, are prone to paludification. In the black spruce forests of the Abitibi and north of Quebec (A/NQ) regions, time-since-last fire, superficial deposit and flat ground surface topography have been reported as the main factors that cause paludification (Laamrani et al., 2014). For effective sustainable land resource management and policy making in northern black spruce forests, an up-to-date and reliable predictive spatial map of paludification at the regional scale is needed. The aim of this study was to predict paludified areas at a regional scale by parametrizing soil organic layer-landscape models using a machine learning method (random Forest) and Maxent models. Organic layer thickness (OLT) was predicted at a regional scale to map paludification. Most important predictive variables were environmental data representing terrain attributes derived from digital elevation models, landscape data derived from remotely sensed data, provincial Forest Inventory data derived from Maps, and data on soil moisture parameters derived from Radarsat-2 data. Training sites were constructed from OLT experimental sites; and the resulting regional map were validated with a set of punctual OLT field-measured observations (~2500 points) spread over the study area. Knowledge of the spatial extent of paludification at the regional scale is of great importance to forest industry and its forest managers because it would allow them to make better cost-effective management decisions that optimize forest productivity and ensure sustainability of the forest.

References:

Crawford, R.M.M., Jeffree, C.E., and Rees, W.G. (2003). Paludification and forest retreat in northern oceanic environments. Annals of Botany, 91: 213–226.

Fenton, N., Lecomte, N., Légaré, S., and Bergeron, Y. (2005). Paludification in black spruce (Picea mariana) forests of eastern Canada: Potential factors and management implications. Forest Ecology and Management, 213(1-3): 151–159.

Laamrani, A., Valeria, O., Fenton, N., Bergeron, Y., and Cheng, L.Z. (2014). The role of mineral soil topography on the spatial distribution of organic layer thickness in a paludified boreal landscape. Geoderma, 221-222: 70–81.

Simard, M., Lecomte, N., Bergeron, Y., Bernier, P.Y., and Pare, D. (2007). Forest productivity decline caused by successional paludification of boreal soils. Ecological Applications, 17(6): 1619–1637.

Vygodskaya, N.N., Groisman, P.Y., Tchebakova, N.M., Kurbatova, J.A., Panfyorov, O., Parfenova, E.I., and Sogachev, A.F. (2007). Ecosystems and climate interactions in the boreal zone of northern Eurasia. Environmental Research Letters, 2(4): 1–7.

Scale-dependent mapping of stand structural heterogeneity from airborne LiDAR data

Collins Byobona Kukunda[1] and Philip Beckschäfer[1]

[1]Chair of Forest Inventory and Remote Sensing, Georg August Universität Göttingen, Germany Corresponding email: ckukund@gwdg.de

Key words: Scaling problems, Forest structure, Mixed effects models, airborne LiDAR, Spatial cofounding

Abstract

Heterogeneity in forest structure, naturally occurring or induced by disturbance, is continuous in space and time. In practice, heterogeneity in structure is quantified from ecological or forest inventory data; often bound to observations made on sample plots. For any given location, the plot-based quantities of structure are known to vary for different plot sizes due to differences in unobserved neighborhoods at plot boundaries. In regression, this scale dependence may confound relationships between the forest structural indices and their predictors affecting the resulting map accuracies. Our study first investigated for plot size effects on variability in forest structure described by forest structural indices. We thereafter explored the relationship between the indices of structure and heterogeneity and the plot sizes in forest stands with varying degrees of structural complexity. Finally, the observed plot size effects were modeled statistically and multiple regressions used to map structural complexity and heterogeneity over unobserved parts of the study area from airborne LiDAR data. Three forest structural indices were considered: the aggregation index of Clark and Evans, the Structural Complexity Index and the Enhanced Structural Complexity Index. We used inventory data from one fully mapped 28.5 ha plot in a semi-natural mature deciduous forest stand and 23 fully mapped one-hectare inventory plots spread in different temperate forest types in central Germany. To study the plot size effects, the structural indices were quantified on the basis of 18 plot sizes from 0.1 to 9.8 ha simulated on the 28.5 ha plot and 10 plot sizes from 0.1 to 1 ha simulated on the 23 one-hectare inventory plots. A fixed effects analysis was used to model plot size effects across levels of stand complexity. In addition, a structural equation model was used to explain the effect of differences in the plot sizes on multiple regressions between LiDAR derived canopy metrics and the forest structural indices. Resultant map accuracies were assessed using the Root Mean Square Error (RMSE) and the True Skills Statistic (TSS) in a leave-one-out cross validation procedures for larger plot sizes and an independent set of data collected on 500 m2 inventory plots. Preliminary results show that all structural indices were influenced by the plot size and LiDAR data is a good predictor of forest structural complexity and heterogeneity (RMSE ≈ 20%). The highest map accuracy so far (TSS ≈ 0.71) has been obtained at the scale shown by the structural equation model to have minimal effects of spatial cofounding. These findings are relevant to optimize plot sizes for efficient inventory of components of forest structure as well as for the design of natural resource inventories. The structural complexity and heterogeneity map produced for the study area will be relevant for guiding further ecological and forest management planning.

Stereo matched very high-resolution satellite images for predictions of forest variables

Persson, H.J., Olsson, H, Fransson, J.E.S.
Department of Forest Resource Management, Swedish University of Agricultural Sciences, Umeå, Sweden, firstname.lastname@slu.se

Keywords: WorldView-2, Pléiades, stereo, forest, stem volume, tree height, basal area

There is a steady need of establishing and updating information about the forest. Airborne laser scanning (ALS) has for more than one decade been considered the most accurate remote sensing technique that in combination with field samples can be used to create wall-to-wall estimations of typical forest variables, like Lorey's mean height (H_L), basal-area or stem volume. Many countries, including Sweden, can now offer complete national digital terrain models (DTMs) based on ALS, which has enabled also other techniques for estimations of this type of variables. One such technique is stereo matching of very high resolution (VHR) satellite images, which often possess resolutions below 1 meter. The matched result is a digital surface model (DSM) from which the DTM can be subtracted to obtain the forest canopy height.

One main advantage of using stereo matched VHR images over ALS data, is the significant lower price ($40/km^2 compared to >$200/km^2).

Studies from Germany and Finland have used stereo matched WorldView-2 images to estimate forest variables, and there are a few similar studies which have considered Pléiades data for estimations of other types of variables.

In the current study, stereo matched WorldView-2 and Pléiades data have been compared for two Swedish test sites (Krycklan, Lat. 64°16'N, Long. 19°46'E, and Remningstorp, Lat. 58°30'N, Long. 13°40'E). Systematic 10 m field plots were distributed at the respective test sites, from which the field variables in question have been computed, using established allometric equations. The estimated variables were HL, basal-area (BA) and stem volume (VOL).

The results show that HL could on plot level be estimated with 8% to 10% RMSE, the basal-area with 24% to 29% RMSE and the stem volume with 30% to 33% RMSE. The results seem robust across the different test sites and across different tree species.

The conclusion is that stereo matching of VHR satellite images is a promising method for estimating forest variables, when a high-resolution DTM is available. The results from this study, indicated that the accuracies fore HL are similar to those achieved from similar ALS based estimations, while the estimations of BA and VOL are not sufficient by using only stereo matched heights.

POSTER

The 2016 NASA AfriSAR campaign for tropical forest structure and biomass measurements: design, execution and first results

Lola Fatoyinbo[1], Christy Hansen[1], Naiara Pinto[2], Michelle Hofton[3], Bryan Blair1, Sassan Saatchi[2], Marc Simard[2], Yunling Lou[2], Ralph Dubayah[3], Scott Hensley[1], Laura Duncanson[1,4], Marco Lavalle[2].

[1]NASA Goddard Space Flight Center, Greenbelt, Maryland
[2] NASA Jet Propulsion Laboratory, California Institute of Technology
[3]University of Maryland, College Park, Maryland
[4]NASA Postdoctoral Program/USRA, Columbia, Maryland

Keywords: Forest Canopy Height, Biomass, SAR, Lidar, Tropical Forests, Airborne Campaigns

Background

The AfriSAR campaign was a joint NASA and ESA airborne campaign conducted in Gabon in support of the upcoming ESA BIOMASS, NASA-ISRO Synthetic Aperture Radar (NISAR) and NASA Global Ecosystem Dynamics Initiative (GEDI) missions. The aim of the campaign was to collect ground, airborne SAR and airborne Lidar data for the development and evaluation of forest structure and biomass retrieval algorithms. The campaign consisted of 2 deployments, the first in 2015 with the ONERA SETHI SAR system and the second in 2016 with the NASA LVIS (Land Vegetation and Ice Sensor) Lidar, the NASA L-band UAVSAR and the DLR F-SAR. In addition, field teams from the Gabon ANPN (Agence Nationale des Parcs Nationaux), University College London and NASA were collecting ground data. Here we focus on the 2016 NASA contributions to campaign.

Aim

The objectives of the ESA/NASA AfriSAR deployments were to: 1) measure forest canopy height, canopy profiles and biomass density under a variety of forest conditions such as primary and degraded forest and a variety of forest types, including tropical rainforest, mangroves, forested freshwater wetlands and savannas 2) acquire detailed measurements of airborne SAR data and Lidar data for cross calibration of NASA and ONERA/DLR instruments and for CAL/VAL support of the BIOMASS, NISAR, and GEDI missions, and 3) conduct technology demonstrations of joint SAR and Lidar applications.

Methods

The NASA AfriSAR campaign involved 2 aircrafts: the LaRC (Langley Flight Research Center) B-200 carrying LVIS and the AFRC (Armstrong Flight Research Center) C-20 carrying the L-band UAVSAR. The aircrafts were based out of Libreville, Gabon for 3 weeks in February 2016, jointly with the DLR aircraft and SAR instrumentation.

Results

A central motivation for the AfriSAR deployment was the common biomass requirement for the three future spaceborne missions and the lack of sufficient airborne and ground calibration data covering the full range of biomass in tropical forest systems. During the campaign, the NASA sensors collected Tomographic SAR, Polarimetric InSAR, Polarimetric SAR and Waveform Lidar data over six joint sites. These sites were the Mondah Forest, Lope National Park, Pongara National Park, Mabounie, Rabi, and the Lower Ogooué River. Additional data was also collected over additional sites and in long transects. In total, over 70 hours of science data were collected. In this presentation, we will present the design and execution of the NASA AfriSAR campaign, and show some of the first results and data products from the campaign.

POSTER

Uncertainty estimation of stand structural variables in LiDAR-based forest inventories at different sample sizes.

Sastre L, Mauro F, Pascual C, Gomez-Roux M, Manzanera JA, Garcia-Abril A.*

Research Group for Sustainable Management SILVANET. FoReStLab. College of Forestry and Natural Environment, Technical University of Madrid, Ciudad Universitaria, 28040 Madrid, Spain.
**: Oregon State University, Corvallis, OR, USA.*
Corresponding author: J.A. Manzanera (joseantonio.manzanera@upm.es).

Keywords: EBLUP, forest inventory, LiDAR, Small Area Estimation, uncertainty estimation.

Abstract:

The aim of this work seeks to analyze an improvement in the quality of the forest attribute estimates of a forest inventory when we include auxiliary data coming from a LiDAR (Light Detection And Ranging) dataset. Multiple regression models were designed for the basal area, density, quadratic mean diameter, dominant height, biomass and volume variables. The estimation errors for these variables were analyzed using random sampling methods, and reducing the number of sample plots. One of the main conclusions of this study is that the inclusion of LIDAR-derived metrics significantly reduces the sampling effort and improves the precision of the estimation. The inclusion of model-based and Empirical Best Linear Unbiased Predictor estimations further improves the accuracy at the plot and stand levels.

Introduction

Forest structure is defined as the spatial distribution of both living and dead vegetation size, age and species, with special emphasis on the arboreal component (Spies & Franklin, 1991). Deepening the characterization of the structure affects the progress of Global carbon cycle studies, forest productivity, use of cover habitat by birds, arboreal mammals and arthropods, interaction between forests and rivers, and in the prediction of fire behavior (Means et al., 2000).

The most relevant aspects of the study of the structure in the forest stands are the distribution of trees, the specific composition both in species diversity and in their distribution in the stand and the differentiation in diameter, height and size of crowns, as well as the Different vertical strata (M. del Río 2003). Forest attributes have traditionally been mapped using passive airborne or satellite sensors and statistical methods (McRoberts and Tomppo 2007). However, optical sensors have important limitations in quantifying vegetation characteristics because they only generate information in two dimensions. In addition, in dense coverage areas, the highly reflected energy tends to saturate the signal captured by the sensor (Lefsky, Cohen, Harding, et al., 2002), making it impossible to make estimates of the different dasometric variables above a certain threshold. In this context, LiDAR technology is able to traverse the forest cover and provide information of its three-dimensional dimension. Since it does not present the problem of signal saturation, LIDAR allows to evaluate the three-dimensional patterns of the arboreal canopy and to estimate the vertical structure of the plant communities (Lefsky, Cohen, Harding, et al., 2002). The three-dimensional information provided by the LiDAR sensor has been used successfully in the estimation of different forest parameters, such as canopy height, wood volume, etc., automatically and with greater accuracy than that achieved with techniques of traditional inventory (Sithole and Vosselman 2005) or other approaches with optical sensors (Maltamo et al., 2006).

Managers need up-to-date information at the time of decision-making on the status, structure and composition of the forest stands, provided individually for each of the management units and subunits. This goal can be achieved by different statistical techniques, such as model-assisted, model-based, indirect estimation fixed or mixed effects estimation (Mauro Gutiérrez et al. 2013, 2015).

Materials and Methodology:

This analysis is carried out on the Peña del Águila, mountainside, located in Fuenfriá s Valley (Cercedilla, Madrid). To this day, the LiDAR flight has been used in 2011 and in two field inventories; one of them was made in 2013/2014, covering 60 sampling plots, and the other one made in 2015, covering 80 sampling plots. Multiple regression models were designed for the basal area, density, quadratic mean diameter, dominant height, biomass and volume variables. The errors committed in estimating these forest attributes were analyzed from models and by using random sampling methods, reducing the number of sampled plots.

Results:

It was found that adding LiDAR´s information significantly reduces the forest inventory errors. Secondly, stand, pixel and mount level estimates were carried out using sampling design and model based techniques and the errors committed were compared. The first technique included the simple random sampling and the model assisted estimation; the second one embraced Small Area Estimation (SAE) techniques. Moreover, the model based estimation allowed to develop a pixel and stand level error mapping.

Finally, outcomes showed that EBLUP estimators (Empirical Best Linear Unbiased Predictor) brought out more accurate estimates tan those coming from sampling design based techniques, in population subunits (stands).

Conclusions:

The main conclusion of this study is that the inclusion of LIDAR-derived metrics significantly reduces the sampling effort and improves the precision of the estimation. The inclusion of model-based and Empirical Best Linear Unbiased Predictor estimations further improves the accuracy at the plot and stand levels.

References.

Lefsky, Michael A, Warren B Cohen, David J Harding, et al. 2002. "Lidar Remote Sensing of above-Ground Biomass in Three Biomes." Remote Sensing of Environment: 393–99.

Lefsky, Michael A, Warren B Cohen, Geoffrey G Parker, and David J Harding. 2002. "Lidar Remote Sensing for Ecosystem Studies." BioScience 52(1): 19–30.

Maltamo, M et al. 2006. "Nonparametric Estimation of Stem Volume Using Airborne Laser Scanning, Aerial Photography, and Stand-Register Data." 436: 426–36.

Mauro Gutiérrez, F., García García, D., García Abril, A., Martín-Fernández, S., Núñez Martí, M.V., Gonzalez García C., Ayuga Téllez E. 2013. "Reducción Del Numero de Parcelas de Muestreo Al Incorporar Información Auxiliar LiDAR En La Estimación de Variables Dasométricas." 6º Congreso Forestal Español: 1–13.

Mauro Gutiérrez, Francisco. 2015. "Estimación de Variables Dasométricas a Partir de Datos LiDAR Y Obtención de Modelos de Referencia Para Las Distribuciones de Alturas Y Diámetros Del Arbolado." PhD Thesis, UPM.

McRoberts, Ronald E., and Erkki O. Tomppo. 2007. "Remote Sensing Support for National Forest Inventories." Remote Sensing of Environment 110(4): 412–19.

Means, Joseph E et al. 2000. "Predicting Forest Stand Characteristics with Airborne Scanning Lidar." 66(11): 1367–71.

Río, M. del. 2003. "Índices de Diversidad Estructural En Masas Forestales." Forest Science (January).

Sithole, George, and George Vosselman. 2005. "Filtering Of Airborne Laser Scanner Data Abstract :" Photogrammetric Engineering and Remote Sensing: 66–71.

Spies, Thomas A, and Jerry F Franklin. 1991. "The Structure of Natural Young , Mature , and Old-Growth Douglas-Fir Forests in Oregon and Washington."

ForestSAT 2016

Forest Modelling

OTERRA
CENTRO DE ESTUDIOS DE RECURSOS NATURALES
UNIVERSIDAD MAYOR

UNIVERSIDAD MAYOR
para espíritus emprendedores

Facultad de Ciencias
ESCUELA DE INGENIERÍA FORESTAL

Data assimilation of InSAR-based estimated forest stand attributes

Lindgren, N.[1], Persson, H.J.[1], Nyström, M.[1], Grafström, A.[1], Nyström, K.[1], Muszta, A.[1], Wallerman, J.[1], Willén, E.[2], Fransson, J.[1], Ståhl, G.[1], Olsson, H.[1]

[1]Department of Forest Resource Management, Swedish University of Agricultural Sciences, Umeå, Sweden, firstname.lastname@slu.se
[2] The forestry research institute of Sweden, Uppsala, Sweden, firstname.lastname@skogforsk.se

Keywords: Data assimilation, TanDEM-X, InSAR, extended Kalman filter, forest inventory, growth functions, time series

Up-to-date, cost-efficient and accurate information of the state of the forest is important to manage and monitor forests. Data assimilation can be used to optimally combine forecasts of previous estimates with new observations of the current state, based on the uncertainties in the forecast and the observations. In other fields of study, such as robotics and meteorology, data assimilation has led to better accuracies and reduced need for reference data. Early studies have also shown a potential for keeping forest stand registers up-to-date, using simulation (Ehlers et al., 2013) as well as empirically with a time series of canopy height data from digital photogrammetry (Nyström et al., 2015).

In the present study, data assimilation through extended Kalman filtering was used to assimilate a series of stand attribute predictions made from TanDEM-X InSAR data. In total a time series of 19 InSAR images acquired between 2011 and 2014 were used in combination with a high-resolution (2x2 m) digital terrain model. Forest variables were predicted for each InSAR image, using empirical regression estimates with forest data from field plots as response variables. Each prediction was assimilated with forecasts from the previous time point.

Both assimilated estimates and estimates based on a single acquisition were evaluated using cross-validation on a set of 137 sample plots with 10 m radius inventoried twice, in 2010 and 2014. Linear interpolation was used to create reference data for the intermediate years, and evaluation was made with the reference data matching the acquisition date.

The results show that, at all assimilated time points, data assimilation resulted in better estimates than estimates based on the single acquisitions. Median reduction in RMSE was 0.4 m for Lorey's mean height, 0.9 m^2/ha for basal area and 15.3 m^3/ha for stem volume. The conclusion is that data assimilation is a promising method for estimating forest stand attributes when multiple data sets from different acquisition time points are available, for example the continuous flow of data from TanDEM-X.

Delineation of forest structure patterns in the circumpolar taiga-tundra ecotone

Paul M. Montesano, Christopher Neigh, Jon Ranson

ForestSat 2016

Interactions between broad-scale climate, local-scale site factors and disturbance history have produced forest patterns in the taiga-tundra ecotone (TTE) that include a range of woody cover from forest cover patches and clusters of shrubs to sparsely arranged individuals. These biome boundary patterns influence ecological processes and are evident at local scales, but are often not apparent in moderate-resolution imagery from most earth observing satellites. Such scale problems have contributed to uncertainties in the extent of the TTE, its structural characteristics, and its net effect on current and future processes in the high northern latitudes. Recent advances using the global archive of Landsat data have provided calibrated tree cover at 30-m resolution, which may help improve TTE delineation. Furthermore, U.S. federal access to sub-meter DigitalGlobe data provides the means to improve estimates of the TTE forest patterns with observations of individual trees and structure from stereoscopic observations. A supercomputer cluster with cloud storage facilitates (1) image-based sampling of the entire TTE domain at the scale of forest structure change, (2) examining detailed forest structure patterns, and (3) exploring novel techniques for capturing horizontal and vertical forest structure. Site-scale (~1 m) maps of forest cover and height in sample strips across the TTE domain will be used to optimize the medium-scale (~30 m) delineation of this biome boundary and examine the spatial variability of detailed forest structure patterns. The resulting products may refine input to ecosystem models while providing insight into the variability of recent structural changes. An overview and early results of our current work will be presented.

POSTER

Detecting the spread of invasive tree species in central Chile with combined Landsat and Sentinel-2 data

Tobias Schmidt[1], Michael Foerster[1], Birgit Kleinschmit[1], Julian Cabezas[2], Fabian Fassnacht[2]

[1] Institute for Landscape Architecture and Environmental Planning, Technical University of Berlin
[2] Institute for Geography and Geoecology, Karlsruhe Institute of Technology (KIT)

Keywords: *One-Class-Classifier, Species Distribution Modelling, Pinus radiata, Ulex europaeus, Acacia dealbata, Sentinel-2, Landsat*

Chile has a large number of endemic species due to its isolated location and is therefore one of the biodiversity hots-spots of the Planet. At the same time a number of invasive species occurred over the last decades and have shown to have a notable negative effect on Chilean ecosystems. Between 2016 and 2018, the project SaMovar (Satellite-based Monitoring of invasive species in central-Chile) will investigate the past and recent spread of selected invasive species.

Ulex europaeus, Acacia dealbata and Pinus radiata have a large impact on local and regional biodiversity in central-Chile. Two objectives of the project are the mapping of the current state of spread and the identification of the historical invasion dynamics of the three species. Moreover, the future spread of the invasive species will be spatially estimated to produce risk maps for management measures. For these objectives the application of multi-temporal and multi-sensor satellite data (especially Sentinel-2 and Landsat) in combination with Unmanned Aerial Vehicle (UAV) data will be pursued.

In a first step, the most recent distribution ranges of the three target species will be detected using the data of both sensors by the application of one-class-classifier (OOC) techniques (e.g. Maxent). Presence information of the target species will be derived from spatial and spectral high resolution UAV data. To increase the model accuracy, the different phenological phases of the species can be considered. Due to the high temporal resolution of both sensors, it is possible to assess which combination of acquisition dates of each sensor is leading to the result with the significantly highest model accuracy. For this purpose the McNemar test will be applied to find significant differences in between multiple combinations of images and the subsequently derived classifications with a semi-exhaustive feature selection approach. As a result we can detect optimal acquisition dates, which will be used to compare the capability of Landsat and Sentinel-2 to distinguish between native vegetation and invasive species. Finally, the information on the classification quality of the different acquisition dates can be used for the identification of the historical spread of the three target species using the Landsat archive. For validating the retrospective classifications historical aerial photos from the last 30 years will be used. .

Together with the disturbance history of the region and additional environmental features (e.g. digital elevation model, climate data) this information will be used as input layer to species distribution models which will be developed to model the future spread of the three target species assuming different climate scenarios.

Preliminary results of the project are presented, especially regarding the identification of Pinus radiata in the natural forest remnants of the Maule Region using the already collected UAV data and first results of the classification using single Landsat and Sentinel-2 images.

How much forest area should be sampled to get accurate biomass estimations at different scales?

Rico Fischer[1], Jessica Hetzer[1], Andreas Huth[1]

[1]Department of Ecological Modelling, Helmholtz Centre for Environmental Research – UFZ, Permoserstr. 15, 04318 Leipzig, Germany

Keywords: Tropical Forest, Biomass, Sampling, Model

Abstract:

Tropical forests play an important role in the global carbon cycle. Field inventory plots were used for understanding forest structure and dynamics at different scales under the assumption that these plots accurately represent their surrounding landscape. Here, we tested at different scales whether inventory plots meet this assumption for biomass estimations in tropical forests. In a first step, we investigated this assumption on a local scale. Using a large 50-ha forest inventory plot from Panama we analyzed how representative 1-ha subplots are for biomass estimations. Results showed that about 6 of these 1-ha subplots are needed to accurate estimate biomass for this region even at its most reliable sampling strategy. Using a mathematical model we found out that for accurate biomass estimations in less homogenous forest sites (such as disturbed forests or montane forests) the number of needed field plots increased by 60-80%. In a second step, we used larger data sets to test different sampling strategies for accurate estimates of forest biomass at regional scale. It turned out that the required number of inventory plots is high. To overcome the limited number of inventory plots for accurate tropical forest biomass estimations the use of inventory plots in combination with high-resolution remote sensing products could be one promising solution.

Lessons Learned – National Individual Tree Species Extent and Parameter Modeling for Insect and Disease Risk Mapping

James Ellenwood [US Forest Service – R&D], Frank Krist [US Forest Service – S&PF/FHTET]

Keywords: Forest modeling, Remote sensing, Landsat, Tree Species Distributions, Insect and Disease Risk

Parameter datasets of presence [Ellenwood 2015 and others], basal area (BA), and stand density index (SDI) were modeled for 289 individual tree species using forest inventory data, Landsat imagery, and several national datasets for the coterminous US and Alaska at a 30-meter resolution to support the 2013-2027 National Insect and Disease Risk Map – NDRIM (Krist and others 2014). NIDRM is a nationwide strategic assessment of potential tree mortality due to insects and diseases. To facilitate local and regional planning efforts and develop models of forest parameters by tree species, USFS Forest Inventory and Analysis (FIA) data were linked to each national data layer and analyzed with See5 and Cubist data mining software (Quinlan 2012). Model outputs were processed into a 30-meter spatial dataset

A number of issues were identified in the completion of this project that would be valuable for future considerations in subsequent projects. Three issues are presented: phenology representation, plot-pixel mis-match, and exceptional areas.

This project utilized three-season Landsat 5/7 imagery to represent vegetation phenology. Though somewhat useful for differentiating conifer and hardwood species, the coarse temporal representation is highly variable with respect to plant phenology. Individual species have different phenological responses and the subtle seasonal changes are not decipherable from the three-season dataset. Observed in the individual species models, reflectance data was seldom selected as a significant variable for most of the 289 species. A possible explanation is the "noise" created by different phenological stages not represented by the three-season images. Newer techniques that composite multiple images to achieve a cloud-free representation may exacerbate this situation. Tools which create time-integrated images as smoothed seasonal representations show promise.

The plot clusters do not represent "whole" pixels. This project attempted to mitigate this by utilizing individual subplots within the cluster as separate samples. Confidence images for each of the parameter rasters indicated a very high degree of variation. It is surmised that a substantial portion of this variation is due to the plot-pixel size mis-match. Options to either increase plot size through two-stage sampling or reducing pixel size through incorporation of "pan" images are examined.

Though the plot design creates a representative sample for the Nation, exceptional areas are difficult to represent, yet the modeling process attempts to apply to all areas. For this project, parameters were limited to no greater than 10% extrapolation. This may not be optimal for biological phenomenon. Creating separate layers of extrapolated parameters may yield insightful information for subsequent product utility.

Citations:

Ellenwood JR, Krist FJ, Romero SA. National Individual Tree Species Atlas. FHTET-15–01. Fort Collins, Colorado: U.S. Department of Agriculture, Forest Service, Forest Health Technology Enterprise Team; 2015.

Krist FJ, Ellenwood JR, Woods M, McMahan A, Cowardin J, Ryerson D, Sapio F, Zweifler M, and Romero SA. 2013–2027 National Insect and Disease Forest Risk Assessment. FHTET-14-01. Fort Collins, Colorado: U.S. Department of Agriculture, Forest Service, Forest Health Technology Enterprise Team; 2014.

Quinlan R. Cubist/See5 [computer programs]. Rulequest, Inc. Available from: URL: http://www.rulequest.com; 2012.

Modeling forest structure and aboveground biomass integrating airborne LiDAR and satellite Radar data

Mariano Garcia[1,2], Sassan Saatchi[1] and Heiko Balzter[2,3]

[1] Jet Propulsion Laboratory (JPL), California Institute of Technology, Pasadena, CA 91109, USA.
[2] University of Leicester, Centre for Landscape and Climate Research, Department of Geography, Leicester, LE1 7RH, UK.
[3] National Centre for Earth Observation, University of Leicester, Leicester, LE1 7RH, UK.

Keywords: LiDAR, SAR, aboveground biomass, extrapolation.

Abstract

Improved spatially explicit information on forest structure and aboveground biomass (AGB) is required to understanding the role of forests in the carbon cycle, for greenhouse gases inventories or for sustainable forest management. This study aims at developing algorithms to allow the extrapolation of LiDAR-based forest height estimates over larger regions using satellite Radar data. We selected two study sites corresponding to a temperate broadleaf and mixed forest. The use of exponential models showed a poor performance for both study sites. Improved results were obtained using a support vector regression (SVR) algorithm. Inclusion of additional information from texture metrics as well as elevation data from SRTM significantly improved the results (R2=0.76 and 0.8; RMSE= 2.63 and 1.72 m for WLEF and Howland, respectively). Regardless of the modeling approach used, model performance improved as the resolution decreased from 25 m to 100 m.

Finally, we evaluated the potential of calibrating a single model for both study sites and compared it to the site-specific calibrated models. No significant differences between the site-specific and the biome model were observed at WLEF with R^2= 0.76 and 0.77 and RMSE= 2.63 and 2.62 m for the site-specific and the biome models, respectively. For Howland, a decrease in R^2 from 0.8 to 0.71 and an increase in RMSE from 1.72 to 2.04 m was observed.

Introduction

Improved spatially explicit information on forest structure and aboveground biomass (AGB) is required to understanding the role of forests in the carbon cycle, for greenhouse gases inventories or for sustainable forest management. Field methods are time consuming and limited in regards the spatial coverage, making difficult capturing the heterogeneity of forest structure. The high variability of forest structure both, at local and landscape scales, hampers extrapolation of forest structure estimates to regional or continental scales (Xu et al., 2016). Remotely sensed data, particularly LiDAR and radar sensors, offers the opportunity to capture this spatial variability in forest structure and improve AGB estimates over larger regions.

Two space LiDAR missions are planned for launch in the coming years, namely the ICESat-2/ATLAS (Gwenzi and Lefsky, 2014) and the Global Ecosystem Dynamics Investigation (GEDI; Dubayah,et al., 2014). Likewise, two satellite radar missions will be launched. The first is the BIOMASS mission, a P-band synthetic aperture radar (SAR), which is part of the ESA's (European Space Agency) Earth Explorers (http://www.esa.int/Our_Activities/Observing_the_Earth/The_Living_Planet_Programme/Earth_Explorers/Future_missions/Biomass). The second is the NASA-ISRO Synthetic Aperture Radar (NISAR), an L-band InSAR mission resulting from the partnership between NASA and the Indian Space Research Organization (ISRO).

The LiDAR sensors will be multi-beam profilers that will provide a dense sampling of the Earth's terrestrial ecosystems; however, in order to provide wall-to-wall estimates of forest structure integration of these data with other satellite borne sensors will be required. This study aims at developing algorithms to allow the extrapolation of LiDAR-based forest height estimates over larger regions using satellite Radar data. We address three research questions: 1) can we extrapolate LiDAR height using L-band SAR polarimetry data? 2) At what scale we obtain the best results? And 3) can we develop a single model for an entire biome or do we need site-specific models?

Methodology

Study sites

We selected two study sites corresponding to a temperate broadleaf and mixed forest. The first study site (WLEF) is located in Park Falls, Wisconsin, USA. The area selected was approximately 13 x 9 km, mainly covered by deciduous and mixed coniferous forests as well as some wetland areas. The second study area is the Howland forest, Maine, USA. This a boreal transitional forests in Howland mixed deciduous-coniferous forest, generally fragmented due to both natural disturbance and logging or management practices. This site covered an area of 8 x 5 km.

Datasets

ALOS-PALSAR

We used the high resolution terrain corrected product developed by the Alaska Satellite Facility from the Advanced Land Observing Satellite/Phased Array L-band Synthetic Aperture Radar (PALSAR). This product combines the radiometric and terrain correction processes to provide gamma naught power images at 12.5 m resolution (Gens, 2015). We selected 4 images for WLEF and 3 images for Howland from 2010, from May to October.

Airborne LiDAR

Our reference data to validate the height estimations from SAR data was the 1 m spatial resolution canopy height model (CHM) product developed by the G-LiHT (Goddard's LiDAR, Hyperspectral & Thermal Imager) team.

Additional data

The additional data consisted of the SRTM V2.1 product, with a spatial resolution of 30 m and a Landsat OLI image.

Data processing

Environmental conditions, like vegetation and soil moisture, have a significant impact in the backscatter signal (Santoro et al., 2006; Saatchi et al., 2011). In order to remove this effect, each pixel value was averaged using all dates available. Subsequently the images were resampled to 25 m, 50 m and 100 m. We also derived texture features from the images (standard deviation and entropy) using 5x5 and 9x9 window sizes. The same texture metrics were derived from the SRTM, which had been resampled to the same resolutions used for the ALOS-PALSAR data. As for the Landsat data, the spectral information was summarized into the brightness, wetness and greenness components of the tasseled cap transformation. The same texture metrics as for the SAR data were derived for each TC component.

Height modeling

We used two different approaches to estimate height from the ALOS-PALSAR data. The first approach used an exponential model fitted using the HH, the HV bands or a combination of both. To fit the models, the mean backscatter value obtained at each 1 m height interval was computed to reduce the noise of the backscatter data.

The second approach used a support vector regression (SVR) machine learning algorithm to estimate the height. We used the LS-SVMlab Toolbox developed by De Brabanter et al. (2011). A radial basis function was used as kernel and the two parameters defining the bandwidth (h) and the regularization parameter (g), which defines contribution of the training data error in the loss function to be minimized, were calculated using a grid search with a ten-fold cross-validation.

We tested different models based on the ALOS-PALSDAR data alone and consecutively adding additional information from the SRTM and the Landsat sensors. Approximately 10% of the data were used for calibration and 90% for validation. Finally, in order to evaluate the possibility of developing a single model for both study sites, a model was trained using sample data from both study sites and compared to the site-specific models.

Results

For both study sites, the exponential model based on HV band gave the best results due to the dominance of volume scattering from the canopy. Regardless of the band used, an increase in R^2 and a decrease of RMSE was observed as the spatial resolution decreased from 25 m to 100 m (Figure 1).

SVR models trained using HV data improved R2 more than 10% (WLEF: 0.43-0.58; Howland: 0.49-0.59 at 100 m) and reduced the RMSE by almost 40% (WLEF: 5.61-3.49 m; Howland: 3.71–2.42 m at 100 m). As for the parametric models, the best results were obtained at 100 m resolution. Inclusion of additional data improve the results significantly at both sites. For WLEF, the use of texture metrics derived using a 9x9 window and the elevation information from the SRTM provided the best results with R^2=0.76 and RMSE 2.63 m. Additional information including texture from SRTM and spectral and textural information from Landsat did not improve the results. For Howland, texture information provided important information for the height estimation given the fragmented landscape of this study site. Therefore, the best results were achieved using ALOS bands and their texture information along with the elevation and texture information derived from the SRTM data. The R^2 obtained for this model at 100 m resolution was 0.8 and the RMSE was 1.72 m. Figure 2 shows the R^2 and the RMSE achieved for each of the models trained.

The calibration of a single model (biome model) for both study sites showed good performance over both sites. Thus, no significant differences between

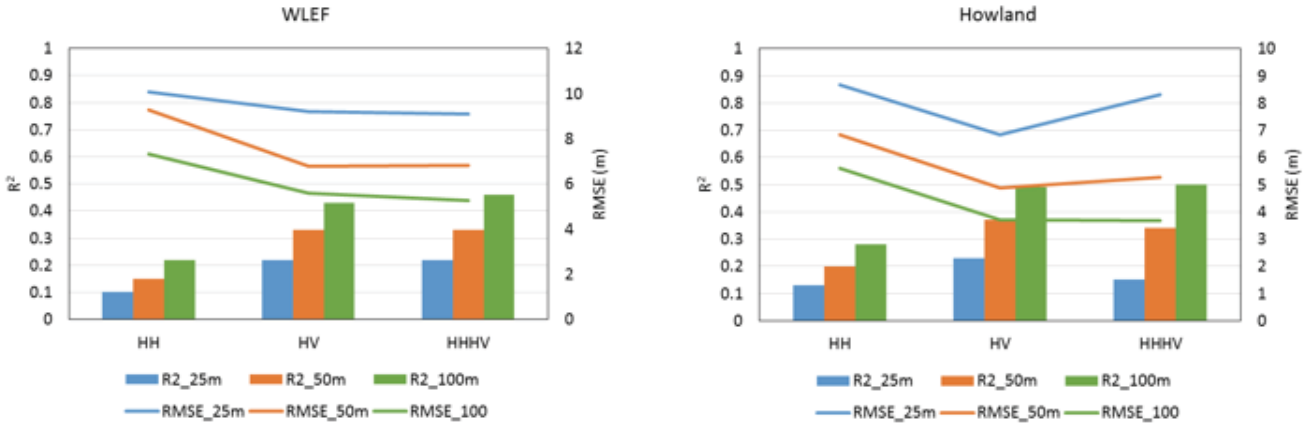

Fig. 1: R2 (bars) and RMSE (lines) values obtained for the each parametric model and spatial resolution at each study site.

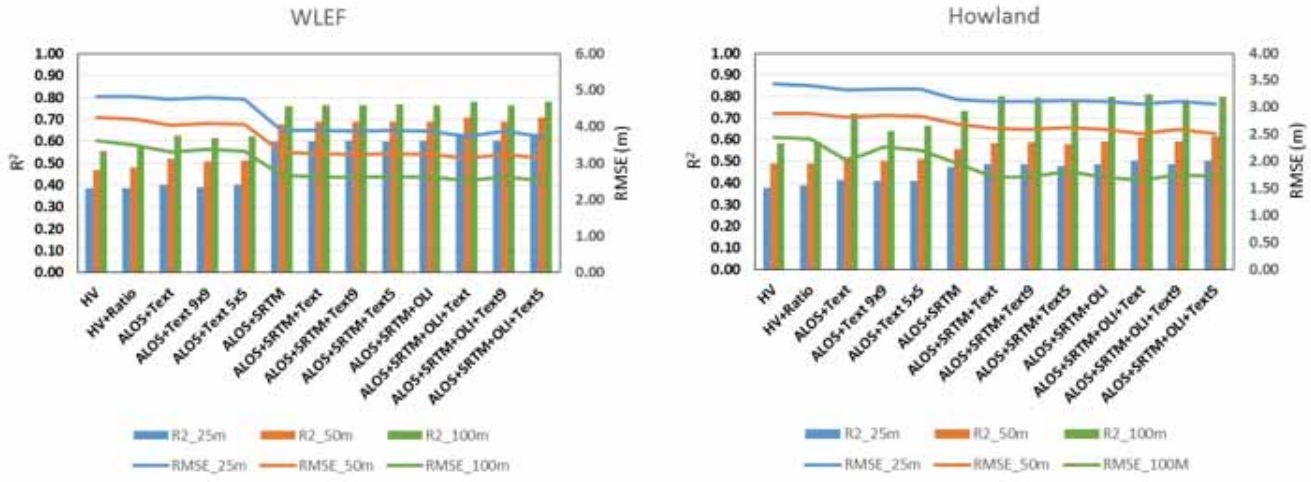

Fig. 2: R2 (bars) and RMSE (lines) values obtained for the each SVR model and spatial resolution at each study site.

the site-specific and the biome model were observed at WLEF with R^2= 0.76 and 0.77 and RMSE= 2.63 and 2.62 m for the site-specific and the biome models, respectively. For Howland, a decrease in R^2 from 0.8 to 0.71 and an increase in RMSE from 1.72 to 2.04 m was observed.

Conclusions

In this study we have demonstrated the LiDAR-based height can be extrapolated to larger areas using L-band SAR data in temperate broadleaf and mixed forests. In order to reduce the effect of environmental conditions on the backscatter signal, multitemporal data are required. NISAR will provide 12 day global observations, which will allow for an improved reduction of the effects of environmental conditions. The use of SRTM data help improve height estimates, particularly over areas with rougher topography, whereas texture information improve results over fragmented landscapes. Non parametric algorithms (SVR) showed greater ability to model canopy height than parametric models, allowing to better capture complex relationships between the backscatter signal and the LiDAR-based height. In all cases, spatial resolution affected significantly the estimations, with the best results achieved at 100 m spatial resolution. Our results are of significance for the integration of data provided by future space missions like GEDI and NISAR.

References

De Brabanter, K., P. Karsmakers, F. Ojeda, C. Alzate, J. De Brabanter, K. Pelckmans, B. De Moor, J. Vandewalle, and J. A. K. Suykens (2011), LS-SVMlab Toolbox User's Guide. Version 1.8, Katholieke Universiteit Leuven. Department of Electrical Engineering, ESAT-SCD-SISTA. Kasteelpark Arenberg 10, B-3001 Leuven-Heverlee, Belgium.

Dubayah, R., Goetz, S., Blair, J.B., Luthcke, S., Healey, S., Hansen, M., et al. (2014a). The Global Ecosystem Dynamics Investigation (abstract). ForestSAT 2014 Conference, Nov. 4-7, 2014, Riva de Garda, Italy.

Gens, R. (2015). ASF radiometric terrain corrected products. Algorithm Theoretical Basis Document.

Gwenzi, D., Lefsky, M.A., Suchdeo, V. P. and Harding, D.J, (2016). Prospects of the ICESat-2 laser altimetry mission for savanna ecosystem structural studies based on airborne simulation data. ISPRS Journal of Photogrammetry and Remote Sensing, 118, 68-82.

Saatchi, S.S., Marlier, M., Chazdon, r. L., Clark, D., B. and Russell, A.E. (2011). Impact of spatial variability of tropical forest structure on radar estimation of aboveground biomass. Remote Sensing of Environment, 115, 2836-2849.

Santoro, M. Eriksson, L., Askne, J. and Schmullius, C. (2006). Assessment of stand-wise stem volume retrieval in boreal forests from JERS-1 L-band SAR backscatter. International Journal of Remote Sensing, 27:16, 3425-3454.

Xu, L., Saatchi, S.S., Yang, Y., yu, Y. and White, L. (2016). Performance of non-parametric algorithms for spatial mapping of tropical forest structure. Carbon Balance and Management, 11-18.

Acknowledgements

Mariano Garcia is supported by a Marie Curie International Outgoing Fellowship within the 7th European Community Framework Programme (ForeStMap - 3D Forest Structure Monitoring and Mapping, Project Reference: 629376). The contents on this paper reflect solely the authors' views and not the views of the European Commission. Heiko Balzter was supported by the Royal Society Wolfson Research Merit Award, 2011/R3 and the NERC National Centre for Earth Observation. The research was carried out at the Jet Propulsion Laboratory, California Institute of Technology, under a contract with the National Aeronautics and Space Administration.

POSTER

Modeling of ALS data statistics in tree-level – application to single tree detection using Bayesian inference

Teemu Luostari[1], Timo Lähivaara[1], Petteri Packalen[2], Aku Seppänen[1]

[1] Department of Applied Physics, University of Eastern Finland, Finland
[2] School of Forest Sciences, University of Eastern Finland, Finland

Keywords: remote sensing, forest inventory, Bayesian inference, uncertainty quantification, modeling, single tree detection

Abstract

The analysis of Airborne Laser Scanning (ALS) data can be divided into two categories: area based methods and single tree detection. While the area based methods aim to predict the plot-level statistics directly from ALS data using regression-type methods, in the single tree detection, the plot-level statistics are derived from individual tree information inferred from the ALS data. The latter approach was taken, e.g., in (Andersen, Reutebuch, & Schreuder, 2002), (Lähivaara et al., 2014), (Micheas, Wikle, & Larsen, 2014), where the detection of individual trees and estimation of their dimensions was based on fitting a set of canopy height models (CHM) to the ALS data. In all these papers, the problem of single tree detection was considered in the framework of Bayesian inference (Kaipio & Somersalo, 2005). The Bayesian framework allows for incorporating prior information on the allometric relations of trees into the ALS based estimates of tree crown shapes. Such information can improve the reliability of the tree detection significantly: In (Lähivaara et al., 2014) the Bayesian approach resulted a success rate of about 70 % in a case where the success rate of a conventional height-based filtering (HBF) method was approximately 50 %.

In the CHM fitting proposed in (Lähivaara et al., 2014), the tree crowns are modeled as rotationally symmetric objects. If the error caused by this idealization is not accounted for, it can result biased estimates for the tree crown parameters and also lead to false detection of trees. In this paper, we aim at improving the Bayesian single tree detection by statistical modeling of errors caused the rotationally symmetric CHMs. The statistics of these modeling errors are computed using a training data set consisting of ALS data and field measured tree locations and sizes. The results show that accounting for the tree-level modeling error statistics improves the Bayesian estimates for the single tree parameters and the success rate of the tree detection.

References

Andersen, H., Reutebuch, S. E., & Schreuder, G. F. (2002). Bayesian object recognition for the analysis of complex forest scenes in airborne laser scanner data. *International Archives of Photogrammetry Remote Sensing and Spatial Information Sciences, 34*(3/A), 35-41.

Kaipio, J., & Somersalo, E. (2005). *Statistical and computational inverse problems* (1st ed.) Springer-Verlag New York.

Lähivaara, T., Seppänen, A., Kaipio, J. P., Vauhkonen, J., Korhonen, L., Tokola, T., et al. (2014). Bayesian approach to tree detection based on airborne laser scanning data. *IEEE Transactions on Geoscience and Remote Sensing, 52*(5), 2690-2699.

Micheas, A. C., Wikle, C. K., & Larsen, D. R. (2014). Random set modelling of three-dimensional objects in a hierarchical bayesian context. *Journal of Statistical Computation and Simulation, 84*(1), 107-123.

Modelling residual stand volume using unmanned aerial vehicles and digital aerial photogrammetry

Tristan Goodbody[1], Nicholas C. Coops[1], Piotr Tompalski[1], Patrick Crawford[2], Ken Day[3]*

[1] Faculty of Forestry, University of British Columbia, 2424 Main Mall, Vancouver, BC, V6T 1Z4, Canada. (604) 822 6452, goodbody.t@gmail.com, nicholas.coops@ubc.ca, piotr.tompalski@gmail.com
[2] Spire Aerobotics, 211-2386 East Mall Vancouver, BC, V6T 1Z3, Canada. (778) 928-4203, patrick@spireaerobotics.com
[3] Alex Fraser Research Forest, 72 South 7th Avenue, Williams Lake, BC, V2G 4N5, Canada. (250) 392-2207, ken.day@ubc.ca
Preference for Oral Presentation Format

Keywords: Unmanned Aerial Vehicles, Forest Inventory, Stereo Photogrammetry, Timber Volume, Predictive Modelling

Abstract

To improve precision management and the cost effectiveness of forest planning and operations, we look to build an enhanced forest inventory. To do so, we utilized an unmanned aerial vehicle (UAV) to collect a digital aerial photogrammetry (DAP) pointcloud to model residual stand volume and identify harvest locations. To do so, UAV collected aerial imagery and field measurements were acquired in 2015 in The Alex Fraser Research Forest near Williams Lake, BC. Tree height, diameter at breast height (DBH), and species were measured from systematically implemented variable radius plots throughout the study area at the time of imagery collection. DAP pointcloud metrics and field measurements were used to create a DAP volume model using linear regression with an RMSE% and bias% of 18.50 and 1.16 respectively. Results achieved from the DAP volume model indicate strong potential for UAV acquired DAP data to outline the location and estimate the quantity of residual stand volume. The cost effectiveness, ease of deployment, and collection of very high resolution imagery makes UAV collected DAP a strong candidate for incorporation into forest management and enhanced forest inventory practices. Future analysis into the utilization of DAP to gauge the success of applied harvesting regimes and monitoring residual stand behaviour post-harvest are discussed.

Modelling the effect of environmental factors on the height increment of stands with the use of repeated Airborne Scanning data

Jarosław Socha[*1], Radomir Bałazy[2], Marcin Pierzchalski [1], Mariusz Ciesielski[2]*

[1] University of Agriculture in Krakow, Faculty of Forestry, Al. 29 Listopada, Kraków, 32-425 Poland
[2] Forest Research Institute, Braci Leśnej 3, Sękocin Stary, 05 – 090 Poland
[*]Speaker, e-mail: rlsocha@cyf-kr.edu.pl

Keywords: LiDAR, height increment, microsite variability, topography

Abstract

Dynamics of forest communities expressed by height increment may be subjected to environmental gradients. Tree height increment may be subjected to temperature and wetness gradients, provides a quantitative baseline for understanding patterns of resource use, spatial structure and the physiological mechanism of tree reaction ecosystems to climate stress as the factors predisposing to climate affected disturbances.

The dependency between the topography and various environment factors has been observed for a long time (Hess, 1965, Maciaszek et al., 2000). The most commonly used topographic indices are elevation, aspect, slope, slope position, longitude and latitude (Chen et al., 1998; Hägglund and Lundmark, 1977; Seynave et al., 2005; Socha, 2008). Increasing availability of precise ALS based DEM models enable more detailed description of local topography by the use of different indices such as: TPI, SPTPI, TWI (R. Sørensen et al., 2006) or geomorphons (Jasiewicz and Stepinski, 2013). In site evaluation latitude and elevation are used as indirect measures of regional climate, while slope position, slope gradient and aspect are used as measures of local climate (Chen et al., 2002; Monserud and Rehfeldt, 1990; Socha, 2008; Wang and Klinka, 1996). Topographic indices such as Topographic Wetness Index (TWI) may be used as indirect measures of water status of given site (R. Sørensen et al., 2006). Due to the difficulties connected with measurement of height increment on standing trees analyses of height increment and its response to environmental gradients have received so far less attention and were limited mainly to relatively small samples collected from cut down trees (Gamache and Payette, 2004).

This study constitutes the practical application of change detection by airborne laser scanners for wall-to-wall monitoring the effect of environmental factors on the tree height growth over time using repeated ALS data.

The research objectives of this study on the whole elevational and aspect gradients in the Jizera Mountains were to (1) detect the site-dependent variability of mean annual height increments measured using change detection techniques, (2) explore the dominant environmental factors limiting height increment using repeated ALS data. We hypothesized that the limiting effect of water stress and temperature on height growth is affected by topography. Therefore we revealed that elevation, aspect and topographic indices, which by influence on thermal and moisture conditions affect height increment of Norway spruce may be used as indicator of susceptibility of given site to disturbances.

In the study, the data used were acquired: (a) in August and September 2007 via ALTM 3100 Optech laser scanner. (b) in July and August 2012 via LMS-Q680i laser scanner. ALS data had average density of around 6 points per m2, height error up to 15 cm and an X,Y location error below 20 cm. With the interpolation algorithms implemented in TerraScan software based on point cloud, the following models were generated: Digital Terrain Model (DTM), Digital Surface Model (DSM), and normalized Digital Terrain Model (nDSM) with a spatial resolution of 0.5 m. Digital Terrain Model (DTM) developed based on data from the airborne laser scanning was of spatial resolution equal to 0.5 m and covered whole area. Based on ALS data, digital surface models were generated for the years 2007 and 2012. Then, with through the raster difference (DSM – DTM) in map algebra Crowns Height Models (CHM) were established.

In the analysis the relationships between height increment obtained by change detection techniques and predictor variables were investigated using generalized additive models (GAM, Hastie & Tibshirani1990). Optimal amount of smoothing was estimated based on cross-validation. Graphs of smoothing spline functions of GAM models was used in order to illustrate the effect of individual predictor variables on height increment. Model GAM describing height increment within the period 2007 - 2012 as a function of site and stand characteristics explain about 62,5 % of height increment variability (R2adj=0,625). It was found that height increment was significantly affected by site characteristics including: altitude, slope, transformed aspect and other DTM products such as TWI and TPI.

Nationwide airborne laser scanning based models for volume, biomass and dominant height in Finland

*Eetu Kotivuori, Lauri Korhonen & Petteri Packalen**
eetu.kotivuori@uef.fi, lauri.korhonen@uef.fi, petteri.packalen@uef.fi, School of Forest Sciences, Faculty of Science and Forestry, University of Eastern Finland, P.O. Box 111, 80101 Joensuu, Finland. Petteri Packalen is the presenter.

Keywords: Airborne Laser Scanning; LIDAR; area-based approach; remote sensing; regression analysis; calibration; mixed-effect models

The aim of this study was to examine how well stem volume, above-ground biomass and dominant height can be predicted using nationwide airborne laser scanning (ALS) based regression models. The study material consisted of nine ALS inventory projects in different parts of Finland. We used field sample plots and ALS data to create nationwide and regional models for each response variable. The final models contained one or two ALS predictors, which were chosen based on the root mean square error (RMSE), and cross-validated. Finally, we tested how much predictions would improve if the nationwide models were calibrated with a small number of local sample plots. Although forest structures differ in different parts of Finland, the nationwide volume and biomass models performed quite well (leave-inventory-area-out RMSE 22.3% to 33.8%, bias -13.8% to 18.7%) compared with regional models (leave-plot-out RMSE 20.2% to 26.8%, no bias). However, the nationwide dominant height model (RMSE 5.4% to 7.7%, bias -2.0% to 2.8%, with the exception of one region) performed nearly as well as the regional models (RMSE 5.2% to 6.7%). The results show that the nationwide volume and biomass model predictions are likely to be biased, because forest structure and ALS device have a considerable effect on the predictions. Large biases appeared especially in northern Finland. Local calibration decreased the bias and RMSE of volume and biomass models. However, the nationwide dominant height model did not benefit much from calibration.

Predicting the aboveground biomass of individual trees using remote sensing data and new allometric models: a case study in Norway

Michele Dalponte[1], Lorenzo Frizzera[1], Hans Ole Ørka[2], Tommaso Jucker[3], Terje Gobakken[2], Erik Næsset[2], Damiano Gianelle[1]

[1] Dept. of Sustainable Agro-ecosystems and Bioresources, Research and Innovation Centre, Fondazione E. Mach, Via E. Mach 1, 38010 San Michele all'Adige (TN), Italy
[2] Dept. of Ecology and Natural Resource Management, Norwegian University of Life Sciences, P.O. Box 5003, NO-1432 Ås, Norway
[3] Dept. of Plant Sciences, University of Cambridge, Downing Site, Cambridge CB2 3EA, United Kingdom

Keywords: individual tree crowns, aboveground biomass, airborne laser scanning, hyperspectral imagery

Introduction

Allometric models used in forestry to predict tree's aboveground biomass rely primarily on diameter at breast height (DBH) and tree height as inputs. In many forest types such models are species-specific, which means that species must be recorded as well. In particular DBH and species information play an important role as tree height is often predicted as function of these attributes. Nowadays airborne laser scanning (ALS) data provide detailed height measurements, in addition to which individual tree crown (ITC) delineation methods provide a means to determine (for each detected tree) crown dimensions that subsequently can be related to DBH (Hemery *et al.*, 2005). Moreover, with hyperspectral data detailed tree species mapping is possible (Dalponte *et al*. 2012). As DBH cannot be directly measured with airborne remote sensing (ARS) data, it may be useful to develop new allometric models based on tree characteristics that can be directly measured from ARS data. Following this idea, Jucker *et al*. (2016) recently developed allometric models for predicting DBH and aboveground biomass (AGB) based on height and crown diameter using a worldwide dataset of more than a hundred thousand individual trees measurements. The study of Jucker *et al*. (2016) did not involve remote sensing data, focusing exclusively on the development of the allometries. Moreover it focused on developing global and regional allometric models without considering species-specific information. The objective of this study is to develop species-specific models for the prediction of DBH for three main species groups in Norway using field measured height and crown diameters, and to validate the models when remotely sensed data (ALS and hyperspectral data) are used to predict species, height and crown diameter. To achieve this objective we developed the models using data from one dataset and then we validated them on an independent dataset.

Study areas

In this study two datasets collected in two different areas in southern Norway were used. The first dataset collected in Aurskog-Høland municipality was used for the development of the DBH allometric models for Scots pine, Norway spruce and broadleaves species. The dataset consists of 667 field measured trees for which DBH, height, species and crown dimensions were recorded. On this dataset a validation at tree level was done.

The second dataset was used to validate the models at plot level. It was collected in Våler municipality. This dataset comprised 9376 trees distributed on 153 plots of 400 m^2. ALS and hyperspectral data have been acquired over the plots in 2011. Inside each plot the position of all the trees, the DBH and the species were recorded, while the height was measured only for few sample trees in each plot.

Methods

Using the Aurskog-Høland dataset, models that relate DBH to field measured heights and crown diameter were constructed following the methodology of Jucker *et al*. (2016). The models were in the form:

$$DBH = a * (H * CD)^b + \varepsilon \quad (1)$$

where is the diameter at breast height in centimeters, the height in meters, and the crown diameter in meters. The model fitting was done by using a data binning approach and a log normal form of the models. To validate the models at tree level, for each model, the root mean square error (RMSE), average mean difference (D-bar), and coefficient of determination (R^2) were calculated on an independent validation dataset corresponding to 10% of trees selected at random. This randomization procedure was repeated 100 times and for each metric the mean value across the 100 iterations was calculated.

For the Våler dataset, individual tree crowns (ITCs) were delineated using the ALS data and the delineation algorithm of the R package (*itcSegment*). Delineated ITCs were matched to the field data and the matched ITCs were used for species classification using hyperspectral data. 1608 matched ITCs were used as training and 1416 as validation. The hyperspectral pixels inside each ITC that had a NDVI value higher than 0.5 were used in the classification process. The species classification was performed using a Support Vector Machine (SVM) classifier (R library *kernlab*) at pixel level, and then the labels of the pixels inside each ITC were aggregated using a majority rule. This approach was used to predict the species of all the delineated ITCs.

DBH for each ITC was predicted using the model in equation 1. AGB was predicted for each ITC using the models of Marklund (1988) with height from ALS data as one predictor and DBH from equation 1 and species from hyperspectral data as the two other predictors. AGB for the field trees was predicted using the models of Marklund (1988) and field measured height, DBH, and species. Plot level field estimated AGB was obtained summing the values of AGB of all trees inside each plot. Similarly the plot level ARS estimated AGB was obtained summing the values of AGB of all ITCs inside each plot.

Results

In Table 1 the coefficients of the models in equations 1 for the three species considered are presented, along with RMSE, D-bar and R^2. The delineation method used detected more than 90% of the trees with DBH >20 cm, and only 56% of the trees with DBH <20 cm (see Figure 1). The tree species classification accuracy obtained on the validation set were: i) overall accuracy: 87.7%; ii) kappa accuracy: 0.794; and ii) mean class accuracy: 83.6%. Figure 2 shows the results of the AGB estimation at plot level for the Våler dataset.

As it is clear from these results (and by the ones of Jucker *et al*. 2016) it is possible to reverse the allometric models in order to use height and crown diameters as input. The relation of these models with ARS data needs to be considered more carefully as it strongly depends on the forest characteristics. Indeed the main limitation remains, namely that ITC approaches do not detect all trees, and especially not the suppressed ones, and thus there will always be a fraction of the AGB missing (see Figure 2). The tendency of missing trees will increase in multilayer and dense forests. Moreover, dense canopies may create high commission errors in the delineation, resulting in an erroneous increase in the AGB estimate.

Table 1. Coefficients, RMSE, D-bar and R^2 for equation 1 for all the species together, and for the three main species groups.

Species	a	b	RMSE (cm)	D-bar (%)	R^2
All	0.808	0.794	3.6	-3.2	0.79
Spruce	0.952	0.749	2.6	0.9	0.87
Pine	1.365	0.691	3.6	2.0	0.85
Broadleaves	0.795	0.754	2.3	0.3	0.50

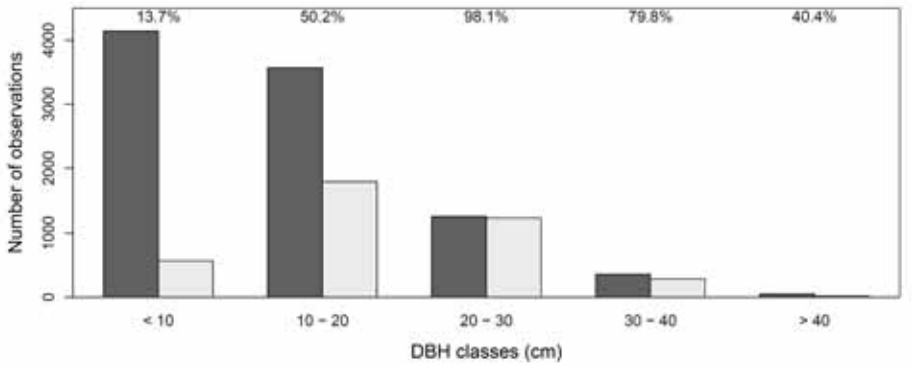

Figure 1. Number of field measured trees (dark gray bars) and number of detected ITCs (light gray) for each DBH class. The numbers at the top of the graph represent the percentage of detected trees.

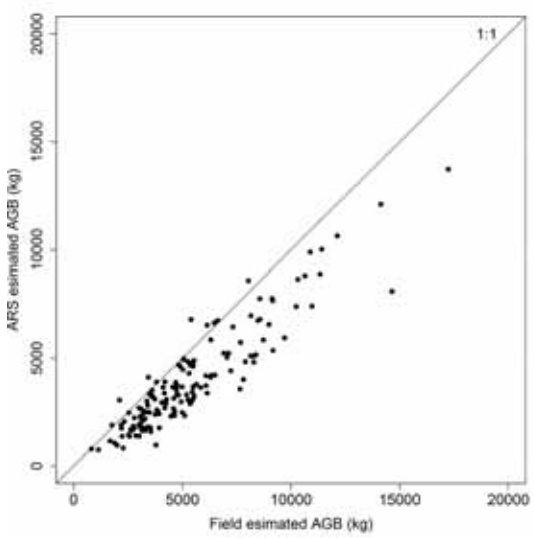

Figure 2. Field estimated AGB and ARS estimated AGB for each field plot in Våler dataset.

References

Dalponte, M., & Coomes, D. A. (2016). Tree-centric mapping of forest carbon density from airborne laser scanning and hyperspectral data. *Methods in Ecology and Evolution*, doi: 10.1111/2041-210X.12575.

Dalponte. M., Bruzzone, L., Gianelle, D. (2012) Tree species classification in the Southern Alps based on the fusion of very high geometrical resolution multispectral/hyperspectral images and LiDAR data. *Remote Sensing of Environment*, 123, 258–270.

Hemery G.E., Savill P.S., & Pryor S.N. (2005) Applications of the crown diameter–stem diameter relationship for different species of broadleaved trees. *Forest Ecology and Management*, 215, 285–294.

Jucker, T., Caspersen, J. P., Chave, J., Antin, C., Barbier, N., Bongers, F., Dalponte, M., van Ewijk, K., Forrester, D., Heani, M., Higgins, S., Holdaway, R., Iida, Y., Lorimer, C., Marshall, P., Momo, S., Moncrieff, G., Ploton, P., Poorter, L., Rahman, A., Schlund, M., Sonké, B., Sterck, F., Trugman, A., Usoltsev, V., Vanderwel, M., Waldner, P., Wedeux, B., Wirth, C., Wöll, H., Woods, M., Xiang, W., Zimmermann, N., & Coomes, D. A. (2016). Allometric equations for integrating remote sensing imagery into forest monitoring programs, Global Change Biology, submitted.

Marklund, L.G., (1988). Biomass functions for pine, spruce and birch in Sweden (Report No. 45). Swedish University of Agricultural Sciences, Umeå.

Prediction of alien species richness in two forest watershed of South-Central Chile: a remote sensing synergistic approach

Mauricio Galleguillos[1,2], Andrés Ceballos[1,2], Antonio Lara[2,3]*

[1]Universidad de Chile, Facultad de Ciencias Agronómicas, Departamento de Ciencias Ambientales y Recursos Naturales Renovables.
[2]Center for Climate and Resilience Research (CR2), Chile.
[3]Universidad Austral de Chile, Facultad de Ciencias Forestales y Recursos Naturales, Instituto de Conservación, Biodiversidad y Territorio.
**Corresponding author: mgalleguillos@renare.uchile.cl*

Keywords: alien species richness, predictive model, spectral index, evaporative fraction, spatio-temporal, textures, exotic forest plantations.

Abstract:

Central Chile is considered one of the biodiversity hotspot and is a highly threatened territory due to land use changes, especially the establishment of exotic industrial plantations of pine and eucalyptus. The intensive short time rotation of these monoculture provide increasingly fragmented landscape configuration that favors the introduction and establishment of alien species. The aim of the research was estimating the spatial distribution of alien species richness by the use of a synergistic approach based on spatio-temporal remote sensing information. We developed a parsimonious and accurate predictive model of alien species richness from *in situ* data taken in two watershed of South-central Chilean coastal range, based on vegetation indexes and evaporative fraction derived from thermal data.

Introduction

Ecosystems of the Chilean Mediterranean biodiversity hotspot are under an increasingly threatened condition mainly due to land use change because of human use competition (Alaniz et al. 2016). The landscapes of South-Central Chile are currently configure by the dynamic of forest plantation systems, and are constitute by a fragmented mosaic of pine and eucalyptus monocultures, shrubs, bare soil, agro-grassland and native forest remnants with high endemism proportion (Miranda et al., 2016). The high rates of change of land cover due to the dynamic of short time rotation of industrial plantations have generated modifications in the floristic composition of plant species, leading to an increase of alien species adapted to conditions of constant change and variability.

The invasion of dangerous alien species can lead to extinction of native species, modifying biodiversity, affecting ecosystems services, modifying the ecosystem metabolism and affecting the landscape (Hobbs 2000). The monitoring of alien species is paramount to prevent this effects, this is why remote sensing has demonstrated to be a valuable tool in this endeavor (Asner and Vitousek 2005). The generation of especially explicit empirical models that allow to identify where those species are grouped, can help to improve the management decision at the landscape level. The investigation present an original predictive modelling methodology based on a synergistic remote sensing approach that make use of spatio-temporal predictors based on vegetation index and evaporative fraction information.

The study area comprise to subcatchments (Purapel y Cauquenes) covered mainly by forest plantations and are located in the coastal range mountains of the Maule and Bio-bio regions (Fig. 1). Land cover maps were computed with the Maximum Likelihood supervised classification from Landsat data for years 2001 and 2013 in order to determine the field sample plots that represent the most representative

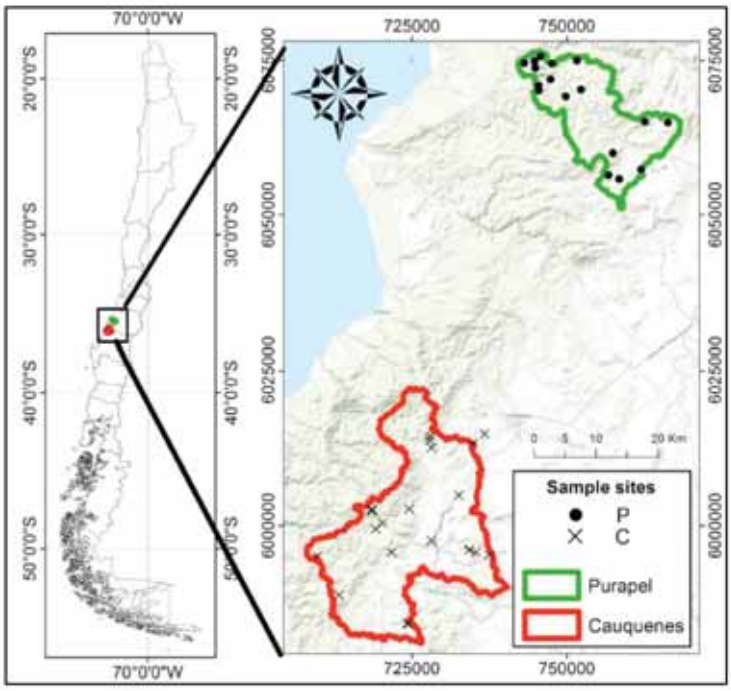

Fig. 1: Study site and sample plots spatial distribution

ecosystem states within the catchments: Early successional; adult pine plantation; adult eucalyptus plantation; mixed-exotic-native; native forest (Fig 2). Field vegetation surveys were accomplished to determine plant vascular species richness, including herbs, shrubs and trees, in 39 plots of 225m^2 each, by using a nested plot design.

Several kind of predictors were considered: topographical, derived from a DEM SRTM; vigor of vegetation derived from spectral indexes (NDVI, GNDVI, NGRDI); and hydric status of vegetation represented by evaporative fraction (EF) computed with thermal data using the Simplified Surface Energy Balance Index (S-SEBI) (Roerink et al. 2000) following the parameterization of Galleguillos et al. 2011. Spectral and thermal predictors were obtained from ASTER Level 2 products of surface reflectance and land surface temperature, spatio-temporal metrics were computed for the latter predictors, and these were obtained from nine and eight scenes spanning the years 2001 to 2014 for Cauquenes and Purapel watersheds. Variables eco-hydrological conditions were covered by the set of available scenes according to the time lapse from the last significant precipitation event. The predictors were submitted to texture analysis with a gray-level co-occurrence matrix, which allowed to characterize the spatial heterogeneity of the landscape. A data mining approach based on the Recursive Feature Elimination (Guyon et al. 2002) algorithm was used to obtain the combination of predictors that explain better the response variable. Then, the selected predictors were used to adjust a Generalized Linear Model with a Poisson distribution (Lopatin et al., 2016).

A parsimonious model was obtained for alien richness prediction (Fig. 3), with an R2 = 0.74, an RMSE = 2.18 and a BIAS = 11.1% considering 4 predictors: the variance between 25 pixels (kernel of 5*5) from a raster that represent the first quartile of the temporal series of NGRDI (spectral-spatial-temporal predictor, NGRDIpc_Vx5), the quotient of the absolute deviation from the median and the median of temporal series of evaporative fraction (temporal-energy flux predictor, EF_cb), the land cover (structural predictor), and the watershed where the alien species belongs (bioclimatic predictor). Representation of the model: glm (Richness ~ NGRDIpc_Vx5 + EF_cb + LandCover + watershed). A bootstrapping validation assessment shows the consistency of the model in the Fig. 3 a,b,c). The selected predictors were coherent with the functional dynamic of alien species in those kinds of ecosystems, and with the inner structural compatibility of each land cover class.

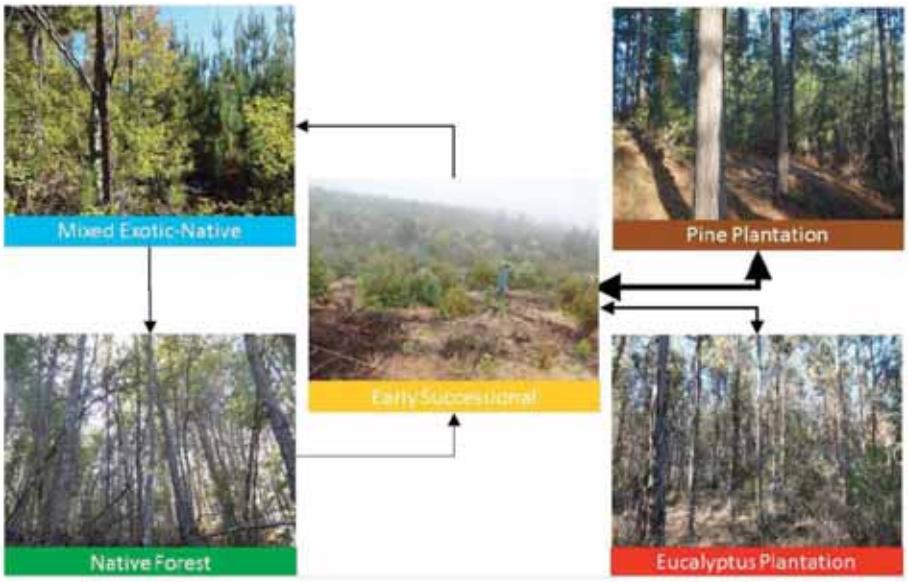

Figure 2. Ecosystems states identifies according to the land cover changes analysis of maps of 2001 and 2013. Arrows represent expected transitions between classes and the width of the arrows represent the frequency of the transition within the catchments.

Results and discussion

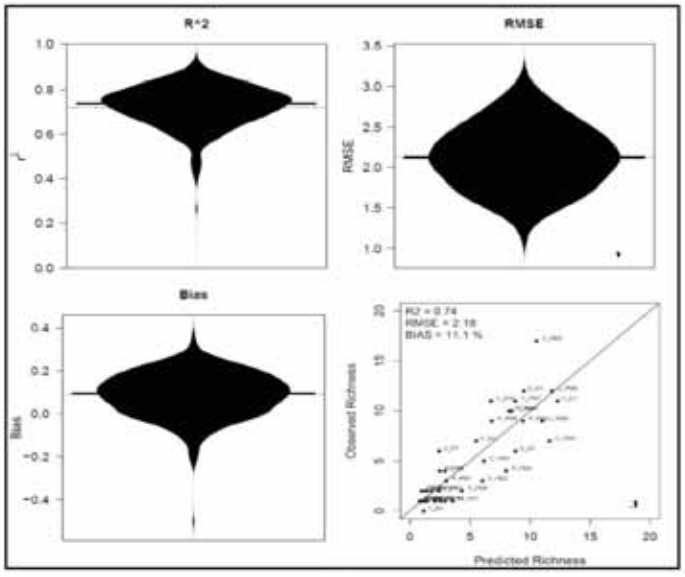

Fig. 3: a,b,c). Coefficient of determination, root-mean-square error and bias bootstraping validation assessment respectively of the predictive model. d) Model representation (predicted alien species richness by the model vs observed alien species richness).

Conclusions

The synergy generated by the contribution of different source of satellite data and the spatio-temporal analysis allowed to obtain an acceptable accurate prediction of alien species richness in forested ecosystems subjected to strong anthropic pressure.

References

Alaniz A., Galleguillos M., Pérez-Quezada J. 2016. Assessment of quality of input data used to classify ecosystems according to the IUCN Red List methodology: The case of the central Chile hotspot. Biological Conservation In press.

Asner G. and Vitousek P.M. 2006. Remote analysis of biological invasion and biogeochemical change. PNAS 102(12): 4383-4386.

Galleguillos M., Jacob F., Prévot L., French A., Lagacherie P., (2011). Comparison of two temperature differencing methods to estimate daily evapotranspiration over a Mediterranean vineyard watershed from ASTER data. Remote Sensing of Environment 115(6): 1326.

Guyon, I., Weston, J., Barnhill, S., (2002). Gene selection for cancer classification using support vector machines. Mach. Learn. 46, 389–422.

Hobbs R.J. (2000) Land-Use changes and invasions. In: Mooney H.A., Hobbs R.J. (eds.) Invasive species in a changing world. Washington, DC. Island Press. p. 31-54.

Lopatin J., Dolos K., Hernández J., Galleguillos M., Fassnacht F. (2016). Comparing generalized linear models and random forest to model vascular plant species richness using LiDAR data in a natural forest in central Chile. Remote Sensing of Environment 173:200–210.

Miranda, A. Altamirano, A. Cayuela, L. Lara, A. González, M. 2016. Native forest loss in Chilean biodiversity hotspot: revealing the evidence. Regional Environmental Change: 1-13.

Roerink, G. J., Su, Z., & Menenti, M. (2000). S-SEBI: a simple remote sensing algorithm to estimate the surface energy balance. Physics and Chemistry of the Earth. Part B: Hydrology, Oceans and Atmosphere, 25(2), 147–157.

Reconciling MODIS satellite with terrestrial forest inventory data to assess forest productivity in Europe

Mathias Neumann[1], Adam Moreno[1], Volker Mues[2], Sanna Härkönen[3], Matteo Mura[4], Olivier Bouriaud[5], Mait Lang[6], Giuseppe Cardellini[7], Alain Thivolle-Cazat[8], Karol Bronisz[9], Jan Merganic[10], Iciar Alberdi[11], Rasmus Astrup[12], Frits Mohren[13], Maosheng Zhao[14], Hubert Hasenauer[1]*

[1] *Institute of Silviculture, Department of Forest and Soil Sciences, University of Natural Resources and Life Sciences, Vienna, 1190, Austria*
[2] *University of Hamburg, Centre for Wood Science, World Forestry, Hamburg, 21031, Germany*
[3] *University of Helsinki, Department of Forest Sciences, Helsinki, 00014, Finland*
[4] *geoLAB - Laboratory of Forest Geomatics, Department of Agricultural, Food and Forestry Systems, Università degli Studi di Firenze, Firenze, 50145, Italy*
[5] *Universitatea Stefan del Mare, Suceava, 720229, Romania*
[6] *Tartu Observatory, Tõravere, 61602, Estonia*
[7] *KU Leuven – University of Leuven, Division Forest, Nature and Landscape, Leuven, 3001, Belgium*
[8] *Technological Institute, Furniture, Environment, Economy, Primary processing and supply, Champs sur Marne, 77420, France*
[9] *Laboratory of Dendrometry and Forest Productivity, Faculty of Forestry, Warsaw University of Life Sciences, Warsaw, 02-776, Poland*
[10] *Czech University of Life Sciences, Faculty of Forestry and Wood Sciences, Prague, 16521, Czech Republic*
[11] *INIA-CIFOR, Departamento de Selvicultura y Gestión de los Sistemas Forestales, Madrid, 28040, Spain*
[12] *Norwegian Institute for Bioeconomy Research, Ås, 1431, Norway*
[13] *Wageningen University, Forest Ecology and Forest Management Group, Wageningen, 6700, The Netherlands*
[14] *Department of Geographical Sciences, University of Maryland, 20742, USA*

* *corresponding author mathias.neumann@boku.ac.at*

Keywords: MODIS, NFI, Europe, trees, climate, modelling, carbon, biomass, bioeconomy

Forests provide important ecosystem services, such as timber production for a growing bio-economy, food, increasing demand biodiversity, water and protection against natural hazards. Forests are also increasingly important in mitigating climate change effects by storing large amounts of carbon. The physiology and productivity of forests are strongly altered by environmental conditions such as climate, soils and management practices. Understanding the response and feedbacks of forest towards historic, current and future environmental change requires a consistent large scale model framework incorporating the biogeochemical processes between vegetation and the atmosphere. Today large scale forest information is provided by earth observing satellite systems which include the Moderate Resolution Imaging Spectroradiometer (MODIS). MODIS data can be used in conjunction with the MOD17 algorithm to produce vegetative productivity estimates. This algorithm combines biogeochemical model principles with temporally--explicit vegetation data and daily climate data to provide productivity measures worldwide on a 1-km resolution. In this study we computed a regional Net Primary Production (NPP) dataset ("MODIS_EURO") by rerunning MOD17 with local European climate data. We next harmonized tree carbon estimation methods from 13 European countries and processed data from 196,434 plots (more than 2 Mio. sample trees) from 13 National Forest inventories to obtain terrestrial NPP. With this reference dataset, we evaluated our previously created remote sensing dataset "MODIS_EURO" across scales and gradients. MODIS EURO shows better agreement with the terrestrial reference NPP from forest inventory data, than the global MODIS NPP estimates that use a global climate data set, highlighting the importance of accurate climate data in remote sensing applications. MOD17 is climate sensitive and local climate data better captures the conditions in Europe. Discrepancies between MODIS EURO and terrestrial data can be explained by differences in forest stand density and the employed tree carbon estimation methods. This new dataset

- the key outcome of this study - provides wall-to-wall NPP estimates for Europe (EU-27 including Norway and Switzerland) and allows spatial and temporal analysis on the impact that environmental change has on vegetative productivity. This study highlights the advantages and disadvantages of two conceptually different approaches for estimating NPP and enhances our understanding of linking terrestrial with remote sensing data.

References:

Moreno, A. & Hasenauer, H. (2015). Spatial downscaling of European climate data. International Journal of Climatology. http://doi.org/10.1002/joc.4436

Moreno, A., Neumann, M., & Hasenauer, H. (2016). Optimal resolution for linking remotely sensed and forest inventory data in Europe. Remote Sensing of Environment, 183, 109–119. http://doi.org/10.1016/j.rse.2016.05.021

Neumann, M., Zhao, M., Kindermann, G., & Hasenauer, H. (2015). Comparing MODIS Net Primary Production Estimates with Terrestrial National Forest Inventory Data in Austria. Remote Sensing, 7(4), 3878–3906. http://doi.org/10.3390/rs70403878

Neumann, M., Moreno, A., Mues, V., Härkönen, S., Mura, M., Bouriaud, O., Lang, M., Achten, W. M. J., Thivolle-Cazat, A., Bronisz, K., Merganic, J., Decuyper, M., Alberdi, I., Astrup, R., Mohren, F.,Hasenauer, H. (2016). Comparison of carbon estimation methods for European forests. Forest Ecology and Management, 361, 397–420. http://doi.org/10.1016/j.foreco.2015.11.016

Neumann, M., Moreno, A., Thurnher, C., Mues, V., Härkönen, S., Mura, M., Bouriaud, O., Lang, M., Cardellini, G., Thivolle-Cazat, A., Bronisz, K., Merganic, J., Alberdi, I., Astrup, R., Mohren, F., Zhao, M., & Hasenauer, H. (2016). Creating a Regional MODIS Satellite-Driven Net Primary Production Dataset for European Forests. Remote Sensing, 8(554), 1–18. http://doi.org/10.3390/rs8070554

Zhao, M. & Running, S. W. (2010). Drought-induced reduction in global terrestrial net primary production from 2000 through 2009. Science, 329(5994), 940–3. http://doi.org/10.1126/science.1192666

Relating forest height structure to virtual ground truth data

Nikolai Knapp[1], Rico Fischer[1], Andreas Huth[1]

[1] Helmholtz-Centre for Environmental Research (UFZ), Leipzig, Germany

Key words: forest structure, dynamic modeling, Lidar simulation, calibration

Recent developments in remote sensing technology have improved our abilities of forest monitoring remarkably. Accurate height maps and even 3D point clouds of forest canopies can be obtained from light detection and ranging (Lidar) and increasingly from synthetic aperture Radar (SAR) satellites (e.g. TanDEM-X, Sentinel-1). However, it remains a challenge to link metrics of height structure to the main variables of interest, such as forest biomass, productivity, carbon turnover, stem size distribution, disturbance patterns or forest age. Usually, large forest inventory datasets are required to establish robust relationships between remote sensing metrics and ground-based metrics. Such inventory-based calibration requires extensive field campaigns and reaches its limits with variables which are difficult to measure at plot scale, like carbon fluxes.
Here, we propose a new approach where we complement real world ground-truth data with virtual forest inventory data generated by forest simulations. Dynamic forest models help us to understand the links between ecological processes and vegetation structure. Hence, joining the fields of remote sensing and forest modeling will lead to mutual benefits, by increasing structural realism of forest models and facilitating the development and calibration of remote sensing approaches.

We used the individual-based forest model FORMIND to simulate the neotropical lowland rainforest of Barro Colorado Island (BCI), Panama, and derived virtual inventory data covering the full range of possible successional states. For each simulated stand we also conducted a virtual remote sensing campaign using a Beer-Lambert-based Lidar model. The simulated datasets were then used to investigate relationships between remote sensing metrics and intrinsic attributes of the forest. We considered metrics of different spatial resolutions to also mimic height data that could be obtained from spaceborne SAR systems.

The presented methodology can serve to better understand how carbon dynamics in forests relate to the measurable structure of forests and how this information can be used for remote sensing based inventories and monitoring. Additionally, the approach allows exploration of the potential of future satellite missions (e.g. GEDI, BIOMASS, Tandem-L) for estimating the different forest attributes.

Temporal and Angular Effects of the Spectral Signal on Deciduous Forest Crown Components

Michael Foerster[1], Ben Somers[3], Kyle Pipkins[1], Laurent Tits[4], Karl Segl[2], Maximilian Brell[2], Birgit Kleinschmit[1], Angela Lausch[5] and Anne Clasen[1, 2]

[1]Geoinformation in Environmental Planning Lab, Technische Universität Berlin, Straße des 17. Juni 145, D-10623 Berlin, Germany
[2]Helmholz Centre Potsdam-GFZ German Research Centre for Geosciences, Telegrafenberg, 14473 Potsdam, Germany
[3]Division of Forest, Nature and Landscape, Department of Earth and Environmental Sciences, KU Leuven, Celestijnenlaan 200E, BE-3001 Leuven, Belgium
[4]Geomatics Lab, Department of Biosystems, KU Leuven, Willem de Croylaan 34, BE-3001 Leuven, Belgium
[5]Department of Compuational Landscape Ecology, Helmholtz Centre for Environmental Research-UFZ, Permoserstrasse 15, D-04318 Leipzig, Germany

Keywords: Unmixing; MESMA; forest; bark; observation angle; phenology.

Abstract

Imaging spectroscopy has proven to be a promising tool to provide information on forest biochemical and biophysical variables. The presented study is investigating crown component fractions in a forest ecosystem on a sub-pixel-basis. In this context, the potential of spectral unmixing to derive information on the distribution of the endmembers 'leaf', 'bark' and 'soil' within a pixel is analyzed.

Close range spectral measurements of the canopy and its components were taken with an ASD FieldSpec instrument mounted to a crane measurement platform situated in a temperate deciduous forest in North-East Germany. Reference fractional abundances of the components were precisely determined from photographs taken simultaneously to the ASD measurements. Unlike most other studies, which only consider two components, mainly 'leaf' and 'soil', this experimental setup facilitated the inclusion of the additional component 'bark' for the unmixing of forest crown components.

Measurements from different stages of the phenological phases were used in this study. In the 2015 field campaign, data was collected on April 21st, June 5th, August 3rd and October 1st. Airborne HySpex data was collected simultaneously on the last three of these dates and on July 7th.

Especially in summer, the dense foliation in this complex vegetation structure causes the problem of saturation effects, when applying broadband vegetation indices. This study illustrates that multiple endmember spectral mixture analysis (MESMA) can contribute to overcoming this challenge. The results indicate that the inclusion of an additional 'bark' endmember clearly improves the accuracy of the unmixing results. When only nadir viewing directions were taken into account, a mean absolute error of 7.9% could be achieved for the fractional occurrence of the 'leaf' endmember and 5.9% for the 'bark' endmember. In order to evaluate the results of this field-based study for remote sensing applications, a transfer to airborne and satellite-based imagery was carried out. All sensors used in this study were capable of unmixing crown components with a mean absolute error ranging between 3% and 21% for the nadir measurements.

However, airborne and spaceborne sensors provide imagery that includes not only nadir viewing directions. Off-nadir viewing zenith angles up to 10° are a common case for sensors with a large swath. This needs to be considered in image processing and the derivation of biophysical parameters. BRDF corrections account for illumination and viewing geometry as well as structural and optical properties of the surface, but commonly, they do not account for variations in the actual visibility of the canopy components at different observation angles. The crane measurement platform allowed for a very detailed view on the changing visibility of the occurring canopy components at different angles.

Use of Random Forest Modeling Techniques to Predict and Detect Shrub Locations Under Canopy using LiDAR Structure and Topography Metric

Caileigh Shoot, Sean Jeronimo, Van Kane, Monika Moskal, Jonathan Kane
University of Washington, School of Environmental and Forest Sciences, Seattle, WA 98195;

Jim Lutz
Utah State University, S. J. & Jessie E. Quinney College of Natural Resources, 5230 Old Main Hill, Logan, UT 84322-5230

Abstract

Shrubs are an important component of forested ecosystems around the globe. Fulfilling many ecological niches, shrubs can be anything from a source of food and habitat, to an understory fuel in wildfire. Shrubs add vital carbon and nutrients to forests, assist in water filtration and storage in forest soils, and can act as a key indicator of overall forest vigor. Despite their importance, shrub distributions are widely unknown across landscapes. In addition, mapping shrub locations in the field is arduous and virtually impossible to implement across entire landscapes. Thus, in order to protect and manage shrubs, it is important that a method for mapping and quantifying shrubs across the landscape is developed. LiDAR has been proven to accurately measure upper canopy features when compared with field measurements, but has not been proven to be a viable method of measuring below-canopy features such as shrubs, despite it's ability to penetrate the forest canopy. This study will create and evaluate a method for detection and prediction of shrub locations across a landscape using Random Forest, a classification and regression machine learning algorithm.

This study was performed on the 25.6 ha Yosemite Forest Dynamics Plot in Yosemite National Park. Medium-resolution (averaging 30 points per m^2) discrete-return LiDAR data was acquired in 2010, and in 2011 field crews mapped and identified the species of all shrub patches >2 m^2. The LiDAR data was analyzed using FUSION, which generates 400+ metrics from the LiDAR data, including both canopy structure and topographic metrics. These metrics were input as predictors into a Random Forest model, and then used to detect and predict shrub locations. With this method, explanatory model accuracies averaged 84% using only topography metrics, 75% using only structure metrics, and 79% using both structure and topography metrics. Predictive model accuracies were shown to be much lower, averaging 33% accuracies for all 3 predictor inputs. These lower accuracies appear to be spatially correlated and may potentially be explained by variables not captured in previous field data collection efforts. In order to better understand and explain these results, further investigation into these errors is needed and will likely be performed in Fall 2016.

Vegetation Chlorophyll estimated from multi-angle MODIS and tower hyperspectral observations: A tool for scaling ecosystem seasonality and leaf demography across Amazonian evergreen forests

Thomas Hilker[1,2], Lênio Soares Galvão[3], Luiz E. O. C. Aragão[3], Yhasmin M. de Moura[3], Cibele H. do Amaral[4], Alexei I. Lyapustin[5], Jin Wu[6], Loren P. Albert[6], Marciel José Ferreira[7], Liana O. Anderson[8], Victor A. H. F. dos Santos[9], Neill Prohaska[6], Edgard Tribuzy[9], João Vitor Barbosa Ceron[9], Scott R. Saleska[6], Yujie Wang[10] José Francisco de Carvalho Gonçalves[9], João Victor Figueiredo Cardoso Rodrigues[7], Maquelle Neves Garcia[9]

[1]Oregon State University, College of Forestry, Corvallis Oregon 97330, USA, [2] University of Southampton, Department of Geography and Environment, Southampton SO17 1BJ, United Kingdom, [3] Instituto Nacional de Pesquisas Espaciais (INPE), São José dos Campos - SP, 12227-010, Brazil, [4] Federal University of Viçosa, Viçosa - MG, 36570-900, Brazil, [5] NASA Goddard Space Flight Center, Greenbelt, MD 20771, [6] University of Arizona, Department of Ecology and Evolutionary Biology, Tucson, AZ 85721, [7] Federal University of Amazonas, Manaus - AM, 69077-000, Brazil, [8]Centro Nacional de Monitoramento e Alertas de Desastres Naturais, São José dos Campos - SP, 12247-016, Brazil, [9] Instituto Nacional de Pesquisas da Amazônia (INPA), Manaus - AM, 69067- 375, Brazil, [10] Joint Center for Earth System Technology, University of Maryland Baltimore County, Baltimore MD

Keywords: leaf pigments; phenology; photosynthetic capacity; MAIAC, tropical ecosystem

Understanding controls on seasonal and inter-annual variability in vegetation phenology is of paramount importance for Earth system modeling. Here, we introduce a new approach for scaling tropical ecosystem phenology by using multi-angle Moderate Resolution Imaging Spectroradiometer (MODIS) observations to invert a fully coupled canopy reflectance model (ProSAIL). Monthly estimates of vegetation leaf pigments derived from the inverse model showed strong seasonal variations across two flux-tower sites in the central Amazon basin with marked increases in chlorophyll concentrations during the early dry season. Remotely sensed chlorophyll concentrations were strongly correlated to field measurements (r^2=0.64 and r^2=0.98). We also utilized hyperspectral data from a camera installed on a tower to scale modeled chlorophyll pigments to MODIS observations (r^2=0.73). Chlorophyll pigment concentrations (Chl_{A+B}) were correlated to changes in the amount of young and mature leaf area per month ($0.59 \leq r^2 \leq 0.64$). Increases in MODIS observed Chl_{A+B} were preceded by increased photosynthetically active radiation (PAR) during the dry season ($0.61 \leq r^2 \leq 0.62$) and followed by changes in net carbon uptake. This allows the conclusion that, at these two sites, seasonality of plant productivity is controlled by vegetation phenology rather than sunlight directly. Remote sensing of leaf pigment concentrations can help to improve our understanding of seasonal changes the photosynthetic leaf area's efficiency to absorb sunlight.

ForestSAT 2016

Forest Monitoring

OTERRA
CENTRO DE ESTUDIOS DE RECURSOS NATURALES
UNIVERSIDAD MAYOR

UNIVERSIDAD MAYOR
para espíritus emprendedores

Facultad de Ciencias
ESCUELA DE INGENIERÍA FORESTAL

A polyalgorithm for land cover trend and change detection

Rishu Saxena[1], Layne Watson[1], Randolph Wynne[2], and ValerieThomas[2]

[1]Department of Computer Science, Virginia Tech.
[2]Department of Forest Resources and Environmental Conservation, Virginia Tech.

Keywords: Time series analysis, satellite images, landsat imagery, change detection

Abstract:

Forest monitoring and management can benefit immensely from satellite images. Time series analysis of satellite imagery is one way of extracting the wealth of information held in these images. Several algorithms to this end have been proposed by different groups in the remote sensing community utilizing different approaches: analytics based, mathematical functions based, some purely temporal, some spatio-temporal, and the like.

However, the design and selection of these algorithms, so far, appears to be predominantly context specific, i.e., most of these proposed methods seem to perform well on the dataset that they are designed for but their performance on randomly picked datasets from across the globe has not been studied. In general, no single algorithm designed so far will work for all regions is highly likely. The same is also indicated by our experiments.

In this talk, we will present a novel time series analysis algorithm, specifically a `polyalgorithm', to circumvent this gap. Our polyalgorithm consists of four different time series analysis algorithms along with a set of metrics for analyzing the requisite results to produce the final result. The algorithms we have chosen are fundamentally unique to each other in their design as well as in the phenomenon they capture. We have experimented with 6 different path/rows of Landsat images, collectively covering a gamut of ecosystems. For scalability and robustness, all the codes are written in Fortran.

Our algorithm will be useful in understanding and monitoring deforestation, urbanization, changes in tree canopy covers and such other processes, both anthropogenic as well as natural. It can thus be directly utilized by the policy makers for managing forests. It will further be of use in a much broader spectrum of applications including but not limited to general Earth monitoring (eg., land usage, land cover), health monitoring and urban transportation.

AFIS - Wildfire Visualisation and Multi-sensor detection capabilities

Philip Frost, CSIR Meraka Institute, South Africa

Keywords: Wildfire, detection, fire danger, burned area, mobile application, dashboard, satellites, camera

The Council for Scientific and Industrial Research (CSIR) lead by die Meraka Institute and supported by partners such as the South African National Space Agency (SANSA), University of Maryland and University of Wisconsin Madison have been involved in the developed of the Advanced Fire Information System (AFIS) over the last 12 years. The original aim of the system was to provide near real time fire information to fire fighters, farmers and forest managers across Southern Africa based on Earth Observation satellite products from Terra and Aqua MODIS and the Geostationary MSG. With the launch of the system in 2004, Eskom (South Africa' and Africa's largest power utility) quickly became the biggest user of the system where more than 300 line managers and support staff all around the country would receive cell phone and email fire alert messages whenever a MODIS or MSG active fire was detected within 2 km of any of the 28 000km of Eskom's transmission lines. Today the system has evolved in to a comprehensive wildfire information system that provides users with information and intelligence around the prediction, detection, monitoring and assessment of wildfires globally. EO satellite wildfire detections are complemented with both crowdsource detections from the AFIS Watchtower app as well as through automated in situ camera detection systems capable of detecting thin smoke plumes up to 20 miles away. Fire Danger models such as the Canadian FWI and Australian McArthur Fire Danger models have been fully integrated in to the system and can be produced for any area globally. A new MODIS burned area product has been produced by merging the standard MCD45 MODIS with the MCD64 BA product from Louis Giglo while a new Landsat 8 and Sentinel 2 algorithm has also been developed to provide higher resolution mapping of new fire events.

The visualization of AFIS has evolved from an online web viewer to a hybrid wildfire dashboard providing situational awareness for any region of interest. The NASA World View integration in to the dashboard has dramatically improved the visualisation component within the dashboard and now provide users with access to not only the Direct readout station data but also all the NASA GIBS data sets.

The AFIS mobile app is available on both the ITunes and Play stores and provides users with access to fire detections, fire weather forecasts and fire history through their mobile devices. The new AFIS Watchtower app allow fire managers to report the location of a new fire through their phone camera and is currently been tested by fire managers in Portugal.

Application of high-resolution satellite data for monitoring forest areas in changeable climatic conditions

Zbigniew Bochenek[1], Dariusz Ziolkowski[1], Maciej Bartold[2,1], Karolina Orlowska[2], Bogdan Zagajewski[2]*

[1] Institute of Geodesy and Cartography, Remote Sensing Centre, Modzelewskiego 27, 02-679 Warsaw, Poland, email: zbigniew.bochenek@igik.edu.pl; dariusz.ziolkowski@igik.edu.pl; maciej.bartold@igik.edu.pl
[2] Department of Geoinformatics, Cartography and Remote Sensing, Faculty of Geography and Regional Studies, University of Warsaw, Poland, email: bogdan@uw.eu.pl; karolina.orlowska@uw.edu.pl
** Corresponding author*

Keywords: climate change, forest monitoring, high-resolution data, vegetation index

Abstract

The main objectives of the research work were to determine usefulness of high-resolution optical satellite data for monitoring various forest parameters and to assess impact of changeable climatic conditions with the use of vegetation indices derived from remotely sensed data. Three types of high-resolution satellite data were used in the study: Landsat TM/OLI, SPOT 5 and Sentinel 2 images. Three forest areas located in a temperate climatic zone in northeastern Poland, differing in environmental conditions were taken into consideration. Five vegetation indices describing various aspects of plant condition and vegetation structure - Normalized Difference Vegetation Index - NDVI, Enhanced Vegetation Index - EVI, Triangular Vegetation Index - TVI, Normalized Difference Infrared Index - NDII, Disease Water Stress Index - DSWI - were derived from satellite images. Their values were analyzed in a temporal profile in four vegetation seasons: 2006, 2014, 2015 and 2016, in conjunction with meteorological parameters – temperature and precipitation. The results of analyses proved that dedicated vegetation indices characterizing water stress in plants – Disease Water Stress Index (DSWI), Normalized Difference Infrared Index (NDII) and Triangular Vegetation Index (TVI) are sensitive to changeable climatic conditions, especially detecting drought impact on forest canopies. The indices are also useful for characterizing types of forest site, tree stand mixture and tree species. In particular they give an opportunity to differentiate dry, fresh and humid forest sites, three levels of mixing conifers and hardwoods, as well as some species within deciduous forests.

Introduction

Forest monitoring with the use of remote sensing techniques is an important topic, both in global and regional scale. As far a global scale is concerned, there were many initiatives aimed at application of low and medium-resolution satellite data for deriving information on forest state and its changes [Boyd and Danson, 2005; Blackard et al., 2008; Soudani el al., 2008; Asner et al., 2009]. The most important international projects dealing with this topic were: TREES, REDD, Geoland Forest Monitoring, GLOBBIOMASS and others [Gibbs et al., 2007; Bicheron et al., 2008; Le Toan et al., 2011] . But parallel to forest monitoring at a global scale numerous projects have been conducted in order to apply high-resolution satellite images for forest mapping and for estimating forest parameters [Puzzolo et al., 2003; Huang et al., 2010; Morton et al., 2011; Miettinen et al., 2014]. Different types of satellite data, both optical and microwave, have been used for this purpose and various aspects of forest monitoring were taken into account. Several practical conclusions on applicability of remotely sensed data for forest monitoring have been already drawn, nevertheless due to complexity of forest environment and its differentiation through various climatic zones there is still a need to further develop and improve the existing methods. The presented work is a contribution to that development,

concentrating on the use of optical high-resolution satellite images for characterizing various forest parameters and for studying impact of climate changes on forest behavior in a temperate zone.

Methodology

Three forest areas located in northeastern Poland have been selected as pilot sites for the presented research work. These are: Bialowieska Forest, Knyszynska Forest and Borecka Forest. Northeastern Poland, where the sites are located, is under influence of continental climate, characterized by impact of polar air masses, shorter vegetation period comparing to the rest of Poland and quite high temperature fluctuations. There are some differences in climatic conditions between sites – Borecka Forest is slightly influenced by oceanic climate which has a certain impact on vegetation development. The selected forest areas are also different, as far as tree species and forest sites are concerned.

Three types of high-resolution satellite images have been used: Landsat TM/OLI images, SPOT 5 images and Sentinel 2 images. Apart from satellite images ground reference data have been collected for the regions of interest. The detailed digital forest maps prepared by Forest Service have been compiled; they comprise comprehensive information on forest, including species, stand mixture and type of forest site. Moreover, ground measurements characterizing real plant condition have been conducted (spectroradiometric, fluorescence, pigment content measurements).

In order to study, if specific vegetation indices derived from high-resolution satellite data are sensitive to variable climatic conditions characterized by changes of meteorological parameters and if they change due to some forest parameters – type of forest site, tree species and tree stand mixture, a set of indices was generated, namely:
Normalized Difference Vegetation Index – NDVI characterizing general plant condition

$$NDVI = (NIR - RED) / (NIR + RED)$$

Normalized Difference Infrared Index – NDII characterizing water content in plants

$$NDII = (NIR – SWIR\ 1) / (NIR + SWIR\ 1)$$

Disease Water Stress Index – DSWI characterizing stress of plants due to water shortage and damage

$$DSWI = (NIR – GREEN) / (SWIR\ 1 + RED)$$

Triangular Vegetation Index – TVI characterizing plant condition and chlorophyll content in red-edge

$$TVI = 0.5 * [120 * (R750 – R550) – 200 * (R670 – R550)]$$

All indices were analyzed in a temporal profile. In order to quantify their changes and to relate them to climatic conditions, simple index characterizing decrease of vegetation index was produced using the following formula:

$$\text{Decrease}_{\text{index value}} = \text{Max}_{\text{index value at peak season}} – \text{Min}_{\text{index value at the end of season}}$$

Regarding tree species six species represented within study areas were selected for the analysis: two coniferous species – spruce and pine and four deciduous species – birch, alder, oak and hornbeam. Three types of forest site were taken into consideration: fresh, humid and dry site, in combination with various tree species – conifers and hardwoods. Tree stand mixture was analyzed at three levels of mixing: pure stands (90 – 100 %), 70 to 90 % of dominant species, 50 to 70 % of dominant species.

In order to study relations between vegetation indices derived from high-resolution satellite data and climatic conditions meteorological information was compiled for the regions of interest, using web-available database http://en.tutiempo.net/climate/poland.html. It comprises various meteorological parameters e.g. mean daily temperature and precipitation. These parameters at first stage of the works were processed in order to produce so-called hydrothermal index, which combines both temperature and precipitation information in 10-day's cycle, characterizing drought conditions for the study area.

Results

At first stage of the works thorough analysis of the selected vegetation indices has been performed, in order to find those which are more useful for differentiating particular tree species and which can respond to variable climatic conditions in a best way. The analysis was done for indices derived from Landsat, SPOT and Sentinel 2 data with the aim to compare usefulness of these types of satellite images for forest studies. Comparative analysis of four vegetation indices – NDVI, NDII, DSWI and TVI revealed that Disease Water Stress Index (DSWI) derived from Landsat images and Triangular Vegetation Index (TVI) derived from Sentinel 2 data are the most sensitive to species differentiation,

analyzed through vegetation season. Both indices demonstrate possibilities of differentiating some tree species, e.g. pine and spruce from coniferous group, as well as alder, birch and hornbeam from deciduous group. Changes of indices for 2015 and 2016 are presented in figure 1.

As both analyzed indices – DSWI and NDII revealed some decreasing trends at the second part of vegetation period, it was decided to verify, if these changes are related to meteorological situation. For this purpose hydrothermal index (HT) which informs on drought has been calculated and next DSWI index based on Landsat data has been computed for all vegetation seasons between 2000 and 2015. Next differences between maximum and minimum DSWI value were determined and correlated with the mean hydrothermal index derived from meteorological data for the years of interest, using Statistica software package for this purpose. Results of correlation analysis revealed, that there is a quite strong relationship between vegetation index derived from remotely sensed data and the index characterizing climatic conditions - the correlation coefficient r was equal to -0.723. The results are presented in graphical form in figure 2.

The second part of the research work was devoted to analysis of impact of type of forest site and stand mixture on values of vegetation indices derived from high-resolution data. The analyses conducted for three types of forest site – dry, fresh and humid site, as well as for three levels of stand mixture revealed that both forest parameters have an influence on values of DSWI and TVI indices, decreasing level of index in case of dry site and increasing its value in case of mixing coniferous forests with deciduous species. These impacts should be taken into account while analyzing relationships between vegetation indices and climatic conditions.d

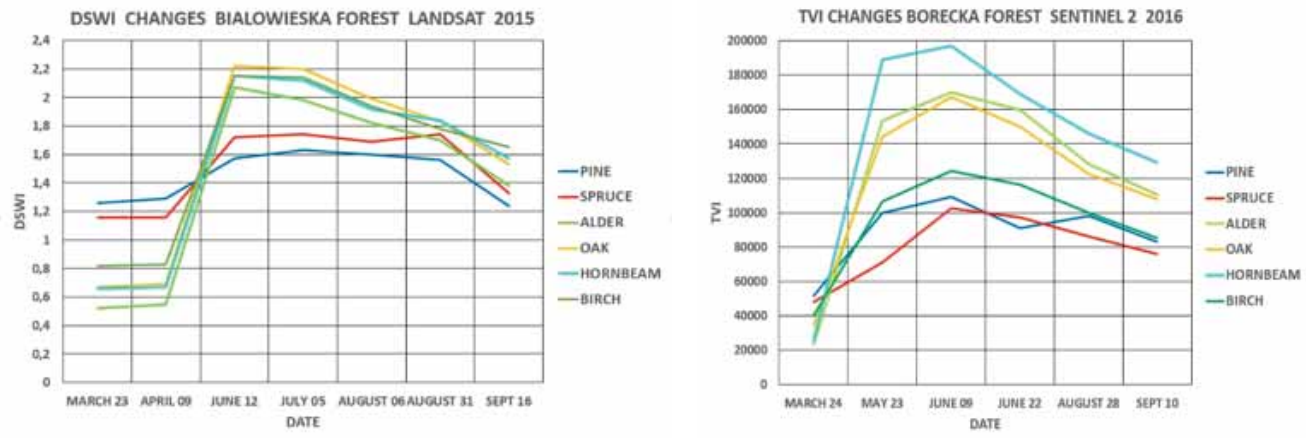

Fig. 1. Changes of vegetation indices - DSWI and TVI for 2015 vegetation season

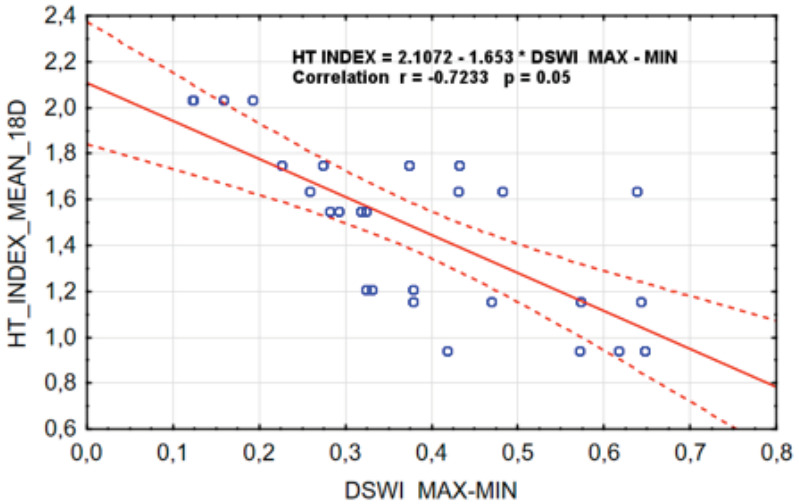

Fig. 2. Results of correlation analysis between changes of DSWI index and hydrothermal index

Conclusions

The main conclusion from the presented study is that there are relations between changeable meteorological conditions and forest condition, expressed by remote sensing based indices, but these relations vary depending on type of forest site and degree of tree species mixture. It was found that vegetation indices derived from high-resolution satellite data, which include information on spectral reflectance both in near infrared and shortwave infrared bands, can be effective for evaluating stress in forest stands due to drought conditions. The second important conclusion is that some basic characteristics of forest stands, such as forest site type and degree of tree species mixture have impact on remote sensing based parameters, while applying adequate vegetation indices, such as Disease Water Stress Index (DSWI) and Triangular Vegetation Index (TVI), which modify the general relations between climatic changes and forest condition. While analyzing relations between EO-based vegetation indices and forest characteristics it was found that deciduous stands are more sensitive to drought conditions, as expressed by changes of DSWI index, than coniferous forests. Comparing forest sites it was proved that coniferous stands located on dry forest site are more resistant to long-term drought than those situated on fresh and humid sites. These conclusions open new possibilities for the detailed forest studies and assessments, but also point out complexity of analysis of satellite images, when applied for forest monitoring. So finally one can conclude, that optical, high-resolution satellite images are useful for assessing impact of climate change and for analyzing main environmental features of forests, but in order to derive more information e.g. on forest structure synergistic use of optical and microwave images should be considered.

References

Asner G.P., Knapp D.E., Balaji A., Paez-Acosta G., 2009. Automated mapping of tropical deforestation and forest degradation: CLASlite. J. Appl. Remote Sens., 3 (2009) 033543, 24p. http://dx.doi.org/10.1117/1.3223675

Bicheron, P., P. Defourny, C. Brockmann, L. Schouten, C. Vancutsem, M. Huc, S. Bontemps, M. Leroy, F. Achard, M. Herold, F. Ranera, and O. Arino. 2008. GLOBCOVER Products Description and Validation Report. MEDIAS-France, ftp://uranus.esrin.esa.int/pub/globcover_v2/global/

Blackard, J.A., Finco M.V., Helmer E.H., Holden G.R., Hoppus M.L., Jacobs D.M., Lister A.J., et al. 2008. Mapping US forest biomass using nationwide forest inventory data and moderate resolution information. Remote Sensing of Environment112 (4): 1658–1677.

Boyd D.S, Danson F.M. 2005. Satellite remote sensing of forest resources: three decades of research development. Prog Phys Geogr 2005; 29(1): pp. 1-26. [doi:101191/0309133305pp432ra]

Gibbs, H.K., Brown S., Niles J.O. and Foley J.A.. 2007. Monitoring and estimating tropical forest carbon stocks: Making REDD a reality. Environmental Research Letters 2(4): 045023.

Huang C., Goward S.N., Masek J.G., Thomas N., Zhu Z., Vogelmann J.E., 2010. An automated approach for reconstructing recent forest disturbance history using dense Landsat time series stacks. Remote Sens. Environ., 114 (2010), pp. 183–198

Le Toan T., Quegan S., Davidson M.W.J., Balzter H., Paillou P., Papathanassiou K., Plummer S., Rocca F., Saatchi S.S., Shugart H., Ulander L., 2011. The BIOMASS mission: mapping global forest biomass to better understand the terrestrial carbon cycle. Remote Sens. Environ., 115 (2011), pp. 2850–2860

Miettinen J., Stibig H.S., Achard F., 2014. Remote Sensing of forest degradation in Southeast Asia – aiming for a regional view through 5-30 m satellite data. Global Ecology and Conservation, Vol. 2 December 2014, pp. 24-36

Morton D.C., DeFries R.S., Nagol J., Souza Jr C.M.., Kasischke E.S., Hurtt G.C., Dubayah R., 2011. Mapping canopy damage from understory fires in Amazon forests using annual time series of Landsat and MODIS data. Remote Sens. Environ., 115 (2011), pp. 1706–1720

Puzzolo V, De Natale F, Giannetti F. 2003. Forest species discrimination in an alpine mountain area using a fuzzy classification of multi-temporal SPOT (HRV) data. Geoscience and Remote Sensing Symposium, 2003 IGARSS '03 Proceedings 2003 IEEE. Int 2003; 4: pp. 2538-40.

Soudani, K., le Maire G., Dufrene E., Francois C., Delpierre N., Ulrich E. and Cecchini S., 2008. Evaluation of the onset of green-up in temperate deciduous broadleaf forests derived from Moderate Resolution Imaging Spectroradiometer (MODIS) data. Remote Sensing of Environment 112 (5): 2643–2655.

Assessing the cumulative climatic effects on regional forest decline dynamics in coniferous forests

David M. Bell, USDA Forest Service, Pacific Northwest Research Station
Warren B. Cohen, USDA Forest Service, Pacific Northwest Research Station
Zhiqiang Yang, Oregon State University, College of Forestry

Keywords: coniferous forests; ecological drought; forest decline; Landsat; TimeSync

Abstract

Protracted, multi-year changes in forest vegetation have become the dominant form of disturbance in the western United States and these forest declines are generally attributed to climate-mediated stressors like drought, insects, and disease. However, climatic effects compound over time (e.g., multi-year droughts), implying that examination of forest declines must incorporate cumulative climatic effects. Our research assesses the contribution of climate to remotely sensed forest decline (RSFD). We leveraged a two-stage stratified random sample of coniferous forests in the western United States and the TimeSync Landsat time series visualization tool to use 30-m multispectral imagery (Landsat TM and ETM+; 1984-2012) and repeat photography (Google Earth) to derive independent plot-based estimates of the presence or absence of RSFD at each sampling location.

Using MaxEnt, a machine learning algorithm for modeling presence data, we found that previous year's precipitation, current year's maximum temperature, and trends in temperature and precipitation during the previous five years all contributed to observed patterns of RSFD, implicating ecological drought (decreasing precipitation and increasing temperature) as a driver of RSFD. Stochastic Antecedent Modeling, a hierarchical Bayesian statistical approach to examining lagged, or cumulative, effects, provided a more nuanced image of climatic influences on RSFD. Preliminary results for a subset of spruce, fir, and mountain hemlock (SFMH) forest locations experiencing decline (n = 50) indicated that maximum monthly spring temperatures (April – June) and total monthly summer precipitation (July – September) exhibited cumulative effects on RSFD timing up to 8 years into the past. SFMH forest decline was most sensitive to cumulative temperature and precipitation in colder climates, highlighting sensitivity of high elevation forests to drought-induced decline. Additionally, RSFD associated with high temperatures was associated with dense, closed canopy forests (i.e., high tasseled-cap wetness), whereas it was associated with sparse forest canopies (i.e., low angle) for low precipitation. These results indicate that forest vulnerability to drought-induced decline will vary regionally, that these declines develop over the course of several years, and that local variation in forest structure will mediate the impact of interannual variation in climate on forest health.

Assessing the predictions of high-resolution climate surfaces: a statistical analysis in a Southern Hemisphere country

Christian Salas[1], Luis Morales[2], Renato Cifuentes[3], Rodrigo Vargas[1], Andres Fuentes-Ramirez[1]

[1] Laboratorio de Biometría, Departamento de Ciencias Forestales, Universidad de La Frontera, PO Box 54-D, Temuco, Chile
[2] Laboratorio de Investigación en Ciencias Ambientales, Departamento de Ciencias Ambientales y Recursos Naturales Renovables, Universidad de Chile, PO Box 1004, La Pintana, Santiago, Chile.
[3] KU Leuven, Department of Biosystems, Division of Crop Biotechnics, Willem de Croylaan 34, BE-3001 Leuven, Belgium

Keywords: temperature, precipitation, interpolation, uncertainty, hypothesis testing.

Climate variables are needed in several disciplines ranging from engineering to natural sciences for management, policy making, and scientific purposes. In order to overcome the problems of rather scatter available climate data in some places, several interpolated climate surfaces (ICS) have been produced worldwide. These climate variable surfaces are spatial grids at high spatial resolution (e.g., 1 km^2), and are currently used for many applications. The WorldClim project is one of the most used ICS because it has been made widely open and is freely available on the Internet. In forestry, ecological, and geographical applications, a ICS is not only used for imputing missing climate variables, but also for mapping and modelling climate change and its effects on related variables, such as, species distribution and population changes. However, neither its uncertainties nor its predictions had been thoroughly analyzed. We assessed the monthly predictions of WorldClim for four climate variables (maximum, mean, and minimum temperature; and precipitation) through all Chile (i.e., over an area of more than 750000 km^2, through an extension of 4270 km) based on a large set of weather station data, to create concurrent observations. We assessed the prediction errors, as well as the performance of WorldClim by conducting statistical hypothesis testing on the estimated parameters of an observed-predicted simple linear regression model. The results indicate that only the maximum temperature is correctly predicted during the entire year by WorldClim. The precipitation is better predicted during summer and spring seasons (i.e., September – February) than during autumn and winter seasons (i.e., March – August). However, there are statistical differences for predicting both the minimum and mean temperature for all months. We point out that WorldClim predictions although have several problems, are quite useful in practice. Nevertheless, we recommend calibrating or validating the climate predictions as much as possible in any study that would heavily rely on climate data. This process will provide insights into the geographic distribution of uncertainties and will allow for improvements of climate variable surfaces at locations of interest. Finally, we demonstrate a statistical assessment based on both prediction capabilities and hypothesis testing.

Assessment of forest productivity from MODIS NPP data in relation to forest management and optimal leaf area index

Mait Lang[1,2], Tiit Nilson[1], Mathias Neumann[3], Adam Moreno[3]

[1] Tartu Observatory, 61602 Tõravere, Tartumaa, Estonia; e-mail: lang@to.ee.
[2] Institute of Forestry and Rural Engineering, Estonian University of Life Sciences, Kreutzwaldi 5, Tartu 51014, Estonia.
[3] Institute of Silviculture, Department of Forest and Soil Sciences, University of Natural Resources and Life Sciences, Vienna, Peter-Jordan-Str. 82, A-1190 Wien, Austria.

Keywords: hemi-boreal forest, optimum LAI, net primary production, Estonia.

Abstract

Global scale maps of terrestrial ecosystem net primary production (NPP) are routinely produced based on coarse spatial resolution satellite data (Zhao, *et al*. 2005). The NPP is estimated by using Monteith hypothesis which states that total photosynthesis product (GPP) is proportional to absorbed photosynthetically active radiation and light use efficiency and limited by air temperature and water vapor pressure deficit. NPP is obtained by subtracting growth and maintenance losses from GPP. It can be expected that the NPP estimates are related to forest growth and disturbances.

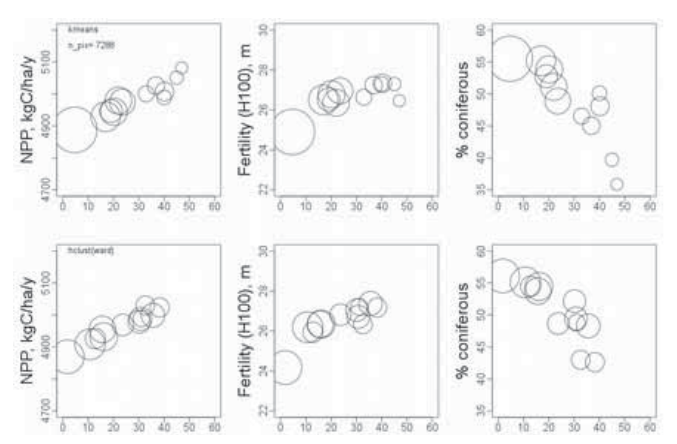

Figure 1. Envisat MERIS data based NPP, site fertility, % coniferous and forest management induced disturbances (1987-2013) for 1km2 pixels clustered according to disturbance signatures.

We used three NPP datasets to assess the impact of forest management induced disturbances to forest productivity in hemiboreal forests in Estonia. Landsat TM based regeneration felling maps (U. Peterson, Tartu Obsevatory) covering years 1987-2013 with about 5-year interval were used to calculate disturbance signatures for 1km2 forested pixels of NPP maps. Three independent NPP estimates were used (Zhao, *et al.* 2005, Nilson et al. 2012, Neumann et al. 2016). The mean NPP estimate was positively correlated with disturbances and site fertility and negatively correlated with the share of coniferous (Figure 1).

The NPP relationship with site fertility can be expected to be positive and negative correlation of NPP with the share of coniferous can be explained by the tree species preferences to sites and also forest spectral signatures and the NPP model constants. However, the positive correlation between NPP and disturbances can be induced by the optimum LAI phenomena in the NPP algorithms (Nilson et al. 2014) happening due to saturating relationship between fAPAR and LAI and increasing maintenance losses with increasing LAI.

References

Neumann, M., Moreno, M., Thurnher, C., Mues, V., Härkönen, S., Mura, M., Bouriaud, O., Lang, M., Cardellini, G., Thivolle-Cazat, A., Bronisz, K., Merganic, J., Alberdi, I., Astrup, R., Mohren, F., Zhao, M., Hasenauer, H. (2016). Creating a regional MODIS satellite-driven Net Primary Production dataset for European forests. Remote Sensing, (In review).

Nilson, T., Rennel, M., Luhamaa, A., Hordo, M., Olesk, A., Lang, M. (2012). MERIS GPP/NPP product for Estonia: I. Algorithm and preliminary results of simulation. Forestry Studies | Metsanduslikud Uurimused 56, 56–78.

Nilson, T., Rennel, M., Lang, M. (2014). MERIS GPP/NPP product for Estonia: II. Complex meteorological limiting factor and optimum leaf area index. Forestry Studies | Metsanduslikud Uurimused 61, 5–26. Zhao, M., Heinsch, F.A., Nemani, R., Running, S. (2005). Improvements of the MODIS terrestrial gross and net primary production global dataset. Remote Sensing of Environment 95, 164–176.

Automatic recognition of burned areas with the use of a support vector machine (SVM) using VNIR spectral bands with multiple satellite sensors.

Manuel Castro[1], Patricio Acevedo[1]

[1] Laboratorio de Teledetección Satelital, Departamento de Ciencias Físicas, Facultad de Ingeniería y Ciencias, Universidad de La Frontera, Casilla 54-D, Temuco, Chile.

Keywords: SVM, burned areas, Automatic recognition, VNIR

Abstract

The increasing need to monitor and oversee burned areas with greater precision has resulted in a series of studies which are focused on improving the accuracy and efficiency of mapping using satellite platforms with high resolution spatial sensors, those which generally only incorporate spectral bands in the visible and near-infrared range (VNIR). Traditionally for the study and detection of burned areas the near-infrared (NIR) and mid-infrared (SWIR) spectral zones have been used, given their sensitivity to this type of land cover, but only the medium and low spatial resolution sensors incorporate SWIR bands, in oriented studies usually at the regional level. The present study seeks to classify burned areas using visible and near-infrared (VNIR) spectral bands, using a support vector machine (SVM). The analysis exclusively considers pixels of the VNIR bands from different satellite platforms such as Fasat-C, SPOT, GeoEyes, WorldView-2, Landsat-8 and Sentinel-2A, as well as some spectral indices derived from this zone of the spectrum. The results of the classification based on pixels from different servers using an SVM indicate that the use of spectral indices combined with VNIR spectral bands, instead of just the VNIR spectral bands, improves the accuracy and reliability of the recognition of burned areas. A SVM is shown effective since using images from different sensors still does not have major problems in detection. Nonetheless, volcanic slag zones tend to be classified as areas affected by burning mainly because the spectral signature is very similar in the VNIR spectral region, but this is solvable applying a mask of non-vegetational soil uses.

POSTER

Barren ground caribou (Rangifer tarandus groenlandicus) behaviour after recent fire events; integrating caribou telemetry data with Landsat fire detection techniques

Gregory J.M. Rickbeil[1], Txomin Hermosilla[1], Nicholas C. Coops[1], Joanne C. White[2], Michael A. Wulder[2]

[1] Integrated Remote Sensing Studio, Faculty of Forestry, University of British Columbia, 2424 Main Mall, Vancouver, BC, Canada, V6T 1Z4; phone: 604-827-4429; fax: 604 822 9106
[2] Canadian Forest Service (Pacific Forestry Centre), Natural Resources Canada, 506 Burnside Road, Saanich, British Columbia, Canada, V8Z 1M5

Keywords: arctic, disturbance, Landsat, mammal, movement, remote sensing, telemetry, ungulate

Abstract

Fire is a major factor affecting access to high quality forage such as terricholous lichens for barren ground caribou (Rangifer tarandus groenlandicus). Herein, we characterize how the size and severity of fires are changing across five barren ground caribou herd ranges occurring in the Northwest Territories and Nunavut, Canada. Additionally, we demonstrate how time since fire, fire severity, and time of year (season) result in complex changes in caribou behavioural metrics estimated using telemetry data. Fire disturbances were identified using novel time series of gap-free Landsat surface reflectance composites from 1985 to 2011 across all herd ranges. Burn severity was estimated using the differenced normalized burn ratio (dNBR). Annual area burned and burn severity were assessed through time for each herd and, using generalized additive mixed models, were related to two behavioural metrics: velocity and relative turning angle. Neither annual area burned nor burn severity displayed any temporal trend within the study period. However, certain herds, such as the Ahiak and Beverly, have more exposure to fire than other herds (i.e. Cape Bathurst had a maximum forested area burned of less than 4 km2). Time since fire and burn severity both significantly affected velocity and relative turning angles. Across all seasons, fire virtually eliminated foraging-focused behaviour for all 26 years of analysis while more severe fires saw a marked increase in movement-focused behaviour compared to unburnt patches. Between seasons, caribou used burned areas as early as one-year post fire, demonstrating complex, non-linear reactions to time since fire and fire severity, and these reactions changed depending on season. In all cases movement-focused behaviour was detected post fire. We conclude that changes in caribou behaviour immediately post-fire are primarily driven by changes in forest structure rather than changes in terricholous lichen availability.

Bringing Earth Observation Services for Monitoring Dynamic Forest Disturbances to the Users – EOMonDis

F.Enßle, T. Haeusler, S. Gomez, C. Storch, M. Pape, H. Ott, T. Wagner, G. Ramminger
GAF AG
Munich, Germany

Keywords: Forest Monitoring, REDD+, Zero Deforestation, Dense Time Series, Tropical Dry Forests

Abstract

The geographical extent and limited accessibility of tropical forest ecosystems hinders accurate estimation and spatial explicit monitoring of forest resources by purely field-based inventories. The spatial explicit representation of forest ecosystem status and changes thereof is a key requirement to protect natural forests, enable effective forest law enforcement and support sustainable management of forest resources. This paper introduces the background of the EOMonDis project, mapping service requirements and the methodological concept for algorithm development and product verification. Furthermore, the processing chain and results for optical based dense time series analysis for one out of four test sites are described.

Introduction

During the last decade, remote sensing has become an integral part of national and international forest policy programmes. An important forest management policy is embedded in the United Nations Framework Convention on Climate Change (UNFCCC) programme Reducing Emissions from Deforestation and Forest Degradation and the role of conservation, sustainable management of forests and enhancement of forest carbon stocks in developing countries (REDD+), which was started in 2005 by an initiative of a few countries. The initial effort was further developed such that the REDD+ mechanism is based on a three phased approach, of which the final phase relates to payments for verified emission reductions. These financial incentives should preserve carbon stored in natural forest ecosystems and reduce emissions from forested lands. An essential component of such a system is a reliable monitoring system of forest resources and changes thereof. At the same time, the private sector companies of the commodity sector want to establish deforestation free production chains. Within this context, a methodological approach was developed to identify areas for potential expansion and identify areas of High Carbon Stocks (HCS) that shall be preserved [1]. Thus, for the successful implementation of forest policies, forest resources have to be mapped spatially and subsequently be monitored to track changes on a regular basis. Mapping of activity data (AD) furthermore provides a valuable information source for a sustainable forest management. With the launch of first satellites of the Sentinel constellation, optical and radar data of high spatial and temporal resolution are freely available. In the near future, the temporal coverage will be even increased by the launch of other satellites complementing the constellation. With the high repetition rate of the Sentinel-2 satellites, complemented by Sentinel-1 data and Landsat sensors, fast response monitoring systems can be implemented with low Earth Observation (EO) data costs. Up-to date information on activity data can thereby be provided to realise an effective forest management.

"Bringing Earth Observation Services for Monitoring Dynamic Forest Disturbances to the Users" project (EOMonDis) is a project supported by the European Commission's Horizon 2020 programme and is being implemented from 2016-2019. The overall aim is to

improve tropical forest monitoring products that are based on satellite borne high-resolution sensor data and of high temporal resolution. The project focuses especially on developing state-of-the-art processing chains based on dense time series and suitable for large area mapping by integration of available optical and radar data with particular emphasis on Sentinel 1 and 2 data.

This paper will present in the next Section the main forest monitoring requirements for the UNFCCC REDD+ policy as well as for the Zero Deforestation (ZD) programmes. Section 3 will summarise the Study Sites that will be used in the current project. The following Section 4 will then present the planned methodological approaches and the paper will end with a concluding section.

Forest Monitoring Requirements

Countries that are willing and able to reduce emissions from deforestation and forest degradation are recommended by the United Nations Framework Convention on Climate Change (UNFCCC) Conference of Parties (COP) to establish robust and transparent forest monitoring systems to account for anthropogenic forest-related greenhouse gas emissions by sources and removals by sinks. The methodological approach proposed by Intergovernmental Panel on Climate Change (IPCC) for carbon emission accounting requires two basic data: (1) activity data (area extent of the activity) and (2) emission factor (carbon stock per unit area). Consequently, potential REDD+ countries need to estimate emissions and changes in forest carbon stocks from deforestation or forest degradation and have a means to establish reference emission levels, against which future emissions can be compared, as well as to address the displacement of emissions.

Additionally the IPCC Good Practice Guidance (GPG) for Land Use, Land Use Change and Forestry (LULUCF) defines 3 Tiers or levels of accuracy for reporting which have to be considered for the REDD services. "Moving from Tier 1 to Tier 3 increases the accuracy and precision of the estimates, but also increases the complexity and the costs of monitoring" [2]. Furthermore, in the case of deforestation the GPG presents three approaches to obtaining areal extents: "(i) only identifying the total area for each land category (approach 1); (ii) tracking of land-use changes between categories (approach 2); and (iii) tracking land-use changes using sampling or wall-to-wall mapping techniques (approach 3). Approach 3 is the only approach that tracks forest and other land conversions on an explicit spatial basis, including gross deforestation and gross change in other land cover classes" (FCCC/TP/2009/1).

For the establishment of baseline or reference emission levels, there is a need for robust and cost-effective methodologies to estimate and monitor changes in forest cover and associated carbon stocks and greenhouse gas emissions. Thus, more specifically countries will need to know:

- The aerial extent of deforestation and forest degradation (hectares),
- For degradation, the proportion of forest biomass lost (percentage),
- Where the deforestation or forest degradation occurred (which forest type),
- The carbon content of each forest type (tons of carbon per hectare), and
- The process of forest loss that affects the rate and timing of emissions.

The Zero Deforestation program is a further development of the High Conservation Value (HCV) approach, addressing concerns that the HCV approach may allow for the conversion of forests, which do not fall under a HCV category, but storing at the same time high amounts of carbon. The ZD program and the effective evaluation of companies' commitments require two different kind of forest monitoring products. For the development of new plantations companies that are committing to ZD have to restrict their expansions to locations of low carbon stocks and preserve areas of high value. With the knowledge of the spatial explicit location of high carbon stocks within the concessions the evolvement of these forests can be monitored over time. An efficient monitoring of forest resources is therefore required to help companies in confirming their ZD commitments. The two main forest monitoring products can be summarised as:

- The aerial extent and amount of forest carbon stocks (tons of carbon per hectare),
- The process of forest loss in areas under protection (hectares).

Study Sites

Within EOMonDis project, study sites in four countries have been established to adequately cover a wide range of tropical forest compositions. The study sites are located in Gabon, Cameroon, Malawi and Peru.

A. Cameroon

Cameroon has a South to North extent from around latitude 2° to 12° N. The transition from North to South is represented by various climatic conditions and land cover types. These can be roughly divided in three major zones. The northern part is mainly covered by croplands and open woody vegetation. The middle part of Cameroon has deciduous woodlands with some areas of mosaic forest and savanna. The southern part has large areas of closed evergreen forests with a transition zone of deciduous woodlands in the west and Mosaic Forest in the east.

The various forest cover types in the Centre province qualified this region for method development in the current project. To demonstrate the feasibility of developed algorithms on different forest cover types, two sites were established. The northern demonstration site has an area of 15,000 km² and is mainly covered by savanna. The second site has an area extend of around 10,000 km² and covers a highly fragmented and divers landscape with the city Yaoundé in the centre of the Area of Interest (AOI).

B. Gabon

Gabon is located on the western side of Central Africa and is intersected by the equatorial line. The vegetation is affected by a typical equatorial climate, characterised by high annual precipitation of more than 2000mm and average daily temperatures of about 24°C - 27°C with very low annual variations.
The selected test site (~38,000 km²) is located at the western side of Gabon. As most of Gabon, the selected site is covered by evergreen dense equatorial forest as well as some part of savanna. The site also includes some of the recent agro-industrial development that have recently been taking place in Gabon leading to substantial deforestation.

C. Malawi

Situated between latitude 9° to 17° S and longitude 30° to 36° E, Malawi has a total area of ~ 120.000 km². Several highlands between 1300 masl and 3000 masl are located in the northern, middle and southern part of the country. The mean annual temperatures in these areas are about 13° C, whereas in the lower regions annual temperatures are up to 25° C. The highlands have at the same time high annual precipitation of more than 1600mm and in the cold dry season precipitation is provided by mist, resulting in a consistent cloud cover in the northern mountain areas near the lake.

The main part of the country consists of flat plateaux with elevations around 750 -1300 masl. Towards the southern part, the elevation declines at around 180 masl. The main forest type is Miombo (*Brachystegia* woodlands) generally found between 600 - 1500 masl with an annual rainfall of 510 mm to 1530 mm. "In Malawi, Miombo woodlands constitute 92.4% of the country's total forested area, and are mainly located in forest and game reserves established for water catchment as well as for soil and biodiversity conservation" [4]. Miombo forest represent an important forest composition with a wide distribution in several African countries with a characteristic leafless period during the dry season. In the sub-Saharan region, Miombo forests cover approximately 17.3 million km² [5] and have large distribution areas in Southern America. Up to now the most Earth Observation (EO) based mapping approaches do focus on humid tropical forest and only few research results for tropical dry forest have been presented.

The Malawian study site of dry tropical forest has an area of ~32.000 km² with highlands in the northern part, the Kaningina Forest Reserve in the middle, Kasungu National Park in the south-west and Nkotakhota Wildlife Reserve in the eastern part.

D. Peru

Situated in the north-western part of South America, Peru covers an area of ~1.285.000km². The Andes significantly affect the climate and ecosystems of Peru. From the coastline on the West the elevation rises to the peak of the Andes and declines towards the Amazon Basin on the Eastern side. Eastern of the Andes, the main forest types can be summarised as lowland evergreen broad leaf rain forest, lower montane forest and upper montane forest. The western part of Peru has low precipitation, resulting in *Sclerophyllous* dry forest and an overall sparse tree cover.

The area size of the Peruvian sites is ~35.000km² and mainly covers forests in the provinces San Martin and Ucayali; both provinces are known as areas where rapid deforestation has occurred. Recent agro-industrial development in relation to the palm oil and cocoa industry led to significant deforestation events in these sites.

Forest Cover Mapping

EOMonDis developments are based on experience from previous projects in the domain of tropical forest ecosystem monitoring and will undergo a permanent improvement process. Especially the method for dense time series analysis, which has been developed within the European Space Agency (ESA) funded Global Monitoring for Environment and Security Service Element for Forest Monitoring (GSE FM) project, builds the starting point for the processing approach. The developed method [6] focuses on tropical dry forest with leaf-on and leaf-off periods. Identification of forest is much more challenging in these ecosystems due to scattered distribution of trees, which causes mixed spectral signatures in the high-resolution EO data domain, hampering precise estimation of canopy cover per area unit. Another drawback is the coincidence of the vegetation period with the season of heaviest cloud cover during the rainy season. Conditions for optical image acquisition are much better during the dry season, but the leaf-off state of deciduous trees hinders an accurate determination of forested areas.

The entire project is realised by a two-phased approach; the first phase comprises a requirement assessment and improved algorithm development, the second phase is dedicated for product enhancements and inclusion of product feedback that is gathered at the end of the first phase. With the knowledge and information gained from the user requirement assessment, the technical developments are targeted towards the product output specifications. These output specifications define the EO input data that can be used to meet pre-defined product requirements. The processing chain therefore has to be adaptable to input data of different type and capable of processing data composites of varying spectral characteristics within the dense time series (e.g. phenology, leaf-on/leaf-off). At the current stage of the project, the automated processing chain is proven for the handling of optical EO data, mainly Sentinel-2 and Landsat data. Having said this the subsequent description applies to forest cover and change mapping based on optical data. The monitoring system is built to start with the baseline year 2010 and provides a continuous monitoring of forest cover and forest cover changes (including IPCC relevant Land Use and Land Use Change classes) from 2015 onwards using multi-sensoral and -temporal satellite data, which are validated with VHR optical data.

E. EO Data Processing

Before entering into the detailed time series analysis, common pre-processing procedures are applied to all input data, namely a) Cloud detection and masking b) Radiometric calibration in-between scenes c) Calculation of Top of Atmosphere (ToA) reflectance d) Geometric validation and e) Tasselled Cap Transformation [7]. Initially, the data will be segmented into image objects with similar spectral properties to reduce data volume and counteract alignment problems in this multi-temporal, multi-source data scenario. In order to derive objects that reflect all different states of the land cover over the entire timeframe under consideration, each individual scene will be investigated separately in a sequential (sub-) segmentation procedure, starting from a master image. The resulting segments then function as a basis for the subsequent image analysis.

Classification of segmented satellite images is performed using a supervised approach with K-Nearest Neighbour algorithm, independently for each image of the time series. Training data is collected by visual interpretation of very high-resolution (VHR) imagery and high-resolution (HR) imagery. A special focus is given to areas with persistent cloud clover to guarantee a sufficient amount of reference data for each scene. Suitable reference locations are these ones, which do not undergo any changes during the period under consideration. These stable locations are used to extract spectral information for each scene individually at object level to train the classificator, image by image, to perform a sequence of land cover classifications. The information content of the chronologically ordered satellite images is then used to a) improve accuracy of each individual classification, b) replace NoData values at a specific point in time by applying logical rule sets and c) determine the location and date of change events.

F. Dense Time Series Analyses

The methodology is based on rating independent classification results in their temporal context, taking account of quality aspects of the specific EO data source and predicted, standardized land-cover-specific dynamics. Prior to the time series analysis, all input scenes are rated according to the time of acquisition (leaf-on or leaf-off-season) and atmospheric conditions (clouds/shadows/haze). Both factors do influence the accuracy of the forest cover classification. Thus, results from a classification performed on a satellite image acquired during leaf-on stage and under clear sky are assumed to be more reliable than results from an image taken under interfered conditions. Contrary to the a priori reliability, the continuity of classification results of a specific object is used to calculate context driven reliability. A moving window, that respects five successive classification results, is used to compare each class assignment with the four adjacent ones in the timeline. The level of agreement is calculated for each segment. The value, denoted as class reliability, considers the consistency of classification results along the time axes. Additionally, a plausibility rating is introduced to consider natural behaviour of forest ecosystems such as time needed until canopy cover is again detectable in satellite imagery and the phenology of trees.

Based on these indicators, the algorithm iteratively optimises the individual classification results by maximising the plausibility of the entire code sequence. The procedure results in logically consistent code sequences that correspond to an expected behaviour of – or transition between - the land cover under consideration.

G. Product Verification Approach

Mapping results have to be validated with statistical sound methods in order to fulfil the stakeholder requirements and enable an unbiased judgement of product quality. There is no doubt, that accuracy assessments shall be always performed with an independent data set. Generation of the reference data to evaluate the quality of single map products can be produced either by field data collection or by visual interpretation of very high-resolution imagery. Satellite and airborne imagery have the great advantage of covering large areas in a continuous manner. Field based observation are most often sample based with a limited extend of coverage. Especially for remote areas, field based reference data collection is not feasible regarding time, cost and efficiency. Recommended land use classes of the IPCC can be reliably interpreted on VHR data. Within EOMonDis, the concept of stratified random sampling with primary sampling units (PSU) and secondary sampling units (SSU) is adopted. Combining a random sampling approach with a systematic grid ensures that the whole area is sampled [8]. The method can be used to generate reference samples for classification and reference samples for accuracy assessments. For this purpose, VHR data should be divided in a northern and southern part to guarantee independent data sets for classification and validation.

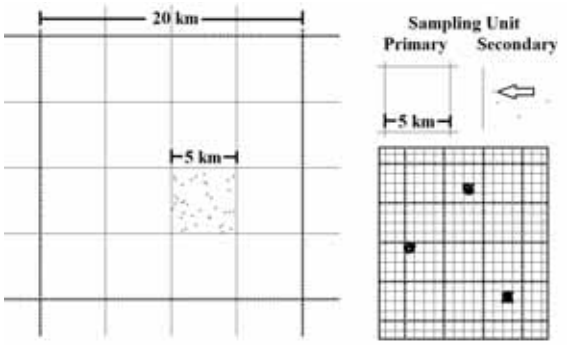

Figure 1 : Example of the sampling design for the selection of primary sampling units (PSU) and secondary sampling units (SSU). A stratification across the PSU can be performed to cover different intensities of deforestation. For each stratum, one PSU per grid cell would be used.

Figure 1 shows the conceptional design of this sampling procedure for a grid with 20km, an area of 25 km² for the PSU and random points within a selected PSU, whereas the points are the SSUs. The design is flexible and adaptable to local conditions. In order to accurately estimate the accuracy of mapping results, a stratification of PSU locations is performed according to their risk of change. The stratification is performed by incorporating global forest change (GFC) data, which contains the yearly change of forests at a spatial resolution of 30m [9]. It is most likely, that new changes will occur in the proximity of former deforestation events. The overall area of changes is calculated for each grid cell and for each PSU. Afterwards the PSUs of each grid cell are equally divided into PSU of high risk of change and PSU of low risk of change

H. Precusor Study Malawi

Within the Malawian test site, a precursor study on the rule based classification methodology was conducted by incorporating Landsat and SPOT EO data in a dense time series analysis with the former described methods. Details of the approach for land cover and land cover change mapping are described in [6]. The main results are presented within this section to illustrate the applicability of the method, which was tested for tropical dry forest. A 10% threshold for canopy cover, a minimum mapping unit of 0.5 hectare and maturity height of 5 m was chosen as forest definition, which is in line with the Food and Agriculture Organisation (FAO) definition of dry forest.

EO data for classification was comprised of 376 Landsat and 28 SPOT5 scenes, covering a time period from the year 2000 until 2014. All EO data was individually pre-processed and classified. Forest losses were classified into one of the Intergovernmental Panel on Climate Change (IPCC) compliant land cover classes: Cropland, Grassland, Settlement, Wetland, Water and Other Land Use. The accuracy assessment was performed with 542 sample points, which were generated by a posteriori stratification and selection of 12 PSUs. Thus, the sample selection is unbiased and independent from reference data that was used for classification.

Figure 2 shows a subset of the result from change date mapping. The classified dense time series that covers the period in between the reference dates for the change map enable the determination of narrow time windows for each specific change event, an important requirement to specify yearly deforestation rates. Beyond that, the existence of a continuous, consistent classified time series allows for filling most data gaps – e.g. related to clouds – in case of stable land cover around a map's reference dates, testified by classification results of adjacent scenes in the timeline. With an overall accuracy of 89.11% for the year 2000 and 86.16% for the year 2014, the entire processing chain is suitable to meet required standards. The low accuracy of change detection (62.28%) can be explained by the use of IPCC categories, a binary evaluation of changes would result in higher accuracies.

I. Conclusion

The EOMonDis project is addressing the need for user tailored, precise and validated forest monitoring products. The basis for method development are the stakeholder requirements from the climate policy, private sector companies in the domain of deforestation free supply chains and governmental institutions at country level that need reliable information on their forest resources and changes thereof. The integration of Sentinel-2 and Sentinel-1

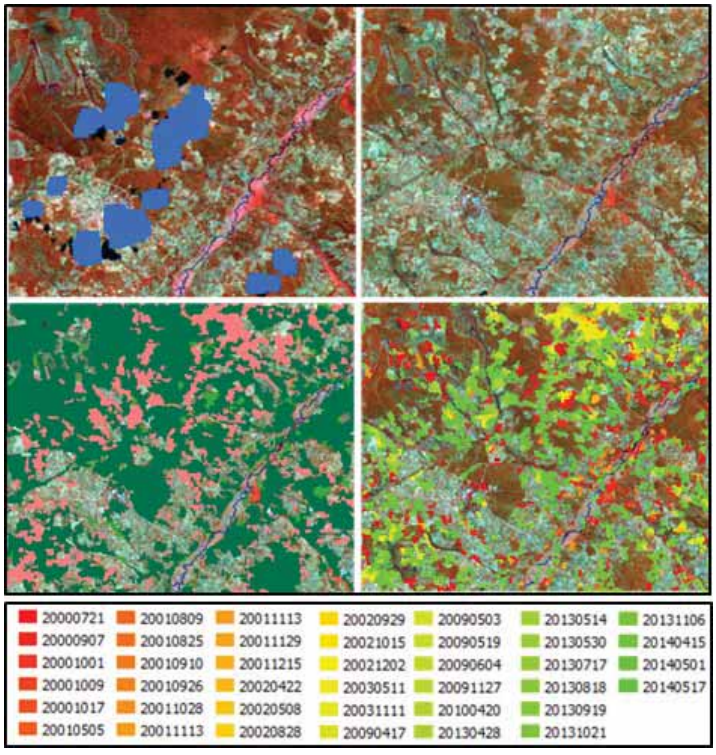

Figure 2 Subset of the Malawian test site. Upper row: Reference data for change detection (Landsat5, RGB = NIR, SWIR, RED). Historic Image with cloud/shadow data gaps (left) and reference date 2015 (right) Lower left: Completed forest change map between the reference dates (upper row), red colour indicates deforestation. Lower right: Deforestation dates derived from EO time series 2000 - 2014 (legend below).

data into dense time series builds the solid basis of the monitoring concept. The variety of forest ecosystems, the knowledge based classification procedure with adaptable rule sets and the validation approach will demonstrate the capabilities of EO data for tropical forest monitoring, accompanied by documented quality assurance.

References

[1] HCS Approach Steering Group, 2015, The HCS approach Toolkit – The High Carbon Stock Approach: No Deforestation in Practice. Version 1.0, Kuala Lumpur. HCS Approach Steering Group.

[2] GOFC-GOLD, 2015, A sourcebook of methods and procedures for monitoring and reporting anthropogenic greenhouse gas emissions and removals associated with deforestation, gains and losses of carbon stocks in forests remaining forests, and forestation. GOFC-GOLD Report version COP21-1, (GOFC-GOLD Land Cover Project Office, Wageningen University, The Netherlands).

[3] UNFCCC, 2009, Cost of implementing methodologies and monitoring systems relating to estimates of emissions from deforestation and forest degradation, the assessment of carbon stocks and greenhouse gas emissions from changes in forest cover, and the enhancement of forest carbon stocks, Technical Paper FCCC/TP/2009/1. UN Framework Convention on Climate Change.

[4] Kachamba, D.J.; Eid, T.; Gobakken, T., 2016, Above- and Belowground Biomass Models for Trees in the Miombo Woodlands of Malawi. Forests 2016, 7, 38.

[5] Chidumayo, E. & Marunda, C., 2010, Defining Dry Forests and Woodlands of Sub-Saharan Africa. In: Chidumayo, E.N. and Gumbo, D.J. (eds) The dry forests and woodlands of Africa: managing for products and services, p. 1. Earthscan Library, London. ISBN 978-1-84971-131-9

[6] Storch, C., Wagner, T., Ramminger, G., Pape, M., Ott, H.,Häusler, T., Gomez S., 2016, Automatic derivation of forest cover and forest cover change using dense multi-temporal time series data from Landsat and SPOT5TAKE5. Proceedings of ESA Living Planet Symposium SP-740, 09-13 May 2016, Prague Czech Republic.

[7] Kauth, R.J. & Thomas, G.S., 1976, The Tasselled Cap -- A Graphic Description of the Spectral-Temporal Development of Agricultural Crops as Seen by LANDSAT. Procs. Symposium on Machine Processing of Remotely Sensed Data, West Lafayette, Indiana, 29 June -1 July 1976 (West Lafayette, Indiana: LARS, Purdue University), 41-51.

[8] Sannier C., McRoberts R.E., Fichet L-V, Massard K. Makaga E., 2014, Using the regression estimator with Landsat data to estimate proportion forest cover and net proportion deforestation in Gabon, Remote Sensing of Environment, Volume 151, Pages 138-148.

[9] Hansen M. C., Potapov, P. V., Moore, R., Hancher, M., Turubanova, S. A.,Tyukavina, A., Thau, D., Stehman, S. V., Goetz, S. J., Loveland, T. R., Kommareddy, A., Egorov, A., Chini, L., Justice, C. O., Townshend J. R., 2013, High-resolution global maps of 21st-century forest cover change. Science 342, 850–853. doi:10.1126/science.1244693.

POSTER

Change Detection in Multitemporal SAR Orthoimages

Rafael A. S. Rosa[1,2], David Fernandes[2], João B. Nogueira Jr.[3] , Karlus A. C. Macedo[1], Juliano Lázaro[1], Dieter Lübeck[1]

[1] Bradar Indústria S.A.
[2]Instituto Tecnológico de Aeronáutica – ITA
[3]Santo Antônio Energia S.A.

Keywords: change detection, multitemporal images, synthetic aperture radar, SAR.

Forest monitoring is a major concern today due to climate changes, conservation of fauna and flora and to the lack of water. Therefore, several environmental monitoring techniques have been developed and used to detect changes in the scenes. However, the main techniques have limitations related to weather conditions and does not have the expected effect. The use of SAR (Synthetic Aperture Radar) seems appropriate to detect changes due to its independence of atmospheric and lighting conditions. The SAR change detection is a process that uses SAR images acquired in the same geometric conditions but in different moment (multitemporal) to identify changes in the surface that occurred between two acquisitions. This work presents a new method of change detection in multitemporal SAR orthoimages using the difference between them. Experimental tests were conducted using real SAR data obtained by the airborne sensor OrbiSAR-2 from Bradar in the Amazon Forest and the results showed a higher accuracy than those found in the literature.

One of the most important topics today is the climate change, and one of its main possible cause is the deforestation of rainforests around the world. Just talking about the Amazon Forest, the last years deforestation average has been 5,000 km²/year. This scenario makes more and more organizations and institutions search surveillance methods for the reduction and prevention of deforestation. The most important Brazilian programs for this purpose are PRODES (Amazon Deforestation Monitoring Program) – the world's biggest forest monitoring program – and DETER (Real Time Deforestation Detection), both from INPE – National Institute for Space Research, doing the monitoring through satellite imagery. These programs have demonstrated their relevance, however they have two limitations due to their sensors: the resolution (15m) and the inability to map regions covered by clouds. At the beginning of these programs, there was a reduction of the Amazon deforestation rate, however after their limitations become known by the deforesters this rate has grown by using invisible techniques to that sensors: selective logging (isolated and scattered lumbering in order to hinder the identification); and the deforestation in rainy periods, when optical imaging sensors have restrictions due to clouds. That is why change detection by radar imaging, mainly SAR (Synthetic Aperture Radar), seems appropriate to equatorial and tropical forest monitoring due to its independence of weather conditions, without losing the high resolution. The purpose of this study was to develop an algorithm able to automatically detect changes in the surface in a time interval using SAR orthoimages from temporally spaced acquisitions, however with identical geometry (multitemporal). The goal was to create an efficient tool able to automatically identify regions where there was some kind of change, such as appearance of gaps in vegetation areas, trails, changes at forests borders, selective logging, growth of pastures, plantations and other dynamic land use. The following figures show examples of SAR orthoimages from the Bradar OrbiSAR-2 airborne sensor, obtained in the region of Porto Velho (Brazil) in 2013, provided by the Santo Antônio Energia S/A, with change indications through the RGB composition. Figure 1 shows three images: (a) and (b) are SAR orthoimages obtained with 1-month interval between them; and (c) shows an RGB composition of these SAR orthoimages, wherein the R-band is composed of the older SAR orthoimage (a) and the G- and B-bands are equal and have the latest SAR orthoimage (b), in this way,

the red regions are areas where there was less return of the radar signal in the second than in the first acquisition, in other words, they are areas where the targets were "disappeared" (cut trees), the cyan regions are areas where the opposite occurred, i.e., they are areas in which the return of the radar signal increased due to the "appearance" of targets (growth of pasture) and the gray regions are areas where there has been no significant change.

Figure 2 shows the SAR ability to detect the selective logging: this figure is also an RGB composition of two SAR orthoimages acquired with 1-month interval between them, generated with the same principle of the image (c) of Figure 1, this means that, the red regions represents the cut trees. In this image, the cyan regions are trees that were hidden in the first imaging and were exposed in the second. Figure 3 (a) shows an RGB composition

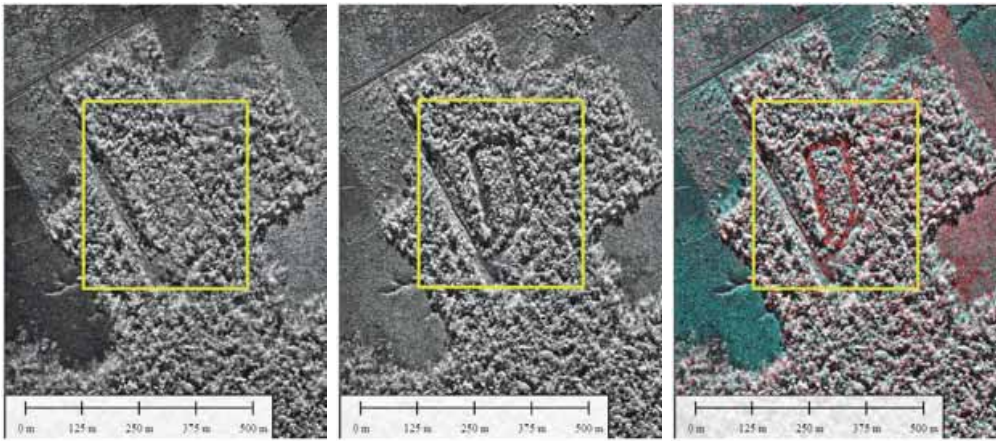

(a) (b) (c)

Figure 1. SAR orthoimages obtained by OrbiSAR-2 sensor at 2012/09/23 (a) and 2012/10/20 (b); and the respective RGB composition (c).

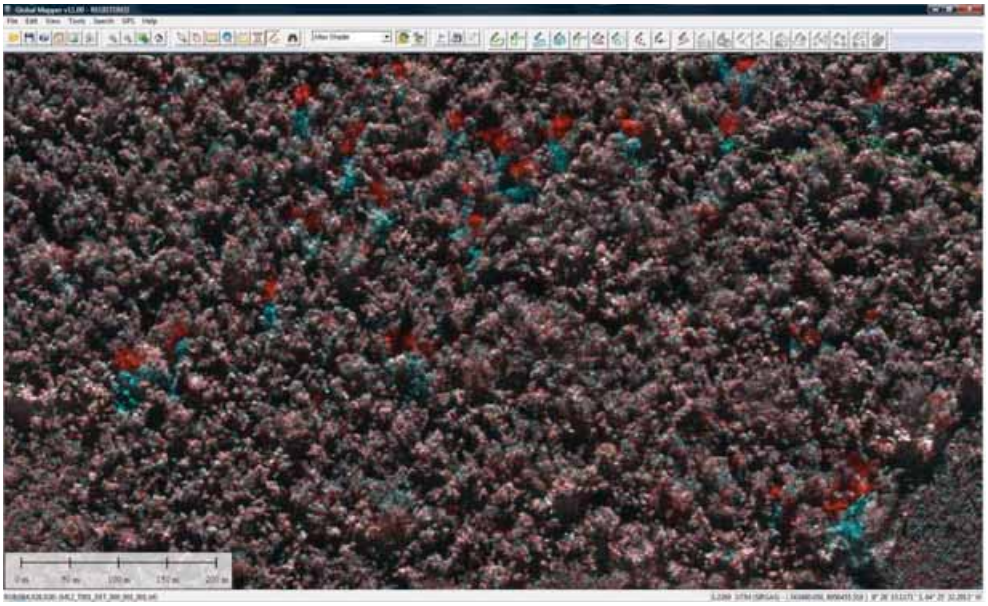

Figure 2. RGB composition of multitemporal SAR orthoimages showing the selective logging in red and the appearance of targets in cyan.

(a) (b)

Figure 3. RGB composition of multitemporal SAR orthoimages showing a deforestation in the region delimited by the yellow contour (a) and corresponding aerial photograph of this deforested area (b).

of two multitemporal acquisitions identifying a deforesting on the Madeira River banks and (b) is an aerial photography of this region obtained after the second of these acquisitions, confirming the detection.

The objective of this work was to create an algorithm that, from multitemporal SAR orthoimages, is able to identify changes between them and to produce binary masks that can be used for creating cartographic vectors.

Changing northern vegetation conditions are influencing barren ground caribou (Rangifer tarandus groenlandicus) behavior

1st: Gregory J.M. Rickbeil[1] 2nd: Txomin Hermosilla[1] 3rd: Nicholas C. Coops[1] 4th: Joanne C. White[2] 5th: Michael A. Wulder[2] 6th: Trevor C. Lantz[3]

[1] Faculty of Forestry, University of British Columbia, Vancouver, BC, Canada, V6T 1Z4
[2] Canadian Forest Service (Pacific Forestry Centre), Natural Resources Canada, Victoria, British Columbia, Canada, V8Z 1M5
[3] School of Environmental Studies, University of Victoria, BC, Canada, V8W 2Y2

Keywords: Arctic, EVI, GPS, Landsat, mammal, movement, productivity, telemetry

Abstract

Aim: To quantify changes in vegetation productivity over the past three decades across five barren ground caribou (Rangifer tarandus groenlandicus) herd ranges and assess how these changes are influencing caribou behavior.
Location: Northwest Territories and Nunavut, Canada

Methods: As an indicator of vegetation productivity, the enhanced vegetation index (EVI) was calculated on newly-developed cloud free, gap free, Landsat surface reflectance image composites representing 1984 to 2012. Changes in EVI were assessed on a pixel basis using Theil-Sen's non-parametric regression and compared across herd ranges and land cover types using generalized least squares regression. Animal movement velocity and turning angle were calculated from caribou telemetry data and generalized additive mixed models were used to link these behavior metrics with changes in vegetation productivity.

Results: Vegetation productivity increased across the five caribou herd ranges examined. The largest productivity increase occurred over the ranges of the most western herds, generally in tundra and shrub habitats. Results indicate that caribou tended to move more slowly and turn at larger angles in tundra habitats with large increases in productivity. Caribou tended to move more slowly through shrub habitats and more quickly through forest habitats with increased levels of productivity; however, caribou did not respond to productivity changes in shrub and forest habitats in terms of turning angles.

Main Conclusions: Over the 3 decades of collected data, barren ground caribou habitats have become more productive, which is consistent with other studies that have documented increases in Arctic vegetation productivity. In particular, increasing levels of productivity in tundra habitats may lead to improved foraging opportunities across barren ground caribou calving and summer ranges. However, shrub habitats which experienced large gains in productivity were associated with decreased foraging behavior, indicating that shrub proliferation may offset the potential benefits of increasing tundra productivity.

POSTER

Characterization of the wildland-urban interface using LiDAR data and OBIA as a tool for fire risk prevention and management at a local scale

Miguel A. Rodríguez-Garrido
José Carlos García-López
*Flor Alvarez-Taboada**

**corresponding author. flor.alvarez@unileon.es*
Affiliation of the authors:
Miguel A. Rodríguez-Garrido and Flor Alvarez-Taboada : GEOINCA research group. Department of Mining Technology, Topography and Structures, University of León, Ponferrada Campus, Avenida de Astorga s/n, 24400, Ponferrada, León, Spain.
José Carlos García López: Head of the Section for Nature Protection (León). Regional Government of Castilla y León, Avd. Peregrinos s/n, 24008, León, Spain.

Key words: LiDAR, woodlands, buildings, forest fire, OBIA

Abstract

The wildland-urban interface (WUI) is the area where buildings are in contact with the forest. Nowadays it is one of the biggest problems regarding wildfire suppression. Thus, establishing measures and proposals to reduce the fire risk in those areas is needed, so it is required to know its location and extension. The main goals in this study are: (i) to identify and map the intervention areas to establish preventive measures against wildfires fires in the WUI, (ii) the classification and mapping of the vegetated areas according to the foreseeable fire behaviour, based on LiDAR data and (iii) to classify the constructions in the WUI depending on the damage risk in case of a wildfire.

The methodology was structured in 3 parts: (i) processing of the LiDAR data, (ii) classification and mapping of the vegetated areas according to the foreseeable fire behaviour in case of a wildfire, and (iii) characterization of the WUI for fire risk prevention and management at a local scale, where the buildings and infrastructures were classified regarding their damage risk.

The use of the normalized digital surface model derived from the LiDAR data and the RGB orthophotographs in the object based image analysis was suitable to identify fuel models defined by the canopy cover fraction and the woody vegetation height, as it stated the overall accuracy of 87.92% (kappa: 0.8554), obtained for the classification of the vegetation by height. It was possible to identify and quantify the extension of the three levels of risk of damage due to a wildfire for the three preventive intervention areas. It was concluded that LiDAR, orthophotographs and the techniques used in this study are appropriate for the characterization of the WUI, critical for fire risk prevention and management at a local scale.

Introduction

The wildland-urban interface (WUI) is defined as the area where buildings are in contact with the forest. Nowadays it is one of the biggest problems regarding wildfire suppression. Thus, establishing measures and proposals to reduce the fire risk in those areas is needed, so it is required to know its location and extension. Galicia (NW Spain) was the Spanish region most affected by wildfires from 2001-

2010, with 72,423 fires, 68 of them were classified as large forest fires (more than 500 ha). In addition to the frequent wildfires in this area, the scattered distribution of the settlements and the large number of buildings located in the wildland-urban interface, brings to light the need to identify the buildings which could be affected if there was a wildfire and to quantify their risk of damage in regards to their location.

The main goals in this study are: (i) to identify and map the intervention areas to establish preventive measures against wildfires fires in the WUI, (ii) the classification and mapping of the vegetated areas according to the foreseeable fire behaviour, based on LiDAR data and (iii) to classify the constructions in the WUI depending on the damage risk in case of a wildfire.

Methodology

The study area covers 16 km² in the surroundings of Pedrafita do Cebreiro (Lugo, NW Spain). Data from the Aerial Orthophotograph National Plan (PNOA) (LiDAR and RGB orthophotographs), cadastral cartography and ground truth points for the validation of the filtering process and for the digital terrain model (DTM) interpolation were used in this project. The LiDAR dataset consisted of 0.5 point/m² data from two different flights: 2009 (Region of Galicia) and 2010 (Region of Castilla y León), while the RGB orthophotographs where gathered in 2009. The methodology was structured in 3 parts (Figure 1): (i) processing of the LiDAR data, (ii) classification and mapping of the vegetated areas according to the foreseeable fire behaviour in case of a wildfire, and (iii) characterization of the WUI for fire risk prevention and management at a local scale, where the buildings and infrastructures were classified regarding their damage risk.

LiDAR data Processing

This first phase includes all the processes required to obtain a normalized digital surface model (nDSM). It involved a visual analysis for outlier removal; a filtering phase to remove all the points which do not belong to the terrain (using a linear prediction algorithm (Kraus & Pfeifer, 1998)); and the interpolation of these filtered data using a 2 m x 2 m cell size to develop a DTM. The results of the filtering process where were validated using ground truth data verified on the images, trying to minimize the omission and commission errors, and trying to keep the same filtering parameters for both flights. The DTM was validated using data measured in the field by GNSS receivers. The criteria to choose the most suitable combination of parameters for the interpolation were: (i) qualitative analysis, (ii) minimizing the 95% error quantile, (iii) minimizing the 68.3% error quantile and (iv) minimizig RMSE. All these steps were carried out by using FUSION tools (McGaughey, 2015) and R. Finally, a 2 m x 2 m nDSM was derived, and it was validated with a random sample of vertical profiles.

Classification and mapping of the vegetated areas according to the foreseeable fire behaviour in case of a wildfire.

The second phase required the definition of 5 fire behaviour fuel models, based on the height and the canopy cover of the woody vegetation (Table 1). The risk of damage for buildings in case of a forest fire was defined for each fire behaviour fuel models (based on the intensity and height of the flames and the propagation speed).

Table 1. Fire behaviour fuel models, based on the height and the canopy cover of the woody vegetation (shrubs and trees).

	Height		
Canopy cover	< 2 m	2 - 8 m	> 8 m
< 20 %	Model 1	Model 1	Model 1
20 % - 60 %	Model 2	Model 2	Model 3
> 60 %	Model 4	Model 4	Model 5

The classification was performed by following an object based image analysis, with two levels of segmentation and a non-parametric classification of the vegetation based on its height. The input data were the RGB images, the green ratio and the nDMS. The process is showed in detail in Figure 1. To validate the results of this classification, an accuracy assessment was performed using data from a random sampling and the global accuracy, omission error, commission error and kappa were calculated. Subsequently, the canopy cover fraction was calculated and the vegetation was classified according to 5 fire behaviour fuel models, which also

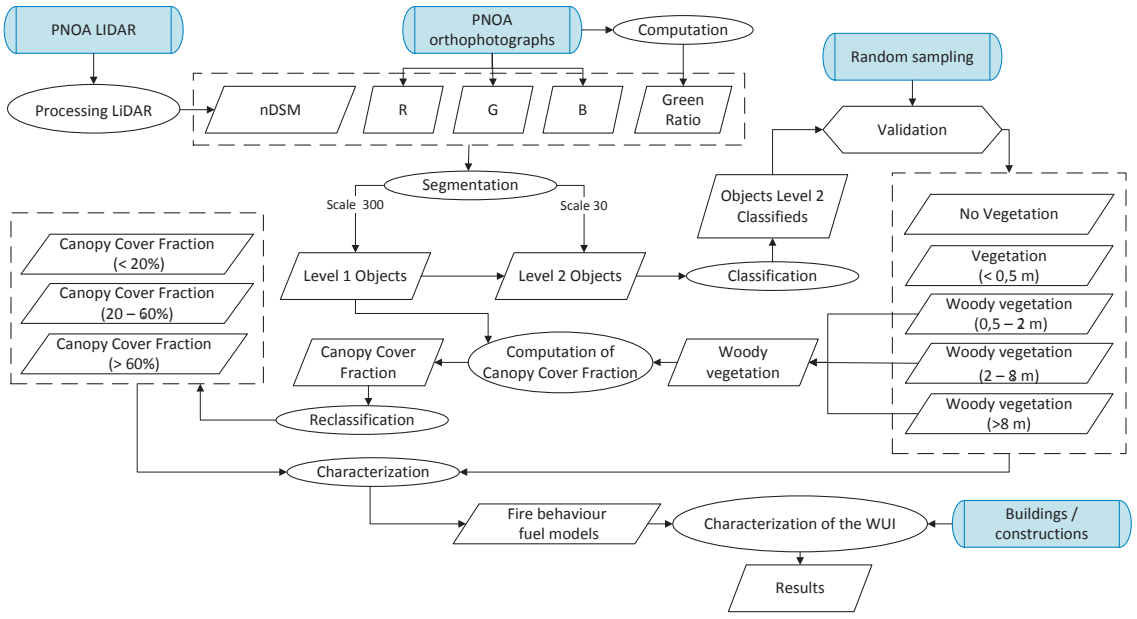

Figure 1. General workflow.

allowed determining the risk of damage due to a wildfire.

Characterization of the WUI for fire risk prevention and management at a local scale.

In this phase, each building and infrastructure was classified regarding their damage risk, taking into account Table 2. The risk assigned was the highest for the vegetation in a radius of 25 m. Moreover, and taking into account different laws, the risk in a radius of 100 m and 400 m were also computed. Those three areas were designated as preventive intervention areas. Once the the risk in the preventive intervention areas was identified and analyzed, then the extension of each risk level (Low, High and Very high) was quantified at two different scales: for the study area and for every building/construction.

Results

The results showed that the most accurate 2 m x 2m DTM was generated using the LiDAR flight data of Castilla y León, removing the outliers, with the filtering parameter values of w=2 and g=-1.5 and the switch 'minimum' in the interpolation process. This DTM reached an accuracy of 1.36 m for the 95% quantile, a root-mean-square error (RMSE) of 0.699 m and a precision= 1.378 m.

The use of the normalized digital surface model derived from the LiDAR data and the RGB orthophotographs in the object based image analysis was suitable to identify fuel models defined by the canopy cover fraction and the woody vegetation height, as it stated the overall accuracy of 87.92%

Table 2. Area covered by each fuel model.

Fuel Model	Area (ha)	Area with woody vegetation (%)	Total área (%)	Risk of damage due to a wildfire
1	15.38	1.39	0.96	Low
2	77.97	7.03	4.87	High
3	0.97	0.09	0.06	Low
4	822.28	74.09	51.39	Very high
5	193.27	17.41	12.08	Low

(83.70%-91.18%) (kappa: 0.8554), obtained for the classification of the vegetation by. The five fuel models were directly associated to three risk levels in the wildland-urban interface, which allowed to identify and locate the areas affected by the different levels of risk due to fire damage (Table 2). The fuel model number 4 (scrubland and dense young forest) was the one that covered the largest area (882.28 ha), which means that the high risk of fire damage in constructions affects 51.39% of the study area.

It was possible to identify and quantify the extension of the three levels of risk of damage due to a wildfire for the three preventive intervention areas. For the preventive intervention area of 25 m, 3.68 ha were identified and mapped as high risk areas and 9.10 ha as very high risk areas (1.33% of the study area). Related with the characterization of the WUI for fire risk prevention and management at a local scale, more than 99% of the constructions (262) were at high risk or very high risk. To decrease this risk in the preventive intervention area of 25 m, 12.79 ha were identified and mapped and in that area the canopy cover fraction is advised to be reduced by using preventive silviculture, in order to reach a canopy cover fraction lower than 20%, with the aim of obtaining vertical and horizontal fuel discontinuity.

Conclusions

It was concluded that LiDAR, orthophotographs and the techniques used in this study are appropriate for the characterization of the WUI, critical for fire risk prevention and management at a local scale.

References

[1] McGAUGHEY, R.J. *FUSION/LDV: Software for LiDAR data analysis and visualitation*, 2015. United States: Department of Agriculture.

[2] KRAUS, K., PFEIFER, N. Determination of terrain models in wooded areas with airbone laser scanner data. En: *ISPRS Journal of Photogrammetry and Remote Sensing*, 1998, vol 53, pag 193-203.

Combining Sentinel-1, Sentinel-2 and Landsat 8 images for near-real time forest change detection

Ruth Sonnenschein[1], Claudia Notarnicola[1], Carlo Marin[1] & Malcolm Davidson[2]

[1]EURAC, Institute for Applied Remote Sensing, Bozen/Bolzano, Italy
[2]European Space Agency, ESTEC, Nordwijk, The Netherlands

Keywords: Forest change detection, Sentinel-1, Sentinel-2, Landsat-8, near-real time monitoring, continuous change detection

Abstract

Earth observation has become the most important instrument for monitoring forest cover dynamics at high spatial resolution and across large areas. A large variety of change detection approaches has been developed which have been moved from bi-temporal change detection to annual change detection and continuous change detection approaches (Zhu et al., 2012, Zhu and Woodcock, 2014, Zhu et al., 2015) mainly driven by the availability of free and consistent optical Landsat images. Despite the need of timely alerts about illegal logging activities or assessments of the spatial extent and impacts of disturbances caused by natural hazards, near-real time monitoring of forest disturbances has been restricted by the relatively low temporal resolution of the Landsat sensor and the presence of cloud cover. Fusion concepts combining Landsat and the daily MODIS images overcome the low temporal resolution but may miss small-scaled disturbances and furthermore, face similar limitations in areas with persistent cloud cover. Radar images allow forest change mapping in such situations but data access has been mainly restricted until now.

With the launch of ESAs Sentinel missions, earth observation monitoring capabilities have drastically increased by a series of satellite constellations offering complementary technologies and a free and open data access policy. Especially the Sentinel-1 C-band radar sensor and the Sentinel-2 multi-spectral optical sensor with a high spatial and temporal resolution are designed to provide detailed information on land changes over time. Yet, it remains unclear how the near-real time monitoring of forest disturbances benefits from the two Sentinel satellites, the synergies between them and the synergies with the Landsat-8 sensor. Our overall objective was to assess how accurate and timely forest changes can be detected by using a multi-source concept. Based on previous research activities, we further developed the continuous change detection approach (Zhu et al., 2012) and present a methodology that allows detecting forest changes using each Sentinel-1 or Sentinel-2/Landsat-8 image. We fitted band-wise time-series models to each pixel and data source through time considering data availability and temporal variability of the forest ecosystem. We then predicted spectral and backscattering values for each new acquisition date and flagged those pixels which considerable differed from the actual values using the modeling period as reference. By integrating flagged pixels over time and across Sentinel-1 and Sentinel-2 sensors, we finally labeled pixels as forest change. We validated our results by simultaneously interpreting temporal profiles of spectral and backscattering values and image chips following the concept of TimeSync (Cohen et al., 2010). We present a case study to show the benefits and limitations of our multi-source approach together with estimates on how reliable the single flags and their integrations over time are for accurate change alerting and change detection.

References:

Cohen, W. B., Yang Z., Kennedy, R. (2010): Detecting trends in forest disturbance and recovery using yearly Landsat time series: 2. TimeSync — Tools for calibration and validation. Remote Sensing of Environment, 114, 2911-2924.

Zhu, Z., Woodcock, C.E. and Olofsson, P. (2012): Continuous monitoring of forest disturbance using all available Landsat imagery. Remote Sensing of Environment, 122, 75-91.

Zhu, Z. and Woodcock, C.E. (2014): Continuous change detection and classification of land cover using all available Landsat data. Remote Sensing of Environment, 144, 152-171.

Zhu, Z., Woodcock, C.E., Holden, C. and Zhiqiang, Y. (2015): Generating synthetic Landsat images based on all available Landsat data: Predicting Landsat surface reflectance at any time. Remote Sensing of Environment, 162, 67-83.

Developing a U.S. national land use and land cover reference data set to support inter-agency mapping, validation and statistical estimation needs

Todd A. Schroeder[1], Tom R. Loveland[2], Bruce Pengra[3], Warren B. Cohen[4], Sean P. Healey[5], Mark Finco[6], Steve V. Stehman[7], and Zhiqiang Yang[8]

[1]USDA Forest Service, Southern Research Station, Knoxville, TN USA
[2]U.S. Geological Survey (USGS), Earth Resources Observation and Science (EROS) Center, Sioux Falls, SD USA
[3]Stinger Ghaffarian Technologies/USGS Earth Resources Observation and Science (EROS) Center, Sioux Falls, SD USA
[4]USDA Forest Service, Pacific Northwest Research Station, Corvallis, OR USA
[5]USDA Forest Service, Rocky Mountain Research Station, Ogden, UT USA
[6]RedCastle Resources/USDA Forest Service, Geospatial Technology Applications Center (GTAC), Salt Lake City, UT USA
[7]College of Environmental Science and Forestry, State University of New York (SUNY-ESF), Syracuse, NY USA
[8]Department of Forest Ecosystems & Society, Oregon State University, Corvallis, OR USA

Keywords: TimeSync visualization tool, Landsat time series, Reference data, Land use and land cover change, Forest disturbance, Design-based statistical estimation, Map validation

Given the recent influx of moderate resolution imagery from satellites such as Landsat and Sentinel-2, remote sensing has become an effective and affordable tool for monitoring forest dynamics and land use and land cover change over large geographic areas. With data constraints now minimized, many government agencies are turning to new remote sensing approaches to help meet specific mission objectives, such as to produce and deliver maps which resolve current and historical characteristics of landscape condition and change. Although the products developed by different agencies often vary in scope and attributes of interest, one commonality is the need for high quality reference data which can support image classification, map validation and statistical estimation activities. With increased focus on using the full temporal depth of the available satellite archive, the analyst interpretation approach has surfaced as one of the best and only means of collecting reference data which spans the full range (20-40 years) and interval (annual) of most time series applications. Visualization tools such as TimeSync (Cohen et al., 2010) have facilitated the collection of analyst interpretations of disturbance and other land use and land cover variables over space and time, yet the costs associated with measuring a large number of plots (~25,000) remains high. In an effort to mitigate costs and reduce redundancy, the U.S. Geological Survey (USGS) and the U.S. Forest Service (USFS) have recently formed a collaborative partnership to mutually collect a U.S.-wide, nationally consistent reference data set which can meet both individual and shared agency objectives. In this talk we will discuss various facets of this operational data collection effort, including development of a TimeSync-based, joint response design which meets overlapping, but divergent programmatic needs, as well as implementation of a flexible sampling design, which promotes statistical estimation of land use and land cover variables, while also allowing for future sample intensification and addition of new partnering agencies. To shed light on the consistency of data collected by different agencies and interpreters, as well as to examine the utility of the collected variables for assessing map accuracy, results from two initial pilot studies conducted in the Pacific Northwest and Great Lakes regions will be presented. In conclusion, we will assess the future benefits and challenges associated with expanding inter-agency collaboration in the era of rapidly evolving remote sensing technologies.

References

Cohen, W.B., Z. Yang, and R.E. Kennedy. 2010. Detecting trends in forest disturbance and recovery using yearly Landsat time series: 2. TimeSync - Tools for calibration and validation, *Remote Sensing of Environment* 114:2911-2924.

Development of a UAV based platform for monitoring simulated disease expression using time-series airborne laser scanning and high resolution multi-spectral imagery

Jonathan P Dash[1], Marie Heaphy[1], Toby Stovold[1], Michael S Watt[2], Heidi Dungey[1].*

[1]Scion, PO Box 3020, Rotorua, New Zealand
[2]Scion, PO Box 29237, Fendalton, Christchurch, New Zealand

Keywords: UAV, *Pinus radiata*, ALS, multispectral imagery, time-series

Forest products are a vital component of the global economy and play a vital role in climate regulation and the provision of ecosystem services. In New Zealand the plantation forest industry is the country's third largest export earner with exports worth more than $5 billion per annum. Plantation forestry is dominated by the fast-growing conifer species *Pinus radiata* which occupies 90% of the total plantation area. Such reliance on a single species means that the industry is particularly vulnerable to biosecurity incursions and plant pathogens. In New Zealand *Pinus radiata* is affected by a number of pathogens including *Dothistroma pini*, *Cyclaneusma minus* and *Phytophtora pluvialis* and these result in a significant loss in forest productivity. In light of this a range of remote sensing technologies are required for monitoring the spread of endemic infections and detecting outbreaks so that control measures can be implemented. Previous research has shown that large-scale outbreaks of certain foliar pathogens can be detected from high resolution satellite imagery and imagery from manned aircraft. However, detection in this manner may be inadequate for early detection of outbreaks, identification of small outbreaks, and may be too expensive for assessment on a regular basis. Unmanned aerial vehicles (UAV) potentially provide a platform that provides very high resolution data acquisition with a regular return frequency in a cost-effective manner. With the development of appropriate analytics and suitable data acquisition settings this can potentially play an important role in supporting the forest industry and forest research.

Disease outbreaks in a biological system are challenging to predict and so acquiring a time-series dataset that encompasses the early stages of disease expression are difficult to obtain. To address this a trial was initiated where a disease outbreak was simulated through tree poisoning. Poisoning was intended to invoke changes in needle colour and retention that might be consistent with disease expression. Within a 9 ha trial plots were assigned to 5 different treatments, including a control, and for each treatment there were 5 replicates. The treatment defined the number of trees poisoned within each plot and all trees were poisoned in the same manner. The trial was regularly assessed from the ground using conventional tree health scoring by an experienced technician and from a UAV using high density airborne laser scanning (ALS) and 5 narrow band multi-spectral imagery with a 6 cm ground surface distance (GSD). Multi-spectral images were converted from digital numbers to reflectance values using a reflectance panel with known spectral properties and time-series images were converted to like-values through identification of spectrally invariant targets in consecutive images and adjustment using a technique based on robust regression. A series of spectral and textural indices were calculated from the imagery and were available as indicators of progressive discoloration. High density ALS data were processed to provide a point cloud representing the forest canopy and then described using a number of metrics including height percentiles, distribution of height percentiles, ratio metrics and penetration metrics. Metrics describing the point cloud were designed to detect changes in

defoliation. Rasters detailing the remotely sensed data for the trial were resampled to a range of resolutions to provide insight into the utility of lower resolution data to detect the simulated disease expression.

Using data from the highest resolution datasets a random forest model was fitted with the ground assessment as the response variable and all candidate explanatory variables derived from the UAV data. This was used to identify predictors that were most important for describing discolouration and defoliation. Using the rasters of the important predictors a rule set was developed using object based image analysis (OBIA) software to segment healthy and poisoned trees in each image. This allowed the time elapsed since poisoning for detection to be quantified using UAV data and data from traditional ground assessment. A comparison of detection rates across the different sized clusters allowed the detection thresholds to be identified. A comparison of rasters at various resolutions provided insight into the relationship between image resolution and the size of the outbreak that could be detected using the UAV data.

POSTER

Dominant tree species dynamics informed by 30 years of Landsat time series in mountain areas of Northern Spain

Cristina Gómez, Isabel Aulló, Fernando Montes

INIA, Forest Research Centre, Dpt. of Silviculture and Forest Management, Crta. La Coruña km 7,5, 28040 Madrid, Spain

Keywords: annual land cover, Landsat, SVM, species dynamics, colonization, densification, Spain

Abstract

Dominant tree species may change gradually, as result of natural succession or encouraged by fluctuations of average temperatures and precipitation. Species dominance may also change under anthropogenic influence with forest management or use. Landsat data from the TM, ETM+, and OLI sensors, spanning the period from 1984 to 2015 were used in this work to characterize the dominant tree species dynamics in a 300000 ha mountain area englobing Ordesa National Park (NP) in Northern Spain. Land cover types and land cover changes were retrospectively analysed with an almost annual series built with images from the United States Geological Survey (USGS) and the European Space Agency (ESA) archives. A twelve-class land cover classification scheme was specifically designed to identify dominant tree species, accounting the species successional stages and phenological cycles in this region. A Support Vector Machine (SVM) classification rule was trained with reference data from field plots measured in 2013 with ForeStereo and contemporaneous aerial photography, and applied to 28 summery images radiometrically normalized with the Iteratively Re-weighted Multivariate Alteration Detection (IR MAD). The input variables to the classifier included reflectance, Tasseled Cap Transformation (TCT) derived indices, texture features, and features derived from a Digital Elevation Model (DEM). For stabilization of the temporal land cover product (28 land cover maps in a 32 year period) a filter of ecologically feasible annual land cover transitions was applied. The final classification was validated over a reference image (2013) with overall accuracy 75%. Temporal trajectories of the Tasseled Cap Angle (TCA), an index positively related with density variables, and its temporal derivative, the Process Indicator (PI) were analysed to characterize the change and rates of change in forest density. Inference of the tree species changing dominance in mixed forests was based on trends of change in the temporal trajectories of the classification probabilities deployed by the SVM classifier at each annual land cover map. Our results indicate that some areas at high altitudes are progressively being colonized by natural forests of pine. A generalized densification tendency has been observed, particularly since the 1990s, in forest stands without human intervention and those where grazing practices have been reduced or abandoned. Actual conditions seem to favour a growing dominance of *Fagus sylvatica* L. and *Abies alba* Mill. in mixed forests. The dynamics of tree species in the NP and adjacent areas indicate a similar pattern of change, suggesting changes are both resulting from successional processes and changes in human influence. Frequent land cover products derived from a series of Landsat data and supported by ecological knowledge provide valuable insights of diversity and species dynamics.

POSTER

EO-1 SWIR band detection capability and comparison with Landsat

Shannon Franks[1], Christopher Neigh[2]

[1] Stinger Ghaffarian Technologies (SGT), NASA/GSFC, Greenbelt Maryland 20771
[2] NASA/Goddard Space Flight Center, Code 618, Greenbelt Maryland 20771

Keywords: EO-1, Advanced Land Imager, ALI, Shortwave infrared, SWIR, Landsat, Spectral Band Pass

Abstract:

The Earth Observing One (EO-1) satellite has been in orbit for 15 years. The mission was started to test new technologies that could perhaps be incorporated in future earth observation satellites like Landsat. In this study, we test one of those technologies for its usefulness in detecting Tamarack (*Larix laricina*) tree mortality due to attack of Eastern Larch Beetle (*Dendroctonus simplex*) around Park Falls, Wisconsin. The sensitivity of the extra shortwave infrared (SWIR) band (1.2 – 1.3 µm) onboard the Advanced Land Imager (ALI) was studied in comparison to the traditional SWIR bands that are collected from the Landsat satellites. Time series ALI and Landsat imagery calibrated to surface reflectance was used in the study. The locations of the damage was provided by the USFS Forest Health Technology Enterprise Team and was validated with high resolution WorldView 2 data showing the individually attacked trees. Differences in the spectral sensitivity to tree mortality were found in the various SWIR bands and that knowledge could be useful when detecting insect damage. Our results show that the shorter wavelength SWIR band and the longer wavelength band are more sensitive to the damage than the one that is traditionally used in satellite remote sensing.

**** I would prefer a poster presentation

POSTER

Estimación y monitoreo de cobertura de malezas a través de imágenes satelitales

Rodrigo Saavedra [1], Rodrigo Burgos [1], Jorge Requena [2], Mauricio Reyes [3], Cecilia Muñoz[4]

[1]Bioforest S.A, Unidad Bioinformática y División de Silvicultura. Forestal Arauco S.A.
[2]Forestal Arauco Zona Norte, Mensura y Cartografía.
[3]Forestal Arauco Zona Centro, Planificación Silvícola.
[4]Forestal Arauco Zona Sur, Vivero y Planificación Silvícola.

Palabras claves: cobertura de malezas, monitoreo, imágenes satelitales, uso operacional.

Resumen

La presencia de malezas en las plantaciones forestales si bien tiene algunos efectos favorables como la protección del suelo, estas afectan negativamente la sobrevivencia y el crecimiento de las plantaciones. La cobertura de malezas es monitoreada a través de las visitas que realizan los jefes de áreas a cada uno de los predios, sin embargo dado los grandes volúmenes de superficie que manejan anualmente, estos monitoreos pueden ser tardíos para un control oportuno de la vegetación competidora. Es por esto que se propone el desarrollo de un sistema como herramienta de apoyo para uso operacional, que permita la estimación y monitoreo de forma oportuna y masiva de la cobertura de malezas a través de imágenes satelitales.

Este estudio tiene como objetivos 1) Desarrollar metodología para estimar la cobertura de malezas a través de imágenes satelitales y 2) Desarrollar una herramienta de uso operacional como apoyo a la planificación del control de malezas. Para esto se utilizaron imágenes del satélite Landsat 8 (NASA - USGS). Posteriormente se procedió a la evaluación de los predios donde se realizó un muestreo compuesto generándose cuadrantes para la estimación de cobertura de malezas en terreno. Se observó que existe una correlación significativa entre la cobertura de malezas observada en terreno y el índice espectral de vegetación NDVI de 0.71, generándose un modelo que permita la estimación de la cobertura de malezas a nivel patrimonial y con el fin de poder implementar un sistema de apoyo para uso operacional.

POSTER

Exploring remote sensing potential in land use, land use change and forestry (LULUCF) inventories in Aragón

Eva Sevillano Marco[1], Eduardo Notivol Paíno[2],

[1] Regional de Blumenau - Regional University of Blumenau (FURB), Department of Forestry. Rua São Paulo, 3250, 89030-000 Blumenau-Santa Catarina, Brazil evasevillano@yahoo.es.
[2] Agro-food technology and research Centre of Aragón (CITA). Forest Resources and Agriculture Applications Avda. Montañana 930, 50059 Zaragoza, Spain enotivol@aragon.es. *Keywords: Landsat, Classification, Land Use, Change, Forestry, Biomass, Kyoto Protocols*

Abstract

In the Green-house Effect Inventories reports, surfaces estimation and annual changes in land uses could be more accurately calculated by means of the application of remote sensing than with the commonly used methods used by the Regional Government in Aragón (Spain) based on available static maps, including national land cover or forest maps. The objective of the study is the evaluation of the potential application of remote sensing techniques of land cover/land use yearly monitoring. LULUCF categories maps and change detection (i.e., between two years, 2002 and 2009) were obtained from a maximum likelihood supervised classification of Landsat multitemporal scenes (phenologically representative dates throughout the year). Confusion matrices provided global accuracy values of respectively 89.24% and 83.69% in 2002 and 2009.

Introduction

The Kyoto Protocol (IPCC 2000) establishes the requirement of annual inventories submission of all anthropogenic greenhouse gas emissions from sources and removals from sinks. Surfaces and annual changes in land uses could be more accurately estimated than with commonly used methods in the Green-house Effect Inventories reports, based on static maps (i.e., CORINE Land Cover, Information system of land cover in Spain SIOSE and National Forest Map NFM). In this context, Volden et al. (2003) and Romero et al. (2004) mention five European countries –Finland, Italy, Netherlands, Norway, Switzerland- that examined the potential of remote sensing for the evaluating land use and land-use change for the Kyoto Protocol reporting. User-requirements are defined for determining land use, assessing forest areas and estimating aboveground biomass at a minimum spatial resolution for mapping 0.5 ha (Kyoto Protocol requirements). Transparency, reliability and periodicity of data are highlighted features linked to remote sensing methods. Also, a high degree of automation without terrestrial control is desirable Romero et al. (2004). The Landsat series was identified in several test areas as one the most useful generally speaking considering worldwide availability of products, homogenization procedures across inventories and compromise between the medium spatial resolution it provides and the Kyoto requirements. It is advisable to complement the imagery with aerial ortophotographies, climatic and topographic maps. Among the identified weaknesses, the first trials showed overestimation in forestlands surfaces as well as expected issues in small and sparse forest patches. From the LULUCF categories surfaces, a further step in the carbon stocks assessment is the aboveground biomass quantification. Certainly although not a specific requirement in the Kyoto Protocol, it is a key element for the inventories (e.g., land use change in forestalands suchlike afforestation and deforestation), and can be approached by means of remote sensing techniques as well. Therefore, the objective of the present study is the evaluation of the potential application of remote sensing techniques in the methodology definition at regional scale of land cover/land use yearly monitoring for the region of Aragón, in Spain. A first exploration of model fitting techniques is undergoing starting from this study.

Methodology

Aragon is one of the 17 autonomous regions of Spain and covers an area of approximately 47719 km^2. It is located at NE of Iberian peninsula between 39ºN and 43ºN. The orography of the region is characterized by the Ebro Valley depression (altitude ranging from 150 to 300 m above sea level) and two mountain ranges surrounding the valley: the Pyrenees at north with peaks over 3000 m and the Iberian System range with maximum heights over 2000 m. Aragon's climate can be defined as continental moderate. Temperatures are determined mainly by altitude, ranging from cold or very cold in winter and cool in summer in the mountains to the north (Pyrenees) and to the south and west (Iberian range), to mild in winter and hot in summer in the central lowlands. Rainfall is also very variable, with very low mean values in the central areas and increasingly higher values in mountain areas, especially in the high Pyrenees. In the middle of Aragon, which is only 200 metres above sea level, the annual average temperature is around 14 °C To the north and south of the Ebro valley, where the elevation rises to 500 m above sea level, the temperature drops by two degrees. In the mountains, between 600 m and 1000 m observed temperatures are between 11 and 12 °C. The vegetation follows the oscillations of the extreme topography and climate. There is a great variety, both in wild vegetation and crops. In the highlands forests (pines, firs, beeches, oaks) can be found, as well as bushes and meadows, while in the lower altitude areas of the Ebro valley green oak and sabina are the most abundant trees, apart from the agricultural lands.

Groundtruth data was derived from photointerpretation and available products like SIOSE 2005, CORINE 1990, 2000, 2006 and Global Land Cover 2000, and National Forest Map (i.e., Coordination of information on the environment CORINE Land Cover, Information system of land cover in Spain SIOSE and National Forest Map NFM). A compromise between capturing the variability inherent to the thematic category and its characteristic features is needed. The selection criterion has been to prioritize the extraction of pure areas, avoiding usage mixtures and ecotones that could introduce noise to the classification stage. Unchanged areas between the whole time series have been chosen and erosion has been applied therefore minimizing border areas, displacement and topology errors. The sample was split on a 50% basis to obtain the training areas as input for the supervised classification and test areas for the evaluation and validation processes. Avoiding cloud scenes when possible, scenes were selected in phenologically representative dates throughout the year. Between three and six dates per year for each scene are needed. Ideally, considering the regional environmental variables: one scene in between March-April, two between May-June, one between August-September, one between October-December and one between January-February. All the databases have been projected to ETRS 1989 UTM Zone 30N (EPSG 3042) and subset to the area of study. Cloud, shadows and snow have been masked in order to minimize spectral distortions in radiometric corrections (Chávez 1996 method employed, using a 20 m pixel digital elevation model DEM together with the required inputs of Julian day, solar elevation angle, and azimut angle, irradiances, transmissivity, slope-gain and offset-bias). Spectral vegetation índices were derived: Normalized Difference Vegetation Index NDVI, Ratio Vegetation Index RVI, Soil Adjusted Vegetation Index SAVI, and Tasseled Cap. Additionally, from the DEM, slope and aspect layers were generated to be used in the classification process. Finally, to account for the units and ranges diversity of all the scenes, indices and topographic layers, previous to the classification, standardization is required (Spiegel 1991), calculating the mean and standard deviation for each variable.

The legend of six categories follows the classes defined by the United Nations Framework Convention on Climatic Change UNFCCC for LULUCF. After the standardization process abovementioned, 6 spectral bands (optical bands 1,2,3,4,5 and 7 of Landsat 5TM and Landsat 7 ETM+) from 3-6 dates per year, vegetation indices, tasselled cap, slopes, elevations and aspect were stacked to be used in the classification. A supervised classification method (maximum likelihood) generates the corresponding land use thematic cartography for 2002 and 2009. Accordingly, LULUCF categories maps and also the change detection (i.e., between two years, 2002 and 2009) were obtained from classification of Landsat multitemporal scenes. Confusion matrices and signature separability were the evaluation techniques used. A workflow diagram is shown in Figure 1.

Results

The changes between categories between 2002 and 2009 are shown in Figure 2 and Table 1.

At detailed zooms, and legend containing each of the transitions, many other features relevant for the regional management and LULUCF monitoring become intelligible.

Figure 2. Map of Aragón transitions in LULUCF classes between 2002-2009.

Confusion matrices provided global accuracy values of 89.24% in 2002 and 83.69% in 2009. User and producer accuracies are depicted in Table 2.

Most vegetation covers surfaces remain unchanged, as expected in vegetation dynamics in such period.

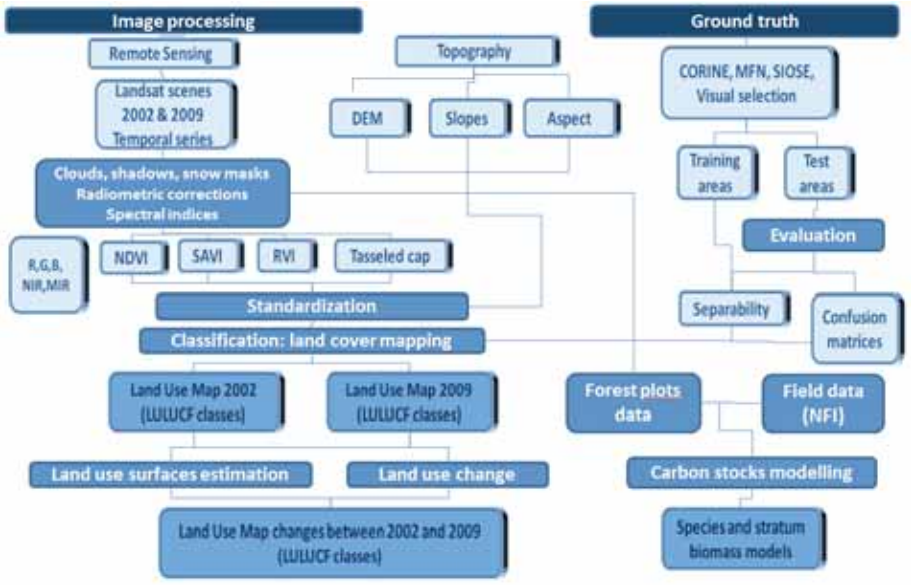

Figure 1. Workflow

Table 1. LULUCF Land use surfaces discriminated by remote sensing and their changes between the considered period (2002-2009)

LULUCF Categories surfaces (km2) and changes	km²	To cropland	1249,37
Forest	12000	To grassland	1313,05
Grassland	878,939	To water	16,81
Cropland	5859,25	To urban	2946,66
Soil	11400	To forest	1896,86
Urban	475,379	To soil	6454,08
Water	309,146	Total changes	13876,83
		Total unchanged	30900,00

Table 2. Kappa indices, producer accuracies and user accuracies for the LULUCF UNFCCC categories in 2002 and 2009 in Aragón (Spain).

2002 /2009	Producer accuracy	User accuracy	Kappa index
Grassland	62.9% / 67.8%	95.4% / 87.8%	0.95 / 0.86
Cropland	93.7% / 79.4%	91.1% / 86.3%	0.89 / 0.83
Soil	98.6% / 80.5%	65.6% / 54.6%	0.61 / 0.48
Urban	76.0% / 75.6%	95.4% / 89.9%	0.95 / 0.72
Water	97.3% / 89.0%	100.0% / 95.4%	1.00 / 0.94
Forest	96.9% / 86.7%	94.7% / 98.0%	0.93 / 0.97

Likewise, the urban growth is clearly evidenced locally. Tuning of methods is subject to availability of updated coherent ground truth and field data in accordance to requirements of classification method and the subsequent definition of categories. After the achievements verified in these first trials, it is strongly recommended that future aims address the automation of processes for a seamless implementation at regional and homogenously at national scales, in order to compile accurate land cover temporal series for annual periods from the reference year 1990 onwards (i.e., IPCC compliant methods state reference year 1990). Such maps can be complemented with more detailed legends, for instance embedding Forest Maps, in order to enable biomass stocks estimation by means of geospatial modelling: e.g., relating stands data to spectral variables or derived indices, resulting from the combination of field data with remote sensing variables. This line of work was initiated by fitting aboveground biomass models from field data (CITA, 2008) and employing the LULUCF spectral variables and derived products as predictors.

Conclusions

This exploration was intended to tailor research to territorial management and provide the regional government with fit-for-purpose resources in the implementation of policies suchlike the Protocol of Kyoto: in particular for the LULUFC sector accounting methods in the Green-house effect gases inventory. In the climatic change study, the continuity of forerunner remote sensing missions, ever increasing availability of products, with enhanced capabilities (spatial and spectral resolutions, temporal coverage), and development of sensors fusion techniques, are relevant in the LULUCF sector accounting methods, allowing for improved accuracy performance, biomass modelling and back-monitoring as tested in this pilot case.

Acknowledgements

This project was co-funded by the European Regional Development Fund (ERDF) and the Farming, Livestock, and Environment Department of the Regional Government in Aragón (Spain), 2007-2013 Objective Regional Competitiveness and Employment, Axis 2: Environment and Risk Prevention, Category 49: Climatic Change Adaptation and Mitigation. The research was assigned by the Regional Government to the Agro-food technology and research Centre of Aragón (CITA), by the 182/2013 Decree 19th November 2013, published in the official regional bulletin 234, 27th November 2013. Research project: Green-house effect gases inventory, emissions and sinks in the Land Use, Land Use Change and Forestry –LULUCF-sector).

References

Chávez P S, 1996. Image-based atmospheric corrections. Revisited and improved. Photogrammetric Engineering & Remote Sensing 62.9 1025-1036

Centro de Investigación y Tecnología Agroalimentaria de Aragón (CITA), 2008. Estudio sobre la funcionalidad de la vegetación leñosa de Aragón como sumidero de CO2: existencias y potencialidad (estimación cuantitativa y predicciones de fijación). Centro de Investigación y Tecnología Agroalimentaria de Aragón, Zaragoza, Spain. Retrieved from: http://www.aragon.es/estaticos/GobiernoAragon/Departamentos/MedioAmbiente/Areas/03_Cambio_climatico/06_Proyectos_actuaciones_Emisiones_GEI/estudio.pdf

Intergovernmental Panel on Climate Change (IPCC). 2000. Watson R, Noble I R, Bolin B, Ravindranath, N H, Verardo D J, Dokken D J (Eds) Land use, Land-use Change, and Forestry: A Special Report. Cambridge University Press. Cambridge, UK.

Romero J, Volz R, Giamboni M, Rüsch W 2004. The role of the forest in the Kyoto Protocol - Estimation of carbon reserve using satellite data). Schweizerische Zeitschrift für Forstwesen 155 (5), pp. 125-133.

Spiegel M R 1991 Statistics. McGraw Hill 556 p.

Volden E, Bruzzone l, Romero J, Lumicisi A, Renda O, La Fortezza R, Tomppo E, Aalde H 2003. Forest environmental reporting services. In: Learning from Earth's Shapes and Sizes. Proceedings of the International Geoscience and Remote Sensing Symposium (IGARSS '03), Vol. 7, July 21-25, 2003, Toulouse, France, pp. 4582-4584.

Fire behavior simulation from global fuel and climatic information

M. Lucrecia Pettinari[1,2], E. Chuvieco[1]

[1.] Department of Geology, Geography and Environment, University of Alcala, Alcalá de Henares, Spain.
[2.] E-mail: mlucrecia.pettinari@uah.es

This study presents a global fire behavior simulation based on a global fuelbed dataset and climatic and topographic information. The simulation was executed using the Fuel Characteristic Classification System (FCCS). The climatic information, extracted from the ERA-Interim Global Reanalysis covered the period 1980-2010, and daily weather parameters were used to calculate the mean monthly fuel moisture content (FMC) and wind speed for the early afternoon period. Also, as the most severe fires occurs with extreme environmental conditions, a worst condition scenario was created using the mean value of the 30 days with lowest FMC during each month of the study period.

The FMC, wind speed and slope information was grouped into classes, and FCCS was used to simulate the reaction intensity, rate of spread and flame length of the fuelbeds in the different environmental conditions. These results were then mapped, showing the variation in surface fire behavior during the different months of the year throughout the world, both due to the climatic conditions and the characteristics of the fuels. The surface fire behavior parameters identified the fuels and environmental conditions that could cause more severe fire events, and could be used as a mean to assess fire danger.
Keywords: global fuel map, FCCS, fuel moisture content, fire behavior

Introduction:

Wildfires occur due to a combination of available fuels, sources of ignition, and environmental conditions (mostly weather), that allow the fire to be sustained and spread. Most regional fire behavior modeling systems consider weather variables to estimate critical parameters such as rate of spread, flame length or the energy released (Rothermel 1983), but only a few consider explicitly the differences in fire behavior due to fuel properties.

The objective of this study was to combine fuel and weather information to obtain fire behavior parameters at a global scale, using a global fuel map previously developed (Pettinari and Chuvieco 2016)

Methodology:

To calculate fire behavior, we used the Fuel Characteristics Classification System (Ottmar et al. 2007). The FCCS was designed to represent the structural and geographic diversity in wildland fuels and combines the fuel properties into "fuelbeds", which include the physical and chemical variables used to model fire behavior and fuel consumption and predict emissions (Riccardi et al. 2007). Based on input environmental variables, the FCCS also predicts surface fire behavior parameters using a reformulation of the Rothermel (1972) fire behavior model (Sandberg et al. 2007).

The fuel distribution and their physical and chemical variables related to fire behavior were extracted from the Global Fuel Dataset developed by Pettinari and Chuvieco (2016). This dataset was developed from different spatial variables, both based on satellite Earth observation products and fuel databases, and is comprised by two products: a global fuelbed map (at a resolution of approximately 300m), developed using land cover and biomes information, and a database that includes the parameters of each fuelbed that are related to fire behavior and effects.
To calculate the fire behavior parameters, FCCS requires information on fuel moisture content (FMC), wind speed and slope. Percentage slope was calculated using the Global 30 Arc-Second Elevation (GTOPO30) product and the different percentages were grouped in three slope classes: 0-5%, 5-45% and >45% slope.

The FMC and wind speed was calculated using the climatic data of the ERA-Interim Global Reanalysis (Dee et al. 2011) of the European Centre for Medium-Range Weather Forecast. The weather information covered a 30-year period, with daily data between 1981 and 2010, with a spatial resolution of 0.5 degrees.

To obtain the FMC, the 10-h fuel moisture content was calculated using the equations of the National Fire Danger Rating System (NFDRS, Cohen and Deeming 1985), and using the following weather variables from the ERA-Interim database: 2 meter temperature, 2 meter dew point, total precipitation, total cloud cover and snow depth. The 10-h FMC obtained was converted to Fuel Moisture Scenarios (FMS, Scott and Burgan 2005) to be input in FCCS. The daily values of FMS obtained from the 1980-2010 climatic data were aggregated in a monthly basis, to obtain the mean FMS for each month in each 0.5° cell, as a proxy to the mean conditions that could be found in that region during that month of the year. However, since severe weather conditions (low FMC and high wind speed) usually cause the most important fire events and largest fires, a "worst conditions scenario" was created, calculating the mean FMS of the 30 days with lowest FMC for the entire period and for each month.

Wind speed was calculated from the 10m U and V wind components of ERA-Interim, and converted to midflame wind speed using a wind adjustment factor of 0.348. The daily values of wind speed were aggregated by month to obtain the mean midflame wind speed for each month in each 0.5° cell, and the resulting wind speeds were grouped in three classes: 0-1 m.s-1, 1-2.5 m.s-1 and 2.5-5 m.s-1. To account for the worst conditions scenario, the midflame wind speed corresponding to the 30 worst-FMC-days was obtained for each month, and the values were averaged and then converted to wind class for those conditions.

The possible FMSs, wind classes and slope classes created 36 combinations of possible environmental scenarios. Each fuelbed from the Global Fuelbed Dataset was run in FCCS version 3.03.203 module inside the Fuel and Fire Tools (http://www.fs.fed.us/pnw/fera/fft/index.shtml, accessed November 2016) in all the scenarios, to obtain all possible rate of spread (ROS), flame length (FL) and reaction intensity (RI) values for each fuelbed. To create the fire behavior maps, each fuelbed pixel in the fuelbed map was assigned the fire behavior results corresponding to the environmental scenario of their location and month that was being evaluated, both for the mean and worst conditions.

Results:

Figure 1 shows, as an example of the results obtained: the mean reaction intensity for the months of January (a) and July (b). The highest values of RI obtained for January were 4664 kJ.m-2.s-1, both in mean and worst conditions and located in the cropland-shrubland belt of Northern Africa. But during worst conditions the geographical distribution of RI values higher than 2000 kJ.m-2.s-1 extended also to the Brazilian Cerrado and South-American shrublands in Argentina, Bolivia and Uruguay, along with the savannas in Southern Africa. Regarding July, the highest RI values obtained were 3835 kJ.m-2.s-1 for the mean conditions, located in Zambia, and 4435 kJ.m-2.s-1 for the worst conditions, located in Argentina. The geographical distribution of the cells with RI > 2000 kJ.m-2.s-1 during July's mean conditions include the Southern-African Savannas and the Brazilian Cerrado, but extend to Northern Africa and South-American shrublands when the worst conditions are considered.

As with the RI, the ROS and FL also showed changes in value according to seasonal weather conditions and fuelbeds. The highest values of ROS were obtained for grassland fuelbeds located mostly in the African continent, and also in the North-American Deserts, along with rice croplands in southern Kazakhstan, reaching to values up to 1.013 m.s-1 for the July's worst conditions. Regarding the FL, the highest values obtained (>6 m) were all located in Africa.

It should be noted that the coarse resolution of the weather information allowed obtaining only a generalized and estimated result of the fire behavior outputs. Wind speed, for example, is highly variable in time and space and affected by sheltering and terrain, which could not be considered at the resolution of the data (0.5°) or even the fuelbed map (approx. 300m). As such, the values used for the analysis are not expected to be realistic in local fire events, but to introduce a coarse variable showing areas and months in which fire could have a more

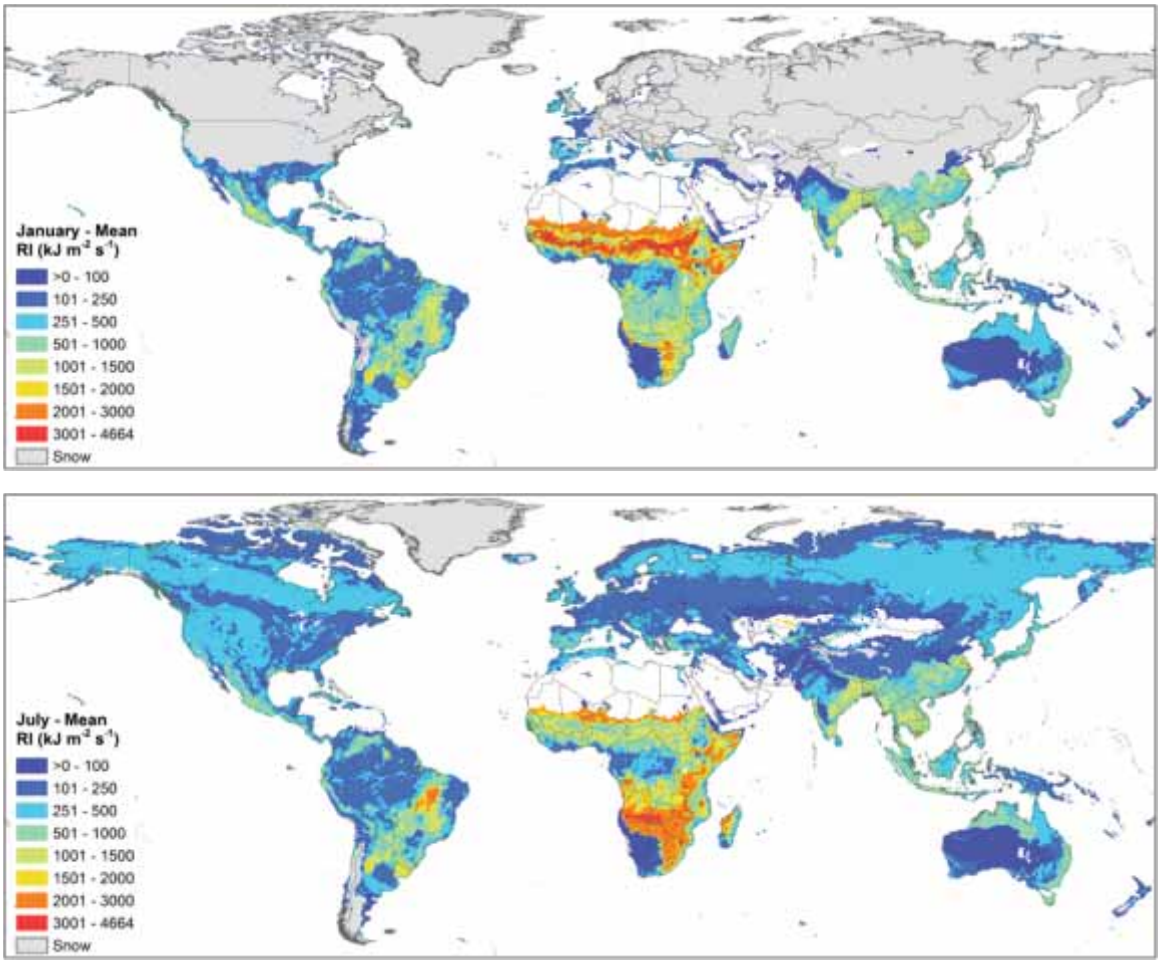

Figure 1: Mean Reaction intensity (RI) for January (a) and July (b) for the study period.

severe behavior due to general wind speeds being higher than in other regions or months.

Still, fire behavior parameters are important because they allow understanding the fire itself, and not only classifying the fire as a binary event (fire – no fire). Fire events are extremely variable, and they produce different effects in the ecosystem. For this reason, the study of the characteristics of the fire events, by means of estimating fire behavior parameters, can help identifying land cover and environmental conditions combinations that could cause severe fires with relevant environmental impacts, thus posing a higher danger.

Conclusions:

The maps showed that the highest values of reaction intensity were found in shrubland fuelbeds in tropical and sub-tropical dry regions, the highest rates of spread were obtained for grasslands in those locations and shrublands in desertic areas, and the highest flame lengths occurred in African savannas. All parameters were highly affected by the environmental conditions, increasing their values up to an order of magnitude with changes in the fuel moisture content of the fuels.

The coarse resolution of the climatic data, though provided information on regional weather conditions, cannot allow predicting accurate local fire behavior, because local conditions of fuel moisture and wind can rapidly change and modify the fire behavior.
Still, the results showed the importance of including detailed fuel information into fire risk assessment systems based on weather parameters, as it could help to better estimate the expected fire behavior and effects.

References:

Cohen J. D. and Deeming J. E. (1985). "The National Fire-Danger Rating System: basic equations." General Technical Report PSW-82. Berkeley, CA, USDA Forest Service, Pacific Southwest Forest and Range Experiment Station. 23 pp.

Dee D. P., Uppala S. M., Simmons A. J., Berrisford P., Poli P., Kobayashi S., Andrae U., Balmaseda M. A., Balsamo G., Bauer P., Bechtold P., Beljaars A. C. M., van de Berg L., Bidlot J., Bormann N., Delsol C., Dragani R., Fuentes M., Geer A. J., Haimberger L., Healy S. B., Hersbach H., Hólm E. V., Isaksen L., Kallberg P., Köhler M., Matricardi M., McNally A. P., Monge-Sanz B. M., Morcrette J.-J., Park B.-K., Peubey C., de Rosnay P., Tavolato C., Thépaut J.-N. and Vitart F. (2011). "The ERA-Interim reanalysis: configuration and performance of the data assimilation system." Quarterly Journal of the Royal Meteorological Society 137: 553-597.

Ottmar R. D., Sandberg D. V., Riccardi C. L. and Prichard S. J. (2007). "An overview of the Fuel Characteristic Classification System - Quantifying, classifying, and creating fuelbeds for resource planning." Canadian Journal of Forest Research 37(12): 2383-2393.

Pettinari M. L. and Chuvieco E. (2016). "Generation of a global fuel data set using the Fuel Characteristic Classification System." Biogeosciences 13(7): 2061-2076.

Riccardi C. L., Ottmar R. D., Sandberg D. V., Andreu A., Elman E., Kopper K. and Long J. (2007). "The fuelbed: a key element of the Fuel Characteristic Classification System." Canadian Journal of Forest Research 37(12): 2394-2412.

Rothermel R. C. (1972). "A mathematical model for predicting fire spread in wildland fuels." Research Paper INT-115. Odgen, UT., USDA Forest Service, Intermountain Forest and Range Experiment Station. 40 pp.

Rothermel R. C. (1983). "How to predict the spread and intensity of forest and range fires." INT-143. Boise, ID., National Wildfire Coordinating Group, USDA Forest Service Intermountain Research Station. 166 pp.

Sandberg D. V., Riccardi C. L. and Schaaf M. D. (2007). "Reformulation of Rothermel's wildland fire behaviour model for heterogeneous fuelbeds." Canadian Journal of Forest Research 37(12): 2438-2455.

Scott J. H. and Burgan R. E. (2005). "Standard fire behavior fuel models: a comprehensive set for use with Rothermel's Surface Fire Spread Model." RMRS-GTR-153. Fort Collins, CO., USDA Forest Service, Rocky Mountain Research Station. 80 pp.

POSTER

Forest area changes and impact of forest boundary delineation on change detection in forested landscapes in Eastern Europe

Urmas Peterson[1,2] and Jaan Liira[3]

[1] Tartu Observatory, Tõravere 61602, Tartumaa, Estonia, Tel: +3727410152, Fax: +3727410205, E-mail: urpe@aai.ee, web-page: http://www.to.ee
[2] Institute of Forestry and Rural Engineering, Estonian University of Life Sciences, Kreutzwaldi 5, Tartu 51014, Estonia
[3] Institute of Ecology and Earth Sciences, University of Tartu, Lai 40, Tartu 51005, Estonia, Tel and Fax: +3727376222, E-mail: jaan.liira@ut.ee, web-page: http://www.botany.ut.ee

Keywords: Forest mapping, forest change detection, gradual changes, winter images

Boreal and northern temperate forests cover substantial part of European land area. Fine-scale and spatially explicit data on changes of the forested area in Eastern Europe are sketchy. Within the last decades the change of forested area in this region is expressed mostly in a gradual and slow expansion of forested patches on the former agricultural land. Forests at northern latitudes are characterized with winters during which snow covers several months the ground. Winter in boreal and hemi-boreal latitudes is the season with the greatest target to background contrast on predominantly two-class images composed of forest and non-forest classes. In winter, forest patches are surround on all sides by open areas with bright snow cover.

We used imagery of Landsat sensors from the United States Geological Survey (USGS) archive for three time periods: mid to late 1980s, early 2000s and 2010s (years 2011 to 2016). Our study area: three Baltic states, Byelorussia, Ukraine and European part of Russia were covered with winter images on these years in the USGS archive. Results obtained from moderate resolution Landsat images were locally supported with high resolution winter images for error estimates or with national basic map data if available.

The images were classified into "forest" and "non-forest" classes by thresholding pixel radiance values. The optimal edge threshold was defined by looking for a maximum radiance contrast of neighbouring pixels in a forest boundary area. Forest boundary segments were assigned an attribute of cardinal direction according to their relative position at the edge of a forest patch.

Forest boundary locations on images taken in different solar illumination conditions were compared. The aim was to distinguish real changes at forest edges (i.e. forest patch expansion) from those changes in image classification resulting from different solar elevation and atmospheric haze conditions. We found that shade and forest structure affect edge detection on medium resolution satellite images. Regression analysis was used to relate the possible drivers of forest area increase in Eastern Europe.

We found locally extensive increase of forest patch areas on abandoned farmland in the studied region. However, we also found strong differences in the rates and spatial patterns of forest area change among the countries and administrative regions in our study area. The role of local agricultural and forest management activities, distance to local and regional centres, relative forested area and configuration of forested patches are discussed as possible driving factors of forested area change.

Forest monitoring using remote sensing time-series: The case of Colombian Andes Protected Areas

Murillo-Sandoval Paulo J.[1,2] *, Hilker Thomas*[1]
[1] *Oregon State University,* [2] *Universidad del Tolima*

Keywords: Protected Area, NDVI, Trends, MODIS, BFAST, Landsat, time-series

Protected Areas (PA's) are an essential tool for conservation of biodiversity and species maintenance. The tropical Andes have been classified as a "hyper" hotspot for endemism and conservation support, and as a result, monitoring their PAs is a vital requirement for conservation biology. One way to evaluate the ecological integrity of PA's is through monitoring vegetation phenology, degradation and disturbances. However, regular field monitoring of remote areas such as the Andes Mountains is often not feasible due limited accessibility and high costs. Remote sensing therefore provides a key tool for assessing landscape changes over time, but prevailing cloud cover and lack of frequent, high-resolution datasets provides significant challenges. Recently, advances in atmospheric correction and cloud screening have opened new opportunities for remote observations of otherwise challenging areas, such as the Andes. The Multi-angle Implementation of Atmospheric Correction algorithm (MAIAC) is a novel cloud screening technique that can help to increases the quantity of available cloud free observations while reducing noise in land surface reflectance at 1km resolution. These observations, while often too coarse to observe small scale disturbances, such as caused by human intervention, may be combined with complementary medium resolution sensors to allow accurate monitoring of landscape degradation and disturbance in space and time. Here, we combine a time-series (2000-2014) of satellite observations derived from MODIS-MAIAC with 30 meter resolution Landsat imagery. Trends in landscape patterns were evaluated using the Breaks For Additive Seasonal and Trend (BFAST) algorithm in order to compare 15-year vegetation trends inside and outside the "Picachos" Protected area of the Colombian Andes. Our results show a progressive upslope logging inside "Picachos". The combination of low and medium resolution sensors processed by BFAST is a useful technique to obtain reliable information about the contribution of short-term and longer-term shifts on Protected Areas and to detect progressive deforestation patterns at fine spatial scale.

Global fire impacts assessment from long term analysis of burned area products

Emilio Chuvieco[1], Lucrecia Pettinari[1], Itziar Alonso-Canas[1], Marc Padilla[2], Kevin Tansey[2], Chao Yue[3,4], Philippe Ciais[4], Angelika Heil[5], Johannes Kaiser[5], Florent Mouillot[6], Jose Miguel Pereira[7], Duarte Oom[7], Aitor Bastarrika[8], Ekhi Roteta[8], Guido van der Werf[9], Thomas Storm[10], Jose Gomez-Dans[11] and Philip Lewis[11]*

[1]Environmental Remote Sensing Research Group, Universidad de Alcalá, Spain. mlucrecia.pettinari@uah.es, itziar.alonsoc@uah.es,
[2]Department of Geography, University of Leicester, Leicester, UK kjt7@leicester.ac.uk mp489@leicester.ac.uk
[3]Laboratoire de Glaciologie et Géophysique de l'Environnement, UJF, CNRS, Saint Martin d'Hères CEDEX, France. chaoyuejoy@gmail.com
[4]Laboratoire des Sciences du Climat et de l'Environnement, LSCE CEA CNRS UVSQ, 91191 Gif- Sur-Yvette, France, philippe.ciais@lsce.ipsl.fr
[5]Max Planck Institute for Chemistry, Mainz, Germany. a.heil@mpic.de, j.kaiser@mpic.de
[6]UMR CEFE 5175, CNRS/Université de Montpellier/Université Paul-Valéry Montpellier/ EPHE/IRD, France. florent.mouillot@cefe.cnrs.fr
[7]Centro de Estudos Florestais, Instituto Superior de Agronomia, Universidade de Lisboa. Lisboa, Portugal. jmocpereira@gmail.com
[8]University of the Basque Country, Vitoria, Spain. aitor.bastarrika@ehu.es; ekhi.roteta@gmail.com
[9]VUA - Stichting VU-VUmc, Netherlands, guido.vander.werf@vu.nl
[10] Brockmann Consult, Germany, thomas.storm@brockmann-consult.de
[11] University College London, United Kingdom, {j.gomez-dans, p.lewis}@ucl.ac.uk
(*) Corresponding author: Emilio Chuvieco, Environmental Remote Sensing Research Unit, Universidad de Alcalá, Telf: 918854438 / Fax: 918854439; e-mail: emilio.chuvieco@uah.es

Abstract

Biomass burnings (including forest, grassland, peatland and agricultural fires) have important impacts on global terrestrial and atmospheric systems, affecting land cover, surface albedo, and the atmospheric concentration of greenhouse gases, chemically reactive species and aerosols. Several products have been generated in the last years to estimate total burned area, but uncertainties remain, particularly those associated to small and low intensity fires. Impact of climate and societal changes modify traditional fire regimes, extending fire seasons, increasing fire severity or introducing fire in sensitive areas.

The Fire_cci project of the European Space Agency Climate Change Initiative aims to generate consistent time series of burned area products to assess the extents of biomass burnings, as well as their spatial and temporal characteristics. Fire impacts on atmospheric and terrestrial processes are assessed, with particular attention to CO_2, CO and CH_4 emissions, modifications of vegetation patterns and biomass availability.

The global burned area products of the Fire_cci program are being developed from MERIS and MODIS sensors (300 m and 250m of spatial resolution respectively), complemented with a small-fire databased generated from medium resolution sensors (Sentinel-2's MSI, 10-20 m of spatial resolution, and Proba-V, 100-300 m resolution) for the African continent. BA algorithms for new Sentinel-3 sensors (OLCI and SLSTR) will also be developed. Validation of the global products is based on a statistical sampling design of Landsat frames. For these sites, fire reference perimeters are generated based on multitemporal analysis of TM/ETM+/OLI images.

The paper will present the current status of the project and will provide analysis of the first global burned area product based on the full-time series of high resolution MERIS sensor data (at 300 m).

Improving forest change detection in the UK using LandTrendr and TimeSync Landsat analysis tools

Jacqueline Rosette[1], Iain Bye[1], Zhiqiang Yang[2,3], Warren Cohen[3], Dirk Pflugmacher[4], Juan Suárez[5] and Helen McKay[5]

[1] Swansea University, Singleton Park, Swansea SA2 8PP, UK
[2] Forest Ecosystems and Society, Oregon State University, Corvallis, OR 97331, USA
[3] US Forest Service, Pacific Northwest Research Station, Corvallis, OR 97331, USA
[4] Humboldt-Universität zu Berlin, 10099 Berlin, Germany
[5] Forest Research, Northern Research Station, Roslin EH25 9SY, UK

Key words: Landsat, disturbance, change detection, forest management, forest condition

This research explores the innovative application of remote sensing to enhance forestry management and monitoring methods in the UK.

In partnership with the US Forest Service and Oregon State University, the project utilises the unique archive of Landsat imagery, and the advanced LandTrendr and TimeSync time series analysis tools, to investigate changes in forest cover, to identify trends of decline and recovery, and attribution of those trends. Results are verified using subcompartment-level management information, records of tree health and action taken, and sequential lidar data showing changes in growth trajectories.

The project focuses on three study areas which have experienced different predominant forms of disturbance and forest cover.

The Loch Lomond and Trossachs National Park in Scotland has suffered a series of severe storms in recent years which have caused widespread loss from windthrow, and subsequent progression of wind damage through adjacent areas.

Japanese larch plantations in South Wales have been affected by Phytophthora ramorum which expanded from southwest England, and which has been contained through severe management intervention.

The Savernake Forest in England has been designated a Site of Special Scientific Interest, and is derived from ancient wood pasture management containing veteran trees. The timber rights of this private forest are leased to the Forestry Commission, meaning that this area contains a combination of managed stands and ancient woodland.

Figure 1 shows an example of management and condition history for a stand in the Cowal and Trossachs Forest District, detected using LandTrendr time series analysis.

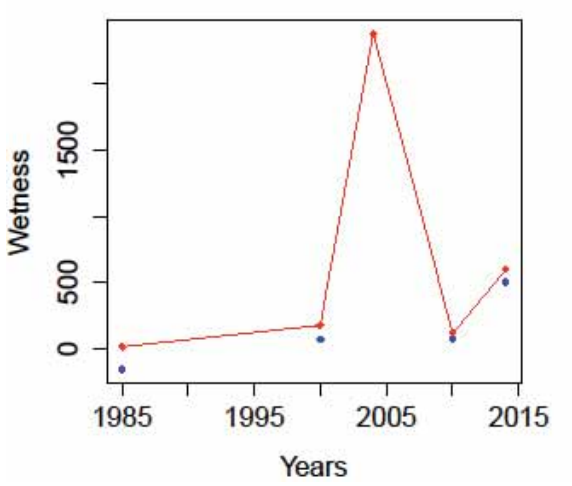

Figure 1. Blue markers represent observed Tasselled Cap Wetness (TCW) values of vertices (identified points of inflection); red points and connecting red lines show fitted trajectories (LandTrendr algorithm). Note that the trend is inverted such that an increase in TCW (y axis values) indicates loss.
Automatic algorithm detection of stability (1985-2000), felling (2003-4), rapid recovery (to 2010) followed by slower decline in condition due to Dothistroma Needle Blight (>2010).

The nature of these sites and their disturbance histories provide the opportunity to investigate the application of time series analysis using the LandTrendr and TimeSync Landsat analysis tools in the UK context, where cloud, seasonality and fragmented forest cover create challenging conditions. The sensitivity of the algorithms to accurately detect forest change of varying intensity and duration (e.g. clear felling or sudden wind loss versus decline and recovery relating to forest condition) is investigated. This is of direct benefit the British Forestry Commission for the accuracy and currency of information regarding the national forest resource.

POSTER

Interpreted high resolution imagery for rapid assessment of land use and land cover changes in the United States - The USDA Forest Service's Image-based Change Estimation (ICE) project

Mark Finco [1], Abigail Schaaf [1], Kevin Megown[2], Paul Patterson[3], Tracey Frescino[3], James Blehm[4]

[1] RedCastle Resources, Inc. under contract to the USDA Forest Service, Salt Lake City, Utah USA
[2] Geospatial Technology and Applications Center, USDA Forest Service, Salt Lake City, Utah USA
[3] Forest Inventory and Analysis, USDA Forest Service, Ogden, Utah USA
[4] Forest Inventory and Analysis, USDA Forest Service, St. Paul, Minnesota USA

Keywords: Change Estimation, Land Cover, Land Use, Interpretation, NAIP

Abstract:

The USDA Forest Service's Forest Inventory and Analysis (FIA) program provides a long-standing, rigorous, field plot-based national forest inventory for the United States. The cycle time for remeasurement of field plots, however, is between 5 and 10 years, and national leadership identified a need for more quickly available land cover and land use change information, even if the level of detail is less than possible with field measurements. The FIA Image-based Change Estimation (ICE) protocols resulted from this need to rapidly create change information.

Fortunately, the United States collects nationwide, high resolution imagery every two to three years through the National Agricultural Imagery Program (NAIP) that is well suited for interpreting broad land cover and land use classes. In collaboration with the Forest Service's Remote Sensing Applications Center (RSAC), FIA developed a two-step interpretation of NAIP over FIA plot locations to quantify the amount and type of land cover and land use changes. The ICE project has been producing data for nearly two years, and this talk will present experiences with the interpretation protocol and preliminary change estimation results.

Landsat reveals the impact of disturbance on carbon storage in the United States National Forest System

Sean Healey[1], Alex Hernandez[2], Chris Garrard[2], James McCarter[3], Crystal Raymond[4]

[1] US Forest Service, [2] Utah State University, [3] North Carolina State University, [4] City of Seattle

Keywords: Landsat, disturbance, carbon

As part of a national strategy to address climate change in the management of US national forests, the US Forest Service has been directed to assess the degree to which disturbances such as fire and harvest have affected the amount of carbon stored in each management unit. Because these assessments are to be used in local forest planning, it is desirable that they be based upon monitoring data that are spatially and temporally specific; model results over hypothetical or generalized landscapes are less useful. The Forest Carbon Management Framework (ForCaMF) was developed to meet this assessment need by combining carbon dynamics built into an empirically calibrated growth model with remotely sensed (Landsat-based) records of historical forest conditions and subsequent disturbance history. Each of these data sources is calibrated by and/or aligned with national forest inventory data. ForCaMF outputs show the degree to which disturbances since 1990 have altered current carbon stocks on each national forest. A novel Monte Carlo error simulation approach integrates uncertainties associated with both model terms and remote sensing inputs to provide confidence boundaries on national forest-level assessments.

ForCaMF results reveal a country facing diverse disturbance threats in different regions. On a per-hectare basis, insects in the Rocky Mountains of Colorado have had the largest local effects on carbon storage, although fires in places as diverse as California, Florida, and Montana have also had a dramatic impact. Root disease is the dominant disturbance process, carbon-wise, in some parts of the Rocky Mountains, while harvest is the most important disturbance factor in many southeastern national forests. ForCaMF allows these impacts to be compared both within and across individual management units. Landsat has unique properties as a monitoring tool that add irreplaceable temporal and spatial context to assessments of forest dynamics. Leveraging this context in highly scrutinized applications such as these carbon assessments will require the kind of uncertainty evaluation and integration with other established monitoring resources that have been built into ForCaMF.

Landsat time series analysis – The impact of forest ecosystem history on biodiversity

Wanda Graf, Paul Magdon, Christoph Kleinn

Keywords: Landsat, times series, forest inventory, forest structure, biodiversity, functional diversity, scales

Forest ecosystems exhibit considerable dynamics which manifest themselves in man-made or natural changes which are either long-term or short term in character (such as windfall or tree felling). The current state of structure, composition and function of a particular forest is the result of its ecosystem, management and conservation history. These dynamics are also mirrored in changes of biodiversity patterns (Pickett & White 1985, Turner 2010).

We investigated the influence of ecosystem history on species richness and functional diversity. Intermediate disturbance regimes are expected to cause highest species richness and functional diversity according to the intermediate disturbance hypothesis (Connell 1978). We hypothesize, significant trends of remote sensing derived vegetation indices point to changes in species diversity and composition as well as functional diversity.

This relationship of ecosystem history and biodiversity is researched within the framework of the "Biodiversity Exploratories" – one of the leading long-term and large-scale projects. The study is carried out at three sites (Schwäbische Alb, Hainich-Dün, Schorfheide-Chorin in Germany) in the temperate mixed forest comprising 150 experimental plots of 100 m by 100 m which feature a land use intensity gradient from conservation to managed forest ecosystems. For all experimental plots data of a full census inventory of woody perennials and herbaceous plants are available among other taxa. Validation is done using an independent forest inventory dataset collection, a systematic grid covering the entire study area.

For exploring the ecosystem history of the experimental plots we used a time series of Landsat 5, 7 and 8 from 1984 to 2016 of over 3000 images. We combined Landsat imageries from the archives of the United States Geological Survey and European Space Agency to gain dense and continuous time series.

We analyze changes in trend (systematic change over time) and disturbance events for the time series of the Normalized Difference Vegetation Index of Landsat surface reflectance imageries for each experimental plot. Surface reflectance of the raw data is calculated with the LEDAPS software (Masek et al. 2013). Among others, we use the Mann-Kendall-Trend test (Mann 1945) for trend analysis and segmentation algorithms to detect disturbance events. First analyses show that disturbance events and trends can be detected in the time series by using these methods. Moreover, long and dense time series as used in this study are required due to the low management intensity and stable nature of these temperate forests. It showed that ecosystem history is related to the observed biodiversity patterns of the experimental plots.

This work helps to better understand the temporal development of forest ecosystem structure, composition and function as well as its impact on species and functional diversity. Thus, this project delivers valuable information for the development of forest management and conservation plans.

References

Connell, H. J., 1978. Diversity in Tropical Rain Forests and Coral Reefs. Science, 199 (1335), 1302-1310.

Mann, H. B., 1945. Nonparametric tests against trend. Econometrica, 13, 245–259.

Masek, J. G., Vermote E.F., Saleous N., Wolfe R., Hall F. G., Huemmrich F., Gao F., Kutler J., Lim, T. K., 2013. LEDAPS Calibration, Reflectance, Atmospheric Correction Preprocessing Code, Version 2. Model product. Available on-line [http://daac.ornl.gov] from Oak Ridge National Laboratory Distributed Active Archive Center,

Oak Ridge, Tennessee, U.S.A. http://dx.doi.org/10.3334/ORNLDAAC/1146

Pickett, S. T. A., White, P. S. (Eds.), 1985. The Ecology of Natural Disturbances and Patch Dynamics. Academic press, New York.

Turner, M. G., 2010. Disturbance and landscape dynamics in a changing world. Ecology, 91, 2833–2849.

POSTER

Monitoring of forests to determine different levels of change

K. Sepp[1], R.G.H. Bunce[1], M. Lang[1], M.Villoslada[1], S. Mucher[2]

[1]Estonian University of Life Sciences, 1 Kreutzwaldi St, 51014 Tartu, Estonia
[2] Alterra, PO Box 47 6700AA Wageningen, The Netherlands

Keywords: Forest habitats, Stratification, LIDAR

Since the first satellite images became available in the 1990's maps of land cover have been produced at varying levels of detail. However, whilst the sophistication of the imagery has increased the problem of detailed evaluation of the map units has remained.
At a strategic level satellite imagery is now routinely used to track changes in tree cover by forest agencies and National parks. There is no doubt that the most recent satellites especially in conjunction with LIDAR, can monitor regeneration, regrowth, encroachment and gap dynamics outside canopies but are unlikely to be able to determine changes in ground vegetation and changes in species. The latter are needed in the assessment of biodiversity and the methodology that will be described in the paper provides a solution to the problem.

The methodology that has been developed over the last 30 years is that of classification, using the multivariate statistical analysis technique ISOCLUSTER on environmental data, mainly climate and topography, usually recorded from one kilometer squares. The squares are classified into relatively homogeneous strata at national or international levels. The strata can then be used to describe the range of variation within the domain and can also be used to select dispersed random samples for in situ surveys of habitats, vegetation and other ecological parameters. The initial surveillance can then be repeated to monitor change. A long term monitoring example is the Countryside Survey of Britain which was originally based on 32 strata which have been increased to 40 so that separate figures can be produced for England, Wales and Scotland. The survey has reported on the changes in all habitats, including forests, as well as species composition at ten year intervals since 1978. For example, between 1990 and 2007 the area of broadleaved woodland increased but the number of species declined by 9.3%. The full results, including the flows between different habitats over time, are given in www.countrysidesurvey.org.uk. The integration between records of forest cover and other habitats enables planners to assess the changes that are taking place in the entire countryside and develop appropriate policies for conservation. Comparable studies have been carried out in Portugal, Sweden and Northern Ireland.

The methodology has also been used to develop an integrated program for monitoring biodiversity in Europe using a classification with 72 environmental strata based on climatic and topographic data. The methodology will be described in the paper and is described in EBONE website (http://www.wageningenur.nl/en/Expertise-Services/Research-Institutes/alterra/Projects/EBONE-2.htm). The framework has also been used to assess the implications of climate change, for example showing that Fagus sylvatica may expand northwards in Sweden under the most likely scenarios.

Recently, a comparable classification has been constructed for Estonia producing eight classes. These have been validated by applying orthogonal regression to the axes of Principal Component Analysis of the satellite land cover map of Europe and DECORANA on species distributions in Estonia. The correlation coefficients were over 0.7 and were very significant. The strata are now being used to survey vegetation and species in Estonian habitats, such as clear fell forests, abandoned fields and patches of invasive species, to provide data for the modelling of potential changes under different climate change scenarios.

Patagonian forests under attack: increasing large-scale insect outbreaks detected from MODIS images

R. O. Chávez[1],, S. A. Estay[2], A. G. Gutiérrez[3], R. Rocco[1]*

[1]Pontificia Universidad Católica de Chile, Instituto de Geografía. Valparaíso, Chile
[2]Universidad Austral de Chile, Instituto de Ciencias Ambientales y Evolutivas. Valdivia, Chile
[3]Universidad de Chile, Departamento de Ciencias Ambientales y Recursos Naturales. Santiago, Chile

Keywords: Patagonian forests, EVI, remote sensing, time series, anomaly

Abstract

Insect outbreaks are considered one of the major disturbances in temperate forests. These natural events have dramatic consequences not only on industry, but also on ecosystem functioning and biodiversity conservation. Worldwide, natural outbreak dynamics have changed in the last decades by global climate change with consequences not fully understood. In this study, we used 16-days MODIS EVI composites to 1) reconstruct the leaf phenology of Chilean Patagonian forests and 2) detect EVI anomalies. Negative EVI anomalies (values below the normal range) are related to green canopy loss caused, among other perturbations, by insect defoliators. We developed a mathematical algorithm (R Script) to calculate the EVI annual phenological cycle and EVI anomalies at the pixel level. By displaying pixel level anomalies, we quantified the intensity, spatial distribution, and temporal spread of insect outbreaks for the whole Aysén Region, Southern Chile (which is about the size of England). The analysis showed that massive outbreaks (> 20,000 hectares) occurred during the growing seasons 2008-2009, 2011-2012, and 2014-2015, showing an increasing trend on the affected area along time. This increasing trend in outbreaks events may lead to extensive carbon loss from one of the largest wilderness forested area in the Southern Hemisphere.

POSTER

Reconstructing forest changes in a fragmented landscape of southwest France from multiple datasources: ecological implications

P.- A. Herrault[1], D. Sheeren[2], M. Fauvel[2], M. Paegelow[3]

[1]*Centre d'études spatiales de labiosphère (CESBIO) UPS/CNRS/IRD/CNES Toulouse, France*
[2]*Université de Toulouse, INP-ENSAT, UMR 1201 DYNAFOR Av. de l'Agrobiopôle, BP 32607, Auzeville Tolosane, 31326 Castanet Tolosan cedex*
[3]Université de Toulouse, UTM, UMR 5602 GEODE 5, al A. Machado, 31058 Toulouse,France

Knowledge about changes in landscape can contribute to better explain the current biodiversity because of a possible time-lag in biological responses. Past disturbances of forests were already shown as a key driver to explain apart of the current species richness of forest insects or plants. Historical maps combined with image time-series data (old aerial photographs and satellite images) are often used to assess the temporal continuity of forests and their spatio-temporal dynamics. However, adequate methods are needed to recostruct automatically past and current states of forests with their trajectory.

In this study, we present a global processing chain to reconstruct forest cover with its changes in a fragmented landscape of south west France. Five spatial data sources from 1850 to 2010 were selected to map the forest evolution: historical maps dating from 1850 and 1900, black and white aerial photographs acquired in 1954 and 1979, and true color orthophotograph of 2010. First, a new registration method based on kernel ridge regression was proposed for georeferencing old maps and managing their geometrical local distortions. Then, animage-processing method was defined to extract and vectorize the forests from the old color map of 1850. The supervised classification approach based on a Gaussian detector relies on a color transformation of the map in the CIELab color space, after a morphological filtering step applied to remove overlapping elements (text, elevations contour lines). An additional GEOBIA method was performed on the orthophotgraph of 2010 to capture the current state of forests. For the others sources, the forests were digitized manually. In a next step, datasets of woodlands produced for the fifth time period were manually matched in order to produce the corresponding relations for estimating changes. Finally, metrics at the object and landscape levels were computed to characterize the spatio-temporal evolutions of the forest cover. This paved the way for measuring effects of history on current species richness of forest hoverflies. Results show high performances for the developed methods and tools. Thiss tudy alsoprovides an interesting methodological framework to drive futur estudies in historical ecology.

Remote sensing of photosynthetic light use efficiency of tropical ecosystems

Celio Helder Resende de Sousa [1] , Thomas Hilker [2] , Yhasmin Mendes de Moura [3]

[1] Forest Ecosystems and Society Peavy Hall 050E Oregon State University, Corvallis, OR 97330
celio.sousa@oregonstate.edu
[2] Forest Ecosystems and Society Peavy Hall 231 Oregon State University, Corvallis, OR 97330
thomas.hilker@oregonstate.edu
[3] Instituto Nacional de Pesquisas Espaciais - INPE Caixa Postal 515 - 12227-010 - São José dos Campos - SP, Brasil
yhas.mendes@gmail.com

Keywords: remote sensing, photosynthesis, photochemical reflectance index, MODIS, MAIAC, Amazon

Abstract

Tropical ecosystems play major roles in the global carbon, water and energy cycles and, as a result, in global climate. The broad goal of this research is to monitor changes in plant physiological parameters, including status of pigments, and water use in connection with drought events in such ecosystems. Specifically, we focus on stress related changes in photosynthetic activity and monitoring of vegetation decline following major stress events by inferring light use efficiency (ε) from measurements of reflectance from the MODIS data using the Photochemical Reflectance Index. To address our objective, we inferred light use efficiency (ε) from measurements of reflectance from the MODIS data from 2000 to 2012. Lower values of PRI were found during the driest months of the year (July, August and September). We also conducted an exploratory analysis to assess the potential climate variables that might drive the changes in photosynthetic activity in the Amazon. We were also able to demonstrate close links between changes in the Photochemical Reflectance Index temperature and precipitation. Our finding show clear seasonality of light use efficiency over tropical forests that are related to dry and wet season cycles and correspond well to flux tower related measurements of photosynthesis. Finally, Multi-angle MODIS observations, while not optimal for measuring short term changes in ε, may provide realistic estimates of photosynthesis over tropical regions.

Satellite-based monitoring of invasive species in Central-Chile

Julian Cabezas[1], Fabian Fassnacht[1], Tobias Schmidt[2], Birgit Kleinschmit[2], Michael Foerster[2]

[1] Institute for Geography and Geoecology, Karlsruhe Institute of Technology (KIT)
[2] Institute for Landscape Architecture and Environmental Planning, Technical University of Berlin

Keywords: Disturbance detection, Nothofagus forest, Landsat, BFAST, Pinus radiate, Ulex Europaeus, Acacia dealbata.

Chile has a large number of endemic species due to its isolated location and is therefore one of the biodiversity hots-spots of the Planet. At the same time a number of invasive species occurred over the last years and have shown to have a notable negative effect on Chilean forest ecosystems. Between 2016 and 2018, the project SaMovar (Satellite-based monitoring of invasive species in central-Chile) will investigate the past and recent spread of selected invasive species.

Most invasive species are ruderal species/strategists and are strongly adapted to certain kinds of disturbances. Therefore, one focus within the project will be the reconstruction of the disturbance history of natural vegetation areas of three administrational regions in central Chile (Maule, Biobio, Isla Chiloe in Los Lagos). The targeted time-period for the analysis will be 1985-2016. Based on time-series analysis using Landsat, MODIS and Copernicus data as well as recent and historic reference information, disturbance occurrences and the type of disturbance will be recorded. The mapping of disturbances will base on the creation of a vegetation mask followed by disturbance mapping based on LandTrendr and BFAST. After the mapping of the disturbances, each disturbed area will be assigned to one of the most common disturbance agents in the study areas. These include forest fires, clear-cutting and biotic agents. Methodically, the assignment to disturbance agents will base on the analysis of the reflectance signal and the shape of the disturbed area. The development of the signal over the first few years after the disturbance will also be considered as additional information.

The disturbance history will subsequently be used as one input layer to species distribution models which will be developed to model the future spread of *Pinus radiata*, *Ulex europaeus* and *Acacia dealbata* assuming different climate scenarios. These three non-native woody species have been observed to have a prominent impact on the natural vegetation of central Chile by invading non-managed areas that often suffered from disturbances briefly before the invasion. Specifically in the Maule Region. Natural Nothofagus forest is being severely invaded by *Pinus Radiata,* especially when the forest fragments are surrounded by pine plantations or when the forests are disturbed, creating opening in the vegetation.
The project thereby methodically targets on 1) the adaptation of the methodical state-of-the-art in remote sensing based mapping of invasive species to the new data delivered by Copernicus and 2) the detection and classification of disturbances as an input to improve the identification and modelling of invasion dynamics. The scientific interest mainly lies in an increased understanding of the invasion dynamics of the three target species in a highly heterogeneous landscape that has undergone drastic land-use changes over the last few decades.
Preliminary results of the project are presented, especially regarding the detections of disturbances (fires, harvesting) in the forest ecosystems of the Maule Region using the BFAST algorithm applied to the available Landsat archive.

Spectral manifestation and signal to noise ratio of forest disturbance and recovery

Zhiqiang Yang, Department of Forest Ecosystem and Society, Oregon State University, Corvallis, OR
Warren Cohen, USDA Forest Service, PNW Research Station, Corvallis, OR
Sean Healey, USDA Forest Service, Rocky Mountain Research Station, Ogden, UT
Noel Gorelick, Google Switzerland GmbH, Zurich CH 8002
Robert Kennedy, College of Earth, Ocean, and Atmospheric Sciences, Oregon State University, Corvallis, OR

Landsat imageries have been widely used in change detection from simple two-date image differencing analysis to complex time series analysis. Understanding how forest disturbance and recovery are manifested spectrally can help making efficient change detection with remote sensing data. In this study, 7200 randomly selected pixel samples in Contiguous United States were interpreted with time series of Landsat images using piecewise linear segmentation and all available aerial photos. For each sample pixels, change processes including harvest, fire, decline, recovery, and stable were recorded. With the identified piecewise linear segments, the noise level for the whole time series for each sample pixels were quantified for all the 6 raw Landsat bands and a series of vegetation indices (Tasseled Cap Brightness, Greenness, Wetness, NBR, NDVI, NDMI) The spectral signals for all identified disturbance were calculated as the segment change in the bands and indices. Both signal and noise varies greatly by bands and spectral indices. Visible bands have lowest level of noise (< 0.01) and also have lowest level signal (<0.03). Shortwave infrared band have relative large noise and signal, resulting in higher signal to noise ratio. In this presentation, we present how signal to noise ratio varies by disturbance types in different spectral bands and indices (2.23 – 16.68). Based on correlations among signal to noise ratio in spectral indices, we present an application of using signal to noise ratio information for forest change detection for Contiguous United States.

Terra-i: A Pantropical Near Real Time Monitoring System for Vegetal Cover Change

1. Louis Reymondin, Terra-i team leader and the system's chief architect, 2. Paula Paz, research assistant, Presenter, 3. Oscar Bautista, research assistant, 4. Jhon Tello, systems analyst

Keywords: Deforestation, near real time monitoring, sensing remote, pan-tropically, neural network.

Abstract

Terra-i is a system for near real time vegetal cover change monitoring using remote sensing and data mining. It aims to detect vegetation loss resulting from human activities at pantropical level and provide up-to-date information about vegetation status with a spatial resolution and frequency, 250 meters and every 16 days, relevant for decision markers. Terra-i is developed by the International Centre for tropical Agriculture CIAT, University of Applied Sciences Western Switzerland HEIG-VD and King´s College London and is currently funded by Global Forest Watch (GFW) and CGIAR consortium. Terra-i data are available free of charge on www.terra-i.org. Data are also available in other platforms as Terra-i is a core partner of Global Forest Watch.

The methodology is based on the premise that natural vegetation follows a predictable pattern of changes in greenness from one date to the next brought about by site-specific characteristics and climatic conditions in the preceding days. We use a Bayesian-probability based neural network to learn how the greenness of a given pixel (MODIS-MOD13Q1) responds to a unit of rainfall (TRMM/GPM), then apply the model to identify anomalies in the time series which can be attributed to human activities.

The tool has been applied as an official early warning system for land cover and land-use change in Peru through the collaborative framework agreement signed between the International Center of Tropical Agriculture (CIAT) and the Peruvian Ministry of Environment (MINAM). Finally, the most outstanding publication based on Terra-i data is a paper published in *Science* in January 2014: Drug Policy as Conservation Policy: Narco-Deforestation. In this paper, a team led by Kendra McSweeney used Terra-i data to show the relationship between drug trafficking and deforestation in eastern Honduras.

The focus of this talk will be on the Terra-i methodology and its potential uses to inform decision making.

About the Author

Paula Paz is a Topographical Engineer from Universidad del Valle, Colombia with understanding and general management of GIS and remote sensing software tools. Paula is currently working as research assistant at CIAT working on the Terra-i project since three years ago. Her main tasks include the downloading, processing and post-processing of data and information for Terra-i to support the monitoring of deforestation in the tropics. Additionally Paula has been involved in projects with the Peruvian government, and has participated of fieldwork to validate of Terra-i data and know the main drivers of deforestation in the Peruvian Amazon.

Time series of Landsat images to determine burned area in the context of the Latin American Network of Forest Fires (RedLatIF).

Jesús A. Anaya[1], Armando M. Rodriguez[2], Walter Sione[3]

[1] Universidad de Medellín. Colombia. Email: janaya@udem.edu.co
[2] Fundación Amigos de la Naturaleza - Universidad Autónoma Gabriel R. Moreno. Bolivia.
[3] Universidad Autónoma de Entre Ríos – Universidad Nacional de Luján. Argentina.

Keywords: Forest fires, time series, Landsat, GEE, burned area.

Abstract

Time series of the Normalized Burn Ratio (NBR) calculated from Landsat data were analyzed at different ecoregions of Colombia and Argentina. The process included removing clouds and cloud shadows from Landsat imagery and masking areas were vegetation was removed without evidence of charcoal. Changes from vegetation to bare soils are usually classified as burned areas and therefore validated as commission errors. Temporal change from prefire to postfire (dNBR) was evaluated using three methods: i) The difference between the prefire and postfire normalized burned radio (dNBR) (Key & Benson 2005); ii) The relative form of dNBR (Miller & Thode 2007), and iii) The dNBR where a composite of the maximum reflectance was used as input for prefire. Each method generated a surface of dNBR and different thresholds were used to classify each dNBR pixel into burned and not burned. Metrics as minimum sum of errors and dice coefficient (Padilla et al. 2014) were considered to define the optimum threshold. The analysis of burned area time series allow identifying the cause of errors and generating prefire statistics. It was found that there is a pattern towards large commission errors when trying to minimize omission and no difference was found from methods i) and ii). Time series are important to replace prefire pixles contaminated by clouds, but other errors arise depending on the metric selected from the time series.

Introduction

Large discrepancies have been found for burned area (BA) estimation using remote sensing images with data sets of medium resolution (500 m – 1 km) as GBA2000, GlobScar, WFA, (Boschetti et al. 2004) or more recently MCD64A1, MCD45A1, GEOLADN-2 (Moreno et al. 2014). Several aspects of remote sensing technology such as spatial and temporal resolution are identified as responsible for inaccuracy (Anaya & Chuvieco Salinero 2012). Indexes derived from spectral bands are commonly used to enhance the detection of BA (Chuvieco et al. 2002; González et al. 2007; Roy et al. 2008). A simple index is the single date of the Normalized Burn Ratio based on NIR and SWIR (Key & Benson 2006) used to determine fire severity. However, the detection improves when the difference between two dates is considered, one date to determine prefire NBR and other date for post fire NBR.

The method to highlight areas affected by fire and the selection of a threshold to classify BA (limit between burned and unburned pixels) is challenging because the large amount of factors affecting prefire and post fire reflectance. Some of these factors are the amount of vegetation, the type of vegetation and the composition and color of soils (e.g. black soils vs. white soils). By the other hand, there are changes not associated to the effect of fire, such as, illuminations and atmospheric differences in the pre and post fire imagery, changes inherent to vegetation phenology and climate conditions. The sum of these factors generates unique per pixel

conditions. The present work aims to decrease the uncertainty generated by changes in reflectance at TOA before and after the fire using NBR and time series of Landsat data.

Methodology

Two values of the NBR were calculated, one for the charcoal signal (postfire) and one for vegetation (prefire). The difference between these NBR values was calculated for every pixel of a Landsat image, for this reason, the result is a surface with dNBR values (difference of the normalized burn ratio index). Reflectance calculated on top of the atmosphere (TOA) was used to calculate NBR; in this phase clouds, shadows and water bodies were removed. Two masks were used to remove the effect of clouds, one for the large reflectance of the aerosol and the other to remove the low reflectivity of their shadow. Clouds were masked with the built-in algorithm of GEE "simple cloud score" and shadows were removed with a threshold for SWIR1. The last pre-processing step was to identify and remove water bodies with the Normalized Difference Water Index (NDWI).

Input data and BA index calculations

Landsat 5 and 8 were used for calculations based on equation 1, 2, 3 and 4.

$$NBR = \frac{(\rho_{NIR} - \rho_{SWIR})}{(\rho_{NIR} + \rho_{SWIR})} \quad \text{eq. 1}$$

dNBR= NBRprefire – NBRpostfire (Miller & Thode 2007) eq. 2

RdNBR= (NBRprefire – NBRpostfire)/NBRprefire eq. 3

$dNBR_{max}$ = NBRprefire(max) – NBRpostfire eq. 4

Where,
SWIR: 2.1-2.3 µm
RdNBR: Relative difference of NBR
NBRprefire(max): maximum NBR from prefire time series

The RdNBR has been considered important when NBR values are low at prefire conditions (eq. 3). For instance, when the amount of vegetation is low, dispersed (with high soil signal) or dry, which is very likely in pastures during the dry season. The maximum value of NBR for prefire conditions (eq. 4) where selected to evaluate the effect of removing clouds using time series. Pixels contaminated with clouds are expected to result in low NBR values. Three dNBR surfaces where generate using equations 2-4. Then each surface was classified into multiple BA maps using thresholds increments of 0.1. When dNBR ≤ 0 it is assumed that the pixel was not affected by fire. Each BA map generated by this semi-automatic method was compared to the reference information to generate accuracy statistics in order to select the best method and optimal threshold.

Results

The extent and size of BA reference information varied notably. The average size of BA polygons for the images of Colombia and Argentina was 4 and 132 ha respectively. With a highly fragmented landscape in Colombia (801 polygons) when compared to Argentina (276 polygons). NBR values behave very similar to NDVI values, with high NBR values at prefire, healthy vegetation, and low values after fire. Figure 1, shows three land cover types of Colombia: grassland, Shrubland (regrowth) and mature amazon forests. The time series show low values of NBR at date 23, when BA reference information was gathered. The NBR values for bare soil and burned areas are very similar in prefire and posfire, for this reason bare soils are likely to be classified as burned areas by the semi automatic method. Other aspect revealed by the time series analysis is the variability of NBR in the Forest class due to phenology and remote sensing artifacts, with a minimum NBR of 0.58 and a maximum of 0.72. This variability is the cause of commission at low threshold values.

The error of commission increases as the BA identification increases. In this regard, it should be noted that the metrics to select the best method should include both, low errors and large BA agreement. Selecting thresholds associated to low sum of errors (commission and omission) heavily influenced by commission will result in extremely low values of BA detection.

No significant differences in accuracy were found when using the relative form of dNBR (equation 3), the best identification of BA with the lowest commission error was found when using equation 4. These preliminary results indicate that time series

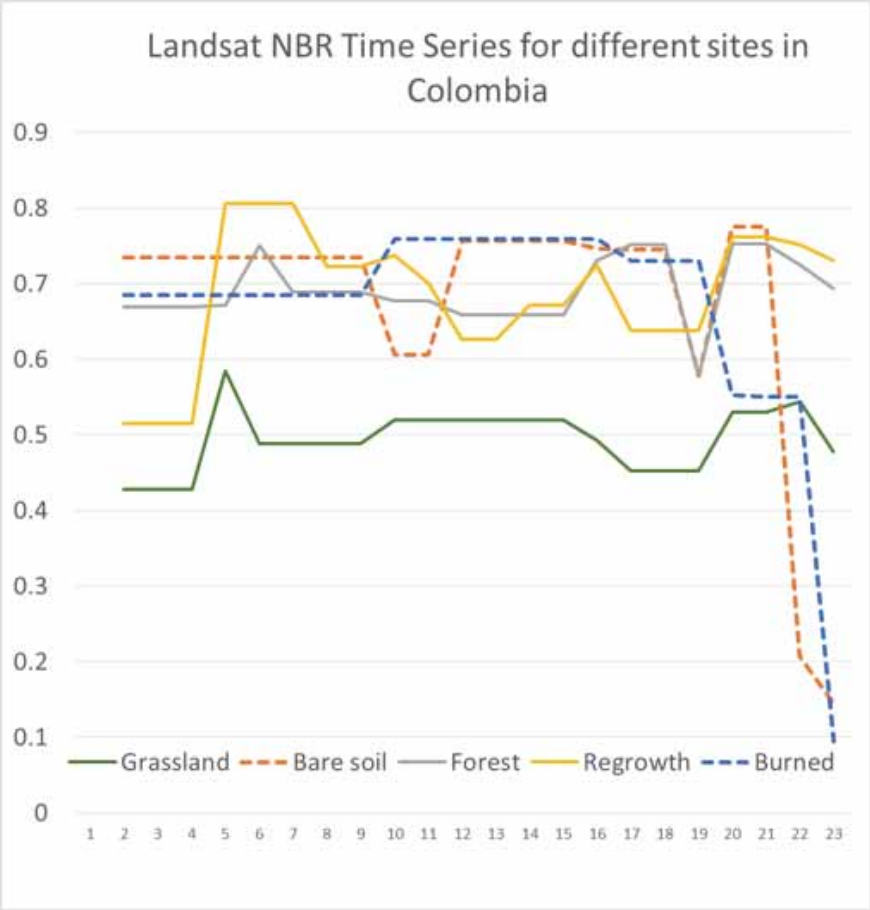

Figure 1. Time series of prefire NBR values and other classes of land cover.

may improve BA classification in areas with heavy cloud content, i.e. when prefire pixels contaminated by clouds are replaced by a time series metric.

Conclusions

The main limitation was the availability of consecutive images with low extent of cloud content. The best burned area map was derived by including soils mask and the maximum composite as input for prefire NBR. This case study has been implemented on the Google Earth Engine platform which allows access to a vast amount of satellite imagery and tools for algorithm development (Patel et al. 2015). This platform was very valuable for the cooperation and interaction among the Latin American Network of Forest Fires (RedLatIF) members.

References

Anaya, J.A., Chuvieco Salinero, E., (2012). Accuracy assessment of burned area products in the Orinoco basin. Photogrammetric Engineering and Remote Sensing 78, 53-60.

Boschetti, L., Eva, H.D., Brivio, P.A., Gregoire, J.M., (2004). Lessons to be learned from the comparison of three satellite-derived biomass burning products. Geophysical research letters 31(L21501), doi:10.1029/2004GL021229.

Chuvieco, E., Martin, M.P., Palacios, A., (2002). Assessment of different spectral indices in the red-near-infrared spectral domain for burned land discrimination. International Journal of Remote Sensing 23, 5103-5110.

González, A.F., S., M.d.M., Cuevas, G.M., (2007). Un nuevo algoritmo para la cartografía de áreas quemadas a partir de información NIR, SWIR y TIR. Revista de Teledetección, 97-105.

Key, C., Benson, N., (2005). Landscape assessment: Ground measure of severity; the Composite Burn Index, and remote sensing of severity, the Normalized Burn Index, in: D. Lutes, R.K., J. Caratti, C. Key, N. Benson, S. Sutherland, L.

Gangi (Ed.), FIREMON: Fire effects monitoring and inventory system. USDA Forest Service, pp. 1-51.

Key, C., Benson, N., (2006). Landscape Assessment (LA) Sampling and Analysis Method, in: Rep., U.F.S.G.T. (Ed.), RMRS-GTR-164-CD, p. 51.

Miller, J.D., Thode, A.E., (2007). Quantifying burn severity in a heterogeneous landscape with a relative version of the delta Normalized Burn Ratio (dNBR). Remote Sensing of Environment 109, 66-80.

Moreno, J.A., Garcia, J.R., del Águila, I., Hernández, P., (2014). Burned Area Mapping in the North American Boreal Forest Using Terra-MODIS LTDR (2001–2011): A Comparison with the MCD45A1, MCD64A1 and BA GEOLAND-2 Products. Remote Sensing 6, 815-840.

Padilla, M., Stehman, S.V., Chuvieco, E., (2014). Validation of the 2008 MODIS-MCD45 global burned area product using stratified random sampling. Remote Sensing of Environment 144, 187-196.

Roy, D.P., Boschetti, L., Justice, C.O., Ju, J., (2008). The collection 5 MODIS burned area product -- Global evaluation by comparison with the MODIS active fire product. Remote Sensing of Environment 112, 3690-3707.

Understanding the large area disturbance history of Australian Sclerophyll forests

Simon Jones [13], Mariela Soto-Berelov [13], Samuel Hislop [13], Trung Nguyen [13], Salahuddin Ahmad [12], Shirley Famelli [1], Andrew Haywood [1234]*

[1] Centre for Remote Sensing, School of Mathematical and Geospatial Sciences, RMIT University, Melbourne, Australia
[2] Department of Environment, Land Water and Planning, East Melbourne, 3002, Victoria, Australia
[3] Coopertive Research Centre for Spatial Information, Carlton, 3053, Victoria, Australia
[4] European Forestry Institute, Kuala Lumpur, Malaysia

Keywords: remote sensing, woody attribution, disturbance history, feature extraction.

Abstract

This paper presents a methodology for attributing and characterising the disturbance history of Sclerophyll forested landscapes over large areas. First we define a set of woody vegetation data primitives (e.g. canopy cover, leaf area index (LAI), bole density, canopy height), which are then scaled-up using multiple remote sensing data sources to characterise woody vegetation features. The advantage of this approach is that vegetation landscape features can be described from composites of these data primitives. The proposed data primitives act as building blocks for the re-creation of past woody characterisation schemes as well as allowing for re-compilation to support present and future policy and management and decision making needs.

A large public land manager –the Victorian Department of Environment, Land Water and Planning set up 786 permanent field plots (VFMP), sampled on a stratified systematic random framework, to measure woody and non-woody forest data primitives. Results are presented of data primitives including: 1) LAI –validated using ground based hemispherical photography, LAI 2200 PCA, CI-110 and terrestrial and airborne laser scanners; 2) canopy height and vertical canopy complexity derived from airborne LiDAR validated using ground plot observations; and, 3) time-series characterisation of disturbance history and associated land cover change using LandTrendr analysis of Landsat LEDAPS data. kNN is then used to link the derived features to the VFMP field plot sites.

Use of New Technologies in Monitoring Mountain Forests' Condition

Radomir Bałazy [1], Mariusz Ciesielski [1], Tomasz Hycza [1], Patryk Waraksa [1]

[1] Forest Research Institute, Braci Lesnej 3 Street, 05-090 Raszyn

Keywords: LiDAR, satellite images, ALS, GIS, mountains, monitoring, remote sensing, deforestation

Mountain ecosystems, though very abundant and diverse, are extremely difficult to monitor. An obstacle during research may not only be large differences in altitudes, but also completely different climatic conditions on various aspects and mountain slopes. It is in such conditions that remote sensing techniques are particularly applicable, which enable fast, precise, though not necessarily cheap, monitoring of the occurring processes.

Upon the request of General Directorate of The State Forests, the greatest monitoring of mountain ecosystems has been carried out in the south of Poland since 2012, which is based, among others, on data obtained from airborne laser scanning (ALS), satellite imaging repeated three times within every growing season (Black Bridge), aerial photographs, and ground measurements including terrain laser scanning (TLS). The application of all those technologies at one place and at a time ensures unparallel possibilities of observing the occurring processes. The project named "Creation of a Forest Information System Covering the Areas of the Sudety and the Western Beskidy Mountains within the Scope of Forest Condition Monitoring and Assessment" is at the same time the greatest GIS project at The State Forests, which has been awarded an ESRI prize in 2014 for exceptional achievements in the scope of GIS.

The purpose of the presented project, apart from the development of a modern GIS system, is mainly monitoring of mountain deforestation process, and an attempt to understand complicated dependencies which influence this process. Several dozen of various analyses have been carried out so far for whole forest stands, as well as for single trees (based on LiDAR data), which have demonstrated many interesting relationships. The presentation will include the results of selected analyses, among others:

- The impact of topography on deforestation process based on the analysis of a detailed terrain model (DTM).
- The dependence of spruce growth (based on ALS measurements of hundreds of thousands of individual trees) on climate conditions, performed treatments and soil in the context of their health condition in the past and today.
- Mechanics of mountains' deforestation processes, their directions, and processes' accompanying dependencies based on ALS data and satellite imaging.
- Relations between selected physical and chemical features of soils and assimilation apparatus based on over 600 circle areas in the context of topography and observed deforestations.

POSTER

Using historical satellite time-series to test an hypothesis of forest susceptibility to the bark beetle outbreak

Martin Hais[1,6], Jan Wild[2,5], Luděk Berec[3], Josef Brůna[2], Robert Kennedy[4], Justin Braaten[4], Kateřina Hellebrandová[6], Zdeněk Brož[1]*

[1] Department of Ecosystem Biology, Faculty of Science, University of South Bohemia, Branišovská 31, 37005 České Budějovice, Czech Republic
[2] Institute of Botany, The Czech Academy of Sciences, CZ-252 43, Průhonice, Czech Republic
[3] Department of Ecology, Institute of Entomology, Biology Centre CAS, Branišovská 31, 37005 České Budějovice, Czech Republic
[4] Department of Forest Ecosystems and Society, Oregon State University, 321 Richardson Hall, Corvallis, OR 97331, United States
[5] Faculty of Environmental Sciences, Czech University of Life Sciences Prague, Kamýcká 129, Praha 6 – Suchdol, CZ-165 21, Czech Republic
[6] Department of Forest Ecology, Forestry and Game Management Research Institute, Strnady 136, 252 02 Jíloviště

Forest disturbances significantly influence the character of forest ecosystems, and many studies have focused on disturbance or post-disturbance processes. However, few studies have investigated whether satellite data can provide insight into precursor conditions for disturbance in forests. Based on experience from the Bavarian Forest and other temperate spruce forests we modelled risk of bark beetle attack based on commonly used environmental predictors together with pre-disturbance spectral trajectories from Landsat Thematic Mapper (TM) imagery. Our study area is located in the central part of the Šumava Mountains, in the border region between the Czech Republic and Germany, Central Europe. The areas of bark beetle attacked forest were delineated from aerial photographs taken in 1991 and every year in the period 1994 -2000. The environmental predictors represent forest stand attributes (e.g. tree density or distance to the attacked forest from previous year) and common abiotic factors like topography-climate variables or geological and pedological background. Pre-disturbance spectral trajectories were defined by the Tasseled Cap linear transformation (Wetness, Brightness) calculated from 16 Landsat TM scenes for the period 1984 – 1999. As pre-disturbance spectral trajectory we consider a slope of linear regression of either Wetness or Brightness index related to years from 1984 until one year before the bark beetle attack. Using logistic regression and multimodel inference, we calculated predictive models separately for any single year in 1994 – 2000 to account for a possible shift in importance of individual predictors during disturbance. Inclusion of pre-disturbance spectral trajectories (Wetness slope and Brightness slope) improved predictive ability of bark beetle attack models. Wetness slope appeared most prominent even in comparison to environmental predictors and relatively stable over the years, while Brightness slope improved the model only in the middle of the disturbance (1996). Moreover, these pre-disturbance predictors were not correlated with other environmental predictors and are therefore able to explain additional data variability. Predictive power of our fitted models expectedly decreased with further in the future, but this trend was slower at the beginning of disturbance. The pre-disturbance spectral trajectories are valuable not only for assessing the risk of bark beetle attack, but also for detection of long-term gradual changes even in non-forest ecosystems.

Validating a Forest Canopy Disturbance Map in North Central USA

Mark D. Nelson (corresponding author)
U.S. Department of Agriculture, Forest Service, Northern Research Station, 1992 Folwell Avenue, St. Paul, MN 55108, USA, phone 651-649-5104, e-mail mdnelson@fs.fed.us

Brian G. Tavernia
The Nature Conservancy, Colorado Field Office, 2424 Spruce Street, Boulder, CO, 80302, USA, phone 720-974 7014, e-mail brian.tavernia@tnc.org

James D. Garner
U.S. Department of Agriculture, Forest Service, Northern Research Station, 1992 Folwell Avenue, St. Paul, MN 55108, USA, phone 651-649-5107, e-mail jamesdgarner@fs.fed.us

Stephen V. Stehman
State University of New York, College of Environmental Science and Forestry, 322 Bray Hall, 1 Forestry Drive, Syracuse, NY, 13210, USA, phone 351-470-6692, e-mail svstehma@syr.edu

Charles H. Perry
U.S. Department of Agriculture, Forest Service, Northern Research Station, 1992 Folwell Avenue, St. Paul, MN 55108, USA, phone 651-649-5191, e-mail charleshperry@fs.fed.us

Keywords: forest canopy disturbance, early successional forest, Landsat Time Series Stack, accuracy assessment

Abstract

The aim of this study was to produce a geospatial dataset of early successional forest (ESF; age 1-20 years) and other land cover classes, and to conduct a comprehensive and robust suite of map validation procedures for estimating accuracy and assessing utility of the dataset. We used summer Landsat time series stacks (LTSS) and a vegetation change tracker algorithm (VCT; Huang et al. 2010) to classify forest canopy disturbance during 1990-2009 in Michigan, Wisconsin, and Minnesota, USA. To reduce commission of ESF we incorporated LTSS of snow covered winter imagery (VCTw; Stueve et al. 2011). Stand age was inferred from year of canopy disturbance and binned into four 5-year age classes that were assigned to forest pixels of the U.S. National Land Cover Database of 2011 (Homer et al. 2015). To reduce omission of ESF, we reclassified a subset of NLCD2011 Shrub/Scrub and Grassland/Herbaceous class to forest where corresponding VCTw pixels were classed as forest (Garner et al. 2016). Land use and stand age data from U.S. Department of Agriculture Forest Service, Forest Inventory and Analysis (FIA) plots (n=27,219) were used to produce estimates of map accuracy and post-stratified estimates of area following "good practices" in Olofsson et al. (2014), which were augmented by additional site- and non-site specific validation assessments. Reported estimates are accompanied by ±95% confidence intervals. Overall accuracy of generalized land cover classes (forest/nonforest/water) increased relative to NLCD2011 from 87.6% (±0.39%) to 89.5% (±0.36%) after reclassifying about 11,000 km2 of NLCD2011 nonforest classes to forest. We estimated 216,563 (±1,532) km2 of forest land area, of which 26,635 (±1,134) km2 was disturbed within the past 20 years. About 12% of total forest area was ESF; 8.5% in Michigan, 10.9% in Wisconsin, and 16.2% in Minnesota. Overall accuracy for seven classes (1-5 year old, 6-10 year old, 11-15 year old, 16-20 year old, persisting forest over 20 years, nonforest, and water), was 84.9% (± 0.42%). Two thirds of the error was attributed to allocation disagreement and one third to quantity disagreement (Pontius and Millones 2011). Producer's accuracies ranged from 15.0% (± 1.89%) for 16-20 year old forest to 91.5% (± 0.45%) for persisting forest class; user's accuracies ranged from 38.8% (± 6.28%) for 1-5 year old forest to 90.4% (± 0.52%) for nonforest class.

Overall accuracy increased insignificantly to 85.6% (± 0.42%) after aggregating the four 5-year age classes into a single 20-year age class. Accuracies for individual 5-year age classes ranged from 15-31% producer's accuracy to 39-45% user's accuracy, changing to 31.0% (± 1.46%) producer's accuracy and 62.4% (± 3.26%) user's accuracy after aggregating the four 5-year age classes into a single 20-year age class. Similarly, accuracies for 5-year age classes improved to 24-36% (producer's accuracy) and 54-68% (user's accuracy) under a fuzzy classification assessment approach whereby neighboring forest age classes in the error matrix were also counted as correctly classified (Gopal and Woodcock 1994). Northwestern subregions had lowest overall accuracies but highest producer's and user's accuracies for ESF age classes. Estimates within equal-area polygons created using a space-filling curve procedure (Lister and Scott 2009) revealed spatial clustering of omission errors. Employing multiple validation assessments across multiple strata improved our understanding of data quality, utility, causes of misclassification, and limitations of validation data.

Water yield dynamics in forested watersheds: Using Landsat annual time series for the assessment of eco services in national forests of the Intermountain West, USA

Alexander J. Hernandez[1], Sean P. Healey[2], R. Douglas Ramsey[1]

[1] Utah State University
[2]United States Forest Service

Keywords: Landsat Time Series; Water Yield, Disturbance; SWAT; Forested Watersheds

Changes in forest structure invariably impact the dynamics of the water balance of a given region. Interception, infiltration, evapotranspiration, and runoff are promptly affected after sudden disturbances (i.e. harvests, fires) that eliminate or reduce canopy cover. Assessment of long-term water effects of disturbance at the catchment level is limited by the lack of continuous, wall-to-wall information about disturbance patterns. Here, we present results of combining highly-detailed disturbance datasets in conjunction with a physically-based hydrologic model to report about water dynamics in forested landscapes. The US National Forest System (NFS) has developed a comprehensive plan for carbon monitoring that requires a detailed temporal mapping of forest disturbances across 75 million hectares. A long-term annual time series that shows the timing, extent, and type of disturbance beginning in 1990 and ending in 2011 has been prepared for the entire NFS using a mix of automated and manual mapping processes. Maps also showed the magnitude of each change event, which was modeled in terms of inter-annual canopy cover loss. This information was used as input to the Soil and Water Assessment Tool SWAT to model water dynamics, with an emphasis in water yield and sediment concentration, and thus gain empirical insight into how disturbance may predispose changes in water at a given outlet in forested watersheds. We developed a hydrologic baseline (business as usual) that included long-term measured climatic variables, topographic relief, soil hydrologic groups, and the National Land Cover Dataset NLCD for the year 1992, 2001, 2006, and 2011. Then, on a yearly basis from 1990, we included our disturbance datasets in the SWAT model to augment the spatiotemporal variability of the land cover input, and modeled streamflow and sediment loads for every year thereafter. This permitted the comparison between undisturbed and disturbed scenarios across the study area. SWAT was calibrated in watersheds where monthly hydrometric records were available. This allowed the estimation of the model efficiency, and thus report on the model uncertainty. The thematic, spatial, and temporal resolution of our disturbance maps allows the estimation of the relative impact of disturbance through time in these watersheds. Our results provide detailed transparent accounts of water yield dynamics, and provide opportunities to assess trends in ungauged watersheds with similar ecological conditions. Water resources are subject to numerous stress agents such as global change, and climatic variability. Our research here quantifies the effects of natural and anthropogenic disturbance on water dynamics that can be used for managers and stakeholders to plan for the future.

ForestSAT 2016

Forested wetland monitoring

OTERRA
CENTRO DE ESTUDIOS DE RECURSOS NATURALES
UNIVERSIDAD MAYOR

UNIVERSIDAD MAYOR
para espíritus emprendedores

Facultad de Ciencias
ESCUELA DE INGENIERÍA FORESTAL

3D mapping of mangrove forests along the Pacific Coasts of Central and South America

Marc Simard[1], Victor H. Rivera-Monroy[2], Edward Castañeda[2], Michael Denbina[1], Hector Tavera Escobar[3], Mireya Cajas Pozo[4], Mariko Burgin[1]

[1]California Institute of Technology-Jet Propulsion Laboratory, Pasadena, California, USA
[2]Louisiana State University, Baton Rouge, Louisiana, USA
[3]Fundación Mar Viva, Bogotà, Colombia
[4]Escuela Superior del Litoral, Guayaquil, Ecuador

Keywords: Mangroves, forests, interferometry, radar, polinsar, height, biomass

Mangrove forests are some of the most productive ecosystems on Earth. In addition to extraordinary carbon sequestration potential, they provide a wealth of socio-economic resources to coastal communities. Thus, it is imperative to generate baseline maps to assess their status and vulnerability to climate change and human activity. We present novel approaches to map mangrove canopy height as well as above ground biomass along the Pacific coasts of central and south America. Mangroves of these regions span a wide variety of structural characteristics and socio-economic contexts, providing a robust assessment of the remote sensing capabilities.

We used several airborne and space-borne instruments. In particular, we use a technique called polinSAR (Polarimetric Interfometric Synthetic Aperture Radar) to map mangrove forests in 3D. In 2013 and 2015, NASA's UAVSAR system, an airborne L-band fully polarimetric radar enabled for repeat-pass interferometry, collected data along the coasts of Costa Rica, Colombia and Ecuador. Using these data, we have developed an adaptive temporal decorrelation algorithm to compensate for changes in environmental moisture and wind conditions between UAVSAR flights. To validate the UAVSAR estimates of canopy height, we also collected coincident in situ data in the Osa Peninsula, the department of Chocó and the Guayas estuary. Furthermore, we used data from Shuttle Radar Topography Mission (SRTM) and the German's TanDEM-X spaceborne instruments to estimate canopy height and cross-validate UAVSAR estimates of canopy height. We obtained height uncertainties in the order of 2m over a 20m pixels. The in situ data was also used to derive canopy height-biomass allometric equations to convert canopy height into above ground biomass maps.

Interestingly, comparison of the new canopy height maps from the UAVSAR and TanDEM-X systems with those derived from the Shuttle Radar Topography (SRTM) acquired in 2000 show strikingly rapid changes in mangrove forest structure. Some forests grew nearly 15 meters in the time interval. We also found the location of the tallest mangrove of the Americas (to be announced during the presentation).

Upcoming spaceborne missions with interferometric capabilities (e.g. NISAR, SAOCOM and BIOMASS) will provide further opportunities to monitor mangrove structure and health. Thus it is crucial to further develop technique adapted to repeat-pass polinSAR and mangrove forests.

Finding the DAM signal: Utilizing time series of all available landsat TM/ETM+ observations to map and monitor beaver-related flooding events

Valerie J. Pasquarella[1,2] and Curtis E. Woodcock[3]
[1] Department of Environmental Conservation, University of Massachusetts Amherst, 160 Holdsworth Way, Amherst, MA 01003; email: valpasq@umass.edu
[2] Northeast Climate Science Center, University of Massachusetts, 233 Morrill Science Center, 611 North Pleasant Street, Amherst, MA 01003
[3] Department of Earth and Environment, Boston University, 675 Commonwealth Ave., Boston, MA 02215

Keywords: Landsat time series, forested wetlands, flood events, disturbance monitoring

Abstract

Multi-temporal imagery from Landsat family of satellites has been widely used to study a variety of change processes common to upland forests, including fire, wind, harvest, and insect damage; however, there have been relatively few studies using Landsat data to specifically map and monitor beaver activity in lowland areas. In this study, time series of all high quality Landsat TM/ETM+ observations from 1985-2014 were used to investigate the spectral-temporal signatures of beaver-related disturbances in Massachusetts, USA. We found evidence of a distinct spectral-temporal flood response consisting of a decrease in mean annual Tasseled Cap Brightness occurring concurrently with a decrease in the seasonal variability of Tasseled Cap Greenness. A targeted change detection algorithm was developed based on this observed response and the algorithm was tested on reference datasets. Results suggest that the timing of detected flood events matches well with records of beaver activity, and the algorithm is flexible enough to identify flood events of different durations and magnitudes. As North American beaver populations continue to expand, dense time series of Landsat observations provide a new source of information for monitoring beaver activity over large spatial extents.

Introduction

North American beaver *(Castor canadensis)* populations, once decimated by overhunting, are returning to the landscapes of the conterminous United States and reclaiming their role as continental-scale agents of change. Like humans, beavers are classic ecosystem engineers, having a disproportionately large impact on their environments and habitats beyond basic needs for food and shelter (Naiman et al. 1988; Rosell et al. 2005). Beaver dams alter the physical and chemical properties of streams, changing currents, temperature, and rates of sedimentation (Butler & Malanson 2005), and this rapid alteration of the abiotic environment often has dramatic impact on riparian and aquatic habitats. Therefore, understanding the spatial and temporal dynamics of beaver activity is important for future management of the beaver population, as well as the management of forest and wetland ecosystems modified by beaver activity.

Multi-temporal imagery from Landsat family of satellites is widely used to study a variety of other land cover change processes common to North American landscapes, including fire, wind, harvest, and insect damage (Cohen & Goward 2004; Wulder et al. 2012). Flooding is often recognized as a driver of vegetation change (Nielsen et al. 2008; Cohen et al. 2016), and previous Landsat-based studies of land cover change have quantified conversions from forest to open water (Drummond and Loveland 2010) and among wetland types (Kayastha et al. 2012; Fickas et al. 2015). However, most previous efforts to quantify beaver activity at landscape scales have relied on expert interpretation of a series of high-resolution aerial photos to identify beaver-related wetland changes, and there have been relatively few studies using Landsat imagery to specifically map

and monitor beaver activity (Finn and Howard 1981; Townsend, Walsh & Butler 1995; Townsend & Butler 1996).

With free and open access to the Landsat archive now provided by the USGS, there has been growing interest in using Landsat time series to analyze ecological processes (Kennedy et al. 2014; Gomez et al. 2016). Given the widespread, potentially continental-scale impacts of growing beaver populations, there is a critical need to acknowledge beavers as an agent of change similar to other widely studied patch-altering disturbances and to investigate how time series of remotely sensed observations, as opposed to individual images, can be used to automate detection of spatial and temporal patterns of beaver activity. In this study, time series of all high quality Landsat observations were used to explore the spectral-temporal signature of beaver activity and develop an algorithm that can be used to map beaver activity over large areas.

Methodology

To investigate spectral-temporal responses to flooding events caused by beaver activity in Massachusetts, we utilized stacks of all available Landsat TM and ETM+ imagery with < 80% cloud cover. Analysis was restricted to images acquired from January 1984 through December 2014 to ensure that full years of data were used in the calculation of annual statistical metrics, resulting in a 30-year time series for each pixel. To facilitate the interpretation of reflectance data, Landsat's six optical bands were transformed into three Tasseled Cap (TC) components—Brightness (TCB), Greenness (TCG) and Wetness (TCW) (Crist 1985).

From a change detection perspective, flooding events associated with beaver activity typically consist oftwo concurrent events—(1) a flood event following initial damming and (2) changes in vegetation cover and condition due to stress and die-off of flood-intolerant plant species. While harvest, fire, or insect infestation may also cause declines in vegetation conditions, these agents of change typically produce a post-disturbance increase in reflectance (Schroeder et al. 2011; Senf et al. 2015), with removal or die-off of vegetation revealing a bright soil background. Flooding, however, would be expected to *decrease* post-disturbance reflectance, as vegetation succumbs to inundated conditions resulting in an open water or "ponded" state. Thus, flooding events should have a spectral-temporal trajectory that is distinct from other types of forest change and wetland conversions. In comparing the TCB, TCG and TCW trajectories of locations impacted by beavers, a decrease in both TCB and TCG was observed in all examples.

Using the observed relationship between TCB and TCG, we developed an algorithm for identifying beaverrelated flooding events using Landsat time series. Mean TCB, maximum TCG, and minimum TCG were computed for each year in the time series using all clear observations for that year. Simple conditional evaluations were then used to determine whether or not a flood event had occurred (or remains in progress) in a given year (Table 1). The first set of conditions identifies abrupt change, as indicated by a large, negative year-to-year change in the mean of TCB, combined with a decrease in the seasonal range of TCG. The second set of conditions identifies long-term (cumulative) changes, as indicated by a large negative decrease in the cumulative annual difference in mean TCB combined with a decrease in the seasonal range of TCG. Ultimately, a flood event is flagged when the annual OR cumulative annual difference in mean TCB from the previous year is greater than a threshold (TCB_{diff} or TCB_{cusum}) AND the annual range of TCG in the current year is less than some percentage of the starting range of TCG (TCG_{stress}). In the most general sense, this algorithm is used to test the hypothesis that there is a detectable, directional relationship between TCB and TCG associated with beaver-related flooding.

Results

The proposed algorithm was tested on several sites with a history of beaver activity, including Mass Audubon's Broadmoor Wildlife Sanctuary, located in Natick, MA. Mapping flood events in the Broadmoor wetlands by year (Figure 1) shows the timing and extent of flooding associated with two beaver dams. In 1990, a large area of change is detected in the wetland upstream of Dam 1. The flooding event caused by Dam 1 persists from 1990 through 1994, with other potential events in 1998, 2005 and 2013. The effects of Dam 2 first appear in 2003, with a flood event persisting through the end of the time series. The timing and location of flooding events is generally in agreement with sanctuary records of

Table 1: General descriptions of key algorithm parameters and specific values used in this study

Threshold	Description	Value
TCB_{diff}	Year-to-year change in mean TCB, captures abrupt flooding	-0.05
TCB_{cusum}	Cumulative sum of the year-to-year change in mean TCB, captures gradual flooding	-0.05
TCG_{stress}	Range of TCG calculated as percent of range in year 1, captures vegetation stress	$TCG_{t=1}$ * (1 - 0.3)

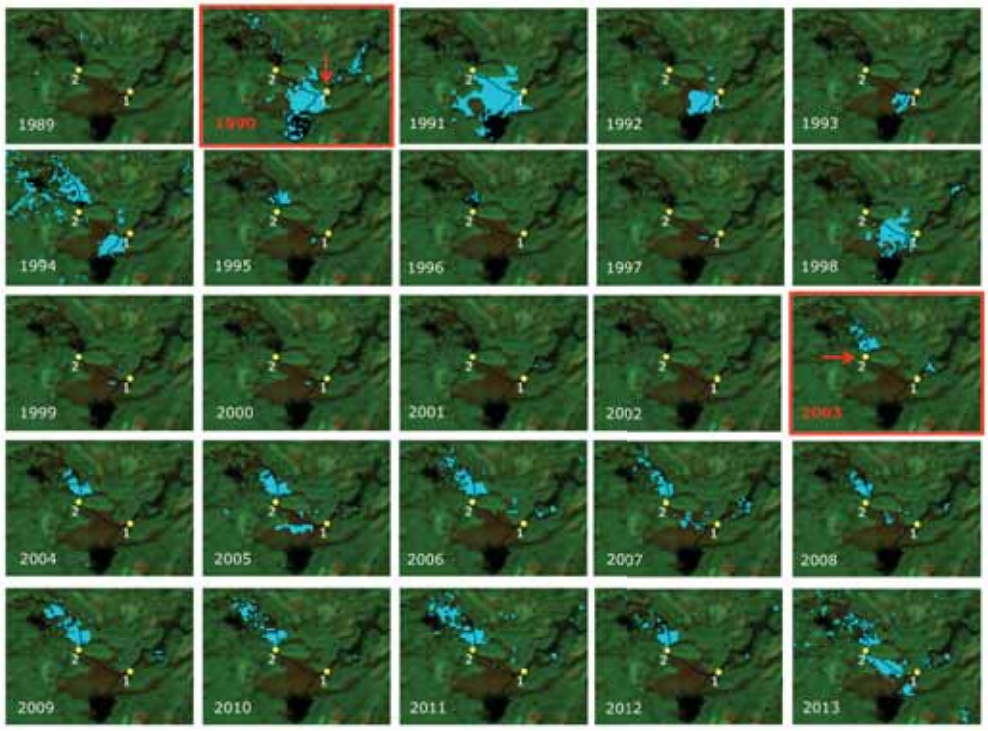

Figure 4: Mapped results for Broadmoor, 1989-2013. Blue areas correspond to flood events detected in a given year.
Known beaver dams are indicated by yellow circles. Landsat base image acquired 11-October 2008.

beaver
activity. The algorithm is able to detect year-to-year variability in the extent of flooded area, and is sensitive to both short-term and longer-term events. Furthermore, flood events are generally concentrated in wetland areas with limited commission in upland areas. These results suggest that flood events do have a distinct spectral-temporal signature and can be mapped and monitored an annual time step using Landsat time series.

Conclusions

This study advances uses of time series of all high quality Landsat observations to identify beaver-related flooding events at an annual time step. We have identified a spectral-temporal relationship that distinguishes flooding from other types of change events. To test this hypothesized spectral-temporal response, we developed an algorithm that can be used to detect timing, persistence and location of flooding events. Unlike more complex segment-based approaches (e.g. Kennedy et al. 2010; Zhu et al. 2014; Czerwinski et al. 2014), we use year-to-year variability in key spectral features to detect change events at an annual time step. Testing indicates that the timing of flood events detected by our algorithm matches well with records of beaver activity, and the algorithm is flexible enough to identify flood events of different durations and magnitudes. Furthermore, algorithm parameters are easily interpretable and tunable, and should be generalizable to other study areas. As the North American beaver population continues to expand, dense time series of Landsat

observations provide a new source of information on the long-term large-scale impacts of these industrious ecosystem engineers.

References

Butler, D. R., & Malanson, G. P. (2005). The geomorphic influences of beaver dams and failures of beaver dams. *Geomorphology,* 71(1-2), 48–60.

Cohen, W. B., & Goward, S. N. (2004). Landsat's Role in Ecological Applications of Remote Sensing. *BioScience,* 54(6), 535.

Cohen, W. B., Yang, Z., Stehman, S. V., Schroeder, T. A., Bell, D. M., Masek, J. G., et al. (2016). Forest disturbance across the conterminous United States from 1985–2012: The emerging dominance of forest decline. *Forest Ecology and Management, 360*(C), 242–252.

Crist, E. P. (1985). A TM tasseled cap equivalent transformation for reflectance factor data. Remote *Sensing of Environment,* 17(3), 301–306.

Czerwinski, C. J., King, D. J., & Mitchell, S. W. (2010). Mapping forest growth and decline in a temperate mixed forest using temporal trend analysis of Landsat imagery, 1987–2010. *Remote Sensing of Environment, 141,* 188–200.

Drummond, M. A., & Loveland, T. R. (2010). Land-use Pressure and a Transition to Forest-cover Loss in the Eastern United States. *BioScience, 60*(4), 286–298. http://doi.org/10.1525/bio.2010.60.4.7

Fickas, K. C., Cohen, W. B., & Yang, Z. (2015). Landsat-based monitoring of annual wetland change in the Willamette Valley of Oregon, USA from 1972 to 2012. *Wetlands Ecology and Management,* 1–21.

Finn, J. T., & Howard, R. (1981). Modeling a beaver population on the Prescott Peninsula, Massachusetts: Feasibility of LANDSAT as an input. NASA. Goddard Space Flight Center Eastern Reg. Remote Sensing Appl. Conf.; p 155-162

Gómez, Cristina, White, J. C., & Wulder, M. A. (2016). Optical remotely sensed time series data for land cover classification: A review. *ISPRS Journal of Photogrammetry and Remote Sensing,* 116(C), 55–72.

Kayastha, N., Thomas, V., Galbraith, J., & Banskota, A. (2012). Monitoring Wetland Change Using Inter-Annual Landsat Time- Series Data. *Wetlands,* 32(6), 1149–1162.

Kennedy, R. E., Yang, Z., & Cohen, W. B. (2010). Detecting trends in forest disturbance and recovery using yearly Landsat time series: 1. LandTrendr--Temporal segmentation algorithms. *Remote Sensing of Environment, 114*(12), 2897–2910.

Kennedy, R. E., et al. (2014). Bringing an ecological view of change to Landsat-based remote sensing. *Frontiers in Ecology and Environment,* 12, 6, 339-346.

Naiman, R. J., Johnston, C. A., & Kelley, J. C. (1988). Alteration of North American streams by beaver. *BioScience,* 753–762.

Nielsen, E. M., Prince, S. D., & Koeln, G. T. (2008). Wetland change mapping for the U.S. mid-Atlantic region using an outlier detection technique. *Remote Sensing of Environment,* 112(11), 4061–4074.

Rosell, F., Bozser, O., Collen, P., & Parker, H. (2005). Ecological impact of beavers Castor fiber and Castor canadensis and their ability to modify ecosystems. *Mammal Review*, 35(3□4), 248-276.

Schroeder, T. A., Wulder, M. A., Healey, S. P., & Moisen, G. G. (2011). Mapping wildfire and clearcut harvest disturbances in boreal forests with Landsat time series data . *Remote Sensing of Environment,* 115(6), 1421–1433.

Senf, C., Pflugmacher, D., Wulder, M. A., & Hostert, P. (2015). Characterizing spectral–temporal patterns of defoliator and bark beetle disturbances using Landsat time series. *Remote Sensing of Environment, 170*(C), 166–177.

Townsend, P. A., Walsh, S. J., & Butler, D. R. (1995). Beaver pond identification through a satellite-based ecological habitat classification. In Proc., *American Society for Photogrammetry and Remote Sensing and the American Congress on Survey and Mapping Annual Meeting, Charlotte, NC* (pp. 102-111).

Townsend, P. A., & Butler, D. R. (1996). Patterns of landscape use by beaver on the lower Roanoke River floodplain, North Carolina. *Physical Geography, 17*(3), 253-269.

Wulder, M. A., Masek, J. G., Cohen, W. B., Loveland, T. R., & Woodcock, C. E. (2012). Opening the archive: How free data has enabled the science and monitoring promise of Landsat. R*emote Sensing of Environment, 122*(C), 2–10.

Zhu, Z., & Woodcock, C. E. (2014). Continuous change detection and classification of land cover using all available Landsat data. *Remote Sensing of Environment, 144*(C), 152–171.

Multi-Scale Remote Sensing of Mangrove Structure and Biomass/Blue Carbon

Emanuelle Feliciano[1, 2], Temilola Fatoyinbo[1], David Lagomasino[1, 3], Seung Kuk Lee[1, 3]

[1]Biospheric Sciences Laboratory, NASA Goddard Space Flight Center, 8800 Greenbelt Road, Greenbelt, MD 20771, United States.
[2]NASA Postdoctoral Program, Universities Space Research Association, 7178 Columbia Gateway Dr., Columbia, MD 21046, USA.
[3]Goddard Earth Sciences, Technology and Research (GESTAR), Universities Space Research Association, 7178 Columbia Gateway Dr., Columbia, MD 21046, USA.

Abstract

Coastal blue carbon ecosystems such as mangroves have the highest total carbon densities of all ecosystems. The high carbon sequestration coupled with the high risk of destruction make mangroves a prime candidate for carbon mitigation initiatives such as the United Nations Collaborative Programme on Reducing Emissions from Deforestation and Degradation in Developing Countries (UN-REDD and REDD+). Our wetland group at NASA is investigating the use of multi-scale remote sensing techniques coupled with ground measurements at various mangrove sites around the world including Africa, Bangladesh and the United States. As part of these projects we have been working with local governments, scientific institutions and international organizations such as the WWF, the UN-REDD programme, USAID, and SilvaCarbon among others. The study areas of our case studies include the mangrove forests of Mozambique in Africa, the Sundarbans in Bangladesh and the Everglades National Park in the United States. To study the structure and health of the mangrove forests we are using remote sensing data from airborne LiDAR (ALS) in conjunction with TanDEM-X (TDX) and WorldView (WV) satellites to estimate canopy height. Our research strategy consists in using ALS to upscale field estimates of biomass to a larger scale and enable validation of TDX and/or stereo WV derived estimates of canopy height and biomass. This enable us to estimate and model above ground biomass (AGB) as it has a proportional relationship with canopy height.

For Mozambique (Zambezi Delta), we are presenting results that include (1) the validation and comparison of independent mangrove canopy height measurements from ALS, TDX and WV, (2) AGB modeling and total AGB estimation using ALS data and field measurements. For the Sundarbans in Bangladesh we show preliminary results of canopy height, AGB and below-ground biomass for the largest continuous mangrove forest in the world. For the Everglades National Park in the United States we present results of canopy height and AGB estimation using a combination of ALS, TDX and mangrove allometry. Furthermore, we present results of AGB estimation using Terrestrial Laser Scanning (TLS) in the Everglades. TLS is a tool that could help us reduce AGB uncertainty in the near future. In addition to the findings of these case studies, we present preliminary results of mangrove growth rates using a combination of Landsat data and canopy height data for test sites in Africa and Bangladesh. The research of our wetland group is of upmost importance if a carbon monitoring system (CMS), such as the proposed NASA CMS needs to be developed in blue carbon ecosystems for monitoring, reporting and verification (MRV) activities.

P-Band DInSAR time series of river bank erosions: Preliminary results and comparisons with field measurements

Karlus A. C. de Macedo[1], Thiago L. M. Barreto[1], Leandro Matos[1], Dieter Lübeck[1], Carlos T. C. Gamba[2]* and, Daniel S.N.A. Albarelli [2], Pedro R. Crisma[2], Adalberto A. Azevedo[2] and João Bosco Jr.[3]**

[1]Bradar Remote Sensing , Brazil
[2]Instituto de Pesquisas Tecnológicas do Estado de São Paulo (IPT), Brazil
[3] Santo Antônio Energia, Brazil
**Corresponding authors: karlus.macedo@bradar.com.br, carlosgamba@ipt.br, joaobosco@santoantonioenergia.com.br*

Keywords: P-band, synthetic aperture radar, SAR, differential interferometry, DInSAR, time series, terrain movement, forest, river banks, erosion processes.

Abstract

P-band differential interferometric (DInSAR) data were acquired from August 2015 until July 2016, along 240km downstream from Santo Antônio Energia dam in Madeira River (Amazon Basin). The objective is to measure and monitor erosions along the river banks, especially in forested areas, with DInSAR. We present the processing methodology and time series analysis applied to this data set. Preliminary field and radar measurements are compared in order to evaluate and validate the proposed methodology.

Introduction

Differential synthetic aperture radar interferometry (DInSAR) and further time series analysis are established techniques and they have been applied successfully to spaceborne remote sensing. Recently, it has been demonstrated that airborne DInSAR at L- or P-bands are able to deliver coherent dense-grid of high-resolution measurements over vegetated terrain along time, overcoming the limitations of spaceborne DInSAR [de Macedo et al., 2012 ; Jones et al, 2012]. Nowadays, further airborne DInSAR investigations and developments are being carried on at L or P-band. This is because, the centimeter accuracy and long-term coherence, which are achieved when using these bands, are very appropriate to measure processes such as erosion, sedimentation occurring in forested areas [de Macedo and Wimmer, 2015] and landslides [Delbridge, 2015]. This work investigates how terrain movements associated with erosions along vegetated river banks can be measured, identified and monitored by P-band DInSAR.

Methodology

A sequence of 11 airborne SAR high-resolution images at P-band were acquired from August 2015 until July 2016, along 240km downstream from Santo Antônio Energia dam in Madeira River (Amazon Basin). The P-band data were acquired and were processed with the OrbiSAR airborne system, of Bradar, Brazil. Details on the airborne DInSAR requirements and processing can be found in de Macedo et al. [2012].

We conducted the field campaigns to measure the terrain movements synchronized with the week of the very first flight in order to guarantee the same reference readings (to) for both field and SAR measurements. Further readings occurred synchronized with the week of the second, fourth, seventh, ninth and eleventh acquisition flights. The timeseries analysis applied to our interferometric data set is based on the work published in de Macedo et al. [2015]. The preliminary time series of the accumulated terrain movements here presented are obtained via the direct-integration.

Results

Fig. 1 shows the DInSAR mosaic of the whole surveyed region in order to understand the magnitude, location and area extesion of the terrain movements seen by the radar. A ROI (region o interest) of the surveyed area was selected. Fig. 2 shows the field and DInSAR time series of the ROI, overlaid with the X-band SAR amplitude and contour lines from the X-band elevation model, obtained from the same airborne sensor.

Both SAR and field measurements show that the terrain is moving downwards. Fig. 2(j,l) show photos, where a process of piping can be clearly identified. Fig. 3 shows a preliminary statistical analysis over 95 field stakes. The scatterer plot shows that the correlation factor between the DInSAR and field measurements is 0.28. Although weak, we can conclude that there are correlation between the radar and field measurements.

Reasons for the weak correlation are: (1) The field measurements are pointwise, while the radar measures the average movements within a resolution cell of 17mx17m. (2) In field, we measure the vertical movements and the planimetric movements relative to the river banks, which is mostly oriented to the East-West plane. While the radar, measures only in the LOS (line-of-sight) direction, and are affected by both horizontal and vertical movements within the North-South Plane. Therefore, only the vertical movements are sensed by both the radar and field measurements. (3) The assumed reference stable stake for the field measurements, some times, are located within the area of movement, as revealed by the DInSAR images in Fig. 2. In such cases, the field measurements are possibly underestimating the movements. (4) Its is important also to note the external sources of interference in the radar measurements, like soil moisture. Its is not fully understood up to now, the degree of contribution of soil moisture in the DInSAR measurements [Zwieback et al. 2015].

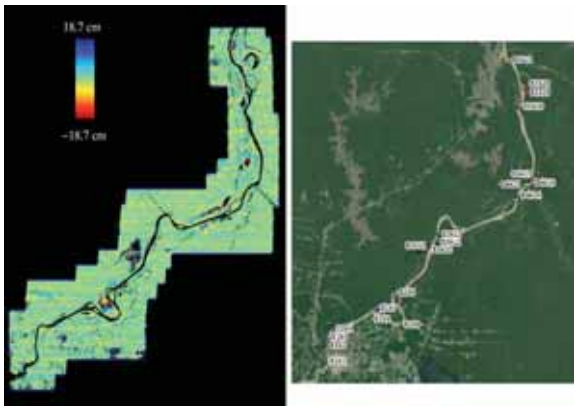

Fig. 1: DInSAR Mosaic (left) and corresponding Google Earth® Imagery (right)

Conclusions

The preliminary conclusion is that the P-band DInSAR is sensible and precise enough to detect and track the terrain movements along river banks, such the ones caused by erosion processes. This unique data set comparison between DInSAR and field data allowed us to gain knowledge about the accuracy and sources of interference for movements sensed at P-band in dense forested areas. Further improvements in the processing chain, such as the generation of the redundant network of interferograms, are being implemented.

References

de Macedo K.A.C., Wimmer C., Barreto, T. L., Lubeck D., Moreira, J. R., Rabaco L.L.M., Oliveira W.J. (2012). Long-term airborne DInSAR measurements at X-and P-Bands: A case study on the application of surveying geohazard threats to pipelines. IEEE Journal of Selected Topics in Applied Earth Observations and Remote Sensing, 5(3), 990-1005.

de Macedo K.A.C., Wimmer C. (2015, July). Time series of airborne DInSAR data over the Amazon flooded vegetation: Water level changes. In 2015 IEEE International Geoscience and Remote Sensing Symposium (IGARSS) (pp. 5252-5255). IEEE.

Delbridge B., Bürgmann R., Fielding E., Hensley S., (2015, July). Kinematics of the slumgullion landslide from UAVSAR derived interferograms. In 2015 IEEE International Geoscience and Remote Sensing Symposium (IGARSS) (pp. 3842-3845). IEEE.

Jones. C.E, Bawden G., Deverel S., Dudas J., Hensley S.,. Yun S. H. (2012, November). Study of movement and seepage along levees using DINSAR and the airborne UAVSAR instrument. In SPIE Remote Sensing (pp. 85360E-85360E). International Society for Optics and Photonics.

Zwieback, S., Hensley, S., Hajnsek, I. (2015). Assessment of soil moisture effects on L-band radar interferometry. Remote Sensing of Environment, 164, 77-89.

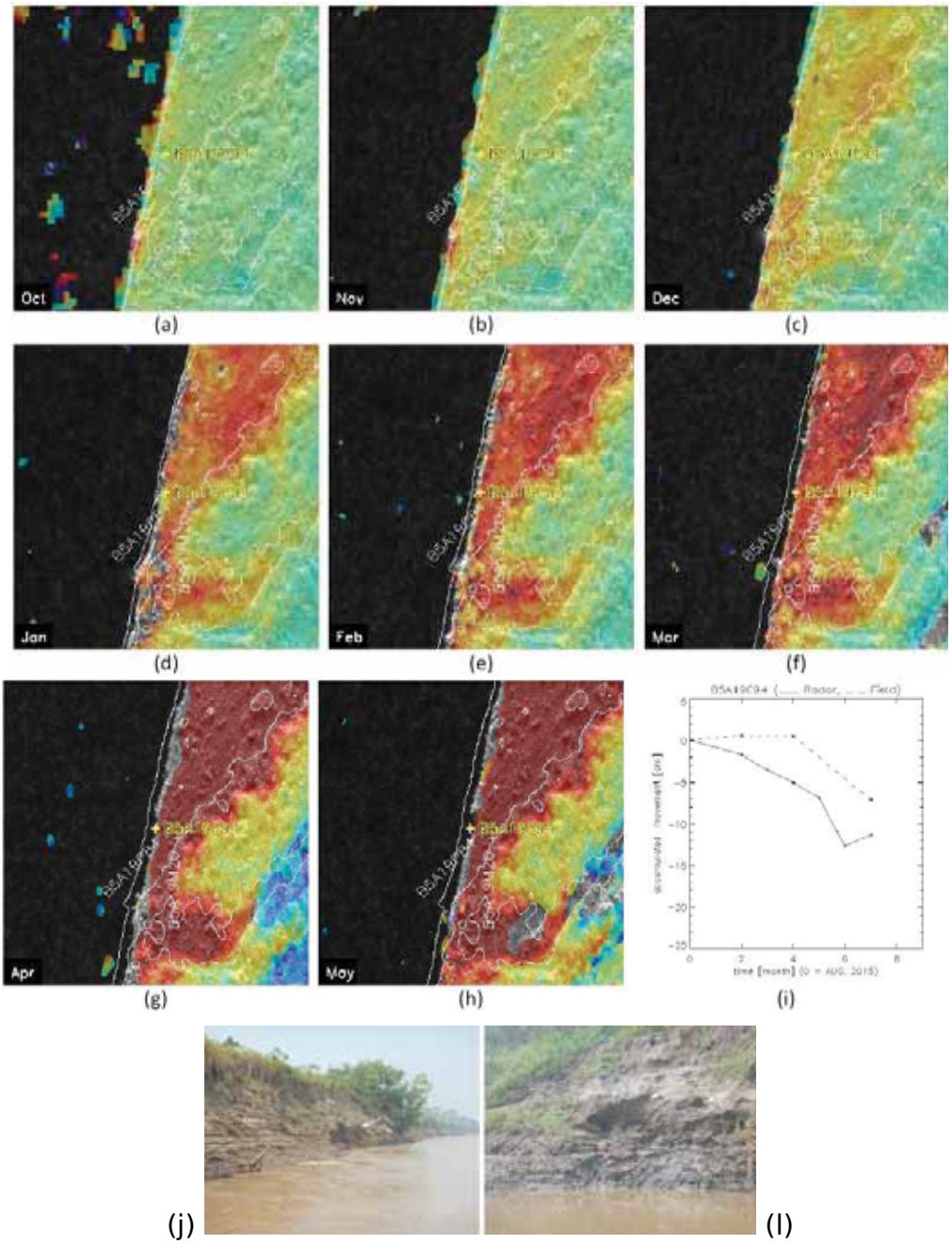

Fig. 2: DInSAR and field time series and photo of the geodynamic process.

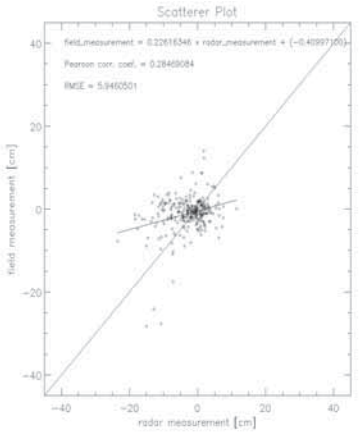

Fig. 3: Preliminary radar vs. field measurement comparisons

Poster Presentation, ForestSat 2016, Santiago, Chile.

Statistical correction of Lidar-Derived digital elevation models with multispectral airborne imagery

Kevin J. Buffington, Oregon State University and US Geological Survey
Bruce D. Dugger, Oregon State University
Karen M. Thorne, US Geological Survey
John Y. Takekawa, Audubon California

Vertically accurate digital elevation models (DEMs) are necessary for studying low-slope ecosystems and hydrology. The biogeomorphology of coastal wetlands are largely controlled by tidal inundation; as sea levels rise, accurate wetland DEMs are critical for modeling into the future. Airborne light detection and ranging (lidar) is a valuable tool for collecting vast amounts of elevation data across large areas; however, the limited ability to penetrate dense vegetation with lidar increases the vertical uncertainty. Methods to correct lidar-derived elevation data exist, but a reliable method that requires limited field work and maintains spatial resolution is lacking. We present a novel method, the Lidar Elevation Adjustment with NDVI (LEAN), to statistically correct lidar digital elevation models (DEMs) with vegetation indices (NDVI) from multispectral airborne imagery (NAIP) and survey-grade GPS measurements. Across 17 tidal marshes along the Pacific coast of the U.S., we achieved an average root mean squared error of 0.072 m, with a 40-75% improvement in accuracy from the lidar bare earth DEM. Results from our method compared favorably with results from three other methods (minimum-bin gridding, mean error correction, and vegetation correction factors), and a power analysis applied to our extensive GPS dataset (>17,000 ground points) showed that on average 118 points were needed to calibrate a site-specific correction model for tidal marshes along the Pacific coast. By using readily available imagery and field surveys, we found that lidar-derived DEMs can be adjusted for greater vertical accuracy while maintaining high (1 m) horizontal resolution. While developed in tidal marshes, the LEAN model approach could be applied to any ecosystem where vertical accuracy of DEMs is important and survey-grade GPS measurements can be collected.

ForestSAT 2016

Forestry & Forest Management

OTERRA
CENTRO DE ESTUDIOS DE RECURSOS NATURALES
UNIVERSIDAD MAYOR

UNIVERSIDAD MAYOR
para espíritus emprendedores

Facultad de Ciencias
ESCUELA DE INGENIERÍA FORESTAL

Analysing the relations between landscape structural changes and hydrological response at subcatchment scale in temperate forest basins: the case of Maule's inner dryland

Benjamín Sotomayor[*1,2], *Mauricio Galleguillos*[1,2], *Christian Little*[3], *Antonio Lara*[2,4]

[1] *Laboratoy of Ecology of Ecosystems, School of Agronomical Sciences, University of Chile*
[2] *Center for Climate and Resilience Research (CR)2, Santiago, Chile.*
[3] *Instituto Forestal, Valdivia, Chile.*
[4] *Instituto de Conservación, Biodiversidad y Territorio, Universidad Austral de Chile, Valdivia, Chile*
**Corresponding author: benjasotomayor@ug.uchile.cl -- Santa Rosa Avenue #11315, La Pintana, Santiago, Chile.*

Keywords: Landscape composition, configuration, change, hydrologic response, land cover, correlation.

Abstract

We generated 8 land cover maps for the 2000-2014 period in Cauquenes and Purapel catchments, located in Maule region's inner dryland, Central Chile, to test for relations between landscape structural and configurational changes and runoff coefficients at annual and seasonal scale at subcatchment level. Overall accuracies ranged from 85% to 100%. A Spearman's Correlation Matrix revealed several positive and negative statistically significant correlations between landscape configuration and structure metrics, suggesting that the landscape's configurational and structural dynamic driven by anthropic forestry management could have an impact in hydrological response at short term.

Introduction

South-central Chile inner dryland and coastal range is a landscape composed of a matrix of extensive industrial pine and eucalyptus plantations, degraded shrubland and growingly fragmented native forests patches, where industrial forestry has expanded rapidly and intensively since mid-1970's (Echeverria et al., 2006). Today, this activity is the main driver that triggers the landscape's inner spatial dynamic, driven by the short rotation period applied to industrial plantations (10 to 20 years) (Armesto et al., 2007). Several studies conducted in Chile and elsewere have shown the effects that fast-growing species plantations have on hydrological response by analysing landscape composition, defined as the total surface per land cover class, changes in the long term (Leblanc et al. 2008, Little et al. 2009). However, until now it's unclear whether landscape configuration dynamics, understood as the landscape patches arrangement and position changes over time, in short term could have any significant effect over hydrological response at subcatchment scale. The main objective of this investigation is to test for relations between landscape structural changes and the hydrological response at two forested catchments in coastal Maule region, Chile, between 2000 and 2014.

Methods

The study area is located in the inner dryland of the Maule Region and comprises the Purapel (270 km^2) and Cauquenes (619 km2) subcatchments, both characterized by a pluvial hydrologic regime and Mediterranean climate. Natural vegetation consists of a mixture of deciduous *Nothofagus* forest

and thorny schlerophyllous shrubs (Luebert and Pliscoff, 2006), but in present days, the landscapes is dominated by a matrix of fast-growing *Pinus radiata* and *Eucalyptus spp.* plantations and isolated fragment of native forests in remote places and heavily degraded anthropogenic savannas in the lower reaches (Echeverria et al. 2006, Van de Wouw et al. 2011). Landscape composition for 2000-01, 2001-02, 2004-05, 2005-06, 2006-07, 2008-09, 2010-11 and 2013-14 summer seasons was represented using Landsat-derived land cover maps using the Maximum Likelihood Classifier (MLC), including a 1985-86 map as a reference situation. Six land cover classes were established based on previous field data: Agricultural-Meadows (A), Bare Soil (BS), Industrial Plantations (P), Native Forest (NF), Shrubland (SH) and Impervious land (I). 20 training zones per class were defined per class through Google Earth images interpretation and previous field reference data. We used Landsat VNIR+SWIR bands from the Landsat Climate Data Record (CDR) plus 3 vegetation indices (Summer NDVI, GNDVI and $\Delta NDVI_{winter\text{-}summer}$) to enhance spectral separability among classes, and topographic correction was applied with the C-Correction method as proposed by Hantson and Chuvieco (2011). Accuracy assessment was conducted with a Confusion Matrix using 10 validation zones per land cover class for each date and study site. Landscape configuration was represented through the land cover's general position in the landscape using a Topographic Position Index-based landscape landform classification (Weiss, 2001) derived from an SRTM 1-arcecond DEM. Hydrological response was represented with the Runoff Coefficient (RC), calculated as the ratio between accumulated rainfall and runoff at annual and seasonal (four-month) scale. Finally, the existence of relationships between runoff coefficients and landscape configuration features was addressed using Spearman's Correlation Matrix with a significance level of 0.05.

Results and Discussion

Overall accuracies of the land cover maps ranged from 85% to 100%, indicating a strong agreement with the reference data. An intense land use/land cover change process was observed in the 1985-2000 period in both catchments. In 1985-86, the landscape composition was dominated by a matrix of degraded Shrubland and Bare Soil in both catchments, but by 2000-01, it had changed significantly due to the explosive expansion of Industrial Plantations, which increased by 461% in Cauquenes and 680% in Purapel (figure 1). On the other hand, Native Forest shrunk by 43% in Cauquenes and 53% in Purapel at an annual

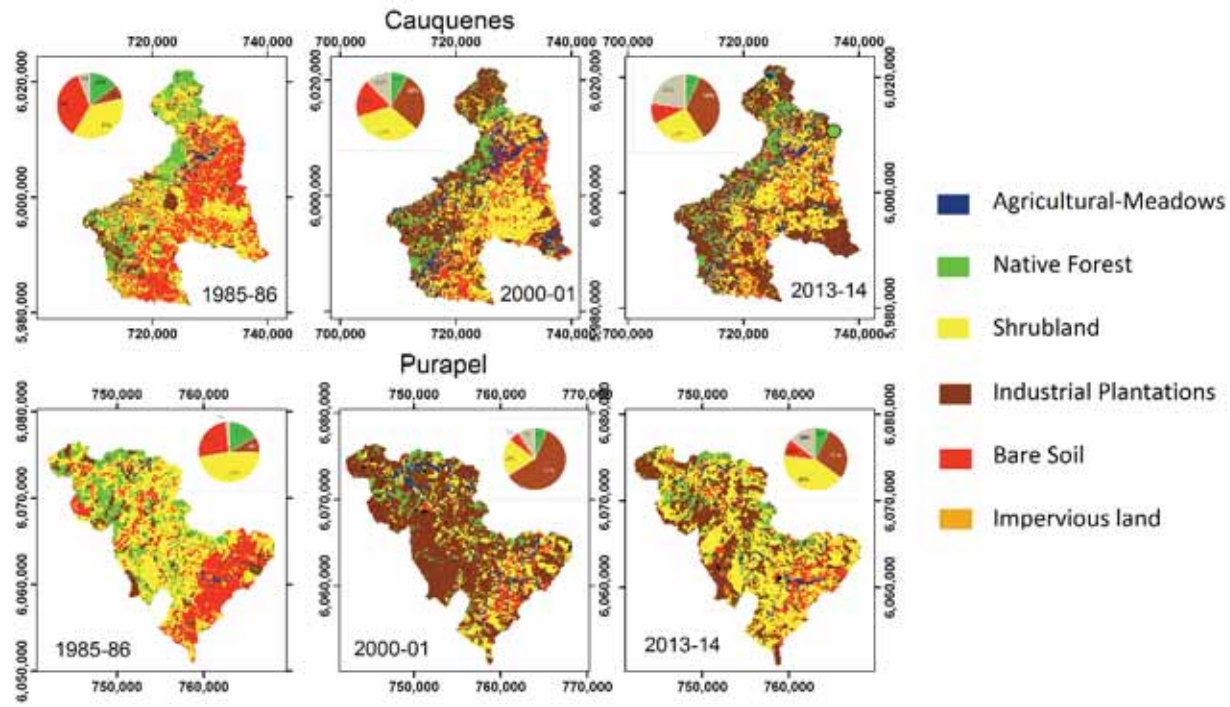

Fig.1: Land cover maps between 1985-2000-2015 in Cauquenes and Purapel catchments

rate of -3.63% and -6.29%, respectively. In the 2000-2014 period, the intensity of this process decreased, being the dominant matrix a mixture of Industrial Plantations and Shrubland (figure 1). In fact, no significant trend in total surface was observed in any land cover in both catchment in this period (figure 2), indicating that the landscape has stabilized in a functioning state defined as Dynamic Equifinallity by Patterson y Hoalst-Pullen (2011). An exception was found in the case of Industrial Plantations in Purapel, where a significant decrease in surface was observed in this period due to extensive harvest operations. Nevertheless, this specific land use has a strong spatial persistence (Miranda et al. 2015) so it is expected to increase in surface as trees grow older and can be precisely classified by remote sensing methods.

A negative and significant correlation was observed between the surface of Industrial Plantations at Hillsides and the annual and autumn runoff coefficient in Cauquenes (figure 3). CONAF (2011) indicated that the majority of newly stablished industrial plantations in the study area between 1999 and 2008 were set in shrublands and abandoned cropland, and in that sense, Farley et al. (2005) and Huber et al. (2008), analysing the effects of replacing shrubs and prairies with *Pinus* radiata over hydrological cycle, reported a decrease runoff generation mainly due to increase in interception, percolation and evapotranspiration at local scale. The correlation obeys to stochastic behaviour of plantations due to the lack of integrated management at catchment level, as can be seen by analysing the temporal distribution of data in the correlation (figure 3). This wasn't observed in Purapel because of the significant reduction in this land cover's surface due to extensive harvests operations (figure 2).

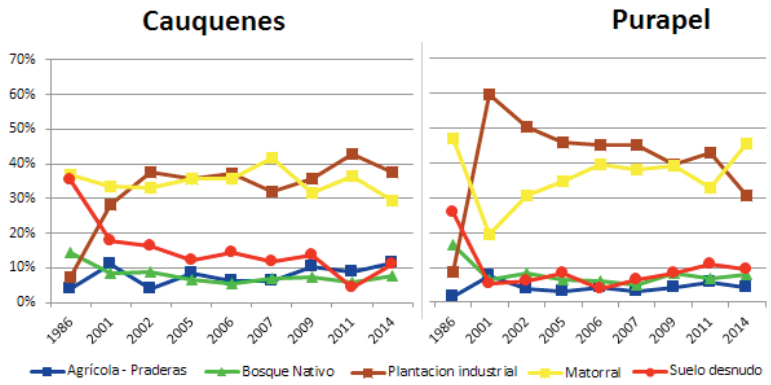

Fig. 2: Composition trend per land cover class in 2000-2014 period in Cauquenes and Purapel catchments.

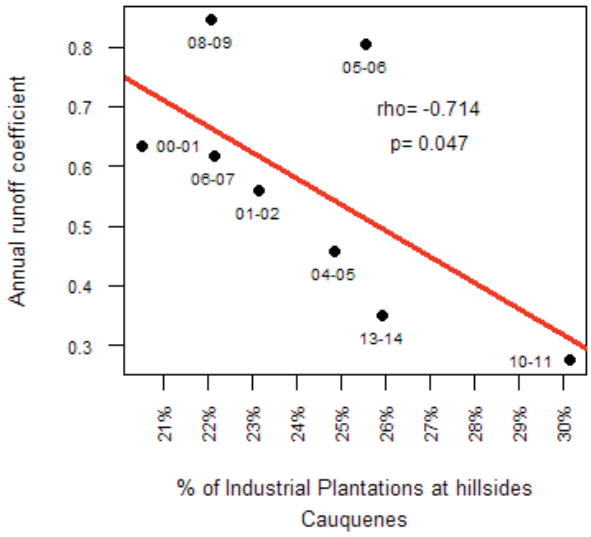

Fig. 3: Statiscally significant correlations between landscape structural features and runoff coefficients in Cauquenes and Purapel between 2000-2014.

Conclusion

Statistically significant correlations were detected at annual and seasonal scale in Cauquenes subcatchment and suggest that the landscape's inner configurational dynamic triggered by the extensive and intensive forestry use could affect hydrological response in the short term in the context of highly anthropized landscapes. The investigation only shows preliminary exploratory results, hence more effort should be done to improve our knowledge about the effect of landscape configuration in hydrology in order to provide a sustainable use of the territories by integrating this effect in the management at catchment level.

References

Armesto, J; Arroyo, M; Hinojosa, L. 2007. The Mediterranean environment of central Chile. The physical geography of South America 2007: 184-199.

Aronson, J; del Pozo, A; Ovalle, C; Avendaño, J; Lavin, A; Etienne, M. 1998. Land use changes and conflicts in central Chile. Landscape disturbance and biodiversity in Mediterranean-type ecosystems 1998: 155-168.

Echeverria, C; Coomes, D; Salas, J; Rey-Benayas, JM; Lara, A; Newton, A. 2006. Rapid deforestation and fragmentation of Chilean Temperate Forests. Biological Conservation 130(4): 481-494.

Farley, KA; Jobbágy, EG; Jackson, RB. 2005. Effects of afforestation on water yield: A global synthesis with implications for policy. Global Change Biology 11(10): 1565-1576.

Hantson, S; Chuvieco, E. 2011. Evaluation of different topographic correction methods for landsat imagery. International Journal of Applied Earth Observation and Geoinformation 13(5): 691-700.

Huber, A; Iroumé, A; Bathurst, J. 2008. Effect of Pinus radiata plantations on water balance in Chile. Hydrological Processes 22(May 2007): 142-148.

Leblanc, MJ; Favreau, G; Massuel, S; Tweed, SO; Loireau, M; Cappelaere, B. 2008. Land clearance and hydrological change in the Sahel: SW Niger. Global and Planetary Change 61(3-4): 135-150.

Little, C; Lara, A; McPhee, J; Urrutia, R. 2009. Revealing the impact of forest exotic plantations on water yield in large scale watersheds in South-Central Chile. Journal of Hydrology 374(1-2): 162-170.

Miranda, A; Altamirano, A; Cayuela, L; Pincheira, F; Lara, A. 2015. Different times, same story: Native forest loss and landscape homogenization in three physiographical areas of south-central of Chile. Applied Geography 60: 20-28.

Patterson, M; Hoalst-Pullen, N. 2011. Dynamic equifinality : The case of south-central Chile's evolving forest landscape. Applied Geography 31(2): 641-649.

Weiss, a. 2001. Topographic position and landforms analysis. Poster presentation, ESRI User Conference, San Diego, CA 64: 227-245.

Van de Wouw, P; Echeverría, C; Rey-Benayas, JM; Holmgren, M. 2011. Persistent acacia savannas replace Mediterranean sclerophyllous forests in South America. Forest Ecology and Management 262(6): 1100-1108.

POSTER

Large area tree species mapping in mixed temperate forests from multi-temporal RapidEye satellite images and LiDAR data.

Paul Magdon[1], Collins Kukunda[1], Hans Fuchs[1] and Christoph Kleinn[1]
[1] Chair of Forest Inventory and Remote Sensing, Georg-August University of Göttingen

Keywords: Forest management, multi-temporal, RapidEye, RandomForest

The importance of forests particularly in densely populated areas of Central Europe has clearly shifted from a pure source of timber, wood and other tangible products towards a source of multiple ecosystem services including water protection, carbon sequestration, biodiversity preservation, recreational functions, and also production of wood. Close-to-nature forest management and conservation practices have been developed and adopted to manage forest lands sustainably so that the long-term provision of this suite of environmental, ecological and economic services is secured, simultaneously on the same piece of land. Current forest management emphasizes specific silvicultural practices that include natural regeneration, selective logging, dead wood management, habitat tree conservation and economic target tree identification. Consequently, forest structure in many regions has changed away from the traditional age-class forests towards highly complex – closer to nature – forest stands with trees of different species, ages/development stages and dimensions. In order to implement these management and conservation practices, as well as to effectively monitor their impact on the ecosystem services, high quality inventory data is essential. Stand inventory approaches were so far based on compartments as the basic spatial management units, for which a homogenous forest structure was assumed. However, with increasing complexity and with more diverse silvicultural practices that focus on individual trees instead of entire compartments, new challenges arise for forest monitoring. Remote sensing techniques can operationally support the development of forest management and conservation plans when the demanded target variables can be observed or modelled with sufficient accuracy. Tree species composition and spatial distribution is among the fundamental input information for forest management and conservation planning and decisions in these close-to-nature forest types.

In this study we research into the potential of combining multi-temporal RapidEye satellite images and LiDAR canopy height models (CHM) to create maps of the main European tree species. We analyze the seasonal changes in the spectral signatures of the species in order to i) identify seasonal characteristics that can be utilized to differentiate between the species, ii) to identify the seasons /dates which are most important for the discrimination and iii) to evaluate the minimum number of acquisition required per vegetation period.

This work is part of the DFG funded "Biodiversity Exploratories" Priority Program, a large collaborative research project that covers different forest types across three regions (each ~1000km²) in Germany. We base our analysis on 78 RapidEye L1B satellite images collected between 2014 and 2015, which were orthorectified with a high quality local elevation model and a systematic set of field survey GCPs resulting in a subpixel accuracy of the image co-registration. Cloud detection and atmospheric corrections were applied using ATCOR software and in-situ spectral reflectance measurements. The training dataset was compiled from a full census of trees on 32 plots with a size of one hectare each, where a total number of n=12,144 trees of 28 tree species were recorded in 2015. The tree species information from the field observations was merged with tree crown delineations derived from the LiDAR CHM using seed growing and watershed segmentation methods. From each of the segments RapidEye pixels were extracted and fed into a spectral signature database. Using graphical

and statistical analysis methods we identify the species specific characteristics and compare the intra- and inter-species variation. Furthermore, we research into the impact of the crown architecture on spectral reflection by extracting 3D crown shapes from the LiDAR CHM. Doing so we wish to contribute to the understanding of the sources of variability of canopy reflectance measurements by separating the signal variation into species specific variation and variation caused by the crown structure. Finally, non-parametric RandomForest models are trained to produce tree species distribution maps for all three regions. The validation of the maps is done with an independent sample based forest inventory which covers all three regions based with a randomly placed systematic grid.

Given the large and systematic set of images, training and validation data and the extent of the study area, we assume that the results from this study will contribute to the development of remote sensing assisted forest monitoring systems of highly complex mixed temperate forests, which are urgently demanded by forest managers, conservation planners and researchers.

Remote Sensing Contributions to Indicators of Biological Diversity in the U.S. National Report on Sustainable Forests—2015

Mark D. Nelson
U.S. Department of Agriculture, Forest Service, Northern Research Station, 1992 Folwell Avenue, St. Paul, MN 55108, phone (651) 649-5104, e-mail mdnelson@fs.fed.us,

Curtis H. Flather
U.S. Department of Agriculture, Forest Service, Rocky Mountain Research Station, 240 West Prospect Road, Fort Collins, CO, 80526, phone (970) 498-2569, e-mail cflather@fs.fed.us,

Kurt H. Riitters
U.S. Department of Agriculture, Forest Service, Southern Research Station, 3041 East Cornwallis Road, Research Triangle Park, NC, 27709, phone (919) 549-4015, e-mail kriitters@fs.fed.us,

Carolyn Sieg
U.S. Department of Agriculture, Forest Service, Rocky Mountain Research Station, 2500 South Pine Knoll Drive, Flagstaff, AZ, 86001, phone (928) 556-2151, e-mail csieg@fs.fed.us, and

James D. Garner
U.S. Department of Agriculture, Forest Service, Northern Research Station, 1992 Folwell Avenue, St. Paul, MN 55108, phone (651) 649-5107, e-mail jamesdgarner@fs.fed.us,

Guy Robertson
U.S. Department of Agriculture, Forest Service, National Program for Sustainability Assessment, 1400 Independence Ave., SW, Washington, DC 20250, phone (703) 605-1071 e-mail grobertson02@fs.fed.us,

Keywords: biological diversity, land use, land cover, remote sensing

Abstract:

Forest biological diversity contributes to human welfare through multiple ecosystem services. The Montréal Process (MP) provides a standard international framework for assessing a set of criteria and indicators (C&I) of the sustainability of temperate and boreal forest ecosystems and their ecological, social, and economic components in twelve countries, including the United States. The *National Report on Sustainable Forests—2015* relies on the MP C&I to organize and present data relevant to U.S. forests. The first of seven criteria addressed in the 2015 Report is Conservation of Biological Diversity, which is organized into nine indicators that address three sub-criteria: ecosystem diversity, species diversity, and genetic diversity. The aim of this presentation is to report results for U.S. 2015 indicators of forest conservation of biological diversity, with emphasis on remote sensing and geospatial contributions and challenges.

Ecosystem diversity indices of U.S. forest land use, composition, and structure are based on national forest inventory (NFI) field observations, post-stratified by satellite image-based land cover datasets to increase estimate precision. Protected vegetation land cover classes are assessed by combining 30-m Landfire existing vegetation types with a protected areas geospatial database. Landscape metrics of forest fragmentation are obtained from 30-m National Land Cover Databases of 2001 and 2011. Total area of forest land use increased by 14 million acres since the previous report. Timberland area increased by 14 million acres in large diameter size classes and decreased by 7 million acres in

medium and small diameter size classes. Woodlands (41%) and forest (31%) have a higher percentage of area protected than other natural vegetation cover types (16%). Between 2001 and 2011, net loss of interior forest cover varied from 7 to 20 percent depending on the landscape scale of measurement.

Indices of species and genetic diversity are based on national biological field inventories. Forest-associated taxa showed a general increase in the proportion of possibly extinct or at-risk species since 2003. Greatest declines in number of forest bird species occurred in oak ecoregions of the southern Appalachians, pine and northern hardwood ecoregions of the upper Midwest and Great Lakes, and montane and arid high plains ecoregions in the intermountain West.

Declining populations and shrinking geographic ranges provide indirect indications of genetic diversity loss. Between 1966 and 2011, about 19% of forest-associated bird species increased in populations and 20% decreased; decliners include species associated with early successional or wetland habitats. Ten percent of forest-associated species no longer fully occupy their former range; substantially higher rates of range shrinkage occur for infraspecies than for species.

Harmonization across indices is challenging due to different definitions in remote sensing and field inventory datasets, e.g., land cover versus land use. Understanding the interaction among indicators and the potential causes of indicator dynamics will necessarily involve linking indicators spatially and exploring patterns of covariation. Indicators derived from traditional on-the-ground surveys (e.g., species richness, species imperilment) could be modeled using indicators of habitat that are traditionally derived from remotely sensed imagery (e.g., area, configuration, and composition of land uses and land cover).

Potential of using data assimilation to support forest planning

Rami Saad, Peichen Gong, Tomas Lämås and Göran Ståhl

Keywords: uncertainty; suboptimal loss; remote sensing; combining data; Bayesian statistics.

Abstract

Uncertainty in forest information typically results in economic losses in addition to other losses as a consequence of suboptimal management decisions. Several techniques have been proposed to handle such uncertainties; however, these techniques are often complex and costly. Data assimilation (DA) has recently been advocated as a tool which may reduce the uncertainty and thereby reduce complexity in implementing techniques to handle uncertainty in forest planning. It offers an opportunity to make use of all new sources of information in a systematic way, and thus provide accurate and up-to-date information to forest planning. New remote sensing techniques can deliver information about forest stands with short intervals at low cost; DA offers a unified framework to make use of these new sources of forest information. In this study we review the literature on handling uncertainties in forest planning as well as related literature from other scientific fields in order to assess the potential benefits of using DA in forest planning. We identify five major potential benefits: (*i*) The accuracy of the information will be improved, (*ii*) The information will be kept up-to-date, (*iii*) The DA procedure will provide information with known accuracy, (*iv*) Bayesian decision making can be applied, whereby the accuracy of the information can be utilized in the decision making process and (*v*) DA data and Bayesian decision making allow for the analysis of optimal data acquisition decisions.

Use of remotely sensed data to spatially predict optimal final stand density, value and the economic feasibility of pruning for even age plantation forests

Michael S Watt[1], Mark O Kimberley[2], Jonathan P Dash[2], Duncan Harrison[2]

[1]Scion, PO Box 29237, Fendalton, Christchurch, New Zealand
[2]Scion, PO Box 3020, Rotorua, New Zealand

Keywords: 300 Index; LiDAR; productivity surfaces; pruning; radiata pine; Site Index; stocking

Two of the key end-uses for which forest plantations are grown are clearwood timber, in which the lower branches of the trees are removed (pruned) and structural grade timber in which trees are not pruned. Forest managers in many plantation growing regions have to determine the relative profitability of growing for clearwood or structural grade to ascertain whether pruning will be cost effective. Regardless of the regime chosen managers also need to determine the final crop stand density (S_{opt}) that will maximise value. Using a comprehensive series of simulations extracted from a New Zealand growth model for *Pinus radiata* a model of optimal S_{opt} that maximises the volume and value of clearwood and structural grade regimes was developed. At its core this model uses either GIS surfaces, satellite imagery or LiDAR data to predict two site productivity indices (Site Index, 300 Index) which in turn are used to spatially predict S_{opt}. Using log prices over the last 21 years the model was used to spatially predict variation in S_{opt} for New Zealand's largest plantation forest (Kaingaroa Forest) and throughout New Zealand. The model was also used to predict the relative value of clearwood *vs*. structural regimes, through time.

Of the three remotely sensed data sources LiDAR data most accurately predicted both Site Index and 300 Index and the final models had respective R^2 values of 0.88 and 0.79. The wide predicted variation in S_{opt} for Kaingaroa forest and at the national level was clearly a function of the two productivity indices 300 Index and Site Index. For all three regimes the highest values of S_{opt} (ca. 500 – 700 stems ha-1) were found on sites with high 300 Index (high volume) and low to moderate Site Index (moderate height). The lowest stand densities (ca. 200 – 300 stems ha-1) were found on sites with low to moderate 300 Index and moderate to high Site Index. Mean predicted Sopt for the existing plantation resource within New Zealand was 603 stems ha-1 for the structural regime and 569 and 449 stems ha-1, for the two clearwood regimes, that, respectively, targeted production of small and large diameter pruned log.

Temporal analyses show pruning profitability has declined markedly over the last two decades in New Zealand primarily in response to reductions in the pruned log premium. Spatial analyses show pruning to be profitable within at least 95% of plantations using values from 1995-2000 and unprofitable within at least 95% of plantations using values from 2011-2015. The most profitable areas for pruning were found to be located in regions where 300 Index ranges from moderate to high and Site Index is relatively low.

This research clearly shows an application of precision forestry that can use LiDAR or satellite imagery to guide management operations at both broad spatial scale and fine resolution. The application of the presented model suggests there is considerable scope for increasing plantation value through optimising S_{opt} by site to values that are higher than those generically prescribed and highlighting sites where pruning is likely to be most profitable.

ForestSAT 2016

Latin American Forests

OTERRA
CENTRO DE ESTUDIOS DE RECURSOS NATURALES
UNIVERSIDAD MAYOR

UNIVERSIDAD MAYOR
para espíritus emprendedores

Facultad de Ciencias
ESCUELA DE INGENIERÍA FORESTAL

Comparing Generalized Linear Models and random forest to model vascular plant species richness using LiDAR data in a natural forest in central Chile

Javier Lopatin[1,2], Klara Dolos[1], H.J. Hernández[2], M. Galleguillos[3], Fabian Ewald Fassnacht[2]

[1] Institute of Geography and Geoecology, Karlsruhe Institute of Technology (KIT), Kaiserstraße 12, 76131 Karlsruhe, Germany
[2] Laboratory of Geomatics and Landscape Ecology, Faculty of Forest and Nature Conservation, University of Chile, 11315 Santiago, Chile.
[3] Department of Environmental Sciences, School of Agronomic Sciences, University of Chile, 11315 Santiago, Chile.

Keywords: *Species richness, LiDAR, GLM, random forest, alpha-diversity, bootstrap validation.*

Biodiversity is an essential element of the Earth system, related to many important ecosystem services. Cost-efficient and precise monitoring systems are needed to support the conservation of biodiversity in a quickly changing world. Here, we tested the suitability of airborne discrete-return LiDAR data for estimating vascular plant species richness of second growth native forest ecosystems in central Chile. We modelled the vascular plant richness of four layers (total, tree, shrub and herb richness) using twelve LiDAR-derived variables. As species richness values are typically non-normally distributed count data, the corresponding asymmetry and heteroscedasticity in the error distribution has to be considered. We therefore compared the suitability of random forest (RF) and a Generalized Linear Model (GLM) with a negative binomial error distribution. In both cases, a feature selection to identify the most relevant LiDAR predictors was applied as a first step. In both model types, the three most important predictors for all four layers were altitude above sea level, standard deviation of slope and mean canopy height. This agreed with our preconception of LiDAR's suitability for estimating species richness which we hypothesized to be its capacity to capture three types of information: micro-topographical, macro-topographical and canopy structural. Generalized Linear Models showed higher performances (r^2: 0.66, 0.50, 0.52, 0.50; nRMSE: 16.29%, 19.08%, 17.89%, 21.31% for total, tree, shrub and herb richness respectively) than RF (r^2: 0.55, 0.33, 0.45, 0.46; nRMSE: 18.30%, 21.90%, 18.95%, 21.00% for total, tree, shrub and herb richness, respectively). In addition, the best GLM models were more parsimonious (three predictors) and less biased than the best RF models (twelve predictors). We explain this with the mentioned non-symmetric error distribution of the species richness values, which RF could not capture properly.

From an ecological perspective, the predicted diversity maps agreed well with the known vegetation composition of the area. High species numbers were found at low elevations and along riversides. In these areas, overlapping distributions of thermophile sclerophyllos species, water demanding Valdivian evergreen species and species growing in Nothofagus obliqua forests occur. Our three main conclusions were: 1) appropriate model selection is important when working with biodiversity count data; 2) RF has troubles when applied to data with non-symmetric error distributions; and 3) structural and topographic information derived from LiDAR data is useful for predicting local plant species richness.

Detection of low density natural forest in the Andes region using LANDSAT 8 imagery

Author: Vega Isuhuaylas, Luis Alberto.
Affiliation: Forestry and Forest Products Research Institute (FFPRI)
Co-author: Hirata, Yasumasa.
Affiliation: Forestry and Forest Products Research Institute (FFPRI)

Keywords: Andean forest, remote sensing, forest detection, spectral test, Landsat 8

Abstract

Andean ecosystems in South-America are among the most diverse and threatened ecosystems in the world. Due to a long history of exploitation that still continues, the remaining natural forests in the Andes region are relict tree populations in inaccessible locations and open forests with low density of individuals. From the perspective of forest conservation, the detection via remote sensing techniques of such low density forests in large areas with freely available medium resolution satellite data constitutes a challenge.

This study aims to evaluate the detection of Andean natural forests by remote sensing techniques according to forest density using LANDSAT 8 satellite data, and to determine the most effective detection variables.

The selected study area is the department of Cuzco (Peru). Field data on Andean forest condition was gathered by plotless sampling survey in several locations and the forest stand density was calculated. Low density forest was defined at different values for testing purposes. Next, spectral separability tests between low density forest and other land cover classes were carried out using the mean values of reflectance, vegetation indexes and other factors estimated via PCA and Tasseled cup analysis. Finally, a land cover classification is carried out using the variables with better separability results and the accuracy of classification is calculated.

Effect of lidar pulse density on the prediction of aboveground biomass change in Brazilian Amazon Rainforest

Carlos Alberto Silva[1,2,3], Andrew Thomas Hudak[2], Lee Vierling[1], Carine Klauberg[2], António Ferraz[3], Mariano Garcia Alonso[3], Michael Keller[4], Sassan Saatchi[3]

[1] Department of Natural Resources and Society, College of Natural Resources, University of Idaho, (UI), 875 Perimeter Drive, Moscow, Idaho, 83844, USA
[2] USDA Forest Service, Rocky Mountain Research Station, RMRS, 1221 South Main Street, Moscow, ID, 83843, USA
[3] Jet Propulsion Laboratory, California Institute of Technology, Pasadena, CA 91109, USA
[4] USDA Forest Service, International Institute of Tropical Forestry, San Juan, PR, 00926, USA

Keywords: Airborne Lidar, Biomass, Tropical Forest, Forest Inventory, Pulse densit

Tropical forests are an important component of global carbon stocks, but the response of tropical forest biomass to climate is not sufficiently studied or understood. Airborne lidar (Light Detection and Ranging) is well suited for quantifying tropical forest carbon stocks, however trade-offs exist between lidar pulse density and acquisition cost. Our objective was thus to evaluate the effect of lidar pulse density on aboveground biomass (AGB) change prediction using airborne lidar and field plot data in a tropical rain forest located near Paragominas, Pará, Brazil. Forest attributes such as tree density and diameter at breast height were measured in 84 square field plots of 50x50m in 2014. Using previously published allometric equations, tree AGB was computed and then summed to calculate total AGB at each sample plot. The lidar data were acquired 2012 and 2014, and for each dataset the pulse density was downscaled from its original density to lower densities of 12, 10, 8, 6, 4, 2, 1, 0.8, 0.6, 0.4 and 0.2

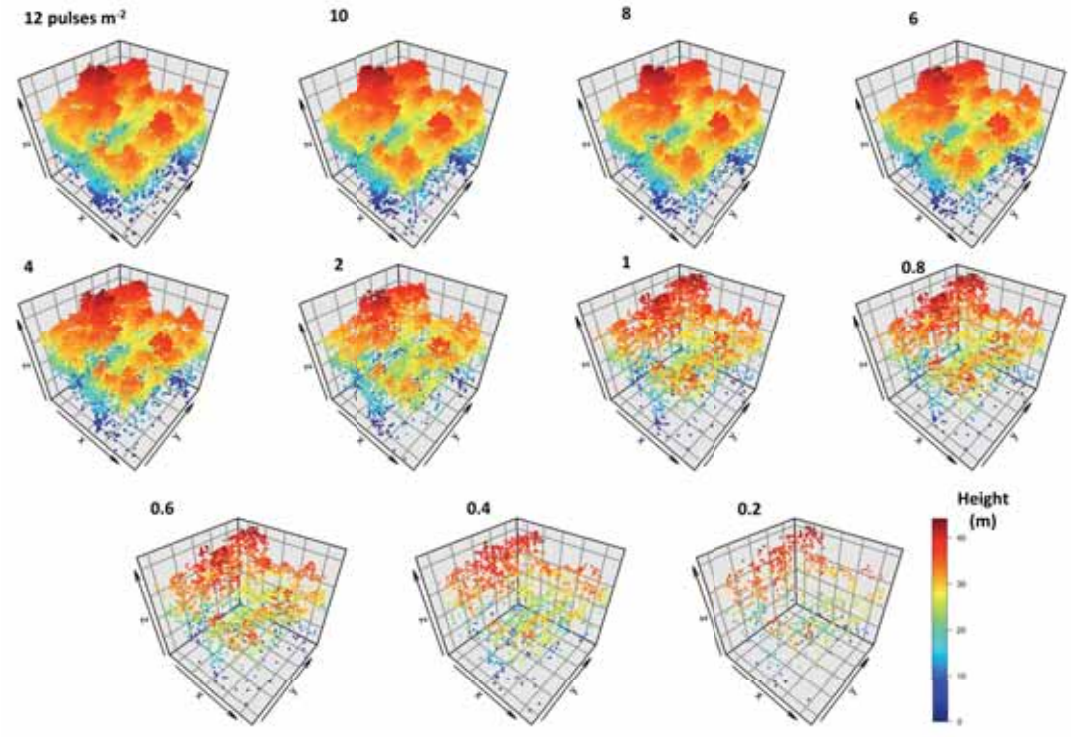

Figure 1. Lidar point cloud by target pulse density. The 3d points are coloured by height.

pulses/m^2. The effect of pulse density on the AGBC prediction was evaluated under two scenarios i) lidar data both from 2012 and 2014 were normalized to height-aboveground using the DTMs created from each density dataset; and ii) To simulate the effect on subsequent acquisition, the DTM generated at highest pulse density (12 pulse/m^2) from 2012 was used to normalize height-aboveground for downscaled lidar datasets both from 2012 and 2014. For both scenario, we clipped the point cloud into the sample plots to compute mean canopy height (MCH). A power model was used to model AGB from MCH in 2014, and to predict AGB for 2012 and 2014. Leave-one out cross validation was applied and the models were assessed according to the coefficient of determination (R^2), relative root mean square error (RMSE,%) and Bias (%). The AGB change was then computed as the difference between AGB predicted from 2012 and 2014. To achieve consistent results; we repeated all procedures 30 times. Our findings showed that for both scenarios the AGB change prediction was only slightly affected by pulse density. For models in scenario 1, the mean RMSE and Bias slightly increased from 15.01 to 15.99%, 0.09 to 0.16% and the R^2 slightly decreased 0.75 to 0.72 as pulse density decreased from 12 to 0.2 pulses/m^2. For scenario 2 the mean RMSE (%) increase from 14.91 to 15.20%, the Bias (%) stayed constant at 0.09, and the R^2 decreased from 0.76 to 0.75 as pulse density decreased as well. Moreover, as pulse density decreased from 12 to 0.2 pulses/m^2, the mean AGB change prediction across sample plots slightly decreased from 4.22 to 3.84 Mg/ha and from 6.12 to 5.82 Mg/ha, for scenario 1 and 2, respectively. This study showed that a DTM generated from either low or high pulse density lidar can be used to normalize height aboveground for predicting AGB changes in tropical forest. We therefore, we conclude that there is good potential to monitor carbon pools in Brazilian Tropical Rain Forest using airborne lidar data with low pulse density.

Estimating of the leaf area index in a forest fragment of mixed ombrophilous forest in Brazil, using remote sensing techniques

Bruna Nascimento de Vasconcellos Schiavo[1]
Ângela Maria Klein Hentz[1]
Ana Paula Dalla Corte[2]
Carlos Roberto Sanquetta[2]

[1] PhD student, Federal University of Paraná, Department of Forest Engineering – Curitiba, Parana state, Brazil
[2] PhD, Federal University of Paraná, Department of Forest Engineering – Curitiba, Parana state, Brazil

The leaf area index (LAI) is considered as a component of the most sensitive part in forest structure, because the canopy leaves regulate the fundamental processes in forest productivity. This study was conducted to estimate the leaf area index, in a fragment of Mixed Ombrophilous Forest, located in São João do Triunfo, Paraná state, Brazil, using remote sensing techniques. The LAI was generated from orbital images of Pleiades sensor, based on the relationship between some vegetation indices tested in this work. First, the orbital images were corrected for atmospheric and radiometric distortion, then two vegetation indices (VI) NDVI and SAVI were generated. The vegetation indices were used to test the models proposed in the literature by the Manual for the Energy balance algorithms of the earth's surface (SEBAL, 2002) that uses the IV SAVI and Duchemin (2006) using the IV NDVI. In addition, 312 samples were distributed in the study area, where the LAI was estimated from the terrestrial sensor IC-110 Plant Canopy Analyzer, considered the real value as control. The data obtained by the remote sensing techniques were correlated with the data obtained from the field, using the Pearson's correlation coefficient. The VI NDVI present a correlation with the control of r = 0.32, and the SAVI presented a correlation of r = 0.78. It was observed that the model proposed by SEBAL (SAVI) was highly correlated with the control data (r = 0.66). However, the model proposed by Duchemin (NDVI) did not present correlation (r = 0.23), so is considered inefficient to estimate LAI in the Mixed Ombrophilous Forest. In addition, both models presented an underestimation compared to the real value. The LAI estimated by terrestrial and orbital sensors presented an ample variability among the data, a factor possibly related to species diversity, a characteristic of native forests. Among of these variations, it was possible to identify the different canopies in these models, so the pixels with the highest values of the LAI correspond to the area with a predominance of hardwoods. The remote sensing techniques and the images of the Pleiades sensor performed well to estimate the leaf area index in the forest fragment of Mixed Ombrophilous Forest.
Keywords: Araucaria Forest; Pleiades; CI-110 Plant Canopy Analyzer;

Introduction

Woodgate et al. (2015) considers that leaf area index (LAI) is a primary descriptor of vegetation structure and is an essential climatic variable. It is considered as part of the most sensitive structure of the forest, because canopy leaves regulate some ecophysiological processes, such as photosynthesis and transpiration, which are considered as fundamental elements of forest productivity (LARCHER, 2004; BAMBI, 2007). There are many feasible methods and equipment for the non-destructive estimation of leaf area index and photosynthetically active radiation, so that isolated tree, planting, direct biometric measurements of leaves or indirect measurements can be considered using regression models based on branches, trunks Or productivity in general (Guimarães et al., 2013). The two main methods of estimation of leaf area index through remote sensing are based on the empirical relationship between vegetation indexes and LAI, or between models of radiation transfer using passive sensors or neural networks (MA, 2014).

The objective of this study was to test sensing techniques to estimate leaf area index in a fragment of the Mixed Ombrophilous Forest in the state of Paraná, Brazil.

Methodology

The study was carried out at the Rudi Arno Seitz Experimental Station of the Federal University of Paraná, located in the city of São João do Triunfo, in the Center-South Region of the state of Paraná, Brazil. 312 sample points were distributed in the study area, where the LAITERRESTRIAL was estimated from the CI-110 Plant Canopy Analyzer sensor, considered as field truth (witnesses). The CI-110 Plant Canopy Analyzer is a passive ground sensor, used to measure the amount of incident solar radiation in the visible spectrum. According to Meyer Junior (2014) the CI-110 is composed of a rod with 24 sensors, and at the tip of the rod, is the fish eye lens that allows to calculate the LAI, the coefficient of transmission for penetration Diffuse, the canopy opening index, the average leaf angle and the canopy extinction coefficient.

LAIORBITAL was estimated through vegetation indices, which are mathematical formulas developed to evaluate the vegetation cover qualitatively and quantitatively, using spectral measurements. Atmospheric and radiometric correction of the image of the Pléiades sensor was performed, and the NDVI and SAVI vegetation indices were tested, which subsidized the LAIORBITAL estimation tests by the models of SEBAL (2002) and Duchemin (2006).

The Pearson correlation analysis was performed between the leaf area index obtained from the CI-110 Plant Canopy Analyzer (LAITERRESTRIAL), considered as field truth and obtained from the orbital image (LAIORBITAL).

Results

The data obtained through the techniques of Remote Sensing were correlated with the data obtained in the field through the Pearson correlation coefficient. The value of the leaf area index for the Mixed Ombrophilous Forest fragment obtained in this study ranged from 6.01 to 8.01. The value of leaf area index for forests, as presented in the literature, varies from 0.40 for a low density of individuals and 16.9 for old stands. The highest values reported are for conifers, with maximum values between 6 and 8, for deciduous forests (JONCKHEERE et al., 2004). Regarding the correlation of the vegetation indices with the field truth, the NDVI presented r = 0.32, the SAVI presented the correlation r = 0.78. Although several studies have demonstrated the functionality of NDVI in estimating vegetation properties, many atmospheric influences and vegetation itself restrict their use globally. Thus, improved indexes, such as EVI and SAVI, incorporate an adjustment factor for soils or atmospheric conditions, generating by-products that have a greater reliability related to the field truth. It was found that the model proposed by SEBAL (SAVI) presented a high correlation with the field truth (r = 0.66). However, the model proposed by Duchemin (NDVI) showed no correlation (r = 0.23), being considered inefficient for the estimation of LAI in Mixed Ombrophilous Forest. In addition, both models presented an underestimation of the truth of the field. The LAI estimated by the terrestrial and orbital sensors showed a great variability between the data, a factor that may be related to the diversity of species, characteristic of native forests. Among these variations, it was possible to identify the different canopies in these models, so that the pixels with the highest LAI values correspond to the predominantly hardwood area. As in the LAI estimated through the CI-110 equipment, the LAI values generated by the orbital method also presented a great variability between the plots. This factor may be related to the different forest dykes predominant in the Rudi Arno Seitz Station.

Conclusion

Remote Sensing techniques and the images of the Pleiades sensor presented a good performance to estimate the leaf area index in a Mixed Ombrophilous Forest Fragment. The SEBAL and Duchemin models presented an underestimation of the field truth, but the SEBAL model was considered efficient due to the strong correlation with the control.

Reference

BAMBI, P. **Variação sazonal do índice da área foliar e sua contribuição na composição da serapilheira e ciclagem de nutrientes na floresta de transição no norte do Mato Grosso**.

111f. Dissertação (Mestrado em Física e Meio ambiente), Universidade Federal do Mato Grosso, Cuiabá, 2007.

DUCHEMIN, B.; HADRIA, R.; ERRAKI, S.; BOULET, G.; MAISONGRANDE, P.; CHEHBOUNI, A.; ESCADAFAL, R.; EZZAHAR, J.; HOEDJES; J.C.B.; KHARROU, M.H.; KHABBA, S.; MOUGENOT, B.; OLIOSO, A.; RODRIGUEZ, J.C.; SIMONNEAUX, V. Monitoring wheat phenology and irrigation in Central Morocco: On the use of relationships between evapotranspiration, crops coefficients, leaf area index and remotely-sensed vegetation indices. **Agricultural Water Management**, v. 79, p.1-27, 2006.

GUIMARÃES, M.J.M., FILHO, M.A.C., PEIXOTO, C.P., JUNIOR, F.A.G., OLIVEIRA, V. V. M. Estimation of leaf area index of banana orchards using the method LAI-LUX. **Water Resources and Irrigation**, v.2, n.2, p.71-76, 2013.

JONCKHEERE, I., FLECK, S., NACKAERTS, K., MUY, B., COPPIN, P., WEISS, M. BARET, F., Review of methods for in situ leaf area index determination Part I. Theories, sensors and hemispherical photography. **Agricultural and Forest Meteorology**, v. 121, 19–35, p.2004.

LARCHER, W. **Ecofisiologia Vegetal**. Ed. Rima. São Carlos. 2004. 531p.

MA, H.; SONG, J.; WANG, J.; XIAO, Z.; FU, Z. Improvement of spatially continuous forest LAI retrieval by integration of discrete airborne LIDAR and remote sensing multi-angle optical data. Agricultural and Forest Meteorology, v. 189-90, p. 60-70, 2014.

SURFACE ENERGY BALANCE ALGORITHMS FOR LAND (SEBAL). **Advanced Training and Users Manual – Version 1.0**. 2002. Disponível em <ftp://ftp.funceme.br/Cospar_Funceme_2010/CLASS_DAY_04.11.2010/LAB/quixere/quixere/Final%20Sebal%20Manual.pdf>. Acesso em: 20 out. 2014.

WOODGATE, W., JONES, S.D., SUAREZ, L., HILL, M., ARMSTON, J.D., WILKES, P., BERELOV ,M.S., HAYWOOD, A., MELLOR, A.; Understanding the variability in ground-based methods for retrieving canopy openness, gap fraction, and leaf area index in diverse forest systems. **Agricultural and Forests Meteorology**, p.83-95, 2015.

Evaluating the ecological vulnerability of the remaining of Araucaria Forest – Southern Brazil

Henrique Luis Godinho Cassol[1]; Bete Caria Moraes[1]; Yosio Edemir Shimabukuro[1];*

[1] National Institute for Space Research, Remote Sensing Division, Avenida dos Astronautas, 1.758 - Jd. Granja, São José dos Campos, SP, CEP 12227-010; {bete;yosio@dsr.inpe.br}.
** Corresponding author: henrique@dsr.inpe.br +55(12)32086458*

Key-words: Deforestation; Araucaria Forest; Landscape Metrics; Ecological Vulnerability; Landscape Ecology;

Abstract

Nowadays Araucaria Forest is highly fragmented and disconnected, which gives it great susceptibility and an extreme risk of biodiversity loss. However, just few studies have tried to establishing their actual ecological vulnerability using landscape metrics and indices. Thus, we asked: What is the current ecological vulnerability degree of the Araucaria Forest? And what is the distribution pattern of forest patches? To answer these questions, we choose the southeast region of Parana State as study case. The region showed around 15,000 ha of deforestation identified between of 2000 to 2010. The pattern distribution of forest patches was calculated through landscape metrics, whereas the ecological vulnerability degree was assessed by interpreting results. The results suggest higher ecological vulnerability on this region due to its highly fragmented landscape. The region contains 90% of forest patches less than 100 ha area, isolated in mean at more than 1.7 km and only 7% of the remaining forest is under protection.

Introduction

Araucaria forest is one of the seven phytophysiognomies of the Atlantic forest - the luxurious forest of the Brazilian coast. As occurred throughout the Atlantic Forest, Araucaria forest was extensively explored not only due to the high value of the Brazilian Pine, but also to give place to agriculture lands, pastures and recently forestry (HIGUCHI et al. 2012). Nowadays, the remaining forest is susceptible and fragmented. For instance, some researchers estimate their actual covering lying between 10 to 20% of the original forest cover (GALINDO-LEAL & CÂMARA, 2003; RIBEIRO et al. 2009; IESB et al. 2007).

The loss of forest has serious impact on the ecosystem, such as biodiversity decline, habitat loss, fragmentation and decreasing environmental condition as water quality and soil fertility (GALINDO-LEAL & CÂMARA, 2003; RIBEIRO et al. 2009). The fragmentation extent, including variations in connectivity (distance between forest patches), is an important factor to assessing the state of ecological vulnerability of an ecosystem. So, the impact of deforestation and its fragmentation may be indirectly measured by landscape metrics, as number and area of forest patches, connectivity between them, and other useful landscape metrics (TURNER, 1989).

In this context, the ecological vulnerability degree of an ecosystem is given by its exposure, sensitivity and resilience (FORMAN & GODRON, 1986). The exposure is related to the structure of the forest as size of fragments and edge effects. Sensitivity is related to the ecosystem function such as interactions among plants and animals or trophic chains and finally, the resilience can be associated to the environment changes, i.e., the ability of forest to return to the previous state (UUEMAA et al. 2013). Thus, a small change in one of them may increase the vulnerability of the whole forest ecosystem.

In this way we ask: what is the current ecological vulnerability degree of the remaining Araucaria Forest? And what is the pattern distribution of forest patches?

Methodology

The study area comprises a Southeast region of Paraná State, Brazil, as a study case (Figure 1). The original forest cover of Araucaria Forest was 78% of SE region (~17,000km²), and remainder of Deciduous forest (20%) and Grasslands (2%) (IPARDES, 2004). The main species of Araucaria forest is the emergent Brazilian pine (*Araucaria angustifolia* Bertz. O. Ktze), co-occurring with other broadleaf species as *Ocotea porosa* (Mez.) L. Barroso, *Ilex paraguariensis* St. Hil, *Cedrela fissilis* and members of Lauraceae and Myrtaceae (STEFENON, 2009).

Dataset

Forest patches of 2000 and 2010 were downloaded from SOS Mata Atlântica/INPE, (2010) in shapefile format. The polygons were converted to reference system WGS84 and reprojected to coordinate system UTM Zone 22 South. Scale format was 1:50000 meaning that the smallest forest patches < 5 ha were not computed. Conservation Units (CU) areas were obtained in shapefile format from Ministry of Environment in scale 1:250000, *datum* WGS84, (www.icmbio.gov.br; ICMBIO, 2013). Rivers channels were downloaded from Institute of Land, Cartography and Geosciences of Paraná (www.itcg.pr.gov.br; ITCG/PR, 2010).

Ecological Vulnerability of Araucaria Forest

In order to evaluate the current ecological vulnerability of the remaining of Araucaria Forest, we applied some landscape metrics to the structure, shape and connectivity of the forest patches (RIBEIRO et al. 2009). Forest cover data and metrics were computed in ArcGIS 9.3, Patch Analyst 5.0 (REMPEL et al., 2012).

Major landscape metrics chosen were: patch size, structural connectivity, shape index, mean isolation, distance to Conservation Units and distance to river channel (Table 1). We utilize the multiscale approach to assess the landscape metrics. In this approach, each metric will be separated in class rules.

The distribution of the fragments into size classes allows us to measure a forest cover in each of the classes and their distribution in the total area. The shape index refers to the complexity of the shape of the fragments. Shape index assumes value one for geometric forms and values greater than one for more irregular and complex shapes. This parameter is very useful, because more irregular forms tend to have a greater edge effect, which may be limiting for a survival of some species (UUEMAA et al., 2013). In structural connectivity we interested of "probable" distance to find a given fragment size class.

In mean isolation, the smallest forest patches are successively removed from analysis to estimate the minimum distance of a random point to the nearest forest patch (RIBEIRO et al. 2009). This index is used to infer the importance of small fragments in the landscape and its connectivity to larger forested areas (stepping stones).

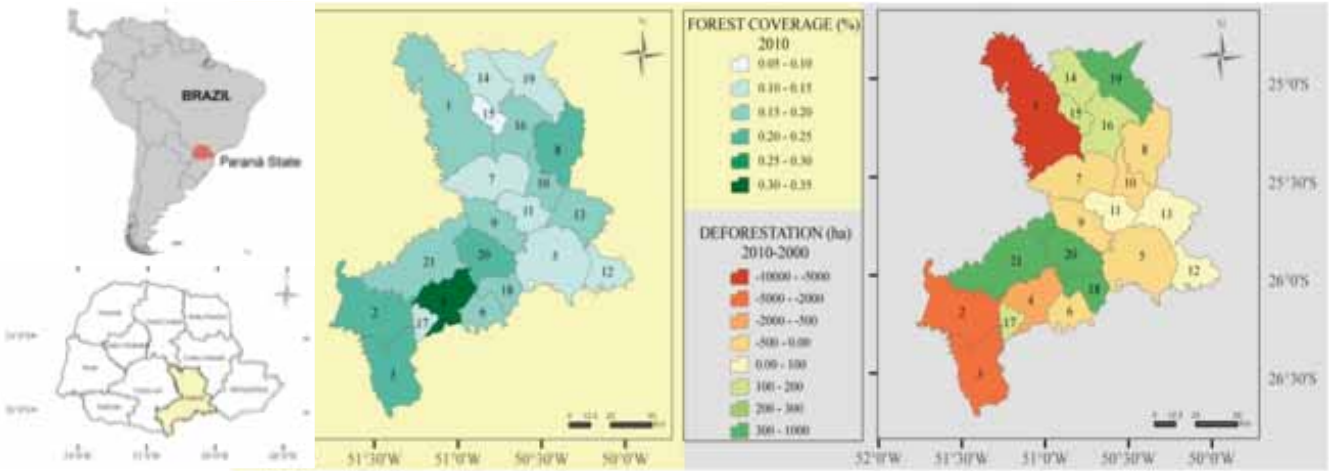

Figure 1. Location of Southeast region of Paraná State, Brazil. In detail, relative coverage of forest for each municipality area, and forest losses and growth from 2000 to 2010.

Table 1. Major landscape metrics applied to assess the ecological vulnerability degree of Araucaria Forest.

Index	Description	Class rules
Patch size	Number of forest patches and percentage of forest cover for different size classes	Patch size classes: 0-50ha; 50-100ha; 100-250ha; 250-500ha; 500-1000ha; 1000-2500ha; 2500-5000ha; >5000ha
Structural Connectivity	Mean area of interconnected forest patches considering minimum distance classes	Linkage distances: 0-200m; 200-500m; 500-900m; 900-1400m; 1400-2000m; 2000-2700m
Shape index	Shape index per forest patches size. Closer to one more geometric is its shape	Patch size classes: 0-50ha; 50-100ha; 100-250ha; 250-500ha; 500-1000ha; 1000-2500ha; 2500-5000ha; >5000ha
Mean isolation	Mean isolation of random points to the nearest forest patch. To evaluate isolation the smallest forest patches were successively removed	Size of forest patches removed: 0-50ha; 50-100ha; 100-250ha; 250-500ha; 500-1000ha; 1000-2500ha;
Distance to CU	Minimum distance of any forest patch to the nearest Conservation Unit	Distance class: 0m (inside CU); 0-500m; 5000-1000m; 1.000-2.000m; 2.000-5.000m; 5.000-10.000m; 10.000-20.000m; 20.000-50.000m; >50.000m
Distance to rivers	Minimum distance of any forest patch to the nearest river channel	Distance class: 0m (touch the river channel); 0-50m; 50-100m; 100-250m; 250-500m; 500-1000m; 1000-2500m; >2500m

Results and Discussions

Remaining forest cover of SE region is 17.5 % and 9% of Araucaria Forest estimated by Ribeiro et al. (2009). The Figure 2 shows the relative distribution of forest patches by number and area against size class, respectively, and the minimum distance of any forest patch to the nearest river channel by distance classes. We can see that 76% of forest patches have less than de 50 ha area, but it represents only 26% of the forested area (Fig. 2a). The largest forest fragments are located in the CU of Serra da Esperança (A > 5000 ha), between the municipalities of Cruz Machado, Mallet and União da Vitória, corresponding to 8% of remaining forest area (Fig. 2a).

We also noticed that 36% of forest patches are distant less than 50 m of any channel river, but its represents only 6 % of forest area (Fig. 2b). This situation is worrying because the areas close to the rivers are protected by law and are a refuge of the wild allowing the flow of plants and animals.

a)

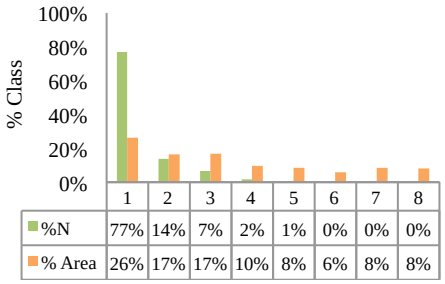

b)

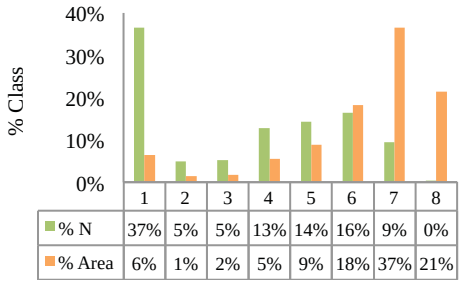

Figure 2. a) Distribution of forest patches by frequency and area by size classes: (1) 0-50ha; (2) 50-100ha; (3) 100-250ha; (4) 250-500ha; (5) 500-1000ha; (6) 1000-2500ha; (7) 2500-5000ha; (8) >5000ha. b) Distance (m) of any forest patch to the nearest river channel by relative frequency and area by distance classes: (1) 0m (touch the river channel); (2) 0-50m; (3) 50-100m; (4) 100-250m; (5) 250-500m; (6) 500-1000m; (7) 1000-2500m;(8) >2500m.

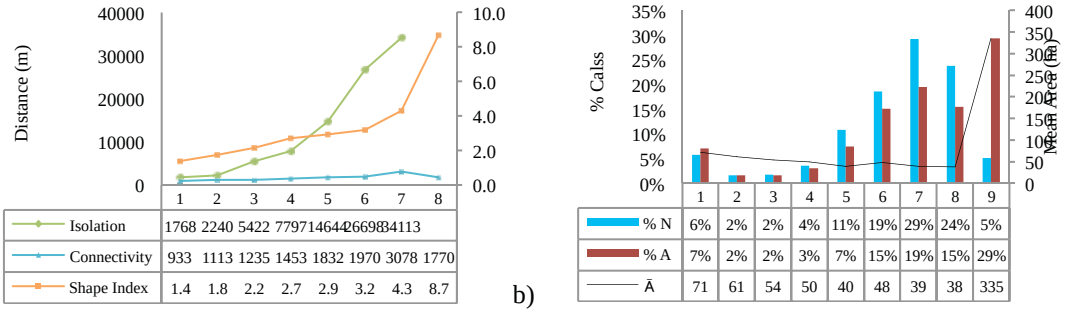

Figure 3. a) Mean isolation (m) of forest patches by size class (ha); mean distance (m) of structural connectivity among forest patches with the same size class, and shape index (unitless) by size class (ha). Size classes: (1) 0-50 ha; (2) 50-100 ha; (3) 100-250 ha; (4) 250-500 ha; (5) 500-1000 ha; (6) 1000-2500 ha; (7) 2500-5000 ha e (8) >5000 ha. b) Minimum distance to of any forest patch to the nearest Conservation Unit by frequency and area by distance class: (1) om (inside CU); (2) 0-500m; (3) 5000-1000m; (4) 1.000-2.000m; (5) 2.000-5.000m; (6) 5.000-10.000m; (7) 10.000-20.000m; (8) 20.000-50.000m; (9) >50.000m. Continuous line refers to mean area (ha) of forest patch by distance class.

Figure 3a presents mean isolation, strutural connectivity and shape index by size of forest patches. The mean isolation between a random point to any forest patch was more than 1700m. If the smallest patches were lost the average isolation would raise exponentially. Structural connectivity between forest patches with less than 50 ha was calculated in 933 meters. As expected, small forest patches are squared while biggest ones showed more complex shapes (Fig. 3a).

The size, shape, proximity and isolation affects directly the structure, function and biodiversity of the remaining forest (GALINDO LEAL, 2003). Small forest patches reduce diversity of birds (ANJOS, 2001), tree species (SCHESSL et al. 2008) and specially great mammals (CHIARELLO, 1999). Considering the isolation and level of fragmentation, species less generalist and with greater need of area are the first to disappear (PARDINI et al., 2009).

The isolation of species due to fragmentation has also negative effect to genetic conservation of *Araucaria angustifolia* by increasing the endogamic reproduction (STEFENON et al. 2009). Small forest patches are not able to provide the self-reproduction of individuals of Brazilian Pine, suggesting that the colonization of border areas or abandoned areas may not be sufficient for the conservation of this important forest species (SOUZA et al. 2008).

In relation to the minimum distance to Conservation Units, 5.75 % of remaining forests are contained in any CU (7% of forest area), it means they are under protection. The mean area size under protection is only 71 ha (Figure 3b). These *circa* 6% of protection is below the recommended 10% that must be necessary to hotspots conservation by Secretariat of the Convention on Biological Diversity (2002). On this scenario, the creation of new CUs should be priority to reduce the losses of biodiversity.

Conclusions

The Araucaria forest is highly fragmented and susceptible: 91% of their fragments have less than 100 ha area; they are isolated in mean to 1.7km and structural connectivity between forest patches are above 900 m. Nevertheless, the Southeast of Paraná State has still 17% of original forest cover; 7% of which are inside of Conservation Units. The major challenge is connect the forest patches with ecological corridors and above all connect them with river channels (only 6 % of patches are less than 50 m of any river stream) combining the protection of water sources with the possibility of animal movement in these areas.

References

ANJOS, L. Bird communities in five atlantic forest fragments in southern Brazil. **Ornitologia Neotropical**. v.12. p. 11–27. 2001.

CHIARELLO, A. G. Effects of fragmentation of the Atlantic Forest mammal communities in southeastern Brazil. **Biological Conservation**. v. 89: p.71–82. 1999.

GALINDO-LEAL, C., CÂMARA, I.G., 2003. Atlantic Forest hotspot status: an overview. In: GALINDO-LEAL, C., CÂMARA, I.G. (Eds.), **The Atlantic Forest of South America: Biodiversity Status, Threats and Outlook**. CABS and Island Press, Washington, p 3–11. 2003.

HIGUCHI, P.; SILVA, A.C.; FERREIRA, T.S.; SOUZA, S.T.; GOMES, J.P.; SILVA,K.M.; SANTOS, K.F. Floristic composition and phytogeography of the tree component of Araucaria Forest fragments in southern Brazil. **Brazilian Journal of Botany**, v. 35. n.2 p. 145-157. 2012.

INSTITUTO DE TERRAS, CARTOGRAFIA E GEOCIÊNCIAS DO PARANA (ITGC/PR). Secretaria do meio ambiente do estado do Paraná. 2010. Available: www.itgc.pr.gov.br. Accessed: 20/07/2013.

INSTITUTO DE ESTUDOS SOCIOAMBIENTAIS DO SUL DA BAHIA (IESB). Instituto de Geociências da Universidade Federal do Rio de Janeiro (IGEO/UFRJ), Departamento de Geografia da Universidade Federal Fluminence (UFF), 2007. Levantamento da Cobertura Vegetal Nativa do Bioma Mata Atlântica. Relatório final. PROBIO 03/2004, Brasília, 84p.

INSTITUTO PARANAENSE DE DESENVOLVIMENTO ECONÔMICO E SOCIAL (IPARDES). Leituras regionais: mesorregião geográfica do Sudeste do Paraná. Curitiba, 2004. 134p.

PARDINI, R.; FARIA, R.; ACCACIO, G.M.; LAPS, R.R.; MARIANO-NETO, E.; PACIENCIA, M.L.B.; DIXO, M.; BAUMGARTEN, J. The challenge of maintaining Atlantic forest biodiversity: A multi-taxa conservation assessment of specialist and generalist species in an agro-forestry mosaic in southern Bahia. **Biological Conservation**, v. 142. p. 1178–1190. 2009.

REMPEL, R.S., D. KAUKINEN., AND A.P. CARR. 2012. Patch Analyst and Patch Grid. Ontario Ministry of Natural Resources. Centre for Northern Forest Ecosystem Research, Thunder Bay, Ontario. [online: http://www.cnfer.on.ca/SEP/patchanalyst/].

RIBEIRO, M.C.; METZGER, J.P.; MARTENSEN, A.C.; PONZONI, F.J.; HIROTA, M.M. The Brazilian Atlantic Forest: How much is left, and how is the remaining forest distributed? Implications for conservation. **Biological Conservation**, v. 142. p. 1141–1153. 2009.

SCHESSL, M.; SILVA, W.L.; GOTTSBERGER, G. Effects of fragmentation on forest structure and litter dynamics in Atlantic rainforest in Pernambuco, Brazil. **Flora**. v. 203. p. 215–228. 2008.

SOS Mata Atlântica. Shapefiles dos remanescentes florestais 2000 e 2010. Available: http://mapas.sosma.org.br/dados/. Accessed: 23/07/2013.

SOUZA, A.F.; FORGIARINI, C.L.; SOLON, J.; BRENA, D.A. Regeneration patterns of a long-lived dominant conifer and the effects of logging in southern South America. **Acta Oecologica**, v. 34, n. 2, p. 221–232, Sep. 2008.

STEFENON, V.M.; STEINER, N.; GUERRA, M.P.; NODARI, R.O. Integrating approaches towards the conservation of forest genetic resources: a case study of Araucaria angustifolia. **Biodiversity and Conservation**, v. 18. p.2433–2448. 2009.

TURNER, M.G.; O'NEILL, R.V.; GORDON, R.H.; MILNE, B.T. Effects of changing spatial scale on the analysis of landscape pattern. **Landscape Ecology**, v.3, p.153-162. 1989.

UUEMAA, E.; MANDER, U.; MARJA, R. Trends in the use of landscape spatial metrics as landscape indicators: A review. **Ecological Indicators**. v.28. p. 100–106. 2013.

Improving Observations of Tropical Forests with Optimized Terrestrial Lidar Scanners

Crystal Schaaf[1], Ian Paynter[1], Edward Saenz[1], Daniel Genest[1], Francesco Peri[1], Zhan Li[1], Alan Strahler[2], David Clark[3], Deborah Clark[3], William Miranda[4], Leonel Campos[4]

[1] School for the Environment, University of Massachusetts Boston, USA
[2] G eography Department, Boston University, USA
[3] Department of Biology, University of Missouri St. Louis
[4] La Selva Biological Station, Sarapiqui, Costa Rica

Terrestrial lidar scanners (TLS), which utilize light detection and ranging (lidar) to create 3D representations of environments, are increasingly being used to capture properties of interest, such as tree volume for deriving biomass, in a variety of ecosystems. Tropical ecosystems present particular challenges to TLS observation. The high level of geometric complexity and the vertical stratification of tropical forests creates complex occlusion, and the inaccessibility, difficult weather conditions and other deployment constraints limit observation opportunities. TLS optimized for scanning speed, portability and resilience, such as the Compact Biomass Lidar (CBL, University of Massachusetts Boston) can be used to meet these challenges and facilitate high quality TLS observation of tropical forests over meaningful spatial extents. The rapid (33 second) scans permit a large number of scan positions to be acquired in a single acquisition effort, in order to mitigate occlusion. The light weight (3.6kg) of the instrument enables deployment on an 11 meter high tripod, which facilitates sampling at multiple heights at each scanning location.

Herein we present results from TLS observations of a long-term CARBONO site at La Selva Biological Station, Costa Rica. These data have been explored through novel analysis techniques to describe forest structure, as well as describe the TLS observation density and quality. Occlusion patterns are described, and used to infer sampling techniques that will further improve observation quality. The contribution of scans of different heights reveal that vertical scan positions offer not only unoccluded observations above the sub-canopy but also provide unique information about the sub-canopy due to the complexity of view-angles possible in the tropical environment.

Mapping forest degradation in the Valdivian Temperate Rainforest ecorregion

Díaz-Hormazábal I.[1], Chávez R. O. [2], Gutiérrez A. G. [1]

[1] Universidad de Chile, Facultad de Ciencias Agronómicas, Departamento de Ciencias Ambientales y Recursos Naturales, Av. Santa Rosa 11315, La Pintana, Santiago, Chile.
[2] Pontificia Universidad Católica de Valparaíso, Instituto de Geografía, Av. Brasil 2241, Valparaíso, Chile.

Key words: Forest gaps, forest degradation, image segmentation, WorldView3.

Governments have committed to mitigate climate change by reducing forest deforestation and degradation. In developing regions such as southern South America, where large tracks of primary forests still exist, this task is increasingly needed, as people subsistence demands the use of intact forests. However, there is a knowledge gap on 1) where primary forests are located and 2) where forest degradation is occurring. Such information is necessary to support decision making for planning forest management. Here, we present an approach for mapping degradation of primary forests in the Valdivian Temperate Rainforest ecorregion in south-central Chile (39-40°S). We based our analysis on forest gap structure of primary forests using 1) ground-based sampling, 2) automatized identification of gaps using high-resolution satellite images, and 3) upscaling gaps metrics to regional scale using lower resolution Landsat images. We used sub-metric satellite images (50 cm) from four study sites representing primary forests. We segmented the panchromatic band using the Mean-Shift algorithm. We then calculated the Enhanced Vegetation Index (EVI) for each segment and classifyied segments with low EVI as potential gaps. We calculated area of segments distinguished as gaps for each forests. Gap segmentation had an average of 78% concordance with gaps identified in the field. We found a good relation between gap areas estimated from high resolution images to vegetation index obtained from Landsat-8 images allowing us to map the location of forests with low gap areas (i.e. low degradation). Intact forests often had lower gap frequency (e.g. gap area <10% of total forest area). Our analyses suggest that 57.3% of old-growth forests in the study area have some degree of degradation. We propose that primary forests have a canopy structure that make them distinghishable from degraded old-growth forests. Our work is a step forward towards monitoring forests at large spatial scales and a contribution for lowering forest degradation in developing countries.

Modeling aboveground biomass from individual tree LiDAR-derived metrics in tropical forest

Carlos Alberto Silva[1,2,3], Andrew Thomas Hudak[2], Lee Vierling[1], Carine Klauberg[2], António Ferraz[3], Mariano Garcia Alonso[3], Michael Keller[4], Sassan Saatchi[3]

[1] Department of Natural Resources and Society, College of Natural Resources, University of Idaho, (UI), 875 Perimeter Drive, Moscow, Idaho, 83844, USA
[2] USDA Forest Service, Rocky Mountain Research Station, RMRS, 1221 South Main Street, Moscow, ID, 83843, USA
[3] Jet Propulsion Laboratory, California Institute of Technology, Pasadena, CA 91109, USA
[4] USDA Forest Service, International Institute of Tropical Forestry, San Juan, PR, 00926, USA

Keywords: Tree detection, Airborne LiDAR, Biomass, Tropical Forest, Forest Inventory

Tropical forest play an important role in mitigating global warming. Airborne LiDAR (Light Detection and Ranging) has been used to predict aboveground biomass in tropical forest. However, few studies have modeling and predicting tropical forest AGB at plot-level from individual tree LiDAR-derived metrics. The aim of this study was to model and predict AGB at plot-level from individual tree LiDAR-derived metrics in a Brazilian tropical forest. Forest attributes such as tree density and diameter at breast height were measured in 2014 at 84 square plots of 50x50m located in Paragominas, Pará, Brazil. Using previously published allometric equations, tree AGB was computed and then summed to calculate total AGB at each sample plot (TAGB). The LiDAR data also acquired in 2014 were normalized to height aboveground, and individual trees were detected using the Adaptive Mean Shift 3D (AMS3D) algorithm. Individual tree metrics, such as height (TH), crow length (CL), crown radius (CRd), crown ratio (CRt), crown based height (CBH), crown projected area (CPA) and crown volume (CV),

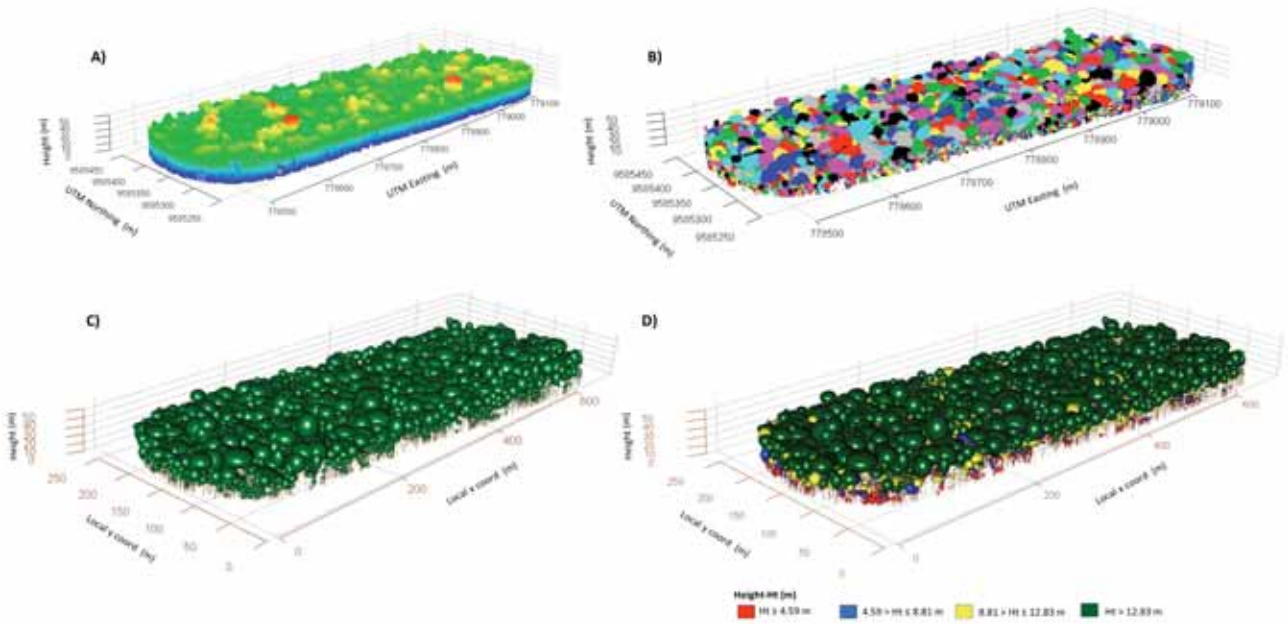

Figure 1. LiDAR point cloud with colour coded by height A) and tree id derived from individual tree detection B); Virtual Forest representation with trees colours coded by a single colour C) and by height D).

were calculated to each single tree using the rLiDAR package, and summarized at plot-level as maximum tree height (MAXTH), mean tree height (MEANTH), mean crown length (MCL), mean crown radius (MCRd), mean crown ratio (MCRr), mean crown based height (MCBH), total crown volume (TCV), and total projected area (TPA). Regression models predicting TAGB from the individual tree LiDAR-derived metrics were developed and evaluated for predictive power and parsimony. The best model from a family of six models was selected based on corrected Akaike Information Criterion (AICc) and assessed through a leave-one out cross validation by the adjusted coefficient of determination (adj.R^2), relative and absolute root mean square error (RMSE) and BIAS. Our findings showed that MAXTH, MCBH, MCRd, and TCV were the most important metrics to predict TAGB, with overall model adj.R^2 of 0.73, absolute and relative RMSE and BIAS of 26.9 and 0.29 Mg/ha and 16.2 and 0.17%, respectively. This study showed that individual tree LiDAR-derived metrics can be used to predict TAGB in tropical forest with acceptable precision. Therefore, we conclude that there is good potential to monitor carbon sequestration in Brazilian Tropical Rain Forest using airborne LiDAR data and individual tree LiDAR-derived metrics.

POSTER

Phenological observations from a hyperspectral camera in the Amazonian Tapajos National Forest

Yhasmin M. de Moura[1], Lênio Soares Galvão[1], Thomas Hilker[2], Cibele H. do Amaral[3], Scott R. Saleska[4], Jin Wu[5], Luiz E. O. C. Aragão[1]

[1]Instituto Nacional de Pesquisas Espaciais (INPE), São José dos Campos - SP, 12227-010, Brazil, [2]University of Southampton, Department of Geography and Environment, Southampton SO17 1BJ, United Kingdom, [3]Federal University of Viçosa, Viçosa - MG, 36570-900, Brazil, [4]University of Arizona, Department of Ecology and Evolutionary Biology, Tucson, AZ 85721, USA, [5]Environmental & Climate Sciences Department, Brookhaven National Lab, Upton, New York, NY, 11973

Keywords: phenology; hyperspectral camera; principal component analysis; tropical ecosystem; mixture model

Understanding seasonal and inter-annual variability of vegetation phenology plays a major role for Earth system modeling. However, scaling field observations of changes in vegetation traits to satellite remote sensing is often challenging due to a mismatch in scale. Near surface camera based phenology can help bridging this gap by using optical principles similar to those used by satellite sensors, but still allowing an interpretation similar to that made by field observations. In this study, we utilized data from a tower-mounted, hyperspectral phenocam imaging system (SOC-710, Surface Optics Corporation, San Diego, CA, US) located at the Tapajós National Forest near Santarem, Pará, Brazil (2.85˚ S, 54.97˚ W) to observe the phenological behavior of a tropical forest ecosystem during the dry season. Seventeen images (4-nm resolution between 385 to 1050 nm) were carefully selected and screened for data quality and clear sky conditions. Reflectance measurements were calibrated using a teflon panel, which was permanently installed within the field-of-view of the camera. Images were acquired at an angle of 45° off-nadir around solar noon to minimize differences of shading effects within the canopy. Principal component analysis (PCA) showed that variations in leaf flushing between July 27 and September 29, 2012 were species-dependent. Using a linear mixture model, we confirmed that differences observed from PCA were expressed in the green vegetation fraction of the hyperspectral images. We conclude that the data analysis of tower-mounted hyperspectral cameras contributes to a better understand of the seasonal phenological signal observed by satellites.

Recent trends of Land Surface Temperature and Vegetation Indexes over the Temperate Rain Forest in Chile

V. Olivares-Contreras, C. Mattar, J.C. Jiménez-Muñoz and A. Gutiérrez.

[1]Laboratory for Analysis of the Biosphere (LAB), Dept. of Environmental Sciences and Natural Renewable Resources, University of Chile, Av. Santa Rosa 11315, La Pintana, Santiago, Chile.
[2]Global Change Unit/Image Processing Laboratory, University of Valencia, Valencia 46980, Spain.
[3]Dept. of Environmental Sciences and Natural Renewable Resources, University of Chile, Av. Santa Rosa 11315, La Pintana, Santiago, Chile.

Key words: Temperate rain forest, land surface temperature, vegetation indexes, Modis, Aysen, Chile.

The current global warming has affected several ecosystems at global scale generating different consequences such as the decrees in carbon stocks and productivity, the increase in mortality and the persistent increment of fire risk. In Chile, one of the most pristine ecosystems is the temperate rain forest located in the Aysén region (43° - 50°S). This rain forest covers more than 4.82 millions of hectare which are mainly located in island and isolated peninsula. This forest has suffered a strong anthropogenic impact during the 30' based on the government policy to introduce grassland through conversion plans from forest to agriculture terrains. More than 6 millions of hectare were burned or affected decreasing the forest land cover and generating a dramatic change in this ecosystem.

The impact of the global warming over the temperate rain forest is unknown. Thus, the aim of this work is to analyze the spatial and temporal land surface temperature and vegetation indexes trends by using MODIS data (MOD11 and MOD13 products) for the period covering 2002 – 2015. The LST, NDVI and EVI were used to estimate the non-parametric trends in the Aysén region (43° - 50°S ; 71 – 77°W) by using the Sen's slope test and to determine the statistical significance applying the Mann-Kendall test. Trends and statistical significance were retrieved pixel by pixel at monthly mean and seasonal periods assuming Summer (December, January and February), Autumn (March, April and May), Winter (June, July and August) and Spring (September, October and November).

Results shown a generalized warming between 43° and 47°S estimated in 1°C/decade. Southern the 47°S the land surface temperature trends were also positive although it was noticed some effects of the spatial resolution of MOD13 generating an impact in te statistical confidence of the trend. In relation to the vegetation indexes, at overall, the trends are positive in the whole region at evaluating NDVI and EVI. Nevertheless, a negative and statistical significance trends were evidenced between 46° – 48°S mainly in 73°W is also retrieved. These results contribute to better understand the dynamic of the Aysén Temperate forest and to show the impact of global warming in the land surface temperature and vegetation trends in this Austral zone of Chile.

ForestSAT 2016

RDD+FREL-FRL and MRV

OTERRA
CENTRO DE ESTUDIOS DE RECURSOS NATURALES
UNIVERSIDAD MAYOR

UNIVERSIDAD MAYOR
para espíritus emprendedores

Facultad de Ciencias
ESCUELA DE INGENIERÍA FORESTAL

Assessing the carbon and water balance of Boreal forests using a process-based model driven by satellite images

Minunno F., Mutanen T., Aurela M, Häme T, Liski Y, Vesala T, Mäkelä A.

Keywords: Process-based modelling, Satellite Images, Carbon and water balance, Boreal forests, data assimilation.

Abstract

Earth Observation (EO) data can potentially be used to drive vegetation models and improve simulated carbon and water fluxes over large areas.

The objective of this work is to test the reliability of a process-based model in predicting the carbon and water balance of Boreal forests when driven by EO measurements. We used a carbon-balance based growth model combined with a soil carbon model.

After being calibrated and tested with ground data from various data sources the combined model was run using LANDSAT data collected in 2015 at 20m resolution. Model predictions were validated at two eddy-covariance sites: Hyytiälä in southern Finland and Sodankylä in Finnish Lapland.

At Hyytiälä, model predictions of annual gross primary production (GPP, 1143.9 gC m^{-2} y^{-1}), annual net ecosystem exchange (NEE, -205.6 gC m^{-2} y^{-1}) and evapotranspiration (ET, 314.6 mm y^{-1}) were within the ranges measured at the eddy-site.

At Sodankylä GPP (573.1 gC m^{-2} y^{-1}) and ET (236.4 mm y^{-1}) predictions were consistent with the measurements, while NEE (-87.27 gC m^{-2} y^{-1}) was overestimated.

On this basis, we discuss the opportunities and challenges of using EO data for large scale simulations with the aim of monitoring carbon and water fluxes.

Comparison of local EO-based dense humid and dry forest cover and change area estimates in the southwest forest massif of Central African Republic using the UMD global dataset

Christophe Sannier[1], Ron Mc Roberts[2], Loïc Faucqueur[1] & Hajar Benelcadi[1]

[1] SIRS, Parc de la Cimaise I, 27 rue du Carrousel 59650 Villeneuve d'Ascq France
[2] Northern Research Station, U.S. Forest Service, Saint Paul, Minnesota, USA

Keywords: Model assisted regression, REDD+, national forest monitoring systems

The southwest forest massif of Central African Republic is covered by dense humid forest but also by substantial dry forest areas. Most of current forest monitoring studies focuses on tropical rain forest because of their ecological interest and high carbon stocks. But about 42% of tropical forests around the world are considered as seasonally dry. Therefore, dry Forest monitoring should not be overlooked because it is found over very large areas and is one of the most seriously threatened forest types. Indeed, the removal of dry forests potentially contributes to a significant proportion of the 7-20% of the total greenhouse gas emissions known to originate from deforestation and forest degradation. However, monitoring of dry forest from remote sensing is a challenge due to its phenological variability and the lack of hard boundaries between forest and non-forest.

An EO-based, IPCC compliant Land Use classification of the area was developed that distinguished between dense humid and dry forest classes was developed for an area of approximately 70,000km² in southwest CAR in collaboration with the Ministry of environment. In addition, a probability sample was developed to calibrate the identification of the lower boundary of the forest category (i.e. 30% forest cover) based on the visual estimation of percent tree cover from Very High Spatial Resolution satellite imagery. This dataset was also used to calibrate the University of Maryland (UMD) Global Forest Change (GFC) data and optimal thresholds were determined based on the comparison of tree cover percentage calibration data with map data to match the selected national forest definition. Then, a model assisted regression was developed based on a separate probability sample over the study area.

Wall-to-wall mapping provides a comprehensive assessment of forest resources and input to land use plans for management purposes, but wall-to-wall approaches require specialized equipment and staff that are often not available. The UMD GFC map products provide an alternative for tropical countries wishing to develop their own wall-to-wall forest monitoring map products but without the resources to do so. However, these maps were produced at global scale and cannot be used directly for national/regional mapping because they need to comply with a selected forest definition. This study provides an approach on how the UMD GFC map can be used locally and a quantification of the loss of precision is made. Initial results suggest that the number of sample units would need to be increased by 44% for the area estimates based on the UMD GFC to be equivalent to the locally based map. The cost of collecting these additional samples is discussed with a view to providing guidelines on whether the additional cost is worthwhile in relation to (i) the additional income generated through a performance based payment scheme, and (ii) the cost of developing a local based capacity to map forest cover.

Comparison of local EO-based dense humid and dry forest cover estimates with the UMD global dataset in the Central African Republic

Hajar Benelcadi[1], Christophe Sannier[1], Loïc Faucqueur[1] & Ron Mc Roberts[2]

[1] SIRS, Parc de la Cimaise I, 27 rue du Carrousel 59650 Villeneuve d'Ascq France
[2] Northern Research Station, U.S. Forest Service, Saint Paul, Minnesota, USA

Keywords: REDD+, Model Assisted Regression, forest estimates, dry forest, UMD GFC, relative efficiency

Abstract

This study provides an approach on how the UMD GFC map can be used locally and a quantification of the loss of precision is made. Initial results suggest that the number of sample units would need to be increased by 48% for the area estimates based on the UMD GFC to be equivalent to the locally based map. The cost of collecting these additional samples is discussed with a view to providing guidelines on whether the additional cost is worthwhile in relation to (i) the additional income generated through a performance based payment scheme, and (ii) the cost of developing a local based capacity to map forest cover.

Introduction

Most of current forest monitoring studies focuses on tropical humid forest because of their ecological interest and high carbon stocks. But about 42% of tropical forests around the world are considered as seasonally dry. Therefore, dry Forest monitoring should not be overlooked because it is found over very large areas and is one of the most seriously threatened forest types. The removal of dry forests potentially contributes to a significant proportion of the total greenhouse gas emissions known to originate from deforestation and forest degradation. However, monitoring of dry forest from remote sensing is a challenge due to its phenological variability and the lack of hard boundaries between forest and non-forest. The REDD+ mechanism is included in the Paris agreement representing the main outcome of the UNFCCC COP21 after a long round of negotiations, as a key instrument to enhance the forests sinks and preserve the forest. Many countries having the tropical forest biome engaged or willing to engage under the REDD+ mechanism are developing a National Forest Monitoring System to assess and monitor their forests. However REDD+ is a result based mechanism. Meaning that the payments will be made to countries providing convincing evidence that reduction targets have been achieved. The evidence must include accurate and precise estimates of forest area that will be submitted by countries as reference emissions levels to be reviewed as part of the Monitoring Reporting and Verification process of the REDD+ mechanism. Wall-to-wall mapping provides a comprehensive assessment of forest resources and input to land use plans for management purposes, but wall-to-wall approaches require specialized equipment and staff that are often not available. The UMD GFC map products provide an alternative for tropical countries wishing to develop their own wall-to-wall forest monitoring map products but without the resources to do so. However, these maps were produced at global scale and cannot be used directly for national/regional mapping because they need to comply with a selected forest definition. Therefore, this paper aims to assess if global datasets such as the University of Maryland (UMD) Global Forest Change (GFC) data can be used to fast track the development of National Forest Monitoring Sys-

tem (NFMS) in countries with complex landscapes such as the Central African Republic in which several biomes including dense tropical rainforest and dry forest are present.

Study site

The study area is located in the southwest forest massif of Central African Republic represented by 3 provinces: Sangha Mbaéré, Lobaye, Ombella-M'Poko. The total area is ~ 70 000 km². The study site was selected because covered by dense humid forest but also by substantial open dry forest areas. This was part of the European FP7 project that was conducted in collaboration with GAF AG and with the local Ministry of Environment and Ecology (MEE). The adopted forest definition is as follow: 1ha minimum area, >30% tree cover, tree height >5m at maturity. Tree plantations are excluded from forest area.

Data

A set of VHR data was acquired circa 2010 as part of the FP7 REDDAF project through the ESA Data Warehouse according the location of Primary Sample Unites (PSUs) from the probability sampling design. All VHR Data were pan-sharpened and resampled to an output pixel size of 0.5 meters to provide a homogeneous dataset optimized for visual interpretation.

Methodology

An IPCC compliant Land Use classification was developed that distinguished between dense humid and dry forest classes. In addition, a probability sample was implemented to calibrate the identification of the lower boundary of the forest category (i.e. 30% forest cover) based on the visual estimation of percent tree cover from Very High Spatial Resolution satellite imagery. This dataset was also used to calibrate the University of Maryland (UMD) Global Forest Change (GFC) data and optimal thresholds were determined based on the comparison of tree cover percentage calibration data with map data to match the selected national forest definition as suggested by Sannier et al (2016). Then, a model assisted regression (McRoberts et al. 2012) was developed based on a separate probability sample over the study area.

Processing of UMD GFC data to match selected forest definition in CAR for 2010

To process the UMD GFC dataset the following chain is applied:

1) Application of the 30% tree cover percentage threshold to the 2000 UMD GFC tree cover percentage map data 2000
2) Integration of « Forest Gains» within the NF class defined
3) Integration of « Forest Losses » within the F class defined
4) The circa 2010 F/NF map results from the combination of the 2000 F/ NF map with the forest gain and losses
5) A 1 ha MMU filter is applied to both the F and NF class

VHR data sampling design

The probability sampling design was performed with simple random selection of sample units. A total of 46 segment of 5*5km based on an unaligned systematic random sample over the study area (~1.5%). From 46 segments: a) 16 segments to calibrate the GFC dataset and b) 30 segments to estimate the forest cover proportion. A set of 10 segments of 1 hectare were randomly selected within each 25 originals 5*5km segments for a total of 250 plots of 1ha. A

Table1: VHR data acquired circa 2010 processed and photo interpreted as an alternative of ground truth data

Sensor	Number of scenes	Resolution (m)
GEOEYE	22	MS: 1.65/Pan:0.41
Ikonos	4	MS 3.2/Pan:0.82
Worldview2	18	MS: 1.85/Pan:0.46
QuickBird	2	MS: 2.4/Pan:0.61

number of 49 systematic pixels by plots were selected to be interpreted into Tree/ No-Tree to extract an estimation of the tree cover within each 1ha plots

Results

Adjustment of the GFC Forest threshold

The VHR tree cover data and the GFC tree cover data set were correlated to determine the adjusted forest threshold of GFC data corresponding to 30% tree cover over the VHR data (Sannier et al. 2016).

Once the threshold determined (figure 1), we apply it to the GFC tree cover map of the year 2000. And to match the 2010 national data, we integrate the gain and the forest losses and we apply a 1 ha MMU so that the adjusted GFC map can be conform to the adopted national forest map definition. The GFC threshold of 51% appears to be better corresponding to a tree cover of 30%.

Area uncertainty estimates for National and GFC maps and the relative efficiency

Maps suffer from bias and the method of model assisted regression (Sannier et al. 2014) takes it into consideration and correct the estimate of forests. Forest cover and forest cover change estimates can be produced based on samples alone (Direct estimate). Observations from reference samples and the map can be combined to improve the precision of

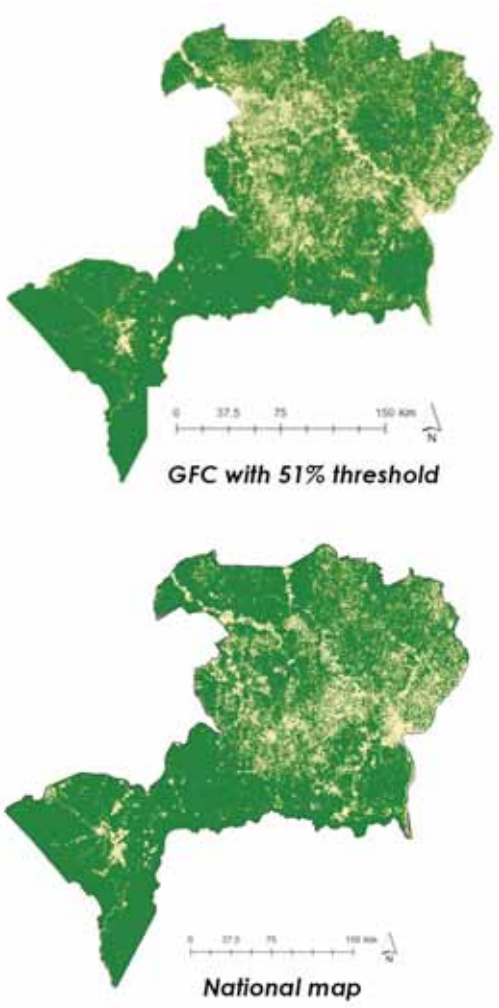

Figure2: The national map with 30% tree cover and the equivalent GFC map adjusted to 51% tree cover

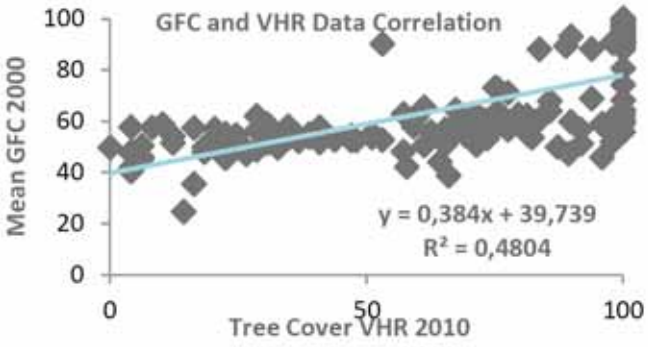

Figure1: Scatterplot of average GFC values over 1ha plots against estimated tree cover values from VHR imagery

estimates (Model Assisted Regression), see (1) and (2):

$$\hat{\mu}^{MAR} = \hat{\mu}^{map} - B\hat{i}as\left(\hat{\mu}^{map}\right) \quad (1)$$

$$V\hat{a}r\left(\hat{\mu}^{MAR}\right) = \frac{1}{m(m-1)} \sum_{i=1}^{m} \left(\Delta_i - \overline{\Delta}\right)^2 \quad (2)$$

The ratio between the variances of the direct area estimate and the map based estimate gives the relative efficiency (McRoberts et al. 2016) of the map which is:

$$t_1 = \frac{V\hat{a}r(\mu)}{V\hat{a}r(\mu_{map})}, \qquad t = \frac{V\hat{a}r(\mu_{GFCmap})}{V\hat{a}r(\mu_{Nationalmap})}$$

With the national map we are underestimating the forest area with nearly 4205 km², but this is less than applying the 30% threshold uncalibrated GFC global map which is overestimating the forest proportion with 8491km². However we have a relative efficiency of more than 2, which mean that direct estimate variance of the national map is higher than the model assisted estimate and the number of sample units would need to be increased by a factor of 2 if the same level of precision was to be achieved with samples alone as compared to the model assisted approach combining the sample units with the national map (table2). The calibrated GFC seems to reduce the map bias compared to the national map. This means that the calibration procedure effectively works. However, the 95% Confidence intervals are considerably wider compared with the National map resulting in a lower relative efficiency (Table2). In fact it is possible to compute the relative efficiency of the adjusted GFC map versus the national map, we would need 48% more samples to have the same level of uncertainty to that of the national map.

The Cost of collecting Additional reference data set

The use of UMD GFC will be economically efficient if the cost of collecting the additional n1-n samples is greater than the cost of the National map minus the cost of GFC data processing, given by:

$$n(t-1)p > M$$

		National	GFC30	GFC51
Study area	(km²)	70 391		
Direct Estimate	(km²)		6010 8	
	(%)		85,4	
Direct Estimate at 95% Confidence Interval	(km²)		±857	
	(%)		±1,21	
Map Bias	(km²)	-4205	8491	-3699
	(%)	5,97	12.06	5.26
MAR Estimate	(km²)	61 328	59 429	60 402
	(%)	87.1	84,4	85.8
MAR Estimate at 95% Confidence Interval	(km²)	±529	±802	±645
	(%)	±0.75	±1.14	±0.91
Relative efficiency without map		2.62	1.13	1.76
Relative efficiency of national vs GFC51		1.48		

Table2: Results of the Model Assisted regression estimates and the relative efficiency to compare the National map, the GFC at 30% threshold and the adjusted GFC

t<1, then μ_{GFCmap} has smaller variance than $\mu_{Nationalmap}$ and $\mu_{Nationalmap}$ is less efficient than μ_{GFCmap}.

n is the original sample size, p is the cost of acquiring each additional sample observation and M is the additional cost of producing the national map compared to GFC.

For this case study:

- n=30 segments, t=1.48,
- With an image costs= 25 $ /km2, (min 25km2 for archived image + sample interpretation) or 35$/km2 and (min 100 km2 for new acquisition+ sample interpretation).
- P= 17500-98000 this covers quite a range depending on whether the VHR imagery is available from an archive or new acquisition need to be programmed.

The use of the UMD GFC data will be economical if P is less than the cost of producing the national map minus the cost of processing the UMD GFC data

Conclusions

UMD GFC data set can be processed for producing national forest cover estimates. In addition, the calibration procedure is effective and reduces substantially map bias. 95% Confidence Intervals greater by about 20% compared with that of national data for forest cover area. To reach the same level of accuracy and so additional reference data is required. UMD GFC is economical if the cost of producing the national map minus the cost of processing the UMD GFC is greater than acquiring and processing new reference samples. However, additional benefits may still be gained from producing the map at national level such as the development of a national capacity in this field, sovereignty and increase level of details.

References:

McRoberts, R. E., Vibrans, A. C., Sannier, C, Næsset, E, Hansen, M. C, Walters, B. F., Lingner, D.V. (2016). Comparison of methods toward multi-scale forest carbon mapping and spatial uncertainty analysis: combining national forest inventory plot data and landsat TM images. Revue canadienne de recherche forestière, 2016, 46(7): 924-932, 10.1139/cjfr-2016-0064

McRoberts, R. E., & Walters, B. F. (2012). Statistical inference for remote sensing-based estimates of net deforestation. Remote Sensing of Environment, 124, 394–401

Sannier C, McRoberts RE, Fichet L-V. 2016. Suitability of Global Forest Change data to report forest cover estimates at national level in Gabon. Remote Sens. Environ. 173: 326-338

Sannier C, McRoberts R A, Fichet LV and Massard K. Makaga R. (2014) Using the regression estimator with Landsat data to estimate proportion forest cover and net proportion deforestation in Gabon.

Disentangling recent patterns in litter fall of European forests with remote sensing data across a continental scale

Mathias Neumann[1], Hubert Hasenauer[1]*
[1] Institute of Silviculture, Department of Forest and Soil Sciences, University of Natural Resources and Life Sciences, Vienna, 1190, Austria

Key words: climate change, NPP, evapotranspiration, LAI, decomposition, nutrients, MODIS, satellite

Remote sensing data is increasingly used for studying the Earth's vegetation across large scales. Forests are particular interesting due to their key role in the global carbon cycle and ongoing climate change. By conducting photosynthesis forests allocate atmospheric carbon absorbed via the stomata and water and nutrients over the roots into their organs such as stem, branches or foliage. Litter fall is important for relocating nutrients from the canopy back into the soil and thus plays an important role in the global carbon cycle by accounting for approximately one third of Net Primary production within forests. Although the role of litter and its decomposition process is evident, it remains a poorly understood process due its high stochasticity and effort to obtain litter fall data. In this study we describe the current spatial and temporal patterns of litter fall data in Europe, test state-of-the-art methods in assessing litter fall estimates and provide a method to enhance the accuracy of litter fall predictions with remote sensing data. For our analysis we obtain litter fall data from the ICP Forests Level 2 network across European forests covering 323 plots and the time period 2000 to 2012. This data set has never been used for such an analysis. After a quality control and a data harmonization, we calculated a mean annual litter fall (total and foliage) of 214 gram carbon m^{-2} $year^{-1}$, equal 38 % of Net Primary production (NPP) for European forests (foliage litter fall 129 gC m^{-2} $year^{-1}$ equal 22%). We detected a significant positive trend between 2000 to 2012 (increase per year 3.4 gC m^{-2} $year^{-1}$, $p<0.001$) which is consistent with observations from the 20th century. Our results suggest that there is an ongoing increase in litter fall over the last 100 years which could be due to climate change impacts. The results support previous research that air temperature may be a predictor for litter fall both spatially and temporally. Combining our data with the latest remote sensing products (Leaf Area Index, NPP and Evapotranspiration using MODIS data) reveal, that remote sensing data may be used to enhance spatial predictions of litter fall, which would allow temporal explicit assessments of litter fall in the global carbon cycle.

References:

Holland, E. A., Post, M. W., Matthews, E., Sulzman, J., Staufer, R., & Krankina, O. (2015). A Global Database of Litterfall Mass and Litter Pool Carbon and Nutrients. Data set. Available online [http://daac.ornl.gov] from Oak Ridge National Laboratory Distributed Active Archive Center, Oak Ridge, Tennessee, USA. http://doi.org/10.3334/ORNLDAAC/1244

Liu, C., Westman, C. J., Berg, B., Kutsch, W., Wang, G. Z., Man, R., & Ilvesniemi, H. (2004). Variation in litterfall-climate relationships between coniferous and broadleaf forests in Eurasia. Global Ecology and Biogeography, 13(2), 105–114. http://doi.org/10.1111/j.1466-882X.2004.00072.x

Mu, Q., Zhao, M., & Running, S. W. (2011). Improvements to a MODIS global terrestrial evapotranspiration algorithm. Remote Sensing of Environment, 115(8), 1781–1800. http://doi.org/10.1016/j.rse.2011.02.019

Neumann, M., Moreno, A., Thurnher, C., Mues, V., Härkönen, S., Mura, M., Bouriaud, O., Lang, M., Cardellini, G., Thivolle-Cazat, A., Bronisz, K., Merganic, J., Alberdi, I., Astrup, R., Mohren, F., Zhao, M., & Hasenauer, H. (2016). Creating a Regional MODIS Satellite-Driven Net Primary Production Dataset for European Forests.

Remote Sensing, 8(554), 1–18. http://doi.org/10.3390/rs8070554

Pitman, R., Bastrup-Birk, A., Breda, N., & Ratio, P. (2010). MANUAL on methods and criteria for harmonized sampling, assessment, monitoring and analysis of the effects of air pollution on forests Part XIII Sampling and Analysis of Litterfall (p. 16).

Estimating the dynamics of carbon stocks in forests with remote sensing data

Michele Dalponte, Lorenzo Frizzera, and Damiano Gianelle

Dept. of Sustainable Agro-ecosystems and Bioresources, Research and Innovation Centre, Fondazione E. Mach, Via E. Mach 1, 38010 San Michele all'Adige (TN), Italy

Forest aboveground biomass is increasing and consequently the carbon stored in these ecosystems. This increase is due to many factors. In the Alps, for example, a reduction in the agricultural exploitation of mountain areas decreased the areas used as grasslands or pastures, and new forest areas appeared. Climate change issues have also responsibilities: as an example the increase of nitrogen depositions and/or CO_2 increased forest productivity. Remote sensing data can be really useful in predicting the changes of aboveground biomass (and thus carbon) over time. In this study we will estimate forest growth, and carbon stocks dynamics, of a forest area in the Alps.

The study site, an evergreen forest, is located in Lavarone (Trento) in the Italian Alps. In this area 50 field plots were located and a survey of DBH, height, and species was carried out in 2007, and it will be repeated in summer 2016. Moreover in 20 trees the annual growth was continuously monitored by means of dendrometers. The main species are *Picea abies* L. Karst., *Abies alba* Mill., and *Fagus sylvatica* L.. Remote sensing data were acquired over the study site in 2007, 2011, and 2015. In particular airborne laser scanning (ALS) data with more than 10 pts/m^2, and hyperspectral data were acquired in all the three dates. Other remote sensing data (SAR) will be also acquired from data archives.

The forest increment will be estimated at plot level and at individual tree crowns (ITC) level. The individual tree crowns delineation will be carried out on the airborne laser scanning (ALS) data using the R library *itcSegment*. The variation in time will be estimated directly or by means of comparison among estimations at different dates. Different remote sensing data will be used both alone and combined together.

Linking Landsat 8 and forest inventory data for local biomass mapping in open canopy woodlands

Belachew Gizachew[1a], Svein Solberg[1], Erik Næsset[2], Terje Gobakken[2], Ole Martin Bollandsås[2]; Johannes Breidenbach[1]; Eliakimu Zahabu[3], Ernest William Mauya[3]

[1]Norwegian Institute of Bioeconomy Research, Post Box 115, 1431, Ås, Norway
[2]Norwegian University of Life Sciences, Department of Natural Resource Management, Post Box 5003, 1432 Ås, Norway
[3]Sokoine University of Agriculture, Faculty of Forestry and Nature Conservation, P.O. Box 3009, Chuo Kikuu, Morogoro, Tanzania.
[1a]Corresponding author

Keywords: AGB, Mapping, Modeling, Miombo woodlands, REDD+, EVI

Abstract

REDD+ implementation requires estimates of forest biomass, an input to estimate carbon emissions. Field inventory and or remote sensing are the expected sources of data for a functional Monitoring, Reporting and Verification (MRV) in the context of REDD+. By linking Landsat 8 derived spectral indices to forest inventory data, a linear mixed effects models for the above ground biomass (AGB) was developed. The model is then applied to composite images of selected districts in Miombo woodlands in Tanzania, to further develop a 30 m resolution AGB map. Inventory data consisted of tree measurements from 500 plots, and the Landsat 8 data comprised two Climate Data Record (CDR) images covering the inventory area. Among a list of spectral indices and band responses tested, the Enhanced Vegetation Index (EVI) correlated most strongly (rho = 0.44) to the AGB. The linear model between the AGB and Landsat 8 derived EVI had a RMSE of 25 t/ha (49%). We mapped the distribution of AGB in 13 sub-districts and compared the AGB density to that of default values of the IPCC, and three recent pan-tropical AGB maps. The low biomass in the miombo woodlands, and the absence of a spectral data saturation problem suggested that Landsat 8 data are suitable sources of auxiliary information for carbon monitoring for low-biomass, open-canopy miombo woodlands.

Mapping historical canopy cover change and recovery using Landsat time series imagery (1972-2015)

Jody C. Vogeler [1], Justin D. Braaten [2], Michael J. Falkowski [3], Robert A. Slesak [4]

[1] Department of Forest Resources, University of Minnesota, St. Paul, MN, USA
[2] Department of Forest Ecosystems and Society, Oregon State University, Corvallis, OR, USA
[3] Department of Ecosystem Science and Sustainability, Colorado State University, Fort Collins, CO, USA
[4] Minnesota Forest Resources Council, St. Paul, MN USA

Keywords: Landsat time series, forest canopy cover, forest disturbance mapping, Minnesota

Monitoring historic trends in change and recovery of forest canopy cover can provide insights into multiple aspect of ecosystem health and functioning. Information on disturbance and recovery events through time may help predict the effects of management and climatic change on forest systems into the future as well as aiding in the modeling and monitoring of current wildlife habitat relationships and historic populations trends. The objectives of this study were to: (1) create historic maps of annual predicted forest canopy cover using Landsat time series imagery from 1972-2015 for the state of Minnesota; and (2) characterize historic trends in forest change and recovery for the study area.

Our project utilizes the full value of the Landsat archive by calibrating and incorporating imagery dating back to 1972 to provide >40 years of comparable annual spectral trends for the state of Minnesota. We introduce an R package, LandsatLinkr, which automates the pre-processing steps necessary for annual cloud-free atmospherically and geographically corrected tasseled cap indices calibrated between Landsat platforms including the early MSS sensors. We used the LandTrendr algorithm to smooth and segment the tasseled cap trends. These smoothed annual tasseled cap composite images were then correlated with Minnesota Forest Inventory and Analysis plots and 4-band NAIP imagery to model forest canopy cover. The best model was then applied to the entire stack of time series Landsat composites to map annual predicted forest canopy cover for over 4 decades. In addition to the creation and validation of these annual canopy cover maps, the cover model was also incorporated into the change labeling portion of the LandTrendr algorithm to better characterize trends in forest change and recovery rates.

The products from this project include statewide annual predicted forest canopy cover maps for the past 4 decades in addition to maps of classified forest change (e.g. fast, slow, high intensity, low intensity) and rates of recovery from the various magnitudes of disturbance. These mapping products are currently being incorporated into a range of forest ecosystem research and management applications including: modeling wildlife habitat and population trends; effects of various harvest methods and patterns on post-harvest forest characteristics and recovery rates; and creating maps classifying the agent of disturbance (e.g. harvest, fire, insect, windfall, urbanization, etc.) for the state of Minnesota.

Resumen Ejecutivo de Nivel de Referencia de Emisiones Forestales / Nivel de Referencia Forestal Subnacional de Chile

Javier Cano Martin , Angelo Sartori Ruilova[2]
Unidad de Cambio Climático y Servicios Ambientales (UCCSA), Gerencia de Desarrollo y Fomento Forestal (GEDEFF), Corporación Nacional Forestal (CONAF).

Profesional Responsable Contabilidad de Carbono y Sistema MRV, UCCSA, GEDEFF. javier.cano@conaf.cl
[2] Jefe UCCSA, GEDEFF, CONAF. angelo.sartori@conaf.cl

Justificación

Cambio Climático

Según la Organización Meteorológica Mundial la concentración atmosférica media mundial de CO_2 ha aumentado en un 41% en los últimos 50 años, superando la barrera de las 400 ppm de concentración de CO_2 lo que representa la mayor concentración en los últimos 800.000 años.

El Panel Internacional de Expertos de Cambio Climático (IPCC) ha identificado variaciones en indicadores meteorológicos derivados del aumento de concentración de Gases de Efecto Invernadero (GEI) durante el Siglo XX, destacando el aumento general de temperatura, días calurosos, precipitaciones fuertes y frecuencia e intensidad de las sequías y una disminución de los días de frío y heladas, estos indicadores en las variaciones climáticas han sido estudiados ampliamente, existiendo un consenso científico general.

En Chile estas alteraciones han sido percibidas durante los últimos años, provocando un aumento de concientización en la sociedad ante las potenciales amenazadas producto de variaciones climáticas derivadas de las actividades humanas que alteran la composición de la atmósfera global y conllevan al denominado cambio climático.

El Rol de los Bosques

La principal causa del aumento de CO_2 (principal Gas de Efecto Invernadero) en la atmósfera es el uso de combustibles fósiles, mientras que la deforestación y degradación de los bosques representa, según IPCC, el 17.3% de las emisiones GEI a nivel mundial.
Para el caso de América Latina, la representatividad de las emisiones de CO_2 producto de la deforestación y degradación de los bosques supera el 40% (CEPAL, basado en datos del World Resources Institute, 2010) Este porcentaje adquiere mayor relevancia si se une a la capacidad de los bosques para capturar y fijar carbono atmosférico su relevancia como medio de suministro de servicios ecosistémicos, provocando que muchos de los esfuerzos realizados a nivel global se concentren en identificar y poner en práctica estrategias que frenen la deforestación, degradación de los bosques, fomento de la conservación, manejo forestal sustentable e incremento de masas forestales.

REDD+

En el marco internacional, durante los últimos 20 años la estructura de estas políticas ha establecido organismos e institucionalidad globales que marcan las políticas a seguir. De especial interés para Chile son las directrices establecidas en el Marco de REDD+ de Varsovia, que determinan que cualquier país que quiera acceder al pago por resultados basados en desempeño, en términos de reducción de emisiones y/o incremento de absorciones de carbono forestal, deberá desarrollar cuatro ejes centrales que se corresponden con: 1) contar con una estrategia país que defina los enfoques de políticas para promover incentivos positivos, 2) elaborar un nivel de referencia de carbono forestal, 3) diseñar e implementar un sistema de monitoreo de emisiones y capturas de carbono y 4) velar por el cumplimiento de consideraciones sociales y ambientales, conocidas como salvaguardas en el contexto global.

ENCCRV

En este contexto, con el objetivo de apoyar la recuperación y protección del bosque nativo y

formaciones xerofíticas, así como potenciar el establecimiento de formaciones vegetacionales en suelos factibles de ser plantados como medidas de mitigación y adaptación a los efectos del cambio climático y lucha contra la desertificación, CONAF, está desarrollando e implementando la Estrategia Nacional de Cambio Climático y Recursos Vegetacionales (ENCCRV) que pretende alcanzar dicho objetivo mediante el diseño e implementación de un mecanismo estatal que facilite el acceso de las comunidades y propietarios de bosques, formaciones xerofíticas y suelos factibles de ser plantados, a los beneficios asociados a los servicios ambientales de estos ecosistemas. Paralelamente, la ENCCRV, pretende satisfacer los compromisos internacionales que ha asumido Chile en materia de cambio climático asociado a los bosques y lucha contra la desertificación, donde destaca el compromiso del Gobierno ante la CMNUCC de manejar sustentablemente y recuperar 100.000 hectáreas de bosque, así como forestar otras 100.000 hectáreas, principalmente con especies nativas, en el período 2016/2030.

Nivel de referencia

Los sistemas forestales/vegetacionales chilenos
Chile, debido a sus características geográficas (suelo, clima, latitud, distribución de la población, entre otras) posee una fuerte diversidad de ecosistemas forestales, con presencia de pequeños bosques de altura en el altiplano y formaciones xerofíticas en la zona norte; bosques esclerófilos en zona central; bosques dominados por especies caducifolias del género Nothofagus en la zona de clima húmedo templado, donde se insertan formaciones dominadas por coníferas milenarias como la Araucaria y el Alerce, para transitar a bosques compuestos por especies perennes, denominado siempreverde, en el área de la Selva Valdiviana y grandes extensiones de bosques de lenga en las regiones más australes del país.

Cada uno de estos bosques y formaciones xerofíticas representan un valioso aporte para la mitigación, en base a la reducción de emisiones e incremento de capturas de CO_2, y la adaptación a los efectos del cambio climático como medio de provisión de agua y refugio, conservación de la biodiversidad, retención de suelo, limitante del avance de la desertificación, etc.

Significado y relevancia

El Nivel de Referencia de Emisiones Forestales / Nivel de Referencia Forestal (NREF/NRF), tiene como objetivo caracterizar las emisiones históricas de Gases de Efecto Invernadero (GEI) por Deforestación y degradación de los bosques, así como las absorciones producto del aumento de existencias de reservas de carbono forestal, la conservación y el manejo sustentable de los bosques y las proyecta hacia el futuro, con la intención de medir el desempeño del enfoque de políticas asociadas a REDD+.

Durante el mes de enero de 2016, Chile consignó el NREF/NRF de carácter subnacional, ante la Convención Marco de las Naciones Unidas sobre Cambio Climático (CMNUCC), que caracteriza las emisiones históricas de GEI por Deforestación y Degradación de los bosques, así como las absorciones producto del aumento de existencias de reservas de carbono forestal, la conservación y el manejo sustentable de los bosques y las proyecta hacia el futuro, para las regiones del Maule a Los Lagos entre los años 1997 y 2013, con la intención de medir el desempeño del enfoque de políticas asociadas a REDD+.

El NREF/NRF fue elaborado siguiendo los criterios determinados por el Panel Intergubernamental de Expertos en Cambio Climático (IPCC) y mantiene congruencia con el Inventario Nacional de Gases de Efecto Invernadero (INGEI) utilizando las mismas fuentes de información, principalmente el Catastro de Bosque Nativo y sus actualizaciones, el Inventario Forestal Continuo y Estadísticas de Incendios Forestales.

En la actualidad el documento presentado está siendo sometido a revisión de expertos internacionales independientes que propondrán mejoras y ajustes para optimizar los métodos e identificar las brechas de información existentes. Durante este período de revisión, CONAF, en conjunto con el equipo de apoyo técnico, tomará las acciones pertinentes para satisfacer las demandas de la CMNUCC CMNUCC entre las que ya se han identificado las de mayor relevancia, como son: 1) la creación de un sistema de registro espacial para la delimitación de áreas bajo Manejo Forestal que permitan estimar el flujo de

carbono y estimar el Nivel de Referencia de Manejo Sustentable, y 2) levantar información espacial de uso de la tierra, complementaria al Catastro, para homogeneizar la temporalidad de los datos y el periodo de referencia.

De forma paralela se trabajará para extender el Nivel de Referencia de escala subnacional a escala nacional, con el objetivo de presentar el NREF/NRF que registre las emisiones y absorciones de las cinco actividades REDD+ a nivel nacional.

Equipo Técnico

El NREF/NRF Subnacional de Chile ha sido elaborado por CONAF, a través de un trabajo conjunto liderado por la Unidad de Cambio Climático y Servicios Ambientales (UCCSA) y el Departamento de Monitoreo de Ecosistemas Forestales, con el apoyo técnico del Banco Mundial, la Consultora Winrock Internacional, el Instituto Forestal (INFOR), la Universidad Austral de Chile (UACH) y las agencias de Naciones Unidas, FAO, PNUMA y PNUD, adscritas al Programa de REDD de Naciones Unidas (UN-REDD).

Área de contabilidad

CONAF, ha decidido focalizar los esfuerzos para la generación del Nivel de Referencia subnacional en la zona Centro-Sur de Chile, desde la Región del Maule hasta la Región de Los Lagos, área que cuenta con una alta concentración y la mayor diversidad de bosques del país, una fuerte presión antrópica y con gran potencial para la reducción/absorción de emisiones de GEI relacionadas con los bosques y capacidad de producir beneficios ambientales no relacionados con el carbono.

Conceptos clave

Bajo el contexto de REDD+, que rige el NREF/NRF, Chile definió como bosque aquellas tierras establecidas como Bosque Nativo en la legislación vigente y determinó los conceptos nacionales para las cinco actividades REDD+: Deforestación, Degradación, Aumento de existencias, Conservación Forestal y Manejo Sustentable.

- Para el cálculo de emisiones por Deforestación fue estimada la superficie de bosque nativo convertida a otros usos.
- En el caso de la Degradación Forestal se consideraron las emisiones por pérdida de biomasa en los bosques que permanecen como tal, las emisiones de CH_4 y N_2O producto de la combustión en incendios forestales, así como las emisiones por sustitución de bosque nativo por plantaciones monoespecíficas de carácter industriales.
- El Aumento de existencias registra aquellas absorciones producto de la forestación y la restitución de bosque nativo, así como las absorciones producidas por los bosques que permanecen bosques durante el periodo analizado.
- Para determinar el Nivel de Referencia de Conservación Forestal, fue analizado el flujo de carbono en los bosques que permanecen bosques en áreas bajo conservación formal.
- Debido a la falta de información oficial del país que permita localizar y delimitar espacialmente las áreas sujetas a Manejo Sustentable, esta actividad no fue integrada en el NREF/NRF, si bien las emisiones y absorciones producto de manejo sí son registradas dentro de las actividades de Degradación y Aumento de Existencias.

Métodos

El NREF/NRF fue elaborado siguiendo los criterios determinados por el Panel Intergubernamental de Expertos en Cambio Climático (IPCC) y mantiene congruencia con el Inventario Nacional de Gases de Efecto Invernadero (INGEI) utilizando las mismas fuentes de información, principalmente el Catastro de Bosque Nativo y sus actualizaciones, el Inventario Forestal Continuo y Estadísticas de Incendios Forestales.

La disponibilidad de información, hace que no se pueda contar con un período de referencia estandarizado para las cinco regiones, pero se estandarizaron los datos para determinar las emisiones y absorciones de CO_2e entre los años 1997 y 2013.

Los métodos aplicados siguen las directrices IPCC de mayor precisión y exactitud, aplicando Enfoques de grado 3 (espacialmente expliciticos), para el cálculo de datos de actividad y factores de emisión de Nivel 2 y 3, (creados en base a datos, inventarios y modelos, desarrollados en el país a escala nacional o subnacional). Se aplicaron metodologías diferenciadas para estimar emisiones y absorciones en áreas de bosques que permanecen como tal y áreas que registran cambios de uso de la tierra.

En el caso de los bosques que permanecen como tal las emisiones por degradación, así como las absorciones producto del aumento de biomasa, fueron calculadas mediante una metodología que, utilizando datos del Inventario Forestal Continuo y análisis de imágenes satelitales, calcula el área basal y número de árboles en una retícula continua

de celdas de una hectárea, permitiendo identificar la situación de degradación o aumento de existencias y el contenido exacto de CO_2e emitido a la atmósfera o absorbido por el bosque durante el periodo.

Para la estimación de emisiones y absorciones que implican cambio de uso de la tierra, como la sustitución, restitución o forestación se analizaron las matrices de cambio del Catastro y se establecieron valores derivados del Inventario Forestales Continuo, de la misma forma que se aplica en el INGEI.

Para determinar las emisiones de Gases de Efecto Invernadero producto de la combustión en incendios forestales se aplicaron factores estándar.

Resultados generales

El NREF/NRF subnacional de Chile representa un flujo de carbono correspondiente a absorciones de carbono 1,5 millones de Toneladas de CO_2e anuales. Este se divide en cuatro principales actividades:

- Deforestación; con 3,5 millones de Ton de CO_2e anuales emitidas, para una superficie superior a las 6.000 ha anuales
- Degradación Forestal; con 9,2 millones de Ton. CO_2e anuales emitidas, para una superficie superior a las 500.000 hectáreas entre 2001 y 2010.
- Aumento de existencias; con 10,0 millones de Ton.CO_2e anuales absorbidas, para una superficie superior a las 700.000 hectáreas entre 2001 y 2010
- Conservación Forestal; con 2,4 millones de Ton. CO_2e anuales absorbidas, para una superficie cercana a 1.450.000 hectáreas de bosques catalogados como áreas de conservación.

Es importante mencionar que el NREF/NRF no contabiliza las absorciones y emisiones que se producen en bosques nativos que se mantienen en un umbral de resiliencia o recuperación natural así como los flujos que se producen en las plantaciones forestales. Estos flujos son recopilados, sin embargo, en el Inventario de Gases de Efecto Invernadero de Chile.

Cronología de ampliación

Durante el año 2016 el Nivel de Referencia será ampliado a las regiones de Valparaíso, Metropolitana y O'Higgins, donde ya se cuenta con una serie de trabajos que han permitido tener avances puntuales. Se prevé que durante 2017 el Nivel de Referencia se extienda a nivel Nacional.

Relevancia del NR

Contar con un Nivel de Referencia ha sida un punto clave para el proceso de elaboración de la ENCCRV, ya que si bien, los principales causales de la deforestación y degradación forestal a nivel nacional e incluso a escala regional, como los incendios y el uso insustentable de la biomasa (principalmente la leña) son conocidos por todos los actores involucrados, hasta la fecha no ha existido una cuantificación específica, así como una identificación detallada de áreas con mayor nivel de afección.

En el marco de la ENCCRV han sido planteadas una serie de medidas de acción que tienen por objetivo combatir los principales causales de Deforestación y Degradación forestal, así como promover la Conservación, el Manejo Forestal y el Aumento de carbono en los bosques, la identificación de las áreas prioritarias para cada tipo de intervención, así como el control y monitoreo de los resultados de la implementación de estas medidas serán analizados en base al Nivel de Referencia.

La adecuada ejecución de estas medidas de acción, deberán ser monitoreadas, reportadas y verificadas ante entes internacionales, lo que permitirá a los ejecutores recibir pagos por resultados, incrementando la plusvalía de los bosques y mejorando las condiciones de vidas de aquellos que mantienen una relación directa con el bosque nativo chileno.

	NREF/NRF			
Actividad REDD+	**Deforestación**	**Degradación**	**Conservación**	**Aumentos**
Maule	84.982	608.976	-14.780	-1.182.162
Biobío	396.645	1.209.890	-72.359	-1.282.143
La Araucanía	1.059.067	1.907.344	-334.741	-1.517.894
Los Ríos	644.696	1.373.080	-710.081	-2.022.041
Los Lagos	1.267.494	4.050.103	-1.298.478	-4.007.772
Total	3.452.884	9.149.392	-2.430.439	-10.012.012

Tabla 1. NREF/NRF subnacional de Chile

POSTER

Synergistic use of sar and optical datasets for forest biomass retrieval and characterization of forests in temperate zone – a national case study Poland

Hoscilo Agata[1], Ziolkowski Dariusz[1], Lewandowska Aneta[1], Sterenczak Krzysztof[2], Bochenek Zbigniew[1], Bartold Maciej[3]

[1]Remote Sensing Centre, Institute of Geodesy and Cartography, Warsaw, Poland
[2] Forest Research Institute, Sekocin, Poland
[3] University of Warsaw, Faculty of Geography and Regional Studies, Warsaw, Poland

Hoscilo, A.: E-mail: agata.hoscilo@igik.edu.pl, Tel: +48 223291976

Keywords: biomass, SAR, carbon, temperate, forest parameters

Abstract

Assessment of forest above-ground woody biomass is essential for national and regional forest carbon stocks and carbon stock changes estimation and reporting. The use of remotely sensed data supports countries in advancing approaches to forest monitoring and management. It helps to obtain accurate data on the status of forest resources and forest carbon stocks and support implementation of national and international policies. The aim of this research is to develop methodology for the forest above-ground woody biomass retrieval at the temperate forest, based on remotely sensed data. The biomass assessment was conducted in the framework of the European Space Agency (ESA) funded GlobBiomass project, which aims to better characterize and to reduce uncertainties of above ground biomass estimates by developing an innovative synergistic mapping approach in five regional sites (Sweden, Poland, Borneo, Mexico, South Africa) for the epochs 2005, 2010 and 2015 and one global map for the year 2010. The authors present the approach for the biomass retrieval at the national level over Poland – temperate forest. A synergy of radar ALOS PALSAR (L-band) and optical Landsat missions data have been used to derive forest above-ground woody biomass at the national level. The backscattering at HH and HV polarization, texture and ratios have been tested. The National Inventory of Forest Condition (inventory plots) has been used as the reference data for the biomass retrieval. The growing stock volume was converted into woody biomass using the IPCC approach based on biomass expansion factors (BEFs) and wood density following IPCC guidelines. The method used for biomass estimation in Poland was based on a machine-learning Random Forest regression. The Random Forest models were calibrated separately for coniferous and deciduous forest using a set of training plots located over the entire forested area except steep slopes in the mountains. The overall accuracy of the biomass retrieval is around 50 tons per hectares; the accuracy of coniferous is better than for broadleaf forest. The information on the spatial distribution of forest biomass was then related to the forest parameters (tree species, type of forest site, forest composition) described by vegetation spectral indices derived from high-resolution Landsat and SPOT5 images. The aim of this analysis was to examine the relationship between forest biomass and various features characterizing forest canopies within the selected area of interest. Remotely sensed forest parameters were determined within WICLAP project, conducted within Polish-Norwegian Research Programme, financed by the National Centre for Research and Development.

Using leaf-on and leaf-off airborne LiDAR to model vegetation structure and above-ground carbon storage in the critical zone

Kristen Brubaker
Hobart and William Smith Colleges, Geneva, NY

Keywords: understory biomass, critical zone, forest structure, lidar

Understanding patterns of above-ground carbon storage across forest types is increasingly important as managers adapt to the threats of climate change. Although airborne lidar has been used extensively to model above-ground carbon storage, it has not been extensively used to understand the difference between tree and shrub carbon storage in closed canopy forests. We compared the fine-scale above ground carbon storage in two watersheds; one watershed was underlain by sandstone bedrock and the other by shale. We measured tree and shrub biomass across three topographic positions for both watersheds, and calculated the carbon stored in each. We then used leaf-on and leaf-off airborne lidar datasets to construct a model for carbon storage for each component across the watershed, using a combination of terrain and point cloud metrics from lidar. Since overstory vegetation can obscure the understory vegetation from LiDAR, a correction factor was applied using percent overstory canopy cover. Using RandomForest, we modeled shrub and tree forest carbon across both watersheds, using a combination of leaf-on and leaf-off LiDAR point cloud metrics and topographic metrics. We found that there is an inverse relationship between tree carbon storage and shrub carbon storage across sites, and that LiDAR can be used to model these relationships across a broader, watershed scale. We also found differences in the tree carbon and shrub carbon ratios between bedrock types. Watersheds underlain with sandstone had a higher proportion of their carbon stored in shrubs, while watersheds underlain with shale had a higher proportion of their carbon stored in trees.

Using satellite data to estimate gas emissions into the atmosphere by burning biomass in Mexico

Maria Isabel Cruz Lopez

National Commission for Knowledge and Use of Biodiversity (CONABIO),
Liga Periferico –Insurgentes Sur 4903, Col. Parques del Pedregal
C.P 14010 Tlalpan, Mexico D.F., icruz@conabio.gob.mx

Keywords: Emissions, Forest fire, satellite data

Mexico is a biodiverse country as result of geographical conditions. One of the most recurrent threats to biodiversity are forest fires, which among its consequences are emissions of greenhouse gases (GHGs), which affect the nature, health and human activities, and they have influence in the global warming. These effects are expressed in different spatial levels: local, regional and global, so it becomes a relevant issue to national and international context.

Internationally, the issue of fires emissions has been analyzed on different ways and techniques; one of the most widely models used to estimate emissions require calculating four main parameters: burned area, amount of existing biomass, burning efficiency (biomass consumed by fire) and emission factor. Different authors have applied the model using statistical data and satellite data. One of the most difficult parameters to estimate is the efficiency of burning, some authors have proposed alternatives using satellite imagery, but the uncertainty is still high.

Therefore the main objective of the research is to develop a method for calculating the burning efficiency with remote sensing data in three representative sites of forest eco-regions of Mexico, as input for the estimation of gas emissions from the burning of biomass and know their spatial distribution.

In order to make predictions of this variable in dynamic form, it uses statistical learning methods, as decision trees, and satellite products to find the spatial and temporal relationships between environmental features (18 variables of biomass, vegetation, topography) and the burning efficiency (field data, provided by Dr. German Flores). The preliminary results show some patters to select the main variables and introduce others, as fuel moisture, and increase the accuracy of prediction.